1-1-2012

Lightweight Self-consolidating Concrete: Statistical Modelling, Mixture Design And Performance Evaluation

Abdurrahmaan Lotfy
Ryerson University

LIGHTWEIGHT SELF-CONSOLIDATING CONCRETE: STATISTICAL MODELLING, MIXTURE DESIGN AND PERFORMANCE EVALUATION

By

Abdurrahmaan Lotfy

Master of Applied Science in Civil Engineering

Ryerson University, 2006

A dissertation presented to Ryerson University
in partial fulfillment of the requirements for the degree of

Doctor of Philosophy

in the Program of Civil Engineering

Toronto, Ontario, Canada, 2012

AUTHOR'S DECLARATION

AUTHOR'S DECLARATION FOR ELECTRONIC SUBMISSION OF A DISSERTATION

I hereby declare that I am the sole author of this dissertation. This is a true copy of the dissertation, including any required final revisions, as accepted by my examiners.

I authorize Ryerson University to lend this dissertation to other institutions or individuals for the purpose of scholarly research

I further authorize Ryerson University to reproduce this dissertation by photocopying or by other means, in total or in part, at the request of other institutions or individuals for the purpose of scholarly research.

I understand that my dissertation may be made electronically available to the public.

Abdurrahmaan Lotfy

Abstract

Lightweight Self-Consolidating Concrete: Statistical Modelling, Mixture Design and Performance Evaluation

Abdurrahmaan Lotfy

2012, PhD, Department of Civil Engineering, Ryerson University

A response surface method based experimental study was carried out to model the influence of key parameters on properties of Lightweight Self-Consolidating Concrete (LWSCC) mixtures developed with various types of lightweight aggregates namely, furnace slag (FS), expanded clay (EC), and expanded shale (ESH). Three key parameters were selected to derive mathematical models for evaluating fresh and hardened properties. Water/binder ratio of 0.30 to 0.40, high range water reducing agent (HRWRA) of 0.3 to 1.2% (by total content of binder) and total binder content of 410 to 550 kg/m^3 were used for the design of LWSCC mixtures. Slump flow diameter, V-funnel flow time, J-ring flow diameter, J-ring height difference, L-box ratio, filling capacity, bleeding, fresh air content, initial and final set times, sieve segregation, fresh/28-day air/oven dry unit weights and 7- and 28-day compressive strengths were evaluated. Utilizing the developed model, three optimum LWSCC mixes with high desirability were formulated and tested for mechanical, mass transport and durability characteristics. The optimized industrial LWSCC mixtures were produced in lab/industrial set-up with furnace slag, expanded clay, and expanded shale aggregates. The mixtures were evaluated by conducting compressive/flexural/split tensile strength, bond strength (pre/post corrosion), drying shrinkage, sorptivity, absorption, porosity, rapid chloride-ion permeability, hardened air void (%), spacing factor, corrosion resistance, resistance to elevated temperature, salt scaling, freeze-thaw

resistance, and sulphuric acid resistance tests. It was possible to produce robust LWSCC mixtures that satisfy the European EFNARC criteria for Self-Consolidating Concrete (SCC).

The proposed mix design model is proved to be a useful tool for understanding the interactions among mixture parameters that affect important characteristics of LWSCC. This understanding might simplify the mix design process and the required testing, as the model identifies the relative significance of each parameter, provides important information required to optimize mix design and consequently minimizes the effort needed to optimize LWSCC mixtures, and ensures balance among parameters affecting fresh and hardened properties.

LWSCCs with FS, EC and ESH lightweight aggregates can reduce the construction pollution, increase the design solutions, extend the service life of the structure and hence, promote sustainability in construction industry.

Acknowledgement

I would like to express my deepest gratitude to my supervisors, Dr. Mohamed Lachemi and Dr. Anwar Hossain, for their guidance, support and patience during the development of this dissertation. During my years at Ryerson they have been there for me without hesitation.

My sincere gratitude and respect goes to my dedicated supervisor, Professor Mohamed Lachemi, for his patience, guidance, sound advice, encouragement and continual support throughout my time at Ryerson - you have always been an inspiration to me not only in research but also in my personal life. To me, you are a great mentor, a passionate researcher, and a caring friend and overall a key factor in me achieving my PhD degree.

I would like to thank Dr. Anwar Hossain for willingness to always help along with patience, kind words and belief in me, which pulled me through this thesis. His countless proof readings, corrections and support made this document possible, and will not be forgotten.

I am also grateful to Dr. Medhat Shehata for his motivation, advice and assistance. He led me to believe that I have a lot of ability and can accomplish anything I set in my mind.

My heartfelt appreciation goes to my doctoral dissertation committee members for their precious time and valuable comments.

I deeply appreciate the remarkable cooperation and technical support of the postdoctoral fellows, Dr. Erdogan Ozbay and Dr. Okan Karahan. In addition, I would like to thank Nidal Jaalouk and Mohamad Aldardari for their technical support during the experimental program of this dissertation.

Finally, I like to acknowledge the contributions of my family. My eternal gratitude to my mother and father for their unconditional love, to my brothers and sisters for their encouragement and support. They have been always by my side and shown their confidence in me. Special appreciation goes to my wife, without her support, sacrifices and believe my successes would not be possible.

Dedication

To My Family

&

To those who guided me on my path

Table of Contents

AUTHOR'S DECLARATION ..... **ii**

Abstract ..... **iii**

Acknowledgement ..... **v**

Dedication ..... **vi**

Table of Contents ..... **vii**

List of Tables ..... **xii**

List of Figures ..... **xv**

List of Notation ..... **xxv**

CHAPTER ONE **1**

1 INTRODUCTION **1**

1.1 General 1

1.2 Background of SCC 3

1.3 Definition of Lightweight Concrete 4

1.4 Development of LWC and Its Applications 4

1.5 Research Significance and General Objectives 5

1.6 Specific Objectives of the Thesis 6

1.7 Thesis Structure 7

CHAPTER TWO **9**

2 LITERATURE REVIEW **9**

2.1 Introduction 9

2.2 Lightweight Concrete (LWC) 10

2.2.1 Introduction *10*

2.2.2 Types of Lightweight Aggregates *11*

2.2.3 Lightweight Aggregate Manufacturing *11*

2.2.4 Absorption properties of lightweight aggregate *14*

2.2.5 Internal Curing 15
2.2.6 Lightweight Concrete Proportioning and Mix Design 16
2.2.7 Mechanical and Mass Transport Properties of Lightweight Concrete 18
2.3 SELF - CONSOLIDATING CONCRETE (SCC) 22
2.3.1 Introduction 22
2.3.2 Materials for Normal Weight SCC 24
2.3.3 Fresh Properties of SCC 25
2.3.4 Mechanical Properties of SCC 31
2.3.5 Durability of Self-Consolidating Concrete 32
2.3.6 Statistical Models of Self-Consolidating Concrete 35
2.4 LIGHTWEIGHT SELF- CONSOLIDATING CONCRETE (LWSCC) 44
2.4.1 Introduction 44
2.4.2 Mixture Design Procedures for LWSCC 44
2.4.3 Factors Affecting Fresh and Hardened Characteristics of LWSCC 53
2.4.4 Durability and Long Term Performance of Self-Consolidating Lightweight Concrete 56
2.4.5 Previous studies related to LWSCC 57
CHAPTER THREE 67
3 EXPERIMENTAL PROGRAM 67
3.1 SCOPE OF THE EXPERIMENTAL PROGRAM 67
3.2 MATERIALS PROPERTIES 69
3.2.1 Properties of Cement, Mineral and Supplementary Cementing Materials (SCM) ... 69
3.2.2 Aggregates 71
3.3 PARAMETRIC CRITERIA 75
3.3.1 Key Parameters 75
3.3.2 Aggregates Testing - Packing Density 76
3.4 MIX DESIGN METHODOLOGY AND MIXTURE PROPORTION 81
3.5 EXPERIMENTAL PROCEDURES 90
3.5.1 Measured Responses 90

3.5.2 Casting of Test Specimens *90*
3.5.3 Testing Procedures *93*

CHAPTER FOUR **97**

4 ASSESSMENTS OF FRESH AND HARDENED PROPERTIES OF STATISTICALLY DERIVED LWSCC MIXTURES **97**

4.1 INTRODUCTION 97
4.2 RESULTS AND DISCUSSIONS 97
4.2.1 Fresh Properties of LWSCC Mixtures *97*
4.2.2 Density and Compressive Strength of LWSCC Mixtures *98*
4.2.3 Discussions *105*
4.3 SUMMARY 118

CHAPTER FIVE **120**

5 THE RESPONSES OF LWSCC MIXTURES AND STATISTICAL EVALUATION OF RESULTS **120**

5.1 INTRODUCTION 120
5.2 RESULTS AND DISCUSSIONS 120
5.2.1 Effects of Mix Parameters on the Slump Flow *121*
5.2.2 Effects of Mix Parameters on the V-Funnel Flow Time *122*
5.2.3 Effects of Mix Parameters on the L- Box Ratio *122*
5.2.4 Effects of Mix Parameters on the Segregation Resistance *123*
5.2.5 Effects of Parameters on Other Responses *124*
5.2.6 Statistical Evaluation of the Test Results *138*
5.2.7 Mathematical Formulation of LWSCC Properties *138*
5.2.8 Statistical Analysis of the Response Models *140*
5.2.9 Repeatability of the Test Parameters *148*
5.3 SUMMARY 150

CHAPTER SIX 163

6 MIX PROPORTION OPTIMIZATION AND VALIDATION OF THE STATISTICAL MODELS 163

6.1 INTRODUCTION 163
6.2 LWSCC MIXTURE OPTIMIZATION 164
6.3 VERIFICATION OF STATISTICAL MODELS 176
6.4 VERIFICATION EXPERIMENT FOR AN OPTIMUM MIX DESIGN 190
6.5 SUMMARY 194

CHAPTER SEVEN 195

7 EVALUATION OF THE MECHANICAL AND MASS TRANSPORT PROPERTIES OF LWSCC MIXTURES 195

7.1 INTRODUCTION 195
7.2 TESTING PROGRAM 195
7.2.1 Casting of Test Specimens 197
7.2.2 Testing Procedures 200
7.3 LWSCC MECHANICAL PROPERTIES RESULTS AND DISCUSSION 204
7.3.1 Effect of LWA on LWSCC Compressive Strength 204
7.3.2 LWSCC Compressive Strength 207
7.3.3 LWSCC Unit Weight 213
7.3.4 LWSCC Flexural Strength 217
7.3.5 LWSCC Split Tensile Strength 221
7.3.6 LWSCC Bond Strength and Discussion 226
7.4 LWSCC MASS TRANSPORT PROPERTIES RESULTS AND DISCUSSION 238
7.4.1 LWSCC Porosity and Water Absorption 238
7.4.2 LWSCC Sorptivity 241
7.4.3 Rapid Chloride Permeability (RCP) of LWSCC 246
7.4.4 LWSCC Drying Shrinkage 250
7.5 SUMMARY 253

CHAPTER EIGHT 255

8 EVALUATION OF DURABILITY ASPECTS OF LWSCC MIXTURES .. 255

8.1 INTRODUCTION 255

8.2 LWSCC DURABILITY PERFORMANCE 255

8.2.1 LWSCC Corrosion Resistance 255

8.2.2 Resistance LWSCCs against Elevated Temperatures 263

8.2.3 Salt Scaling Resistance of LWSCCs 276

8.2.4 Hardened Air Void Analysis of LWSCC 281

8.2.5 Sulphuric Acid Attack Resistance of LWSCC 283

8.2.6 Freeze-Thaw Resistance of LWSCC 289

8.3 SUMMARY 297

CHAPTER NINE 298

9 CONCLUSIONS 298

9.1 SUMMARY 298

9.2 CONCLUSIONS 300

9.3 RECOMMENDATIONS FOR FURTHER RESEARCH 308

APPENDIX 310

APPENDIX A 310

REFERENCES 345

List of Tables

Table 2.1- Allowable lightweight aggregate densities 14
Table 2.2 - Lightweight aggregate saturation test (ESCSI 2004) 15
Table 2.3 - SCC mix proportions for Pearson International Airport in Toronto, Canada (Lessard et al. 2002)..... 23
Table 2.4 - SCC testing methods (EFNARC 2005; ACI 237R 2007; JSCE 1998)..... 26
Table 2.5 - Typical ranges of SCC specified by European guidelines (EFNARC 2005)..... 29
Table 2.6 - SCC proportioning trial mixture parameters (ACI 237R 2007) 29
Table 2.7 - Coarse aggregate content for JSCE ranking (JSCE 1998)..... 30
Table 2.8 - SCC Mix design characteristics (Koehler and Fowler 2006) 31
Table 2.9 - Example of mix proportions using two-level fractional factorial design method (Khayat et al. 2000)..... 37
Table 2.10 - Example of limit and coded value of factors (variables) - (Patel et al. 2004) 40
Table 2.11 - Range of code values F composite factorial design (Sonebi et al. 2007) 41
Table 3.1 - Chemical and physical properties of cement, fly ash and silica fume..... 70
Table 3.2 - Grading and physical properties of aggregates..... 73
Table 3.3 - Chemical analysis of Furnace Slag, Expanded Clay, Expanded Shale..... 74
Table 3.4 - Summary of the optimum aggregate content by volume, weight and void ratio..... 80
Table 3.5 - Limit and coded value of factors 84
Table 3.6 - Statistical analysis factors - Central composite design (CCD) method..... 85
Table 3.7 - Mixture proportions for FS-LWSCC (Furnace Slag LWSCC)..... 87
Table 3.8 - Mixture proportions for EC-LWSCC (Expanded Clay LWSCC)..... 88
Table 3.9 - Mixture proportions for ESH-LWSCC (Expanded Shale LWSCC)..... 89
Table 4.1 - Test results on fresh properties of FS mixes..... 99
Table 4.2 - Test results on fresh properties of EC mixes 100
Table 4.3 - Test results on fresh properties of ESH mixes..... 101
Table 4.4 - Compressive strength and unit weight test results of FS mixes 102
Table 4.5 - Compressive strength and unit weight test results of EC mixes..... 103

Table 4.6 - Compressive strength and unit weight test results of ESH mixes 104
Table 4.7 - LWSCC performance criteria 106
Table 4.8 - Comparison of the 28-day compressive strength results of the developed mixes.....115
Table 4.9 - Comparison of the 28- day air dry unit weight results of the developed mixes 119
Table 5.1 - Analysis of GLM - ANOVA model for FS- LWSCC properties..... 151
Table 5.1 Cont'd - Analysis of GLM - ANOVA model for FS- LWSCC properties 152
Table 5.2 - Analysis of GLM - ANOVA model for EC-LWSCC properties 153
Table 5.2 Cont'd - Analysis of GLM - ANOVA model for EC-LWSCC properties..... 154
Table 5.3 - Analysis of GLM - ANOVA model for ESH-LWSCC properties..... 155
Table 5.3 Cont'd - Analysis of GLM - ANOVA model for ESH-LWSCC properties 156
Table 5.4 - Mathematical Formulation of FS -LWSCC properties 157
Table 5.5 - Mathematical Formulation of EC - LWSCC properties 158
Table 5.6 - Mathematical Formulation of ESH- LWSCC properties..... 159
Table 5.7 - Repeatability of test parameters for FS- LWSCC mixtures..... 160
Table 5.8 - Repeatability of test parameters for EC-LWSCC mixtures 161
Table 5.9 - Repeatability of test parameters for ESH -LWSCC mixtures..... 162
Table 6.1 - EFNARC SCC classification..... 165
Table 6.2 - Classification of responses goal and limits of FS- LWSCC mixtures 168
Table 6.3 - Classification of responses goal and limits of EC- LWSCC mixtures 169
Table 6.4 - Classification of responses goal and limits of ESH- LWSCC mixtures..... 170
Table 6.5 - Mixture proportions for FS-LWSCC (Furnace Slag LWSCC)..... 176
Table 6.6 - Mixture proportions for EC-LWSCC (Expanded Clay LWSCC)..... 177
Table 6.7 - Mixture proportions for ESH-LWSCC (Expanded Shale LWSCC)..... 177
Table 6.8 - Test results of FS- LWSCC mixes used to validate statistical models 178
Table 6.9 - Test results of EC- LWSCC mixes used to validate statistical models..... 179
Table 6.10 - Test results of ESH- LWSCC mixes used to validate statistical models 180
Table 6.11 - FS-LWSCC - Theoretically optimum mix proportions and experimental results .. 191
Table 6.12 - EC-LWSCC- Theoretically optimum mix proportions and experimental results... 192
Table 6.13 - ESH-LWSCC - Theoretically opt mix proportions and experimental results..... 193
Table 7.1- Mix parameters and fresh properties of LWSCC..... 196

Table 7.2 - Summary of tests selected for LWSCC evaluation 199
Table 7.3 - Compressive strength results of LWSCC mixtures 208
Table 7.4 - Unit weight results of LWSCC mixtures 214
Table 7.5 - Flexural strength results of LWSCC mixtures 218
Table 7.6 - Split tensile strength results of LWSCC mixtures 223
Table 7.7 - 28-day bond strength results of LWSCC mixtures 229
Table 7.8 - Comparison of LWSCC bond strength using various code equations 237
Table 7.9 - Absorption and porosity results of LWSCC mixtures 239
Table 7.10 - RCPT results of LWSCC mixtures 247
Table 8.1 - LWSCC specimen detail for accelerated corrosion test 256
Table 8.2 - Bond strength loss and weight loss of steel rebar after corrosion of LWSCC specimens 262
Table 8.3 - Deicing salt surface scaling test results of LWSCC blocks 277
Table 8.4 - LWSCC hardened air void and spacing factor analysis 282

List of Figures

Figure 2.1 - Classification of lightweight concrete and types of aggregates used (Harding 1995) 11
Figure 2.2 - Process flow diagram for lightweight aggregate manufacturing (Environmental Protection Agency 1985) 13
Figure 2.3 - Internal pore structure of lightweight aggregate 13
Figure 2.4 - Modulus of elasticity for different types of concrete (ACI 213R, 2003) 19
Figure 2.5 - Creep for different types of concrete (ACI 213R 2003) 20
Figure 2.6 - increase of SCC usage in Japan (Ouchi, 2003) 22
Figure 2.7- Relationship between slump flow, slow time, and filling capacity of mixture made with different w/cm and Vca values (Khayat et al. 2000) 38
Figure 2.8 - Presentation of modelled region of experimental plan 42
Figure 2.9 - Examples of measured properties versus predicted from statistical models of slump flow and v-funnel (Sonebi 2003) 43
Figure 2.10 - Scheme of compacted aggregate and concrete mixture (Shi and Wu 2005) 47
Figure 2.11 - Effect of coarse-to-total aggregate volume ratio on bulk density and void volume (Shi and Wu 2005) 48
Figure 2.12- Densified aggregate to reduce (Hwang and Hung 2005) 49
Figure 2.13 - The loose density, packing density ratio and void of blended aggregate mixture (Hwang and Hung 2005) 50
Figure 2.14 - Proportioning lightweight self-consolidating concrete by DMDA (Hwang and Hung 2005) 52
Figure 3.1 - Various phases of experimental program 68
Figure 3.2 - Coarse and fine lightweight aggregates used in the study 72
Figure 3.3 - Grading curves for both fine and coarse aggregates 74
Figure 3.4 - Optimum bulk density and % of void of coarse and fine lightweight furnace slag aggregates 78
Figure 3.5 - Optimum bulk density and % of void of coarse and fine lightweight expanded clay

aggregates 79
Figure 3.6 - Optimum bulk density and % of void of coarse and fine lightweight expanded shale aggregates 80
Figure 3.7 - Presentation of modelled region of experimental plan 82
Figure 3.8 - Structure of the three-variable factorial plan of experiment 82
Figure 3.9 - Drum rotating mixer 91
Figure 3.10 - Aggregates 72 hrs pre-soaking 91
Figure 3.11 - Draining excess water form pre- soaked fines and coarse aggregates 92
Figure 3.12 - Pre-weight mixture proportions 92
Figure 3.13 - Standard mixing sequence 92
Figure 3.14 - Mixture temperature and slump flow test - measure of flowability 93
Figure 3.15 - V- Funnel test and filling capacity test 94
Figure 3.16 - J-ring and J- ring height test 94
Figure 3.17 - L- Box test and bleed test 94
Figure 3.18 - Fresh density test and Fresh density test 95
Figure 3.19 - Sieve segregation resistance test and air content test (volumetric method) 95
Figure 3.20 - Penetration resistance test (set time test) and moulds casting 95
Figure 3.21 - Wet burlap curing in the first 24 hrs and compressive strength test 96
Figure 4.1 - Comparison of the slump flows of the developed mixtures 107
Figure 4.2 - Comparison of the L-Box ratios of the developed mixtures 107
Figure 4.3 - Comparison of the filling capacities of the developed mixtures 108
Figure 4.4 - Comparison of the segregation indexes of the developed mixtures 108
Figure 4.5 - Relation of slump flow and segregation index of the developed mixtures 110
Figure 4.6 - Relation of V-Funnel time and segregation index of the developed mixtures 110
Figure 4.7 - Relation of slump flow and V-Funnel time of the developed mixtures 111
Figure 4.8 - Relation of slump flow and J-ring flow of the developed mixtures 111
Figure 4.9 - Relation of J-ring flow and J- ring height different of the developed mixtures 112
Figure 4.10 - Comparison of the 7-day compressive strength of the developed mixtures 113
Figure 4.11 - Comparison of the 28-day compressive strength of the developed mixtures 113
Figure 4.12 - Comparison of the fresh unit weight test results of the developed mixtures 116

Figure 4.13 - Comparison of the 28-day air dry unit weight test results of the developed mixtures 117
Figure 4.14 - Comparison of the 28-day oven dry unit weight test results of the developed mixtures 117
Figure 5.1 - Contours of slump flow changes of FS-LWSCC mixes with w/b, total binder content and HRWRA at 0.75 % 126
Figure 5.2 - Contours of slump flow changes of EC-LWSCC mixes with w/b, total binder content and HRWRA at 0.75 % 126
Figure 5.3 - Contours of slump flow changes of ESH-LWSCC mixes with w/b, total binder content and HRWRA at 0.75 %..... 127
Figure 5.4 - Effect of w/b, HRWRA and total binder content at 480kg/m^3on the slump flow of FS-LWSCC mixes 127
Figure 5.5 - Effect of w/b, HRWRA and total binder content at 480kg/m^3 on the slump flow of EC-LWSCC mixes 128
Figure 5.6 - Effect of w/b, HRWRA and total binder content at 480kg/m^3 on the slump flow of ESH-LWSCC mixes..... 128
Figure 5.7 - Effect of w/b, HRWRA and total binder content at 480kg/m^3 on the V-funnel time of FS-LWSCC mixes..... 129
Figure 5.8 - Effect of w/b, HRWRA and total binder content at 480kg/m^3 on the V-funnel time of EC-LWSCC mixes 129
Figure 5.9 - Effect of w/b, HRWRA and total binder content at 480kg/m^3 on the V-funnel time of ESH-LWSCC mixes..... 130
Figure 5.10 - Contours of V-funnel changes of FS-LWSCC mixes with w/b, total binder content and HRWRA at 0.75 % 130
Figure 5.11 - Contours of V-funnel changes of EC-LWSCC mixes with w/b, total binder content and HRWRA at 0.75 % 131
Figure 5.12 - Contours of V-funnel changes of ESH-LWSCC mixes with w/b, total binder content and HRWRA at 0.75 %..... 131
Figure 5.13 - Effect of w/b, HRWRA and total binder content at 480kg/m^3on the L-Box of FS-LWSCC mixes..... 132

Figure 5.14 - Effect of w/b, HRWRA and total binder content at 480kg/m^{3}on the L-Box of EC-LWSCC mixes 132
Figure 5.15 - Effect of w/b, HRWRA and total binder content at 480kg/m^{3}on the L-Box ratio of ESH-LWSCC mixes 133
Figure 5.16 - Contours of L- Box ratio changes of FS-LWSCC mixes with w/b, total binder content and HRWRA at 0.75 % 133
Figure 5.17 - Contours of L- Box ratio changes of EC-LWSCC mixes with w/b, total binder content and HRWRA at 0.75 % 134
Figure 5.18 - Contours of L- Box ratio changes of ESH-LWSCC mixes with w/b, total binder content and HRWRA at 0.75 % 134
Figure 5.19 - Contours of segregation resistance changes of FS-LWSCC mixes with w/b, total binder content and HRWRA at 0.75 % 135
Figure 5.20 - Contours of segregation resistance changes of EC-LWSCC mixes with w/b, total binder content and HRWRA at 0.75 % 135
Figure 5.21 - Contours of segregation resistance changes of ESH-LWSCC mixes with w/b, total binder content and HRWRA at 0.75 % 136
Figure 5.22 - Effect of w/b, HRWRA and total binder content at 480kg/m^3 on the SSR of FS-LWSCC mixes 136
Figure 5.23 - Effect of w/b, HRWRA and total binder content at 480kg/m^3 on the SSR of EC-LWSCC mixes 137
Figure 5.24 - Effect of w/b, HRWRA and total binder content at 480kg/m^3 on the SSR of ESH-LWSCC mixes 137
Figure 6.1- Various phases of the validation and optimization program 164
Figure 6.2 - Effect of w/b, HRWRA and total binder content at 494kg/m^{3}on the desirability function of FS-LWSCC- 1 mixture (EFNARC SCC class 1) 171
Figure 6.3 - Effect of w/b, HRWRA and total binder content at 520kg/m^{3}on the desirability function of FS-LWSCC- 2 mixture (EFNARC SCC class 2) 172
Figure 6.4 - Effect of w/b and HRWRA on the desirability function of FS-LWSCC- 3 mixture (EFNARC SCC class 3) 172
Figure 6.5 - Effect of w/b, HRWRA and total binder content at 526kg/m^{3}on the desirability

function of EC-LWSCC- 1 mixture (EFNARC SCC class 1) 173
Figure 6.6 - Effect of w/b, HRWRA and total binder content at 544kg/m^{3}on the desirability function of EC-LWSCC- 2 mixture (EFNARC SCC class 2) 173
Figure 6.7 - Effect of w/b and HRWRA on the desirability function of EC-LWSCC- 3 mixture (EFNARC SCC class 3) 174
Figure 6.8 - Effect of w/b, HRWRA and total binder content at 476kg/m^{3}on the desirability function of ESH-LWSCC- 1 mixture (EFNARC SCC class 1) 174
Figure 6.9 - Effect of w/b, HRWRA and total binder content at 486kg/m^{3}on the desirability function of ESH-LWSCC- 2 mixture (EFNARC SCC class 2) 175
Figure 6.10 - Effect of w/b and HRWRA on the desirability function of ESH-LWSCC- 3 mixture (EFNARC SCC class 3) 175
Figure 6.11 - Predicted vs. measured slump flow values of FS-LWSCC model 182
Figure 6.12 - Predicted vs. measured V-funnel values of FS-LWSCC model 183
Figure 6.13 - Predicted vs. measured J-ring values of FS-LWSCC model 183
Figure 6.14 - Predicted vs. measured J-ring height diff values of FS-LWSCC model 184
Figure 6.15 - Predicted vs. measured L-box values of FS-LWSCC model 184
Figure 6.16 - Predicted vs. measured filling capacity values of FS-LWSCC model 185
Figure 6.17 - Predicted vs. measured bleed water values of FS-LWSCC model 185
Figure 6.18 - Predicted vs. measured segregation index values of FS-LWSCC model 186
Figure 6.19 - Predicted vs. measured air content values of FS-LWSCC model 186
Figure 6.20 - Predicted vs. measured initial set time values of FS-LWSCC model 187
Figure 6.21 - Predicted vs. measured final set time values of FS-LWSCC model 187
Figure 6.22 - Predicted vs. measured 7-day compressive strength of FS-LWSCC model 188
Figure 6.23 - Predicted vs. measured 28-day compressive strength of FS-LWSCC model 188
Figure 6.24 - Predicted vs. measured fresh unit weight of FS-LWSCC model 189
Figure 6.25 - Predicted vs. measured 28-day air dry unit weight of FS-LWSCC model 189
Figure 6.26 - Predicted vs. measured 28-day oven dry unit weight of FS-LWSCC model 190
Figure 7.1 - Fixed horizontal industrial pan mixer 198
Figure 7.2 - Preparation of LWSCC elevate temperature and salt scaling specimens 201
Figure 7.3 - Preparation of LWSCC shrinkage prisms and elevate temperature specimens 201

Figure 7.4 - Preparation of LWSCC specimens 202
Figure 7.5 - Preparation of LWSCC specimens 202
Figure 7.6 - Preparation of LWSCC specimens 202
Figure 7.7 - Preparation of LWSCC freeze – thaw prisms and cylinders for bond test 203
Figure 7.8 - Casting and preparing LWSCC specimens 203
Figure 7.9 - Casting initial curing of LWSCC specimens 203
Figure 7.10 - Water tanks for curing LWSCC specimens 204
Figure 7.11 - SEM view of lightweight aggregate closely bonded with cement matrix (x 75) (Lo and Cui 2004) 205
Figure 7.12 - View of the lightweight aggregate concrete showing diffusion of cement paste into the aggregate surface (x 75) (Lo and Cui 2004) 206
Figure 7.13 - The ITZ showing ettringite formed on surface of porous lightweight aggregate (x 5000) (Lo and Cui 2004) 206
Figure 7.14 - Comparison between the 28-day comp strength of FS and EC- LWSCC mixtures against the ESH-LWSCC mixtures 209
Figure 7.15 – Coarse FS aggregate fracture in the broken specimens 210
Figure 7.16 – Coarse ESH aggregate fracture in the broken specimens 210
Figure 7.17 - Comparison of compressive strength gain with age for the three different LWSCC mixtures 212
Figure 7.18 - Comparison of (%) increase of compressive strength with age for different LWSCC mixtures 212
Figure 7.19 - Comparison of compressive strength of three types of LWSCC mixtures at different ages 213
Figure 7.20 - Comparison of the unit weights values of three types of LWSCC mixtures 215
Figure 7.21 - Comparison of the reduction percentages of unit weights of three types of LWSCC mixtures 215
Figure 7.22 - Comparison between compressive strength and dry unit weight density of different types of LWSCC mixtures 216
Figure 7.23 - Flexural test (4- point loading) of LWSCC beams 217
Figure 7.24 - Flexural test (4- point loading) of LWSCC beams 218

Figure 7.25 - Comparison of the flexural strength of different types of LWSCC mixtures at different ages 219
Figure 7.26 - Comparison of the flexural strength gains with age for different types of LWSCC mixtures 219
Figure 7.27 - Comparison of (%) increase of flexural strength with age for different LWSCC mixtures 220
Figure 7.28 - Relationship between the 28-day compressive strength and flexural strength of LWSCC mixtures 221
Figure 7.29 - Split tensile strength test of LWSCC cylinder 222
Figure 7.30 - Comparison between split tensile strength of different types of LWSCC mixtures at different ages 224
Figure 7.31 - Comparison between split tensile strength gains with age for different types of LWSCC mixtures 224
Figure 7.32 - Comparison of (%) increase of tensile strength with age for different LWSCC mixtures 225
Figure 7.33 - Relationship between the 28-day compressive strength and split tensile strength of LWSCC mixtures 226
Figure 7.34 - Schematic representation of pullout test specimen 227
Figure 7.35 - Pull-out test of LWSCC cylinders 228
Figure 7.36 - Pull-out test set up and LWSCC specimens after testing 228
Figure 7.37 - Comparison between the 28-day bond strength of the three different types of LWSCC mixtures 230
Figure 7.38 - The 28-day bond strength reduction of FS and EC- LWSCC mixtures against the ESH-LWSCC 230
Figure 7.39 - Bond failure due to splitting with cracks forming at approximately 120^{o} 231
Figure 7.40 - Bond failure due to splitting with cracks forming at approximately 120^{o} 231
Figure 7.41 - Load-slip behaviour depending on type of rebar (Lachemi et al. 2009) 233
Figure 7.42 - Load-slip behaviour of LWSCC mixtures 233
Figure 7.43 - Relationship between the 28-day compressive strength and bond strength of LWSCC mixtures 234

Figure 7.44 - Absorption and porosity test of LWSCC specimens 238
Figure 7.45 - Comparison between the absorption (%) of the three different types of LWSCC mixtures 240
Figure 7.46 - Comparison between the porosity (%) of the three different types of LWSCC mixtures 241
Figure 7.47 - Schematic diagram showing differences between porosity and permeability (EuroLightCon 1998) 242
Figure 7.48 - Sorptivity measure of LWSCC 243
Figure 7.49 - LWSCC samples during sorptivity test 243
Figure 7.50 - Comparison between the 28-day and 91-day of sorptivity index of LWSCC mixtures 245
Figure 7.51 - Comparison between the 91-day sorptivity index reductions of LWSCC mixtures 245
Figure 7.52 - RCPT setup and samples preparation 247
Figure 7.53 - LWSCC samples undergo RCPT and “Germann Proove-it” software screen 248
Figure 7.54 - LWSCC samples after RCPT test 248
Figure 7.55 - Comparison between the 28-day and 91-day RCP values of LWSCC mixtures 249
Figure 7.56 - Drying shrinkage test of LWSCC prisms 251
Figure 7.57 - Comparison between the drying shrinkage values of LWSCC mixtures 251
Figure 8.1 - Schematic representation of the accelerated corrosion test 256
Figure 8.2 - Current–time history for LWSCC mixtures 258
Figure 8.3 - LWSCC specimens after accelerated corrosion test 260
Figure 8.4 - LWSCC specimens after accelerated corrosion test 260
Figure 8.5 - Corroded steel rebars after undergoing the accelerated corrosion test 261
Figure 8.6 - Comparison between theoretical and actual mass loss for all LWSCC mixtures 263
Figure 8.7 - Heating rate curves and duration of steady state temperatures 264
Figure 8.8 - Comparison between the residual compressive strength of LWSCC mixtures after exposure to different temperatures 265
Figure 8.9 - Comparison between the reductions in compressive strength of LWSCC mixtures after exposure to different temperatures 266

Figure 8.10 - LWSCC specimens during elevated temperatures test..... 269
Figure 8.11 - Controlled furnace used during elevated temperatures test 269
Figure 8.12 - LWSCC specimens after undergoing elevated temperatures test at 900^0C..... 269
Figure 8.13 - EC-LWSCC specimens after undergoing elevated temperatures tests..... 270
Figure 8.14 - Discoloration of EC-LWSCC specimens after undergoing the 900^0C temperatures test 270
Figure 8.15 - Surface map cracks on FS-LWSCC specimens after the 900^0C exposure test 271
Figure 8.16 - Discoloration of LWSCC specimens after specimens after the 900^0C exposure tests 271
Figure 8.17 - ESH-LWSCC specimens after the 300 and 600^0C exposure tests 272
Figure 8.18 - Surface map cracks on ESH-LWSCC specimens after the 900^0C exposure test .. 272
Figure 8.19 - Comparison between weight losses of LWSCC mixtures after exposure to different temperatures 273
Figure 8.20 - Relationship between the weight loss and reduction in compressive strength of FS-LWSCC mixtures 274
Figure 8.21 - Relationship between the weight loss and reduction in compressive strength of EC-LWSCC mixtures 275
Figure 8.22 - Relationship between the weight loss and reduction in compressive strength of ESH-LWSCC mixtures 275
Figure 8.23 - LWSCC mixtures - Cumulative amount of scaled materials over 50 cycles 278
Figure 8.24 - Controlled freezer used salt scaling test..... 280
Figure 8.25 - ESH-LWSCC specimens undergoing salt scaling test 280
Figure 8.26 - FS/EC LWSCC specimens after undergoing salt scaling test 280
Figure 8.27 - LWSCC specimens specimen after undergoing salt scaling test..... 281
Figure 8.28 - FS/EC/ESH LWSCC specimens after undergoing salt scaling test 281
Figure 8.29 - Comparison between weight losses of LWSCC mixtures after different duration of exposure to sulfuric acid 285
Figure 8.30 - Comparison between strength losses of LWSCC mixtures after different duration of exposure to sulfuric acid 287
Figure 8.31 - LWSCC specimens undergoing exposure to sulfuric acid 288

Figure 8.32 - LWSCC specimens under evaluation after exposure to sulfuric acid 288
Figure 8.33 - LWSCC specimens under evaluation after exposure to sulfuric acid 289
Figure 8.34 - Comparison between weight losses of LWSCC mixtures during freeze-thaw test291
Figure 8.35 - Comparison between the relative dynamic modulus of LWSCC mixtures..... 292
Figure 8.36 - LWSCC specimens before freeze-thaw test 294
Figure 8.37 - LWSCC specimens undergoing freeze-thaw cycles..... 295
Figure 8.38 - Evaluating LWSCC specimens during freeze-thaw test 295
Figure 8.39 - Evaluating LWSCC specimens during freeze-thaw test 295
Figure 8.40 - Evaluating LWSCC specimens during freeze-thaw test 296
Figure 8.41 - Evaluating ESH-LWSCC specimens after freeze-thaw test..... 296
Figure 8.42 - Evaluating EC-LWSCC specimens after freeze-thaw test 296
Figure 8.43 - Failed LWSCC specimens during freeze-thaw test..... 297

List of Notation

a	Factor Means
a_0	Equation Coefficient
A	*w/b* (Water -to- Binder Ratio)
A	Total Aggregate
AAR	Alkali Aggregate Reaction
A_b	Area of Individual Bar
A/b	Aggregate-to-Binder Ratio by Mass
ACI	American Concrete Institute
AEA	Air Entrained Admixtures
Al_2O_3	Aluminium Oxide
ASTM	American Society for Testing and Materials
b	Range of Factorial Values
B	Total Binder
C	(%) High Range Water Reducing Admixtures
CAF	Coarse Aggregate Fraction
CaO	Calcium Oxide
$Ca(OH)_2$	Calcium Hydroxide
C_3A	Tricalcium Aluminate
C_2S	Dicalcium Silicate
C_3S	Tricalcium Silicate
CCD	Central Composite Design
CEC	Coarse Expanded Clay

CES	Coarse Expanded Shale
CFRP	Carbon Fiber Reinforced Polymer
CFS	Coarse Furnace Slag
CI	Confidence Interval
Cl	Chloride
CM	Cementitious Materials Content
cm	Centimetres
COV	Coefficient of Variation
CSA	Canadian Standards Association
C/S	Calcium -to- Silicate Ratio
C–S–H	Calcium Silicate Hydrate
d	Days
d_b	Nominal Diameter of Bar
d_{cs}	The Distance From the Closest Concrete Surface to the Centre of the Bar
Dj	Desirability Functions
DIBt	German Institute of Construction Engineering in Berlin
DMDA	Densified Mixture Design Algorithm Method
DOF	Degree of Freedom
EC	Expanded Clay
EC-LWSCC	Expanded Clay LWSCC
E-Clay	Expanded Clay
EFNARC	European Federation of National Associations Representing Producers and Applicators of Specialist Building Products for Concrete
ES	Expanded Furnace Slag

E-Shale	Expanded Shale
ESH	Expanded Shale
ESH-LWSCC	Expanded Shale LWSCC
ESCSI	Expanded Shale Clay and Slate Institute
Eq	Equation
F	Faraday's constant (F = 96,487 Amp.sec)
F	Statistic Test
fs_f	Flexural Strength
f_u	Ultimate Strength of Bar
f_y	Specified Yield Strength
FA	Fly Ash
FAF	Fine Aggregate Fraction
F.C	Filling Capacity
FEC	Fine Expanded Clay
FES	Fine Expanded Shale
Fe_2O_3	Iron Oxide
FFS	Fine Furnace Slag
Fig	Figure
F.T	Flow Time
f_b	Bond Stress/Strength
f_c'	Compressive Strength of Concrete
f_r	Modulus of Rupture
f_{st}	Splitting Tensile Strength
F-Slag	Furnace Slag

FS	Furnace Slag
FS-LWSCC	Furnace Slag LWSCC
JSCE	Japanese Society of Civil Engineers
G	Mass of the Aggregate Plus the Measure
gm	Gram
GGBF	Ground Granulated Blast Furnace Slag
GLM-ANOVA	General Linear Models for Analysis of Variance
GPa	Giga Pascal (unit)
GU	General Use
h	Hour
h_2/h_1	L-box blocking ratio
HPC	High Performance Concrete
HRWRA	High Range Water Reducing Admixtures
ICAR	International Center for Aggregates Research
i	The Current Passed (Amperes)
ITZ	Interfacial Transition Zone
k	Number of Design Factors
kN	Kilonewton
Kg	Kilograms
K_{tr}	The Factor of the Contribution Due to Confinement
l_d	The Development Length
LOI	Loss on Ignition
LWAC	Structural Lightweight Aggregate Concrete
LWSCC	Lightweight Self-Consolidating Concrete

LWC	Lightweight Concrete
LWA	Lightweight Aggregate
LWA/Sand	Lightweight Coarse Aggregate-to-Sand
LWC	Light Weight Concrete
LWF	Lightweight Fine Aggregate
M	Bulk Density of the Aggregate
M	Atomic Weight (iron *M* = 55.847 g/mol)
m	Meter
ml	Millilitre
MgO	Magnesium Oxide
MnO	Manganese Oxide
MPa	Mega Pascal (unit)
m^3/m^3	Unit Absolute Volume of Coarse Aggregate
N	Number of Trials
n	Number of Observation
n_c	Center Point Portion
n_f	Fraction Factorial Portion
Na	Sodium
Na_2O	Sodium Oxide
NaOH	Sodium Hydroxide
NaC1	Sodium Chloride
NC	Normal Concrete
NF	Number of Fractional Factorial Points
n	Number of Variables

No.	Number
NSA	National Slag Association
NWA	Normal Weight Aggregate
P	Pullout Load
PA	Passing Ability
PCI	Prestressed Concrete Institute
pcf	Pounds per Cubic Foot
PFA	Pulverized Fly Ash
Pkg	Package
psi	Pounds per Square Inch
p	Probabilities
pH	Hydrogen Ion Concentration
RCPT	Resistance to Chloride-ion Penetration
RCP	Rapid Chloride Permeability
R	Correlation Coefficient
Sec	Seconds
s	Seconds
S	Bulk Specific Gravity
S/*A*	Sand -to- Total Aggregate Ratio
SCC	Self - Consolidating Concrete
SCLC	Self- Compacting Lightweight Concrete
SCM	Supplementary Cementing Materials
SEM	Scanning Electron Microscope
SF	Silica Fume

S/Pt	Sand-to -Paste Volume
SRA	Shrinkage Reducing Admixtures
SSD	Saturated Surface Dry
SiO_2	Silica - Silicon Dioxide
SO_3	Sulphur Trioxide
SP	Superplasticizer
SSR	Sieve Segregation Resistance
t	Time Passed
T	Mass of the Measure
TiO_2	Titanium Oxide
t_{min}	The Less Thickness of Cement Paste
u	Bond Stress
UPV	Pulse Velocity
V	Volume of the Measure
V	Viscosity
V_a	Volume of Total Aggregates
V_{ca}	Volume of Coarse Aggregate
V_{ca}/V_a	Volume of Coarse Aggregate to Volume of Total Aggregates Ratio
V_g	Volume of Coarse Aggregate
VEA	Viscosity Enhancing Admixtures
VMA	Viscosity Modifier Admixture
VOC	Volatile Organic Compounds
V	Voltage
Vol	Volume

V_p	Volume of Cement Paste
VSI	Visual Stability Index
V_v	Volume Void
W	Density of Water [998 kg/m^3]
w/b	Water -to- Binder Ratio
w/c	Water- to- Cement Ratio
w/cm	Water-to- Cementitious Ratio
w/p	Water-to-Powder Ratio
X	Actual Value (Original Measurement Scale)
X_h	Actual Upper Limit
X_l	Actual Lower Limit
Y	Model Response
z	Ion Charge (Assumed 2 for $Fe \rightarrow Fe^{2+} + 2e^-$)
μ	Mean Value of the Observation
%	Percentage
μm	Micrometer
Ø	Strength Reduction Factor
σ	Standard Deviation

CHAPTER ONE

1 INTRODUCTION

1.1 General

Self-consolidating concrete (SCC) technology has numerous advantages over conventional concrete. SCC does not require external or internal compaction, as it compacts under its self-weight. It can spread and fill every corner of the formwork, purely by means of its self-weight, thus eliminating the need of vibration or any type of consolidating effort (Okamura 2003). Self-consolidating concrete, in its current reincarnation, was originally developed at the University of Tokyo, Japan, in collaboration with leading concrete contractors in the late 1980s. Flowable, self-leveling, self-consolidating slurry has been gaining increasing acceptance since the mid-1980s (Naik et al. 1990).

During the last decade, significant improvements have been achieved in terms of rheological and mechanical characteristics of concrete, particularly in self-consolidating concrete. Since its introduction, different types of SCCs have been developed to meet the builder's requirements. One of the latest innovations in SCC technology is lightweight SCC (LWSCC).

It is estimated that 10~15% of concrete sales in some European countries and 75% of the precast concrete in the USA is SCC. Self-consolidating concrete is known to save up to 50% of labor cost due to its 80% faster pouring speed and reduced wear or tear of formwork (NSA 2006). However, the use of SCC in building structures is sometimes limited because of its high self-weight compared to other construction materials. Therefore, the combination of SCC with lightweight aggregate to produce LWSCC can maximize the applications and benefits of SCC (Karahan et al. 2012; Kim et al. 2010; Kilic et al. 2003).

For over 100 years, structural lightweight aggregate concrete (LWAC) has been widely used as a building component. The density of structural LWAC typically ranges from 1400 to 2000 kg/m^3.

Lightweight aggregate concrete has obvious advantages such as higher strength/weight ratio, better strain capacity, lower coefficient of thermal expansion, and superior heat and sound insulation characteristics due to the presence of air voids in lightweight aggregate (LWA) (ACI 211.2 1998). Furthermore, reduction in the dead weight of a building due to the use of lightweight concrete could lead to a considerable cost saving associated with the decrease in the cross-section of steel reinforced columns, beams, plates and foundation (Topcu 1997). Light weight concrete (LWC) may be produced by using either natural lightweight aggregates such as pumice, scoria, volcanic cinders, tuff and diatomite, or by using artificial lightweight aggregates, which can be produced by heating clay, shale, slate, diatomaceous shale, perlite, obsidian, and vermiculite (Hossain et al. 2011; Hossain 2009, 2006, 2004a,b; Hossain and Lachemi 2007, 2005; Lachemi et al. 2009). Industrial cinders and blast-furnace slag that have been specially cooled can also be used (Topcu 1997).

Despite all the above-mentioned advantageous and the increasing global demand, there are still many difficulties related to the segregation of coarse aggregate and relatively lower compressive strength of LWC compared to ordinary concrete (Chia and Zhang 2004). In practice, since lightweight aggregates often have lower particle densities than the mortar matrix in concrete, the unbalanced density of the mixture can lead to upward segregation of the coarse aggregate. The opposite occurs in conventional concrete with normal weight aggregates where coarse aggregate may sink to the bottom in unbalanced mixtures.

Traditionally, the production method of lightweight aggregate concrete is typically accompanied with segregation problems in the mixture due to the low density of aggregate. On the other hand, the use of large volume of powder in the production of SCC results in more balanced and cohesive mixture with better resistance to segregation at the fresh stage. Therefore, it is believed that the incorporation of lightweight aggregate in SCC can enhance the concrete quality while preventing the segregation of lightweight aggregate (Kim et al. 2010; Hwang and Hung 2005; Caijun and Yanzhong 2005; Wang 2009).

1.2 Background of SCC

The notion behind developing SCC was the concerns regarding the homogeneity and compaction of conventional cast-in-place concrete within intricate (i.e., heavily-reinforced) structures and to improve the overall strength, durability, and quality of concrete (Naik et al. 2005).

Self-consolidating concrete is highly workable concrete that can flow under its own weight through restricted sections without segregation or bleeding. Such concrete must maintain its homogeneity during transportation, placing and curing to ensure adequate structural performance and long term durability. The successful development of SCC must ensure a good balance between deformability and stability. Therefore, it is generally necessary to use superplasticizers in order to obtain high fluidity. Adding a large volume of powder material or viscosity modifying admixture can eliminate segregation. The powder materials that can be added include slag, fly ash, volcanic ash, silica fume, limestone powder, glass filler and quartzite filler.

Since, self-compactability is largely affected by the characteristics of materials and the mix proportions, it becomes necessary to evolve a procedure for mix design of SCC. Researchers have proposed guidelines for mixture proportioning of SCC, which include i) reducing the volume ratio of aggregate to cementitious materials (Khayat et al. 2000; Lachemi et al. 2003); (ii) increasing the paste volume and water-cement ratio (w/c); (iii) carefully controlling the maximum coarse aggregate particle size and total volume; and (iv) using various viscosity enhancing admixtures (VEA) (Aggarwal et al. 2008).

Okamura and Ouchi (1995) have proposed a mix proportioning system for SCC. In this system, the coarse aggregate and fine aggregate contents are fixed and self-compactability is to be achieved by adjusting the water/powder ratio and superplasticizer dosage. The coarse aggregate content in concrete is generally fixed at 50 percent of the total solid volume, the fine aggregate content is fixed at 40 percent of the mortar volume and the water/powder ratio is assumed to be 0.9-1.0 by volume depending on the properties of the powder and the superplasticizer dosage.

The required water/powder ratio is determined by conducting a number of trials (Aggarwal et al. 2008).

1.3 Definition of Lightweight Concrete

Lightweight concrete for structural applications refers to concrete with a density less than 1840 kg/m^3 and a minimum compressive strength of 17.2 MPa made with LWA whose unit weight should not exceed 1120 kg/m^3, as per ACI Committee 318 requirements (ACI 318 2008).

According to EuroLightCon (1998), there are mainly two categories of lightweight aggregate (LWA). The first comprises artificially produced lightweight aggregates such as expanded clay, expanded shale, expanded slate, expanded perlite, exfoliated vermiculite, sintered pulverized-fuel ash, foamed blast furnace slag, expanded glass and so forth. The second category of LWA is natural materials and other types that include pumice, scoria, diatomite as well as wood particles and plastic (EuroLightCon 1998; Hossain 2004, 2009). Low-density concrete generally produced with perlite or vermiculite aggregates rarely exceeds 800 kg/m^3 and has very low compressive strengths in the range of 0.7 to 6.7 MPa. Structural lightweight concretes are typically produced with expanded shale, clay, slate and slag. They can also be made with pumice or scoria, which are naturally occurring volcanic aggregates (Hossain 2004, 2009; Hossain and Lachemi 2007, 2011). Moderate strength concretes fall somewhere in between low-density and structural lightweight concrete. For comparison, normal weight concretes have a typical dry unit weight of 2300 to 2400 kg/m^3.

1.4 Development of LWC and Its Applications

Even though the history of the use of lightweight aggregate (LWA) stems from the early days of the Roman Empire (EuroLightCon 1998; Hossain 2004, 2009), the earliest structural use of lightweight concrete in the USA was in the construction of concrete ships in 1919. In 1922, the first highway bridge was constructed using concrete with expanded shale aggregate. Since then, over 200 concrete and composite bridges containing LWAs had been built in the United States and Canada because of the benefits, such as 25 to 35% of reduction in dead loads and over 10-

20% cost savings (Ries et al. 2010). Lightweight concrete may cost more per unit volume than normal weight concrete, due to higher relative cost of producing lightweight aggregates and the preparations needed prior to their use in concrete. In structural applications, the self-weight of the concrete structure is important because it represents a large portion of the total load. The reduced self-weight of lightweight concrete will reduce gravity load and seismic inertial mass, resulting in reduced member size and foundation force (Kowalsky et al. 1999). Hence, the structure may cost less as a result of reduced dead load and lower foundation costs.

Lightweight concrete has been used for a number of applications and is also known for its good performance and durability (ACI.213 2003). The rapidly growing use of lightweight concrete suggests that the long-term behavior of a lightweight concrete structure is at least comparable to that built with conventional concrete. The use of lightweight concrete can also be of interest in retrofit applications where a concrete column jacket is desired due to architectural reasons over other methods such as steel or composite jackets. In that situation, a normal-weight concrete jacket might result in additional loads that would require expensive foundation retrofit where as a lightweight concrete jacket may not require a footing retrofit. Also, one of the most common uses for lightweight concrete is in commercial and residential slabs, columns, roofs and bridge decks; others include pavement systems, masonry blocks and offshore oil structures. Successful developments and applications of structural LWC have been practical, especially in Europe, to structures ranging from commercial and residential slabs to spans of bridges with achieved compressive strength of 60 MPa at 28-day (EuroLightCon 1998).

1.5 Research Significance and General Objectives

Lightweight concrete is being more and more widely used due to its better structural and durability performance. Several design procedures and statistical modelling for self-consolidating normal weight concrete have been published (Khayat 1998; Patel et al. 2004; Sonebi 2004). But to date, to the best of our knowledge, no published work has dealt with the mixture design and statistical modelling of lightweight self-consolidating concrete (LWSCC). The objective of this research is to demonstrate the feasibility of using a statistical experimental design approach to identify the relative significance of primary mixture parameters and their

coupled effects on relevant properties, including detail investigations on the durability aspects of LWSCC mixtures. Expanded furnace slag, expanded clay, and expanded shale are used as both coarse and fine lightweight aggregates to develop and evaluate LWSCC. The developed statistical models can be used to evaluate the potential influence of mixture variables on fresh state, hardened and durability characteristics required to ensure successful development of LWSCC. Such simulation can help identify potential mixtures with a given set of performance criteria that can be tested in the laboratory, hence simplifying the test protocol needed to optimize LWSCC mixtures.

1.6 Specific Objectives of the Thesis

The specific objectives of this thesis are described as follows:

- To develop statistical design models for LWSCC mixtures, incorporating three types of lightweight aggregates: furnace slag (FS), expanded clay (EC), and expanded shale (ESH), used as both coarse and fine aggregates.
- To assess the influence of adjusting three key design parameters: water (w) to binder (b) ratio (w/b), high range water reducing admixture (HRWRA) dosages and total binder content (b) on LWSCC fresh and hardened characteristics.
- To utilize the developed models in optimizing LWSCC mixtures and theoretically develop three industrial classes of LWSCC as per EFNARC guideline (EFNARC 2005). Subsequently, produce the optimized LWSCC mixtures in the lab/industrial set-up with each of furnace slag, expanded clay, and expanded shale aggregates – a total of nine mixes based on the proposed statistical models.
- To validate whether the theoretically proposed optimum mix design parameters, w/b, HRWRA (%), and total binder can produce LWSCC mixtures with the desired fresh and hardened properties.
- To evaluate the fresh, mechanical, mass transport and durability characteristics of the produced optimized industrial LWSCC mixes using furnace slag, expanded clay, and shale aggregates by conducting slump flow, V-funnel flow time, J-Ring flow, J-Ring height difference, L-box, filling capacity, bleeding, air content, initial/final setting time,

sieve segregation resistance, fresh unit weight, 28-day air dry unit weight, 28-day oven dry unit weight, compressive/flexural/split tensile strength, bond strength (pre/post corrosion), drying shrinkage, sorptivity (rate of water absorption), absorption, porosity, rapid chloride-ion permeability, hardened air void (%), spacing factor, corrosion resistance, resistance to elevated temperature, salt scaling, freeze-thaw resistance, and sulphuric acid resistance tests.

1.7 Thesis Structure

This thesis consists of 9 chapters. Chapter 1 provides an introduction and objectives of the research. Chapter 2 presents a literature review which summarizes the history of SCC and LWC, SCC mix design methodology, key parameters affecting mix design and mix performance, statistical design models and materials properties required for LWSCC. The chapter also discusses the background of LWSCC, highlighting the latest research associated with LWSCC technology and concludes with a comprehensive overview of the most relevant LWSCC fresh and hardened properties.

Chapter 3 presents the experimental program. The use of the response surface method fractional factorial design models and the criteria for three key parameters affecting LWSCC mixture performance are described. Material properties, mixture proportions, and testing procedures are outlined. The development of statistical models is described in three parts, illustrating the use of expanded furnace slag, expanded clay, and expanded shale as lightweight aggregates in SCC mixtures.

Chapter 4 presents the results of the fractional factorial design approach and the derived models which are valid for LWSCC mixtures proportioned with w/b ranging from 0.30 to 0.40, HRWRA dosages varying from 0.3 to 1.2% (by total content of binder) and binder content varying from 410 to 550kg/m^3.

Chapter 5 discusses the effects of mix parameters (w/b, HRWRA and binder content) on the responses of slump flow, V-funnel flow, J-Ring flow, J-Ring height difference, L-box, filling capacity, bleeding, fresh air content, initial and final setting times, sieve segregation, fresh unit weight, 28-day air dry unit weight, 28-day oven dry unit weight, and 7- and 28-day compressive strengths, followed by statistical evaluation of the test results. It also presents the established relationships (given in mathematical formulation) describing the responses of LWSCC in fresh and hardened states.

Chapter 6 presents the mix proportion optimization process. In this study, optimization was performed to develop mixtures that satisfy EFNARC industrial classifications for SCC. Moreover, the chapter also presents the results of additional experimental study to examine whether the theoretically proposed optimum mix design parameters such as w/b, HRWRA (%), and total binder can yield the desired fresh and hardened properties (responses).

Chapter 7 describes the mechanical and mass transport properties of the produced optimized industrial class LWSCC mixtures based on compressive/flexural/split tensile strength, bond strength, drying shrinkage, sorptivity, absorption, porosity and rapid chloride-ion permeability, including a comparison of the performance of LWSCC mixtures with three aggregates types.

Chapter 8 describes the detailed durability investigation of the produced optimized industrial class LWSCC mixtures based on bond strength (pre/post corrosion), corrosion resistance, hardened air void, spacing factor, resistance to elevated temperature, salt scaling, freeze-thaw resistance, and sulphuric acid resistance tests, including a comparison of the performance of LWSCC mixtures with three aggregates types.

Chapter 9 presents the conclusion of the research by highlighting an overview of the main parameters that affect the fresh, hardened and durability characteristics of LWSCC mixtures. Recommendations for aggregate type, materials constituents and mix design of LWSCC are also provided. Performance based guidelines for fresh, hardened and durability properties of LWSCCs are summarized. Finally, possible recommendations/suggestions for continued research are listed.

CHAPTER TWO

2 LITERATURE REVIEW

2.1 Introduction

Lightweight self-consolidating concrete (LWSCC) is one of the latest innovations in concrete technology. This new type of concrete was developed to offer enhanced workability and durability due to its self-consolidation ability. Similar to normal self-consolidating concrete (SCC), these special fresh properties allow LWSCC to penetrate through formwork with complex geometry as well as through highly-congested reinforcing. Hence, LWSCC provides a better quality in the construction of the structural members with reduced labor. In addition, LWSCC also has a further impact on the construction cost by reducing the total dead load of the structural members up to 25%, and requiring less maintenance than a similar steel structure (Bardhan-Roy 1993; Lachemi et al. 2009). This may represent considerable savings in large scale construction that could not otherwise be attained with the use of standard self-consolidating concrete (SCC). LWSCC can achieve better strength and durability while offering excellent workability (Hwang and Hung 2005), and its mechanical properties are in general either competitive or superior to those in conventional lightweight concrete (LWC) and SCC (Karahan et al. 2012; Lo et al. 2007).

LWSCC has already been implemented successfully in large scale bridge construction (Ohno et al. 1993; Melby et al. 1996) and its manufacturing process and rational mix-design methods, as well as testing and acceptance criteria have undergone substantial progress in recent years. Nevertheless, LWSCC structures remain rare due to the relative novelty of the material and the lack of guidance in construction and building codes.

This chapter, divided into three main parts, includes review of structural lightweight concrete, SCC and statistical modelling of SCC/LWSCC, and previous research studies related to LWSCC.

2.2 Lightweight Concrete (LWC)

2.2.1 Introduction

Structural lightweight concrete (LWC) is an important and versatile material in modern construction. It has been used in many and varied applications such as multi-story building frames and floors, bridges, offshore oil platforms, and prestressed or precast structural elements of all types. Many architects, engineers, and contractors recognize the inherent economies and advantages offered by this material, as evidenced by the many impressive lightweight concrete structures found today throughout the world (ACI 213R 2003). Structural lightweight aggregate concrete solves weight and durability problems in buildings and exposed structures. Lightweight concrete has strengths comparable to normal weight concrete, yet is typically 25% to 35% lighter.

Structural lightweight concrete offers design flexibility and substantial cost savings by providing: less dead load, improved seismic structural response, longer spans, better fire ratings, thinner sections, decreased story height, smaller size structural members, less reinforcing steel, and lower foundation costs (Hossain 2003; Hossain 1999). Moreover, lightweight concrete precast elements offer reduced transportation and placement costs (www.escsi.org).

There are many types of aggregates available that are classified as lightweight and their properties cover wide ranges. Elastic properties, compressive and tensile strength, time dependent properties, durability, elevated temperature resistance, and other properties of LWC are dependent on the type of lightweight aggregate utilized in the concrete (ACI 213R 2003). LWC is defined as concrete that is made with lightweight aggregates complying with ASTM C 330 (2009) and has a compressive strength in excess of 17.25 MPa at 28-day, and an air dry density of less than 1840 kg/m^3 as per (ASTM C 567 2011; ACI 211.2 1998). High performance lightweight concretes are typically produced using rotary kiln expanded clay, shale or slate. These lightweight aggregates are relatively “light” in weight due to the cellular structure of the individual aggregate particles. This cellular structure within the particles is formed at high temperatures, generally 1,100°C or higher, by the rotary kiln process.

2.2.2 Types of Lightweight Aggregates

There are several types of material that can be used for aggregates in structural lightweight concrete. They are divided into two main categories, natural lightweight aggregate and manufactured lightweight aggregate. Natural lightweight aggregates include pumice, scoria, volcanic cinders, tuff and diatomite - these materials are volcanic materials. Manufactured lightweight aggregates include expanded shale, clay, slate, fly ash, and expanded slag. These materials are more consistent in their properties and provide more predictable mechanical properties of the hardened LWC. Other artificial lightweight aggregates include perlite, obsidian and vermiculite. Figure 2.1 presents the classification of lightweight concrete and types of aggregates (Harding 1995).

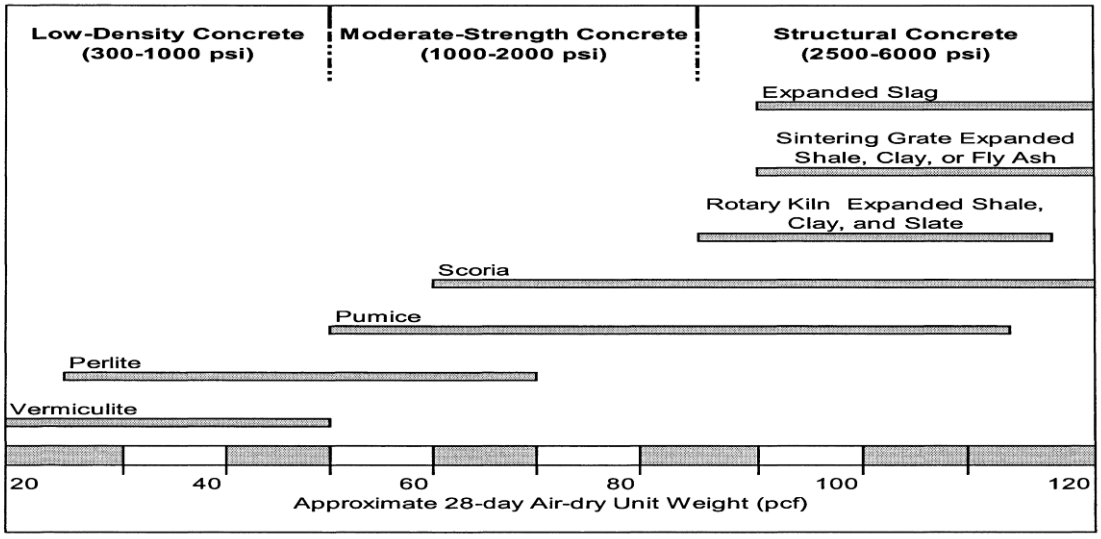

Figure 2.1 - Classification of lightweight concrete and types of aggregates used (Harding 1995)

2.2.3 Lightweight Aggregate Manufacturing

Most lightweight aggregate is produced from materials such as clay, shale, or slate. Blast furnace slag, natural pumice, vermiculite, and perlite can be used as substitutes. To produce lightweight aggregate, the raw material (excluding pumice) is expanded to about twice its original volume.

The expanded material has properties similar to natural aggregate, but is less dense and therefore, yields a lighter concrete product.

The production of lightweight aggregate begins with mining or quarrying the raw material. The material is crushed and screened for size. Oversized material is returned to the crushers, and the material that passes through the screens is transferred to hoppers. From the hoppers, the material is fed to a rotary kiln, which is fired with coal, coke, natural gas or fuel oil to temperatures of about 1200°C. As the material is heated, it liquefies and carbonaceous compounds in the material form gas bubbles, which expand the material. In the process, volatile organic compounds (VOC) are released. From the kiln, the expanded product (clinker) is transferred by conveyor into the clinker cooler where it is cooled by air, forming a porous material. After cooling, the lightweight aggregate is screened for size, crushed if necessary, stockpiled, and shipped. Figure 2.2 illustrates the lightweight aggregate manufacturing process.

Although the majority of plants use rotary kilns, traveling grates are also used to heat the raw material. In addition, a few plants process naturally occurring lightweight aggregate such as pumice. On the other hand, expanded slag is made from blast furnace slag. The slag is quenched in water while in molten state, so as to preserve the lightweight aggregate characteristics. Figure 2.3 shows the pore structure that is created during the manufacturing process which gives the lightweight aggregate its unique characteristic of reduced density. The maximum density allowed for lightweight aggregates as per ASTM C330 and C331 is given in Table 2.1.

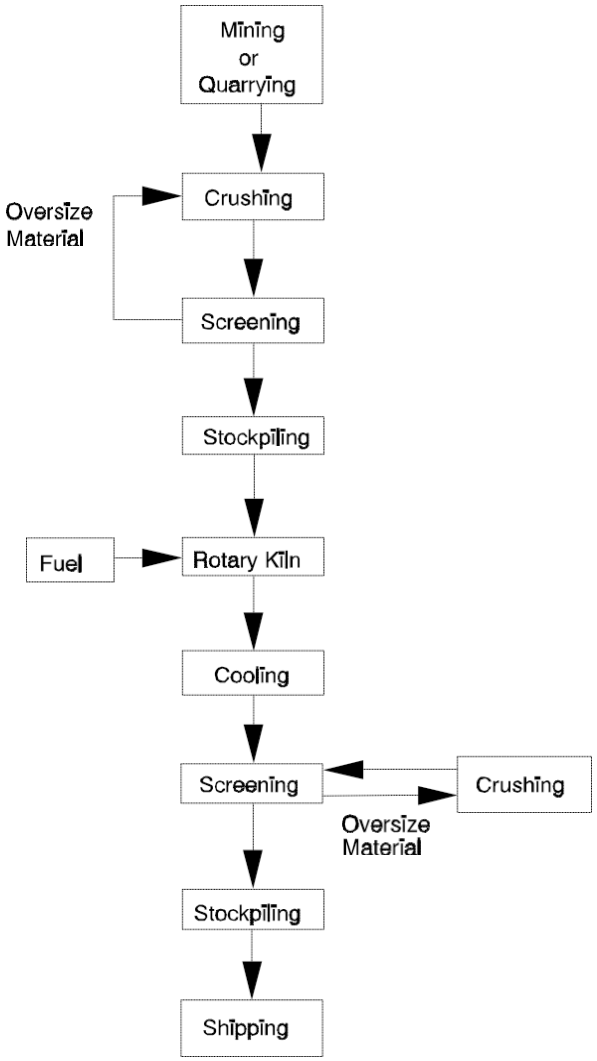

Figure 2.2 - Process flow diagram for lightweight aggregate manufacturing (Environmental Protection Agency 1985)

Figure 2.3 - Internal pore structure of lightweight aggregate

Table 2.1- Allowable lightweight aggregate densities

Aggregate Size and Group ASTM C330 and C331	Maximum Density kg/m^3
Fine Aggregate	1120
Coarse Aggregate	880
Combined Fine and coarse Aggregate	1040

2.2.4 Absorption properties of lightweight aggregate

Due to their porous nature, lightweight aggregate absorb more water compared to normal weight aggregate. Based upon the 24-hour absorption test conducted in accordance with the procedures of ASTM C127 (2007) and ASTM C128 (2007), structural-grade lightweight aggregates will absorb from 5 to more than 25 percent moisture by mass of dry aggregate. By contrast, ordinary aggregates generally absorb less than 2 percent of moisture (ESCSI 2004). This high absorption rate creates two distinct benefits when aggregate is properly prewetted prior to mixing into the concrete matrix. The water present in the aggregate at the time of mixing can help reduce plastic shrinkage (early shrinkage due to unfavorable drying conditions) and provide water for internal curing which allows for more complete hydration of the cement, resulting in better long term strength gain. This process of internal curing is particularly effective when the moisture content of the lightweight aggregate at the time of mixing is in excess of that achieved in a 24 hour soaking (ESCSI 2004). Proper prewetting is required to control the extended workability and water to cementitious material ratio (w/b). If the aggregate has pores near the surface that are water deficient, free mix water will be absorbed while changing the plastic properties and starving cement with a low w/c for hydration. For concrete production, sprinkling of lightweight aggregates can be performed wherever the aggregates are stockpiled. This involves spraying the aggregate stockpile with water for hours to weeks depending on the type and properties of the aggregate. Different lightweight aggregates exhibit different rates at which saturation occurs. Table 2.2 shows an example of saturation test results of lightweight clay aggregate, which shows that at 24 hours the aggregate only obtained 31% of complete saturation. Also, this shows even

after 2 years, 100% saturation was not achieved. This is due to the non-interconnected pore structure of the lightweight aggregate (ESCSI 2004).

Table 2.2 - Lightweight aggregate saturation test (ESCSI 2004)

Immersion Time	Water Absorption (% Mass)	Degree of Saturation	Percentage of 24-Hour Soak
0 min	0	0	0
2 min	5.76	0.17	55
5 min	6.15	0.18	59
15 min	6.75	0.2	64
60 min	7.74	0.23	74
2 hours	8.32	0.24	79
1 day	10.5	0.31	100
3 days	12.11	0.35	115
28 days	18.4	0.54	175
4 months	23.4	0.69	223
1 year	30	o.88	285
2 years	30	0.88	285

2.2.5 Internal Curing

Lightweight aggregate batched at a high degree of saturation may be substituted for normal weight aggregate to provide internal curing in concrete containing a high volume of cementitious materials. High cementitious concretes are vulnerable to self-desiccation and early-age cracking, and benefit significantly from the slowly released internal moisture.

Time dependent improvement in the quality of concrete containing prewet lightweight aggregate is greater than that with normal weight. The reason is better hydration of the cementitious fraction provided by moisture available from the slowly released reservoir of absorbed water within the pores of the lightweight aggregate. The fact that absorbed moisture in the lightweight was available for internal curing has been known for more than five decades. Klieger (1957) studied in detail the role of absorbed water in lightweight aggregates on extended internal curing.

The principal contribution of internal curing results in the reduction of permeability that develops from a significant extension in the time of curing. Powers et al. (1959) reported that extending the time of curing increased the volume of cementitious products formed which caused the capillaries to become segmented and discontinuous. Additional benefits from a reduced concrete permeability are the improved abrasion resistance and increased corrosion resistance of the steel reinforcement (Holm and Bremner 2000). Researches have also conclusively demonstrated reduced sensitivity to poor curing conditions in high strength normal weight concrete containing an adequate volume of high moisture content LWA (Weber and Reinhardt 1995). Since 1995, a large number of papers addressing the role of water entrainment influence on internal curing and autogenous shrinkage have been published (Şahmaran et al. 2009; Hossain 2009).

The benefits of internal curing are increasingly important when pozzolans such as silica fume, fly ash, metokoalin, calcined shales, clays and slates, as well as the fines of lightweight aggregate (LWA) are included in the mixture. It is well known that the pozzolanic reaction of finely divided alumina-silicates with calcium hydroxide liberated as cement hydrates is contingent upon the availability of moisture. Additionally, internal curing provided by absorbed water minimizes the plastic shrinkage due to rapid drying of concrete exposed to unfavorable drying conditions (Holm 1980).

2.2.6 Lightweight Concrete Proportioning and Mix Design

There are three different procedures established by the American Concrete Institute for designing and proportioning lightweight concrete (ACI 213R 2003; ACI 211R 1998). The first is the weight method (specific gravity pycnometer), which is to be used with lightweight coarse

aggregate and normal weight fine aggregate. Estimating the required batch weights for the lightweight concrete involves determining the specific gravity factor of lightweight coarse aggregate with a pycnometer. This allows the conversion of aggregate volume to batch weights, with the lightweight materials in their current absorption state. The following lists the steps involved with this procedure.

1. Choose slump appropriate for the conditions in which concrete will be used.
2. Choose maximum size of lightweight aggregate.
3. Estimate mixing water and air content. The quantity of water per unit volume of concrete required to produce a given slump is dependent on the nominal maximum size, particle shape and grading of the aggregates, amount of entrained air, and inclusion of chemical admixtures. A table is provided in ACI 211.2-5 to approximate the mixing water and air contents for different slumps
4. Select approximate water to cement ratio (w/c). Because different cements and aggregates produce different strengths at the same w/c ratio, it is desirable to have or develop the relationship between strength and w/c for the materials actually used. In the absence of such data, a table is provided in ACI 211.2-5.
5. Calculate cement content. The required cement is equal to the estimated mixing water content (Step 3) divided by the w/c ratio (Step 4).
6. Estimate lightweight coarse aggregate content. This volume is determined by the maximum coarse aggregate size and the fineness modulus of the sand. A table provided in ACI 211.2-5 gives the volume per m^3.
7. Estimate fine aggregate content. After the completion of step 6, all constituents of the concrete have been determined except the fine aggregate quantity. This is established by taking the difference in concrete weight and all other ingredients. The estimated weight of the concrete is either known from previous experience or estimated from a table provided in ACI 211.2-5. This will establish the proportions for trial mixes. Determining the yield of the concrete mix and making the appropriate adjustment will determine the final sand content.

The second procedure is the volumetric method (Damp Loose Volume) which is used for proportioning all lightweight aggregate or a combination of lightweight and normal weight aggregates. This procedure is used to proportion concrete mixes from aggregate manufacturer or historical data. The mix proportions given are loose unit volumes of aggregate and weight for cement and water. The loose unit volumes of coarse and fine aggregates are known and the oven dry unit weight of the aggregate is known. The "as is" condition of the aggregate must be determined. The aggregate stockpile is tested to determine the "as is" loose unit weight. The "as is" unit weight is multiplied by the required loose volume to determine the weight required for the aggregate. The amount of aggregate moisture that contributes to the batch water is also determined from this information. The oven dry batch weight is subtracted from the "as is" batch weight to determine the amount of moisture present. The percentage of absorbed water is determined and the remaining water is subtracted from the mix water.

The third procedure is the absolute volume method. Here, the volume of fresh concrete produced by any combination of materials is considered equal to the sum of the absolute volumes of cementitous materials, aggregates, net water, and entrained air. Proportioning by this method requires the determination of water absorption and the particle relative density factor in an as-batched moisture condition. This procedure represents the most widely used method of proportioning for normal weight concrete mixes as it is more practical and easier to apply.

2.2.7 Mechanical and Mass Transport Properties of Lightweight Concrete

Lightweight concrete exhibits a limited strength that may be obtained with a reasonable amount of cement and a particular aggregate. This concept is referred to as "strength ceiling". A mixture is near its strength ceiling when additional amounts of cement only slightly increase the concrete strength. This is predominantly controlled by the lightweight coarse aggregate, so reducing the coarse aggregate size can increase the obtainable concrete strength. The strength ceiling for some lightweight aggregates may be quite high, approaching that of some normal weight aggregates. Design strength of 21 to 35 MPa is common with lightweight concrete. In precast and prestressing plants, design strengths above 35 MPa are usual (ACI 213R 2003).

The modulus of elasticity of concrete depends on the relative amounts of paste and aggregate and the modulus of each constituent. Normal weight concrete has a higher modulus of elasticity, because the moduli of normal weight aggregate are greater than the moduli of lightweight aggregates. Generally, the modulus of elasticity of lightweight concrete is considered to vary between ½ to ¾ that of normal weight concrete of the same strength (ACI 213R 2003). Comparison and ranges for the elastic modulus is presented in Figure 2.4.

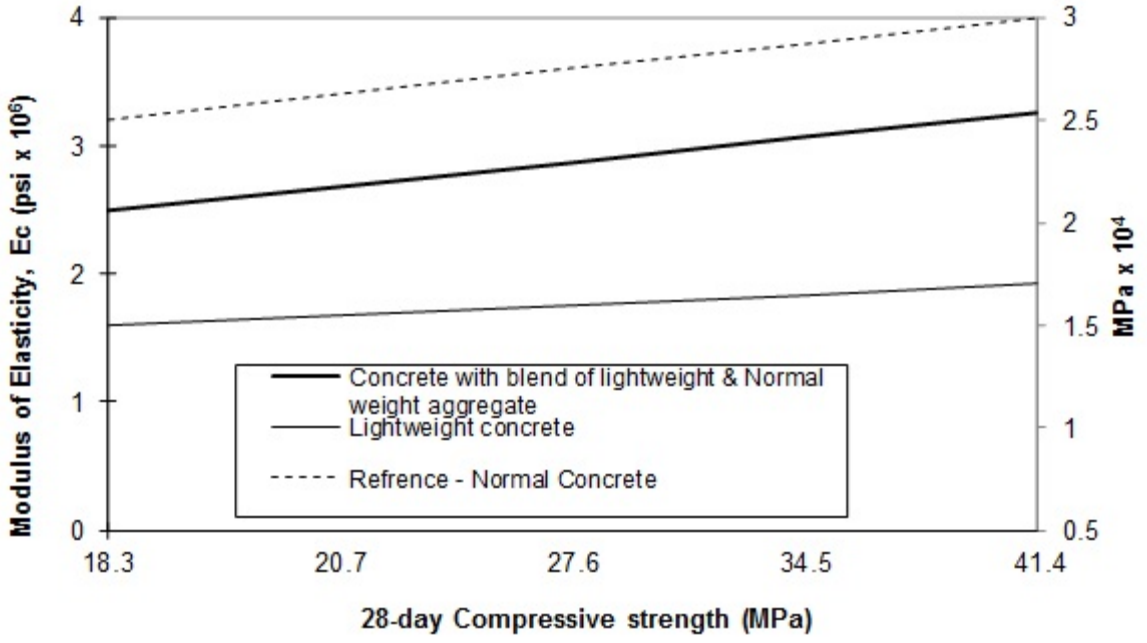

Figure 2.4 - Modulus of elasticity for different types of concrete (ACI 213R, 2003)

Creep is the increase in strain due to an applied stress that may lead to excessive long-term deflection. Creep can be affected by many factors, such as the type of aggregate, and cement, grading of aggregate, water content of the mixture, moisture content of aggregate at the time of mixture, amount of entrained air, age at initial loading, magnitude of applied stress, method of curing, size of specimen or structure, relative humidity of surrounding air, and period of sustained loading (ACI 213R 2003).

Figure 2.5 shows the range in values of specific creep (creep per psi of sustained stress) for normally cured concrete, as measured in the laboratory (ASTM C 512 2010), when under

constant loads for 1 year. As shown in this figure, lightweight concrete exhibits more creep than normal weight concrete at lower strengths, but can be significantly reduced by increasing the compressive strength of the concrete.

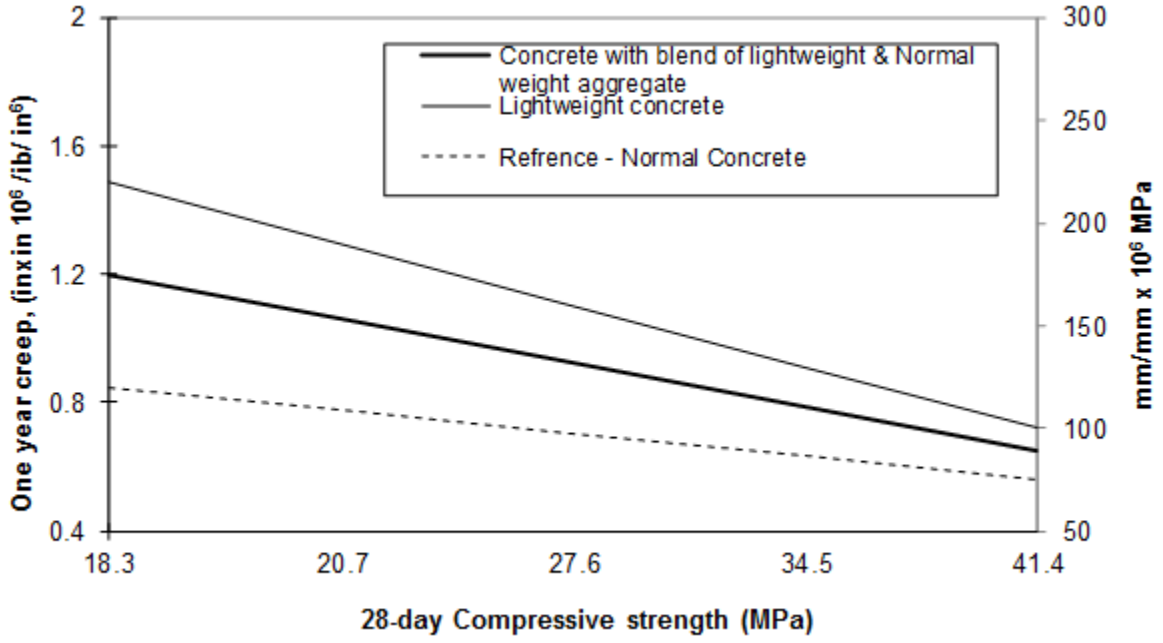

Figure 2.5 - Creep for different types of concrete (ACI 213R 2003)

The modulus of rupture (ASTM C78) is a measure of the tensile strength of concrete (ASTM C78 2010). A concrete specimen is subjected to a three point bending load and the extreme fiber stress at rupture is calculated to determine the modulus of rupture (f_r). ACI 318 requires a reduction in the normal weight modulus of rupture calculation ($f_r = 7.5\sqrt{f_c'}$) by 0.75 for all lightweight concrete, and 0.85 for sand lightweight concrete (ACI 318R 2011).

Permeability of concrete is an important issue, especially in structures where the reinforcing steel can be influenced by external factors such as bridge decks with deicing chemicals and offshore structures where salt water can corrode the reinforcement. Permeability investigations conducted on lightweight and normal weight concrete have been reported in previous research studies (Hossain et al. 2011; Hossain 2009, 2007, 2006, 2005, 2004; Hossain and Lachemi 2007, 2006;

Nishi et al. 1980; Bremner et al. 1992). It is concluded that despite the wide variations in concrete strength, testing media (water, gas, and oil) and testing techniques, lightweight concrete had equal or lower permeability than normal weight concrete. Further, it was reported that the lower permeability of lightweight concrete was attributed to the elastic compatibility of the constituents and the enhanced bond between the coarse aggregate and the matrix (ACI 213R 2003).

Mehta (1986) observed that the permeability of a concrete composite is significantly greater than the permeability of either the continuous matrix system or the suspended coarse aggregate fraction (See also ACI 213R 2003). This difference is primarily related to extensive micro-cracking caused by mismatched concrete components. In addition, channels develop in the interfacial transition zone surrounding normal weight coarse aggregate, giving rise to unimpeded moisture movements (ACI 213R 2003). The contact zone, which is the interface between the aggregate and the cement binder, is superior in lightweight concrete due to the porous nature of the aggregate. This porous media interface allows for hygrol equilibrium to be reached between the two phases, thus eliminating weak zones caused by water concentration (ACI 213R 2003).

Resistance against elevated temperature is an important mechanical property of any structure for the protection of lives as well as property. Lightweight concrete is more resistant to elevated temperatures than normal weight concrete because of its lower thermal conductivity, lower coefficient of thermal expansion, and inherent fire stability of an aggregate already heated to over 1100^{o}C during production (ACI 213R 2003; PCI 1995; ESCSI 2004). The lower thermal conductivity of the lightweight concrete allows the concrete reinforcement to be better insulated from high temperatures, thus allowing longer structural stability. Spalling is a failure in the concrete by cracking and material being separated from the main structural element. This usually occurs in an explosive manner, when internal energy due to vapor pressure is released. The occurrence of spalling is related to the rate of increase in temperature. The more rapid the increase in temperature, the more likely concrete will exhibit spalling.

2.3 Self - Consolidating Concrete (SCC)

2.3.1 Introduction

Placement of concrete generally requires consolidation by vibration in the forms. Self-consolidating concrete (SCC) has been defined as a highly flowable, yet stable concrete that can spread readily into place and fill the formwork without any consolidation (Khayat et al. 2000).

An alternative definition suggests SCC as "a flowing concrete without segregation and bleeding, capable of filling spaces and dense reinforcement or inaccessible voids without hindrance or blockage". The use of SCC in the actual structure has steadily increased in the recent years and presents an excellent alternative to conventional concrete (JSCE 2008). SCC can also be pumped from the bottom of a form or dropped from the top. Figure 2.6 shows the increase of SCC usage in Japan (Ouchi et al. 2003). Many agencies worldwide have shown interest and are working towards developing tests, specifications and adopting SCC.

One of the largest projects to utilize SCC technology in Canada was the expansion of the Pearson International Airport in Toronto. About 2100 m^3 of ready-mix SCC was successfully placed in 180 columns, 13 m tall by 71 cm in diameter (Lessard et al. 2002). There was insufficient overhead clearance to allow placement of conventional concrete. Due to this, the concrete had to be pumped from the bottom of the columns and this could only be achieved by using SCC.

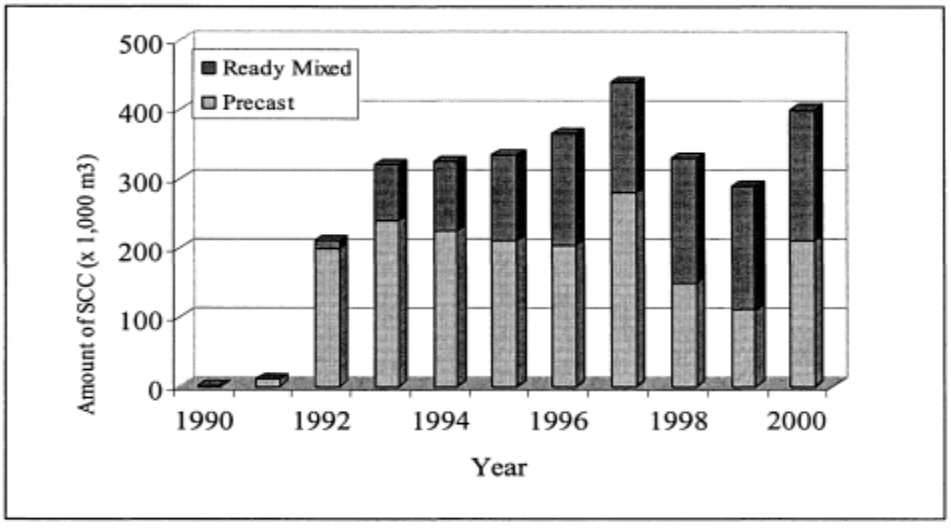

Figure 2.6 - increase of SCC usage in Japan (Ouchi, 2003)

The SCC mixture design is shown in Table 2.3. The compressive strength requirement at 28-day was 30 MPa and the slump flow was required to be between 650 and 700 mm. The average measured cylinder compressive strength was 55 MPa and the average compressive strength of the cores from the columns was 64.5 MPa. The cores from different points within the column showed that the aggregate was evenly distributed throughout. The concrete was pumped into the bottom of a steel column reinforced with a steel rebar cage made of 12 to 30 rebars attached at 35 cm intervals. The concrete was pumped through a 125 mm opening with pressure not exceeding 7 MPa. Each column consisted of 12 m^3 and was filled at a rate of 1 m^3 per minute. SCC clearly met the challenge for this difficult concrete placement. The traditional placement method would have been to fill the column through portholes at different levels, with no assurance of the overall quality of the concrete inside the column. This method would have incurred additional cost and a longer placement window (Lessard et al. 2002).

Table 2.3 - SCC mix proportions for Pearson International Airport in Toronto, Canada (Lessard et al. 2002)

Mixture Proportions	**kg/m^3**
Cement GU	315
Slag	135
Coarse Aggregate	900
Fine Aggregate	825
Water	190
w/cm	0.42
Admixtures	
Type A Water Reducer	300ml/100kg
Type D Retarder	125ml/100kg
Superplasticizer	4.0 L/m^3
VMA	2.1 L/m^3

2.3.2 Materials for Normal Weight SCC

High Performance Concrete (HPC) is generally achieved by lowering the w/c of the concrete mix while using mineral admixtures or chemical admixtures to maintain the workability of the concrete. The same concept is applied to SCC except that the aggregate proportions are also adjusted to achieve maximum flowability while keeping the mix from segregating (separation of paste and aggregates). Aggregate gradation also plays an important role in the workability of SCC mixes. Assaad et al. (2003) studied the significance of aggregate packing density on the fresh properties of SCC. The authors investigated 32 mixes using both discontinuously and continuously graded aggregates. The gradation of the fine and coarse aggregate combinations is quantified using the aggregate packing density. The study determined that by optimizing the packing density or improving the overall gradation of the combined aggregate system, the viscosity of the cement paste could be reduced. Therefore, it could lower the amount of water reducing admixture (superplasticizer) needed to obtain the desired spread and, thus, lower material costs.

Concrete admixtures are additional ingredients in concrete that enhance the plastic and hardened properties of the material such as workability, set time, chloride resistance, and air content. In general, there are two types of admixtures used in concrete production, i.e., mineral admixtures and chemical admixtures. The most common mineral admixtures used today are fly ash, silica fume, and ground granulated blast furnace slag (GGBFS). These materials improve quality of the concrete while also reducing the cement content and save costs. Most SCC mixes employ some volume of fly ash and/or silica fume to increase the workability of the fresh concrete, and to reduce chloride permeability of the hardened material.

Fly ash (FA) is collected from the combustion of pulverized coal in electric power generating plants. The particle sizes of fly ash vary from less than 1 μm to more than 100 μm with the typical particle size measuring less than 20 μm. The spherical nature of FA particles reduces the friction between aggregates and increases the workability of concrete. More recently volcanic ash has also been used to produce SCC (Hossain and Lachemi 2010).

Silica fume (SF) is a by-product of industry producing silicon metal or ferrosilicon alloys. The initial interest in the use of silica fume in concrete was mainly caused by the strict enforcement of air-pollution control measures in various countries to stop release of the material into the atmosphere. More recently, the availability of high range water-reducing admixtures (HRWRA) has opened up new possibilities for the use of silica fume as part of the cementing material in concrete to produce very high strength or very high levels of durability or both (ACI 234R 1996). The individual particles are extremely small, approximately $1/100^{th}$ the size of an average cement particle. Because of high degree of fineness, large surface area, and high amorphous (non-crystaline) SiO_2 content, silica fume is a very reactive pozzolanic material when used in concrete. Silica fume is also used for protection of concrete in contact with chlorides from deicing salts and marine environments.

The replacement amounts for mineral admixtures are unique to each SCC application and should be evaluated to meet specific performance criteria. Chemical admixtures are used for water reduction, air entrainment, acceleration, retardation, and viscosity modification. Water reducers are the key chemical admixtures that give SCC its self-consolidating quality. The water reducing agents in SCC are generally known as superplasticizers. The superplasticizer cause dispersion of the cement particles, releasing the water molecules trapped in the cement conglomerations, and thus, improves workability.

Superplasticizer technology has improved over the past few decades. The most commonly used superplasticizers in the concrete industry today are based on polycarboxylate ethers which rely on electrosteric stabilization for particle dispersion. Electrosteric stabilization combines two mechanisms by first introducing a negative charge to repel the cement particles from each other and then using steric stabilization to keep them apart. Steric stabilization occurs when the cement particles adsorb the polymer chains and give steric hindrance for the agglomeration of particles (SCI 2003).

2.3.3 Fresh Properties of SCC

SCC in its fresh state exhibits much different characteristics than conventional concrete. It should be able to flow under its own weight without the need for mechanical vibration, and

completely fill formworks and surround any steel reinforcement that exists in the forms. In order for a concrete mixture to be classified as SCC, it must exhibit adequate filling ability (to fill a form under its own weight), passing ability (to flow through reinforcing bars or other obstacles without segregation and without mechanical vibration), stability (segregation resistance-static and dynamic stability), surface quality and finish ability in its fresh state (ACI 237R 2007).

2.3.3.1 Self-consolidating concrete testing

There are several test procedures that have been developed throughout the world to evaluate the properties of SCC. All of the testing procedures and apparatus that have been introduced either measure one or two of the required SCC properties. Table 2.4 shows most common SCC tests and its measured properties according to different guidelines.

Table 2.4 - SCC testing methods (EFNARC 2005; ACI 237R 2007; JSCE 1998)

Test Method	**Measured Characteristic**				**Accepted by Guidelines**		
	Filling Ability	Stability	Passing Ability	Relative Viscosity	ACI	JSCE	Europe
Slump Flow	x				x	x	x
Visual Stability Index (VSI)		x			x		x
J-Ring			x		x		
T 500	x	x		x	x	x	x
L-Box			x		x	x	x
Column Segregation Test		x			x		
V-Funnel	x		x	x		x	x
U-Box	x		x			x	
Filling Vessel Test Method	x		x				
Orimet	x		x	x			

Extensive studies investigating the workability of SCC have been conducted in North America and Europe (Khayat et al. 2004; Assaad et al. 2004; Ding et al., 2008; Hossain and Lachemi 2010; Lachmei et al. 2007, 2004, 2003; Patel et al. 2004).

L-box, U-box, and J-ring tests can be used to evaluate the passing ability of SCC and, to a certain extent, the deformability and resistance to segregation (Khayat et al. 2004). When combined with the slump flow test, the L-box test is very suitable for quality control of on-site SCC. The visual stability index, wet sieve segregation test, and penetration test are usually used to estimate the resistance of SCC to segregation.

For SCC to exhibit adequate filling ability it must be able to completely fill the formwork including areas of complex reinforcement under its own weight. Two methods are available to ensure that the concrete will exhibit proper filling ability. Balancing the w/c with the superplasticizer dosage increases the deformability of the paste. Also, the inter-particle friction within the mix can be minimized by reducing the amount of coarse aggregate and increasing the volume of paste (Sonebi et al. 2007; Bailey et al. 2005).

Passing ability is another property of freshly mixed SCC that describes its flowability through obstacles such as steel reinforcement. Khayat et al. (2006) suggest three parameters to consider when evaluating the passing ability of the concrete, namely, the geometry and density of reinforcement, the stability of the fresh concrete, and the maximum aggregate size and content. These should be optimized so that the SCC has no blockage at the areas of congested reinforcement and no segregation (Hwang et al. 2006; Bailey et al. 2005; EFNARC 2005).

To improve resistance to blocking or passing ability, Khayat et al. (2004) recommend that the segregation be reduced using either viscosity modifier admixtures (VMAs) or low w/c. In order to assess the passing ability of the mix; several tests have been developed including the L-box and filling capacity box.

The third requirement for freshly mixed SCC is the resistance to segregation, i.e., separation of aggregates from paste. In order for the concrete to exhibit sufficient filling ability and passing ability, the shear stress in the paste must be reduced. However, when the shear stress in the paste

is reduced too much severe segregation can occur, which leave large pockets of aggregate that can jeopardize the integrity of the structure. During the casting of a structure, segregation can form around the reinforcement, which is related to the passing ability of the concrete. Also, after the concrete has been poured, settlement of the aggregates can occur and cause weak surfaces and cracking in some elements (EFNARC 2005).

To improve segregation resistance, Bailey et al. (2005) suggests minimizing "bleeding due to free water" and reducing the segregation of solid particles. These can be accomplished by using VMAs and/or lowering the w/c of the mix. VMAs essentially reduce the viscosity of the paste and make the mix more stable. To assess the segregation resistances of the fresh concrete, tests such as the bleeding test, sieve segregation resistance, static segregation column test, orimet test, and the visual stability index (VSI) have been developed (JSCE 1998). These tests aim to quantify the dynamic stability as well as the static stability of the concrete.

2.3.3.2 SCC mix proportioning methods

SCC generally requires high fine content and or viscosity modifying admixtures (VMAs). One important factor affecting SCC rheological behaviour is the sand to total aggregate ratio (S/*A*). Conventional concrete has a typical S/*A* ratio ranging from 0.35 to 0.45 by volume. Such conventional concrete can be made flowable using appropriate admixtures but generally has very poor segregation resistance.

There are several procedures that have been published for the design of SCC mixture. European Guidelines for Self-Consolidating Concrete, American Concrete Institute, and the Japanese Society of Civil Engineers (JSCE) have published guidelines of proportioning SCC mixture. The European guidelines for SCC mix proportioning are presented in Table 2.5.

Table 2.5 - Typical ranges of SCC specified by European guidelines (EFNARC 2005)

Constituent	Typical range by Mass (kg/m^3)	Typical Range by Volume (l/m^3)
Powder	380-600	-
Paste	-	300-380
Water	150-210	150-210
Coarse Aggregate	750-1000	270-360
Fine Aggregate	Content balances the volume of the other constituents, typically 55-68% of total aggregate volume	
Water/Powder Ratio by Volume		0.85-1.10

The proposed proportions for the ACI SCC mix design proportioning are presented in Table 2.6.

Table 2.6 - SCC proportioning trial mixture parameters (ACI 237R 2007)

Absolute volume of coarse aggregate	28 to 32% (> 12.5 mm nominal maximum size) 50% (<12.5 mm nominal maximum size)
Paste fraction (calculated on volume)	34 to 40% (total mixture volume)
Mortar fraction (calculated on volume)	68 to 72% (total mixture volume)
Typical w/cm	0.32 to 0.45
Typical cement (powder content)	386 to 475 kg/m^3

When using the Japanese society of civil engineers (JSCE) guidelines for SCC mix design proportioning, the self-compactability rank of SCC mixture must be chosen. The rank is based on the difficulty of the application. Rank 1 is for highly congested reinforcement with complex shapes, whereas Rank 3 is for shallow elements with minimum reinforcement such as slabs. The JSCE guidelines for SCC mix proportioning are presented in Table 2.7

Table 2.7 - Coarse aggregate content for JSCE ranking (JSCE 1998)

Self-Compactability	Unit absolute volume of coarse aggregate (m^3/m^3)
Rank 1	0.28-0.30
Rank 2	0.30-0.33
Rank 3	0.32-0.35

The SCC European guideline offers wider range of powder with upper limit suggested at 600 kg/m^3 allowing variety of ranges and workability classes of SCC. Moreover, the increased powder provides stability and further segregation resisting to the mixture. The suggested coarse to fine aggregate ratio (32- 45%) is suitable for achieving high passing ability in highly congested reinforced element.

The ACI guidelines for designing SCC mixture overestimate the coarse aggregate volume in the mix and suggest 50% sand and 50% stone, when using stone size less than 12.5 mm. The suggested proportion can lead to poor flowability and passing ability with increased viscosity. Further, with the limited suggested powder content at 475 kg/m^3, high flowability (above 720 mm) and segregation resistance (< 15%) would be difficult to achieve. On the other hand, the JSCE guideline is more structured toward field applications where the difficulty of application/ placement is known, with very limited mix propositioning guidelines for starting mix development.

This research seeks the assessment of wide range of LWSCC industrial class; therefore, the European guideline was chosen to be followed for mix design guidelines.

Table 2.8 shows the effects of changing constituents of SCC mixture on slump flow, viscosity, passing ability, filling ability and segregation resistance (Koehler and Fowler 2006). A balanced mix proportion will result in high quality SCC mixture that satisfies the needed characteristics for the application.

Table 2.8 - SCC Mix design characteristics (Koehler and Fowler 2006)

		Slump Flow	Viscosity	Filling Ability	Passing Ability	Segregation Resistance
Aggregates	Maximum Size ↑	↓	↑	↓	↓	↓
	Grading	Higher pkg. Density;	Higher pkg. Density;	Finer Grading	Finer Grading	Uniform or finer grading:
	Improved Shape	↑	↓	↑	↑	↑
	Increased Angularity	↓	↑	↓	↓	↑
Paste Volume ↑		↑	↓	↑	↑	↑
Paste Composition	Water/Powder ↑	↑	↓	↑	↑	↓
	Fly Ash	↑	↓	↑	↑	↑ ↓
	Slag	↑ ↓	↑ ↓	↑ ↓	↑ ↓	↑ ↓
	Silica Fume	↓	↑	↓	↓	↑
	VMA	↓	↑	↑	↑	↑
	HRWRA	↑	↓	↑	↑	↓
	Air	↑	↓	↑	↑	↑ ↓

↑ increase, ↓ decrease, ↑↓ neutral effect

2.3.4 Mechanical Properties of SCC

SCC and conventional concrete of similar compressive strength and with the same raw material sources have comparable properties, and if there are differences, these are usually covered by the safe assumptions on which the design codes are based (EFNARC 2005).

As with conventional concrete, the compressive strength of SCC is determined by the w/c. Since most SCC mixtures have a low w/c, the compressive strengths for SCC are greater. Conventional concrete calculations based on amount of cement and w/c can be used, but may be somewhat conservative, because at the same w/c, properly designed SCC can exhibit higher compressive strength (ACI 237R 2007; Lachemi et al. 2006). This is due to the reduction of the risk of bleeding and segregation along with the lack of mechanical vibration that further promote a more

uniform microstructure and less porous interfacial transition zone between the cement paste and aggregate (Zhu et al. 2001). Other factors that can influence the rate of development and ultimate compressive strength are sand to total aggregate ratio, the type/amount of supplementary cementitious material and fillers, and the combination of chemical admixtures.

The elastic modulus of the constituents and the proportions of each can control the modulus of elasticity of concrete. The aggregate has the most influence on the concrete's modulus of elasticity, because the aggregate usually makes up the largest volume of the concrete. So, selecting an aggregate with an increased modulus will increase the modulus of the concrete while increasing the paste amount could decrease the modulus. Since SCC usually has a higher paste volume, the modulus of elasticity may be somewhat lower. Some observations have shown that for equal compressive strength, the elastic modulus of SCC can be as much as 10 to 15% lower than that of conventional concrete of similar compressive strength due to the required adjustments of mixture proportions to make SCC (Bennenk 2002).

When SCC is properly designed to minimize any segregation or bleeding, the mechanical properties exhibited by the material are comparable to conventional concrete. In some cases the mechanical properties are superior due to the increased quality in the microstructure and the interfacial bond between the aggregate and paste. Special attention should be given to mechanical properties that could be affected by an increase in paste, when compared to conventional concrete.

2.3.5 Durability of Self-Consolidating Concrete

SCC containing supplementary cementing materials (SCM) is known for its superior durability performance. Using SCM along with low w/c to produce SCC increases the density and decreases the total porosity and permeability of the concrete (Aitcin and Nevile 1993; Midgley and Illston 1983; Lessard et al. 1992; Mehta 1980, 1986; Sarkar and Aitcin 1987). In most cases, the production of SCC involves the use of SCM such as fly ash, silica fume, limestone and/or ground blast furnace slag. However, the proportioning of SCC mixture is different from high performance concrete (HPC).

Khayat et al. (2000) suggests that optimized SCC mixtures have favorable air-void systems and excellent durability resistance to freezing and thawing. Also, SCC mixtures with fly ash and silica fume have substantially lower rapid chloride-ion and water permeability than mixtures without SCMs. SCC mixes with the same strength grade as normal concrete have lower values of permeability coefficient and sorptivity (rate of water absorption). Further, chloride diffusivity is much dependent on the type of additional powder used in SCC. Use of pulverized fly ash (PFA) in SCC lowers values of chloride migration (Zhu and Bartos 2003). SCC mixtures made with high-volumes of cement replacement (such as fly ash, silica fume and slag) can achieve very low chloride ion permeability compared to the conventional concrete. They can also achieve good workability, high long-term strength, moderate salt scaling resistance, and low sulfate expansion (Nehdi et al. 2004).

Hassan et al. (2009) concluded in their full-scale reinforced SCC beams study that SCC beams exhibited superior rebar corrosion protection compared to its normal concrete (NC) counterpart. Distinct advantages of SCC over NC in terms of corrosion protection were revealed from the results of current measurements with time, crack widths and patterns, half-cell potential measurements, chloride ion contents near the bar surface and the rebar mass loss/diameter reduction. However, cracks in SCC beams were easily propagated and extended compared to NC beams. SCC beams exhibited breaking and spalling of concrete cover, even at locations which had lower crack widths compared to NC beams. This inferior quality was attributed to the presence of a lower volume of coarse aggregate in SCC beams (25% less than NC), causing lower crack arresting capacity that induces concrete spalling even at locations with lower crack widths.

Autogenous shrinkage, which occurs during setting and is caused by the internal consumption of water during hydration, can be particularly high in mixtures made with a relatively low water-to-cementitious ratio (w/cm), high content of cement, and supplementary cementitious materials exhibiting a high rate of pozzolanic reactivity at an early age. Special attention should be given to protect SCC at early ages to minimize desiccation (ACI 237R 2007). Drying shrinkage is caused by the loss of water from the concrete to the atmosphere. Generally this loss of water is from the cement paste. Drying shrinkage is relatively slow, and the stresses it induces are

partially balanced by tension creep relief (EFNARC 2005). High paste volumes and reduction in aggregate content can lead to greater potential for drying shrinkage (ACI 237R 2007). SCC drying shrinkage has been reported to be similar to or lower than that of conventional concrete of similar compressive strength (Sonebi et al. 1999; Persson 1999). SCC should also be protected from plastic shrinkage cracking because the mixtures may exhibit little or no bleed water (ACI 237R 2007).

Creep, which is the gradual increase in deformation (strain) with time for a constant applied stress, is expected to be higher in SCC when compared to conventional concrete, due to the higher volume of cement (EFNARC 2005; Raghaven et al. 2002). Creep takes place in the cement paste, and it is influenced by the porosity, which is directly related to the w/c. During hydration, the porosity of the cement paste decreases and hence for a given concrete creep decreases as strength increases. As the aggregates restrain the creep of the cement paste, the higher the volume of aggregate and the higher the elastic modulus of the aggregate, the lower the creep will be (EFNARC 2005).

The elevated temperature resistance of SCC has been reported to be similar to conventional concrete (Noumowe et al. 2006). However, SCC could be more susceptible to spalling, due to the low permeability and increased paste volume. This depends upon the aggregate type, concrete quality, and moisture content (Persson 2003, 2004; Cather 2003; Hans and Michael 2006). The use of polypropylene fibres in SCC has been shown to be effective in improving its resistance to spalling. The mechanism is believed to be due to the fibers melting and being absorbed in the cement matrix. The fibre voids then provide expansion chambers for steam, thus reducing the risk of spalling (Cather 2003; Hans and Michael 2006).

In summary, using adequate cement paste in SCC mix design, with proper aggregates packing density, lower water-to-binder ratio (w/b) and pozzolanic material, it is possible to reduce the mixing water, enhance the durability characteristics of SCC such as chloride penetrability, drying shrinkage, electric resistance and resistance to sulfate attack and alkali-aggregate reaction.

2.3.6 Statistical Models of Self-Consolidating Concrete

2.3.6.1 Introduction

The optimization of SCC mixture necessitates carrying out several trial batches to achieve adequate balance between deformability, stability, and mechanical properties. Typically, mixture optimization involves a regression approach where one parameter is changed at a time to assess its influence on properties of interest. This however does not permit the understanding of the relative influence of mixture parameters and their interactions on concrete characteristics (Khayat et al. 2000). Whereas design guidelines (step by step) and statistical modelling for self-consolidating concrete have been published (Khayat et al. 1998; Patel et al. 2004; Sonebi 2004a, 2004b), there is no enough research for lightweight self-consolidating concrete (LWSCC).

The statistical models can be used to evaluate the effects of a group of variables on key responses of SCC or LWSCC and trade-offs among various parameters required to secure similar responses. The models are also useful to establish relationships between various responses that can be determined with different constraints on material performance.

2.3.6.2 Review of previous work on SCC statistical models

Importance of statistical models in proportioning self-consolidating concrete

Several researches address the development of statistical models using a factorial design approach to understand the effect of mixture parameters on key responses of self-consolidating concrete, including slump flow, theological parameters, filling capacity, V-funnel flow time, surface settlement, and compressive strength. The models are valid for mixtures with certain range of w/b, binder, coarse aggregate, viscosity-enhancing agent, and high-range water reducer.

Although the predicted response changes with the deviation from material characteristics used in establishing the models, the models remain quite useful in determining the significance of mixture parameters and their interactions on self-consolidating concrete properties. Khayat et al. (2000) demonstrated one of the useful models in establishing trade-offs among mixture parameters necessary for mixture optimization and compares the effect of changes in such parameters on key self-consolidating concrete responses.

Factorial design models for proportioning self-consolidating concrete

Khayat et al. (2000) selected five key mixture parameters that can have significant influence on mixture characteristics of SCC to derive statistical models for evaluating relevant properties of SCC. The five variables included the concentrations of viscosity modifier admixture (VMA) and HRWR, the w/cm, the content of cementitious materials (CM), and the volume of coarse aggregate (Vca). The modelled concrete responses were the slump flow, and rheological parameters to evaluate the deformability of concrete in a non-restrained area, as well as the filling capacity and V-funnel flow time to evaluate the deformability in a restrained area that reflect its deformability and resistance to blocking. The other modelled responses included the surface settlement, segregation resistance, and compressive strength (f_c') after 7 and 28-days.

A 2^{n-1} statistical experimental design was used to evaluate the influence of two different levels for each of the five mixture variables (n = 5) on the relevant concrete properties. Such a two-level factorial design requires a minimum number of tests for each variable. The initial levels of the five selected mixture variables were carefully chosen after reviewing the demand constraints imposed by the targeted concrete properties. Responses were modelled in a quadratic manner to enable the evaluation of the five selected mixture parameters with five distinguished levels: codified values of -α, -1, 0, 1, and α. The α value was chosen so that the variance of the response predicted by the model would depend only on the distance from the center of the modelled region. According to Khayat et al. (2000), the value α is equal to $NF^{1/4}$ where NF is the number of fractional factorial points $2^{5-1} = 16$ (or $= 16^{1/4} = 2$).

Example of two-level fractional factorial design and four variables with 21 mix combinations and their code and actual values are shown in Table 2.9. The code factors of variables are calculated as follows:

Coded Factor = (Actual value - Factor means)/(Range of the factorial values/2)

For example:

Coded W/C = (Actual W/C - 0.45) /0.05 & Coded SF = (Actual SF - 7.5) / 2.5

Table 2.9 - Example of mix proportions using two-level fractional factorial design method (Khayat et al. 2000)

	Mix	Coded values				Absolute values			
		SF	SP	Sand	W/C	SF	SP	Sand	W/C
Level of factors	1	-1	-1	-1	-1	5	0.6	50	0.4
	2	1	-1	-1	1	10	0.6	50	0.5
	3	-1	1	-1	1	5	1.2	50	0.5
	4	1	1	-1	-1	10	1.2	50	0.4
	5	-1	-1	1	1	5	0.6	100	0.5
	6	1	-1	1	-1	10	0.6	100	0.4
	7	-1	1	1	-1	5	1.2	100	0.4
	8	1	1	1	1	10	1.2	100	0.5
Centre points	9	0	0	0	0	7.5	0.9	75	0.45
	10	0	0	0	0	7.5	0.9	75	0.45
	11	0	0	0	0	7.5	0.9	75	0.45
	12	0	0	0	0	7.5	0.9	75	0.45
	13	0	0	0	0	7.5	0.9	75	0.45
Points of verification	14	-0.6	0.7	-1.0	0	6	1.1	50	0.45
	15	-0.2	0.3	0	0.6	7	1	75	0.48
	16	-1.0	0.7	1	0.4	5	1.1	100	0.47
	17	0.2	0	0.2	0.4	8	0.9	80	0.47
	18	0.6	1	1	0	9	1.2	100	0.45
	19	-0.2	1	0	-0.4	7	1.2	75	0.43
	20	-0.6	0	-0.6	0.6	6	0.9	60	0.48
	21	-1	0.7	-0.1	-0.8	5	1.1	50	0.41

Testing the effect of mixture parameters on various responses

The statistical models can be used to evaluate the impact of mixture composition on SCC properties. Although the models are derived for a specific set of materials, variations in material characteristics will change the estimate of the response. However, the general tendencies regarding the relative impacts of mixture parameters on given responses should remain relevant and hence useful to select directions in the mixture proportioning of SCC.

For example, the effect of increasing HRWR on changes in slump flow, V-funnel flow time, and filling capacity are illustrated in Figure 2.7 for two mixtures. The increase in HRWR lowers the internal resistance to flow and increases the slump flow. Both flow time and filling capacity increase with slump flow, reaching peak values at around 700 mm.

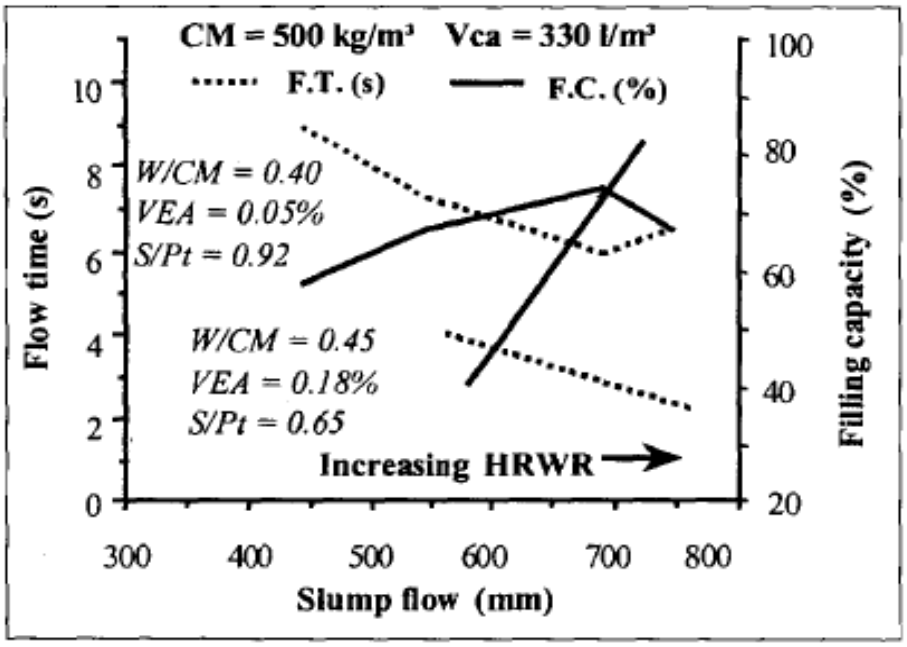

**Vca: voulme of corase aggreates; CM: cementitious materials content; VEA: Viscosity modifier admixture, S/Pt: sand – to – paste volume, F.T: flow time, F.C: Filling capacity*

Figure 2.7- Relationship between slump flow, slow time, and filling capacity of mixture made with different w/cm and Vca values (Khayat et al. 2000)

The developed SCC statistical model by Khayat et al. (2000) can be a guiding tool for establishing LWSCC model. The SCC model covers wide range of variables (VMA, HRWRA, the w/cm, the content of cementitious materials, and the volume of coarse aggregate), two of these variables, namely, VMA and volume of coarse aggregate, are not compatible with LWSCC development. VMA is typically used in the case of poor aggregate gradation, and instability in the SCC mixture. Most industrial designs of SCC avoid the use of VMA because of its complexity of use and lack of compatibility with other chemicals, such as new generations of HRWRA and air entrained admixture. The variation of the coarse aggregate volume is much different in case of LWSCC mixtures, where the aggregate density, optimum aggregate packing density and the stability of the mixture dictate a fixed volume percentage to be used.

Central composite design (CCD) method

The central composite design (CCD) method was used by Patel et al. (2004) to optimize the design of FA self-consolidating concrete mixtures with desired properties. Four input factors were used in the test program: X1 (total binder content), X2 (percentage of FA as cement replacement by mass), X3 (percentage of solid mass of HRWRA as a percentage of mass of cementing materials), and X4 (water-binder ratio: w/b). The CCD method consists of three portions: the fraction factorial portion, the center portion, and the axial portion. They represent how to vary the independent variables and how many runs are required for the experiment. The factorial portion is fractional factorial of the number of factors, and it is not effective if the response is nonlinear. The central portion is useful to estimate experimental error, and the axial portion allows the estimation of curvature or nonlinear modelling.

Fraction factorial portion n_f is where the factors are set at two levels and the number of runs (mixtures) is decided by 2^{k-1}, where k is the number of factors. The total number of mixtures for fraction factorial portion is kept at 2^{k-1} with a different combination of coded value varying between +1 and –1, example shown in Table 2.10.

Center point portion n_c is where enough center points are needed to get good estimation of pure experimental error and to maintain orthogonality. According to Schmidt and Launsby (1994), the

minimum number of n_c can be obtained from: 4 x $\sqrt{n_f}$ +1 -2k. Typically, a total of five runs (mixtures) is kept for the center point portion (Table 2.10) with '0' coded value.

Axial portion is where number of runs for axial portion are set at 2k for the experimental program. The coded value of portion is set at $(n_f)^{1/4}$, where n_f is the number of runs in fraction factorial portion of the design. The final coded value is set at five different levels such as -α, -1, 0, 1, and α (–1.68, –1, 0, +1, +1.68 in Table 2.10). This way, the total number of runs (mixtures) is established and the sequence of mixes was randomized (Patel et al. 2004).

Table 2.10 - Example of limit and coded value of factors (variables) - (Patel et al. 2004)

Factor	**Range**	**Coded value**				
		-1.68	-1	0	+1	+1.68
X_1	350 to 450	350	370	400	430	450
X_2	30 to 60%	30	36	45	54	60
X_3	0.1 to 0.6%	0.1	0.2	0.35	0.5	0.6
X_4	0.33 to 0.45	0.33	0.355	0.39	0.425	0.45

CCD portion	Mixture	Factors			
		X_1	X_2	X_3	X_4
Fractional factorial	6,8,10,11,13 ,17,20,21	± 1	± 1	± 1	± 1
Center point	1,2,9,15,18	0	0	0	0
Axial	7,4,3,12,14, 16,5,19	0,±1.68	0,±1.68	0,±1.68	0,±1.68

By trial-and-error method, the best-fit models shall be identified from different probability distribution functions such as Normal (Gaussian), Gaussian inverse, Gamma, Poisson, and Binomial with different link functions such as identity, log, and power. The "t" test and/or "chi square" test are then implemented to decide statistical significance of the variables. The null hypothesis is checked for all the estimated coefficients such as a_0, a_1, and a_3. The null hypothesis is a presupposition that the true value of the coefficient is zero. In other words, the variable(s)

associated with that coefficient are statistically not significant with no influence on the response Y. If the probability greater than "t statistics" or "chi square statistics" is less than 0.1 (10%), the null hypothesis (the coefficient value is zero) is rejected and it is established that the variable(s) with the estimated coefficient have significant influence on response. If the probability greater than "t statistics" or "chi square statistics" is more than 0.15 (15%), the null hypothesis (the coefficient value is zero) is accepted and it establishes that the variable(s) with the estimated coefficient have no influence on the response. Hence, that variable(s) should not be included in the model (Patel et al. 2004).

The simplicity and the wide range of the measured fresh, hardened and durability responses of the developed SCC statistical model by Patel et al. (2004) makes it a useful tool for creating a similar LWSCC model. Patel's SCC model focuses on the influence of FA percentage on the fresh, hardened and durability characteristics of SCC. The variation of FA percentage may not be the main focus when building LWSCC statistical model, rather having fixed amount of SCMs would simplify the modelling process and the number of trial batch needed for establishing such a model.

Sonebi et al. (2007) suggested that for SCC statistical experimental design (three factors at two levels) should be used to evaluate the influence of two different levels for each variable on the relevant concrete properties. Three key parameters that can have significant influence on mixture characteristics of SCC can be selected to derive statistical models for evaluating the filling ability and passing properties. Example of experimental levels of the variables (maximum and minimum) water content, HRWRA dosage, and the volume of coarse aggregate are defined and given in Table 2.11.

Table 2.11 - Range of code values F composite factorial design (Sonebi et al. 2007)

Coded values	**-1.68**	**-1**	**0**	**+1**	**+1.68**
Water, l/m^3	181	188	198	208	215
HRWRA, l/m^3	3.1	3.75	4.75	5.75	6.43
Volume of coarse aggregate, kg/m^3	173	220	290	360	409

The dosages of water and HRWRA can be varied, the ratio between the coarse aggregate fractions 4/8 and 8/16 mm shall be kept constant at 0.43. The volume of sand should be adjusted to compensate for the increase or decrease of the coarse aggregate (Sonebi et al. 2007).

The variation of the parameters is chosen to obtain a wide range of characteristics in the fresh state. A two-level factorial design requires a minimum number of tests for each variable. Given the fact that the expected responses do not vary linearly manner with the selected variable and to enable the quantification of the prediction of the responses, a central composite plan is selected where the response could be modelled in a quadratic manner.

Because the error in predicting the responses increases with the distance from the center of the modelled region, it is advisable to limit the use of the models to an area bound by coded values corresponding to $-\alpha$ to $+\alpha$ limits. The area bound by the circle with a radius of 1.68 (in the example) on the two-dimensional presentation shown in Figure 2.8 is recommended as a modelled region rather than the outer square region. This can eliminate the four outer regions approaching the edges of the modelled region presenting the furthest points from the center. To ensure the accuracy of the model, a minimum of six replicate central point's mixes shall be prepared to estimate the degree of experimental error for the modelled responses (Sonebi et al. 2007).

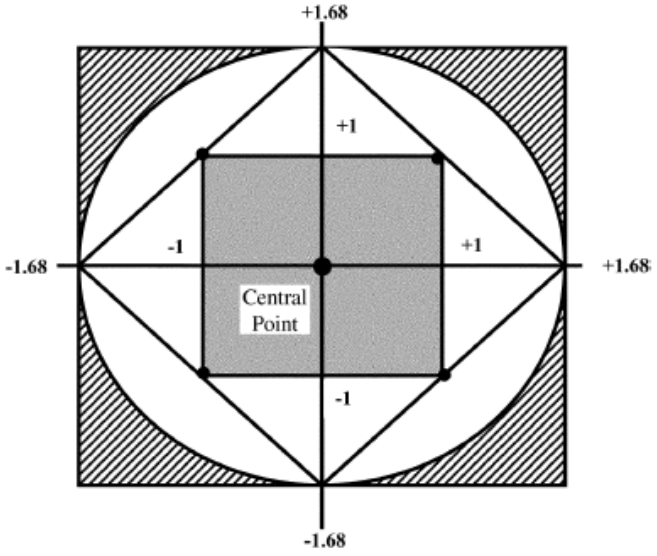

Figure 2.8 - Presentation of modelled region of experimental plan

Validation of statistical models

To validated SCC developed model, number of SCC mixtures shall be selected randomly to verify the ability of the proposed models to predict the responses. These tests shall be carried out with the same materials and under the same testing conditions of the modelled mixtures used for the development of statistical models. For example, the test slump flow and compressive strength (1 and 28-day) of the concrete mixtures shall be compared with the prediction of the respective models.

Accuracy of the proposed models

The accuracy of each of the proposed models can be determined by comparing predicted-to-measured values obtained with mixes prepared at the centre of the experimental domain. For example, the predicted-to-measured values for slump flow and V-funnel are shown in Figure 2.9, with the estimated errors corresponding to a 95% confidence limit (dotted lines). Sonebi (2003) found that for SCC developed models, the ratio of predicted-to-measured values ranged between 0.98 and 1.01, thus indicating good accuracy for the established models to predict the filling ability, passing ability, segregation and compressive strength. In general, Sonebi (2003) proposed SCC models appear to be satisfactory in predicting the flowability, passing ability, segregation resistance and strength, with low scattering between the measured and predicted values.

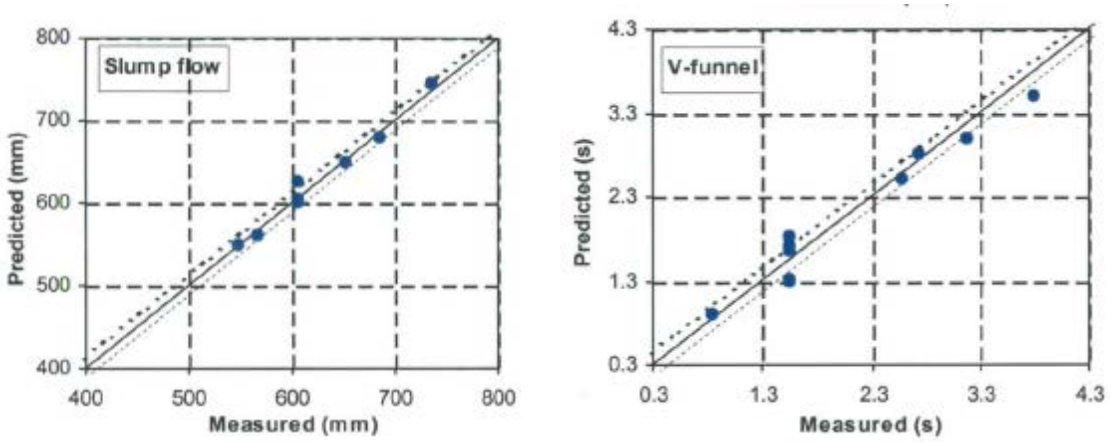

Figure 2.9 - Examples of measured properties versus predicted from statistical models of slump flow and v-funnel (Sonebi 2003)

2.4 Lightweight Self- Consolidating Concrete (LWSCC)

2.4.1 Introduction

Lightweight self-consolidating concrete (LWSCC) is a new class of concrete developed by combining the favorable properties of lightweight concrete (LWC) and self- consolidating concrete SCC. Practical applications of structural LWSCC are in increase. The first reported usage of LWSCC dates back to 1992 when it was used for the construction of a cable stayed bridge main girder in Japan (Okamura 2003). Other applications include: precast panels (Umehara et al. 1994; Garrecht et al. 2010); a thin precast C-shaped wall (Shi and Yang 2005); stadium walkway structural elements; precast stadium benches (Hubertova and Hela 2007); a 20 m prestressed beam (Dymond 2007); precast panels with internal reinforcement of carbon fiber reinforced polymer (CFRP) meshes (Yao and Gerwick 2006); and composite floor slabs (Mechtcherine et al. 2010).

2.4.2 Mixture Design Procedures for LWSCC

For self-consolidating concrete, most mixes can be “converted” into lightweight mixes by replacing some or all of the normal weight aggregate with lightweight aggregate. Often the coarse fraction is replaced with lightweight aggregate and the fines are normal weight sand. In some cases, some or all the fine aggregate may be lightweight. Since these aggregates absorb moisture at a greater rate than other aggregates, pre-wetting is required. As lightweight aggregates have a cellular structure and are therefore, more porous than ordinary crushed stone, they take longer time to reach saturated surface dry (SSD) condition. Therefore pre-soaked aggregates are recommended for trial or production batches. As such, lightweight aggregates absorb and hold more moisture than ordinary stone. Because of its greater porosity, extra care is exercised when designing the LWSCC mix and when dosing the mix water. In fact, lightweight aggregates (LWA) absorb water for hours, days and even weeks after first being wetted (The Concrete Countertop Institute 2006).

While the surface texture and aggregate shape may have an affect on the workability, rougher - angular particles result in a mix that has lower workability than smooth - rounder particles. Most lightweight aggregates weigh about 0.50 to 0.66 the weight of normal aggregate. On average, 1

kg of gravel can be replaced with slightly more than ½ kg of lightweight aggregate. The volume of aggregate stays the same, but the weight is reduced.

Evaluation of the fresh properties for LWSCC is essentially carried out in the same way as for SCC. Numerous investigations on the workability of SCC performed in North America and Europe have shown that L-box, V-funnel, J-rings, and the slump flow tests in conjunction with the visual stability index (VSI) test or sieve segregation resistance (SSR) test are very effective to evaluate the workability of the SCC mix. However, investigations on resistance to segregation of lightweight aggregate (LWC) and volume stability of LWSCC are still ongoing.

Workability is an important factor that affects the application and rheological properties of LWSCC, where the LWSCC mixture is required to have high fluidity, deformability, filling ability, and fairy high resistance to segregation. To ensure that reinforcement can be encapsulated and that the formwork can be filled completely, a favorable workability is essential for fresh LWSCC. In addition, aggregate particles in LWSCC are required to have uniform distribution in the specimen with minimum segregation risk during transportation and placement (Wu et al. 2009).

Choi et al. (2006) designed the mix proportion for LWSCC by adopting a modified method proposed by Su and Miao (2003). The slump flow, V-funnel and U-box tests were then used to evaluate the workability of LWSCC. Similarly, Shi and Wu (2005) used the slump flow, V-funnel, and L-box tests, and the visual observation method to study the properties of LWSCC.

Müller and Haist (2002) proposed three mix proportions for LWSCC and assessed self-consolidated properties by the slump flow, J-ring, V-funnel, and L-box tests. It was found that, compared to SCC, there was no significant difference in the mix proportion design except for the type of aggregates used.

2.4.2.1 Design methods

LWSCC design methods are similar to those used for SCC. Several design approaches based on scientific theories or empirical expressions derived from experiences have been proposed for LWSCC. In general, these procedures fall into the following two categories:

1) Combination of high-range water-reducing admixture and high content of mineral powders;

2) Combination of high-range water-reducing admixture and viscosity-modifying admixture (VMA) with or without defoaming agent.

Figure 2.10 illustrates the general principles for the design of LWSCC, as considered from the excess paste theory. The conventional concrete design method begins with the determination of the amounts of water and cement, and ends up with the calculation of the amount of aggregates. Because aggregates are much less expensive and more stable than cement pastes, a quality concrete should contain as much aggregate and less cement paste as possible. Thus, the most reasonable approach to determine the amounts of cement pastes for the concrete should be based on the characteristics of the aggregates used and of the concrete designed.

Shi and Wu (2005) reported a procedure to design LWSCC using a combination of the least void volume for a binary aggregate mixture, excess paste theory, and ACI 211.2-98 “Standard Practice for Selecting Proportions for Structural Lightweight Concrete”. Figure 2.10(a) shows compacted aggregate particles. In order to obtain a concrete mixture with proper workability, it is necessary not only to have sufficient amount of cement paste to fill the voids among aggregate particles, but also enough paste to form a thin layer of coating on the surface of aggregates to overcome friction between aggregate particles, as shown in Figure 2.10(b). Without a film of cement paste around aggregates as a lubricant, the movement between aggregates would be difficult. To further increase the workability of the concrete mixture to become a self-consolidating concrete, it is necessary to increase the volume of excess paste or the distance between aggregate particles, as shown in Figure 2.10(c). The required volume of excess paste is dependent on gradation, shape, and surface texture of the aggregates used, and can be determined through laboratory experiments for concrete mixtures with desired properties.

LWSCC mixtures with optimum amount of paste and with aggregates that have high packing density, would result in mixtures that have high strength efficiency, high electrical resistance, and low chloride ion penetrability capacity (Hwang and Hung 2005).

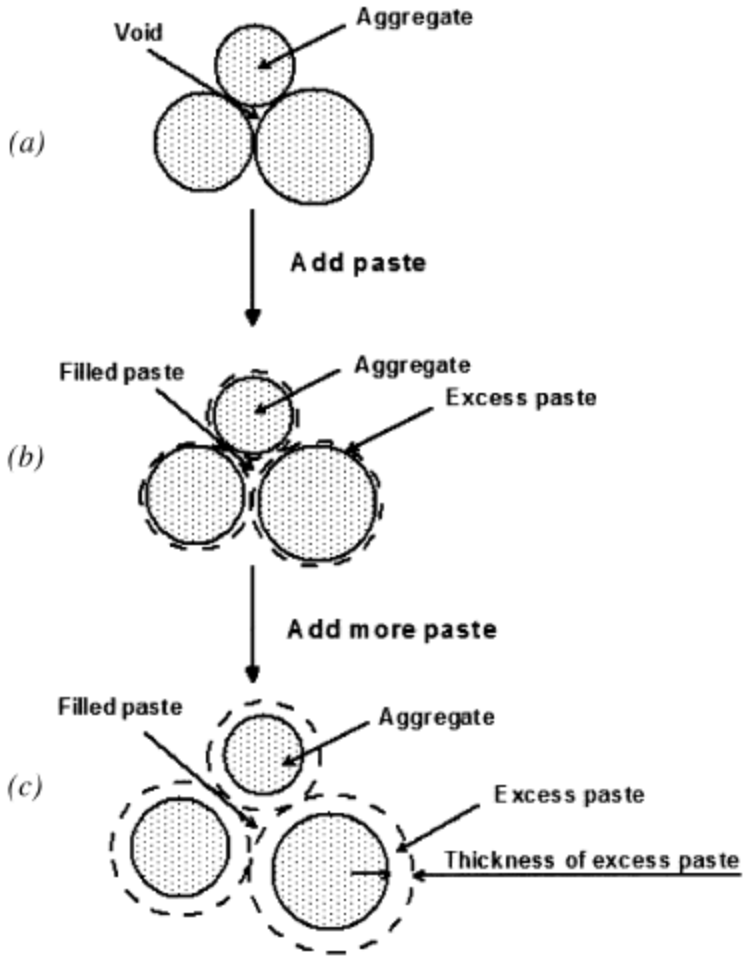

Figure 2.10 - Scheme of compacted aggregate and concrete mixture (Shi and Wu 2005)

2.4.2.2 Packing density

To determine the volume of filled paste and excess paste, the void volume of the dry binary aggregate (fine and coarse) mixtures should be calculated first. The relationship between void volume or density of combined aggregates and coarse-to-fine aggregate volume ratio can be established by packing different amounts of coarse and fine aggregates following ASTM C 29 (2009) as shown in Figure. 2.11.

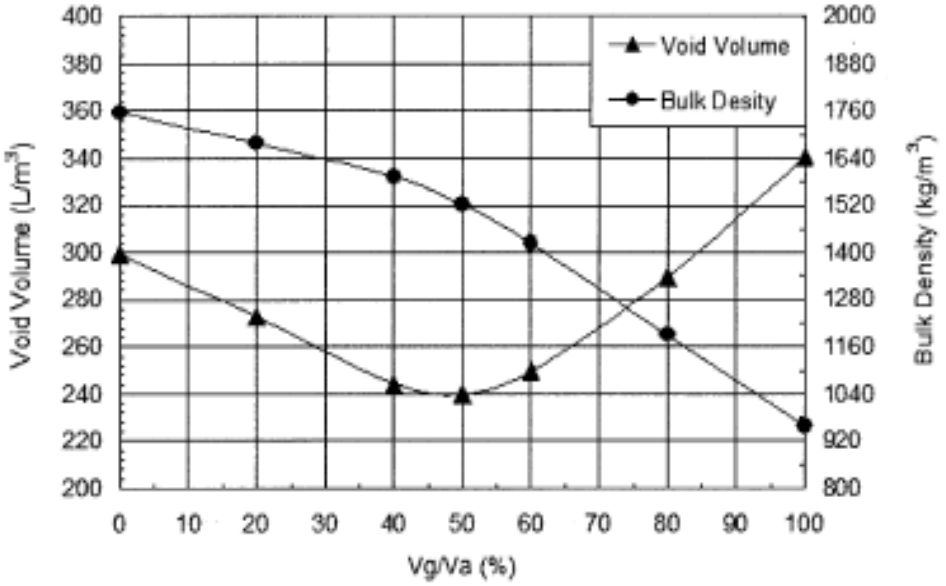

Figure 2.11 - Effect of coarse-to-total aggregate volume ratio on bulk density and void volume (Shi and Wu 2005)

It can be seen from Figure. 2.11 that the lowest void volume for the combined coarse and fine aggregates used in this example is around 240 l/m^3 when the coarse-to-fine aggregate volume ratio is 0.5. In the case of lightweight SCC, one of the main objectives is to develop concrete mixtures with low unit weights. As the coarse-to-fine aggregate volume ratio is increased from 0.5 to 0.6, it does not increase the void volume by much (from 240 to 250 l/m^3) but decreases the density of the combined aggregates significantly (from 1520 to 1420 kg/m^3) (Hwang and Hung 2005).

ACI 211.2 (1998) provides guidelines on relationships between compressive strength and cement content, and relationship between compressive strength and water to cement ratio (w/c). Shi and Yang (2005) used a cement content of 420 kg/m^3 and a w/c of 0.48 to develop LWSCC. The volume of excess paste was determined by experiments. Different volumes of combined aggregates were replaced by cement paste with the same property. It was found that a replacement of 20% aggregate (by volume) by using the excess paste theory gave the concrete the required flowability and segregation resistance. The workability of the concrete mixture was adjusted by using a high-range water-reducing admixture (HRWRA).

2.4.2.3 Proportioning of lightweight self-consolidating concrete

Hwang and Hung (2005) developed the design concept of densified mixture design algorithm (DMDA), motivated by the hypothesis that the physical properties of a mixture will be optimum when the physical density is at its highest. For volume stability, coarse LWA, normal sand and pozzolanic materials (fly ash) are densely packed to reduce the amount of cement paste required. For chemical strengthening of low concrete permeability, pozzolanic material (fly ash) is used to fill void of blended aggregates, and through pozzolanic reaction to strengthen interface between aggregates and cement paste.

The mixture proportion algorithm is divided into aggregate and paste phases. The aggregate phase includes coarse lightweight aggregate, normal weight fine aggregate and fly ash; while the paste phase includes cement, slag, water and superplasticizer (SP). In the DMDA method, the aggregates phase forms the major skeleton by filling coarse particles with fine ones to minimize porosity (Vv), as shown in Figure 2.12, and to increase density of solid materials, thus reducing the amount of cement paste, as shown in Figure 2.13. The paste phase is for lubricating and filling pores to achieve concrete workability as shown in Figure 2.14.

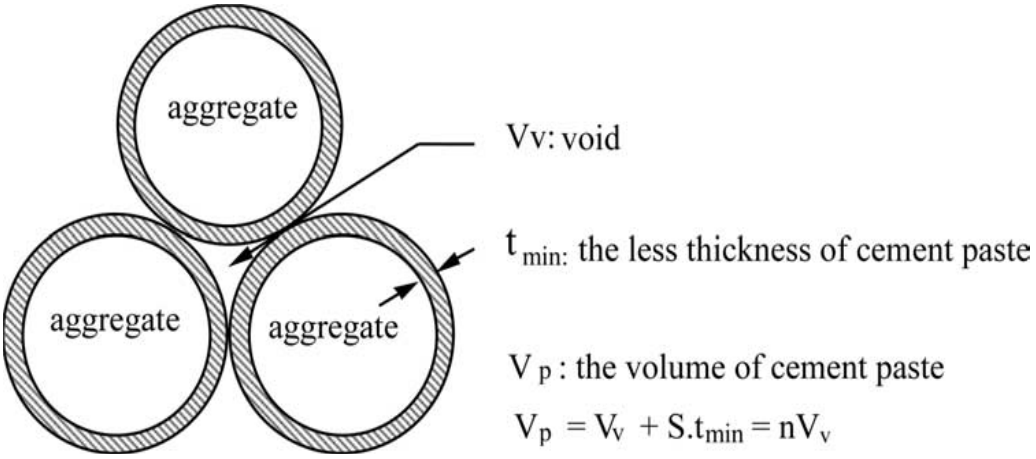

Figure 2.12- Densified aggregate to reduce (Hwang and Hung 2005)

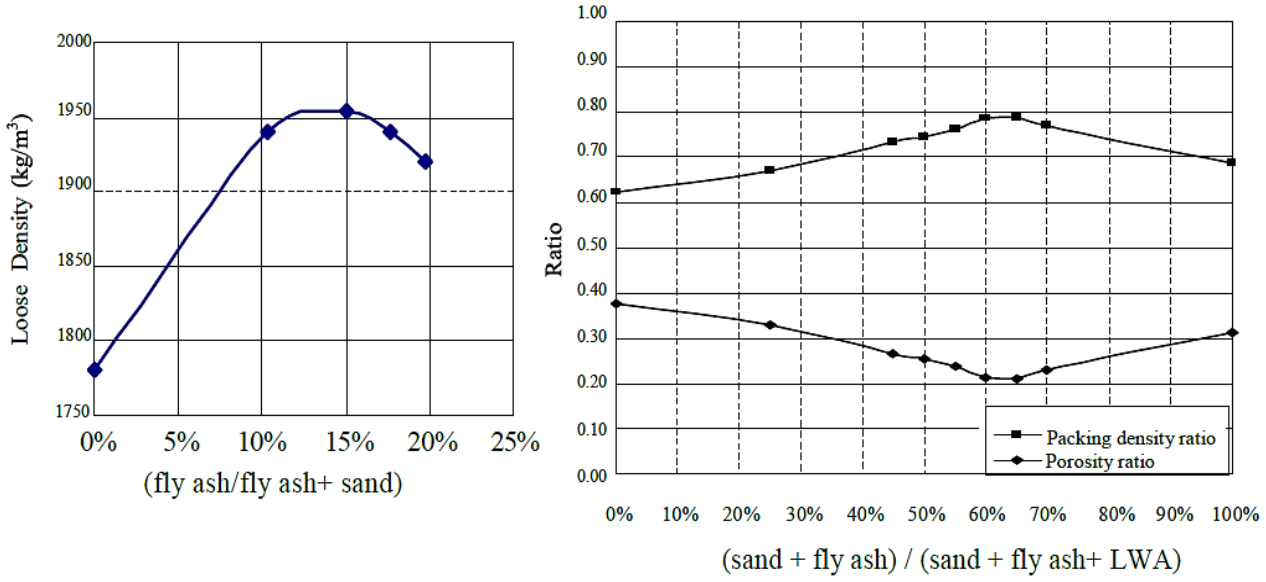

Figure 2.13 - The loose density, packing density ratio and void of blended aggregate mixture (Hwang and Hung 2005)

Design criteria and purpose of DMDA

According to Hwang and Hung (2005) there is some design consideration that needed to be followed when designing LWSCC using the DMDA method.

- Expected strength of LWC is matched with actual data for choosing the proper w/cm. The strength of structural lightweight concrete is not only dependent on the cement paste, but also on all constituting materials. For lightweight high strength concrete, the importance of the physical property of LWA should be stressed.
- The density of structural lightweight concrete is affected by the specific gravity of aggregate. The gradation and shape of LWA affects the packing density of aggregates and the amount of LWA.
- The water content is suggested to be below 160 kg/m^3, but should be enough for cement hydration to ensure the volume stability of concrete.
- The w/c is higher than 0.42 to prevent autogenous shrinkage or chemical contraction due to cement hydration and/or pozzolanic reaction.

- Use as little cement as possible to reduce the supply of alkali and C_3A as well as C_3S to reduce the harmful expansion or swelling of concrete due to alkali aggregate reaction (AAR) or sulfate attack.

The suggested DMDA method for designing LWSCC mixtures by utilizing the physical packing density of aggregate is beneficiation method for water and cement content reduction. This reduction may result in lower permeability and higher electrical resistance of LWSCC mixtures. However, this method focus on introducing fly ash to enhance the aggregates packing density, where it should rather only include the optimum packing density of the coarse lightweight aggregate and normal/light weight fine. Fly ash can be introduced as part of the optimum paste design phase, so that the availability of specific SCM (fly ash) would have no impact on the aggregate design phase. Moreover, w/c of 0.4 or higher may lead to poor mechanical and durability performance. Therefore, proposing low workability classes of LWSCC mixture (slump flow 550 to 650 mm) might be a suitable way for managing poor aggregate packing density rather than increasing the w/c to 0.4 or higher.

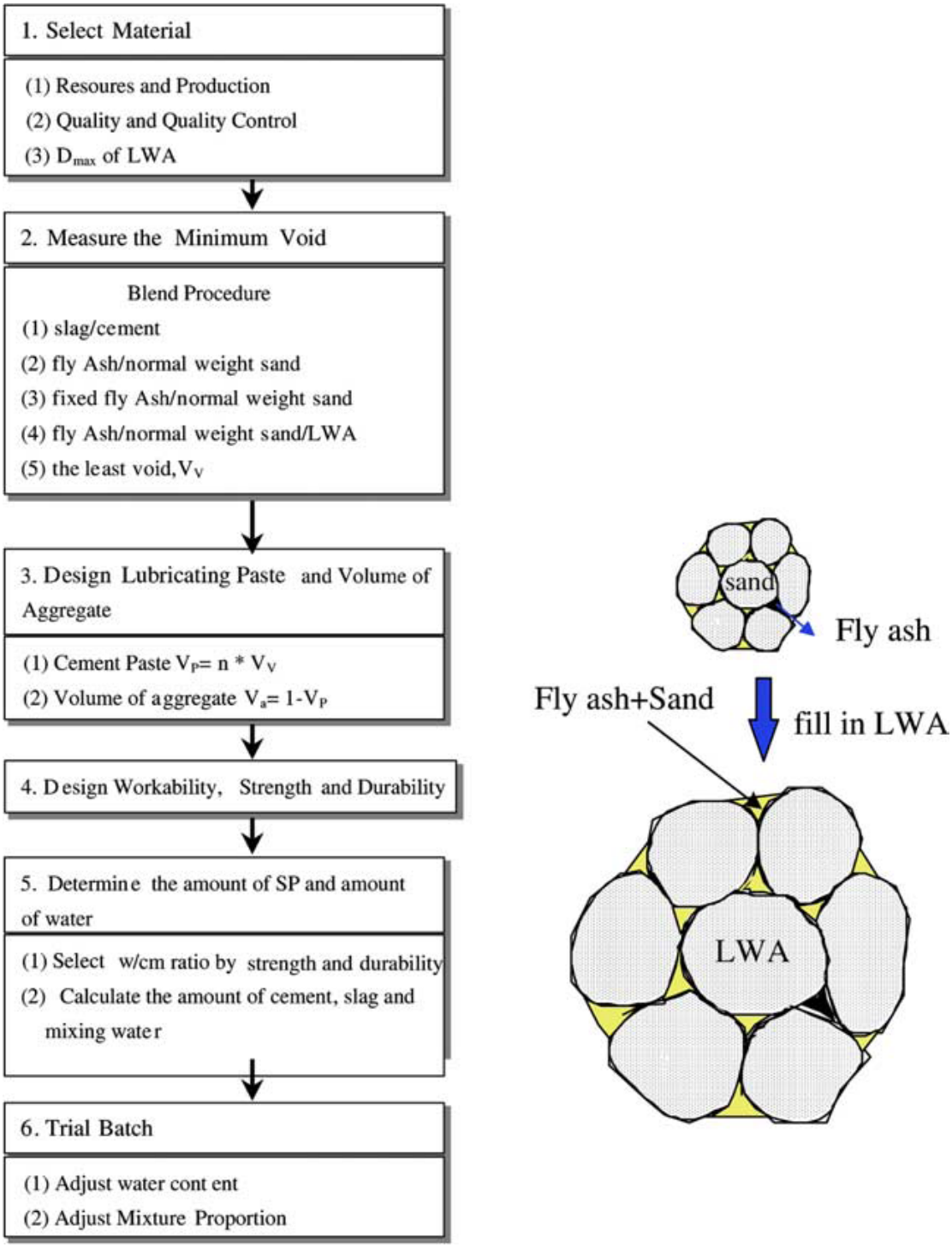

Figure 2.14 - Proportioning lightweight self-consolidating concrete by DMDA (Hwang and Hung 2005)

2.4.3 Factors Affecting Fresh and Hardened Characteristics of LWSCC

Several researchers reported that the development of LWSCC with the following characteristics: low density, high flowability and deformability, high self-compactability and high stability against separation of concrete ingredients (Hwang and Hung 2005; Choi et al. 2006; Lo et al. 2007; Lachemi et al. 2009; Wu et al. 2009; Kim et al. 2010; Gamal 2007; Karahan et al. 2012). However, these advantages may be influenced by many factors such as dosage of high range water reducing agent (HRWRA), concrete mix proportions water- to- cement ratio (w/c), water-to-powder ratio (w/p) and lightweight coarse aggregate-to-sand ratio (LWA/Sand)) and inclusion of normal weight aggregate as a partial replacement of LWA. Gamal (2007) conducted in-depth tests with regard to factors effecting fresh and hardened characteristics of LWSCC using expanded clay.

2.4.3.1 Effect of LWA to sand ratio

Gamal (2007) studied the flowability and air satiability of LWSCC made with 0.30 w/c, 0.80% HRWRA (by weight of cement) and different LWA to sand ratio (2.00, 1.50 and 1.00). It was found that reducing the LWA to sand ratio improved the various fresh parameters of LWSCC such as flowability, deformability and self-compactability. The slump flow increased with the decrease of LWA to sand ratio and the amount of increase reached about 20% as a result of using LWA to sand ratio of 1.0 instead of 2.0. On the other hand, the air content is significantly reduced with the reduction of LWA to sand ratio. The lowest value of air content was obtained when a ratio of LWA to sand of 1.0 was considered. Here the amount of reduction in air content was about 60% compared to the corresponding mixes made with LWA to sand ratio of 2.0.

The improvement in the fresh concrete properties due to reduction of LWA to sand ratio may be attributed to the decrease in friction between concrete ingredients - produced from the interlocking effect between coarse aggregate particles leading to an increase of the degree of flowability and deformability of LWSCC. The amount of air content was reduced because the enhancement occurred in the cohesion of concrete which might have increased with the increase in the amount of sand in LWSCC (Gamal 2007).

The LWA to sand ratio had slight effects on both compressive strength and homogeneity of LWSCC. The compressive strength and ultra-sonic pulse velocity (UPV) increased from 205 kg/cm^2 to 220 kg/cm^2 and from 2700 to 2760 m/s, respectively, when LWA to sand ratio decreased from 2.0 to 1.0. A significant increase in the SSD density of LWSCC was observed due to reduction of LWA to sand ratio. The density increased from 1260 to 1550 kg/m^3 as a result of utilizing a ratio of LWA to sand 1.0 instead of 2.0. On the other hand, considerable reduction in the porosity of LWSCC with decreasing LWA to sand ratio was observed. The amount of reduction reached about 40% for concrete made with LWA to sand of 1.50, compared to the concrete made with 2.0 (Gamal 2007).

The reduction in the porosity may be attributed to the increase in the packing effect, which increased as sand content is increased. Reduction of LWA to sand ratio can cause the voids to be filled with fine sand grains, hence decreases the amount of pores in concrete. The amount of pores also decreased with the decrease of amount of LWA in ordinary Portland cement matrix, thus reducing the porosity and increasing density (Gamal 2007).

2.4.3.2 Effect of w/c

Hwang and Hung (2005) and Gamal (2007) studied the effects of w/c on both fresh and hardened properties of LWSCC. According to Gamal, the air content in LWSCC was remarkably reduced when w/c was decreased from 0.35 to 0.30 (while maintaining the same air dosage) and the amount of reduction reached about 60%. On the other hand, the slump flow was slightly affected (10 mm reduction) by changing the w/c of LWSCC mix.

The study concluded that the w/c had significant roles in enhancing the 28-day compressive strength and pore structure of LWSCC. The compressive strength increased with the decrease of w/c and the porosity decreased with the decrease of w/c. The enhancements in compressive strength and porosity reached about 75% and 60%, respectively, as a result of lowering the w/c ratio from 0.35 to 0.25. Both homogeneity and unit weight of LWSCC were slightly increased with the decrease of w/c (increase of 150 m/s and 115 kg/m^3, respectively). These effects may be attributed to the significant effect of w/c on altering the porosity of LWSCC, thus leading to various alterations in concrete properties.

Hwang and Hung (2005) studied the performance of LWSCCs mixtures under different water-to-binder ratio with different cement paste content using a coated reservoir fine sediment aggregate (750 kg/m^3 of dry loose density). The 91-day compressive strength was 42.5 MPa when cement content was 375 kg/m^3 (w/c = 0.40) using ASTM type I cement and ASTM C618 Class F fly ash. With w/c ratio of 0.32 and cement content of 468 kg/m^3, the 91-day compressive strength was about 50 MPa. It was concluded that LWSCC could achieve high strength, flow-ability and excellent durability.

2.4.3.3 Effect of partial replacement of LWA with normal weight aggregate

As an attempt for improving the hardened characteristics of LWSCC, especially compressive strength, the impacts of partial replacement of lightweight aggregate (LWA) with normal weight aggregate (NWA) on compressive strength, ultra-sonic pulse velocity (UPV) and porosity were studied by Gamal (2007). The research reported that both compressive strength and UPV substantially increased with the increase of the portion of NWA in LWSCC. The increase in compressive strength reached about 15, 30, 50 and 90%, when 35, 50, 60 and 100% NWA were used as a partial replacement of LWA.

This increase in strength was accompanied by a significant increase in the density of concrete, i.e. to enhance the mechanical properties of LWSCC using this approach, an increase in the density of concrete has to be regarded and accepted. The density increased dramatically with increasing the percentage of replacement of LWA with NWA and reached about 2230 kg/m^3 when LWA was fully replaced with NWA. However, the maximum content of LWA to be partially replaced by NWA in LWAC mixes should not exceed one-half of LWA content, to fulfill density criteria for manufacturing structural LWC, as stated by ACI 211.2 (ACI 211 1998).

Gamal (2007) also reported that the partial replacement of LWA with NWA resulted in improvement in the porosity of LWSCC. The porosity of SCC made with 100% LWA is approximately twice that made with 100% NWA. This reduction in the porosity agreed with the resulted improvements in compressive strength and UPV and can be attributed to the decrease of the amount of pores.

Lachemi et al. (2009) investigated LWSCC mixes with normal and lightweight furnace slag sand. It was noted that mixes with normal weight sand, exhibited higher flowability, passing ability and stability/resistance to segregation with lower viscosity than mixes made with lightweight furnace slag sand. The compressive strength and bond strength of the examined lightweight sand mixes were lower compared to mixes made with normal weight sand.

2.4.4 Durability and Long Term Performance of Self-Consolidating Lightweight Concrete

2.4.4.1 Review of previous work

Chia and Zhang (2002) studied the water permeability and chloride penetrability of lightweight concrete (LWC) using expanded clay. The water permeability of the LWC was lower than that of the corresponding normal concrete (NC) but the resistance of the LWC to chloride penetration was similar or higher to that of the corresponding NC. They concluded that for a given 28 -day strength, the LWC would have higher resistance to water penetration and equivalent chloride-ion penetration resistance to NC mixes.

Hwang and Hung (2005) conducted in-depth research to compare the performance of lightweight concrete under different water-to-cementitious material ratio (w/cm) and different cement paste content. The slump flow spread of fresh LWSCC was designed to be within 550–650 mm. The test results indicated that using adequate cement paste with a proper packing density of aggregate yielded dense LWSCC mixture with high strength and the low chloride ion penetrability.

A reduction in cement paste and in water content can reduce large drying shrinkage, while cement paste with SCMs can minimize sulfate attack and alkali-aggregate reaction, as well as reduce the heat of hydration. The w/c must be greater than 0.42 to prevent autogenous shrinkage of cement paste (Mindess and Young 1981). Physical dense packing is needed for volume stability while coarse LWA, normal sand and pozzolanic materials are densely packed to reduce the amount of cement paste required.

2.4.4.2 Durability enhancement

For low concrete permeability, pozzolanic material is used to fill voids in blended aggregates, and strengthen interface between aggregates and cement paste through pozzolanic reaction.

Her-Yung (2009) reported the use of pozzolanic material to decrease the quantity of pores and reduce the mixing water volume, thus enabling durability enhancement and erosion prevention of LWSCC. Dredged silt, fly ash, slag and superplasticizer were used in the study. Three different water to binder) ratios (0.28, 0.32 and 0.40) were used to manufacture the LWSCC. It was concluded that fresh LWSCC can meet the requirements of high flowability. Moreover, with different water to binder ratios, LWSCC can reach 70% or more of its compressive strength at 7-day. Given the same density and mixing water volume, LWSCC with a lower water-to-binder ratio has higher compressive strength. Owing to the limitations of aggregate strength, LWSCC had splitting tensile strength of 1.2-1.9 MPa and increased to 1.5-2.2 MPa at 91-day. For fixed water content and different water to binder ratios, it was found that the lower the water to binder ratio, the better the ultrasonic pulse velocity, electrical resistivity and anti-erosion ability of LWSCC mixtures. LWSCC with lower water to binder ratios showed lower chloride penetration and less weight loss.

2.4.5 Previous studies related to LWSCC

In this section a comprehensive review of published scientific work on the design, properties and applications of LWSCC is provided.

Yanai et al. (1999) first studied the influence of the type and proportions of lightweight aggregates - LWA (namely, artificial perlite of various densities and coal ash), and of the water-to powder volume ratio on the fresh properties such as workability, passing ability, and mix stability, strength characteristics and resistance to freeze-thaw cycles of LWSCC. The results of the study showed that LWSCC could be developed with excellent flowability, passing ability, and segregation resistance by adjusting the unit quantity of LWA and water-to-powder volume ratio according to the properties of LWA. It was observed that the use of high density LWA's resulted in the increase of both the mixtures flowability and filling abilities and their compressive

strengths. This was attributed to the minimization of the density difference between aggregates and paste.

Mechtcherine et al. (2001) experimented with aggregate structures compromising coarse expanded slate or expanded clay and normal weight (river) or lightweight (expanded clay or blast furnace slag) sand. They based the development of LWSCC mixtures on the investigation of the effect of varying water-to-paste volume ratios on the rheological characteristics (yield strength and viscosity) of both the paste (cementitious materials + sand powder + water + HRWRA) and the mortar (paste + sand + viscosity modifying agent (VMA)) phases. The effect of different paste contents in mortars was also investigated. This procedure led to the production of five mixtures with densities ranging from 1440 kg/m^3 to 1880 kg/m^3, while using pre-wetted aggregates as a counter-acting measure for mixing water absorption by their porous structure. Despite the fact that the development mixtures provided slump flow measures that corresponded to the usual values for normal weight SCC, values for spreading time T_{500} and V-funnel flow time were too high to qualify the developed mixture as SCC (these values increased with decrease in density). Finally, the brittle fracture behaviour of LWSCC was mitigated by the addition of steel fibers (0.5% by cement volume).

A critical fresh-state property which can be advantageous for LWASCC is its pumpability, although it has received rather limited research attention. In an investigation by ***Haist et al. (2003),*** the authors assert that the high fines/mortar content makes LWSCC an ideal material for pumping provided the major problem of water absorption by the LWAs under pressure (higher than the atmospheric) is treated through careful composition of the slurry (suspension of fine particles in water). In particular, the content and distribution of fines with a diameter comparable to the magnitude of the lightweight aggregates surface pores is considered crucial in the pumping absorption procedure. To assess the performance of LWASCC mixtures during pumping three mixtures were produced: a SCC, a LWSCC comprising normal weight sand, and an all LWASCC (fine and coarse lightweight aggregates).

By evaluating the workability properties (through slump-flow and V-funnel tests) of all mixtures after passing through a closed pumping system several times, the all-LWASCC exhibited the

highest workability retention characteristics, whereas the LWSCC mixture with normal weight sand exhibited the lowest. This performance was mainly attributed to the open porous structure of the lightweight sand and, consequently, to its ability to exchange slurry content depending on pressure conditions, keeping the mixture fluid and segregation resistive.

A comprehensive work on LWSCC is reported by ***Müller and Haist (2004)***. This work (in which the term used is SCLC, i.e. Self-Consolidating Lightweight Concrete, in place of LWSCC) summarized the findings of an extensive experimental study aimed at the development of SCLC and its technical approval by the German Institute of Construction Engineering in Berlin (DIBt), for implementation in the building code. A wide range of SCLCs was developed with fresh material densities ranging from 1500 kg/m^3 to 2000 kg/m^3. Apart from the use of artificial lightweight coarse aggregate (expanded clay), the adjustment of the mixtures fresh density was achieved by substitution of the normal weight sand by either lightweight expanded clay or bottom ash sand.

The authors highlighted the importance of a careful regulation of both the powder and the mortar matrix's rheological properties in the development of a high quality SCLC, underlining the fact that the minimization of density difference between the powder paste matrix and the lightweight aggregates alone cannot ensure sufficient mixture stability and resistance to segregation. Under this light, the compositions of powder and mortar should be the result of a process that aims to optimize their rheological performance so that the yield stress and the plastic viscosity values are on one hand, low enough to ensure high flowing and passing properties, but on the other hand, high enough to prevent blocking of the lightweight aggregates.

Shi and Wu (2005) investigated the effect of coal fly ash and glass powder addition on the rheological, mechanical and durability features of LWASCC containing a binary aggregate mixture consisting of expanded shale coarse aggregate and natural siliceous sand. The LWSCC was designed based on: (i) the least voids volume for the binary aggregate mixture, (ii) excessive paste theory, and (iii) ACI standard practice for selecting proportions for structural (air-entrained) lightweight concrete. The optimum coarse-to-fine aggregate ratio was found equal to

50/50 while the produced mixtures were based on a 60/40 ratio in order to achieve minimum density. All designed mixtures exhibited satisfactory properties.

Hwang and Hung (2005) evaluated the performance of LWSCC mixtures containing sintered bottom ash, for varying w/c and cement paste content. The slump and the slump-flow for the fresh LWSCC were designed to be 230 - 270 mm and 550 - 650 mm respectively. Experimental results showed that LWSCC compressive strength at 91 -day reached values as high as 56 MPa with cement and water content of 386 kg/m^3 and 150 kg/m^3, respectively. Thirteen mixes were designed with the densified mixture design algorithm method (DMDA). The main goal of this method is to obtain high strength along with a high flowing concrete. The approach taken during this investigation was to use fly ash to fill voids of aggregate instead of replacing part of the cement as in traditional mix design methods. Thus, fly ash will physically fill the voids, densify the mixture of aggregate and act chemically as a pozzolanic material to strengthen the microstructure.

In a work conducted by ***Hela and Hubertova (2005),*** it was highlighted that in the case of truck-mixed LWSCC it is necessary to further increase the quantity of additional water (accounting for the quantity of water absorbed by the LWAs during mixing) also by the amount of water which is soaked into the LWAs during transport and placing, taking into consideration the absorption under high pressure. The authors also suggest the addition of stabilizer to avoid segregation.

Choi et al. (2006) gave special consideration to the investigation of the influence of replacing either the coarse or the fine fraction of normal weight aggregates (NWA) with artificial lightweight ones (being of rhyolitic/lava/Magma origin) on the mechanical and rheological properties of the concrete. Slump flow and T_{500} values of all mixtures were found to be within the commonly accepted limits for SCC, whereas V-funnel and U-box values were unsatisfactory (in regard to the JSCE second class rating standards), especially for the mixtures in which the fine NWA were partially or fully replaced by lightweight sand. This supports the argument made by Yanai et al. (1999) in relation to the density difference between aggregates and paste, which in the previously described mixtures was increased.

Choi et al. (2006) focused on the evaluation of high strength LWSCC (HLWSCC). Fresh properties and fluidity of the mix were analyzed as well as mechanical properties of the paste in its hardened state. Fluidity was studied according to the second class rating of JSCE and divided in three categories: flowability, segregation resistance ability and filling capacity of fresh concrete. Mechanical properties monitored during the research included compressive strength with elapsed age, splitting tensile strength, elastic modulus and density, all after 28 -day. HLWSCC at its fresh state was rated with less than 50% lightweight fine aggregate (LWF) and 75% lightweight coarse aggregate (LWC), hence satisfying the second class standard of JSCE. Compressive strength at 28 -day resulted in values over 40 MPa for all mixes with the exception of lightweight coarse aggregate (LWC) 100%. Also, structural efficiency (compressive strength vs. density) showed a proportional increment when the mixing ratio of lightweight fine aggregate (LWF) increased.

Lo et al. (2007) presented a comparison between workability and mechanical properties of SCC and LWSCC. A self-consolidating lightweight mix with 500 - 600 kg/m^3 binder content and a density of 1650 kg/m^3 was produced using less superplasticizer and viscosity agent along with a lower water/binder ratio than for normal SCC. Bulk density was reduced to 75% of SCC to obtain a similar compressive capacity. Also, the elastic modulus for the LWSCC mix was around 85% of normal SCC. Results indicated that LWSCC was excellent in workability, can attain high compressive strength with relatively small reductions in the elastic modulus while offering the advantages of a material with a lower density. Workability and mechanical properties of both concretes were evaluated using results from slump flow tests, L-box tests, compressive strength, modulus of elasticity and concrete density.

It was concluded that, LWSCC with similar slump flow to that of normal SCC can be produced using less super-plasticizer and viscosity modifying agent along with a lower water/binder ratio to obtain a similar flowability to that of normal SCC with a binder content of 500 - 650 kg/m^3. LWSCC compressive strengths were within the 40 - 58 MPa range, which are similar to the compressive capacity of a SCC concrete with 2200 kg/m^3 density. LWSCC can attain a higher compressive strength than normal SCC at the same water/binder ratio with a 25% reduction in density. The elastic modulus of LWSCC and SCC increased with the increase of binder content.

The elastic modulus of SCC were in values in the 29.5 - 31.5 GPa range and within 22.7 - 27.2 GPa which corresponds to a reduction of 15% for LWSCC.

Hubertova and Hela (2007) studied the development of LWSCC with expanded clay aggregates focusing on the effects of adding metakaolin and silica fume on the properties of this type of concrete. Initially, it was concluded that the use of pre-wetted lightweight aggregates resulted in concretes with better workability, higher workability retention and higher compressive strengths and resistance to freeze-thaw cycles, compared to mixtures comprising dry aggregates. Taking into account the fresh-state test results received at 60 min and 90 min after mixing, the authors suggested the limits for T_{500} and Orimet tests to be revised to 5-10 sec (from 2-5 sec) and to 4-10 sec (from l-5 sec), respectively.

The main reason for this suggested revision is the critical difference in kinetic energy (related to the concrete density) between SCC and LWSCC. The addition of silica fume or metakaolin (10% by cement weight) was found to improve the 28-day compressive strength by 30% and 15%, respectively; the freeze-thaw resistance of the silica fume or metakaolin modified mixtures was also improved.

Uygunoglu and Topcu (2009) investigated the effect of the aggregate type on the coefficient of thermal expansion by comparing SCC and LWSCC mixtures made with pumice. In general, the LWSCC was more durable, and had higher coefficient of thermal expansion. ***Papanicolaou and Kaffetzakis (2009)*** presented the development of all-LWSCC mixtures using pumice focusing on the effect of coarse-to-fine aggregate ratio on the material's rheological and mechanical properties. In an extensive work ***Topcu and Uygunoglu (2007)*** studied the effect of different natural LWA types (pumice, volcanic tuff and diatomite) on the mechanical and physical properties of LWASCC. The use of diatomite produced the highest slump-flow results. On the other hand, pumice LWSCC mixtures exhibited the highest compressive strength. This is due to the excellent interaction between these aggregates and the cement paste, as evidenced through microscopy of the interfacial transition zone.

Her-Yung (2009) developed LWSCC using recycled LWAs made of dried dredged silt of different densities (800 kg/m^3 or 1100 kg/m^3). Low flowability test results were provided for all

produced mixtures (510 mm - 580 mm). Special consideration was given to the investigation of the durability characteristics of this type of concrete. These were assessed through ultrasonic pulse velocity, electrical resistivity, rapid chloride penetration and anti-corrosion tests.

Wu et al. (2009) investigated workability of LWSCC and its mix proportion design using expanded shale aggregates. Two mix proportions for LWSCC according to the water absorption of lightweight aggregate (LWA) were designed. Both mixes had fixed fine and coarse aggregate contents using the volumetric method. Slump flow test, V-funnel, Lbox, U-box, wet sieve segregation, and surface settlement tests were applied to evaluate workability of the concrete in its fresh condition. Column segregation tests and cross section images were used to assess the uniformity distribution of LWAs throughout the specimens. Experimental results indicated that both types of fresh LWSCCs had adequate fluidity, deformability, filling ability, uniform aggregate distribution and minimum resistance to segregation. This study demonstrated that water absorption of the LWA can be used effectively along with fixed aggregate contents in volumetric method to design mix proportions for LWSCC mixture. Increasing the paste content of the mix will increase the shear flow velocity but it will reduce resistance to segregation.

Lachemi et al. (2009) studied the bond behavior of reinforcing steel bars embedded in LWSCC. Three different classes of LWSCC mixtures were developed with two different types of lightweight aggregates. In addition, one normal weight SCC was developed and used as a control mixture. A total of twenty four pullout tests were conducted on deformed reinforcing bars with an embedded length of either 100 or 200 mm and the load-slip responses, failure modes and bond strengths of LWSCC and SCC were compared. Based on the results of this study, the bond strength of deformed bars for LWSCCs was found to be less (between 16 and 38%) as compared to SCC. Under the conditions of equivalent workability properties and compressive strength, bond slip properties were shown to be significantly influenced by the type of lightweight aggregate used.

It was suggested that the load-slip relationships of deformed bars embedded in both normal and lightweight SCC specimens exhibited similar pre- and post- peak responses. The expected failure of lightweight SCC mixtures in bond test was due to splitting. The use of two different types of

lightweight aggregates (slag and expanded shale) in the development of LWSCC with the same compressive strength showed that bond slip properties are significantly influenced by the type of the lightweight aggregate used. The use of expanded shale aggregate as a coarse aggregate showed significantly better performance than using slag aggregate. The average ultimate bond strength increased with increasing embedment length.

Kim et al. (2010) studied the characteristics of self-consolidating concrete using two types of lightweight coarse aggregates with different densities, mostly semi-lightweight (2000 kg/m^3 - 2300 kg/m^3). Nine mixes were evaluated in terms of flowability, segregation resistance and filling capacity of fresh concrete. The mechanical properties of hardened LWSCC, such as compressive strength, splitting tensile strength, elastic modulus and density were assessed.

The experimental results indicated that flowability improved with decreasing density of the lightweight coarse aggregate, while the segregation resistance decreased. The difference in aggregate density did not affect the fillingability of LWSCC mixture. The 28-day compressive strength of LWSCC with 75% of lightweight coarse aggregate was 10% lower than a SCC control mix. For LWSCC mix with 100% lightweight coarse aggregate replacement (with aggregate density of 2070 kg/m^3), the compressive strength was 20% lower than SCC control mix, and 31% lower with an aggregate density of 1580 kg/m^3.

The relationship between the compressive strength and the splitting tensile strength was found to be similar to the expression presented by CEB-FIP model code (1993) for conventional concrete, and the relationship between the compressive strength and the elastic moduli was found to be similar to the expression suggested by ACI 318-11 which takes into consideration the density of concrete. The density of the lightweight aggregate SCC decreased by up to 14% compared to the control SCC, and the specific strength decreased by 20%.

Recently ***Karahan et al. (2012)*** studied the influence of silica fume and metakaolin on mechanical and durability properties of LWSCC. The addition of silica fume or metakaolin was found to improve the strength and the freeze-thaw resistance of LWSCC mixtures.

The following conclusions are inferred from the aforementioned studies:

1. The use of lightweight aggregates in SCC increases the workability, flowability, filling ability and passing ability of the mixture, while increasing the risk of segregation and instability of the mixture.
2. The brittle fracture behaviour of LWSCC can be mitigated by the addition of steel fibers (0.5% by cement volume).
3. Partial or full replacement of normal-weight sand by lightweight sand in LWSCC mixtures resulted in high viscosity and the mixtures failed to qualify as LWSCC.
4. Finding a balance between paste and lightweight aggregates volume is critical to designing robust LWSCC mixture. The yield stress and the plastic viscosity should be low enough to ensure acceptable flowability and passing ability, while preventing blocking or segregation of the lightweight aggregates.
5. LWSCC can achieve high strength, flowability and durability using the densified mixture design algorithm method (DMDA). Due to physical packing of aggregate, reducing the water content as well as the cement content will result in better electrical resistance and lower permeability of LWSCC.
6. When using LWSCC, the concrete density can be reduced by 63 to 83% while maintaining similar strength capacity. However, the elastic modulus for the LWSCC mix is approximately 70 to 85% of normal SCC, while the bond strength is expected to be 15 to 35% less than similar SCC mixture.
7. The addition of silica fume or metakaolin is expected to improve the 28-day compressive strength and the freeze-thaw resistance of LWSCC mixtures.
8. Higher coefficient of thermal expansion is expected for LWSCC mixtures over SCC.
9. LWASCC mixtures (with both fine and coarse aggregates) can exhibit high workability retention and ease of pumpability when the aggregates are pre-wetted.

Despite the listed findings, the following deficiencies were recorded in the LWSCC literature review:

1. The majority of the previous works focused on the study of structural lightweight SCC mixes containing normal weight sand and lightweight coarse aggregates. This type of SCC has a dry density that generally ranges between 1800 kg/m^3 and 2000 kg/m^3, whereas the respective range of all lightweight aggregate SCC goes from 1400 kg/m^3 to 1700 kg/m^3. This range of true lightweight SCC needs further investigation.
2. The influence of key mix design parameters such as (w/b, total binder, and HRWRA) on the fresh and hardened properties of LWSCC was not investigated for different types of lightweight aggregates.
3. No systemic optimization process was established for LWSCC mix design. The current literature lacks guidelines for designing wide range of LWSCC using different types of lightweight aggregates. Further, no statistical model was established for LWSCC where workability, passing ability, mix stability, resistance to segregation, fresh/ dry unit weights, compressive strength were taken in account.
4. Most of the reported studies used only one type of lightweight aggregates for mix performance evaluation. Comparison of fresh, hardened and durability performance of lightweight SCC mixture made with different types of aggregates was not studied.
5. The development of LWSCC mixtures with wide range of workability suitable for different industrial classes/applications was not investigated. The slump flow values ranged mostly between 600 mm and 700 mm.
6. The previous works lack in-depth comparative analysis of mechanical, mass transport and durability performance of LWSCC, such as flexural strength, spilt tensile strength, porosity and water absorption, sorptivity, rapid chloride permeability, drying shrinkage, in-depth corrosion resistance, elevated temperature resistance, salt scaling resistance, sulphuric acid attack resistance and freeze and thaw resistance for all lightweight aggregate SCC mixtures.

Current research is designed to address these issues so that it can contribute significantly to the existing knowledge of LWSCC technology.

CHAPTER THREE

3 EXPERIMENTAL PROGRAM

3.1 Scope of the Experimental Program

This study seeks to assess the feasibility of using a statistical experimental design approach to identify the relative significance of primary mixture parameters and their coupled effects on relevant properties of lightweight self-consolidating concrete (LWSCC), including the mechanical and durability aspects. Expanded furnace slag (FS), expanded clay (EC), and expanded shale (ESH) were used as both coarse and fine lightweight aggregates in this research to develop and evaluate LWSCC mixtures.

The detailed experimental program was divided into five phases (Figure. 3.1) and described in various chapters of the thesis for clarity of presentation. “Phase I: experimental design of LWSCC mixtures” (subject matter of Chapter 3) includes determination of material characteristics, description of a parametric criteria affecting fresh and hardened properties, mixture proportioning, and presentation of the fractional factorial design approach.

Phase II (subject matter of Chapter 4) presents the test results on fresh and hardened properties of 60 laboratory trials LWSCC mixtures derived from three factorial design models incorporating expanded furnace slag, expanded clay, and expanded shale aggregates.

In Phase III (Chapter 6), three types of LWSCC mixtures were statistically optimized to satisfy three classes of EFNARC industrial classifications and their performances were validated through the assessment of fresh and hardened properties (EFNARC 2005). Further, the chapter presents the results of additional experimental study, where ten LWSCC mixtures from each derived model in Phase I were randomly chosen and their performances were validated through the assessment of fresh and hardened properties. Phase IV (Chapter 7) and Phase V (Chapter 8) describe the mechanical and durability properties, respectively, of the optimized industrial class LWSCC mixtures with three lightweight aggregates types.

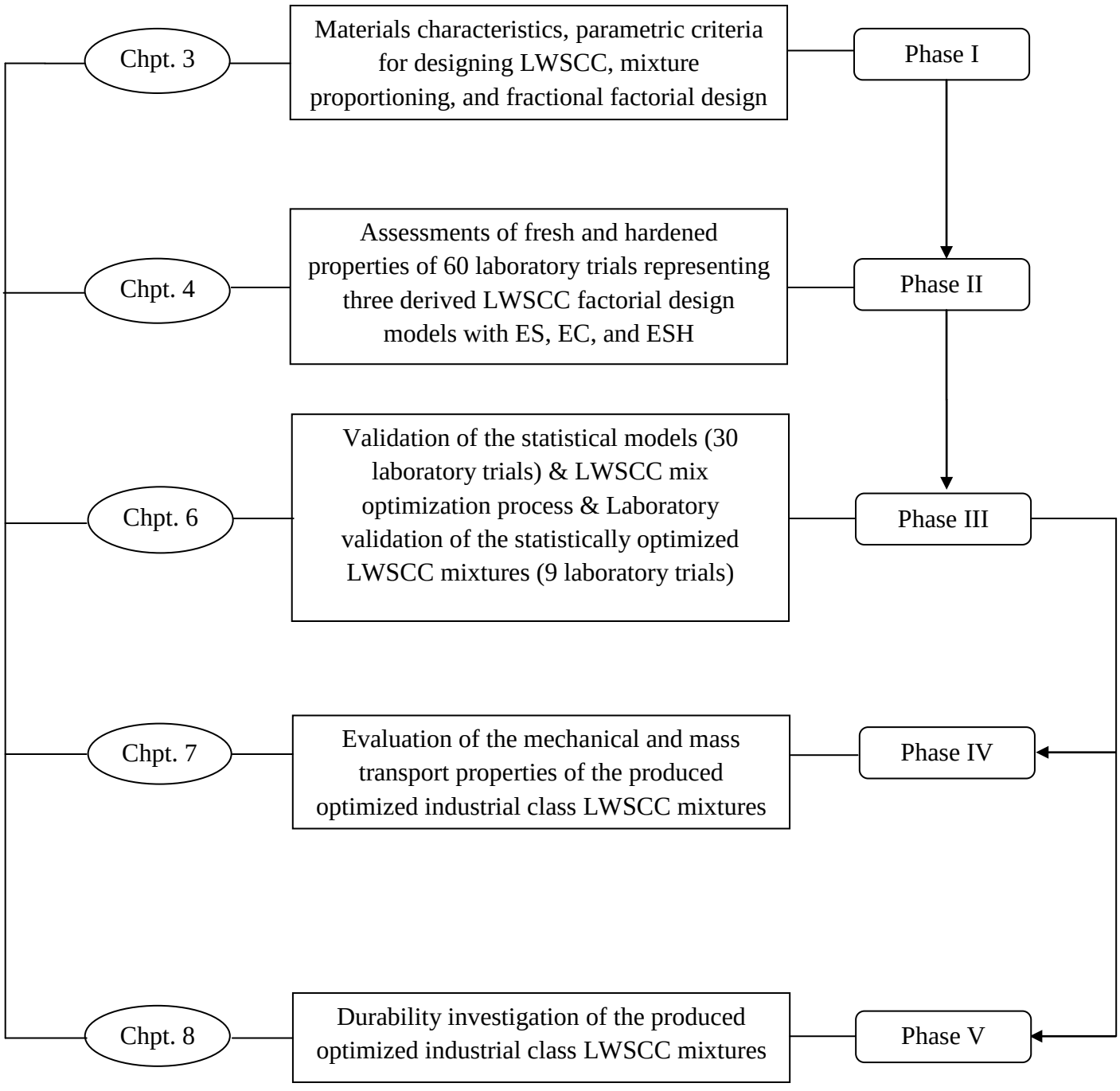

Figure 3.1 - Various phases of experimental program

3.2 Materials Properties

3.2.1 Properties of Cement, Mineral and Supplementary Cementing Materials (SCM)

The cement used was Type GU, hydraulic cement for general construction use. Fly ash (FA) is the most widely used supplementary cementing material (SCM) in concrete. In this research, Class F fly ash according to CSA classification with a calcium oxide (CaO) content of less than 8%, a typical bulk density value of 540 ~ 860 kg/m^3 and a specific gravity of 2.6 was used,

Fly ash has been reported to improve the mechanical properties and durability of SCC when used as a cement replacement material (Patel et al. 2004; Malhotra 2004). Fly ash is expected to be useful in generating the flow and for segregation resistance. Usually concrete containing FA is sufficiently air entrained for freezing and thawing; as the amount of FA increases, more air entraining is required. This can be attributed to the typical problem where high surface area of carbon absorbs air-entraining agent from the concrete mixture. It is difficult to determine the adequate amount of air-entraining admixture. This problem is also associated with lightweight aggregate (LWA) with high absorption rate. Therefore, air entraining was omitted in the development of SCC with LWA. Moreover, use of FA was limited to 15% because a higher value impairs scaling resistance of concrete. This research had also considered the fact "FA addition improves transition zone" by reducing the degree of orientation of calcium hydroxide crystals in the matrix.

For this study, a dry-densified silica fume (SF) powder was used to develop a sticky but flowable mixture with enhanced segregation resistance (Yeginobali et al. 1998). SF was used to increase concrete compressive and flexural strengths, increase durability, reduce permeability and improve hydraulic abrasion erosion resistance. The silica fume used in this study had a specific gravity of 2.2. Chemical and physical properties of cement, FA and SF are presented in Table 3.1.

The proposed LWSCC mixtures contained no viscosity-modifying admixture (VMA), with fixed 20% SCM replacement (FA+SF) of the total binder (B), 5% of which was silica fume and 15% was fly ash type "F". The use of VMA is associated with reduction in paste volume which is believed to be detrimental to the LWSCC mixture stability, passing ability, filling ability and

segregation resistance. Further, many successful LWSCC mixtures were developed without the use of VMA (Karahan et al 2012; Kim et al. 2010; Lachemi et al. 2009). The use of silica fume enhances the fresh properties of LWSCC as it helps to improve the cohesiveness and homogeneity of the LWSCC mixture; holding the lightweight coarse aggregate in place, and preventing them from floating. Further, fly ash and silica fume enhance the durability characteristics of the mixture (Wang 2009).

Table 3.1 - Chemical and physical properties of cement, fly ash and silica fume

Chemical composition	**Cement**	**Fly Ash**	**Silica Fume**
SiO_2 (%)	19.6	46.7	95.21
Al_2O_3 (%)	4.9	22.8	0.21
Fe_2O_3 (%)	3.1	15.5	0.13
CaO (%)	61.4	5.8	0.23
MgO (%)	3	-	-
SO_3 (%)	3.6	0.5	0.33
Alkalis as Na_2O (%)	0.7	0.7	0.85
LOI (%)	2.3	2.2	1.97
Physical			
Blaine (cm^2/g)	3870	3060	21000
+ 45 µm (%)	3.00	17	2.85
Density (g/cm^3)	3.15	2.48	2.20

Based on the optimum materials packing density, the ratio between the coarse aggregate fraction (CAF) and the fine aggregate fraction (FAF) should be kept constant. For example the optimum CAF/FAF ratio was found to be 0.89 when using local furnace slag. Both fine and coarse furnace slag, expanded clay and expanded shale were used as lightweight aggregates in this research.

A polycarboxylate ether type high range water reducing admixture (HRWRA) meeting ASTM C 494 (2011) Type A and Type F with a specific gravity of 1.05 and total solid content of 26% was used as superplasticizer (SP). The pH level for the SP was 7 ± 2 with a Cl^- ion content of less than 0.1%. According to the manufacturer, the used SP combined the function of workability retention and water reduction. It also provides high medium and long term strength development of concrete.

3.2.2 Aggregates

Three types of aggregates were used to develop the LWSCC mixtures: screened air-cooled blast furnace slag from an Ontario source, expanded clay from Erwinville, Louisiana, US, and expanded shale from Denver, Colorado, USA. These lightweight aggregates had nominal sizes of 4.75 mm and 10 mm and were used as fine and coarse aggregates (Figures 3.2). Table 3.2 presents specifications for coarse and fine lightweight aggregate gradation according to ASTM C330 (2009), as well as the gradations and physical properties of fine and coarse lightweight aggregates of furnace slag (F-Slag), expanded clay (E-Clay) and expanded shale (E-Shale).

Figure 3.3 shows grading curves constructed from the sieve analysis of aggregates. Table 3.3 presents the chemical properties of lightweight furnace slag, expanded clay and expanded shale.

According to Lafarge Canada Inc., the porosity of air-cooled blast furnace slag provides excellent mechanical bond with Portland cement paste resulting in up to 10% higher compressive strength with about 30% lighter concrete than normal gravel aggregate mixes (http://www.lafarge-na.com).

The expanded clay, according to Big River Industries Inc. USA, is “GRAVELITE” clay. GRAVELITE expanded clay lightweight aggregate is a structural grade aggregate for use in ready-mix concrete products, as well as asphalt paving and geotechnical engineering projects. The aggregate is produced by mining clay from deposits found on plant property and calcining the clay at a temperature of 2000 ^{0}C in rotary kilns. The resulting lightweight aggregate is graded to conform to the requirements of ASTM C330 (2009).

The expanded shale, produced by TXI aggregate company, USA, is approximately 550 million years old. Shale is, first, removed by drilling and blasting, and transported by dump vehicles to a roll impact crusher. The shale is expanded in an oil fired rotary kiln where temperature is maintained between 1900 ^{0}C and 1200 ^{0}C. At this temperature, the shale is in a semi-plastic state at which entrapped gases are formed and expansion results creating individual non-connecting air cells. After discharged from the kiln, it is cooled and stored. Due to this process and its

intrinsic nature, their fire resistance is greater than natural aggregates and superior abrasion resistance to natural aggregates.

10mm Coarse furnace slag (CFS)

Fine furnace slag (FFS)

10mm Coarse expanded clay (CEC)

Fine expanded clay (FEC)

10mm Coarse expanded shale (CES)

Fine expanded shale (FES)

Figure 3.2 - Coarse and fine lightweight aggregates used in the study

Table 3.2 - Grading and physical properties of aggregates

Sieve size (mm)	% Passing							
	ASTM C-330 Specification		F-Slag		E-Clay		E-Shale	
	Fine	Coarse	Fine	Coarse	Fine	Coarse	Fine	Coarse
13.20	100	100	100	100	100	100	100	100
9.50	80-100	100	100	90.3	100	83	100	91
4.75	5-40	85-100	100	23.2	87	19	100	18.8
2.36	0-20	-	81.2	10.2	63	2	95	2.5
1.18	0-10	40-80	49	-	40	1	65	1.6
0.60	-	-	26.5	-	18.5	0.7	41	0.6
0.30	-	10-35	15.3	-	10.6	0.2	23.5	0.1
0.15	-	5-25	9.5	-	5.5	0	14.7	0
Bulk specific gravity (Dry)	-	-	2.17	1.61	1.22	1.21	1.40	1.33
Bulk specific gravity (SSD)	-	-	2.20	1.75	1.51	1.41	1.81	1.71
Dry loose bulk density (kg/m^3)	1120 (Max)	880 (Max)	1356	950	760.9	621.5	1070	862
Absorption (%)	-	-	6.0	8.0	17.6	16.2	13	14

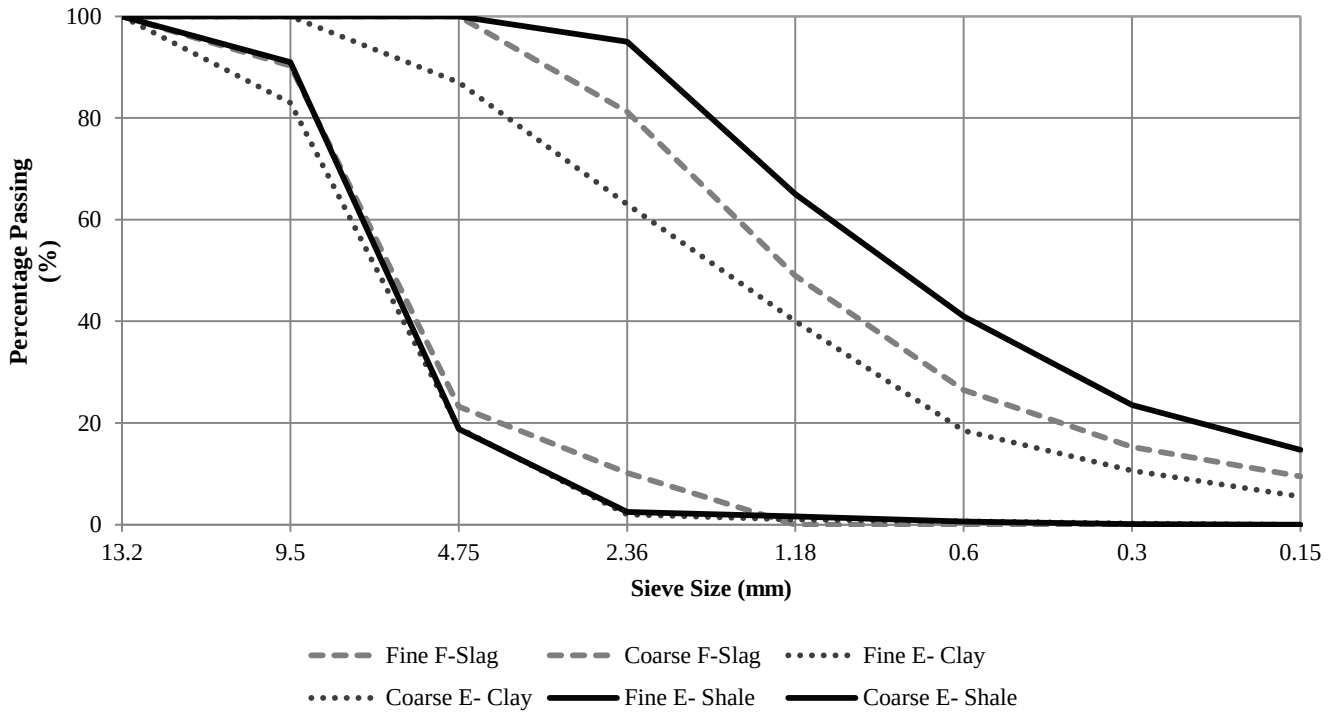

Figure 3.3 - Grading curves for both fine and coarse aggregates

Table 3.3 - Chemical analysis of Furnace Slag, Expanded Clay, Expanded Shale

Chemical Name	Furnace Slag[1]	Expanded Clay [2]	Expanded Shale[3]
	(%)	(%)	(%)
Silica (SiO_2)	37.1	64.6	67.6
Alumina (Al_2O_3)	8.8	20.6	15.1
Iron Oxide (Fe_2O3)	1.9	6.5	4.1
Titanium Oxide (TiO_2)	-	0.8	0.6
Calcium Oxide (CaO)	40.0	1.5	2.2
Magnesium Oxide (MgO)	11.5	2.9	3.5
Alkalies*	0.8	-	3.7
Sulphur Trioxide (SO_3)	-	0.5	0.24
Manganese Oxide (MnO)	0.6	0.1	0.07
Loss on Ignition	1.99	0.3	3.06

1: source: Lafarge Canada Inc. (http://www.lafarge-na.com)
2: source: Big River Industries, Inc. (www.bigriverind.com)
3: source: TXI (www.txiesc.com)
**sodium oxide equivalent*

All the aggregate properties were tested several times to obtain higher confidence level for their accuracy. The saturated surface dry (SSD) bulk densities of fine and coarse aggregates were 2170 kg/m^3 and 1750 kg/m^3, 1510 kg/m^3 and 1410 kg/m^3, 1810 kg/m^3 and 1710 kg/m^3, for furnace slag, expanded clay and expanded shale lightweight aggregates, respectively. The expanded clay aggregates were the lightest with the highest water absorption at 17.6 and 16.2% for fine and coarse particles, respectively.

Due to different porosity and voids in aggregate itself, in this research, SSD density was used to calculate the quantities of aggregates as the lightweight aggregates (LWA) were pre-soaked before use. For the mix design, SSD density was used and water adjustment was made according to the water absorption of aggregates and the moisture content at the time of actual mixing. It is well known that the water adjustment for a concrete with LWA is difficult to control. Grubl (1979) and Muller-Rochholz (1979) recommended adjusting water content by the absorption of LWA in 30 minutes while stored in water. Due to different absorption rate and void ratio of aggregates, the proposed methods for adjusting water content of LWA were difficult to adapt. In this research, numerous trial mixes proved that adjusting water content according to the difference between actual moisture content and water absorption of aggregates was effective and efficient.

3.3 Parametric Criteria

3.3.1 Key Parameters

While design procedures and statistical modelling for self-consolidating normal-weight concrete have been examined (Khayat et al. 1998; Patel et al. 2004; Sonebi et al. 2004), there is a great need for research in the field of lightweight self-consolidating concrete (LWSCC), and particularly in the domain of statistical modelling. In this research a statistical experimental design consisting of two-level fractional factorial design and three variables was used to evaluate the influence of two different levels for each variable on the relevant concrete properties. Three key parameters that have significant influence on mixture characteristics were selected to derive statistical models for evaluating the concrete fresh, hardened and durability characteristics required to ensure successful development of LWSCC. Experimental levels of the variables at

three input factors were used in the test program: X1 (water to binder ratio: w/b), X2 (percentage of HRWRA as a percentage of mass of total binder content), and X3 (total binder content). Based on LWSCC literature review, experience, recommendations of chemical manufacturers, durability considerations and initial laboratory trials, the ranges of the input factors were set and the factors were considered at two levels, as follows:

- X1: Water to binder ratio (w/b): 0.30 to 0.40;
- X2: Percentage of HRWRA: 0.3 to 1.2%
- X3: Total binder content: 410 to 550 kg/m^3

3.3.2 Aggregates Testing - Packing Density

To determine the volume of paste in LWSCC mixtures, the void volume between the aggregate particles of dry fine and coarse aggregates was determined first. The relationship between density of combined aggregates and coarse-to-fine aggregate volume ratio can be established by packing different amounts of coarse and fine aggregates according to ASTM C 29/C 29M (2009). The unit weight and voids in aggregates were determined by measuring the weight of different combination of aggregates in a cylindrical metal measure of a known volume. With the weight of aggregates in the measure, the volume of the measure, and the bulk specific gravity of the aggregate materials, the unit weight of the aggregates (kg/m^3) and percentage of voids can be determined. The unit weight (bulk density) was determined by Equation (3.1)

$$M = (G - T) / V \quad (3.1)$$

where M = bulk density of the aggregate, [kg/m^3], G = mass of the aggregate plus the measure, [kg], T = mass of the measure, [kg], and V = volume of the measure, [m^3].

The bulk density determined by this test method was for aggregate in an oven-dry condition. The void percentage is determined by Equation (3.2).

$$\% \text{ Voids} = 100 [(SW) - M] / (SW) \quad (3.2)$$

where M = bulk density of the aggregate [kg/m^3], S = bulk specific gravity (oven-dry basis) as determined in accordance with Test Method ASTM C 127 or Test Method ASTM C 128, and W = density of water [998 kg/m^3].

Each type of aggregate combination was tested with varying volumes of coarse aggregate to fine aggregate to determine the effects on the percentage of voids and unit weight. Three types of aggregates combinations were used in 60 LWSCC mixtures with three models (A, B and C) - each had 20 mixtures. Furnace Slag LWSCC (FS-LWSCC) mixes “model A” (mixes 1 to 20) used LWCFS and LWFFS and Expanded Clay LWSCC (EC-LWSCC) mixes “model B” (mixes 1 to 20) used LWCEC and LWFEC. Expanded Shale LWSCC (ESH-LWSCC) mixes “model C” (mixes 1 to 20) used LWCESH, and LWFESH.

In this study, the aggregate unit weight for the combination of FS aggregates ranged from 923 kg/m^3 to 1345 kg/m^3. For LWSCC mixes, the choice of aggregate composition in terms of coarse-to-total aggregate volume ratio (V_{ca}/V_a) was based on both the void percentage and the density of the aggregates. The aggregate composition that yields the smallest void percentage will require the addition of the least amount of paste to fill the voids. This is an important step in deriving the most economical mix for the aggregate being used. The aggregate density should also be considered when choosing the aggregate composition. The density of the concrete will depend on the density of the aggregate and the volume of aggregate per volume of concrete used. So, the selection of the aggregate composition should balance the required density of the concrete and void percentage.

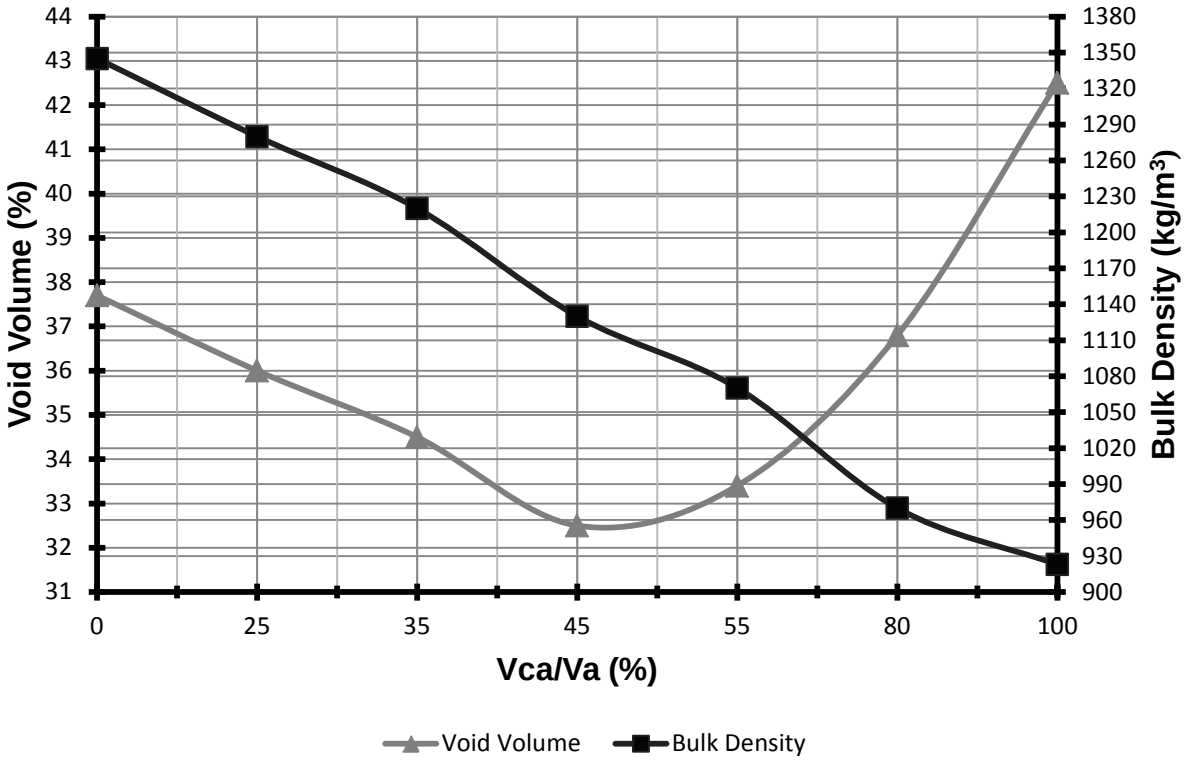

Figure 3.4 - Optimum bulk density and % of void of coarse and fine lightweight furnace slag aggregates

It can be seen from Figure 3.4 that the lowest void volume (%) for the combined coarse and fine aggregates lightweight furnace slag is around 32.4% when the coarse-to-total aggregates volume ratio is 0.47. In the case of LWSCC, one of the main objectives is to develop concrete mixtures with low unit weight. As the coarse-to-total aggregate volume ratio is increased from 0.45 to 0.47, it does not increase the void volume by much (from 32.4 to 32.5%) but it decreases the density of the combined aggregates by 20 kg/m^3 (from 1130 to 1110 kg/m^3). On the other hand, the expanded clay is much coarser compared to the fine fraction of furnace slag which resulted in high void volume when using both coarse and fine expanded clay as aggregates in LWSCC mixture. As illustrated in Figure 3.5, the void volume is increased to 34.5% while the optimum coarse-to-total aggregates volume ratio remained the same at 0.47. This indicates the need for more paste to fill the voids between the aggregates particles.

As for the expanded shale aggregates, the sand fraction is much finer than both expanded clay and furnace slag, which yielded better packing density resulting in lower void volume at 25% while the optimum coarse-to-total aggregates volume ratio reduced to 0.40 as presented in Figure 3.6. This low void volume implies less paste requirement to fill the voids between the aggregate particles, allowing for more excess paste that would give the concrete the required flowability and segregation resistance. Table 3.4 summarizes the optimum aggregate content by volume, weight and void ratio (%), where the lowest void ratio was recoded for ESH aggregates. These test results were affected predominately by the gradation and the particle shape rather than the source of the aggregate.

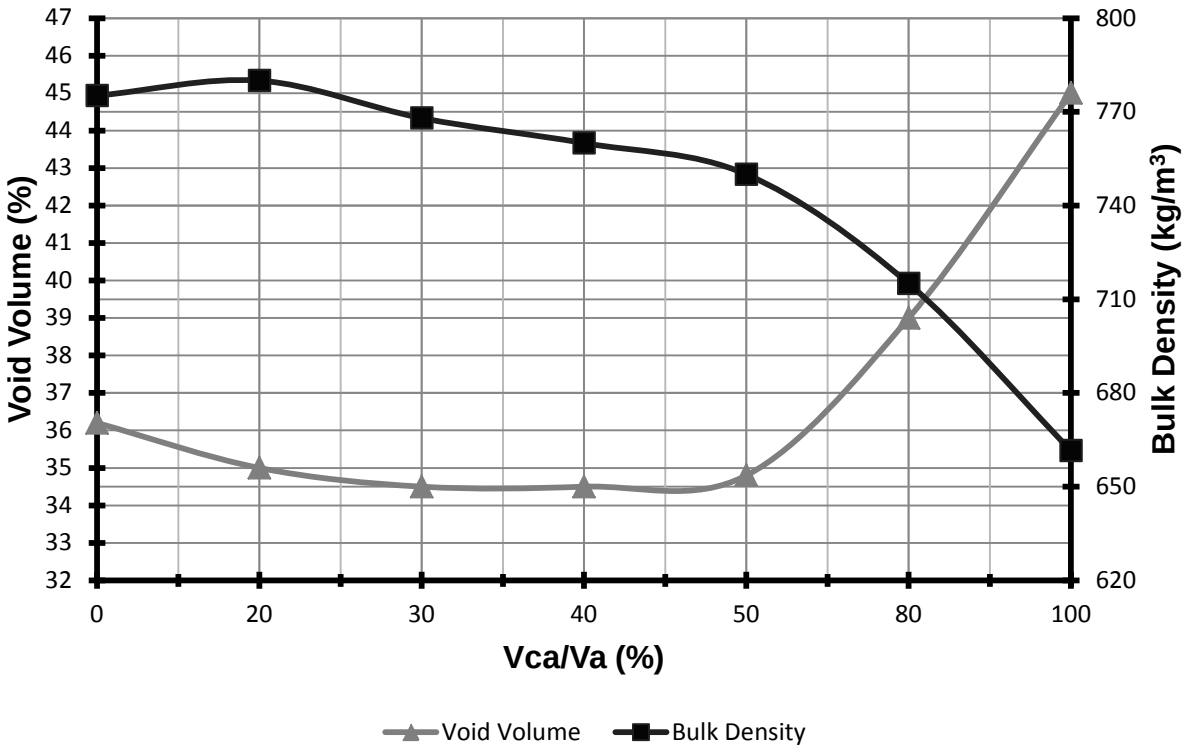

Figure 3.5 - Optimum bulk density and % of void of coarse and fine lightweight expanded clay aggregates

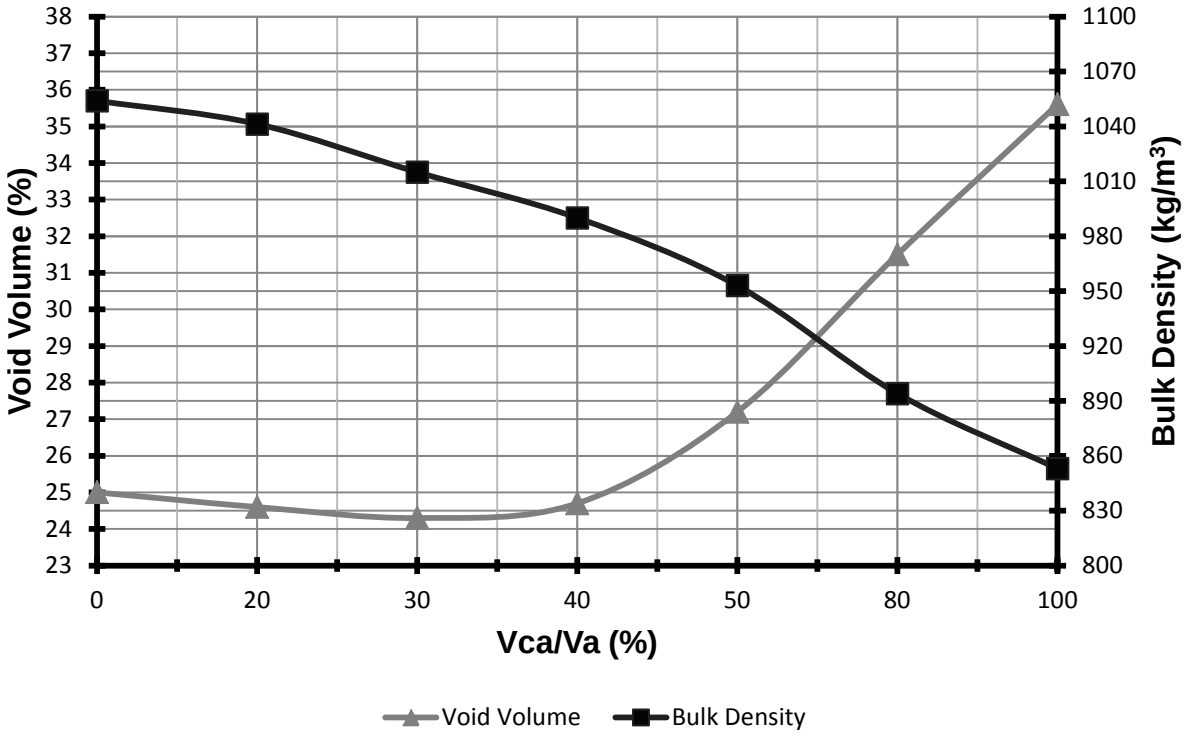

Figure 3.6 - Optimum bulk density and % of void of coarse and fine lightweight expanded shale aggregates

Table 3.4 - Summary of the optimum aggregate content by volume, weight and void ratio

Mix ID	Aggregates content* by volume (%)	Weight (kg/m^3)	Void ratio (%)
Furnace Slag	Coarse F-Slag[1] (47*) Fine F-Slag[2] (53*)	1110	32.5
Expanded Clay	Coarse E-Clay[2] (47*) Fine E-Clay[2] (53*)	648	34.5
Expanded Shale	Coarse E-Shale[3] (40*) Fine E-Shale[3] (60*)	830	25

1: Furnace slag lightweight aggregates
2: Expanded clay lightweight aggregates
3: Expanded shale lightweight aggregates

3.4 Mix Design Methodology and Mixture Proportion

Using three different LWA types (furnace slag, expanded clay and expanded shale) as coarse and fine aggregates, three experimental models (A, B and C) were designed. Each model consisted of twenty concrete mixtures, which were designed using the Box-Wilson central composite design (CCD) method, one of the simplest and widely available modelling design methods (Schmidt and Launsby 1994). The three input factors were X_1 (water to binder ratio: w/b), X_2 (percentage of HRWRA as a percentage of mass of total binder content), and X_3 (total binder content). The ranges of the input factors were set at 0.30 to 0.40 for X_1, 0.3 to 1.2% for X_2, and 410 to 550 kg/m^3 for X_3. The CCD method consists of three portions: the fraction factorial portion, the center portion, and the axial portion. The three portions represent how to vary the independent variables and how many runs are required for the experiment. The factorial portion is fractional factorial of the number of factors, and it is not effective if the response is nonlinear. The central portion is useful to estimate experimental error, and the axial portion allows the estimation of curvature or nonlinear modelling. Presentation of the modelled region is shown is Figure 3.7, while the structure of a central composite design model for three factors are illustrated in Figures 3.8. Limits and coded value of factors are presented in Table 3.5. Table 3.6 presents the statistical analysis factors based on CCD method.

Fraction factorial portion n_f, is where the factors are set at two levels and the number of runs (mixtures) is decided by 2^k, where k is the number of factors. The total number of mixtures for fraction factorial portion is kept at 2^k mixtures with a different combination of coded value varying between +1 and –1.

Center point portion n_c, is where enough center points are needed to get good estimation of pure experimental error and to maintain orthogonality with ‘0’ coded value. As for the axial portion runs, the number of runs are set at 2k.

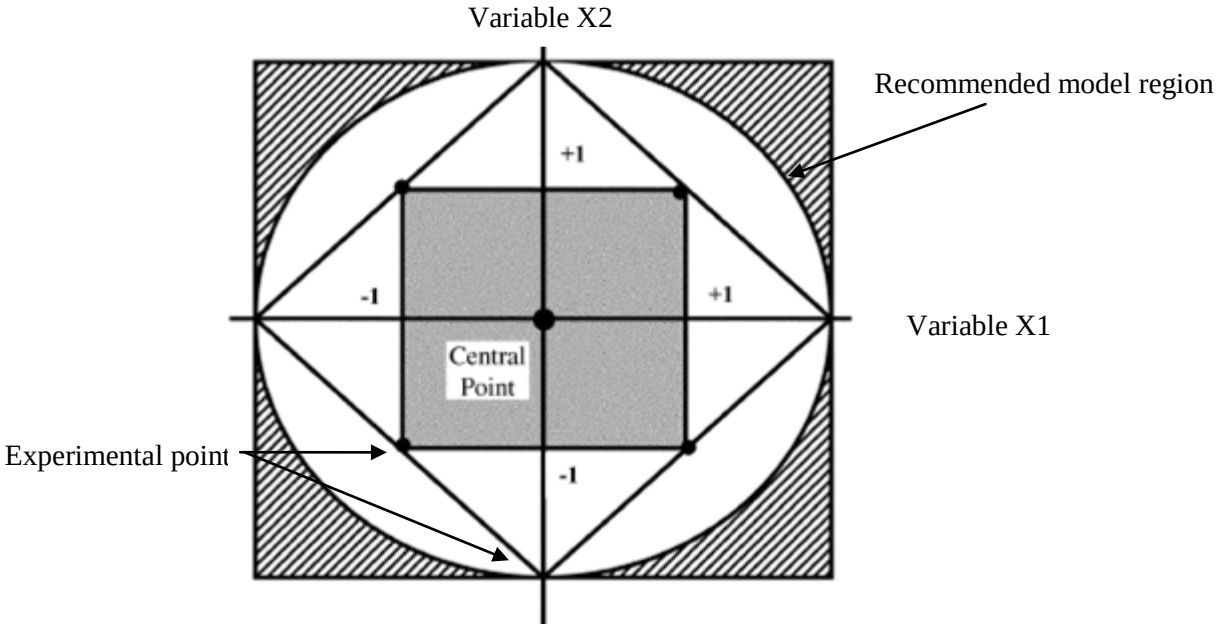

Figure 3.7 - Presentation of modelled region of experimental plan

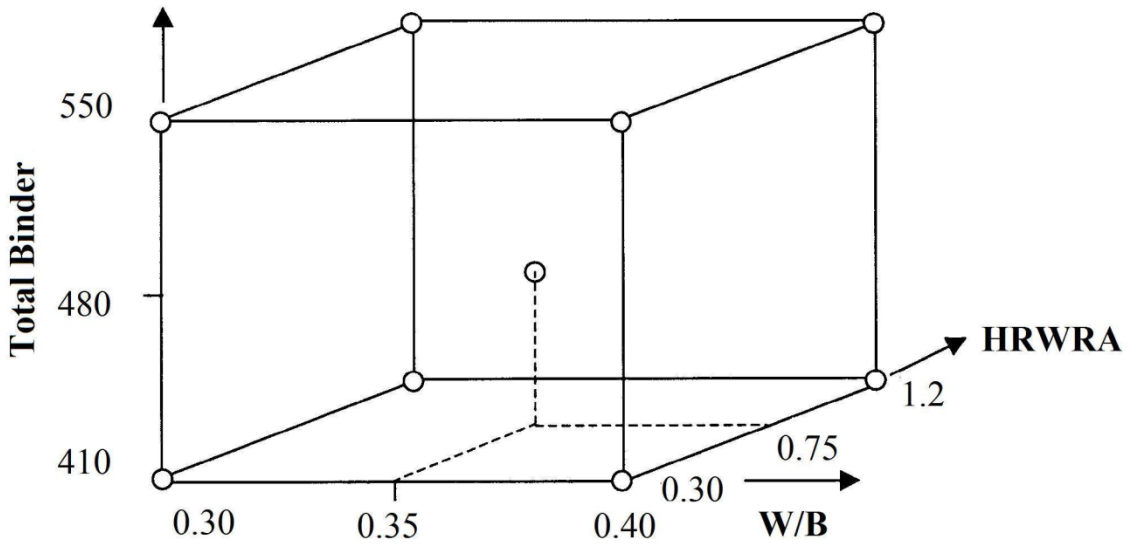

Figure 3.8 - Structure of the three-variable factorial plan of experiment

For this experimental program, the number of trials (N) was based on the number of the design factors (k) as follows:

If k = 3; Trials $N = 2^k + 2k + 6 = 20$

k: Number of factors (3 in this study)

- Fraction factorial portion (n_f): $2^k = 8$ mixtures

- Center point portion (min): $n_c = 4 \times \sqrt{n_f} + 1 - 2k = 6$ mixtures (replicate runs)

- Axial portion: 2k = 6 mixtures

Such a two-level factorial design requires a minimum number of tests for each variable. Given that the expected responses do not vary in linear manner with the selected variable and to enable the quantification of the prediction of the responses, a central composite plan was selected where the response could be modelled. Since the error in predicting the responses increases with the distance from the center of the modelled region, it is advisable to limit the use of the models to an area bound by coded values corresponding to - α to + α limits. The parameters were carefully selected to carry out composite factorial design where the effect of each factor is evaluated at five different levels in codified values of - α, -1, 0, + 1, and + α. The α value is chosen so that the variance of the response predicted by the model would depend only on the distance from the center of the modelled region (Sonebi 2001).

Code Factor Levels were used to transform the scale of measurement for a factor so that the high value becomes +1 and the low value becomes -1. Coding is a simple linear transformation of the original measurement scale. If the "high" value is X_h and the "low" value is X_L (in the original scale), then the scaling transformation takes any original X value and converts it to:

Coded Factor = (Actual value - Factor means) / (Range of the factorial values/2) (3.3)

$= (X - a)/b,$

where X = actual value, a = factor means , b = range of factorial values, $a = (X_h + X_L)/2$ and $b = (X_h - X_L)/2$, X_h = actual upper limit, X_L = actual lower limit.

To retrieve the original measurement scale (X), a coded value is multiplied by "b" and the product is added to “a":

$$X = b\ (\text{coded value}) + a$$

The value coded of portion is $(n_f)^{1/4}$ (3.4)

Using Equations 3.3 and 3.4, the final coded value was set at five different levels -α, -1, 0, 1, and α (–1.414, –1, 0, +1, +1.414; presented in Table 3.6). This way, the total number of runs (mixtures) was established and the sequence of mixes was randomized.

Table 3.5 - Limit and coded value of factors

Factor	**Range**	**Coded Value**				
		-1.414	**-1**	**0**	**+1**	**+1.414**
X_1 = (w/b)	0.30 to 0.40	0.28	0.30	0.35	0.40	0.42
X_2 = (% of HRWRA)	0.03 to 1.2%	0.11	0.30	0.75	1.2	1.39
X_3 = (Binder) kg/m^3	410 to 550	380	410	480	550	580

Table 3.6 - Statistical analysis factors - Central composite design (CCD) method

Mixture	CCD Portion	X1 (w/b)	X2 (% of HRWRA)	X3 (Binder) Kg/m^3
1	**Fractional factorical**	1	1	1
2		1	1	-1
2		1	-1	1
4		1	-1	-1
5		-1	1	1
6		-1	1	-1
7		-1	-1	1
8		-1	-1	-1
9	**Axial**	1.414	0	0
10		-1.414	0	0
11		0	1.414	0
12		0	-1.414	0
13		0	0	1.414
14		0	0	-1.414
15	**Center point**	0	0	0
16		0	0	0
17		0	0	0
18		0	0	0
19		0	0	0
20		0	0	0

Based on the literature and the proven benefits of using SCMs, the proposed LWSCC mixtures contained fixed amount of 20% SCM replacement of the total binder, 5% of which was silica fume and 15% was fly ash type "F". Use of more than 5% silica fume would result in an increase in water demand and HRWRA, and decrease in mixture workability.

Based on the optimum materials packing density test, the ratio (by volume) between the coarse aggregate fractions and the total aggregates was kept constant. For example, when using furnace slag the optimum V_{ca}/V_a (V_{ca}/V_a: volume of coarse aggregate to volume of total aggregates ratio) was found to be 0.47. ACI 211.2 (1998) provides guidelines on relationships between compressive strength and cement content, and relationship between compressive strength and water to cement ratio (w/c). Based on the strength requirement and ACI 211.2 guidelines, in this research, a total binder content of 410 to 550 kg/m^3 and a w/b of 0.30 to 0.40 were chosen as key parameters in LWSCC mix development.

The mix design and statistical evaluation of the test results were performed using Design Expert v.8.1 software18 (Stat-Ease Corporation 2009). Three models were developed, Model A for FS-LWSCC (Furnace Slag LWSCC) mixes FS1-20, model B for EC-LWSCC (Expanded Clay LWSCC) mixes EC1-20, and finally model C for ESH-LWSCC (Expanded Shale LWSCC) mixes ESH1-20. Tables 3.7, 3.8 and 3.9 present the mixture proportions developed by the software for Model A-FS-LWSCC, Model B-EC-LWSCC and Model C-ESH-LWSCC, respectively.

Table 3.7 - Mixture proportions for FS-LWSCC (Furnace Slag LWSCC)

Mix no	X1	X2	X3	Cement	FA	SF	HRWRA	Water	F-Slag aggregate	
	w/b	HRWRA	binder	kg/m^3	kg/m^3	kg/m^3	l/m^3	l/m^3	Coarse	Fine
FS1	0.40	1.2	550	440	82.5	27.5	6.6	220	462	656
FS2	0.40	1.2	410	328	61.5	20.5	4.9	164	550	774
FS3	0.40	0.3	550	440	82.5	27.5	1.6	220	467	659
FS4	0.40	0.3	410	328	61.5	20.5	1.2	164	553	780
FS5	0.30	1.2	550	440	82.5	27.5	6.6	165	509	717
FS6	0.30	1.2	410	328	61.5	20.5	4.9	123	586	824
FS7	0.30	0.3	550	440	82.5	27.5	1.6	165	515	724
FS8	0.30	0.3	410	328	61.5	20.5	1.2	123	585	830
FS9	0.42	0.75	480	384	72	24	3.6	201	500	705
FS10	0.28	0.75	480	384	72	24	3.6	134	557	786
FS11	0.35	1.39	480	384	72	24	6.7	168	527	743
FS12	0.35	0.11	480	384	72	24	0.5	168	530	750
FS13	0.35	0.75	580	464	87	29	4.3	203	470	665
FS14	0.35	0.75	380	304	57	19	2.9	133	585	825
FS15	0.35	0.75	480	384	72	24	3.6	168	528	747
FS16	0.35	0.75	480	384	72	24	3.6	168	528	747
FS17	0.35	0.75	480	384	72	24	3.6	168	528	747
FS18	0.35	0.75	480	384	72	24	3.6	168	528	747
FS19	0.35	0.75	480	384	72	24	3.6	168	528	747
FS20	0.35	0.75	480	384	72	24	3.6	168	528	747

Table 3.8 - Mixture proportions for EC-LWSCC (Expanded Clay LWSCC)

Mix no	X1	X2	X3	Cement	FA	SF	HRWRA	Water	E-Clay aggregate	
	w/b	HRWRA	binder	kg/m^3	kg/m^3	kg/m^3	l/m^3	l/m^3	Coarse	Fine
EC1	0.40	1.2	550	440	82.5	27.5	6.6	220	375	450
EC2	0.40	1.2	410	328	61.5	20.5	4.9	164	445	534
EC3	0.40	0.3	550	440	82.5	27.5	1.6	220	379	455
EC4	0.40	0.3	410	328	61.5	20.5	1.2	164	447	537
EC5	0.30	1.2	550	440	82.5	27.5	6.6	165	412	495
EC6	0.30	1.2	410	328	61.5	20.5	4.9	123	472	567
EC7	0.30	0.3	550	440	82.5	27.5	1.6	165	415	498
EC8	0.30	0.3	410	328	61.5	20.5	1.2	123	474	570
EC9	0.42	0.75	480	384	72	24	3.6	201	405	486
EC10	0.28	0.75	480	384	72	24	3.6	134	450	540
EC11	0.35	1.39	480	384	72	24	6.7	168	426	511
EC12	0.35	0.11	480	384	72	24	0.5	168	429	516
EC13	0.35	0.75	580	464	87	29	4.3	203	382	458
EC14	0.35	0.75	380	304	57	19	2.9	133	473	568
EC15	0.35	0.75	480	384	72	24	3.6	168	427	514
EC16	0.35	0.75	480	384	72	24	3.6	168	427	514
EC17	0.35	0.75	480	384	72	24	3.6	168	427	514
EC18	0.35	0.75	480	384	72	24	3.6	168	427	514
EC19	0.35	0.75	480	384	72	24	3.6	168	427	514
EC20	0.35	0.75	480	384	72	24	3.6	168	427	514

Table 3.9 - Mixture proportions for ESH-LWSCC (Expanded Shale LWSCC)

Mix no	X1	X2	X3	Cement	FA	SF	HRWRA	Water	E-Shale aggregate	
	w/b	HRWRA	binder	kg/m^3	kg/m^3	kg/m^3	l/m^3	l/m^3	Coarse	Fine
ESH1	0.40	1.2	550	440	82.5	27.5	6.6	220	385	613
ESH2	0.40	1.2	410	328	61.5	20.5	4.9	164	456	726
ESH3	0.40	0.3	550	440	82.5	27.5	1.6	220	388	618
ESH4	0.40	0.3	410	328	61.5	20.5	1.2	164	459	730
ESH5	0.30	1.2	550	440	82.5	27.5	6.6	165	422	672
ESH6	0.30	1.2	410	328	61.5	20.5	4.9	123	484	771
ESH7	0.30	0.3	550	440	82.5	27.5	1.6	165	426	678
ESH8	0.30	0.3	410	328	61.5	20.5	1.2	123	487	775
ESH9	0.42	0.75	480	384	72	24	3.6	201	415	661
ESH10	0.28	0.75	480	384	72	24	3.6	134	461	734
ESH11	0.35	1.39	480	384	72	24	6.7	168	436	695
ESH12	0.35	0.11	480	384	72	24	0.5	168	440	701
ESH13	0.35	0.75	580	464	87	29	4.3	203	391	622
ESH14	0.35	0.75	380	304	57	19	2.9	133	486	773
ESH15	0.35	0.75	480	384	72	24	3.6	168	438	698
ESH16	0.35	0.75	480	384	72	24	3.6	168	438	698
ESH17	0.35	0.75	480	384	72	24	3.6	168	438	698
ESH18	0.35	0.75	480	384	72	24	3.6	168	438	698
ESH19	0.35	0.75	480	384	72	24	3.6	168	438	698
ESH20	0.35	0.75	480	384	72	24	3.6	168	438	698

3.5 Experimental Procedures

3.5.1 Measured Responses

The responses that were modelled were slump flow diameter, V-funnel flow time, J-ring flow diameter, J-ring height difference, L-box height ratio, filling capacity percentage, bleeding, fresh air content, initial set time, final set time, sieve segregation, fresh unit weight, 28-day air dry unit weight, oven dry unit weight, 7-day compressive strength and 28-day compressive strength of concrete mixtures.

3.5.2 Casting of Test Specimens

All concrete mixtures were prepared in 35 L batches in a drum rotating mixer as shown in Figure 3.9. Due to the high water absorption capacity of the lightweight aggregates, the aggregates were pre-soaked for a minimum of 72 hours, then the excess water was drained and the materials were weighted up (Figures 3.9-3.12). The saturated surface dry lightweight aggregates were mixed for five minutes with 75% of the mixing water, then added to the cementitious materials and mixed for an additional minute. Finally, the remaining water and HRWRA were added to the mixture, and mixed for another 15 minutes. The mixing sequence is illustrated in Figure 3.13. Just after mixing, the slump flow, L-box, V-funnel, J-ring flow, filling capacity, sieve segregation, bleeding, air content, unit weight and setting time tests were conducted. Ten 100 × 200 mm cylinders from each batch were cast for compressive strength determination. All LWSCC specimens were cast without any compaction or mechanical vibration. After casting, all the specimens were covered with plastic sheets and water-saturated burlap and left at room temperature for 24 hours. They were then demolded and transferred to the moist curing room, and maintained at 23 ± °C and 100% relative humidity until testing. The cylinders for the oven dry unit weight test were stored in lime-saturated water for 28 days prior to transfer to the oven at 100°C. The cylinders for the air dry unit weight test were stored in room temperature for 28 days.

Figure 3.9 - Drum rotating mixer

Figure 3.10 - Aggregates 72 hrs pre-soaking

Figure 3.11 - Draining excess water form pre- soaked fines and coarse aggregates

Figure 3.12 - Pre-weight mixture proportions

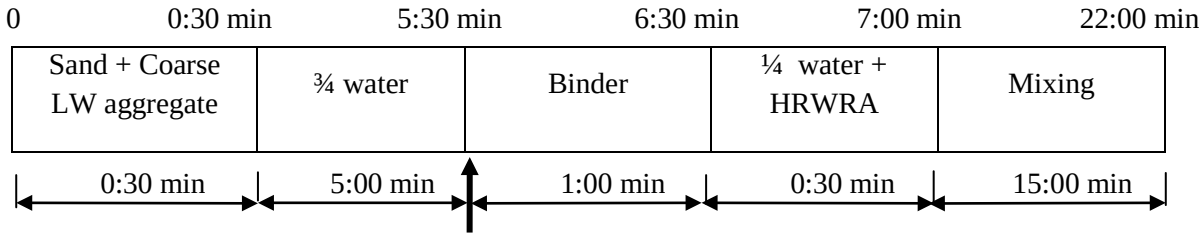

Figure 3.13 - Standard mixing sequence

3.5.3 Testing Procedures

All tests of concrete in the fresh state were conducted as per EFNARC Self-Consolidating Concrete Committee test procedures (EFNARC 2005). The slump flow test was conducted to assess the workability of concrete without obstructions to determine flow diameter (Figure 3.14). The viscosity of LWSCC mixtures was measured using the V-funnel test, where flow time under gravity was determined (Figure 3.15). The filling capacity (Figure 3.15), J-ring (Figure 3.16) and L-box tests (Figure 3.17) determined the passing ability of concrete.

The sieve segregation resistance (SSR) test was conducted according to EFNARC test procedures (Figure 3.19): 5 kg of fresh concrete was poured over 5 mm mesh, and the mass of the mortar passing through the sieve was recorded. The air content of the LWSCC mixture was determined by using the volumetric method, as per ASTM C 173 (2010) procedures (Figure 3.19). The initial set time and final set time of the concrete mixtures were measured as per ASTM C 403 procedures (Figure 3.20). The compressive strength of LWSCC mixtures was determined by using 100 × 200 mm cylinders (Figures 3.20 and 3.21), as per ASTM C 39 (2011). All fresh and hardened testes performed in Phase - I are shown in Figure 3-14 to 3-21.

Figure 3.14 - Mixture temperature and slump flow test - measure of flowability

Figure 3.15 - V- Funnel test and filling capacity test

Figure 3.16 - J-ring and J- ring height test

Figure 3.17 - L- Box test and bleed test

Figure 3.18 - Fresh density test and Fresh density test

Figure 3.19 - Sieve segregation resistance test and air content test (volumetric method)

Figure 3.20 - Penetration resistance test (set time test) and moulds casting

Figure 3.21 - Wet burlap curing in the first 24 hrs and compressive strength test

CHAPTER FOUR

4 ASSESSMENTS OF FRESH AND HARDENED PROPERTIES OF STATISTICALLY DERIVED LWSCC MIXTURES

4.1 Introduction

In this chapter, the results of fresh and hardened properties of sixty fractional factorial designed LWSCC mixtures (Phase I - Experimental program) with furnace slag (FS), expanded clay (EC), and expanded shale (ESH) lightweight aggregates, proportioned with w/b ranging from 0.30 to 0.40, HRWRA dosages varying from 0.3 to1.2% (by total content of binder) and binder content varying from 410 to 550 kg/m^3 are presented, and discussed. In addition, the relationships between responses are established.

4.2 Results and Discussions

The fresh properties of total of sixty FS-LWSCC, EC-LWSCC and ESH-LWSCC mixtures are summarized in Tables 4.1 to 4.3, while the compressive strength and unit weight results are presented in Tables 4.4 to 4.6.

4.2.1 Fresh Properties of LWSCC Mixtures

Tables 4-1 to 4-3 present the slump flow, V-funnel, J-ring flow, J-ring height difference, L-box, filling capacity, bleed, fresh air content, sieve segregation, and initial and final set time test results for FS, EC and ESH mixtures, respectively.

The slump flow range for FS mixtures was between 350 and 810 mm, while between 345 and 760 mm, and between 365 and 850 mm for EC and ESH mixtures, respectively.

The V-funnel flow time ranged between 1.50 and 26 s for FS mixtures, and between 1.9 and 28.7 s for EC and 1.2 and 24 s for ESH mixtures, respectively.

The J-Ring flow ranged between 310 and 800 mm for FS mixtures, and between 305 and 770 mm for EC and 360 and 850 mm for ESH mixtures, respectively. The J-Ring height difference

for FS mixtures ranged between 0 and 16.5 mm, and for EC and ESH mixtures ranged between 0 and 19 mm and 0 and 14 mm, respectively.

The L-box ratio and filling capacity for FS, EC and ESH mixtures ranged between 0.28 and 1 (28 and 100%), between 0.28 and 0.95 (27 and 95%) and between 0.28 and 1 (29 and 100%), respectively.

The sieve segregation resistance test results ranged between 5 and 37%, 5 and 42%, and 4 and 38%, for the bleed water between 0 and 0.108 ml/cm^2, 0 and 0.118 ml/cm^2 and 0 and 0.093 ml/cm^2 and for air content 2.2 and 4.8%, 2.0 and 3.6%, 2.0 and 3.7% for FS, EC and ESH mixtures, respectively.

The initial and final set times for FS, EC- and ESH mixtures ranged between 4:10 and 7:30 h:m (6:15 and 10:20 h:m), between 4:00 and 7:10 h:m (6:05 and 10:40 h:m) and between 3:50 and 7:20 h:m (6:10 and 10:00 h:m), respectively.

4.2.2 Density and Compressive Strength of LWSCC Mixtures

Tables 4.4 to 4.6, present the 7- day and 28-day compressive strength, and fresh, 28-day air dry and 28- day oven dry unit weights for FS, EC and ESH mixtures, respectively.

The fresh unit weight of the FS, EC and ESH mixtures ranged from 1860 to 2020 kg/m^3, from 1563 to1697 kg/m^3, and from 1742 to1892 kg/m^3, respectively. Thus, the three mixtures, as ordered above, may be classified as semi-lightweight concrete, lightweight, and lightweight/semi-lightweight concrete. The 28-day air/oven-dry densities values were generally below the 1840 kg/m^3 limit, classifying the developed mixtures as lightweight concrete, as per ACI Committee 318 requirements (ACI.318 2008).

The 7-day compressive strength of concrete ranged from 18 to 37 MPa, 17 to 36 MPa and 20 to 40 MPa for FS, EC and ESH mixtures, respectively. Whereas, the 28-day compressive strength of concrete ranged from 25 to 49 MPa, 21 to 48 MPa and 28 to 53 MPa for FS, EC and ESH mixtures, respectively.

Table 4.1 - Test results on fresh properties of FS mixes

Mix no	Slump flow (mm)	V-funnel (s)	J-Ring flow (mm)	J-Ring Height Diff (mm)	L-Box ratio	Filling capacity (%)	Bleeding (ml/cm^2)	SSR$^+$ (%)	Air content (%)	Set time (h:m)	
										Initial	Final
1	810	2.1	800	0.0	1.0	100	0.057	17	2.7	06:40	09:10
2*	800	1.5	785	0.0	1.0	100	0.072	37	2.5	07:30	10:20
3*	510	2.3	475	3.5	0.52	55	0.043	7	3.2	05:30	07:10
4*	520	7.0	490	4.5	0.5	55	0.053	25	3.4	06:30	08:30
5*	610	14	585	2.5	0.72	71	0.008	11	2.8	05:30	07:55
6*	625	15	610	3.5	0.59	63	0.01	21	3.0	05:55	08:10
7*	350	24	310	16.5	0.3	28	0.004	5	2.6	04:10	06:15
8*	380	20	340	10.5	0.38	32	0.006	6	2.4	04:25	06:45
9*	780	1.8	765	0.0	1.0	100	0.038	31	2.2	06:20	08:35
10*	390	26	345	10	0.28	32	0.000	7	4.8	04:05	06:10
11*	800	4.2	785	0.0	1.0	100	0.031	25	2.6	06:50	09:20
12*	380	8.0	350	12.5	0.32	28	0.010	8	3.8	04:25	06:20
13*	565	8.2	535	4.5	0.68	69	0.006	7	2.8	04:45	06:30
14*	760	2.4	745	0.0	1.0	100	0.108	31	2.2	05:45	08:20
15	660	4.8	640	2.5	0.89	87	0.011	16	3.2	04:30	06:25
16	690	4.8	670	1.5	0.95	94	0.021	14	3.4	04:50	06:55
17	660	5.3	640	2.0	0.91	90	0.012	13	4.0	05:35	07:10
18	680	4.9	665	1.5	0.93	94	0.019	15	3.8	05:20	07:40
19	670	5.0	660	2.0	0.89	89	0.017	12	3.5	05:30	07:15
20	680	4.7	675	1.5	0.92	95	0.015	13	3.5	05:45	07:20

$^+$*SSR: Sieve segregation resistance test*

**mixture disqualified as LWSCC*

Table 4.2 - Test results on fresh properties of EC mixes

Mix no	Slump flow (mm)	V-funnel (s)	J-Ring Flow (mm)	J-Ring Height Diff (mm)	L-Box ratio	Filling capacity (%)	Bleeding (ml/cm^2)	SSR$^+$ (%)	Air content (%)	Set time (h:m)	
										Initial	Final
1	760	2.7	770	0	0.94	94	0.066	19	2.8	6:00	9:30
2*	755	1.9	765	0	0.94	94	0.086	42	2.6	7:00	10:40
3*	490	3.0	460	5	0.50	53	0.046	8	3.0	5:50	7:25
4*	500	8.6	470	7	0.48	53	0.064	28	3.2	6:40	8:15
5*	580	17.5	550	5	0.68	68	0.009	12	3.0	5:50	7:35
6*	595	18.7	585	5	0.56	60	0.011	24	3.0	5:35	8:40
7*	345	28.7	305	19	0.30	28	0.004	5	2.8	4:25	6:45
8*	385	19.7	340	13	0.39	32	0.007	6	2.4	4:20	6:50
9*	730	2.3	745	0	0.94	94	0.041	36	2.0	6:05	8:40
10*	395	25.7	345	12	0.28	32	0.000	7	3.6	4:20	6:15
11*	740	5.4	765	0	0.93	93	0.035	29	2.8	7:10	9:30
12*	370	11.1	330	16	0.31	27	0.011	9	3.2	4:00	6:30
13*	540	10.9	505	6	0.65	66	0.007	8	2.2	4:35	6:45
14*	720	3.0	735	0	0.95	95	0.118	35	2.4	5:55	8:35
15	650	6.1	650	3	0.87	90	0.024	14	3.0	5:45	6:05
16	645	6.4	635	3	0.84	84	0.013	16	3.2	5:45	6:50
17	630	6.0	655	2	0.90	91	0.014	15	3.4	5:25	6:55
18	655	6.1	585	3	0.85	85	0.017	17	3.6	4:20	7:20
19	620	5.7	645	1	0.89	86	0.019	18	3.4	5:30	7:35
20	630	6.6	625	3	0.85	88	0.021	15	3.4	5:15	7:25

$^+$*SSR: Sieve segregation resistance test*

**mixture disqualified as LWSCC*

Table 4.3 - Test results on fresh properties of ESH mixes

Mix no	Slump flow (mm)	V-funnel (s)	J-Ring Flow (mm)	J-Ring Height Diff (mm)	L-Box ratio	Filling capacity (%)	Bleeding (ml/cm^2)	SSR$^+$ (%)	Air content (%)	Set time (h:m)	
										Initial	Final
1	850	1.6	850	0	1.00	100	0.046	14	2.6	6:00	9:15
2*	810	1.2	770	0	1.00	100	0.060	38	2.2	7:20	10:00
3*	530	1.8	540	2	0.55	58	0.039	6	3.1	5:20	7:05
4*	535	5.6	510	5	0.53	58	0.044	24	3.2	6:25	8:35
5*	640	11.1	650	2	0.77	76	0.007	10	3.1	5:45	7:55
6*	625	11.9	590	4	0.63	67	0.009	20	2.8	5:15	8:20
7*	365	19.7	370	9	0.31	29	0.003	4	2.9	4:45	6:35
8*	380	18.5	360	14	0.37	31	0.005	6	2.0	3:50	6:20
9*	810	1.4	805	0	1.00	100	0.036	30	2.1	6:25	8:10
10*	395	24.0	415	5	0.28	31	0.000	7	3.7	4:35	6:30
11*	820	3.2	795	0	1.00	100	0.026	24	2.4	6:55	9:10
12*	390	6.0	390	8	0.33	29	0.009	7	3.3	4:10	6:10
13*	595	6.5	630	0	0.72	73	0.005	6	2.0	4:15	6:25
14*	755	1.9	715	0	1.00	100	0.093	34	2.5	5:45	8:05
15	675	3.6	680	2	1.00	98	0.011	13	2.6	4:35	7:25
16	705	3.7	710	2	0.98	100	0.016	11	3.3	5:05	6:40
17	685	4.0	680	1	1.00	99	0.011	12	3.2	5:25	6:35
18	700	3.7	700	1	0.97	97	0.017	13	3.2	4:45	6:40
19	685	3.5	680	1	1.00	97	0.013	10	3.2	5:15	7:05
20	705	4.1	700	2	0.99	99	0.015	12	3.0	5:25	7:25

$^+$*SSR: Sieve segregation resistance test*

**mixture disqualified as LWSCC*

Table 4.4 - Compressive strength and unit weight test results of FS mixes

Mix no	Compressive strength (MPa)		Unit weight (kg/m^3)		
	7-day	28-day	Fresh	28-day air dry	28-day oven dry
1	24	32	1922	1802	1762
2	19	26	1950	1815	1756
3	26	35	1965	1845	1785
4	21	29	1975	1858	1805
5	31	43	1985	1865	1805
6	29	40	1993	1873	1823
7	34	46	2000	1880	1820
8	32	43	1870	1720	1672
9	18	25	1890	1770	1680
10	37	49	1930	1780	1733
11	24	36	1940	1798	1740
12	29	42	1900	1764	1712
13	32	45	2020	1885	1846
14	21	29	1860	1740	1710
15	31	44	1930	1810	1746
16	28	39	1910	1790	1713
17	30	42	1900	1780	1720
18	28	40	1903	1783	1723
19	29	40	1908	1775	1705
20	28	41	1922	1789	1735

Table 4.5 - Compressive strength and unit weight test results of EC mixes

Mix no	Compressive strength (MPa)		Unit weight (kg/m^3)		
	7-day	28-day	Fresh	28-day air dry	28-day oven dry
1	22	29	1615	1514	1481
2	18	23	1639	1525	1476
3	24	29	1651	1550	1500
4	20	27	1660	1561	1517
5	30	38	1668	1567	1517
6	29	39	1675	1574	1532
7	34	42	1681	1580	1529
8	31	41	1571	1445	1405
9	17	21	1588	1487	1412
10	36	48	1622	1496	1456
11	24	34	1630	1511	1462
12	28	39	1597	1482	1439
13	29	38	1697	1584	1551
14	20	27	1563	1462	1437
15	27	36	1622	1521	1467
16	28	37	1605	1504	1439
17	27	37	1597	1496	1445
18	27	38	1599	1498	1448
19	29	39	1603	1491	1433
20	30	40	1615	1503	1458

Table 4.6 - Compressive strength and unit weight test results of ESH mixes

Mix no	Compressive strength (MPa)		Unit weight (kg/m^3)		
	7-day	28-day	Fresh	28-day air dry	28-day oven dry
1	27	36	1800	1688	1650
2	21	28	1826	1700	1645
3	29	40	1840	1728	1672
4	23	31	1850	1740	1690
5	34	48	1859	1747	1690
6	31	43	1866	1754	1707
7	38	51	1873	1761	1704
8	34	46	1751	1611	1566
9	20	28	1770	1658	1573
10	40	53	1807	1667	1623
11	26	40	1817	1684	1630
12	32	46	1779	1652	1603
13	36	51	1892	1765	1729
14	22	31	1742	1630	1601
15	31	44	1807	1695	1635
16	34	48	1789	1676	1604
17	32	44	1779	1667	1611
18	31	45	1782	1670	1614
19	33	46	1787	1662	1597
20	31	43	1800	1675	1625

4.2.3 Discussions

In order to qualify as SCC, the mix should satisfy EFNARC industrial classifications, with 550 to 850 mm slump flow (Nagataki and Fujiwara 1995), less than 8 sec of V-funnel time, 80 to 100% of filling capacity, greater than 0.8 of h_2/h_1 ratio of L-box (Sonebi et al. 2000; Petersson and Skarendahl 1999), and less than 20% of segregation resistance (EFNARC, 2005). To be classified as LWSCC, a mix should satisfy EFNARC-SCC industrial classifications as well as it should develop a minimum 28-day compressive strength of 17.2 MPa and attain an air dry unit weight of less than 1840 kg/m^3 (ACI 213R 2003; ACI.318 2005)

The filling capacity test is more relevant for assessing the deformability of SCC among closely spaced obstacles. A filling capacity between 50 and 95% indicates moderate to excellent flowability among closely spaced obstacles (Khayat et al. 2002). For a desirable SCC mixture performance, V-funnel time between 3 and 7 sec is suggested by Bouzoubaa and Lachemi (2001), between 2.2 and 5.4 sec by Khayat et al. (2002) and between 2.1 and 4.2 sec by Ghezal and Khayat (2002).

It is reported that the SCC with L-box ratio (h_2/h_1) greater than 0.8 exhibited good performance without blocking in the structures, hence h_2/h_1 of 0.8 is considered as the lower critical limit for SCC (Sonebi et al. 2000; Petersson and Skarendahl 1999). According to several studies, the L-box and the filling capacity test results should be simultaneously considered to evaluate the concrete passing ability through heavily reinforced sections without the need of vibration.

One of the most important requirements for any SCC is that the aggregates should not be segregated from the paste and the mix should remain homogeneous during the production and placement. It is also equally important that the particles move with the matrix as a cohesive fluid during the flow of SCC. A stable SCC should exhibit a segregation index less than 10% (Khayat et al. 1998).

Table 4.7 presents summary of LWSCC mixtures qualification criteria, focusing of the main key indicators, slum flow diameter, v-funnel time, L-box ratio, percentage of sieve segregation resistance, 28-day air dry unit weight and 28-day compressive strength.

Table 4.7 - LWSCC performance criteria

LWSCC performance criteria	
Slump flow (mm)	550 to 850
V-funnel (s)	0 to 25
Passing ability (L-box)	≥ 0.80
Sieve segregation resistance (%)	0 to 20
28-day Air dry unit weight (kg/m^3)	< 1840
28-day Compressive strength (MPa)	> 17.2

From the results of the present study, mixes FS/EC/ESH 3,4,5,6,7,8,10,12, and 13 exhibited low flowability, poor workability and passing ability, where the slump flow diameter, V-funnel time and L-box ration were below the acceptable EFNARC (2005) performance criteria for SCC, as illustrated in Figures. 4.1 to 4.3, hence these mixtures were disqualified as LWSCC. On the other hand, mixes FS/EC/ESH 2,4,9,11,14 and FS/EC6 are considered segregated mixes due to high segregation index beyond the prescribe limits. Figure 4.4 compares the segregation indexes of the developed mixtures, and it shows EFNARC (2005) segregation limit. Mixes 1, 15, 16, 17, 18, 19 and 20 met all SCC fresh performance criteria outlined by EFNARC, with a balanced density and proper mix proportions.

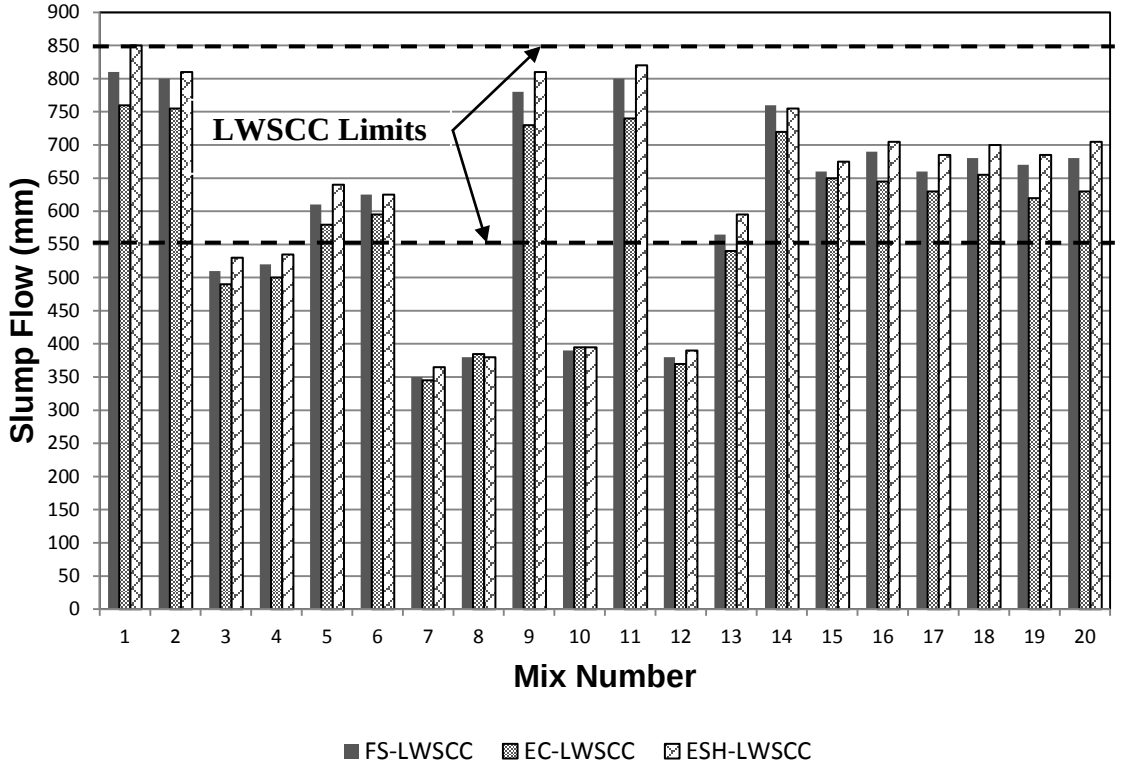

Figure 4.1 - Comparison of the slump flows of the developed mixtures

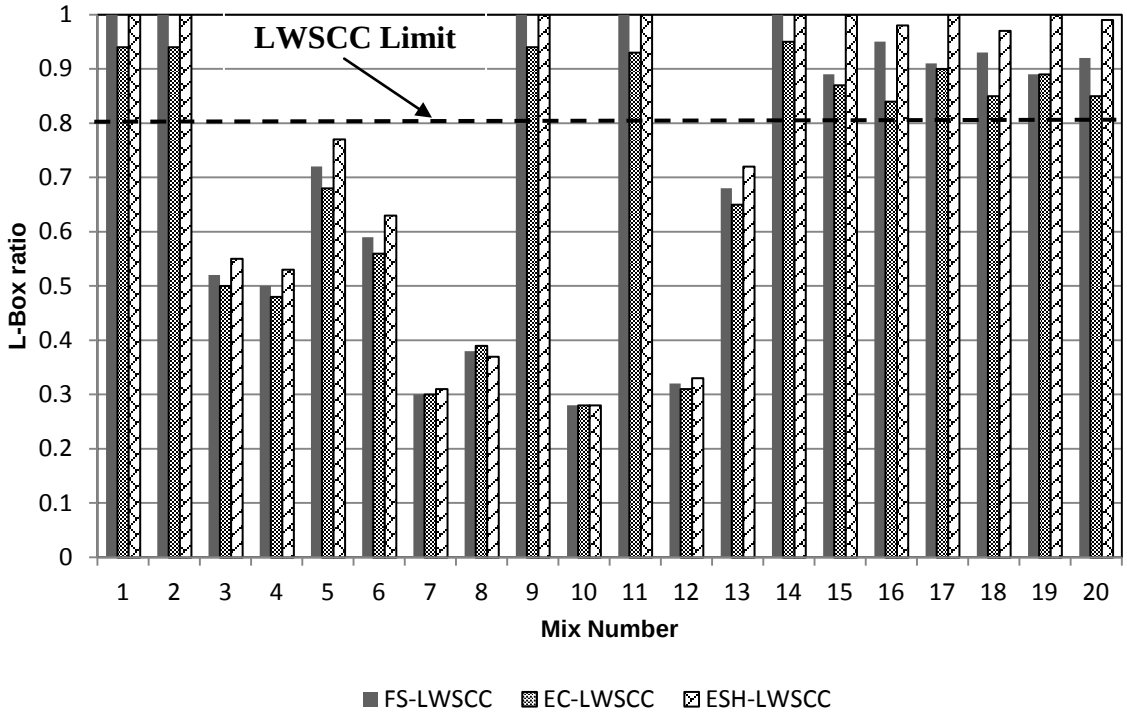

Figure 4.2 - Comparison of the L-Box ratios of the developed mixtures

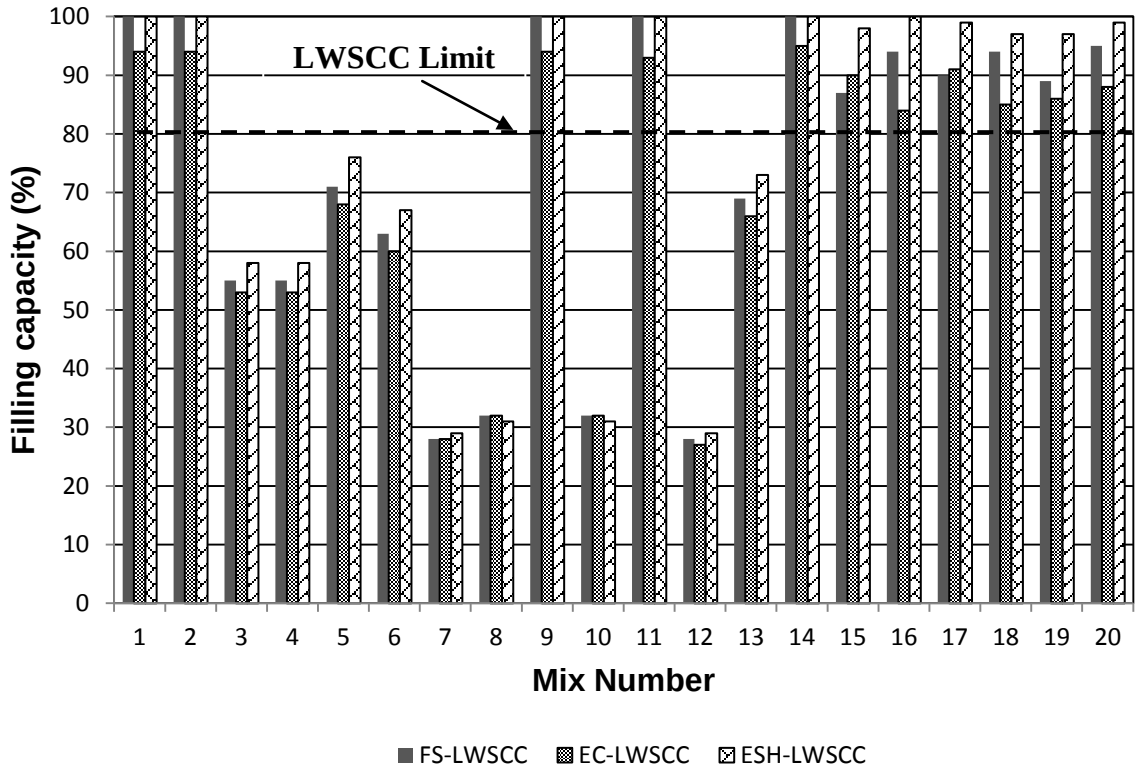

Figure 4.3 - Comparison of the filling capacities of the developed mixtures

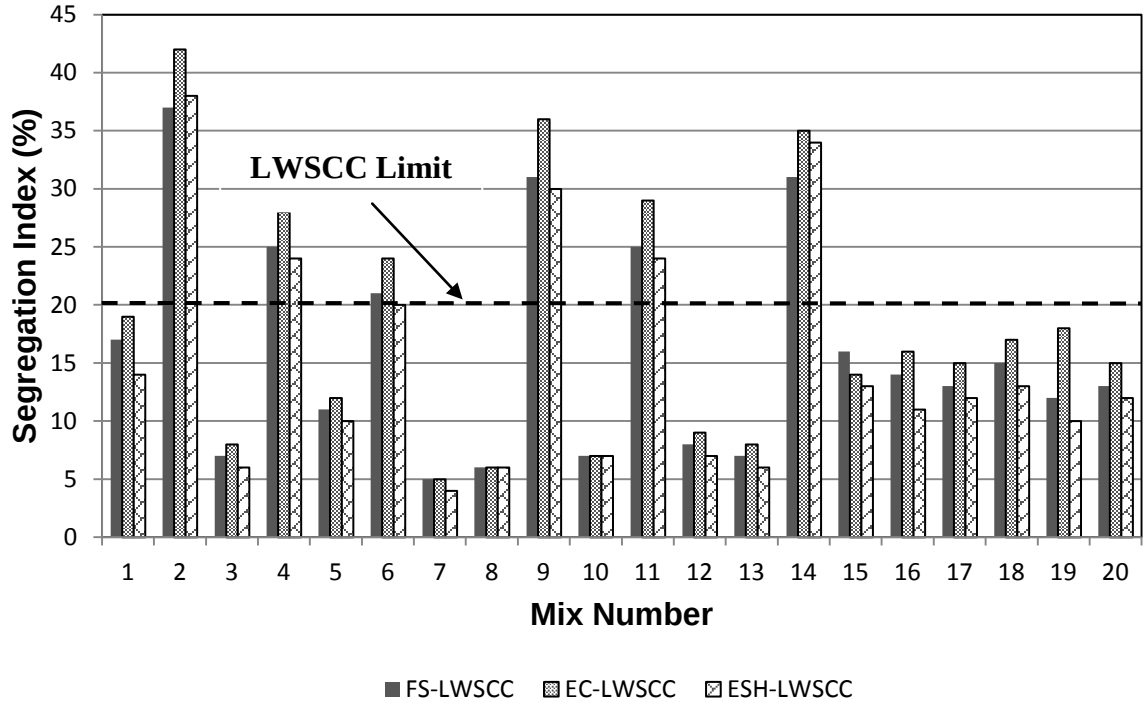

Figure 4.4 - Comparison of the segregation indexes of the developed mixtures

The relation between the slump flow and the segregation index of concrete mixes is illustrated in Figure 4.5. It can be observed that no segregation was found up to a concrete with slump flow of 500 mm. The chances of segregation are very high beyond a slump flow of 750 mm as the segregation index tends to be more than 20% for the developed mixtures. It is always desirable to keep the slump flow between 550 and 750 mm for a stable and homogenous SCC mixture. Based on the materials packing density, for a given mix design where all mix parameters are fixed, the EC mixture will yield lower segregation resistance than both FS and ESH mixtures. On the other hand the ESH mixtures will result in high workability characteristics than both EC and FS mixtures.

Figure 4.6 shows the relationship between V-funnel flow time and the segregation index. It illustrates that there is a higher chance for LWSCC mixture to segregate when the V- funnel flow time is under 6 sec. In another word, as the viscosity of the LWSCC mixtures decrease and the mix constituents get further apart, the tendency of segregation is increased.

Figure 4.7 shows that the slump flow increases as the V-funnel flow time decreases, as expected. The chances of less viscous mix increases beyond a slump flow of 620 mm when V- funnel flow time tends to be under 6 sec. In contrast, a linear relationship is established between the slump flow and the J-ring flow as illustrated in Figure 4.8 (expected for SCC mixtures). Unsurprisingly, J-ring flow height decreases with the increase of J- ring flow of the developed mixtures, as shown in Figure 4.9.

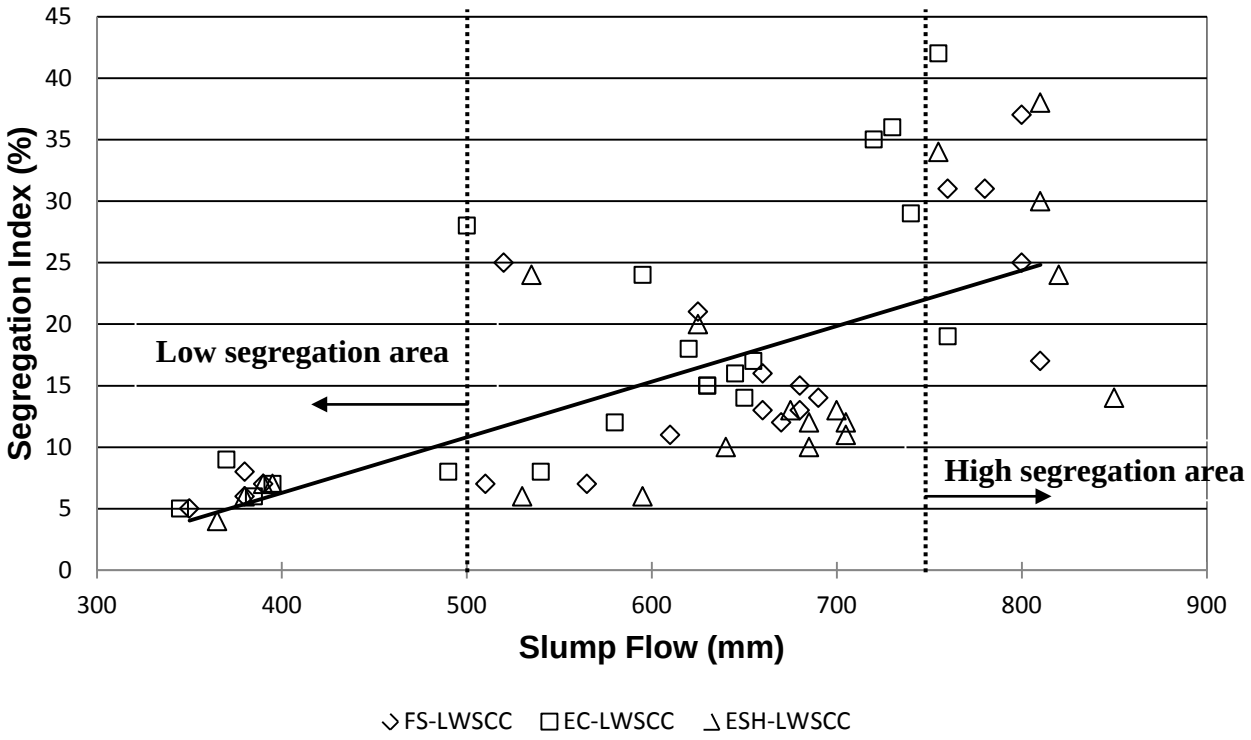

Figure 4.5 - Relation of slump flow and segregation index of the developed mixtures

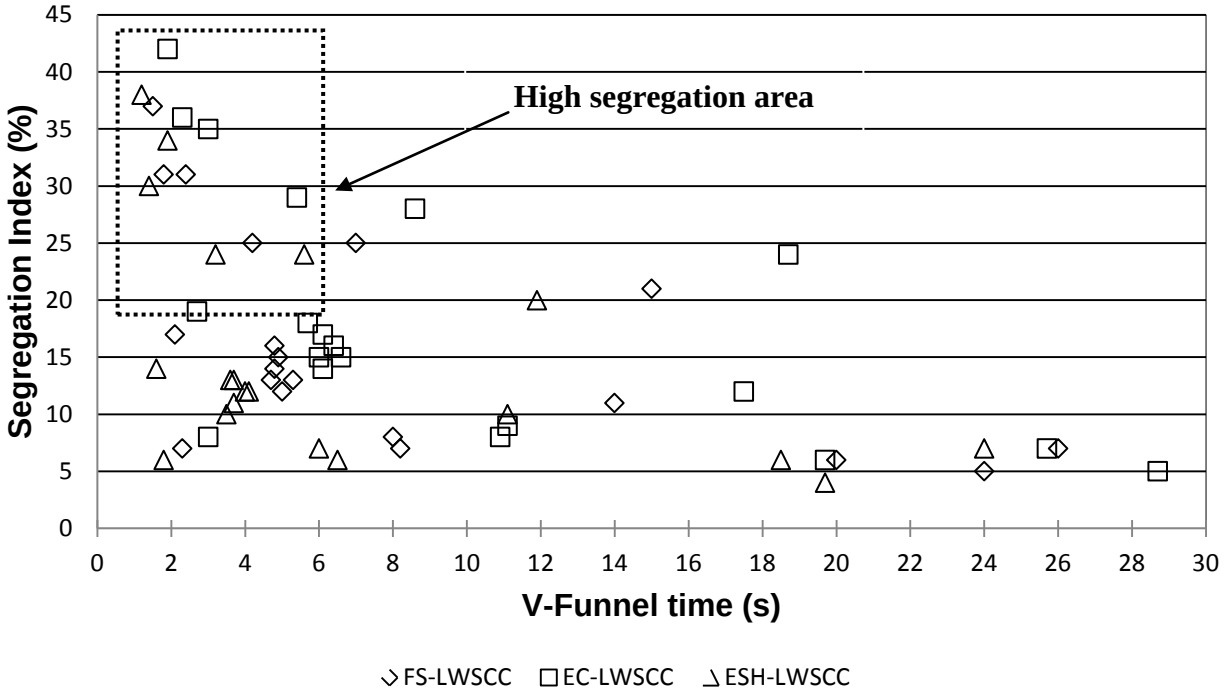

Figure 4.6 - Relation of V-Funnel time and segregation index of the developed mixtures

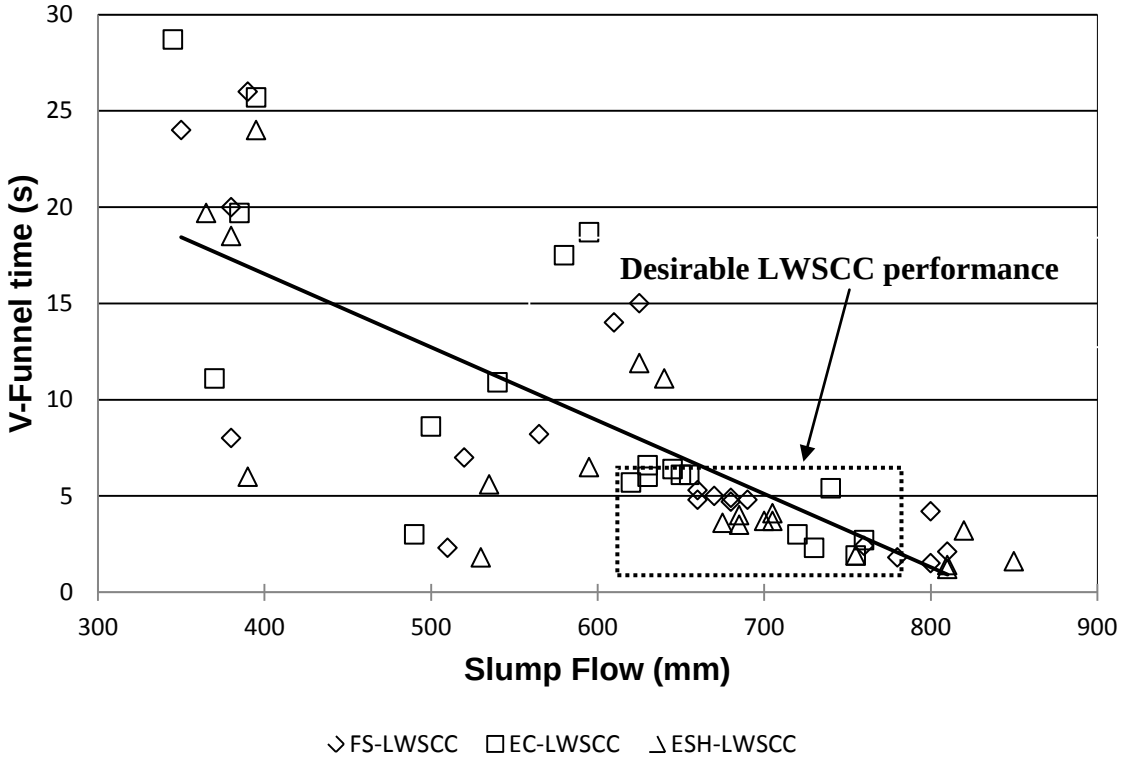

Figure 4.7 - Relation of slump flow and V-Funnel time of the developed mixtures

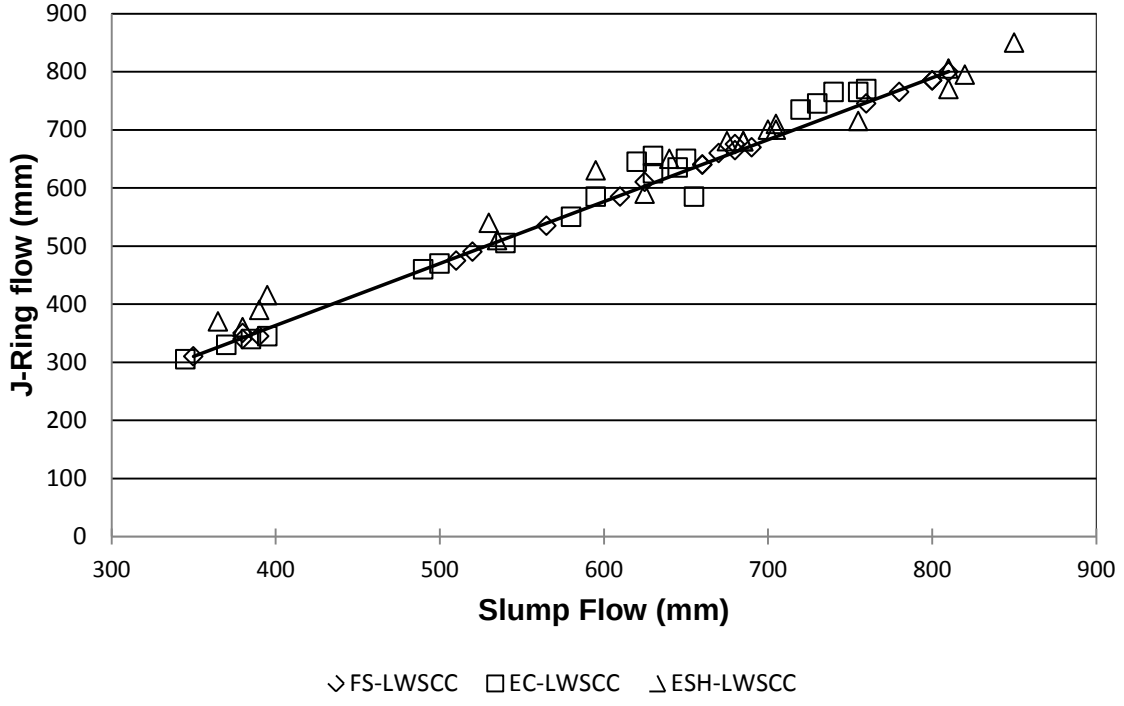

Figure 4.8 - Relation of slump flow and J-ring flow of the developed mixtures

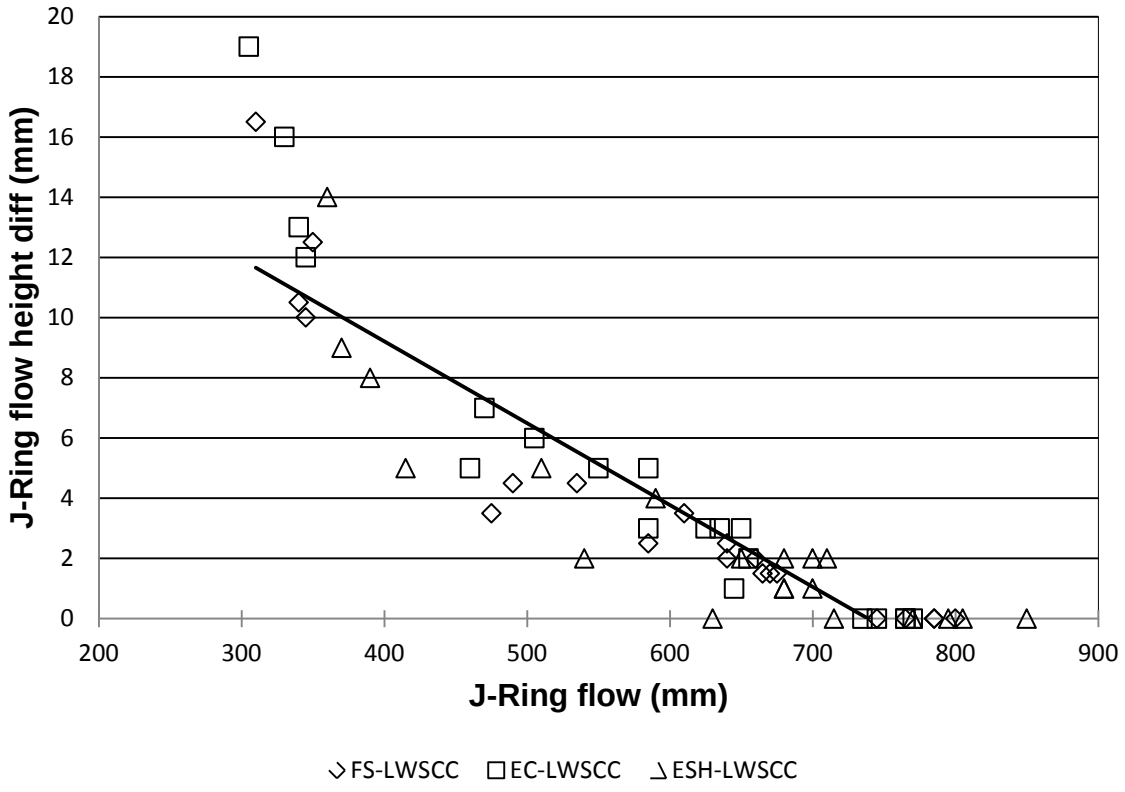

Figure 4.9 - Relation of J-ring flow and J- ring height different of the developed mixtures

All mixes exhibited a 7-day compressive strength greater than 17 MPa and 28-day compressive strength greater than 21 MPa, thus satisfying ACI 213R (2003) for minimum compressive strength of structural lightweight concrete. Figures 4.10 and 4.11 show a comparison of the compressive strength of the developed mixtures with different aggregates type at 7-day and 28-day tests, respectively.

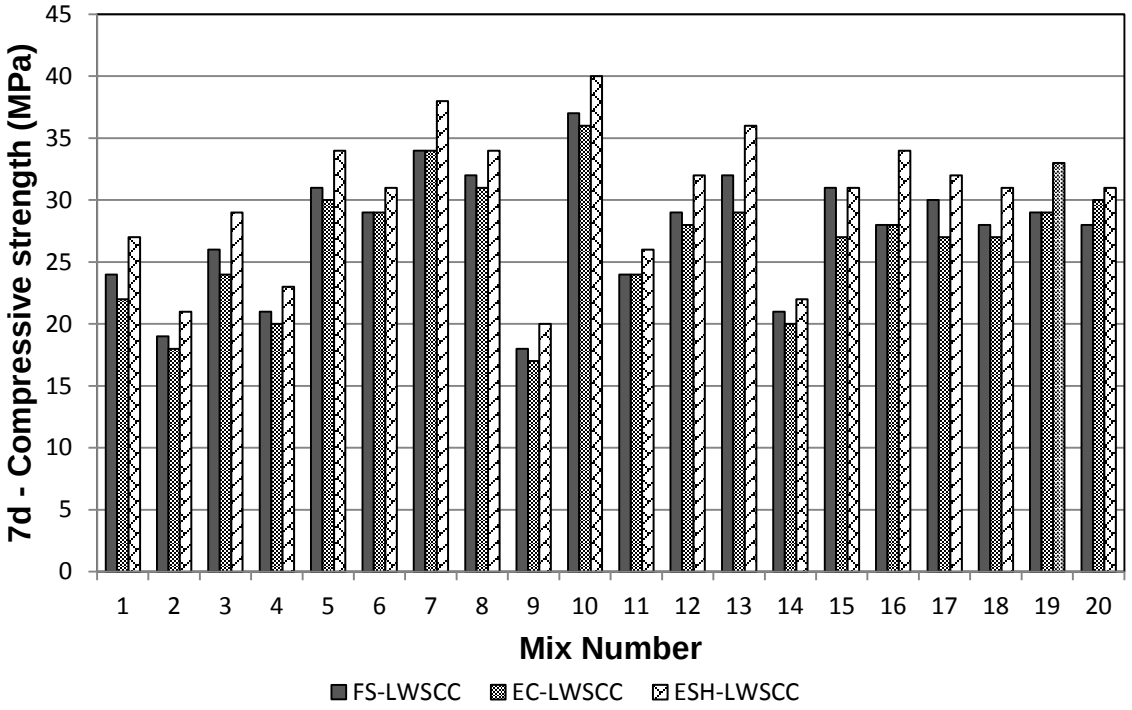

Figure 4.10 - Comparison of the 7-day compressive strength of the developed mixtures

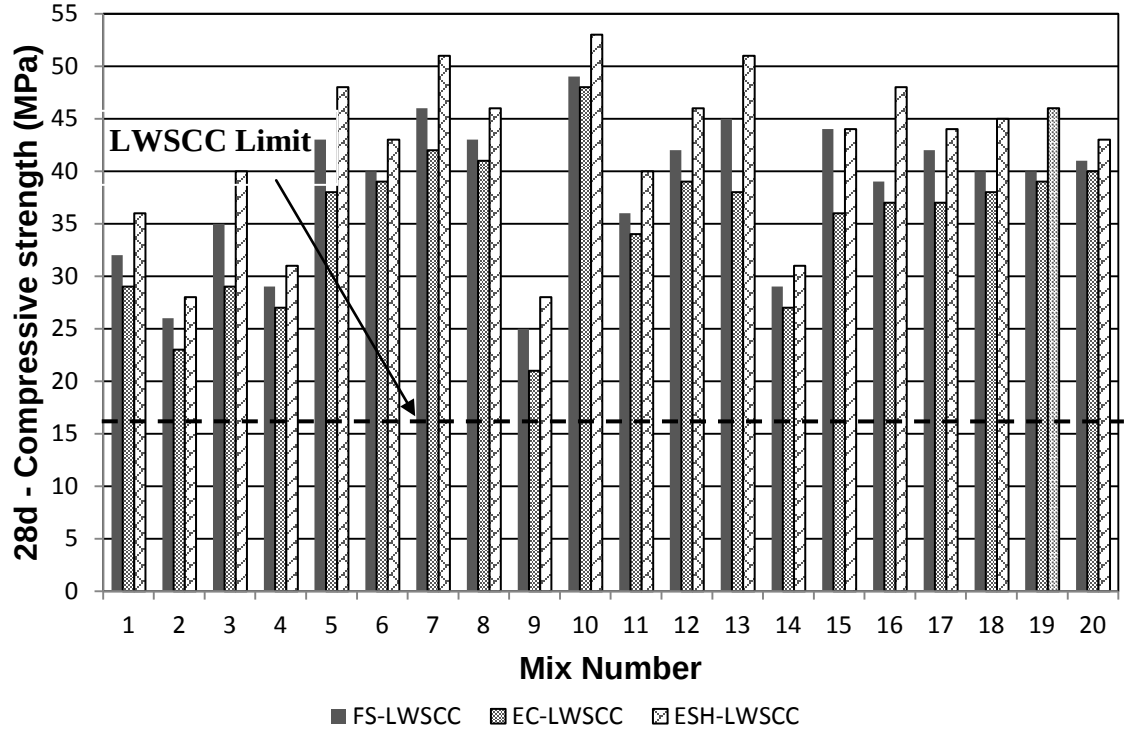

Figure 4.11 - Comparison of the 28-day compressive strength of the developed mixtures

Table 4.8 present compassion of the 28-day compressive strength of the developed mixtures made with the three lightweight aggregates types. The highest strengths were recorded for mixes made with ESH aggregates. These mixes contained a lower volume of coarse lightweight aggregate that helped with attaining higher strength compared to mixes with higher volume of coarse lightweight aggregate (mixes with FS and EC aggregates). The 28-day compressive strength results of FS, EC and ESH mixtures ranged between 25 and 49 MPa, 21 and 48 MPa and 28 and 53 MPa, respectively. The highest strength was obtained when using ESH aggregates and the lowest when using EC. The 28-day compressive strength of the developed mixtures was found to be 29.5 MPa or higher. This difference can be attributed to the influence of the quality and percentage of lightweight coarse aggregate used.

Table 4.8 - Comparison of the 28-day compressive strength results of the developed mixes

Mix no	28-day - Compressive strength (MPa)		
	FS	**EC**	**ESH**
1	32	29	36
2	26	23	28
3	35	29	40
4	29	27	31
5	43	38	48
6	40	39	43
7	46	42	51
8	43	41	46
9	25	21	28
10	49	48	53
11	36	34	40
12	42	39	46
13	45	38	51
14	29	27	31
15	44	36	44
16	39	37	48
17	42	37	44
18	40	38	45
19	40	39	46
20	41	40	43

Figure 4.12 shows a comparison of the fresh unit weight of the developed mixtures. The fresh density varied from 1563 to 2020 kg/m^3. The 28-day air dry and oven dry values were generally below the 1840 kg/m^3 limit, classifying the mixtures as lightweight concrete. Figures 4.13 and 4.14 show a comparison of the unit weight of the developed mixtures with different aggregates type at 28-day air dry and oven dry, respectively. From the figure, it can be seen that the developed EC mixes had the highest reduction in unit weight followed by ESH mixes. This can be attributed to the high aggregates absorption vales for both EC and ESH, which was greater than 13%. In contrast the mixes with FS aggregates had the lowest reduction after drying due to their relative low absorption vales (< 8%).

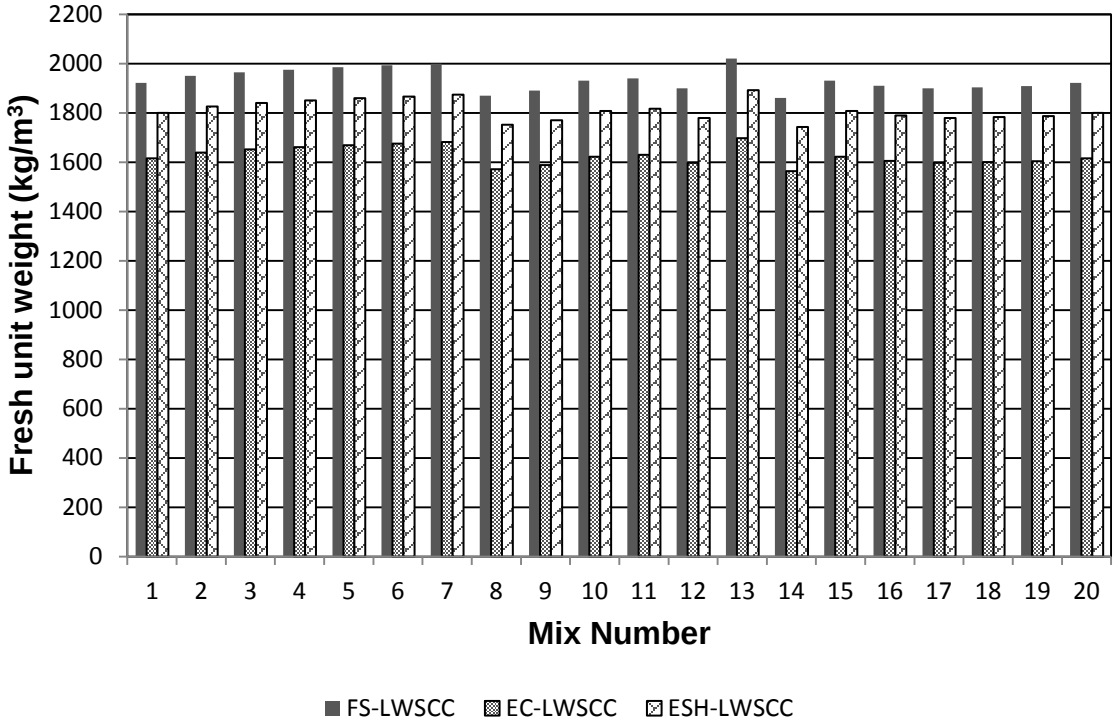

Figure 4.12 - Comparison of the fresh unit weight test results of the developed mixtures

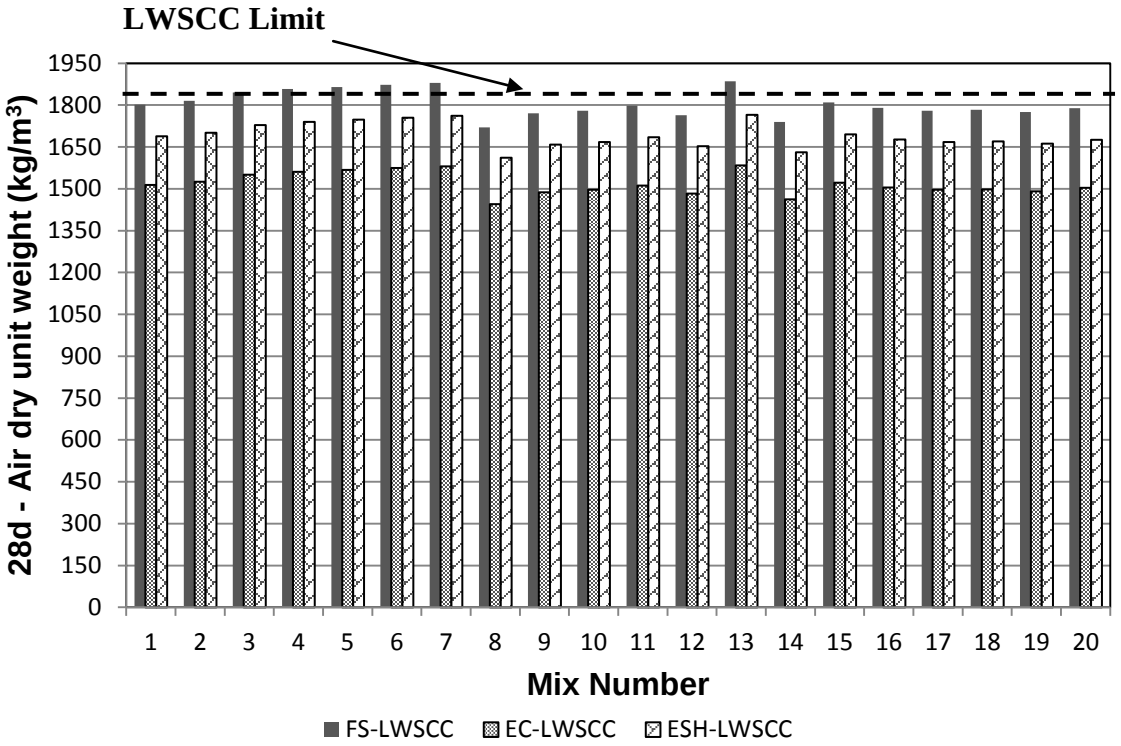

Figure 4.13 - Comparison of the 28-day air dry unit weight test results of the developed mixtures

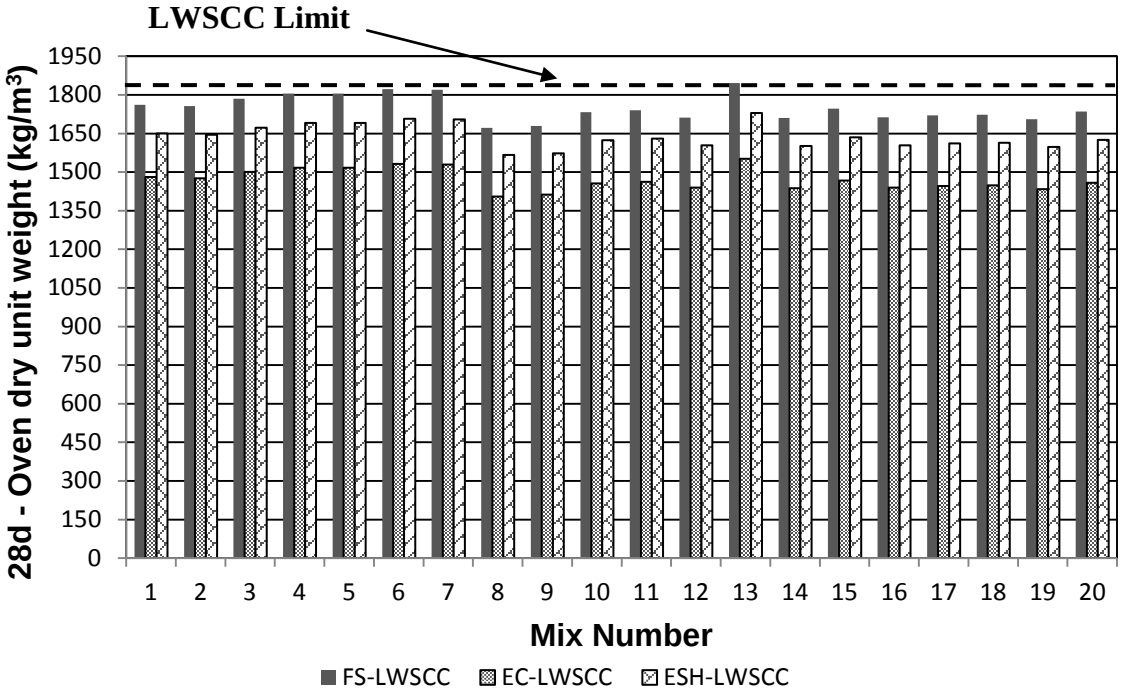

Figure 4.14 - Comparison of the 28-day oven dry unit weight test results of the developed mixtures

A comparison of 28-day air dry unit weight results of the developed mixtures is presented in Table 4.9. The 28-day-air dry unit weight of FS mixtures was the highest ranging from 1720 to 1885 kg/m^3. The EC mixtures had the lowest density ranging from 1445 to 1584 kg/m^3 while the density of ESH mixtures ranged from 1611 to1867 kg/m^3. 28-day air and oven dry unit weight values for the tested EC/ESH mixtures were below the 1840 kg/m^3 limit, classifying these developed lightweight mixtures as lightweight concrete according to ACI 213R (2003). 14 FS mixtures were classified as lightweight and the other six mixtures were classified as semi-lightweight concrete. As expected, the LWSCC density reflects the aggregate density used in each of the developed mixtures (Table 3.2), where the FS aggregates are the heaviest, followed by the ESH and EC aggregates.

4.3 Summary

High packing density of lightweight aggregates (ESH) results in a robust mixture with high workability and segregation resistance. Mixtures made with EC showed the lowest workability, and segregation resistance. Bleeding, air content and set times are affected by the mix parameters not by the aggregate types. The aggregate type affected the LWSCC compressive strength with EC mixtures showing the lowest compressive strength. It was possible to produce LWSCC by using all types of lightweight aggregates.

Table 4.9 - Comparison of the 28- day air dry unit weight results of the developed mixes

Mix no	28-day - Air dry unit weight (kg/m^3)		
	FS	**EC**	**ESH**
1	1802	1514	1688
2	1815	1525	1700
3	1845	1550	1728
4	1858	1561	1740
5	1865	1567	1747
6	1873	1574	1754
7	1880	1580	1761
8	1720	1445	1611
9	1770	1487	1658
10	1780	1496	1667
11	1798	1511	1684
12	1764	1482	1652
13	1885	1584	1765
14	1740	1462	1630
15	1810	1521	1695
16	1790	1504	1676
17	1780	1496	1667
18	1783	1498	1670
19	1775	1491	1662
20	1789	1503	1675

CHAPTER FIVE

5 THE RESPONSES OF LWSCC MIXTURES AND STATISTICAL EVALUATION OF RESULTS

5.1 Introduction

The effects of mix parameters, w/b ranging from 0.30 to 0.40, HRWRA dosages varying from 0.3 to1.2% (by total content of binder) and binder content varying from 410 to 550 kg/m^3 on the responses of fresh and hardened concrete properties such as slump flow, V-funnel flow, J-Ring flow, J-Ring height difference, L-box, filling capacity, bleeding, fresh air content, initial/final setting times, sieve segregation, fresh unit weight, 28-day air dry unit weight, 28-day oven dry unit weight, and 7- and 28-day compressive strengths, are discussed in this chapter, followed by statistical evaluation of the test results. Also, regression analysis for the response of LWSCC fresh and hardened properties is presented.

5.2 Results and Discussions

The effect of the investigated mix design parameters on the variation of key responses (test results) such as slump flow diameter, V-funnel flow time, L-box height ratio and sieve segregation resistance (SSR) are shown in Figures 5.1 to 5.24 and discussed in the following sections.

The influence of the design parameters with statistical details of the models on the rest of responses such as J-Ring flow, J-Ring height difference, filling capacity, bleeding, fresh air content, initial and final setting times, fresh unit weight, 28-day air dry unit weight, 28-day oven dry unit weight, and 7- and 28-day compressive strengths tests is summarized in this chapter. The constructed figures illustrating the effect of the investigated mix design parameters on these responses are presented in **Appendix A**.

5.2.1 Effects of Mix Parameters on the Slump Flow

The slump flow is one of the most important properties of LWSCC. If the slump flow of concrete is between 550 and 750 mm without any segregation, the concrete can be qualified for SCC. Obviously, other fresh concrete tests such as V-funnel flow time, L-box, filling capacity, and SSR are also important to thoroughly evaluate the fresh LWSCC properties. However, one can take decision from slump flow test, if other test set-ups are not available.

Figures 5.1, 5.2 and 5.3 present contour diagrams of the slump flow diameter changes of FS, EC and ESH-LWSCC mixtures depending on the water to binder ratio (w/b) and total binder content (b), respectively. According to Figures 5.1 to 5.3, an increase in the w/b from 0.3 to 0.4 significantly increased the slump flow diameter. However, at fixed HRWRA (%) the slump flow range gets limited with the increase of binder content, for example for FS, EC and ESH mixtures when the HRWRA (%) is fixed at 0.75% and the binder content is increased to 550 kg/m^3, the maximum predicted slump flow is limited to 700 mm, 650 mm and 700 mm, respectively. This is due to the increased demand of HRWRA in order to maintain same slump flow diameter with higher binder content.

The combined effects of w/b and HRWRA have significant influence on the slump flow diameter as shown in Figures 5.4, 5.5 and 5.6. An increase in the HRWRA from 0.3 to 1.2% (by total content of binder) and w/b from 0.3 to 0.4 significantly increases the slump flow diameter when high binder content (480 kg/m^3) is used.

The lowest effect of the coupled parameters (w/b and HRWRA) in increasing the slump flow diameter was observed with the EC-LWSCC mixtures. On the other hand, the greatest effect was observed with the ESH-LWSCC mixtures followed by the FS-LWSCC mixtures. For example, when both parameters (w/b and HRWRA) are maximized at 1.2% and 0.40, the maximum predicted slump flows for FS, EC and ESH mixtures is 800 mm, 750 mm and 850 mm, respectively. This can be attributed to the packing density because a lower amount of fluidity is needed to achieve high workability for high-packing density mixture.

According to Khayat, the w/b is closely related to flowability of concrete. An increase in w/b improves the flowability of the concrete (Assaad and Khayat 2006). Sonebi et al. (2007) states that the SCC fresh properties are significantly influenced by the dosage of water and HRWRA.

5.2.2 Effects of Mix Parameters on the V-Funnel Flow Time

An increase of the w/b from 0.3 to 0.4 significantly reduced the V-funnel flow time whereas an increase of HRWRA from 0.3 to 1.2% (by total content of binder) only slightly reduced the V-funnel flow time. However, combined maximum increase of both w/b and HRWRA parameters resulted in a substantial reduction of the V-funnel flow time (below 2 sec) at given binder content. This observation is in agreement with the conclusion of previous SCC statistical workability study by Sonebi et al. (2007). The V-funnel flow time is indicative of the viscosity of the LWSCC mixture - the higher the flow times the more viscous and less workable is the mix. Changes of V-funnel flow time with w/b and HRWRA are depicted in Figures 5.7, 5.8 and 5.9 for the FS, EC and ESH-LWSCC mixtures.

The effect of w/b and total binder content on the V-funnel flow time of FS, EC and ESH-LWSCC mixtures is plotted in Figures 5.10, 5.11 and 5.12, respectively. From these Figures, it can be concluded that increasing the w/b from 0.3 to 0.4 significantly decreases the V-funnel flow time. However, for both FS and EC-LWSCC mixtures the flow time increases with the increase of binder content at a given HRWRA (%). On the other hand, only a slight increase in flow time was observed with the ESH-LWSCC mixture. This can be attributed to low internal friction (higher excess paste volume) in the ESH mixes (Hwang et al. 2006).

5.2.3 Effects of Mix Parameters on the L- Box Ratio

The L-box height ratio showed a similar trend as slump flow. It is observed that increasing both the w/b from 0.3 to 0.4 and HRWRA from 0.3 to 1.2% (by total content of binder) significantly increased the L-box height ratio when a high binder content of 480 kg/m^3 is used. Figures 5.13, 5.14 and 5.15 present the slump flow diameter changes of FS, EC and ESH-LWSCC mixtures depending on the w/b and HRWRA, respectively.

According to Hwang, a combination of the slump flow and the L-box blocking ratio (h_2/h_1) can be used to assess filling capacity of SCC for quality control and design of SCC for placement in restricted sections or congested elements (Hwang et al. 2006).

Figures 5.16, 5.17 and 5.18 present contour diagrams of the L-box ratio of FS, EC and ESH-LWSCC mixtures depending on the w/b and total binder, respectively. It can be suggested that as the total binder content is increased, the L- box ratio is reduced for a given HRWRA (%).

Similar to the slump flow observation, the lowest effect of the coupled parameters (w/b and HRWRA) was seen with the EC-LWSCC mixtures, while, the greatest effect was seen with the ESH-LWSCC mixtures followed by the FS-LWSCC mixtures. This can be attributed to the high packing density of the mixture and therefore, the lower amount of fluidity needed to achieve high workability. Sonebi et al. (2007) demonstrated the relationship between w/b, HRWRA and volume of coarse aggregate (V_{CA}) and L-box ratio. They concluded that all three parameters significantly influenced the L-box ratio.

5.2.4 Effects of Mix Parameters on the Segregation Resistance

Figures 5.19, 5.20 and 5.21 show that the increase of the binder content appeared to be very effective in increasing the segregation resistance. The increase in binder content enhanced the packing density of mixtures and resulted in a reduction in segregation. This is attributed to the increased cohesiveness and viscosity of the concrete mixture at high binder content. Similar conclusions were drawn in previous SCC statistical studies (Patel et al. 2004; Khayat et al. 2000). Figures 5.22, 5.23 and 5.24 illustrate the trade-off between variation of the w/b and HRWRA on the segregation resistance of FS, EC and ESH-LWSCC mixtures at a given binder content (480 kg/m^3). These contours show that increasing one or both parameters w/b and HRWRA from 0.3 to 0.4 and 0.3 to 1.2% (by total content of binder), respectively, would significantly reduce the segregation resistance of LWSCC mixtures.

Based on the materials packing density, for a given mix design where all mix parameters are fixed, the EC mixture is predicted to yield lower segregation resistance than both FS and ESH mixtures, on the other hand the ESH mixture will result in high segregation resistance and workability characteristics than both EC and FS mixtures.

5.2.5 Effects of Parameters on Other Responses

For all mixes, the filling capacity J-ring flow, and J-ring height difference test results were positively influenced by w/b and HRWRA (%) parameters. An increase of either or both parameters leads to an increase in the measured response. However, an increase in the binder content alone affects the results negatively, showing decrease in the measured responses. Similar to slump flow and L-box results, mixes made with ESH aggregates showed the highest positive increase in response when one or both w/b and HRWRA (%) parameters are increased. As explained before, this is due to the high packing density of such mixtures. Expectedly, mixes made with EC showed the lowest increase when one or both w/b and HRWRA (%) parameters are increased.

Both initial and final setting times were affected by all three parameters. Increase of either or both w/b and HRWRA extended the set time and vice versa. In contrast, an increase in the binder content resulted in shortening of the setting time. No major difference was recorded between comparable mixes (same paste proportion) made with different aggregate types. This can be attributed to the fact that the setting times are governed predominately by the paste design rather than the aggregate types.

For all developed mixes, air content (%) was observed not to be influenced by any of the three investigated parameters. Bleed water was affected by both w/b and total binder content, where an increase in w/b increased the bleed water. On the other hand, an increase in total binder content reduced the bleed water. HRWRA (%) did not affect the bleed water of the concrete mixtures.

As explained in Chapter 4, for all developed mixes, the aggregate density played the major role in affecting the fresh unit weight, where the highest was recorded for FS mixes and the lowest for EC mixes. As for the influence of the examined parameters on the response, the fresh unit weight was influenced mainly by the binder content, as the binder content increased the fresh unit weight increased and vice versa.

For FS mixes, both 28-day air and oven dry unit weights were affected mainly by the w/b and secondarily by the binder content. When the binder content was increased, both 28-day air and oven dry unit weights were increased. An increase in w/b, however, decreased both 28-day air

and oven dry unit weight. Unexpectedly, only the total binder content affected the results of ESH and EC mixtures. An increase in the total binder content increased both unit weights. This behavior might be attributed to the high absorption rate of both aggregates (above 13%) that slowed the evaporation rate of water from the mixture. For all mixes, the HRWRA (%) did not have an effect on the results.

For all developed mixes, 7-day compressive strengths were affected by all three parameters. As the binder increased, the 7-day strength increased. In contrast, as the either or both HRWRA (%) and w/b increased the 7-day strength decreased. Nevertheless, it was expected that HRWRA (%) should not have any influence on the 7-day strength. This is because HRWRA (%) effect is typically weakened away after 24-48 hours. On the other hand, the 28-day compressive strengths were mainly affected by w/b and total binder content. An increase in w/b decreased the 28-day strengths, while an increase in total binder content increased the compressive strength.

As discussed in chapter 4, the developed EC mixtures had lower compressive strength than equivalent mixes with FS and ESH, while mixtures with ESH had the highest compressive strength, which is attributed to the aggregates properties and the quality of interfacial transition zone (ITZ) between the aggregates and the paste.

The figures illustrating the effect of the investigated mix design parameters on discussed responses are presented in **Appendix A**.

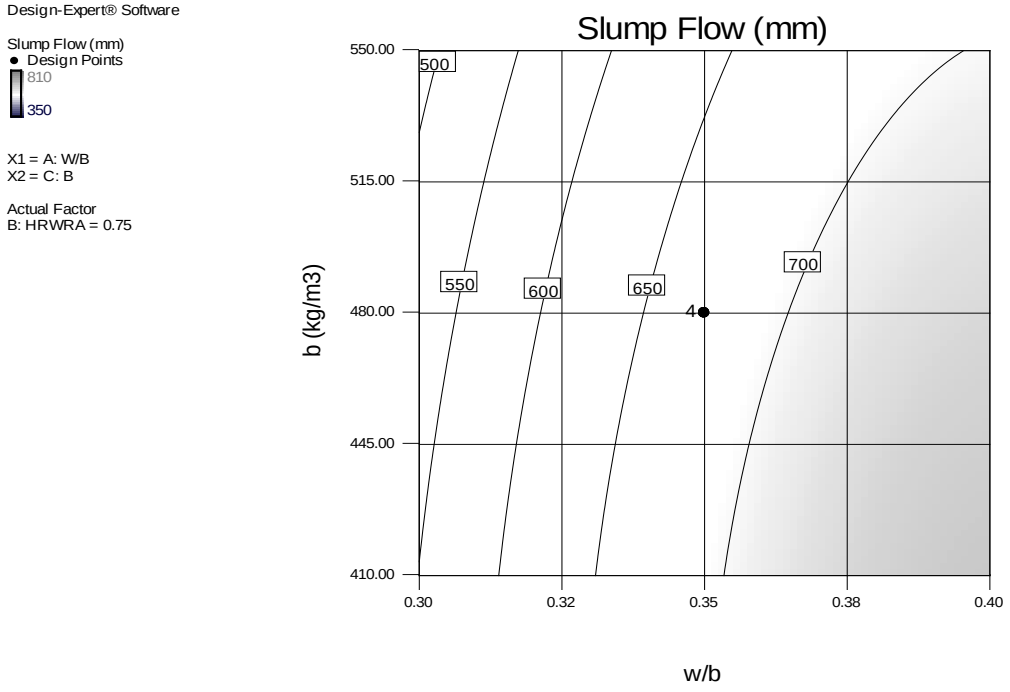

Figure 5.1 - Contours of slump flow changes of FS-LWSCC mixes with w/b, total binder content and HRWRA at 0.75 %

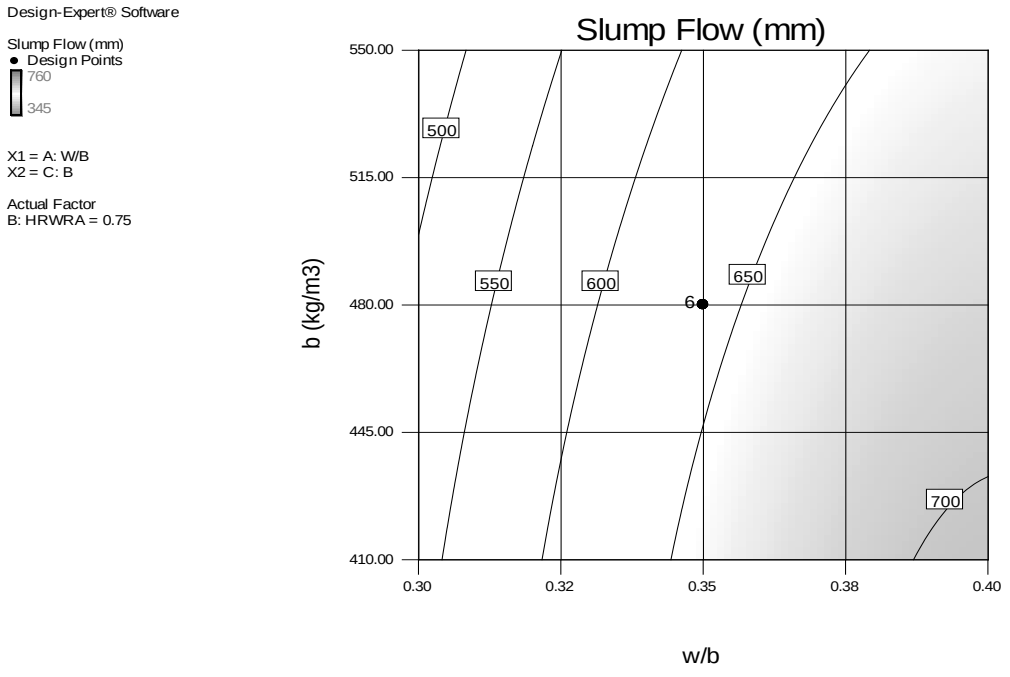

Figure 5.2 - Contours of slump flow changes of EC-LWSCC mixes with w/b, total binder content and HRWRA at 0.75 %

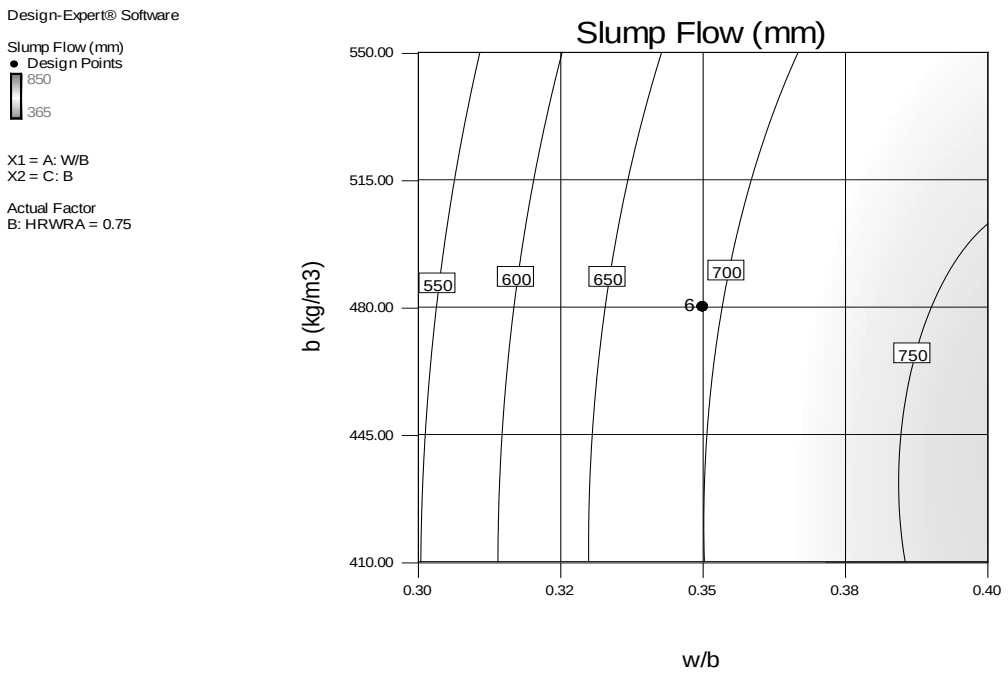

Figure 5.3 - Contours of slump flow changes of ESH-LWSCC mixes with w/b, total binder content and HRWRA at 0.75 %

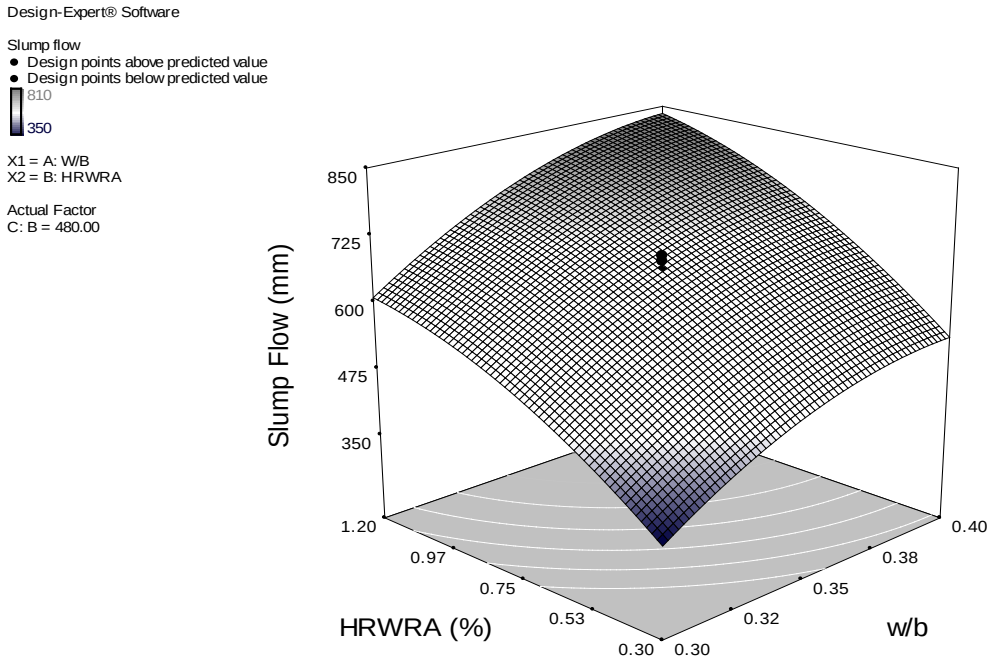

Figure 5.4 - Effect of w/b, HRWRA and total binder content at 480kg/m^{3}on the slump flow of FS-LWSCC mixes

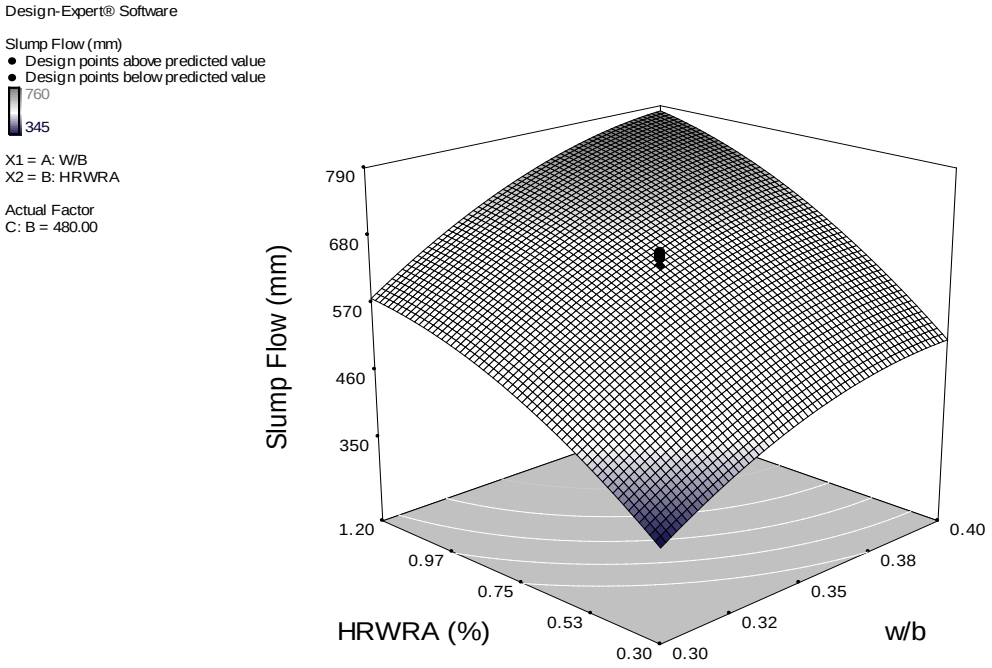

Figure 5.5 - Effect of w/b, HRWRA and total binder content at 480kg/m^3 on the slump flow of EC-LWSCC mixes

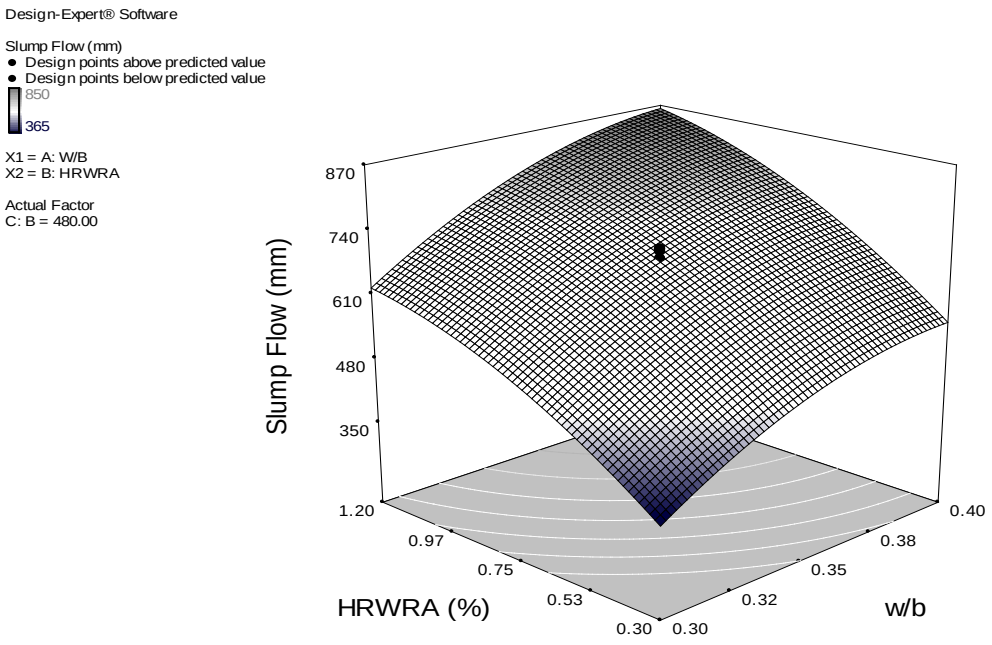

Figure 5.6 - Effect of w/b, HRWRA and total binder content at 480kg/m^3 on the slump flow of ESH-LWSCC mixes

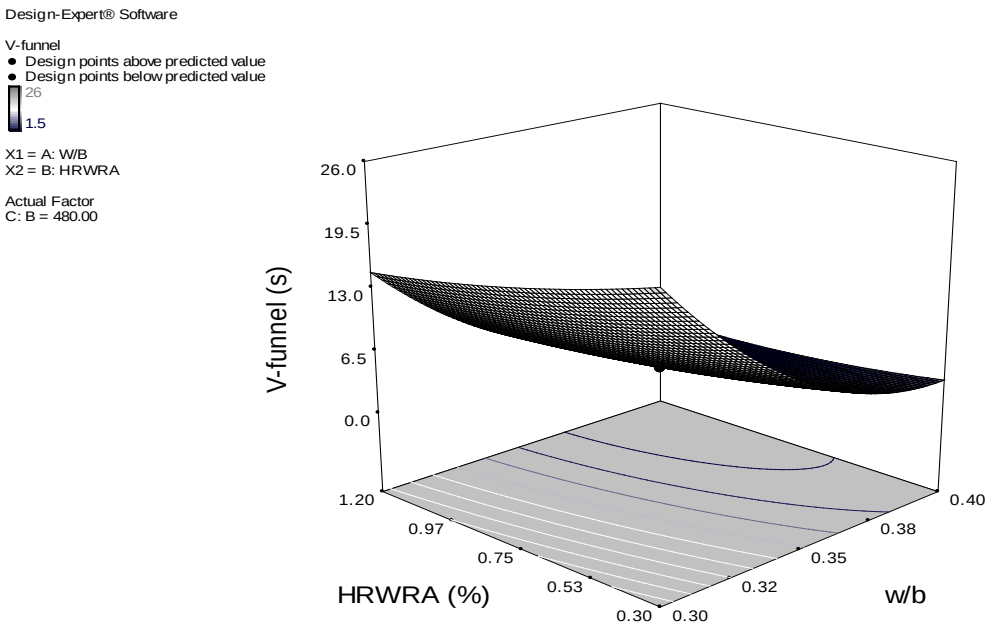

Figure 5.7 - Effect of w/b, HRWRA and total binder content at 480kg/m^3 on the V-funnel time of FS-LWSCC mixes

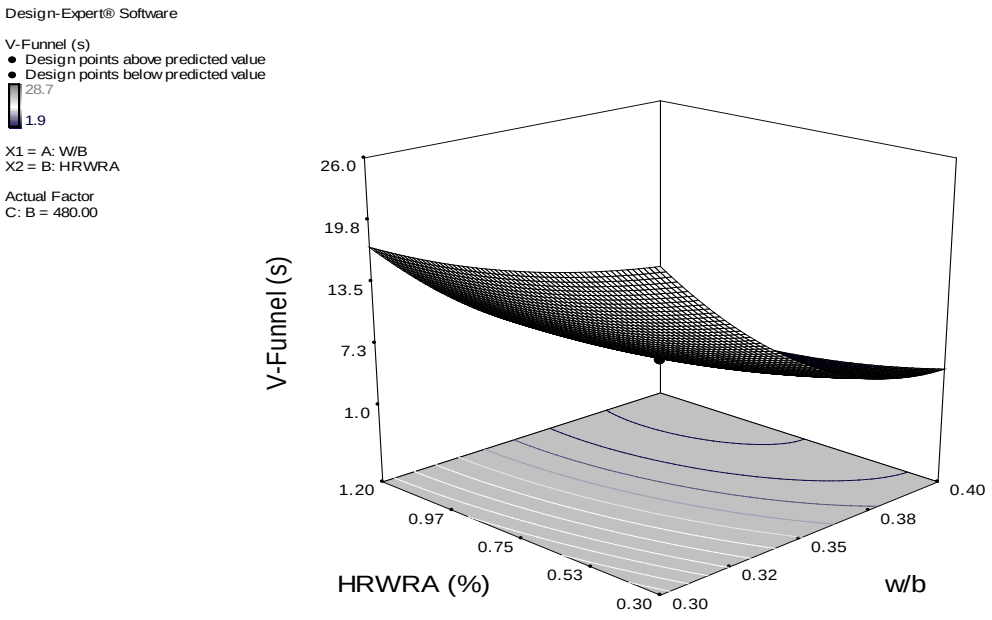

Figure 5.8 - Effect of w/b, HRWRA and total binder content at 480kg/m^3 on the V-funnel time of EC-LWSCC mixes

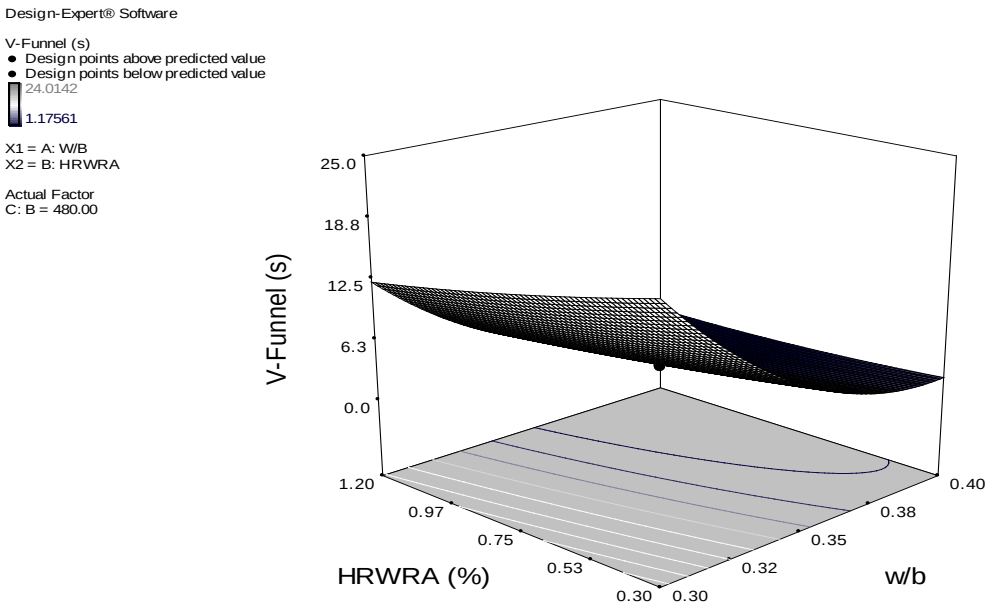

Figure 5.9 - Effect of w/b, HRWRA and total binder content at 480kg/m^3 on the V-funnel time of ESH-LWSCC mixes

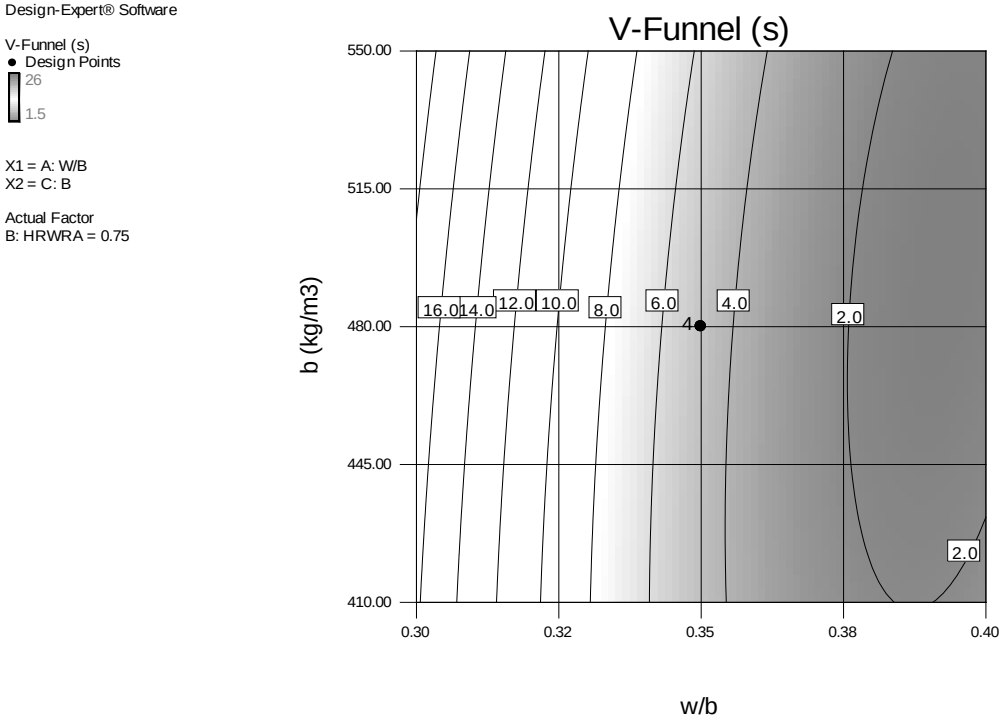

Figure 5.10 - Contours of V-funnel changes of FS-LWSCC mixes with w/b, total binder content and HRWRA at 0.75 %

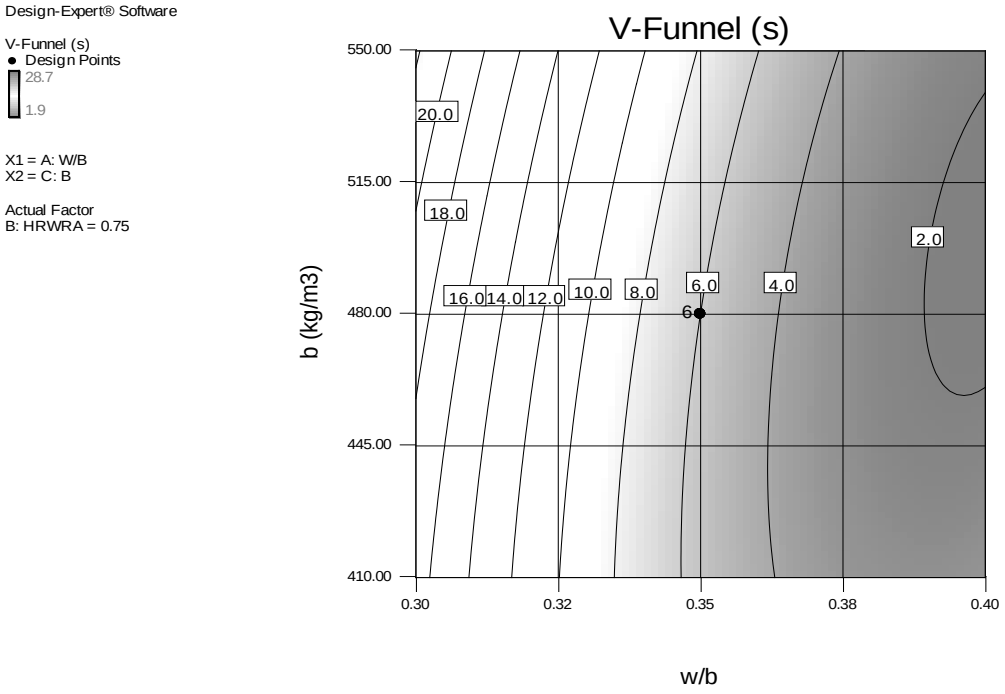

Figure 5.11 - Contours of V-funnel changes of EC-LWSCC mixes with w/b, total binder content and HRWRA at 0.75 %

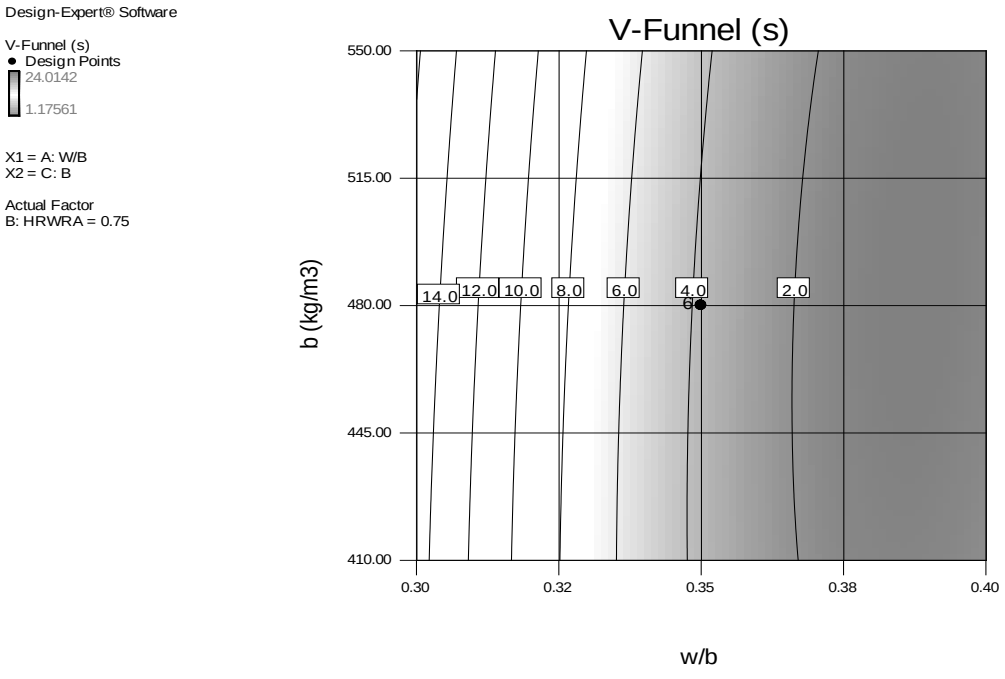

Figure 5.12 - Contours of V-funnel changes of ESH-LWSCC mixes with w/b, total binder content and HRWRA at 0.75 %

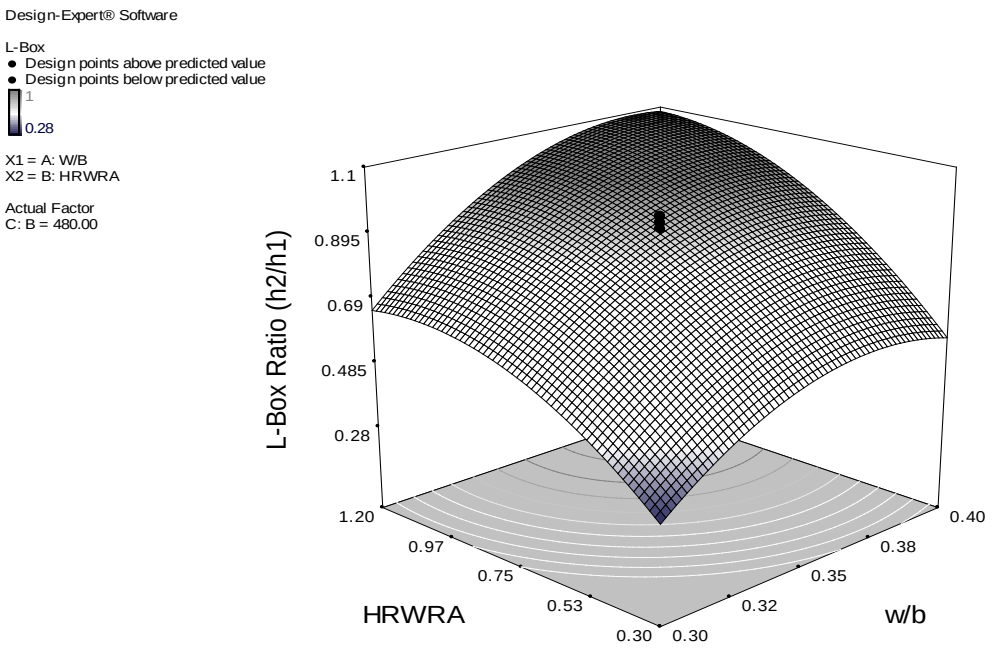

Figure 5.13 - Effect of w/b, HRWRA and total binder content at 480kg/m^{3}on the L-Box of FS-LWSCC mixes

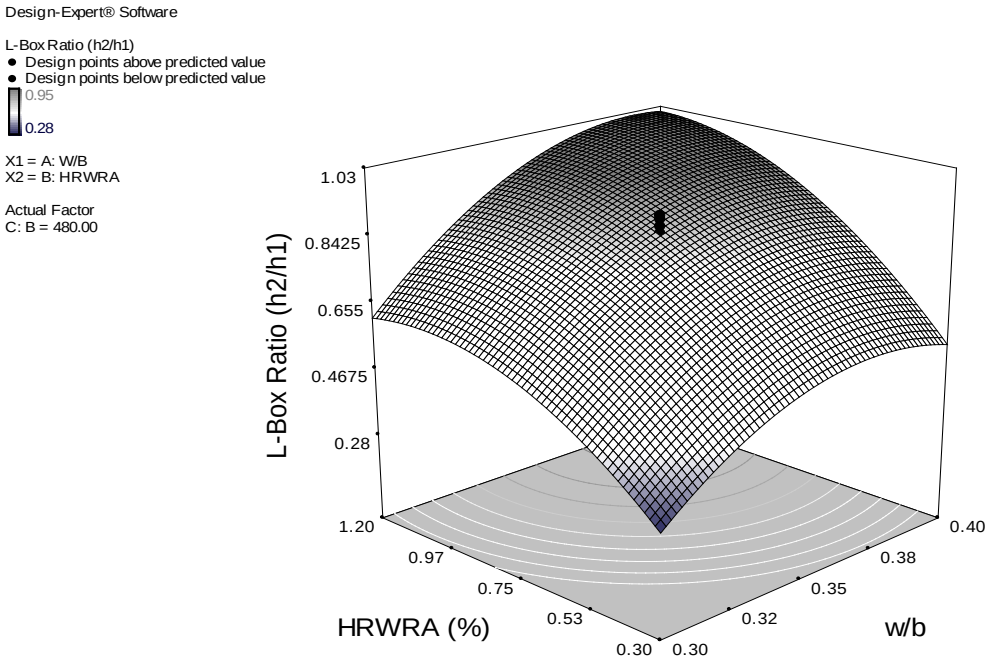

Figure 5.14 - Effect of w/b, HRWRA and total binder content at 480kg/m^{3}on the L-Box of EC-LWSCC mixes

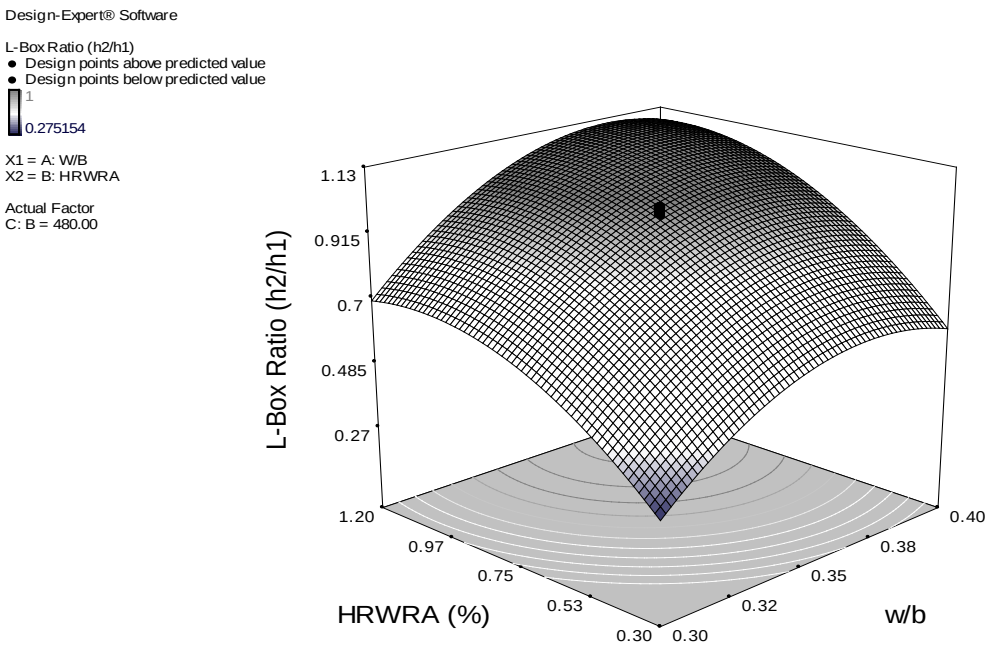

Figure 5.15 - Effect of w/b, HRWRA and total binder content at 480kg/m^{3}on the L-Box ratio of ESH-LWSCC mixes

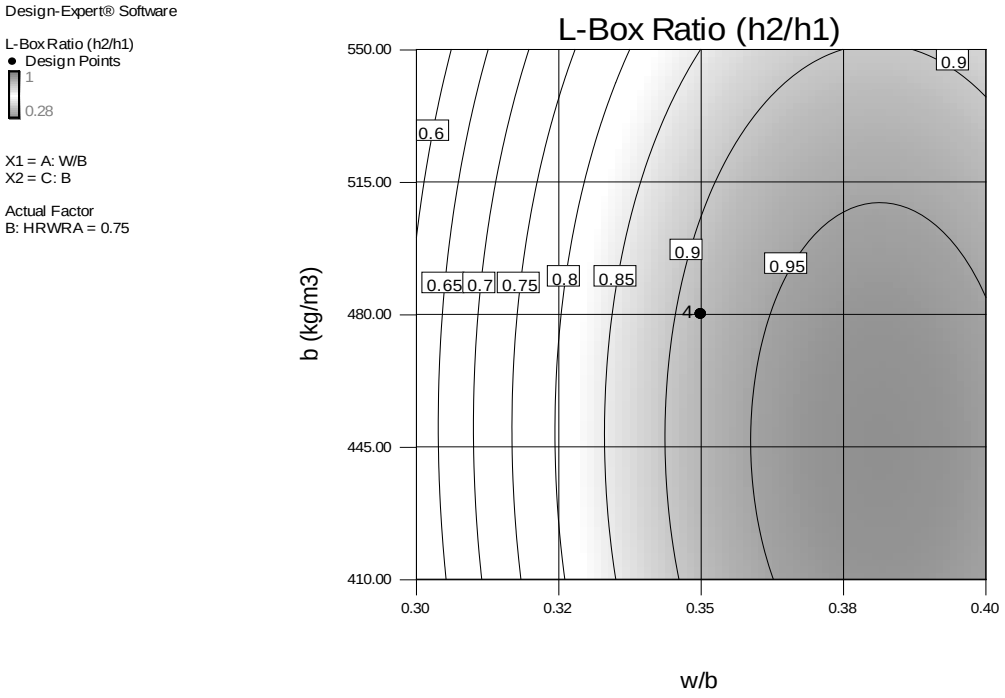

Figure 5.16 - Contours of L- Box ratio changes of FS-LWSCC mixes with w/b, total binder content and HRWRA at 0.75 %

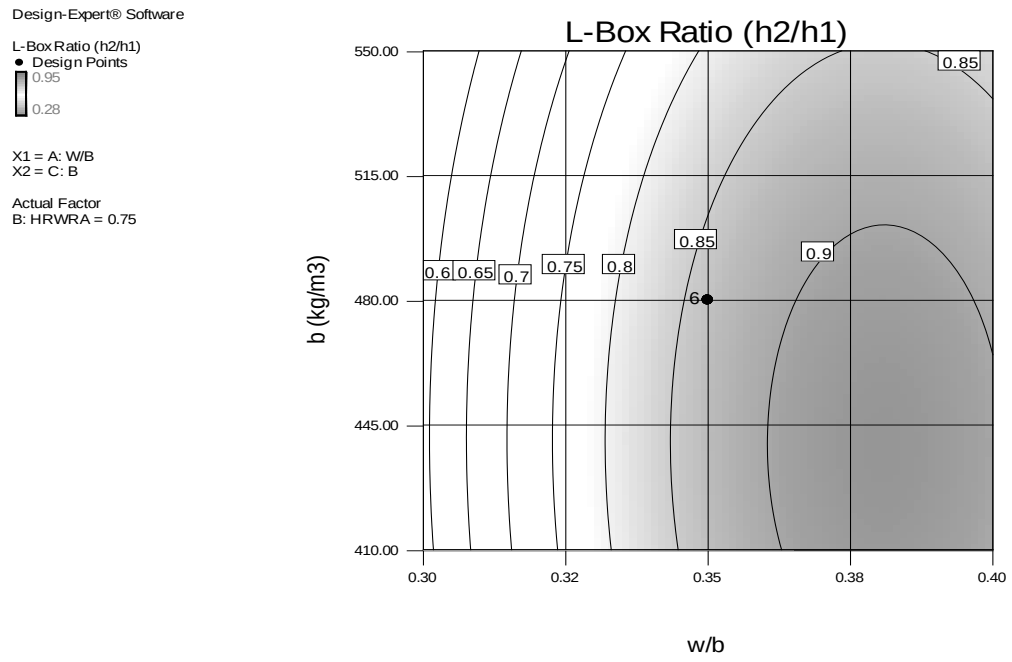

Figure 5.17 - Contours of L- Box ratio changes of EC-LWSCC mixes with w/b, total binder content and HRWRA at 0.75 %

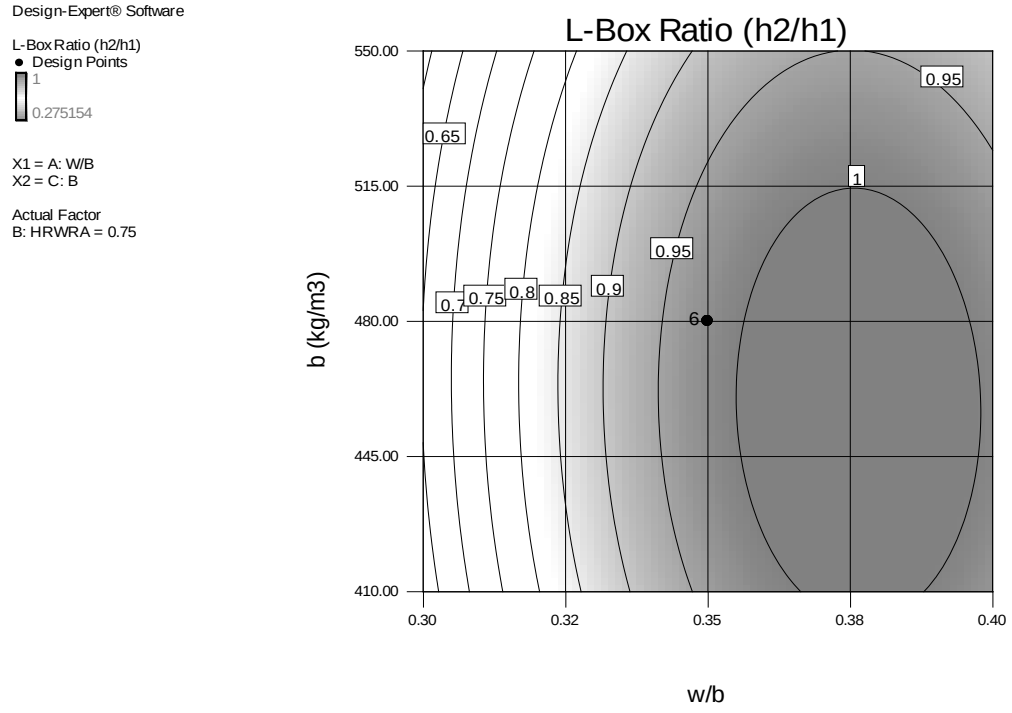

Figure 5.18 - Contours of L- Box ratio changes of ESH-LWSCC mixes with w/b, total binder content and HRWRA at 0.75 %

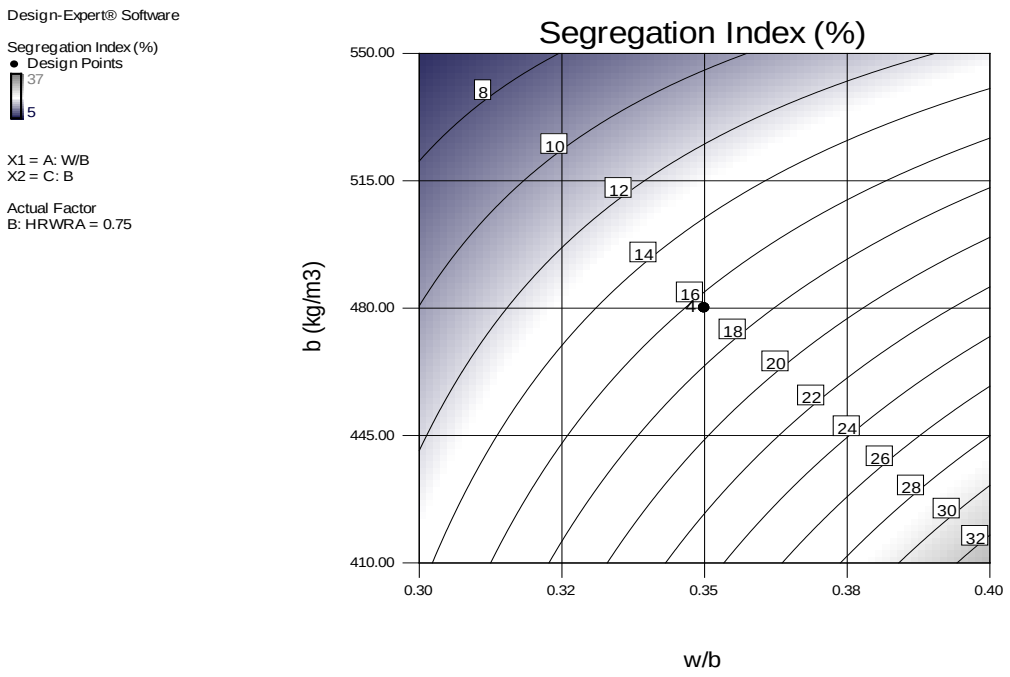

Figure 5.19 - Contours of segregation resistance changes of FS-LWSCC mixes with w/b, total binder content and HRWRA at 0.75 %

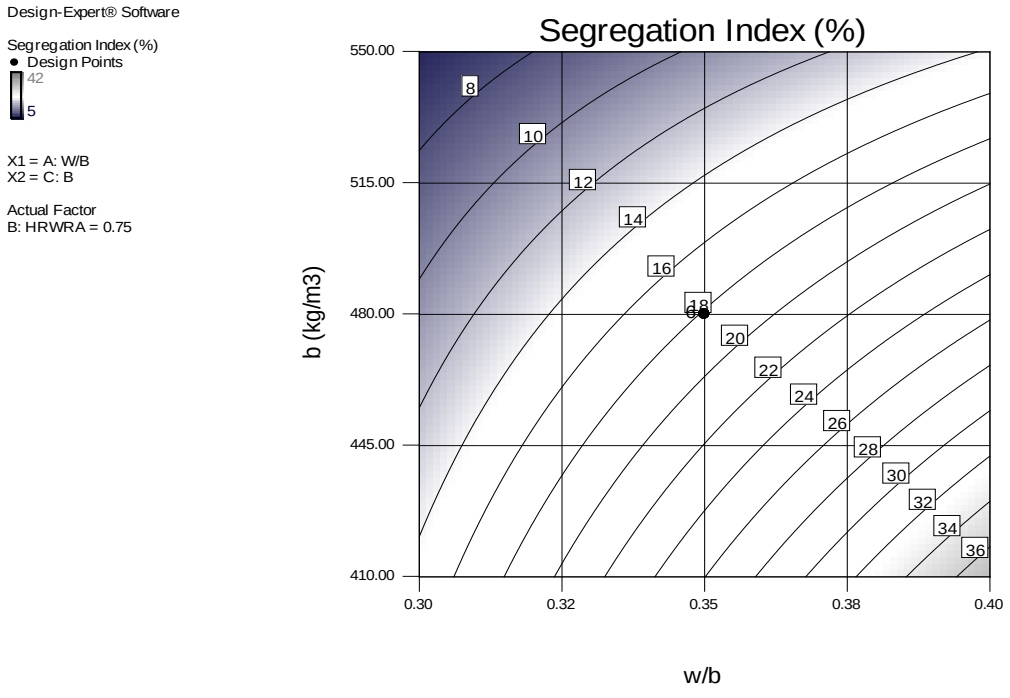

Figure 5.20 - Contours of segregation resistance changes of EC-LWSCC mixes with w/b, total binder content and HRWRA at 0.75 %

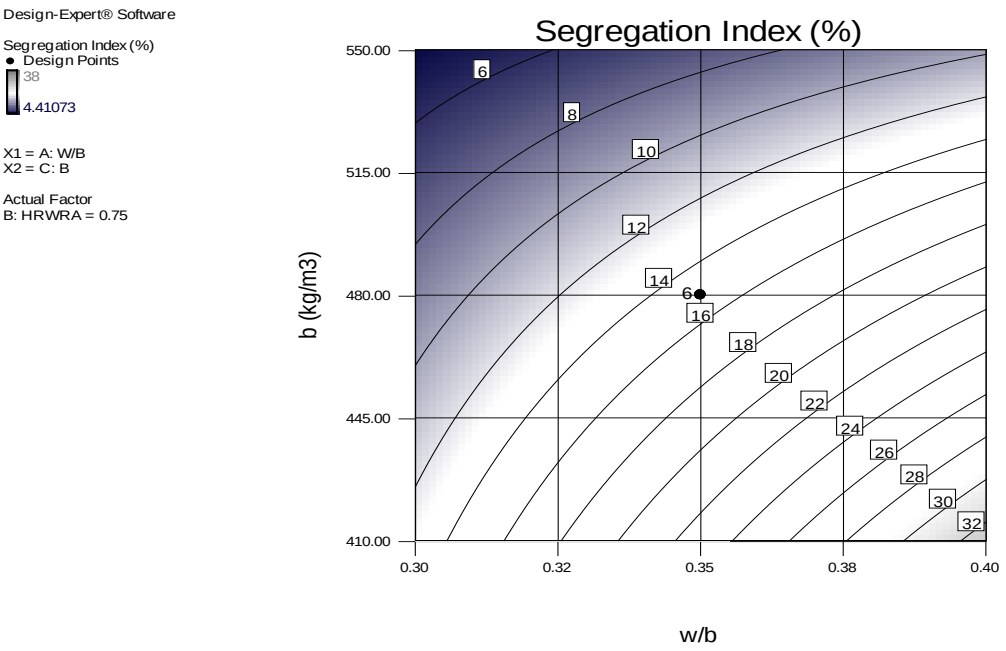

Figure 5.21 - Contours of segregation resistance changes of ESH-LWSCC mixes with w/b, total binder content and HRWRA at 0.75 %

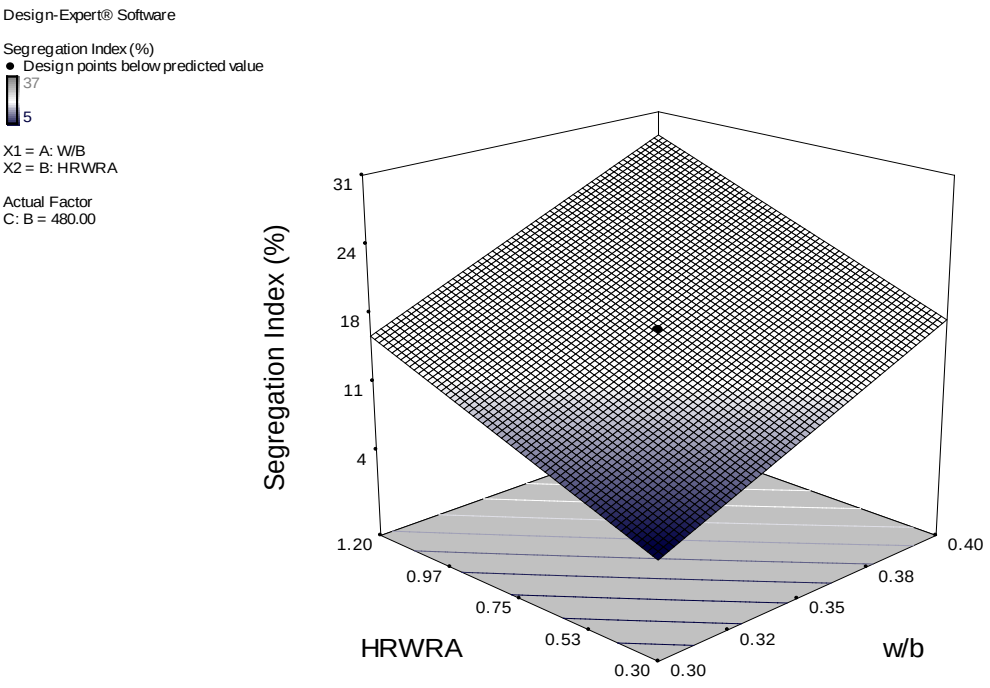

Figure 5.22 - Effect of w/b, HRWRA and total binder content at 480kg/m^3 on the SSR of FS-LWSCC mixes

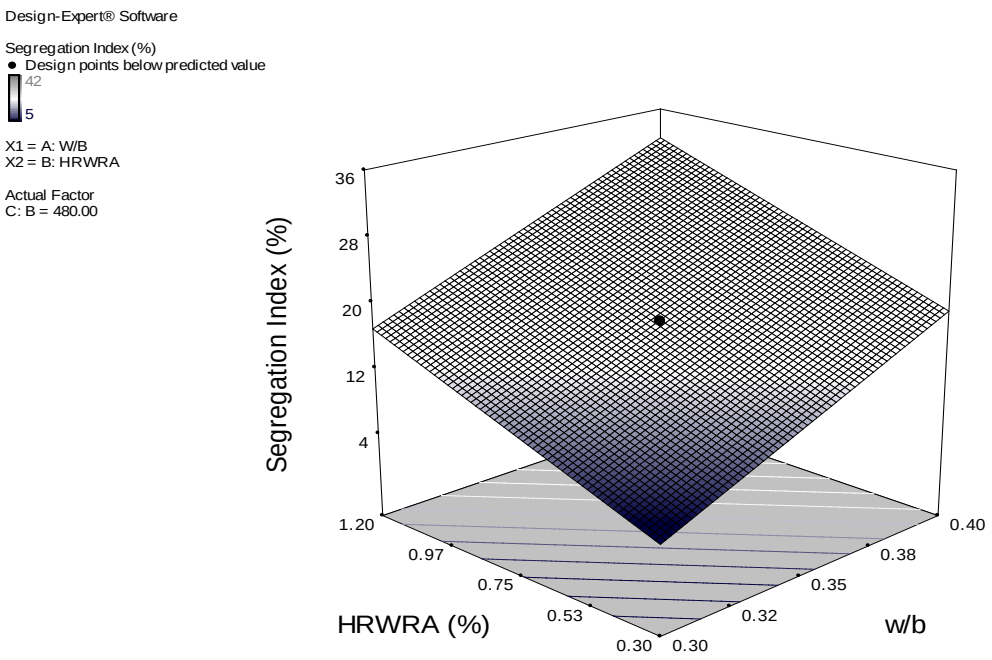

Figure 5.23 - Effect of w/b, HRWRA and total binder content at 480kg/m^3 on the SSR of EC-LWSCC mixes

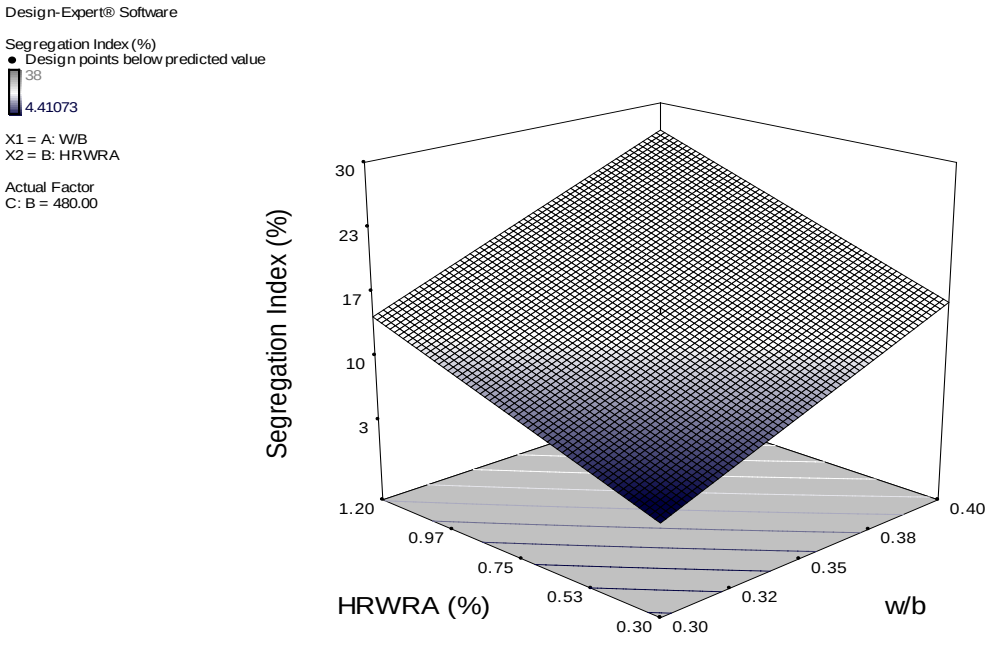

Figure 5.24 - Effect of w/b, HRWRA and total binder content at 480kg/m^3 on the SSR of ESH-LWSCC mixes

5.2.6 Statistical Evaluation of the Test Results

A model analysis of the response was carried out to determine the effective test parameters on the LWSCC. Using general linear model analysis of variance (GLM-ANOVA), the measured fresh and hardened properties of LWSCC such as slump flow, V-funnel flow time, J-Ring flow, J-Ring height difference, L-box, filling capacity, bleeding, air content, initial and final setting time, sieve segregation resistance, fresh unit weight, 28-day air dry unit weight, 28-day oven dry unit weight, and 7- and 28-day compressive strength, were given as the dependent variables while the experimental test parameters (‘‘w/b’’, ‘‘b’’, and ‘‘HRWRA’’) were selected as the independent factors/variables. The GLM-ANOVA was performed and the effect of test parameters and their percent contributions on the above mentioned properties of LWSCC were determined.

The *p*-values in Tables 5.1, 5.2 and 5.3 show the significance of the given test parameters on the test results of FS, EC and ESH LWSCC mixtures. If a system has *p*-value (Probabilities) of $\leq$ 0.05, it is accepted as a significant factor on the test result. If the evidence indicates that the parameter is not zero; the proposed parameter has a highly significant influence on the measured response (Patel et al. 2004; Sonebi 2004a; Sonebi 2004b).

The contributions of each parameter on the measured test results are also presented in Tables 5.1, 5.2 and 5.3 where the effect of the independent parameters on the measured response is calculated. The higher the contribution, the higher the effectiveness of the parameter on the response, and vice versa.

5.2.7 Mathematical Formulation of LWSCC Properties

The mathematical relationship between the independent variables and the responses can be estimated using the model. Linear or quadratic relationships are simplified by using a backward stepwise technique. Evaluating the contribution of each parameter and its significant influence on the response is a key tool used in accepting certain contributions (Whitcom and Anderson 2004; Pradeep 2008).

When establishing a relationship for each response, a regression analysis is performed on the basis of a partial model containing only the terms which are statistically significant ($p \leq 0.05$). Then, t-statistics are calculated and the terms that are statistically insignificant are eliminated. This process is repeated until the partial model contains only the significant terms.

The Design Expert v.8.1 statistical software was used to drive the models by the least square method (Stat-Ease, 2009), where the suggested equation (Eq. 5.1) can be linear, quadratic, cubic or quartic. For example, the structure of quadratic statistical model is as follows:

$$Y = a_0 + a_1X_1 + a_2X_2 + a_3X_3 + a_{12}X_1X_2 + a_{13}X_1X_3 + a_{23}X_2X_3 + a_4X_1^2 + a_5X_2^2 + a_6X_3^2 \qquad (5.1)$$

Where Y represents the model response and X_1, X_2 and X_3 represent the independent variables.

The interaction between the three variables (X_i X_j) and the quadratic effect (X_i^2) of variables were also considered in the proposed models. By trial and error method, the best-fit models were identified from different probability distribution functions such as normal (Gaussian), Gaussian inverse, Gamma, Poisson and Binomial with different link functions such as identity, log, and power. The 't' test and/or 'chi square' test were carried out to decide the statistical significance of variables. The null hypothesis was checked for all estimated coefficients such as a_0, a_1, a_3 etc.

The null hypothesis is a presupposition that the true value of coefficient is zero. In other words, the variable or variables associated with that coefficient are statically insignificant and it has no influence on the response Y. If the probability greater than 't statistics' or 'chi square statistics' is less than or equal to 0.05 (5%), the null hypothesis (the coefficient value is zero), can be rejected and it is established that the variable or variables with the estimated coefficient has significant influence on the response. If the probability greater than 't statistics' or 'chi square statistics' is more than 0.05 (5%), the null hypothesis (the coefficient value is zero), can be accepted and it can be established that the variable or variables with the estimated coefficient has no influence on the response and hence that variable or variables cannot be included in the model.

The experimental data were fed to a statistical model through multiple linear regression analysis which consisted of the terms which were statistically significant at a 0.05 level. R^2 statistic,

which gives a correlation between the experimental data and the predicted response, should be high enough (R^2 = 0.80) for a particular model to be significant (Muthukumar and Mohan 2004).

5.2.8 Statistical Analysis of the Response Models

Analysis of the statistical parameters of the derived models, along with the relative significance, and the contribution % of each parameter on the results are given in Tables 5.1 to 5.3. The R^2 values of the FS, EC and ESH - LWSCC response models for the slump flow, V-funnel flow, J-Ring flow, J-Ring height difference, L-box, filling capacity, sieve segregation resistance, bleeding, fresh air content, initial set time, final set time, 7- day compressive strength, 28-day compressive strength, fresh unit weight, 28-day air dry unit weight, and 28-day oven dry unit weight were found to be (0.96, 0.96, 0.96), (0.97, 0.96, 0.97), (0.95, 0.94, 0.96), (0.96, 0.96, 0.94), (0.93, 0.93, 0.94), (0.95, 0.95, 0.95), (0.94, 0.93, 0.90), (0.58, 0.59, 0.57), (0.53, 0.54, 0.54), (0.93, 0.74, 0.70), (0.95, 0.94, 0.93), (0.88, 0.90, 0.88), (0.86, 0.93, 0.93), (0.73, 0.73, 0.73), (0.54, 0.56, 0.56), and (0.80, 0.75, 0.75), respectively.

Statistically significant models for all three types of lightweight aggregates with a high correlation coefficient R^2 > 0.90 were established for the slump flow, V-funnel, J-ring, J-Ring height difference, L-box, filling capacity, sieve segregation resistance and final set time. A relatively lower R^2 (0.86 to 0.93) was obtained for 7-day and 28-day compressive strength, and R^2 of (0.73 to 0.80) were estimated for the fresh and 28-day oven dry unit weights. Low R^2 of (0.53 to 0.59) was obtained for bleeding, air content (%) and 28-day air dry unit weight.

As for the significance of the parameters on the responses, for example for the slump flow; the order of influence of the test variables is: the dosage of HRWRA, w/b, and the binder content. The dosage of HRWRA had the greatest effect on the slump flow. The effect of binder content was insignificant to the response. This can be attributed to the fact that flowability is driven by HRWRA dose and w/b rather than the binder content. In fact, to secure the same slump flow with more binder content, an increase of both HRWRA and w/b is necessary.

As for the V-funnel time, the order of influence of the test variables on the response is: w/b, the dosage of HRWRA and then binder content. Whereas the dosage of HRWRA, w/b, and the binder content in this order of influence, are contributing to the responses of J-ring flow, J-ring

height different, L-box and filling capacity. The sieve segregation resistance response is greatly influenced by the total binder content, followed by w/b and then the dosage of HRWRA. The contribution % of each parameter on the rest of the results is given in Tables 5.1 to 5.3.

The high correlation coefficient of responses demonstrates excellent correlation, where it can be considered that at least 95% of the measured values can be accounted for with the proposed models (Patel et al. 2004; Sonebi 2004a; Sonebi 2004b).

The derived equations of the modelled responses: slump flow, V-funnel flow time, J-Ring flow, J-Ring height difference, L-box, filling capacity, bleeding, air content, initial and final setting time, sieve segregation resistance test, fresh unit weight, 28-day air dry unit weight, 28-day oven dry unit weight, and 7- and 28-day compressive strength are summarized in Tables 5.4, 5.5 and 5.6 for FS, EC and ESH-LWSCC mixtures, respectively. In these Tables, mixture variables expressed in actual factored values presents a comparison of various parameters as well as the interactions of the modelled responses. The model constants are determined by multi-regression analysis and are assumed to be normally distributed. A negative estimate signifies that an increase of the given parameter results in a reduction of the measured response. For any given response, the presence of parameters with coupled terms, such as $(w/b)^2$ and $(w/b)^3$ indicates that the influence of this parameter (w/b) is quadratic and cubic, respectively.

The key derived models are summarized with the mixture variables expressed in coded values as follows:

Slump Flow

If the slump flow of concrete is between 550 and 850 mm without any segregation, the concrete can be qualified for LWSCC. Of course, other fresh concrete properties such as V-funnel flow time, L-box ratio and segregation index are also important to thoroughly evaluate the fresh LWSCC properties. The proposed slump flow models are as follows:

FS-LWSCC:

$$\text{Slump Flow (mm)} = + 674.04 + 102.21*A + 139.91 * C - 26.78 * B + 9.38 * A * C + 5.62 * A * B + 4.37* B * C - 46.09 * A^2 - 43.59 * C^2 - 7.16 * B^2 \quad (5.2)$$

EC-LWSCC:

$$\text{Slump Flow (mm)} = + 638.81 + 89.68 * A + 124.21 * C - 26.25 * B + 10.00 * A * C + 6.25 * A * B + 5.00 * C * B - 39.69 * A^2 - 42.14 * C^2 - 5.01 * B^2 \quad (5.3)$$

ESH-LWSCC:

$$\text{Slump Flow (mm)} = + 692.94 + 108.72 * A + 143.34 * C - 16.02 * B + 9.38 * A * C + 4.37 * A * B + 9.37 * B * C - 46.84 * A^2 - 44.13 * C^2 - 9.43 * B^2 \quad (5.4)$$

It can be seen in the three slump flow Equations (5.2 to 5.4), that the response is presented in quadratic model. Further a negative estimate before parameter B (total binder content) indicates that increase of B (total binder content) results in a reduction of the measured response, while positive sign before parameters A (w/b) and C (HRWRA %) indicates that increase of either parameter results in increase of the measured response (slump flow).

The highest coefficients for slump flow equation were derived for mixes made with ESH aggregates (a_0 = 692.94, a_1 = 108.72, a_2 = 143.34, a_3 = - 16.02, a_{12} = 9.38, a_{13} = 4.37, a_{23} = 9.37, a_4 = - 46.84, a_5 = - 44.13, a_6 = - 9.43) indicating high expect response of slump flow compared to other types of (LWA), while the lowest coefficients were for mixes made with EC aggregates (a_0 = 638.81, a_1 = 89.68, a_2 = 124.21, a_3 = - 26.25, a_{12} = 10.00, a_{13} = 6.25, a_{23} = 5.00, a_4 = - 39.69, a_5 = - 42.14, a_6 = - 5.01) signifying low predicted response of slump flow for these mixes.

V-Funnel

The proposed V-Funnel models are as follows:

FS-LWSCC:

$$\text{V-Funnel (s)} = +4.82 - 7.87 * A - 2.16 * C + 0.60 * B + 1.15 * A * C - 0.90 * A * B + 0.050 * B * C + 4.67 * A^2 + 0.77 * C^2 + 0.36 * B^2 \quad (5.5)$$

EC-LWSCC:

$$\text{V-Funnel (s)} = +5.99 - 8.49 * A - 2.27 * C + 1.18 * B + 0.65 * A * C - 1.57 * A * B - 0.47 * B * C + 4.33 * A^2 + 1.35 * C^2 + 0.69 * B^2 \quad (5.6)$$

ESH-LWSCC:

$$\text{V-Funnel (s)} = +3.77 - 6.93 * A - 1.97 * C + 0.30 * B + 1.34 * A * C - 0.47 * A * B + 0.28 * B * C + 4.55 * A^2 + 0.40 * C^2 + 0.20 * B^2 \quad (5.7)$$

Based on the derived V-funnel Equations (5.5 to 5.7), the response is presented in quadratic model. A positive estimate before parameter B (total binder content) indicates that increase of B (total binder content) results in a increase of the measured response, whereas negative sign before parameters A (w/b) and C (HRWRA %) demonstrate that increase of either parameter results in decrease of V-funnel time.

L- Box

The following models are proposed for L-Box:

FS-LWSCC:

$$\text{L-Box Ratio (h2/h1)} = +0.92 + 0.17 * A + 0.21 * C - 0.032 * B + 0.044 * A * C - 3.750E-003 * A * B + 0.024 * B * C - 0.13 * A^2 - 0.12 * C^2 - 0.034 * B^2 \quad (5.8)$$

EC-LWSCC:

$$\text{L-Box Ratio (h2/h1)} = + 0.86 + 0.16 * A + 0.19 * C - 0.031 * B + 0.044 * A * C - 1.250E\text{-}003 * A * B + 0.024 * B * C - 0.13 * A^2 - 0.12 * C^2 - 0.027 * B^2 \quad (5.9)$$

ESH-LWSCC:

$$\text{L-Box Ratio (h2/h1)} = + 0.98 + 0.17 * A + 0.22 * C - 0.025 * B + 0.026 * A * C - 6.317E\text{-}003 * A * B + 0.023 * B * C - 0.16 * A^2 - 0.14 * C^2 - 0.046 * B^2 \quad (5.10)$$

Filling Capacity

The filling capacity models are as follows:

FS-LWSCC:

$$\text{Filling Capacity (\%)} = + 90.96 + 17.68 * A + 22.15 * C - 3.33 * B + 2.00 * A * C - 0.50 * A * B + 1.50 * B * C - 12.19 * A^2 - 13.19 * C^2 - 2.88 * B^2 \quad (5.11)$$

EC-LWSCC:

$$\text{Filling Capacity (\%)} = + 87.00 + 16.17 * A + 20.25 * C - 3.10 * B + 1.75 * A * C - 0.50 * A * B + 1.50 * B * C - 11.71 * A^2 - 12.85 * C^2 - 2.69 * B^2 \quad (5.12)$$

ESH-LWSCC:

$$\text{Filling Capacity (\%)} = + 97.47 + 17.53 * A + 22.25 * C - 2.70 * B + 0.18 * A * C - 0.71 * A * B + 1.43 * B * C - 14.84 * A^2 - 15.03 * C^2 - 4.09 * B^2 \quad (5.13)$$

The responses are presented in quadratic model for both L- box and Filling capacity Equations (5.8 to 5.13). A positive sign before parameters A (w/b) and C (HRWRA %) specifies that increase of either parameter results in increase of the measured response (L-box and filling capacity). However, a negative estimate before parameter B (total binder content) indicates that an increase of B (total binder content) results in a reduction of the L-box and filling capacity responses.

Segregation Index

The segregation index can be predicted by flollowing models:

FS-LWSCC:

Segregation Index (%) = +16.44 + 6.41 * A + 5.59 * C - 6.89 * B + 0.13 * A * C - 3.38 * A * B - 1.38 * B * C (5.14)

EC-LWSCC:

Segregation Index (%) = +18.15 + 7.60 * A + 6.51 * C - 7.83 * B + 0.000 * A * C - 3.75 * A * B - 1.75 * B * C (5.15)

ESH-LWSCC:

Segregation Index (%) = + 15.09 + 6.24 * A + 5.45 * C - 7.80 * B + 0.19 * A * C - 3.75 * A * B - 1.89 * B * C (5.16)

For all three models, the segregation index is presented in a linear relationship with the investigated parameters, as shown in Equations (5.14 to 5.16).

7-day Compressive Strength

The 7-day compressive strength models are as follows:

FS-LWSCC:

7-day Compressive Strength (MPa) = + 27.44 -5.24 * A - 1.42 * C + 2.46 * B (5.17)

EC-LWSCC:

7-day Compressive Strength (MPa) = + 26.50 - 5.59 * A - 1.30 * C + 2.06 * B (5.18)

ESH-LWSCC:

7-day Compressive Strength (MPa) = + 30.25 - 5.48 * A -1.55 * C + 3.27 * B (5.19)

The 7-d compressive strength is presented in linear models (Equations 5.17 to 5.19) for all three lightweight aggregates models.

28-day Compressive Strength

The 28-day compressive strength models are as follows:

FS-LWSCC:

28-day Compressive Strength (MPa) = + 38.06 - 7.00 * A - 1.71 * C + 3.38 * B (5.20)

EC-LWSCC:

28-day Compressive Strength (MPa) = + 37.74 - 7.53 * A - 1.42 * C + 1.96 * B + 0.25 * A * C + 1.00 * A * B + 0.25* B * C - 1.50 * A^2 - 0.47 * C^2 - 2.42 * B^2 (5.21)

ESH-LWSCC:

28-day Compressive Strength (MPa) = + 44.83 - 7.31 * A - 1.86 * C + 4.50 * B - 0.023 * A * C + 0.80 * A * B - 0.061* B * C - 2.05 * A^2 - 0.84 * C^2 - 1.75 * B^2 (5.22)

The 28-day compressive strength is presented in linear model for FS-LWSCC (Equation 5.20) and in quadratic models for EC-LWSCC and ESH-LWSCC lightweight aggregates models (Equations 5.21 and 5.22).

Fresh Unit Weight

The following models are proposed for fresh unit weight:

FS-LWSCC:

Fresh Unit Weight (kg/m^3) = +1904.53 - 7.71 * A + 8.05 * C + 25.87 * B - 22.00 * A * C - 20.00 * A * B - 19.50* B * C + 9.08 * A^2 + 14.08 * C^2 + 23.47* B^2 (5.23)

EC-LWSCC:

Fresh Unit Weight (kg/m^3) = +1603.09 -6.51 * A + 6.72 * C + 21.64 * B - 18.50 * A * C - 17.00 * A * B -16.50 * B * C + 6.89 * A^2 + 10.70 * C^2 + 18.64* B^2 (5.24)

ESH-LWSCC:

Fresh Unit Weight (kg/m^3) = + 1786.64 - 7.23 * A + 7.53 * C + 24.23 * B - 20.60 * A * C - 18.73 * A * B - 18.26* B * C + 7.63 * A^2 + 11.83 * C^2 + 20.85* B^2 (5.25)

The fresh unit weight is presented in quadratic models (Equations 5.23 to 5.25) for all three lightweight aggregates models.

28-day Air Dry Unit Weight

The following models are proposed for 28-day unit weight:

FS-LWSCC:

Air Dry Unit Weight (kg/m^3) = + 1844.11 - 27.91 * A - 5.14 * C + 11.75 * B (5.26)

EC-LWSCC:

Air Dry Unit Weight (kg/m^3) = + 1517.55 -2.40 * A +7.08 * C + 23.20 * B - 23.50* A * C - 18.75 * A * B - 17.75 * B * C (5.27)

ESH-LWSCC:

Air Dry Unit Weight (kg/m^3) = + 1691.46 - 2.51 * A + 7.80 * C + 25.82 * B - 26.22* A * C - 20.84 * A * B - 19.67 * B * C (5.28)

The fresh unit weight is presented in linear models for all three lightweight aggregates (Equations 5.26 to 5.28).

The significance of each of the three parameters (w/b, B and HRWARA) on influencing LWSCC properties in each of the above equations is presented in Tables 5.1 to 5.3. Also, these Tables present the effective parameters for each of LWSCC properties.

For all three types of lightweight aggregates, the highest coefficients for the L-box, filling capacity, 7-day compressive strength as well as 28-compressive strength equations were derived for mixes made with ESH aggregates. This indicates that the highest predicted response of these models is achieved when ESH aggregates are used. The lowest coefficients recorded for mixes made with EC-LWSCC mixes signify the lowest predicted response for the L-box, filling capacity, 7-day compressive strength and 28-compressive strength when EC aggregates are used.

For the V-funnel and segregation index equations, the highest coefficients were derived for mixes made with EC aggregates indicating the highest predicted values of these models are obtained when EC aggregates are used. However the lowest coefficients were recorded for mixes made with ESH aggregates, suggesting the lowest predicted values for V-funnel and segregation index with ESH aggregates.

The highest coefficients of both fresh and 28-day air dry unit weights equations were derived for mixes made with FS aggregates indicating the highest values attained for FS mixes. The lowest coefficients were recorded for EC mixes which demonstrates the lowest predicted response.

5.2.9 Repeatability of the Test Parameters

The repeatability is evaluated statistically by means of C.O.V (coefficient of variance) and relative error. The estimated error is calculated using Equation 5.29, according to a 95% confidence interval (CI) using the student's *t*-distribution (Gosset 1908) and relative error using Equation 5.30:

$$\text{Estimated error @ (95\% CI)} = 2.393\ \sigma / (\sqrt{n}) \text{ and,} \quad (5.29)$$

$$\text{Relative error (\%)} = 2.393\ \sigma / (\mu\sqrt{n}) \quad (5.30)$$

where σ = standard deviation; n = number of observation; μ = the mean value of the observation, and 2.39 is the coefficient representing the 95% confidence interval for the student's distribution for n = 6

The statistical mean (μ) is the mathematical average of all the observations collected for a response. It provides reliable idea about the central tendency of the data being collected and it is calculated using Equation 5.31, as follows,

$$\mu = 1/n \sum_{i=1}^{n} x_i \tag{5.31}$$

where, the observed response values are (x_1, x_2, x_3,…, x_n)

The standard deviation (σ) is a measure of the dispersion of a set of observations from its mean; a low standard deviation indicates that the data points tend to be very close to the mean, whereas high standard deviation indicates that the data points are spread out over a large range of values. The standard deviation (σ) is calculated using Equation 5.32:

$$\sigma = \sqrt{\frac{1}{n-1} \sum_{i=1}^{n} (x_i - \mu)^2} \tag{5.32}$$

where n = number of observation; μ = the mean value of the observations, (x_1, x_2, x_3,…, x_n) are the observed values of the response.

The coefficient of variance (C.O.V) is defined as statistical measure of the dispersion of observations in a data series around the mean, and is calculated using Equation 5.33:

$$C.O.V = \sigma/\mu \tag{5.33}$$

The repeatability of test parameters at central points is given in Tables 5.7, 5.8 and 5.9, for mixtures FS, EC and ESH - LWSCC 15 to 20. These tables show the mean results, standard

deviation and coefficient of variance (COV), as well as the standard errors and the relative errors, with 95% confidence limit of measured response of the six repeated mixes measuring: slump flow, V-funnel flow time, J-Ring flow, J-Ring height difference, L-box, filling capacity, bleeding, air content, initial and final setting time, sieve segregation resistance test, fresh unit weight, 28-day air dry unit weight, 28-day oven dry unit weight, and 7- and 28-day compressive strength.

The relative errors at the 95% confidence limit for slump flow, V-funnel flow time, J-Ring flow, L-box, filling capacity, air content, initial and final setting time, sieve segregation resistance test, fresh unit weight, 28-day air dry unit weight, 28-day oven dry unit weight, and 7- and 28-day compressive strength in all three LWSCC models (FS, EC and ESH- LWSCC) are found to be limited to 0.6% - 10%. On the other hand, the relative errors for J-Ring height difference and bleeding ranged approximately between 18.1% and 35.7%. The relative error was defined as the value of the error with 95% confidence limit divided by the mean value.

5.3 Summary

The derived statistical models and response table can be used as tools for predicting the fresh and hardened properties of LWSCC mixtures and further optimizing the mixtures in a simplified and timely fashion (As discussed in Chapter 6).

The relative significance of primary mixture parameters and their coupled effects on relevant properties of LWSCC are established. The developed statistical models can be used to evaluate the potential influence of adjusting mixture variables on fresh and hardened properties.

Table 5.1 - Analysis of GLM - ANOVA model for FS- LWSCC properties

Dependent variable	Source of variation	Statistical parameters					Significant	Contribution (%)
		DOF	Sum of Square	Mean square	F	*p*-value		
Slump Flow	W/B	1	1.25E+05	1.25E+05	51.58	0.0001	Y	34
	HRWRA	1	2.35E+05	2.35E+05	96.66	0.0001	Y	63.7
	Binder	1	8665.92	8665.92	3.57	0.0957	N	2.4
V-Funnel	W/B	1	742.99	742.99	179.0	0.0001	Y	92.5
	HRWRA	1	56.22	56.22	13.54	0.0062	Y	7
	Binder	1	4.39	4.39	1.060	0.3337	N	0.5
J-Ring Flow	W/B	1	1.41E+05	1.41E+05	49.36	0.0001	Y	33.9
	HRWRA	1	2.64E+05	2.64E+05	92.71	0.0001	Y	63.6
	Binder	1	10431.12	10431.12	3.66	0.092	N	2.5
J-Ring Height	W/B	1	127.68	127.68	69.08	0.0001	Y	40.1
	HRWRA	1	181.57	181.57	98.24	0.0001	Y	57.1
	Binder	1	9.00	9.00	4.87	0.0584	N	2.8
L-Box	W/B	1	0.35	0.35	29.52	0.0006	Y	38.3
	HRWRA	1	0.55	0.55	46.53	0.0001	Y	60.4
	Binder	1	0.012	0.012	1.050	0.3360	N	1.4
Filling Capacity	W/B	1	3751.22	3751.22	42.13	0.0002	Y	38.4
	HRWRA	1	5888.51	5888.51	66.14	0.0001	Y	60.2
	Binder	1	134.33	134.33	1.51	0.2542	N	1.4
Sieve Segregation Resistance	W/B	1	493.33	493.33	57.70	0.0001	Y	34.2
	HRWRA	1	374.55	374.55	43.80	0.0001	Y	26
	Binder	1	574.14	574.14	67.15	0.0001	Y	39.8
Bleeding	W/B	1	5.24E-03	5.24E-03	12.22	0.0036	Y	64
	HRWRA	1	4.17E-04	4.17E-04	0.97	0.3411	N	5.1
	Binder	1	2.53E-03	2.53E-03	5.89	0.0293	Y	30.9

Table 5.1 Cont'd - Analysis of GLM - ANOVA model for FS- LWSCC properties

Dependent variable	Source of variation	Statistical parameters					Significant	Contribution (%)
		DOF	Sum of Square	Mean square	F	*p*-value		
Air Content	W/B	1	0.60	0.60	1.25	0.2966	N	54.3
	HRWRA	1	0.44	0.44	0.92	0.3661	N	40
	Binder	1	0.061	0.061	0.13	0.7308	N	5.7
Set Time Initial	W/B	1	6.96	6.96	52.48	0.0001	Y	52.9
	HRWRA	1	5.05	5.05	38.04	0.0003	Y	38.4
	Binder	1	1.15	1.15	8.67	0.0186	Y	8.7
Set Time Final	W/B	1	7.73	7.73	51.72	0.0001	Y	36.8
	HRWRA	1	10.44	10.44	69.84	0.0001	Y	49.7
	Binder	1	2.85	2.85	19.04	0.0024	Y	13.5
7-day Compressive Strength	W/B	1	329.39	329.39	82.80	0.0001	Y	77.2
	HRWRA	1	24.29	24.29	6.10	0.0269	Y	5.7
	Binder	1	73.08	73.08	18.37	0.0008	Y	17.1
28-day Compressive Strength	W/B	1	587.18	587.18	65.96	0.0001	Y	77.2
	HRWRA	1	34.97	34.97	3.93	0.0675	N	4.6
	Binder	1	138.17	138.17	15.52	0.0015	Y	18.2
Fresh Unit Weight	W/B	1	714.08	714.08	0.58	0.4680	N	7.5
	HRWRA	1	777.12	777.12	0.63	0.4497	N	8.1
	Binder	1	8086.73	8086.73	6.57	0.0334	Y	84.4
28-day Air Dry Unit Weight	W/B	1	9349.48	9349.48	13.63	0.0024	Y	82.5
	HRWRA	1	317.23	317.23	0.46	0.5075	N	2.8
	Binder	1	1668.98	1668.98	2.43	0.1411	N	14.7
28-day Oven Dry Unit Weight	W/B	1	12659.7	12659.7	19.58	0.0022	Y	89.7
	HRWRA	1	282.11	282.11	0.44	0.5275	N	2
	Binder	1	1174.93	1174.93	1.82	0.2146	N	8.3

DOF: Degree of freedom, F: Statistic test, p-value: Probabilities, Significant: p <0.050 (Y: Yes), p > 0.050 (N: NO)

Table 5.2 - Analysis of GLM - ANOVA model for EC-LWSCC properties

Dependent variable	Source of variation	Statistical parameters					Significant	Contribution (%)
		DOF	Sum of Square	Mean square	F	*p*-value		
Slump Flow	W/B	1	95869.21	95869.21	65.03	0.0001	Y	33.1
	HRWRA	1	1.859E+05	1.859E+05	126.07	0.0001	Y	64.1
	Binder	1	8325.00	8325.00	5.65	0.0388	Y	2.9
V-Funnel	W/B	1	858.50	858.50	162.56	0.0001	Y	91.6
	HRWRA	1	61.90	61.90	11.72	0.0065	Y	6.6
	Binder	1	16.89	16.89	3.20	0.1040	N	1.8
J-Ring Flow	W/B	1	1.300E+05	1.300E+05	49.16	0.0001	Y	33.6
	HRWRA	1	2.438E+05	2.438E+05	92.17	0.0001	Y	62.9
	Binder	1	13480.79	13480.79	5.10	0.0476	Y	3.5
J-Ring Height	W/B	1	183.74	183.74	74.34	0.0001	Y	39.6
	HRWRA	1	267.42	267.42	108.19	0.0001	Y	57.6
	Binder	1	13.08	13.08	5.29	0.0442	Y	2.8
L-Box	W/B	1	0.29	0.29	34.03	0.0002	Y	38.4
	HRWRA	1	0.45	0.45	53.26	0.0001	Y	60.1
	Binder	1	0.012	0.012	1.40	0.2641	N	1.6
Filling Capacity	W/B	1	3118.44	3118.44	49.17	0.0001	Y	38.2
	HRWRA	1	4937.22	4937.22	77.86	0.0001	Y	60.4
	Binder	1	115.95	115.95	1.83	0.2061	N	1.4
Sieve Segregation Resistance	W/B	1	688.62	688.62	56.02	0.0001	Y	35.5
	HRWRA	1	510.86	510.86	41.56	0.0001	Y	26.3
	Binder	1	740.28	740.28	60.23	0.0001	Y	38.2
Bleeding	W/B	1	6.978E-03	6.978E-03	14.82	0.0014	Y	63.8
	HRWRA	1	6.017E-04	6.017E-04	1.28	0.2749	N	5.5
	Binder	1	3.363E-03	3.363E-03	7.14	0.0167	Y	30.7

Table 5.2 Cont'd - Analysis of GLM - ANOVA model for EC-LWSCC properties

Dependent variable	Source of variation	Statistical parameters					Significant	Contribution (%)
		DOF	Sum of Square	Mean square	F	*p*-value		
Air Content	W/B	1	0.28	0.28	1.58	0.2369	N	91.0
	HRWRA	1	0.027	0.027	0.15	0.7069	N	8.6
	Binder	1	1.08E-03	1.081E-3	6.0E-3	0.9397	N	0.3
Set Time Initial	W/B	1	5.63	5.63	21.72	0.0003	Y	47.7
	HRWRA	1	5.19	5.19	20.05	0.0004	Y	44.1
	Binder	1	0.96	0.96	3.73	0.0715	N	8.2
Set Time Final	W/B	1	7.65	7.65	47.54	0.0001	Y	36.1
	HRWRA	1	10.73	10.73	66.65	0.0001	Y	50.7
	Binder	1	2.80	2.80	17.39	0.0019	Y	13.2
7-day Compressive Strength	W/B	1	372.11	372.11	116.03	0.0001	Y	83.9
	HRWRA	1	20.43	20.43	6.37	0.0225	Y	4.6
	Binder	1	51.14	51.14	15.95	0.0010	Y	11.5
28-day Compressive Strength	W/B	1	676.51	676.51	104.52	0.0001	Y	90.5
	HRWRA	1	24.31	24.31	3.76	0.0814	N	3.3
	Binder	1	46.55	46.55	7.19	0.0230	Y	6.2
Fresh Unit Weight	W/B	1	505.18	505.1	0.71	0.4202	N	7.6
	HRWRA	1	543.79	543.79	0.76	0.4036	N	8.1
	Binder	1	5656.93	5656.93	7.91	0.0184	Y	84.3
28-day Air Dry Unit Weight	W/B	1	68.62	68.62	0.068	0.7978	N	1.0
	HRWRA	1	603.27	603.27	0.60	0.4520	N	8.4
	Binder	1	6502.44	6502.44	6.48	0.0244	Y	90.7
28-day Oven Dry Unit Weight	W/B	1	418.15	418.15	0.50	0.4954	N	6.3
	HRWRA	1	638.69	638.69	0.76	0.4024	N	9.6
	Binder	1	5589.12	5589.12	6.69	0.0271	Y	84.2

DOF: Degree of freedom, F: Statistic test, p-value: Probabilities, Significant: p <0.050 (Y: Yes), p > 0.050 (N: NO)

Table 5.3 - Analysis of GLM - ANOVA model for ESH-LWSCC properties

Dependent variable	Source of variation	Statistical parameters					Significant	Contribution (%)
		DOF	Sum of Square	Mean square	F	*p*-value		
Slump Flow	W/B	1	1.409E+05	1.409E+05	69.88	0.0001	Y	36.0
	HRWRA	1	2.475E+05	2.475E+05	122.73	0.0001	Y	63.2
	Binder	1	3101.39	3101.39	1.54	0.2432	N	0.8
V-Funnel	W/B	1	571.98	571.98	192.66	0.0001	Y	92.3
	HRWRA	1	46.72	46.72	15.74	0.0027	Y	7.5
	Binder	1	1.09	1.09	0.37	0.5574	N	0.2
J-Ring Flow	W/B	1	1.302E+05	1.302E+05	82.89	0.0001	Y	36.4
	HRWRA	1	2.277E+05	2.277E+05	144.89	0.0001	Y	63.6
	Binder	1	283.95	283.95	0.18	0.6798	N	0.1
J-Ring Height	W/B	1	70.55	70.55	45.19	0.0001	Y	38.6
	HRWRA	1	103.91	103.91	66.55	0.0001	Y	56.9
	Binder	1	8.28	8.28	5.30	0.0441	Y	4.5
L-Box	W/B	1	0.34	0.34	35.61	0.0001	Y	37.5
	HRWRA	1	0.56	0.56	58.53	0.0001	Y	61.6
	Binder	1	7.722E-03	7.722E-03	0.81	0.3896	N	0.9
Filling Capacity	W/B	1	3663.64	3663.64	53.31	0.0001	Y	37.7
	HRWRA	1	5964.65	5964.65	86.79	0.0001	Y	61.4
	Binder	1	87.97	87.97	1.28	0.2843	N	0.9
Sieve Segregation Resistance	W/B	1	464.58	464.58	31.88	0.0001	Y	29.9
	HRWRA	1	357.16	357.16	24.51	0.0003	Y	22.9
	Binder	1	734.64	7.34.64	50.41	0.0001	Y	47.2
Bleeding	W/B	1	3.824E-03	3.824E-03	13.59	0.0020	Y	64.8
	HRWRA	1	2.356E-04	2.356E-04	0.84	0.3737	N	4.0
	Binder	1	1.838E-03	1.838E-03	6.53	0.0211	Y	31.2

Table 5.3 Cont'd - Analysis of GLM - ANOVA model for ESH-LWSCC properties

Dependent variable	Source of variation	Statistical parameters					Significant	Contribution (%)
		DOF	Sum of Square	Mean square	F	*p*-value		
Air Content	W/B	1	0.32	0.32	1.49	0.2503	N	50.2
	HRWRA	1	0.26	0.26	1.24	0.2914	N	41.8
	Binder	1	0.051	0.051	0.24	0.6341	N	8.1
Set Time Initial	W/B	1	6.44	6.44	23.88	0.0002	Y	52.4
	HRWRA	1	5.16	5.16	19.14	0.0005	Y	42.0
	Binder	1	0.68	0.68	2.51	0.1329	N	5.5
Set Time Final	W/B	1	6.45	6.45	37.72	0.0001	Y	33.7
	HRWRA	1	10.44	10.44	61.06	0.0001	Y	54.5
	Binder	1	2.26	2.26	13.19	0.0046	Y	11.8
7-day Compressive Strength	W/B	1	357.62	357.62	82.24	0.0001	Y	69.3
	HRWRA	1	28.85	28.85	6.63	0.0203	Y	5.6
	Binder	1	129.55	129.55	29.79	0.0001	Y	25.1
28-day Compressive Strength	W/B	1	637.51	637.51	84.72	0.0001	Y	69.0
	HRWRA	1	41.52	41.52	5.52	0.0407	Y	4.5
	Binder	1	244.55	244.55	32.50	0.0002	Y	26.5
Fresh Unit Weight	W/B	1	622.78	622.78	0.70	0.4212	N	7.4
	HRWRA	1	683.54	683.54	0.77	0.4001	N	8.1
	Binder	1	7092.69	7092.69	8.01	0.0178	Y	84.5
28-day Air Dry Unit Weight	W/B	1	75.35	75.35	0.061	0.8093	N	0.9
	HRWRA	1	733.33	733.33	0.59	0.4561	N	8.3
	Binder	1	8057.00	8057.00	6.48	0.0244	Y	90.9
28-day Oven Dry Unit Weight	W/B	1	546.73	546.73	0.53	0.4852	N	6.6
	HRWRA	1	784.87	784.87	0.75	0.4055	N	9.4
	Binder	1	6989.34	6989.34	6.72	0.0269	Y	84.0

DOF: Degree of freedom, F: Statistic test, p-value: Probabilities, Significant: p <0.050 (Y: Yes), p > 0.050 (N: NO)

Table 5.4 - Mathematical Formulation of FS -LWSCC properties

Parameters	Slump flow	V-Funnel	J-Ring Flow	J-Ring Height	L-Box	Filling capacity	SSR	Bleeding
Constant	-2377.92	277.97	-2682.82	68.77	-8.37	-799.71	-166.73	-0.02
W/B	13865.62	-1379.6	15217.26	-389.8	40.21	3767.67	586.92	0.41
HRWRA	421.31	-29.15	449.37	-36.99	0.35	92.93	31.42	0.01
B	0.35	0.02	0.43	0.11	6.0E-3	0.531	0.27	-2.06E-4
W/B*HRWRA	416.66	51.11	416.66	72.22	1.94	88.88	5.55	-
W/B * B	1.60	-0.25	1.96	-0.21	-1.0E-3	-0.142	-0.96	-
HRWRA * B	0.13	1.58E-3	0.13	-0.02	7.5E-4	0.04	-0.04	-
$(W/B)^2$	-18436.1	1867.64	-20439.5	533.22	-53.92	-4874.51	-	-
$(HRWRA)^2$	-215.26	3.79	-221.47	9.66	-0.6163	-65.11	-	-
$(B)^2$	-1.46E-03	7.33E-5	-1.7E-3	-7.7E6	-6.9E-6	-5.88E-4	-	-
R^2	0.96	0.97	0.95	0.96	0.93	0.95	0.94	0.58

Parameters	Air Content	Initial Set Time	Final Set time	Comp Strength		Fresh Unit Weight	28-day Air Dry Weight	28-day Oven Dry Weight
				7-day	28-day			
Constant	-26.11	9.68	22.52	49.62	66.67	1915.62	1967.47	1811.51
W/B	17.38	-21.81	-37.23	-104.7	-139.9	780.53	-558.25	2269.72
HRWRA	5.29	-0.41	-3.02	-3.16	-3.79	552.97	-11.42	-75.09
B	0.10	-0.01	-0.041	0.03	0.04	-1.76	0.16	-1.36
W/B*HRWRA	-12.22	-2.22	4.72	-	-	-977.77	-	-200
W/B * B	9.58E-16	-0.05	-0.05	-	-	-5.71	-	-1.14
HRWRA * B	-1.55E-17	-1E-17	-5.95E-4	-	-	-0.61	-	-0.10
$(W/B)^2$	-18.12	92.04	106.57	-	-	3630.53	-	-3172.51
$(HRWRA)^2$	-0.96	1.75	2.48	-	-	69.51	-	122.56
$(B)^2$	-1.09E-04	2.82E-5	5.56E-05	-	-	4.78E-03	-	2.06E-03
R^2	0.53	0.93	0.95	0.88	0.86	0.73	0.54	0.8

Table 5.5 - Mathematical Formulation of EC - LWSCC properties

Parameters	Slump flow	V-Funnel	J-Ring Flow	J-Ring Height	L-Box	Filling capacity	SSR	Bleeding
Constant	-1839.4	+236.178	-2395.804	+82.955	-7.36312	-761.4993	-192.232	-0.036086
W/B	+11715	-1187.73	+13809.4	-438.26	+36.9090	+3613.42	+666.299	+0.48389
HRWRA	+356.44	-17.8770	+395.621	-41.316	+0.25145	+90.0893	+41.1386	+0.01570
B	-0.1373	+0.04963	+0.39625	+0.1079	+4.48E-3	+0.49793	+0.30484	-2.383E-4
W/B*HRWRA	+444.44	+28.8888	+638.888	+55.555	+1.94444	+77.7777	+9.7E-14	-
W/B * B	+1.7857	-0.45000	+2.32143	-0.2857	-3.57E-4	-0.14286	-1.07143	-
HRWRA * B	+0.1587	-0.01507	+0.05952	-0.0158	+7.53E-4	+0.04761	-0.05555	-
$(W/B)^2$	-15874	+1731.9	-19019.90	+650.31	-50.1217	-4685.275	-	-
$(HRWRA)^2$	-208.10	+6.6442	-221.1035	+12.680	-0.57582	-63.45234	-	-
$(B)^2$	-1.0E-3	+1.4E-4	-1.802E-3	+1.9E-5	-5.59E-6	-5.499E-4	-	-
R^2	0.96	0.96	0.94	0.96	0.93	0.95	0.93	0.59

Parameters	Air Content	Initial Set Time	Final Set Time	Comp Strength		Fresh Unit Weight	28-day Air Dry Weight	28-day Oven Dry Weight
				7-day	28-day			
Constant	-23.930	+1.34	+30.28	+53.673	-55.3521	+1512.550	-13.5544	+1794.931
W/B	+45.421	+13.74	-58.04	-111.74	+122.71	+888.769	-	+2030.68
HRWRA	+3.1953	+1.45	-2.583	-2.894	-7.40755	+474.8730	+651.758	+503.7415
B	+0.0774	-4.03E-3	-0.059	+0.029	+0.39672	-1.25033	+2.62904	-3.9773
W/B*HRWRA	-8.8888	-	+8.33	-	+11.1111	-822.2222	-1044.4	-972.2222
W/B * B	-0.0142	-	-0.032143	-	+0.28571	-4.85714	-5.3571	-4.32143
HRWRA * B	-1E-18	-	-4.7619E-3	-	+7.93E-3	-0.52381	-0.5634	-0.46429
$(W/B)^2$	-49.978	-	+118.92376	-	-598.373	+2755.89	-	+934.732
$(HRWRA)^2$	-0.1261	-	+2.69968	-	-2.29842	+52.8429	-	+50.3832
$(B)^2$	-7.5E-5	-	+7.0525E-5	-	-4.9E-4	+3.80E-03	-	+6.401E-3
R^2	0.54	0.74	0.94	0.90	0.93	0.73	0.56	0.75

Table 5.6 - Mathematical Formulation of ESH- LWSCC properties

Parameters	Slump flow	V-Funnel	J-Ring Flow	J-Ring Height	L-Box	Filling capacity	SSR	Bleeding
Constant	-2631.74	282.93946	-2803.42	130.55	-10.61	-1020.89	-183.568	-0.0249
W/B	14376.546	-1391.542	13859.24	-479..9	48.58	4597.46	632.705	0.358
HRWRA	356.7146	-32.51110	387.503	-51.01	0.77	136.18	38.001	9.827E-03
B	0.95820	5.826E-03	1.788	0.051	8.8E-03	0.800	0.3084	-1.76E-04
W/B*HRWRA	416.66667	59.47019	333.333	55.55	1.16	7.820	8.2980	-
W/B * B	1.25000	-0.13444	1.428	0.142	-1.8E-3	-0.203	-1.070	-
HRWRA * B	0.29762	9.043E-03	0.39683	0.023	7.3E-04	0.0455	-0.060	-
$(W/B)^2$	-18735.07	1818.468	-18149.1	458.64	-64.59	-5369.08	-	-
$(HRWRA)^2$	-217.9190	1.98610	-259.424	9.077	-0.7061	-74.20	-	-
$(B)^2$	-1.925E-3	4.035E-05	-2.6E-03	-2.8E-5	-9.5E-6	-8.35E-4	-	-
R^2	0.96	0.97	0.96	0.94	0.94	0.95	0.90	0.57

Parameters	Air Content	Initial Set Time	Final Set Time	Comp Strength		Fresh Unit Weight	28-day Air Dry Weight	28-day Oven Dry Weight
				7-day	28-day			
Constant	-21.0232	+0.563	21.84	48.71	-79.42	1697.63	-11.93	1995.35
W/B	24.4648	+14.69	- 43.625	-109.54	319.19	973.54	3681.54	2279.59
HRWRA	4.9689	+1.454	- 1.9452	-3.439	3.38	527.89	724.93	563.21
B	0.0766	-3.37E-03	- 0.0358	0.046	0.328	-1.430	2.920	-4.42
W/B*HRWRA	-13.888	-	3.0555	-	-1.038	-915.71	-1165.45	-1082.20
W/B * B	-0.0321	-	- 0.0589	-	0.229	-5.35	-5.953	-4.81
HRWRA * B	-3.968E-4	-	- 1.3E-3	-	-1.9E-3	-0.579	-0.624	-0.52
$(W/B)^2$	-2.678	-	120.477	-	-821.05	3053.463	-	1012.11
$(HRWRA)^2$	-0.163	-	2.4078	-	-4.14	58.42	-	55.48
$(B)^2$	-6.682E-5	-	5.35E-05	-	-3.6E-4	4.25E-03	-	7.12E-03
R^2	0.54	0.74	0.93	0.88	0.93	0.73	0.56	0.75

Table 5.7 - Repeatability of test parameters for FS- LWSCC mixtures

Test Method	Mean (n = 6)	Standard deviation	C.O.V. (%)	Estimated error (95% CI)	Relative error (%)
Slump Flow (mm)	673.33	12.11	1.8%	11.83	1.8%
V-Funnel (s)	4.92	0.21	4.3%	0.21	4.2%
J-Ring Flow (mm)	658.33	15.06	2.3%	14.71	2.2%
J-Ring Height (mm)	1.83	0.41	22.3%	0.40	21.8%
L-Box (Ratio)	0.92	0.02	2.6%	0.02	2.5%
Filling Capacity (%)	91.50	3.27	3.6%	3.20	3.5%
Sieve Segregation Resistance (%)	13.83	1.47	10.6%	1.44	10.4%
Bleeding (ml/cm^2)	0.02	0.00	24.8%	0.00	24.2%
Air Content (%)	3.57	0.29	8.1%	0.28	7.9%
Set Time Initial (h:m)	5.02	0.49	9.7%	0.48	9.5%
Set Time Final (h:m)	6.94	0.44	6.4%	0.43	6.2%
7-day Comp Strength (MPa)	29.0	1.26	4.4%	1.24	4.3%
28-day Comp Strength (MPa)	41.0	1.78	4.4%	1.75	4.3%
Fresh Unit Weight (kg/m^3)	1912.17	11.57	0.6%	11.30	0.6%
28-day Air Dry Unit (kg/m^3)	1787.83	12.22	0.7%	11.94	0.7%
28-day Oven Dry Unit (kg/m^3)	1723.67	14.85	0.9%	14.52	0.8%

Table 5.8 - Repeatability of test parameters for EC-LWSCC mixtures

Test Method	Mean (n = 6)	Standard deviation	C.O.V. (%)	Estimated error (95% CI)	Relative error (%)
Slump Flow (mm)	638.33	13.66	2.1%	13.35	2.1%
V-Funnel (s)	6.15	0.31	5.1%	0.31	5.0%
J-Ring Flow (mm)	632.50	25.64	4.1%	25.06	4.0%
J-Ring Height (mm)	2.50	0.84	33.5%	0.82	32.7%
L-Box (Ratio)	0.87	0.02	2.8%	0.02	2.7%
Filling Capacity (%)	87.33	2.80	3.2%	2.74	3.1%
Sieve Segregation Resistance (%)	15.83	1.47	9.3%	1.44	9.1%
Bleeding (ml/cm^2)	0.02	0.00	23.3%	0.00	22.8%
Air Content (%)	3.33	0.21	6.2%	0.20	6.1%
Set Time Initial (h:m)	5.13	0.47	9.2%	0.46	9.0%
Set Time Final (h:m)	6.82	0.53	7.7%	0.51	7.5%
7-day Comp Strength (MPa)	28.00	1.26	4.5%	1.24	4.4%
28-day Comp Strength (MPa)	37.83	1.47	3.9%	1.44	3.8%
Fresh Unit Weight (kg/m^3)	1606.83	9.72	0.6%	9.50	0.6%
28-day Air Dry Unit (kg/m^3)	1502.17	10.38	0.7%	10.14	0.7%
28-day Oven Dry Unit (kg/m^3)	1448.33	12.45	0.9%	12.17	0.8%

Table 5.9 - Repeatability of test parameters for ESH -LWSCC mixtures

Test Method	Mean (n = 6)	Standard deviation	C.O.V. (%)	Estimated error (95% CI)	Relative error (%)
Slump Flow (mm)	692.50	12.55	1.8%	12.26	1.8%
V-Funnel (s)	3.77	0.23	6.2%	0.23	6.1%
J-Ring Flow (mm)	691.67	13.29	1.9%	12.99	1.9%
J-Ring Height (mm)	1.50	0.55	36.5%	0.54	35.7%
L-Box (Ratio)	0.99	0.01	1.3%	0.01	1.2%
Filling Capacity (%)	98.33	1.21	1.2%	1.18	1.2%
Sieve Segregation Resistance (%)	11.83	1.17	9.9%	1.14	9.7%
Bleeding (ml/cm^2)	0.01	0.00	18.5%	0.00	18.1%
Air Content (%)	3.08	0.26	8.3%	0.25	8.1%
Set Time Initial (h:m)	4.92	0.41	8.3%	0.40	8.1%
Set Time Final (h:m)	6.78	0.44	6.6%	0.43	6.4%
7-day Comp Strength (MPa)	32.00	1.26	4.0%	1.24	3.9%
28-day Comp Strength (MPa)	45.00	1.79	4.0%	1.75	3.9%
Fresh Unit Weight (kg/m^3)	1790.67	10.78	0.6%	10.54	0.6%
28-day Air Dry Unit (kg/m^3)	1674.17	11.44	0.7%	11.18	0.7%
28-day Oven Dry Unit (kg/m^3)	1614.33	13.85	0.9%	13.53	0.8%

CHAPTER SIX

6 MIX PROPORTION OPTIMIZATION AND VALIDATION OF THE STATISTICAL MODELS

6.1 Introduction

This chapter presents Phase III of the experiential program that included mix proportion optimization process and validation of statistical models. In this study, optimization was performed to develop mixtures that satisfy EFNARC industrial classifications for SCC (EFNARC 2005). Moreover, this chapter also presents the results of additional experimental study to validate whether the theoretically proposed optimum mix design parameters such as water to binder ratio (w/b), high range water reducing admixture (HRWRA) (%), and total binder (b) can yield the desired fresh and hardened properties for lightweight self-consolidating concrete (LWSCC). Diagram illustrating the structure of Chapter 6 is presented in Figure 6.1.

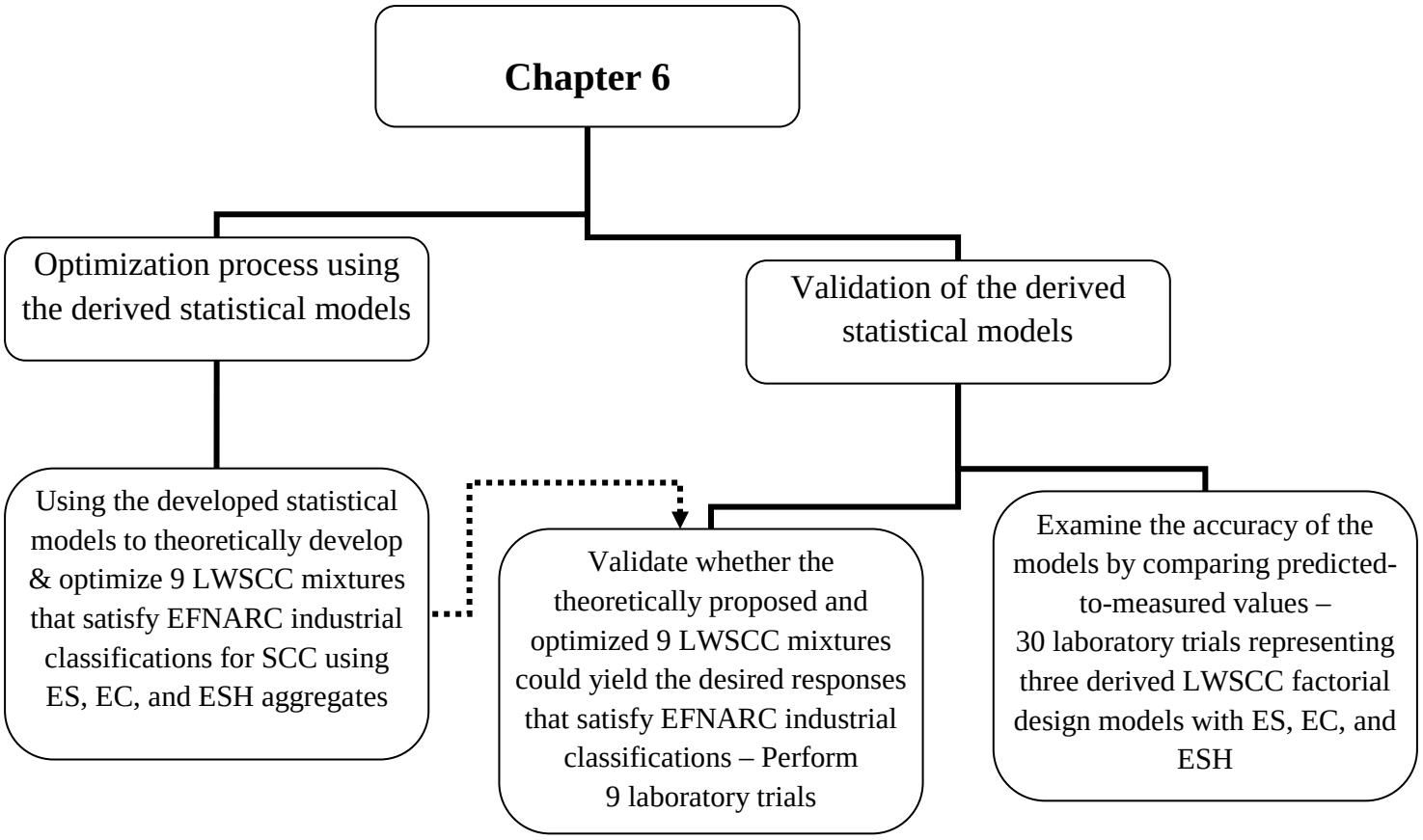

Figure 6.1- Various phases of the validation and optimization program

6.2 LWSCC Mixture Optimization

Based on the developed statistical models and the outlined relationships between mix design variables and the responses (as established in Chapter 5 – Tables 5.4 to 5.6), all independent variables were varied simultaneously and independently in order to optimize the response.

The objective of the optimization process was to obtain the ‘‘best fit’’ for particular response, considering alternating multiple responses concurrently. Optimization was performed to develop mixtures that satisfied EFNARC industrial classifications for SCC (EFNARC 2005). The typical fresh properties of SCC as per EFNARC are presented in Table 6.1.

Table 6.1 - EFNARC SCC classification

EFNARC SCC classification		
Slump flow	**Slump flow (mm)**	
SF1	550 to 650	
SF2	660 to 750	
SF3	760 to 850	
Viscosity	**T500 (s)**	**V-funnel (s)**
VS1/VF1	≤ 2	≤ 8
VS2/V2	> 2	9 to 25
Passing ability (L-box)	**Passing ability ratio (h_2/h_1)**	
PA1	≥ 0.80 with 2 rebars	
PA2	≥ 0.80 with 3 rebars	
Sieve segregation resistance	**Segregation resistance (%)**	
SR1	≤ 20	
SR2	≤ 15	

The mix proportions (independent variables) of FS-LWSCC, EC-LWSCC and ESH-LWSCC mixtures were optimized to yield three classes of LWSCC mixtures with the following fresh properties/classes:

1. LWSCC-1: SF1+VF1+PA2+SR2- Casting by a pump injection system (e.g. tunnel linings) - FS-LWSCC1, EC-LWSCC1 and ESH-LWSCC1.

2. LWSCC-2: SF2+VF1+PA2+SR2- Suitable for many normal applications (e.g. walls, columns) - FS-LWSCC2, EC-LWSCC2 and ESH-LWSCC2.

3. LWSCC-3: SF3+VF1+PA2+SR1- Suitable for vertical applications in very congested structures, structures with complex shapes, or for filling under formwork- FS-LWSCC3, EC-LWSCC3 and ESH-LWSCC3.

VF1 limits were constrained tightly from 4 to 8 seconds for LWSCC -1 & 2 to ensure density stability during application and placement. A numerical optimization technique, using desirability functions (dj) defined for each target response, was utilized to optimize the responses (Whitcomb and Anderson 2004; Pradeep et al. 2008; Ozbay et al. 2010).

Desirability is an objective function that ranges from 0 to 1, where 0 indicates it is outside the range and 1 indicates the goal is fully achieved. The numerical optimization finds a point that maximizes the desirability function. The characteristics of a goal may be altered by adjusting the weight or importance (Ozbay et al. 2010). In this research, target responses were assigned equal weight and importance. All target responses were combined into a desirability function and the numerical optimization software was used to maximize this function. The goals seeking begin at a random starting point and proceeds up the steepest slope to a maximum. There may be two or more maxima because of curvature in the response surfaces and their combinations into desirability functions (Nehdi and Summer 2002).

To perform the optimization process, goals, upper and lower limits for the factors and responses were defined as in Tables 6.2, 6.3 and 6.4. In order to have an equal importance, five predefined responses (slump flow, J-ring flow, V- funnel, L-box and segregation index) in addition to the goal to minimize both J- ring height difference and fresh unit weight response were considered and optimized simultaneously. Furthermore, filling capacity, bleeding, fresh air content, initial and final setting times, 28-day air dry unit weight, 28-day oven dry unit weight, and 7- and 28-day compressive strengths were defined as in the experimental study range.

After running the numerical optimization process for FS-LWSCC-1, EC-LWSCC-1 and ESH-LWSCC-1 mixtures - 38, 28 and 29 solutions were obtained, respectively satisfying the set limits and constrains. The desirability of the proposed solutions ranged from 0.730 to 0.803, 0.750 to 0.811 and 0.732 to 0.810, respectively.

For FS, EC and ESH LWSCC-2 mixtures, 26, 28 and 25 solutions were obtained with desirability ranging from 0.781 to 0.844, 0.787 to 0.835 and 0.798 to 0.864, respectively.

The desirability ranged from 0.860 to 0.898, 0.900 to 0.905 and 0.800 to 0.908, with 11, 8 and 30 solutions that were found for FS, EC and ESH LWSCC-3 mixtures, respectively. The highest desirability function values for FS, EC and ESH LWSCC-1, 2 and 3 mixtures were (0.803, 0.844 and 0.898), (0.811, 0.835 and 0.905) and (0.810, 0.864 and 0.908) for achieving the set, goals and limits as shown in Tables 6.2., 6.3 and 6.4. The minimum acceptable desirability value in this study was 0.8.

Table 6.2 - Classification of responses goal and limits of FS- LWSCC mixtures

Name of responses	Goal	Lower limit	Upper limit	Lower limit	Upper limit	Lower limit	Upper limit
		FS-LWSCC-1	FS-LWSCC-1	FS-LWSCC-2	FS-LWSCC-2	FS-LWSCC-3	FS-LWSCC-3
Slump Flow (mm)	In range	550	650	660	750	760	850
V-Funnel (S)	In range	4	8	4	8	0.0	8
J-Ring Flow (mm)	In range	550	650	660	750	760	850
J-Ring Height (mm)	Minimize	0.0	16.5	0.0	16.5	0.0	16.5
L-Box ratio (h_2/h_1)	In range	0.8	1.0	0.8	1.0	0.8	1.0
Filling Capacity (%)	In range	80	100	80	100	80	100
Sieve Segregation (%)	In range	0.0	15	0.0	15	0.0	20
Bleeding (ml/cm^2)	In range	0.0	0.108	0.0	0.108	0.0	0.108
Air Content (%)	In range	2.2	4.8	2.2	4.8	2.2	4.8
Set Time Initial (h:m)	In range	04:05	07:30	04:05	07:30	04:05	07:30
Set Time Final (h:m)	In range	06:10	10:20	06:10	10:20	06:10	10:20
7-day Comp Strength (MPa)	In range	18	37	18	37	18	37
28-day Comp Strength (MPa)	In range	25	49	25	49	25	49
Fresh Unit Weight (MPa)	Minimize	1860	2020	1860	2020	1860	2020
28-day Air Dry Unit (kg/m^3)	In range	1790	1905	1790	1905	1790	1905
28-day Oven Dry Unit (kg/m^3)	In range	1705	1845	1705	1845	1705	1845

Table 6.3 - Classification of responses goal and limits of EC- LWSCC mixtures

Name of responses	Goal	Lower limit	Upper limit	Lower limit	Upper limit	Lower limit	Upper limit
		EC-LWSCC-1	EC-LWSCC-1	EC-LWSCC-2	EC-LWSCC-2	EC-LWSCC-3	EC-LWSCC-3
Slump Flow (mm)	In range	550	650	660	750	760	850
V-Funnel (S)	In range	4	8	4	8	0.0	8
J-Ring Flow (mm)	In range	550	650	660	750	760	850
J-Ring Height (mm)	Minimize	0.0	19.0	0.0	19.0	0.0	19.0
L-Box ratio (h_2/h_1)	In range	0.8	1.0	0.8	1.0	0.8	1.0
Filling Capacity (%)	In range	80	100	80	100	80	100
Sieve Segregation (%)	In range	0.0	15	0.0	15	0.0	20
Bleeding (ml/cm^2)	In range	0.0	0.118	0.0	0.118	0.0	0.118
Air Content (%)	In range	2.0	3.6	2.0	3.6	2.0	3.6
Set Time Initial (h:m)	In range	04:00	07:10	04:00	07:10	04:00	07:10
Set Time Final (h:m)	In range	06:05	10:40	06:05	10:40	06:05	10:40
7-day Comp Strength (MPa)	In range	17	36	17	36	17	36
28-day Comp Strength (MPa)	In range	21	48	21	48	21	48
Fresh Unit Weight (MPa)	Minimize	1563	1697	1563	1697	1563	1697
28-day Air Dry Unit (kg/m^3)	In range	1445	1584	1445	1584	1445	1584
28-day Oven Dry Unit (kg/m^3)	In range	1405	1551	1405	1551	1405	1551

Table 6.4 - Classification of responses goal and limits of ESH- LWSCC mixtures

Name of responses	Goal	Lower limit	Upper limit	Lower limit	Upper limit	Lower limit	Upper limit
		EC-LWSCC-1	EC-LWSCC-1	EC-LWSCC-2	EC-LWSCC-2	EC-LWSCC-3	EC-LWSCC-3
Slump Flow (mm)	In range	550	650	660	750	760	850
V-Funnel (S)	In range	4	8	4	8	0.0	8
J-Ring Flow (mm)	In range	550	650	660	750	760	850
J-Ring Height (mm)	Minimize	0.0	14.0	0.0	14.0	0.0	14.0
L-Box ratio (h_2/h_1)	In range	0.8	1.0	0.8	1.0	0.8	1.0
Filling Capacity (%)	In range	80	100	80	100	80	100
Sieve Segregation (%)	In range	0.0	15	0.0	15	0.0	20
Bleeding (ml/cm^2)	In range	0.0	0.0931	0.0	0.0931	0.0	0.0931
Air Content (%)	In range	2.0	3.7	2.0	3.7	2.0	3.7
Set Time Initial (h:m)	In range	03:50	07:20	03:50	07:20	03:50	07:20
Set Time Final (h:m)	In range	06:10	10:00	06:10	10:00	06:10	10:00
7-day Comp Strength (MPa)	In range	20	40	20	40	20	40
28-day Comp Strength (MPa)	In range	28	53	28	53	28	53
Fresh Unit Weight (MPa)	Minimize	1742	1892	1742	1892	1742	1892
28-day Air Dry Unit (kg/m^3)	In range	1611	1765	1611	1765	1611	1765
28-day Oven Dry Unit (kg/m^3)	In range	1566	1729	1566	1729	1566	1729

The desirability function changed based on the optimization process and is graphically presented in Figures 6.2 to 6.10. From Figures 6.2, 6.3, 6.5, 6.6, 6.8 and 6.9 for LWSCC mixes of classes 1 and 2 when keeping the binder content constant at 494, 520, 526, 544, 476 and 486 kg/m^3, respectively, it was found that the desirability function increased only for very limited area (highlighted in the figures), and when the w/b and HRWRA (%) are between certain values. However, desirability value decreased drastically to zero out of this limited area indicating that very specific parameter range is needed to achieve high desirability above 0.8 for LWSCC mixtures. According to Figures 6.4, 6.7 and 6.10, high desirability only can be achieved for LWSCC mixes of class 3 when the w/b is kept at 0.4 and for binder content above 500 kg/m^3. Therefore, the "predication" of the highest desirability of LWSCC mixes of classes 3 is graphically presented in a 2D graphs instead of 3D with indication of the chosen point of highest desirability predication.

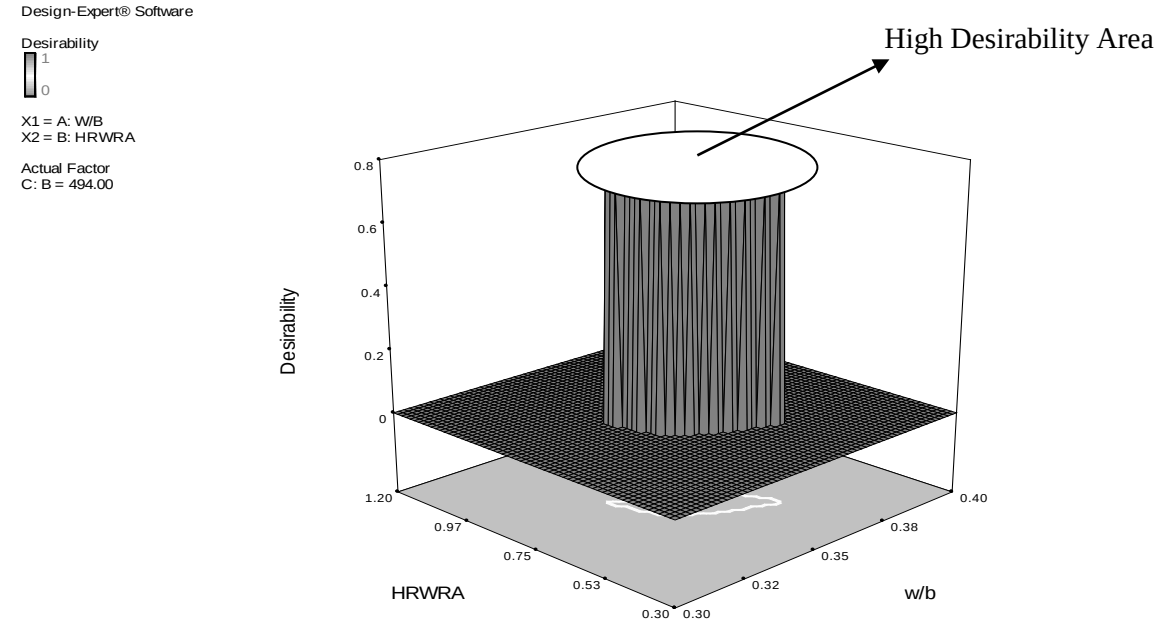

Figure 6.2 - Effect of w/b, HRWRA and total binder content at 494kg/m^{3}on the desirability function of FS-LWSCC- 1 mixture (EFNARC SCC class 1)

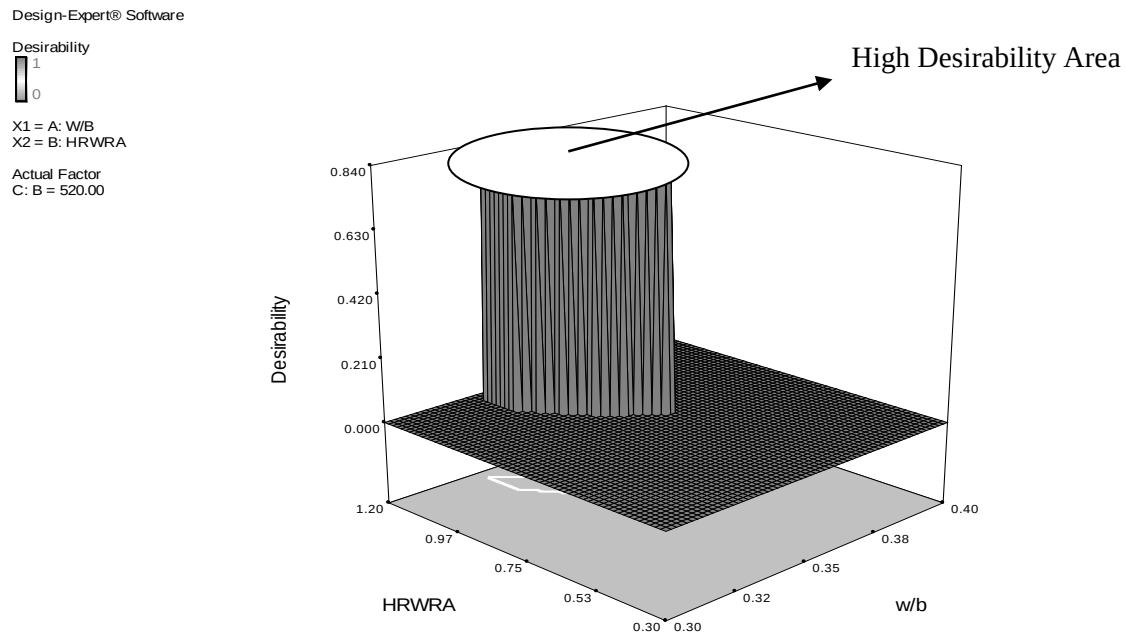

Figure 6.3 - Effect of w/b, HRWRA and total binder content at 520kg/m^{3}on the desirability function of FS-LWSCC- 2 mixture (EFNARC SCC class 2)

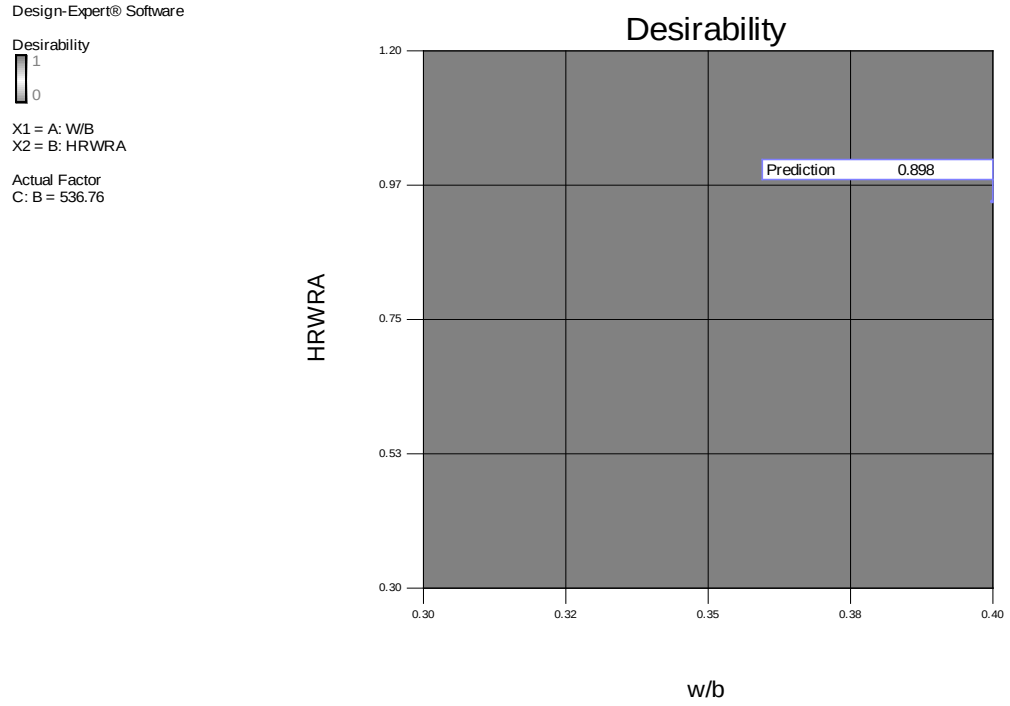

Figure 6.4 - Effect of w/b and HRWRA on the desirability function of FS-LWSCC- 3 mixture (EFNARC SCC class 3)

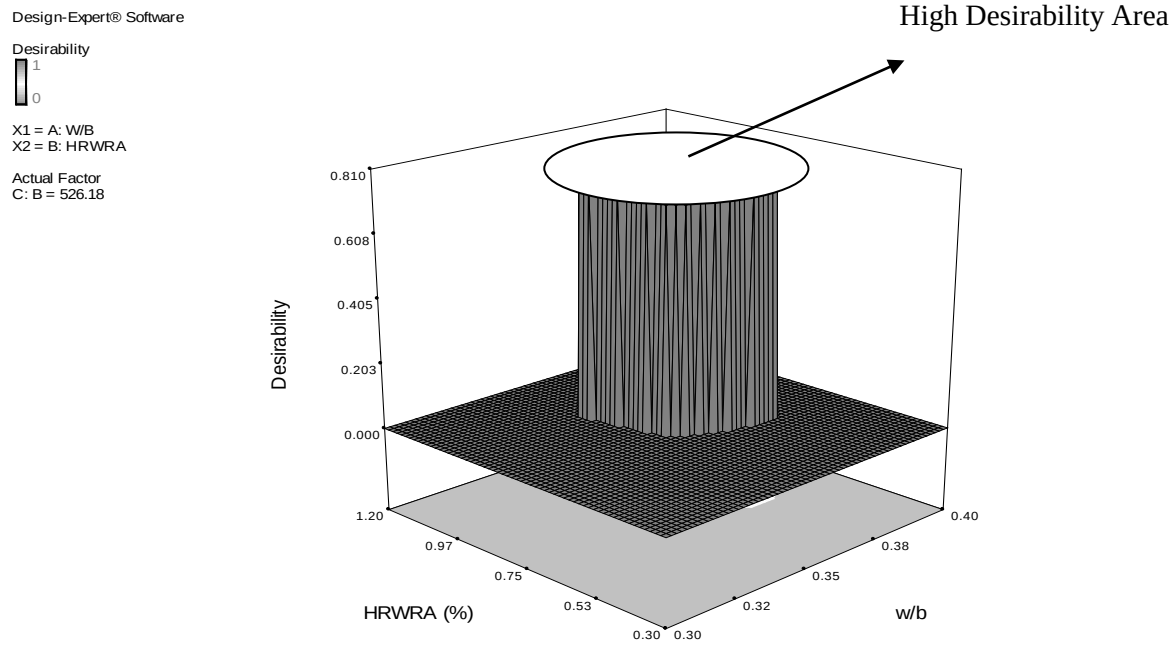

Figure 6.5 - Effect of w/b, HRWRA and total binder content at 526kg/m^{3}on the desirability function of EC-LWSCC- 1 mixture (EFNARC SCC class 1)

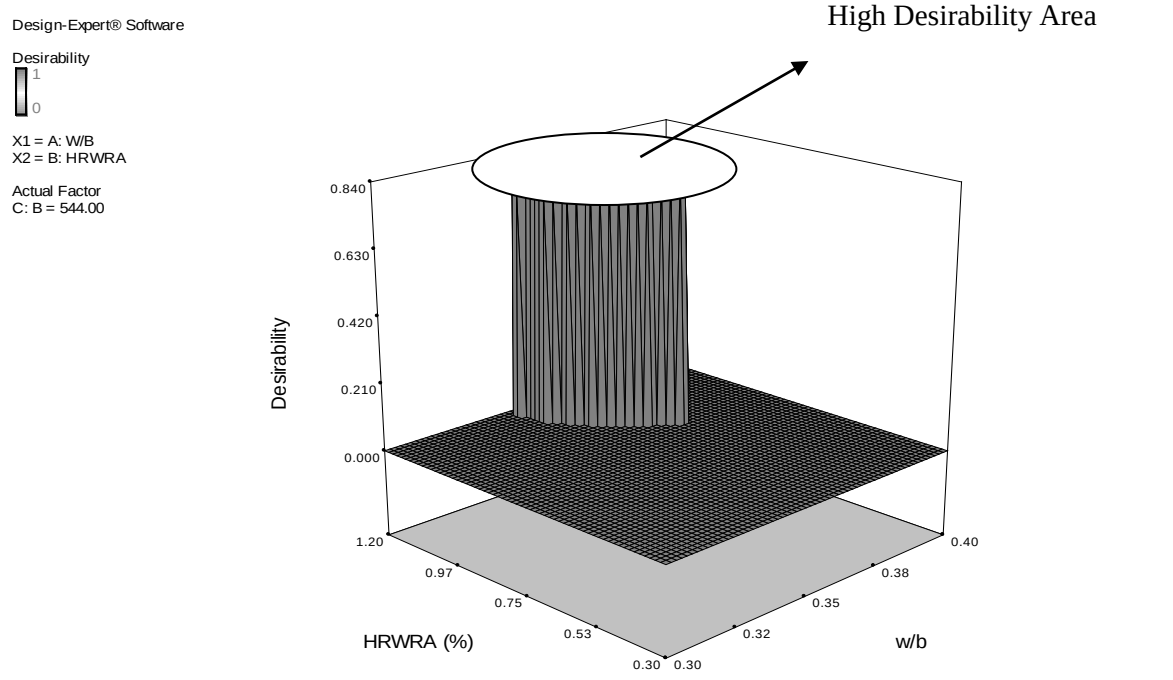

Figure 6.6 - Effect of w/b, HRWRA and total binder content at 544kg/m^{3}on the desirability function of EC-LWSCC- 2 mixture (EFNARC SCC class 2)

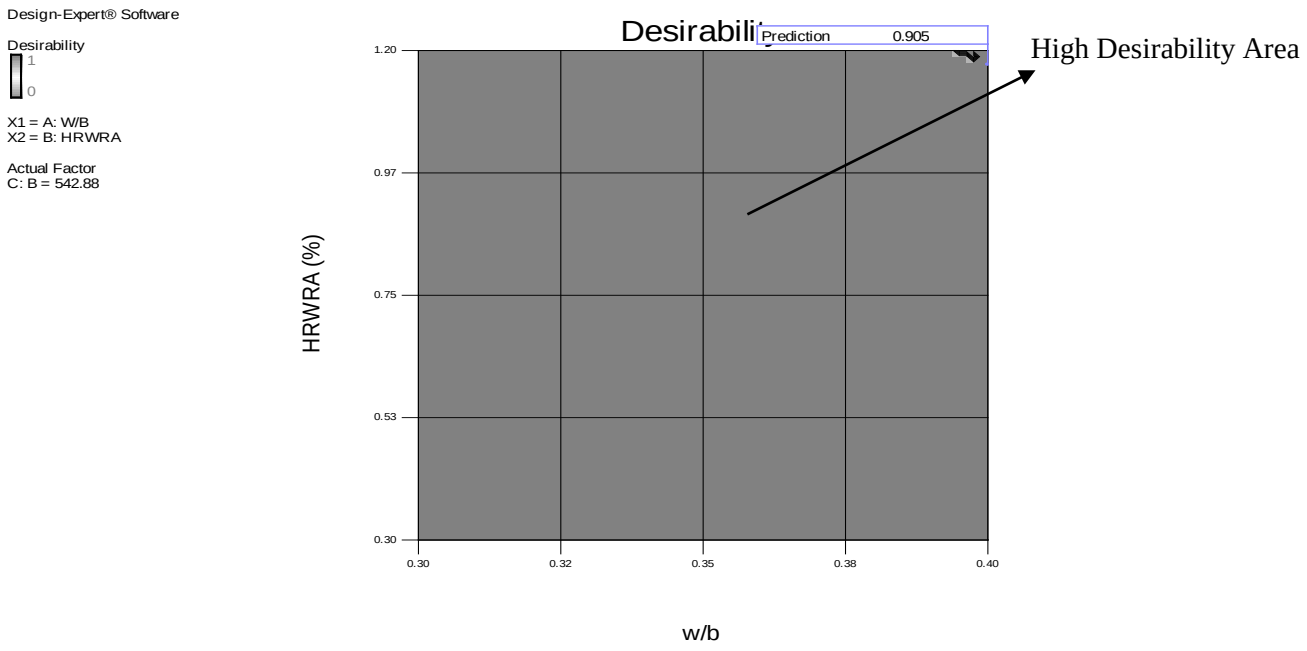

Figure 6.7 - Effect of w/b and HRWRA on the desirability function of EC-LWSCC- 3 mixture (EFNARC SCC class 3)

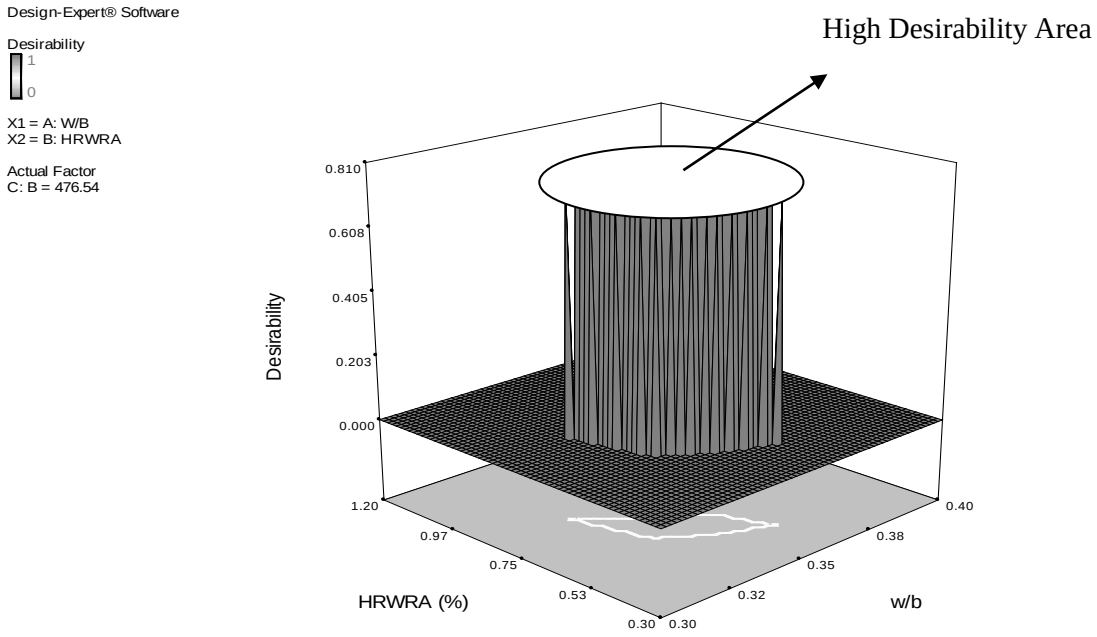

Figure 6.8 - Effect of w/b, HRWRA and total binder content at 476kg/m^{3}on the desirability function of ESH-LWSCC- 1 mixture (EFNARC SCC class 1)

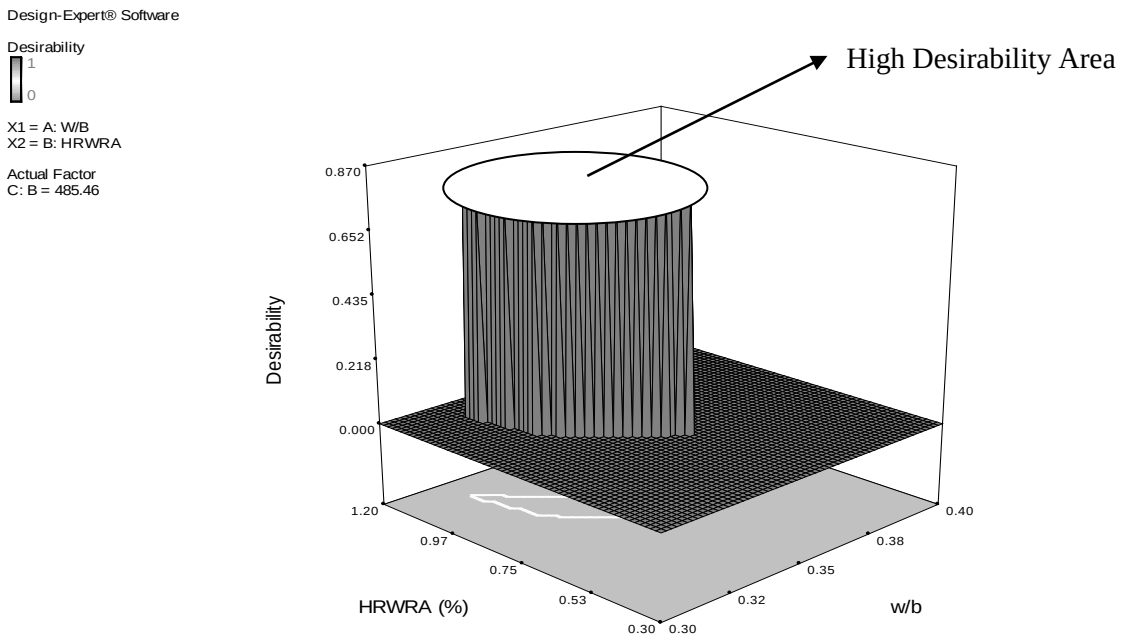

Figure 6.9 - Effect of w/b, HRWRA and total binder content at 486kg/m^{3}on the desirability function of ESH-LWSCC- 2 mixture (EFNARC SCC class 2)

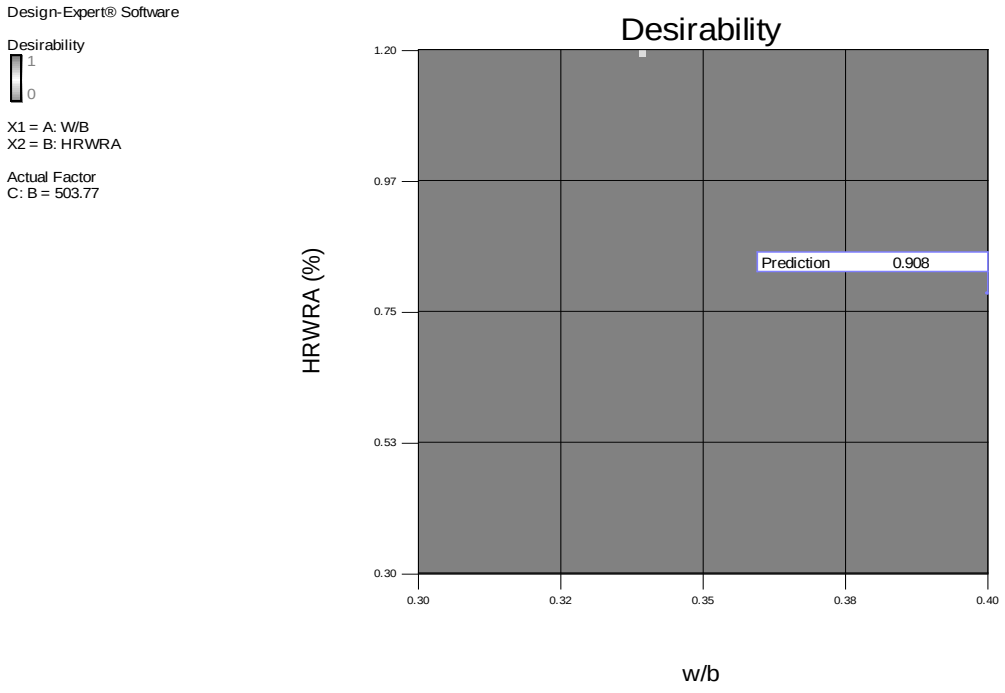

Figure 6.10 - Effect of w/b and HRWRA on the desirability function of ESH-LWSCC- 3 mixture (EFNARC SCC class 3)

6.3 Verification of Statistical Models

The accuracy of each of the proposed models was determined by comparing predicted-to-measured values obtained with mixes prepared at the centre of the experimental domain and five other random mixes.

Mixes 1 to 5 were randomly selected to cover a wide range of mixture proportioning within the modelled region, while mixes 6 to 10 were the centre points of the models. Mixture proportioning and measured responses of theses FS, EC and ESH-LWSCC mixtures are presented in Tables 6.5 to 6.10, respectively.

Table 6.5 - Mixture proportions for FS-LWSCC (Furnace Slag LWSCC)

Mix no	X1	X2	X3	Cement	FA	SF	HRWRA	Water	F-Slag aggregate, kg/m^3	
	w/b	HRWRA	binder	kg/m^3	kg/m^3	kg/m^3	l/m^3	l/m^3	Coarse	Fine
FS1	0.4	0.60	520	416	78	26	2.9	208	485	685
FS2	0.36	0.88	430	344	64	21	3.6	155	555	780
FS3	0.32	0.94	550	440	82	27	4.9	176	503	708
FS4	0.37	0.30	420	336	63	21	1.2	155	558	785
FS5	0.33	1.00	450	360	67	22	4.2	148	551	781
FS6	0.35	0.75	480	384	72	24	3.6	168	528	747
FS7	0.35	0.75	480	384	72	24	3.6	168	528	747
FS8	0.35	0.75	480	384	72	24	3.6	168	528	747
FS9	0.35	0.75	480	384	72	24	3.6	168	528	747
FS10	0.35	0.75	480	384	72	24	3.6	168	528	747

Table 6.6 - Mixture proportions for EC-LWSCC (Expanded Clay LWSCC)

Mix no	X1	X2	X3	Cement	FA	SF	HRWRA	Water	E-Clay aggregate, kg/m^3	
	w/b	HRWRA	binder	kg/m^3	kg/m^3	kg/m^3	l/m^3	l/m^3	Coarse	Fine
EC1	0.4	0.60	520	416	78	26	2.9	208	390	470
EC2	0.36	0.88	430	344	64	21	3.6	155	445	538
EC3	0.32	0.94	550	440	82	27	4.9	176	405	487
EC4	0.37	0.30	420	336	63	21	1.2	155	450	540
EC5	0.33	1.00	450	360	67	22	4.2	148	445	535
EC6	0.35	0.75	480	384	72	24	3.6	168	427	514
EC7	0.35	0.75	480	384	72	24	3.6	168	427	514
EC8	0.35	0.75	480	384	72	24	3.6	168	427	514
EC9	0.35	0.75	480	384	72	24	3.6	168	427	514
EC10	0.35	0.75	480	384	72	24	3.6	168	427	514

Table 6.7 - Mixture proportions for ESH-LWSCC (Expanded Shale LWSCC)

Mix no	X1	X2	X3	Cement	FA	SF	HRWRA	Water	ESH-Clay aggregate, kg/m^3	
	w/b	HRWRA	binder	kg/m^3	kg/m^3	kg/m^3	l/m^3	l/m^3	Coarse	Fine
ESH1	0.4	0.60	520	416	78	26	2.9	208	400	640
ESH2	0.36	0.88	430	344	64	21	3.6	155	455	733
ESH3	0.32	0.94	550	440	82	27	4.9	176	415	665
ESH4	0.37	0.30	420	336	63	21	1.2	155	462	738
ESH5	0.33	1.00	450	360	67	22	4.2	148	455	730
ESH6	0.35	0.75	480	384	72	24	3.6	168	438	698
ESH7	0.35	0.75	480	384	72	24	3.6	168	438	698
ESH8	0.35	0.75	480	384	72	24	3.6	168	438	698
ESH9	0.35	0.75	480	384	72	24	3.6	168	438	698
ESH10	0.35	0.75	480	384	72	24	3.6	168	438	698

Table 6.8 - Test results of FS- LWSCC mixes used to validate statistical models

Mix no	Slump flow (mm)	V-funnel (s)	J-ring Flow (mm)	J-ring height diff (mm)	L-box ratio	Filling capacity (%)	Bleeding (ml/cm^2)	SSR (%)
FS1	648	2.1	625	1.5	0.79	81	0.039	15
FS2	742	2.8	728	0.5	1.00	100	0.044	25
FS3	607	11.7	581	4.0	0.77	77	0.004	9
FS4	540	5.0	513	5.0	0.63	62	0.043	19
FS5	686	8.0	668	2.0	0.87	88	0.028	19
FS6	690	4.8	670	1.5	0.95	94	0.021	14
FS7	660	5.3	640	2.0	0.91	90	0.012	13
FS8	680	4.9	665	1.5	0.93	94	0.019	15
FS9	670	5.0	660	2.0	0.89	89	0.017	12
FS10	680	4.7	675	1.5	0.92	95	0.015	13

Mix no	Air content (%)	Set time (h:m)		Comp strength (MPa)		Unit weight (kg/m^3)		
		Initial	Final	7-day	28-day	Fresh	28-day air dry	28-day oven dry
FS1	3.4	05:35	07:23	24	34	1929	1765	1702
FS2	3.2	05:46	08:17	24	34	1906	1769	1712
FS3	3.2	05:08	07:11	32	45	1977	1809	1759
FS4	3.2	05:28	07:34	25	34	1903	1768	1734
FS5	3.6	05:07	07:33	28	39	1919	1789	1735
FS6	3.4	04:50	06:55	28	39	1910	1790	1713
FS7	4.0	05:35	07:10	30	42	1900	1780	1720
FS8	3.8	05:20	07:40	28	40	1903	1783	1723
FS9	3.6	05:30	07:15	29	40	1908	1775	1705
FS10	3.4	05:45	07:20	28	41	1922	1789	1735

Table 6.9 - Test results of EC- LWSCC mixes used to validate statistical models

Mix no	Slump flow (mm)	V-funnel (s)	J-ring Flow (mm)	J-ring height diff (mm)	L-box ratio	Filling capacity (%)	Bleeding (ml/cm^2)	SSR (%)
EC1	628	2.6	619	2.0	0.77	80	0.043	17
EC2	698	3.8	704	0.5	0.94	95	0.049	28
EC3	578	14.4	554	5.0	0.73	74	0.002	10
EC4	519	6.3	496	7.0	0.61	60	0.048	21
EC5	661	8.6	661	2.0	0.85	86	0.032	22
EC6	645	6.4	635	3.0	0.84	84	0.013	16
EC7	630	6.0	655	2.0	0.90	91	0.014	15
EC8	655	6.1	585	3.0	0.85	85	0.017	17
EC9	620	5.7	645	1.0	0.89	86	0.019	18
EC10	630	6.6	625	3.0	0.85	88	0.021	15

Mix no	Air content (%)	Set time (h:m)		Comp strength (MPa)		Unit weight (kg/m^3)		
		Initial	Final	7-day	28-day	Fresh	28-day air dry	28-day oven dry
EC1	2.8	6:03	7:35	23	30	1620	1526	1462
EC2	3.0	6:22	8:17	24	33	1603	1507	1449
EC3	3.0	5:28	7:07	31	40	1662	1555	1514
EC4	3.0	5:17	7:23	24	32	1600	1490	1451
EC5	3.2	5:53	7:43	27	38	1613	1519	1456
EC6	3.2	5:45	6:50	28	37	1605	1504	1439
EC7	3.4	5:25	6:55	27	37	1597	1496	1445
EC8	3.6	4:20	7:20	27	38	1599	1498	1448
EC9	3.4	5:30	7:35	29	39	1603	1491	1433
EC10	3.4	5:15	7:25	30	40	1615	1503	1458

Table 6.10 - Test results of ESH- LWSCC mixes used to validate statistical models

Mix no	Slump flow (mm)	V-funnel (s)	J-ring Flow (mm)	J-ring height diff (mm)	L-box ratio	Filling capacity (%)	Bleeding (ml/cm^2)	SSR (%)
ESH1	688	1.6	698	0.5	0.86	88	0.033	13
ESH2	715	2.6	698	1.5	1.00	100	0.036	22
ESH3	636	9.4	655	1.0	0.82	82	0.002	7
ESH4	562	3.7	542	5.5	0.69	68	0.037	19
ESH5	708	5.8	695	1.5	0.95	96	0.024	19
ESH6	705	3.7	710	2.0	0.98	100	0.016	11
ESH7	685	4.0	680	1.0	1.00	99	0.011	12
ESH8	700	3.7	700	1.0	0.97	97	0.017	13
ESH9	685	3.5	680	1.0	1.00	97	0.013	10
ESH10	705	4.1	700	2.0	0.99	99	0.015	12

Mix no	Air content (%)	Set time (h:m)		Comp strength (MPa)		Unit weight (kg/m^3)		
		Initial	Final	7-day	28-day	Fresh	28-day air dry	28-day oven dry
ESH1	2.8	5:56	7:23	27	38	1806	1702	1630
ESH2	2.8	5:48	7:35	27	39	1781	1675	1611
ESH3	3.0	5:17	7:19	36	50	1853	1733	1688
ESH4	3.0	5.05	7:21	27	37	1782	1662	1616
ESH5	3.0	5.34	7:33	30	44	1797	1692	1622
ESH6	3.2	5:05	6:40	34	48	1789	1676	1604
ESH7	3.2	5:25	6:35	32	44	1779	1667	1611
ESH8	3.4	4:45	6:40	31	45	1782	1670	1614
ESH9	3.2	5:15	7:05	33	46	1787	1662	1597
ESH10	3.0	5:25	7:25	31	43	1800	1675	1625

Comparisons between predicted and measured values for various FS-LWSCC responses are illustrated in Figures 6.11 through 6.26, where the dashed lines present the upper and lower estimated error at 95% confidence limit (determined in Chapter 6, Tables 5.7 to 5.9). Points found above the 1:1 diagonal line indicates that the statistical model overestimates the measured response.

On average, the predicated-to-measured ratios of slump flow, J-Ring flow, L- box ratio (h_2/h_1), V-funnel flow time, J-Ring height difference, filling capacity %, bleeding, air content %, segregation index %, fresh unit weight, 28-day oven dry unit weight, and 7- and 28-day compressive strengths were 1.0, 1.0, 1.0, 0.98,1.0, 1.03, 0.96, 0.98, 0.99, 1.0, 1.0, 1.01 and 1.03, respectively, indicating an accurate prediction of measured responses within the modelled region. The majority of the data for the measured responses lie close to the 1:1 diagonal line, resulting in the mean value of ratio between predicated-to-measured responses to be 1.00 ± 0.03 (with the exception of the bleeding response). This indicates a high accuracy of the derived model to predicate the response.

On the other hand, the majority of the predicated slump flow, J-Ring flow, L- box ratio- h_2/h_1, V-funnel flow time, J-Ring height difference, filling capacity %, bleeding, air content %, segregation index %, fresh unit weight, 28-day oven dry unit weight, and 7- and 28-day compressive strengths values (Figures 6.11 to 6.19, 6.23, 6.24 and 6.26) are within the acceptable limit of ± 11.83 mm, ± 14.71 mm, ±0.02, ± 0.21s, ± 0.40 mm, ±3.2%, ±0.0038 ml/cm^2, ±0.28%, ±1.44%, 11.30 kg/m^3, ±14.52, ±1.24 MPa and ±1.75 MPa, respectively as reported in Table 5.7 of Chapter 5. These limits constitute experimental errors for the slump flow, J-Ring flow, h_2/h_1, V-funnel flow time, J-Ring height difference, filling capacity %, bleeding, air content %, segregation index %, fresh unit weight, 28-day oven dry unit weight, and 7- and 28-day compressive strengths measurements determined from the repeatability tests.

All of the predicated initial and final setting times and 28-day air-dry unit weight values (Figures 6.20, 6.21 and 6.25) are quite close to the measured values with ratio of the predicated-to-measured value of 1.01, 1.01 and 1.00, respectively. The 10 predicted values for each test are within the 95% confidence limit of the measured response.

As can be seen from the validation investigation, the derived models offer adequate predication of workability, unit weight and compressive strength response within the experimental domain of the modelled mixture parameters. It is important to note that the absolute values of the predicated values are expected to change with the changes in raw material characteristics. However, the relative contributions of the various parameters are expected to be the same, thus facilitating the mix design protocol.

It is worth nothing that comparison between predicted and measured values of various EC-LWSCC and ESH-LWSCC responses are illustrated in **Appendix A**.

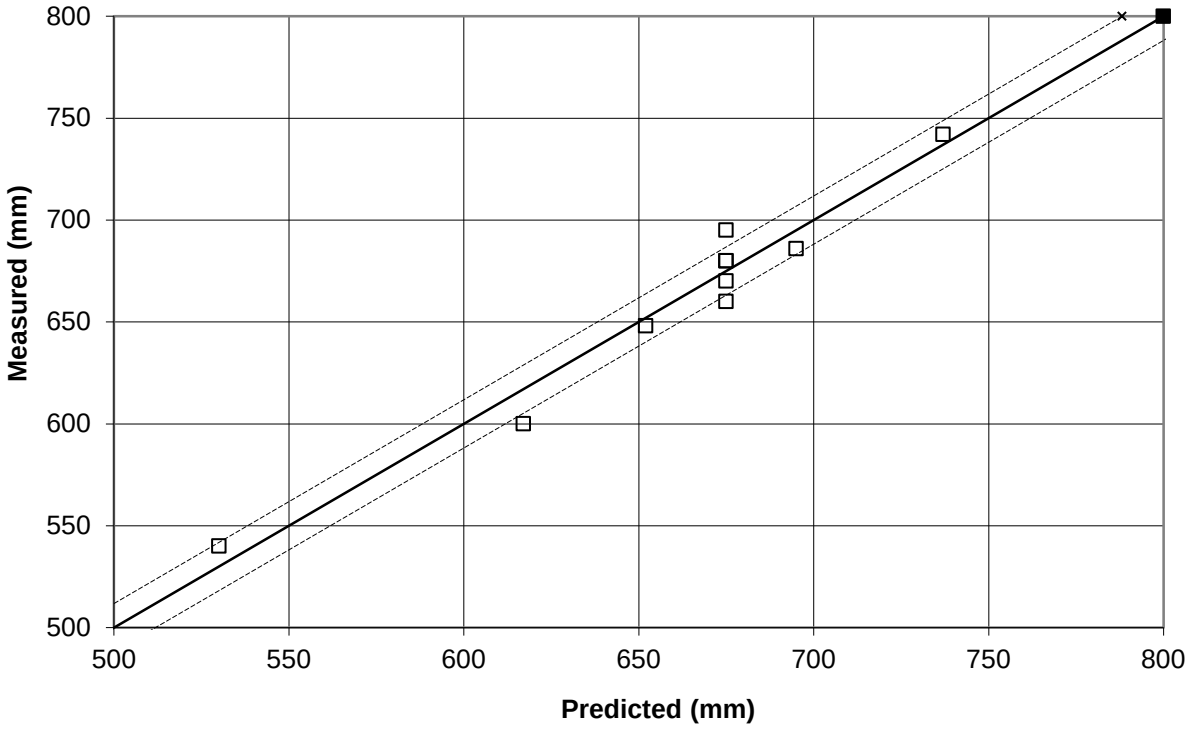

Figure 6.11 - Predicted vs. measured slump flow values of FS-LWSCC model

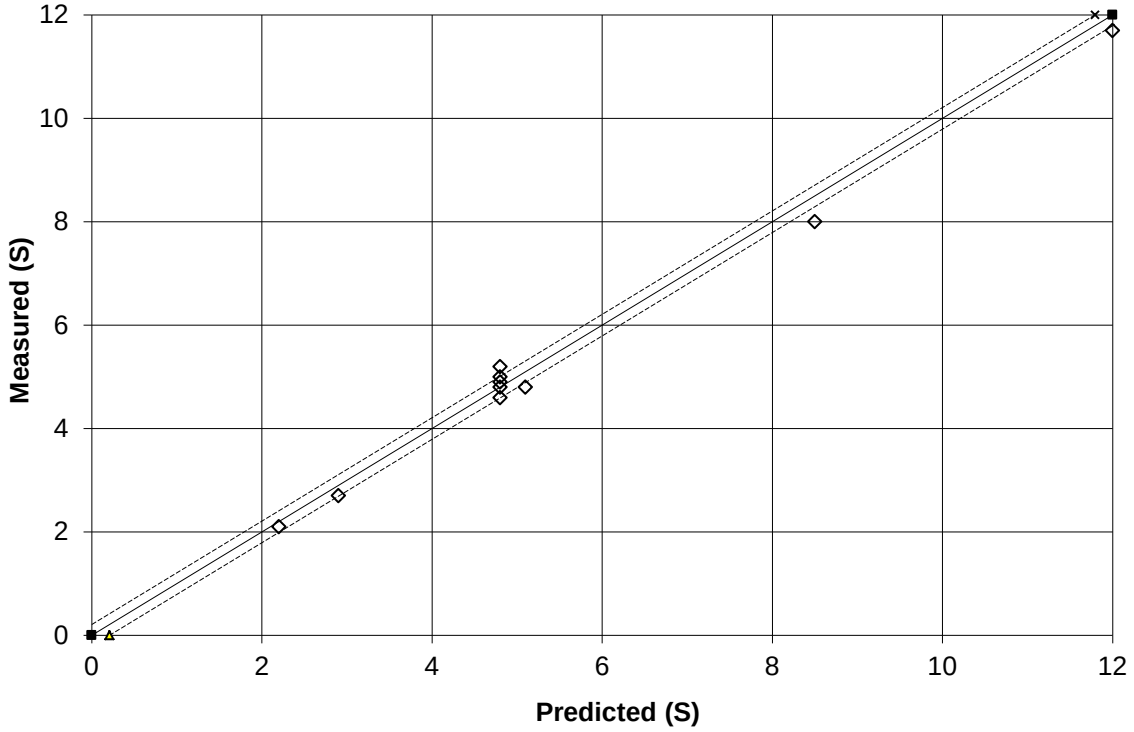

Figure 6.12 - Predicted vs. measured V-funnel values of FS-LWSCC model

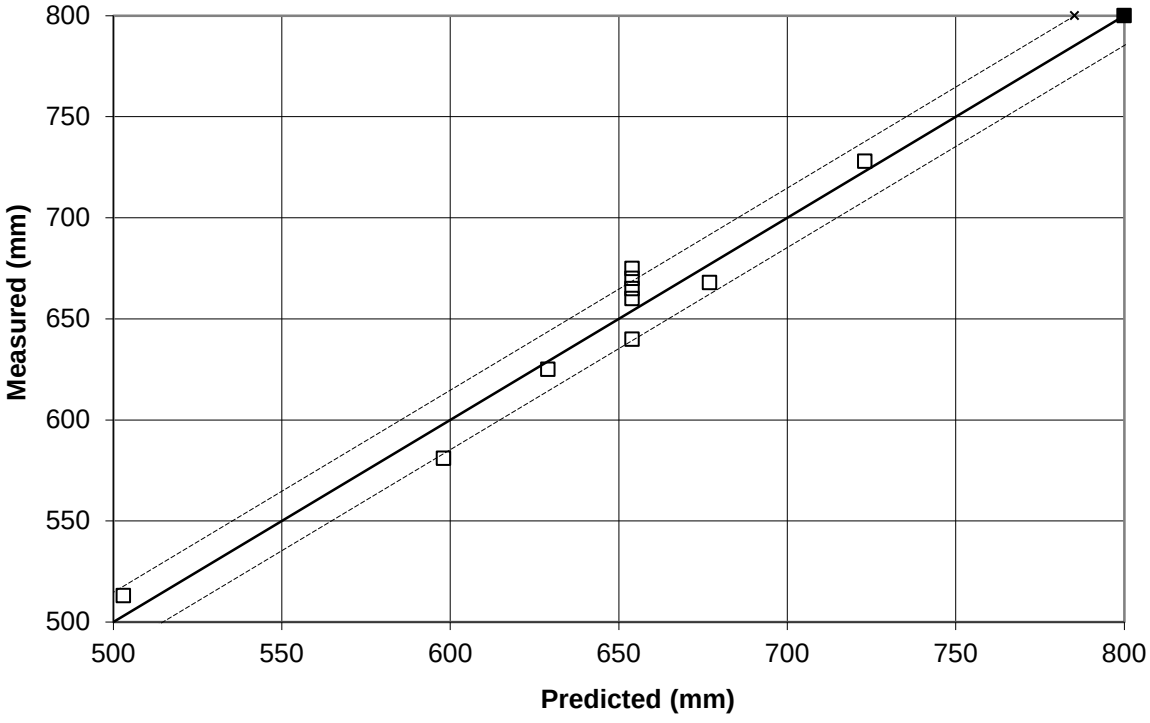

Figure 6.13 - Predicted vs. measured J-ring values of FS-LWSCC model

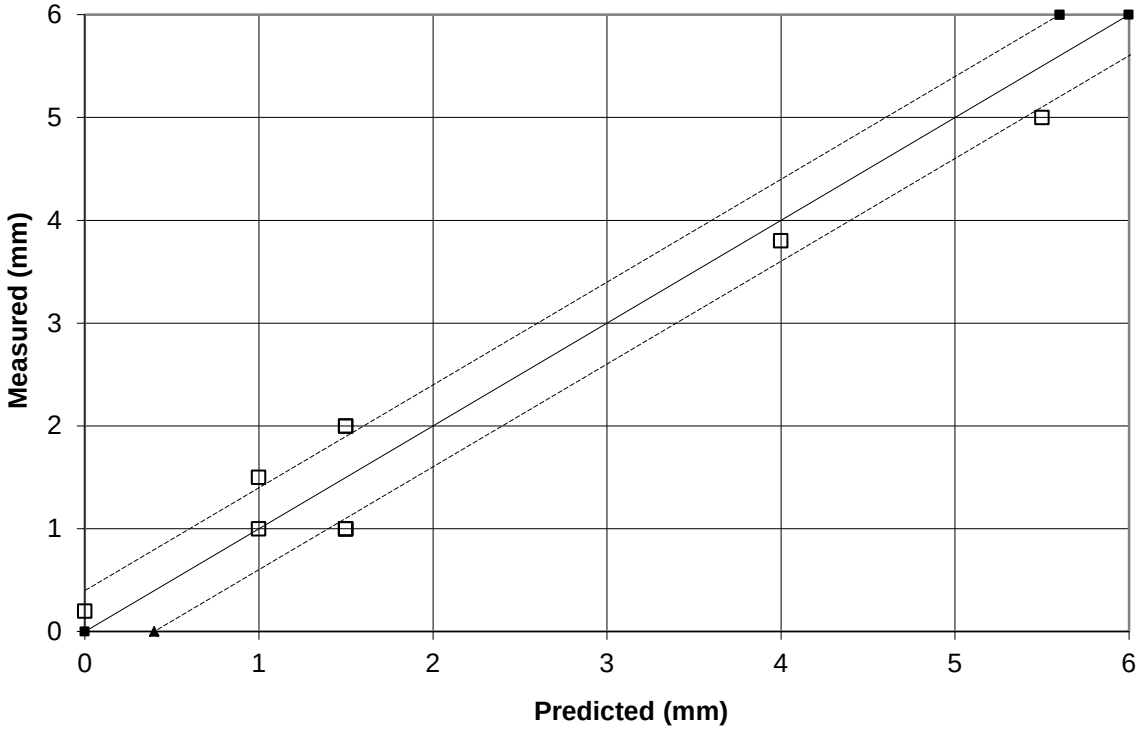

Figure 6.14 - Predicted vs. measured J-ring height diff values of FS-LWSCC model

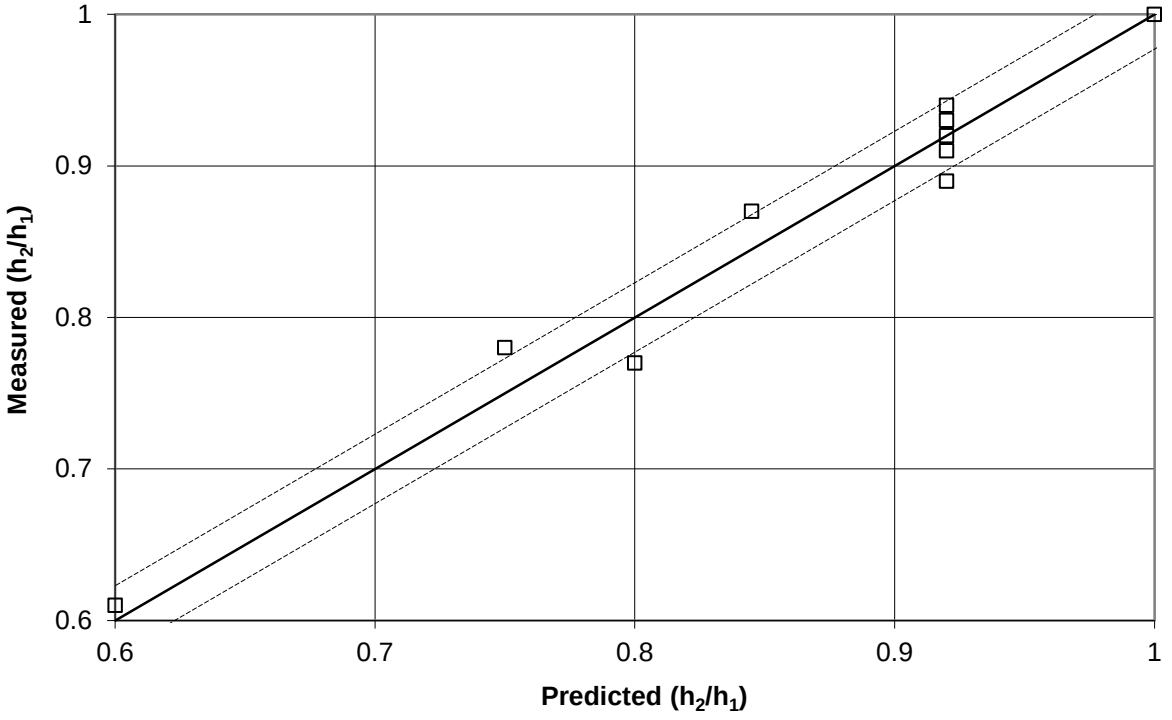

Figure 6.15 - Predicted vs. measured L-box values of FS-LWSCC model

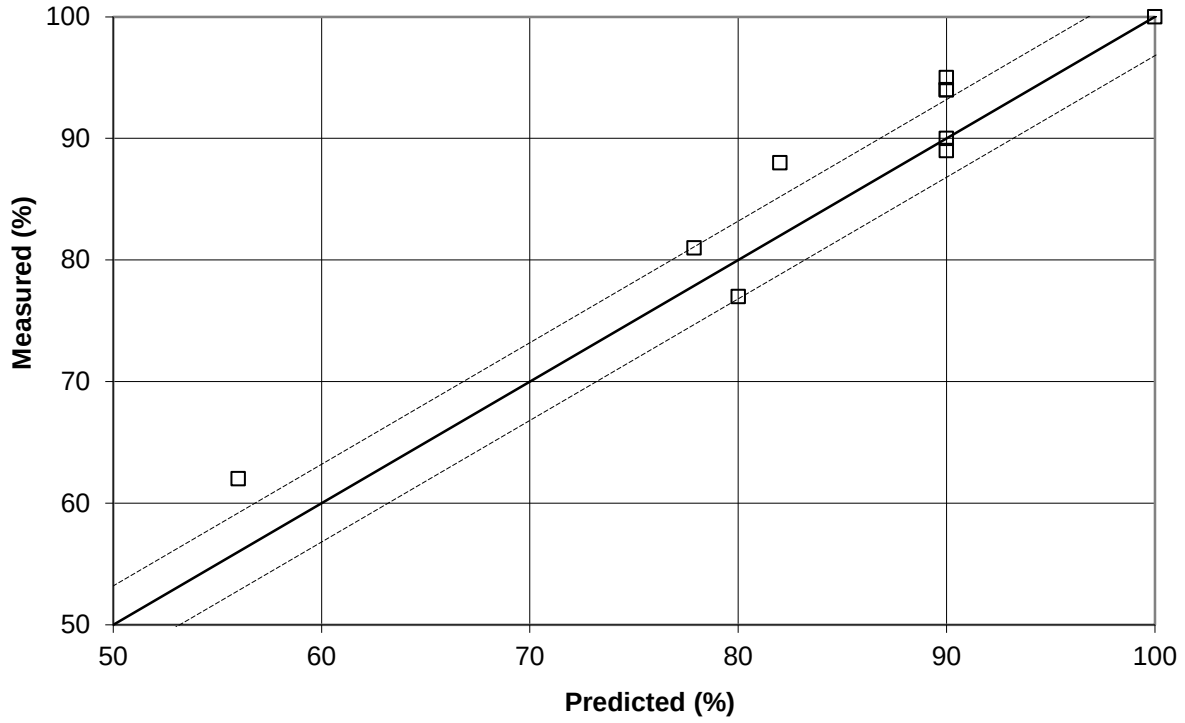

Figure 6.16 - Predicted vs. measured filling capacity values of FS-LWSCC model

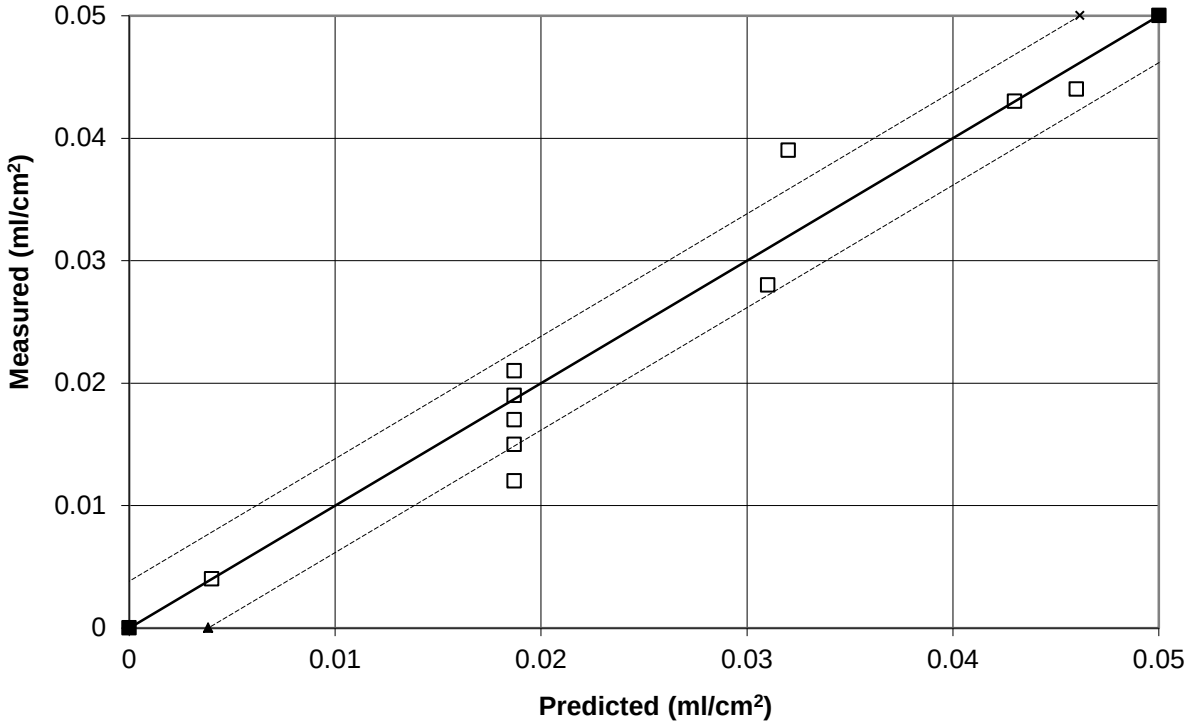

Figure 6.17 - Predicted vs. measured bleed water values of FS-LWSCC model

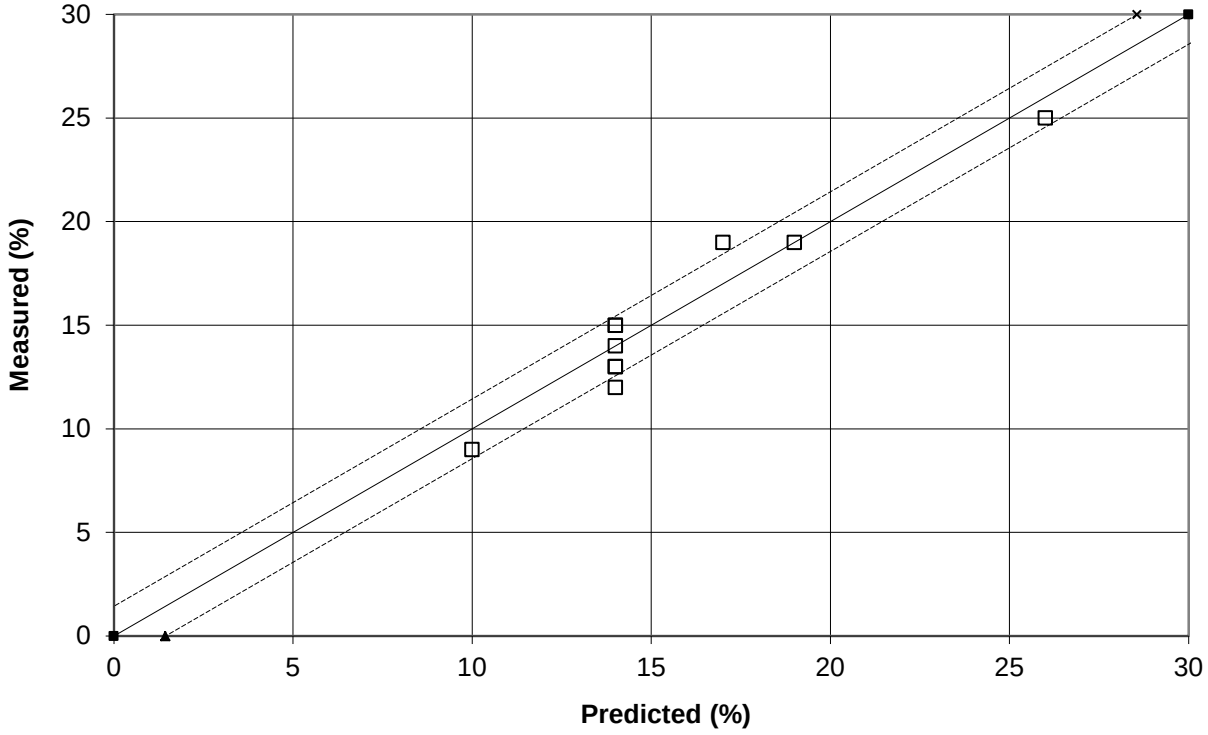

Figure 6.18 - Predicted vs. measured segregation index values of FS-LWSCC model

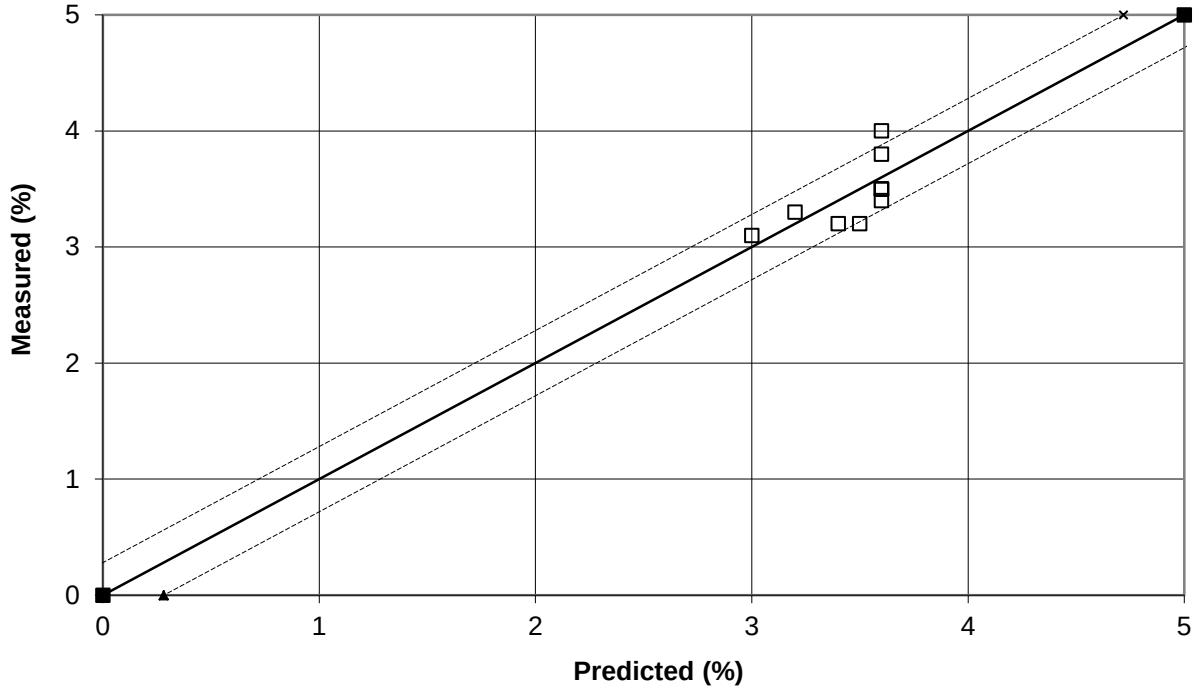

Figure 6.19 - Predicted vs. measured air content values of FS-LWSCC model

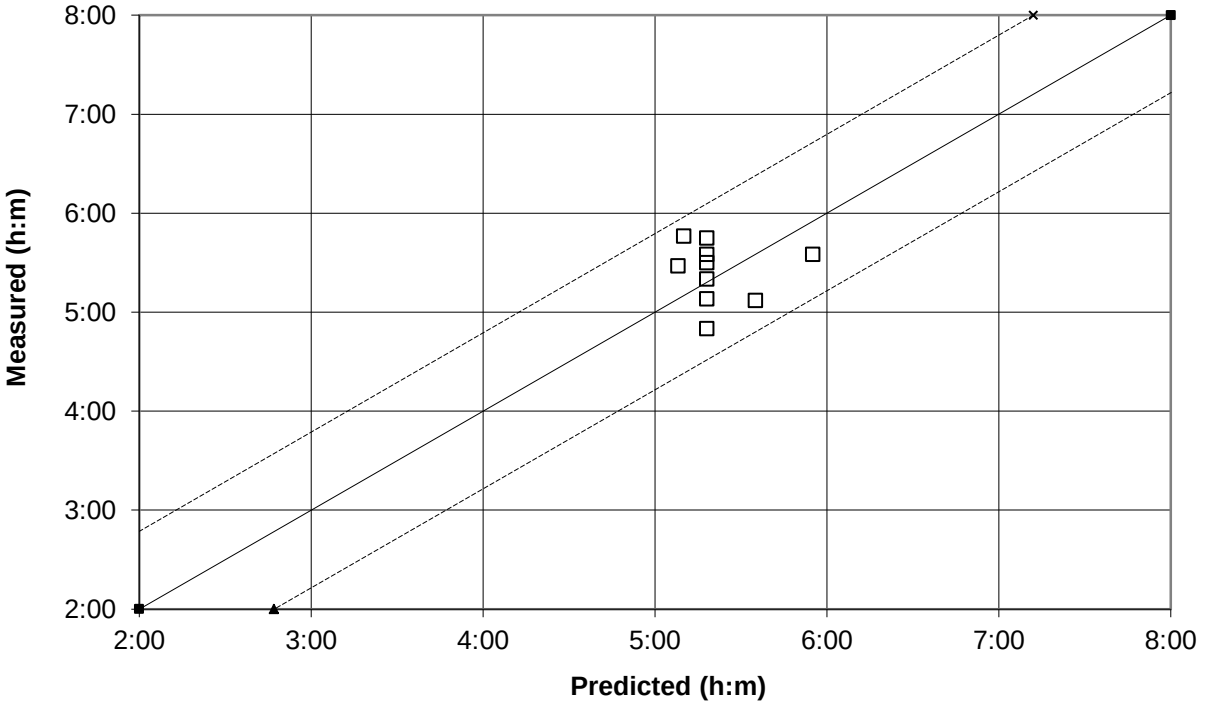

Figure 6.20 - Predicted vs. measured initial set time values of FS-LWSCC model

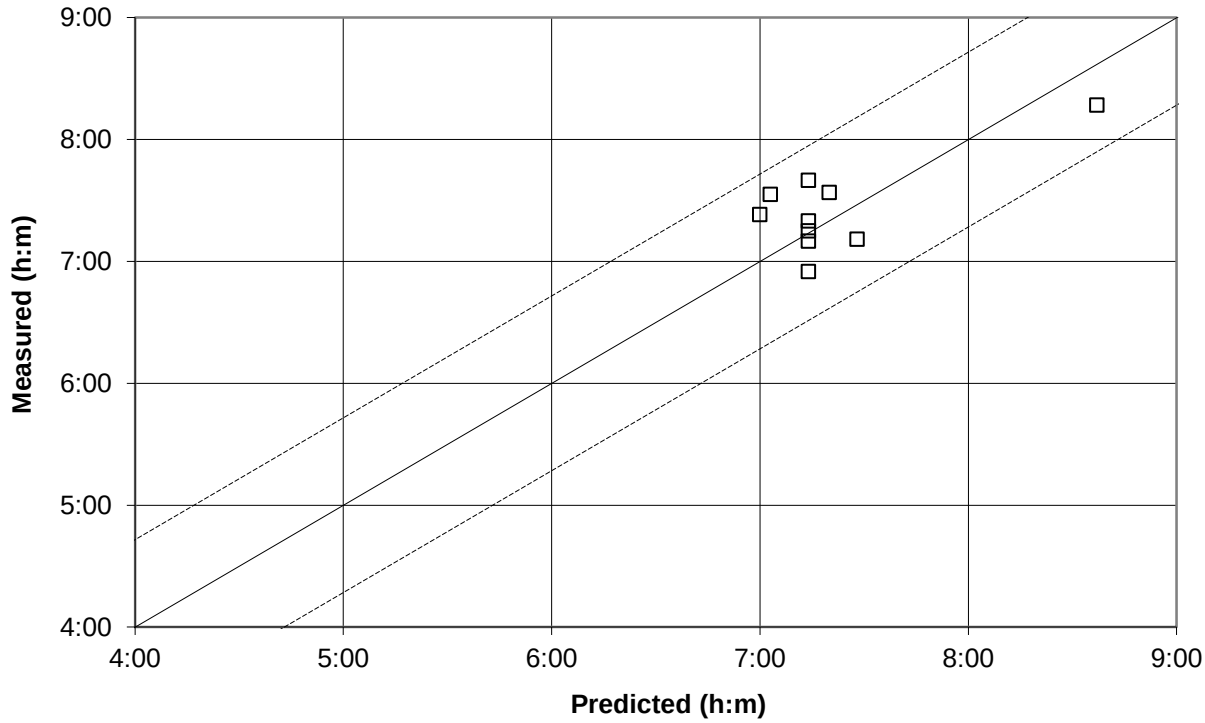

Figure 6.21 - Predicted vs. measured final set time values of FS-LWSCC model

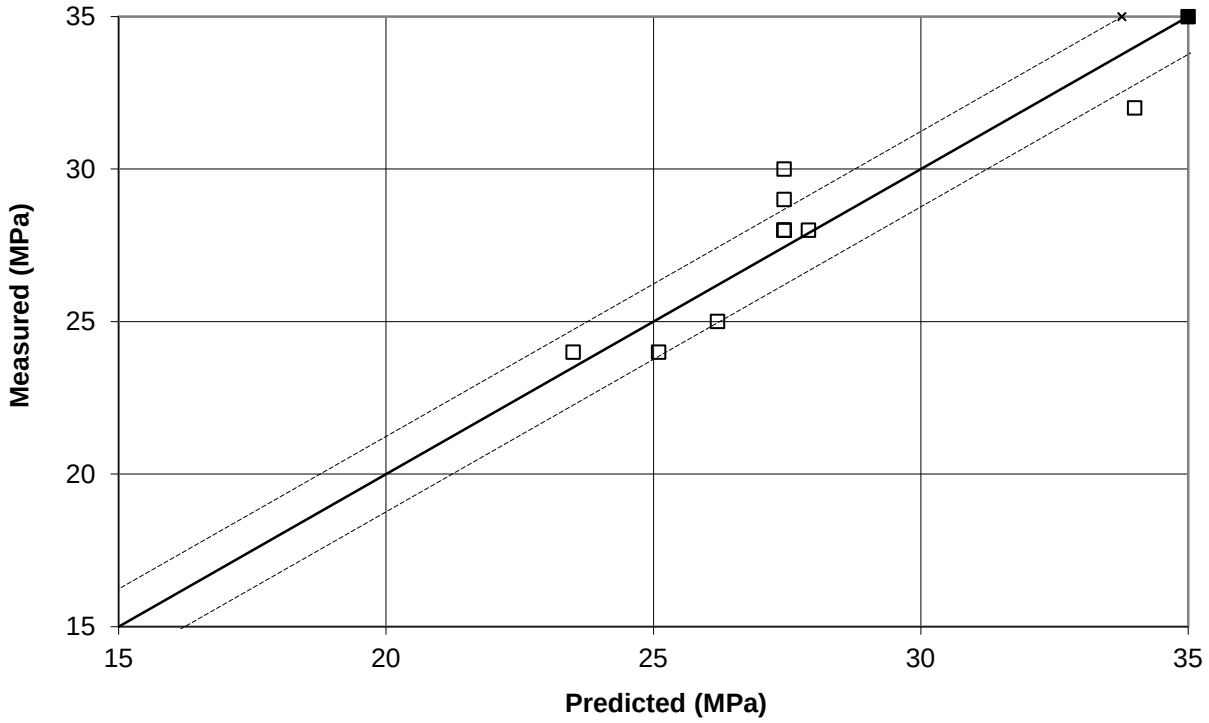

Figure 6.22 - Predicted vs. measured 7-day compressive strength of FS-LWSCC model

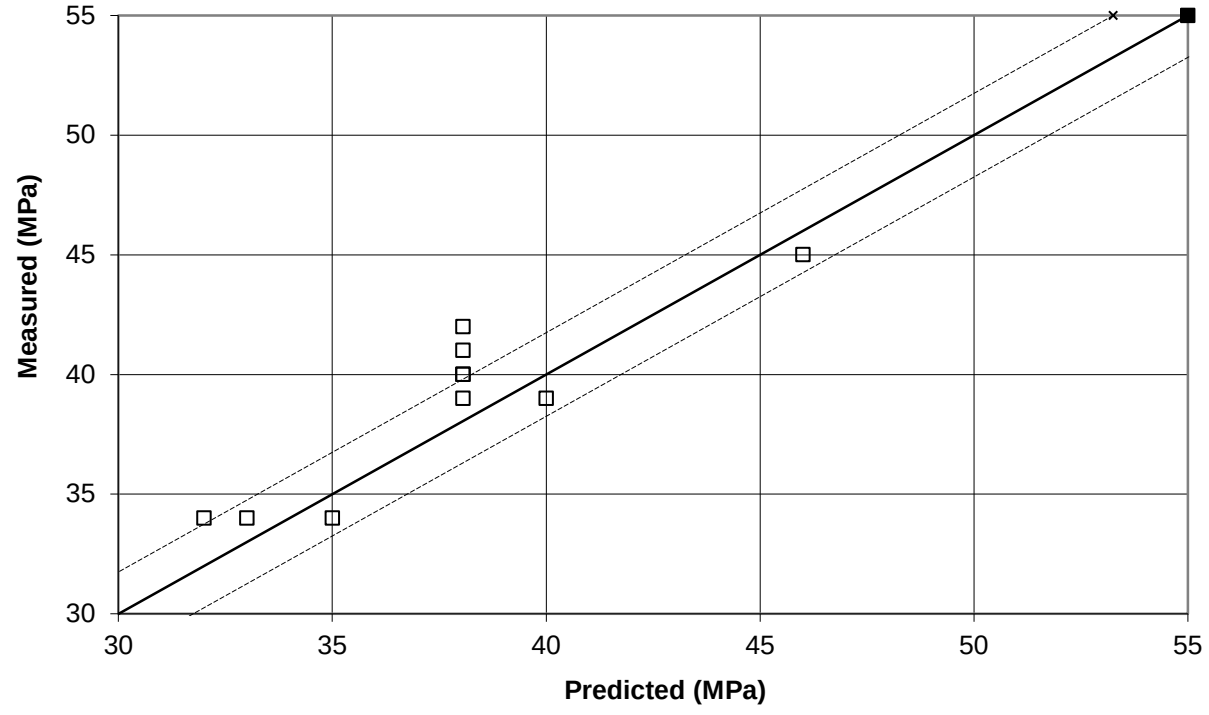

Figure 6.23 - Predicted vs. measured 28-day compressive strength of FS-LWSCC model

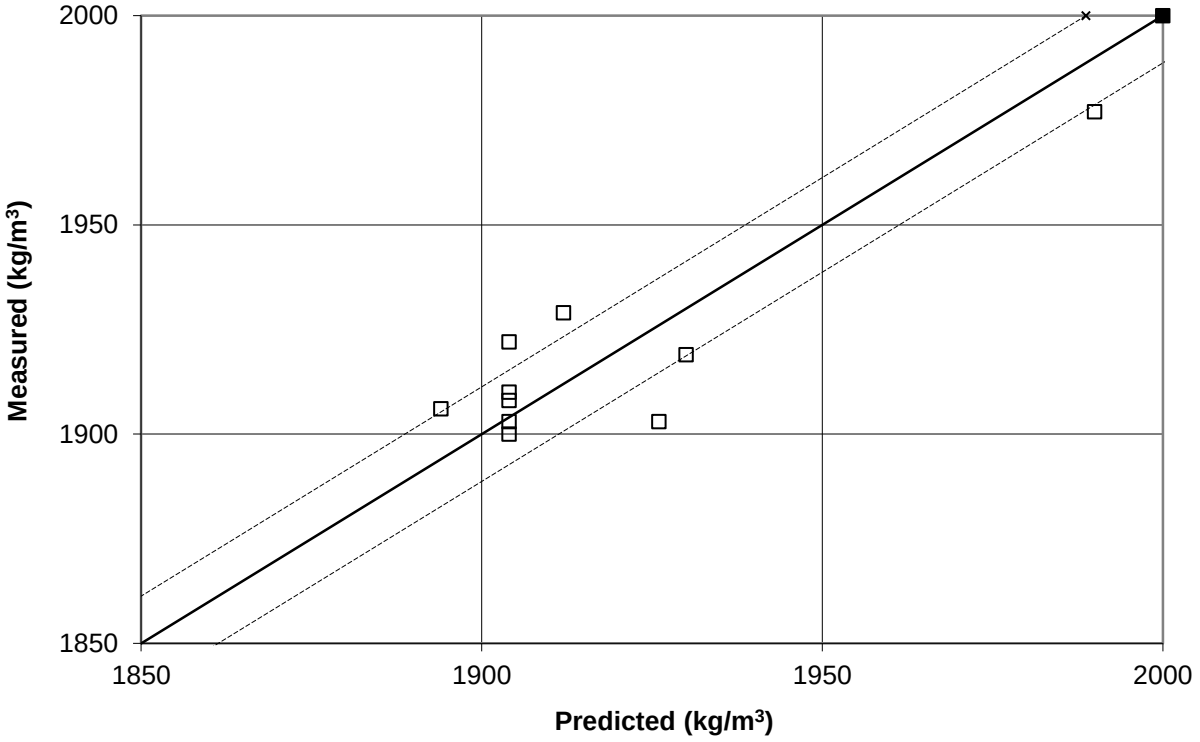

Figure 6.24 - Predicted vs. measured fresh unit weight of FS-LWSCC model

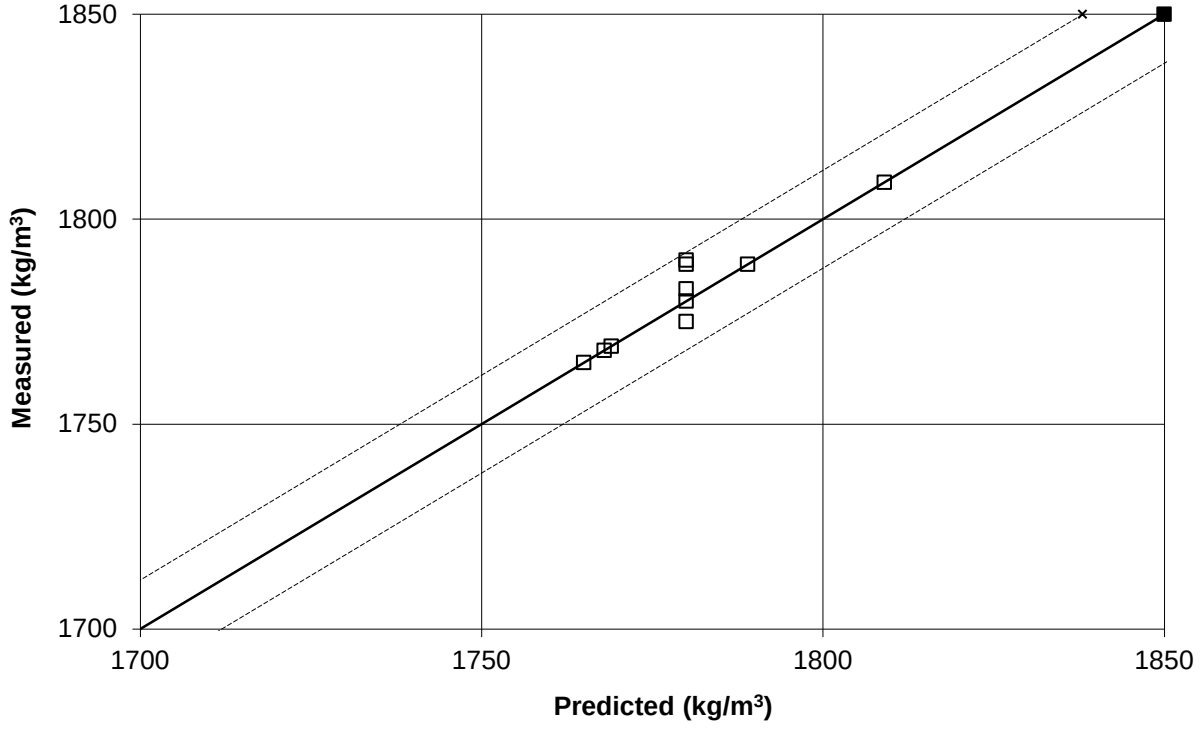

Figure 6.25 - Predicted vs. measured 28-day air dry unit weight of FS-LWSCC model

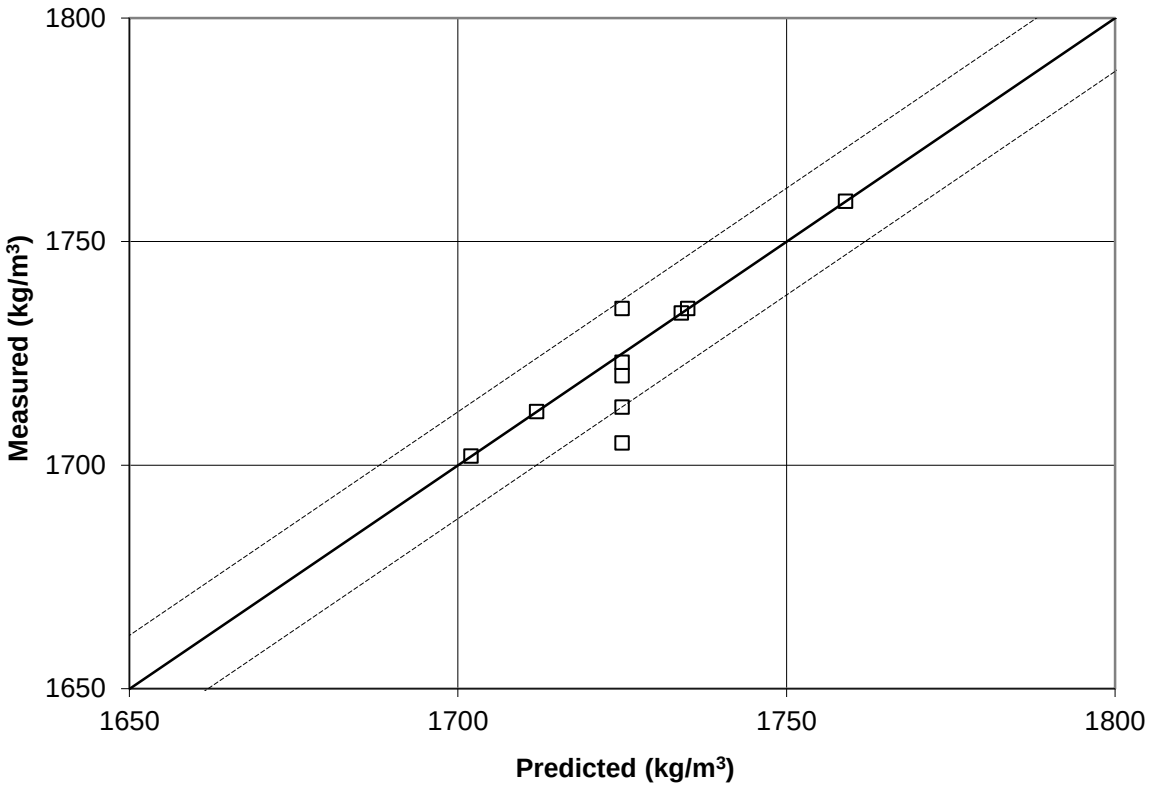

Figure 6.26 - Predicted vs. measured 28-day oven dry unit weight of FS-LWSCC model

6.4 Verification Experiment for an Optimum Mix Design

Utilizing the established high statistical confidence of the developed models, an experimental study was used to validate whether the theoretically proposed optimum mix design parameters such as w/b, HRWRA (%), and total binder (b) could yield the desired responses of three classified EFNARC industrial SCC mixtures. The test was carried out with the same materials and under the same testing conditions. The results are presented in Tables 6.11, 6.12 and 6.13.

Table 6.11 - FS-LWSCC - Theoretically optimum mix proportions and experimental results

Mix No.	FS-LWSCC-1		FS-LWSCC-2		FS-LWSCC-3	
Mix Parameters and responses	**FS-LWSCC-1 Opt values and expected response**	**Experimental results for Opt mix proportions**	**FS-LWSCC-2 Opt values and expected response**	**Experimental results for Opt mix proportions**	**FS-LWSCC-3 Opt values and expected response**	**Experimental results for Opt mix proportions**
w/b	0.36	0.36	0.35	0.35	0.4	0.4
HRWRA	0.64	0.64	0.95	0.95	0.95	0.95
Binder	494	494	520	520	537	537
Slump Flow (mm)	650	635	720	750	765	795
V-Funnel (s)	4	4.55	4	4.2	1.3	2.3
J-Ring Flow (mm)	630	610	700	735	750	770
J-Ring Height (mm)	2.6	3.1	0.8	0	0	0
L-Box (%)	0.87	0.81	0.97	0.92	1	1
Filling Capacity (%)	87	80	97	90	100	100
Sieve Segregation (%)	15	10	15	12	17	18
Bleeding (ml/cm^2)	0.03	0.02	0.02	0.03	0.04	0.07
Air Content (%)	3.6	3	3.3	2.4	2.8	2.2
Set Time Initial (h:m)	04:45	04:20	05:00	05:35	05:45	06:25
Set time Final (h:m)	06:05	06:45	07:10	07:45	08:00	08:40
7-day Comp Strength (MPa)	27	29.61	28	28.3	24	22.2
28-day Comp Strength (MPa)	38	42.61	39	41.1	33	33.24
Fresh Unit Weight (kg/m^3)	1909	1942	1926	1920	1916	1950
28-day Air dry Unit (kg/m^3)	1842	1886	1847	1809	1824	1817
28-day Oven Dry Unit (kg/m^3)	1768	1800	1778	1768	1741	1735
Desirability	0.803	-	0.844	-	0.898	-

Table 6.12 - EC-LWSCC- Theoretically optimum mix proportions and experimental results

Mix No.	EC-LWSCC-1		EC-LWSCC-2		EC-LWSCC-3	
Mix Parameters and responses	**EC-LWSCC-1 Opt values and expected response**	**Experimental results for Opt mix proportions**	**EC-LWSCC-2 Opt values and expected response**	**Experimental results for Opt mix proportions**	**EC-LWSCC-3 Opt values and expected response**	**Experimental results for Opt mix proportions**
w/b	0.37	0.37	0.37	0.37	0.40	0.40
HRWRA	0.75	0.75	0.99	0.99	1.17	1.17
Binder	526	526	543	543	543	543
Slump Flow (mm)	650	630	695	670	760	770
V-Funnel (s)	4.2	4.6	4	3.8	1.3	2.3
J-Ring Flow (mm)	644	625	693	660	770	765
J-Ring Height (mm)	1.75	2	0.426	0	0	0
L-Box (%)	0.87	0.85	0.938	0.9	0.98	0.99
Filling Capacity (%)	88	85	94	89	97	98
Sieve Segregation (%)	12	11	13	12	20	19
Bleeding (ml/cm^2)	0.0291	0.022	0.0269	0.02	0.0465	0.0352
Air Content (%)	3	3.5	2.8	2.4	2.4	2
Set Time Initial (h:m)	5:40	5:30	5:06	4:55	6:40	6:25
Set time Final (h:m)	6:05	6:00	7:04	6:50	9:00	9:25
7-day Comp Strength (MPa)	25.65	26.35	25.91	26.5	21.5	22.75
28-day Comp Strength (MPa)	35	37.2	34.56	35.3	28.11	30.25
Fresh Unit Weight (kg/m^3)	1619	1635	1627	1670	1607	1652
28-day Air dry Unit (kg/m^3)	1527	1539	1524	1570	1488	1528
28-day Oven Dry Unit (kg/m^3)	1465	1476	1479	1505	1454	1438
Desirability	0.81	-	0.83	-	0.90	-

Table 6.13 - ESH-LWSCC - Theoretically opt mix proportions and experimental results

Mix No.	ESH-LWSCC-1		ESH-LWSCC-2		ESH-LWSCC-3	
Mix Parameters and responses	**ESH-LWSCC-1 Opt values and expected response**	**Experimental results for Opt mix proportions**	**ESH - LWSCC-2 Opt values and expected response**	**Experimental results for Opt mix proportions**	**ESH - LWSCC-3 Opt values and expected response**	**Experimental results for Opt mix proportions**
w/b	0.35	0.35	0.35	0.35	0.40	0.40
HRWRA	0.61	0.61	0.83	0.83	0.78	0.78
Binder	476	476	486	486	504	504
Slump Flow (mm)	650	645	708	725	760	770
V-Funnel (s)	4	4.9	4	3.8	1.32	2.1
J-Ring Flow (mm)	650	635	709	715	765	760
J-Ring Height (mm)	2.2	2	0.83	0	0	0
L-Box (%)	0.91	0.87	1	0.98	0.99	0.99
Filling Capacity (%)	90	88	99.4	98	99.99	98
Sieve Segregation (%)	13.1	12.1	14	13	17.75	18.5
Bleeding (ml/cm^2)	0.02357	0.0153	0.021	0.0154	0.0372	0.0254
Air Content (%)	3	2.8	3.033	2.4	2.8	2.1
Set Time Initial (h:m)	5:00	5:20	5:02	5:25	5:40	6:05
Set time Final (h:m)	6:06	6:35	6:08	6:50	7:40	8:00
7-day Comp Strength (MPa)	30.2	32.2	30.6	33	25.8	24.5
28-day Comp Strength (MPa)	44.6	45.75	45.4	47.75	36.95	35.1
Fresh Unit Weight (MPa)	1784	1810	1791	1763	1790	1780
28-day Air dry Unit (kg/m^3)	1688	1653	1695	1708	1689	1650
28-day Oven Dry Unit (kg/m^3)	1606	1585	1614	1602	1610	1590
Desirability	0.81	-	0.86	-	0.91	-

As it can be seen from the optimization/validation process, all three models satisfactorily derived the three desired EFNARC-SCC industrial class mixtures. The optimized mixes satisfy the ranges for slump flow, V-funnel time, L-box ratio and segregation resistance percentage (Tables 6.11 to 6.13).

6.5 Summary

The verification study results showed that the proposed optimum mix proportions satisfied the expected goal responses of slump flow, V-funnel flow time, J-Ring flow, J-Ring height difference, L-box ratio, filling capacity, bleeding, air content, initial and final setting time, sieve segregation test, fresh unit weight, 28-day air dry unit weight, 28-day oven dry unit weight, and 7- and 28-day compressive strengths.

The derived statistical models can therefore be used as useful and reliable tools in understanding the effect of various mixture constituents and their interactions on the fresh properties of LWSCC. The analysis of the derived models enables the identification of major trends and predicts the most promising direction for future mixture optimization. This can reduce the cost, time, and effort associated with the selection of trial batches.

CHAPTER SEVEN

7 EVALUATION OF THE MECHANICAL AND MASS TRANSPORT PROPERTIES OF LWSCC MIXTURES

7.1 Introduction

To date, lightweight self-consolidating concrete (LWSCC) has been successfully used in various applications where conventional concrete is difficult to place and vibrate especially in heavy reinforced structural elements and where reduction in element weight is necessary. Chapter 7 presents Phase IV of the experiential program, where key fresh, mechanical, and mass transport properties of three selected and optimized EFNARC classified LWSCC mixtures made with furnace slag (FS), expanded clay (EC) and expanded shale (ESH) aggregates were investigated.

Tests were conducted to investigate workability, fresh/air dry/oven dry unit weights, setting times, compressive/flexural/splitting tensile strength over time, bond strength, porosity, water absorption, the rate of absorption (sorptivity), resistance to chloride-ion penetration (RCPT), and drying shrinkage.

7.2 Testing Program

Three LWSCC mixtures made with three different lightweight aggregates, furnace slag (FS), expanded clay (EC) and expanded shale (ESH) (total nine mixes) aimed to satisfy EFNARC classes for SCC (1, 2 and 3) as described in Chapter 6 were investigated for fresh, mechanical and mass transport properties.

In order to establish unbiased comparison, LWSCC-1, LWSCC-2 and LWSCC-3 were proportioned with w/b of 0.36, 0.35 and 0.40, total binder content of 494, 520 and 537 kg/m^3, respectively for each class of LWSCC namely FS, EC and ESH. As explained in Chapter 5, the binder content had to be increased for LWSCC-2 and for LWSCC-3 in order to achieve high workable mixes while the HRWRA dosage was adjusted to satisfy the sieve segregation resistance limits (maximum 15% for LWSCC-1 & LWSCC-2 and 20% for LWSCC-3).

Based on the materials packing density (explained in Chapter 4), for a given mix design where all mix parameters are fixed, the EC-LWSCC mixtures will yield lower segregation resistance compared to both FS-LWSCC and ESH-LWSCC mixtures. On the other hand, the ESH-LWSCC mixtures will result in high workability characteristics than both EC-LWSCC and FS-LWSCC mixtures. Table 7.1 summarizes the mix parameters and the key fresh properties of the LWSCC mixtures.

Table 7.1- Mix parameters and fresh properties of LWSCC

Mix Parameters and fresh properties	FS-LWSCC			EC-LWSCC			ESH-LWSCC		
	1	**2**	**3**	**1**	**2**	**3**	**1**	**2**	**3**
w/b	0.36	0.35	0.4	0.36	0.35	0.4	0.36	0.35	0.4
HRWRA	0.64	0.95	0.95	0.57	0.87	0.87	0.57	0.87	0.87
Binder	494	520	537	494	520	537	494	520	537
A^*/b	2.5	2.35	2.13	1.86	1.72	1.56	2.25	2.10	1.90
Slump Flow (mm)	635	750	795	590	655	710	650	750	800
V-Funnel (s)	4.6	4.2	2.3	5.8	6.3	2.0	3.2	3.2	1.6
J-Ring Flow (mm)	610	735	770	570	645	690	660	750	800
L-Box (%)	0.81	0.92	1.00	0.78	0.88	0.89	0.91	1.00	1:00
Filling Capacity (%)	80	90	100	79	89	91	90	100	100
Sieve Segregation (%)	10	12	18	15	15	19.5	9	10	14
Initial Set Time (h:m)	4:20	5:35	6:25	5:13	5:33	6:16	4:33	5:20	6:08
Final Set Time (h:m)	6:45	7:45	8:40	6:54	7:27	8:00	6:45	7:13	8:14

$^*A$ = total aggregate; A/b = total aggregate to binder ratio by mass

When the obtained slump flow diameter, V-funnel flow time, L-box ratio and segregation resistance % are evaluated, mixes LWSCC-1, 2 and 3 with FS and ESH can be classified as

(SF1, VF1, PA2 and SR2), (SF2, VF1, PA2 and SR2), (SF3, VF1, PA2 and SR1), respectively, as per ERNARC consistency classification. EC LWSCC-1 did not satisfy the minimum passing ability lower limit of 0.8 (Table 7.1). Both LWSCC 1 and 2 mixes with EC did not satisfy the minimum slump flow lower limits at 660 and 760 mm, respectively, as outlined in Table 6.1.

7.2.1 Casting of Test Specimens

In Phase IV, all specimens casting was designed to cover investigation on mechanical, transport and durability properties of LWSCC mixtures. As a result, all concrete mixtures were prepared in 125 L big batches in a fixed horizontal industrial pan mixer as shown in Figure 7.1. Same mix preparation and sequence was followed as in Phase I. Just after mixing, the slump flow, L-box, V-funnel, J-ring flow, filling capacity, sieve segregation, unit weight and setting time tests were conducted. Summary of specimen's numbers and test methods is presented in Table 7.2. From each batch, thirty nine 100 × 200 mm cylinders were cast: two for air dry unit weight, two for oven dry unit weight, two for porosity/water absorption, eight for compressive strength, six for split tensile strength, four for sorptivity/resistance to chloride-ion penetration (RCPT), four for bond strength, two for corrosion resistance, one for hardened air void/spacing factor and eight for acid attack resistance tests. Six 75 × 100 × 410 mm beams for flexural strength, six 75 × 75 × 285 mm prisms (three for freezing-and-thawing resistance and three for drying shrinkage test) were cast. In addition, eight 150 × 150 × 150 mm cubes for elevated temperature resistance test, and one 300 × 300 × 75 mm block for scaling resistance test were cast.

All LWSCC specimens were cast without compaction or mechanical vibration. After casting, all the specimens were covered with plastic sheets and water-saturated burlap and left at room temperature for 24 hours. They were then demolded and transferred to the moist curing room, and maintained at 23 ± 2°C and 100% relative humidity until testing. The cylinders for the air dry unit weight test were stored in room temperature for 28 days, while the cylinders for oven dry unit weight test were transferred after curing period to the oven at 110 ± 5°C . The prisms for the drying shrinkage test were stored in lime-saturated water for 28 days prior to transfer to the conditioned chamber maintained at 23 ± 2°C and 50 ± 4% relative humidity. The specimen for scaling resistance was placed in a moist-curing room for 14 day and stored in the air for 14 day at 23 ± 2°C maintained at 45 to 55% relative humidity.

Horizontal industrial pan mixer

Control panel

Discharging chute

Mixing paddles

Figure 7.1 - Fixed horizontal industrial pan mixer

Table 7.2 - Summary of tests selected for LWSCC evaluation

Property	Number of Specimens	Test Method
Slump Flow/ V-Funnel/ /J-Ring Flow, L-Box/ Filling Capacity/ Sieve Segregation	-	EFNARC-2005
Initial/ Final Set Times	2 (150 × 150 mm cylinders)	ASTM C 403-08
Bleed water	-	ASTM C 232-09
Fresh Unit Weight	-	ASTM C 138-10
Unit Weight	4 (100 × 200 mm cylinders)	ASTM C 567-11
Porosity/ Water Absorption	2 (100 × 200 mm cylinders)	ASTM C 642-06
Compressive Strength	8 (100 × 200 mm cylinders)	ASTM C 39-11
Split Tensile Strength	6 (100 × 200 mm cylinders)	ASTM C 496-11
Sorptivity/ Resistance to Chloride-Ion Penetration	4 (100 × 200 mm cylinders) - 50 mm thick disc	ASTM C 1585-11/ ASTM C1202-10
Bond Strength	4 (100 × 200 mm cylinders)	ASTM C 900-06
Corrosion Resistance	2 (100 × 200 mm cylinders)	-
Hardened Air Void/Spacing Factor	1 (100 × 200 mm cylinders)	ASTM C 457-11
Acid Attack Resistance	8 (100 × 200 mm cylinders)	ASTM C 267-06
Flexural Strength	6 (75 × 100 × 410 mm beams)	ASTM C 78-10
Freezing-and-Thawing	3 (75 × 75 × 285 mm prisms)	ASTM C 666-08/ ASTM C 330-09
Drying Shrinkage	3 (75 × 75 × 285 mm prisms)	ASTM C 157-08
Elevated Temperature Resistance	8 (150 × 150 × 150 mm cubes)	ASTM E 119-12
Scaling Resistance	1 (300 × 300 × 75 mm block)	ASTM C 672-03

7.2.2 Testing Procedures

Slump flow, V-funnel, J-ring flow, L-box, filling capacity and sieve segregation tests were conducted as per EFNARC Self-Consolidating Concrete Committee test procedures (EFNARC 2005). The initial and final setting times of concrete mixtures were measured as per ASTM C 403 procedures. The fresh unit weight was tested according to per ASTM C 138 and both air dry and oven dry densities were determined according to ASTM C 567.

The compressive strength and splitting tensile strength of LWSCC mixtures were determined according to ASTM C 39 and ASTM C 496, respectively. A four-point bending test was also performed under displacement control at a loading rate of 0.5 kN/s on a closed-loop servo-controlled hydraulic test system according to ASTM C 78. The bond strength between reinforcing bar and LWSCC mixtures were studied by conducting direct pullout test on a 15 mm diameter deformed bars embedded centrally in the 100 × 200 mm cylinder specimens (as per ASTM C 900). After 28 days of curing, a 50 mm thick disc sample were cut from the 100 × 200 mm cylinder specimens for water porosity, water absorption, water sorptivity and RCPT tests and then tested as per ASTM C 642, ASTM C 1585 and ASTM C 1202, respectively. The shrinkage prisms were tested according to ASTM C 157 where drying commenced after 28 days of curing. The durability tests procedures are outlined in Phase V of the investigation in Chapter 8. Figures 7.2 to 7.9 show the casting and preparation of LWSCC specimens, while Figure 7.10 shows curing of LWSCC specimens in water tanks.

Figure 7.2 - Preparation of LWSCC elevate temperature and salt scaling specimens

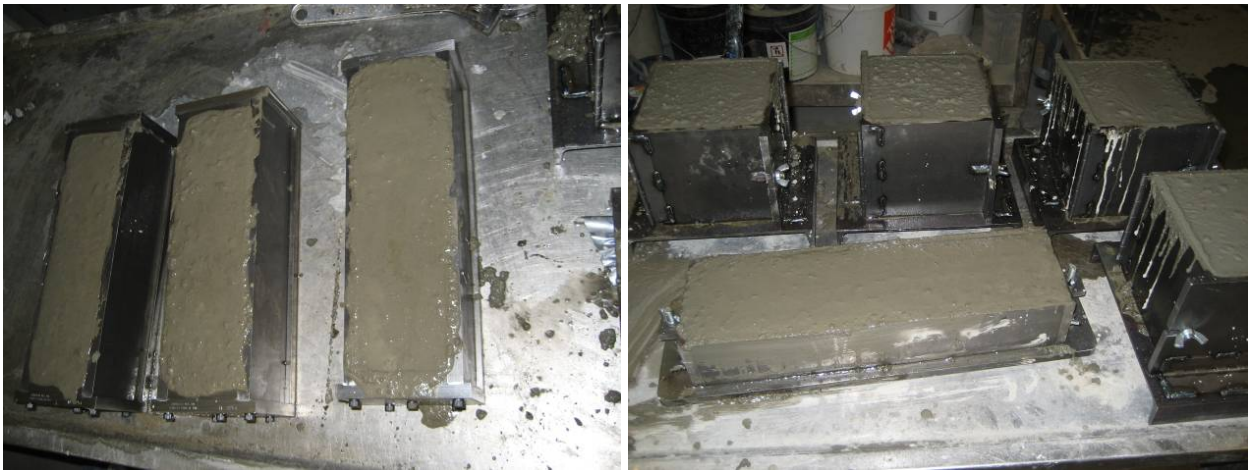

Figure 7.3 - Preparation of LWSCC shrinkage prisms and elevate temperature specimens

Figure 7.4 - Preparation of LWSCC specimens

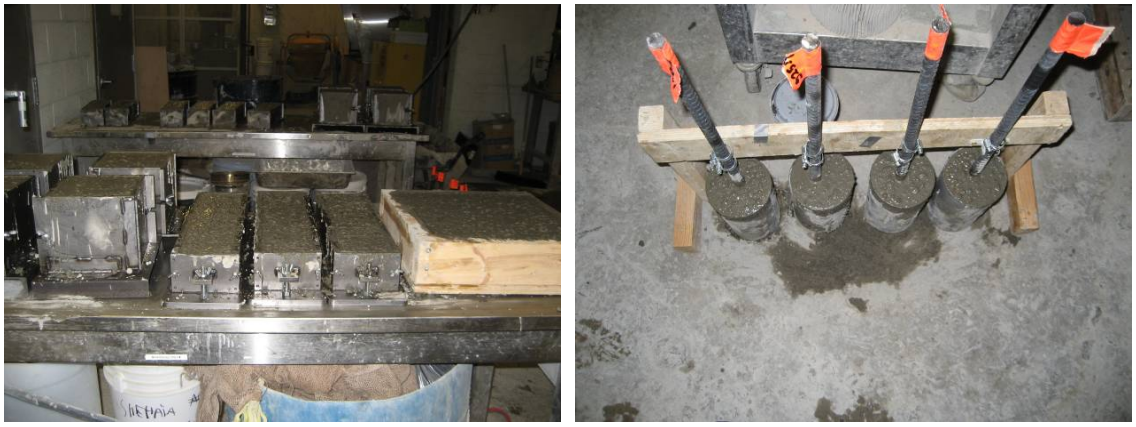

Figure 7.5 - Preparation of LWSCC specimens

Figure 7.6 - Preparation of LWSCC specimens

Figure 7.7 - Preparation of LWSCC freeze – thaw prisms and cylinders for bond test

Figure 7.8 - Casting and preparing LWSCC specimens

Figure 7.9 - Casting initial curing of LWSCC specimens

Figure 7.10 - Water tanks for curing LWSCC specimens

7.3 LWSCC Mechanical Properties Results and Discussion

7.3.1 Effect of LWA on LWSCC Compressive Strength

For typical concrete mixes with lightweight aggregate, the compressive strength decreased with the decrease of density. This can be attributed to the lower strength of the lightweight aggregates. As seen in Figure 7.11, the boundary between the cementitious matrix and the lightweight aggregate shell is not distinct showing that the lightweight aggregates bonds tight and continuous with the cementitious matrix. The well-bonded interfacial transition zone is a characteristic of higher strength development of the lightweight aggregates.

Further, the paste infiltrated the aggregate surface to a certain depth (Figure 7.12). In other words, the 'Wall Effect' that appears in the normal weight concrete does not occur on the Interfacial Transition Zone (ITZ) of the lightweight aggregate. This is because the porous and rough surface of the lightweight aggregates provides sites for the paste to merge across the interfacial transition zone and improves the interaction mechanism between the aggregate and the matrix. The ettringite typically forms on the aggregate shell. At the surface of the lightweight aggregate, cement paste is trapped in the pores as shown in Figure 7.13.

As a result, the strength of the paste and the extend of its arching action over the aggregates really controls the strength of the concrete (Lo and Cui 2004). The strength of the lightweight aggregates is the primary factor that controls the upper strength limit of such concrete mixtures as confirmed by Zhang and Newman (Zhang and Gjorv 1995; Newman 1993).

All aggregates have strength ceilings, and with lightweight aggregates, the strength ceiling generally can be increased by reducing the maximum size of the coarse aggregate, using combination of normal weight coarse aggregate with lightweight fine aggregate and finally, reducing the water-to-binder (w/b) (ACI 213R 2003).

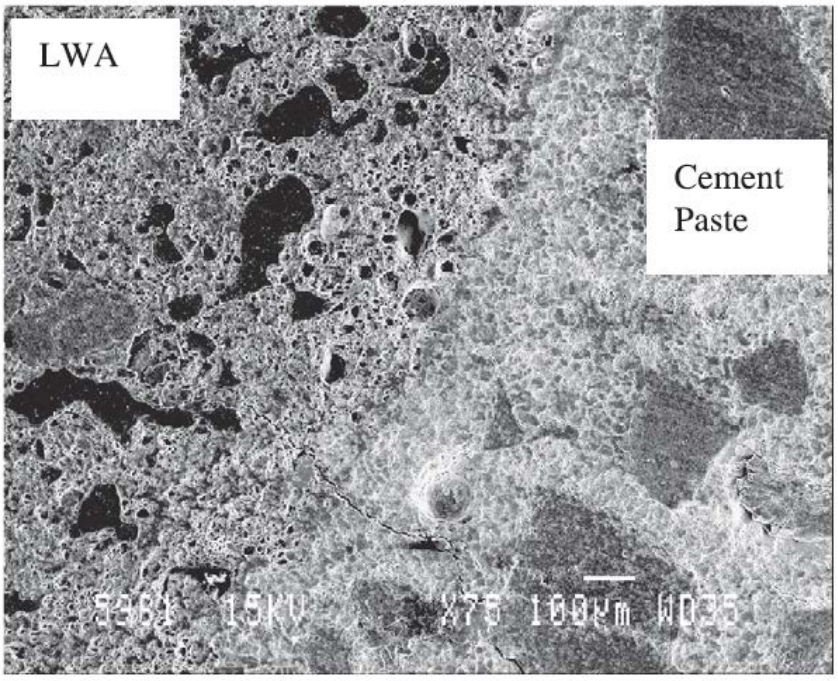

Figure 7.11 - SEM view of lightweight aggregate closely bonded with cement matrix (x 75) (Lo and Cui 2004)

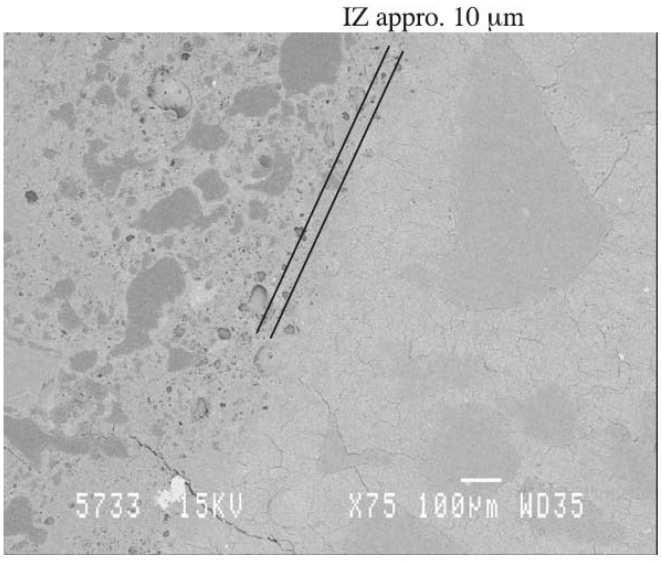

Figure 7.12 - View of the lightweight aggregate concrete showing diffusion of cement paste into the aggregate surface (x 75) (Lo and Cui 2004)

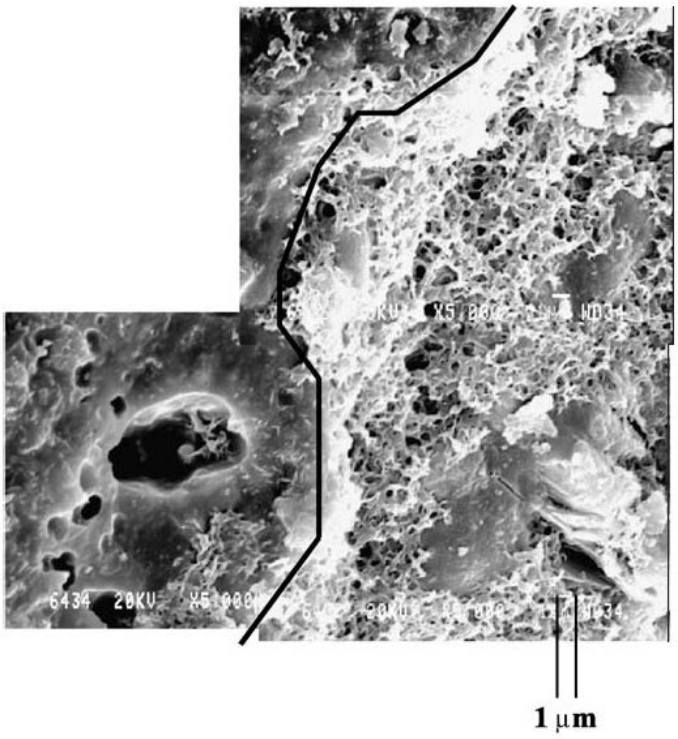

Figure 7.13 - The ITZ showing ettringite formed on surface of porous lightweight aggregate (x 5000) (Lo and Cui 2004)

Generally, the strength increases with an increase in density. The goal of this study is to assess the performance of lightweight SCC made with different types of lightweight aggregates. Therefore, both lightweight fine and coarse aggregates were used in all the examined mixtures, whereas in other studies for developing semi-lightweight SCC mixtures (higher density), use of natural sand may be allowed (Lachemi et al. 2009).

7.3.2 LWSCC Compressive Strength

The variation of compressive strength with age for three groups of LWSCC mixtures (designated as 1, 2 and 3) produced with three different lightweight aggregates is presented in Table 7.3. The 28-day compressive strength of the LWSCC mixes ranged between 29.5 MPa and 52.6 MPa. The highest strengths were recorded by LWSCC mixes 1 and 2 made with ESH aggregates. These ESH LWSCC mixtures contained a lower volume of coarse lightweight aggregate that helped to attain higher strength compared to those FS and EC LWSCC mixes with high volume of coarse lightweight aggregates. The 28-day compressive strength of FS/EC/ESH-LWSCC-1 mixes were 41, 37 and 45 MPa, respectively. LWSCCs with ESH aggregates developed highest strength while those with EC showed the lowest. Moreover, the same trend was observed for LWSCC mixes 2 and 3. The 28-day compressive strength of these LWSCC mixtures was found to be 29.5 MPa or higher. As presented in Figure 7.14, the 28-day compressive strengths of FS-LWSCC mixes 1, 2 and 3 were 8, 9 and 15% lower than equivalent ESH-LWSCC mixtures, respectively. The 28-day compressive strength of EC-LWSCC mixes 1, 2 and 3 were 18, 19, and 25% lower than equivalent ESH-LWSCC mixtures, respectively. The reason for this difference can be attributed to the influence of the quality and percentage of lightweight coarse aggregate used.

Table 7.3 - Compressive strength results of LWSCC mixtures

Mixture No.		Compressive Strength (MPa)		
		7-day	28-day	91-day
FSLWSCC-1	Mean	29.8	41.1	47.2
	C.OV. (%)	1.10	2.10	1.30
FSLWSCC-2	Mean	29.9	42.6	48.1
	C.OV. (%)	1.50	1.20	1.10
FSLWSCC-3	Mean	23.5	33.2	38.8
	C.OV. (%)	1.40	2.70	0.90
ECLWSCC-1	Mean	26.3	36.9	41.7
	C.OV. (%)	0.70	1.70	3.80
ECLWSCC-2	Mean	27.3	37.6	44.0
	C.OV. (%)	0.60	2.70	3.30
ECLWSCC-3	Mean	22.5	29.5	35.2
	C.OV. (%)	2.90	3.70	0.70
ESHLWSCC-1	Mean	33.6	44.9	52.5
	C.OV. (%)	0.60	2.40	0.90
ESHLWSCC-2	Mean	34.0	46.7	52.5
	C.OV. (%)	1.80	2.7	1.30
ESHLWSCC-3	Mean	29.0	39.2	46.6
	C.OV. (%)	2.80	1.40	0.90

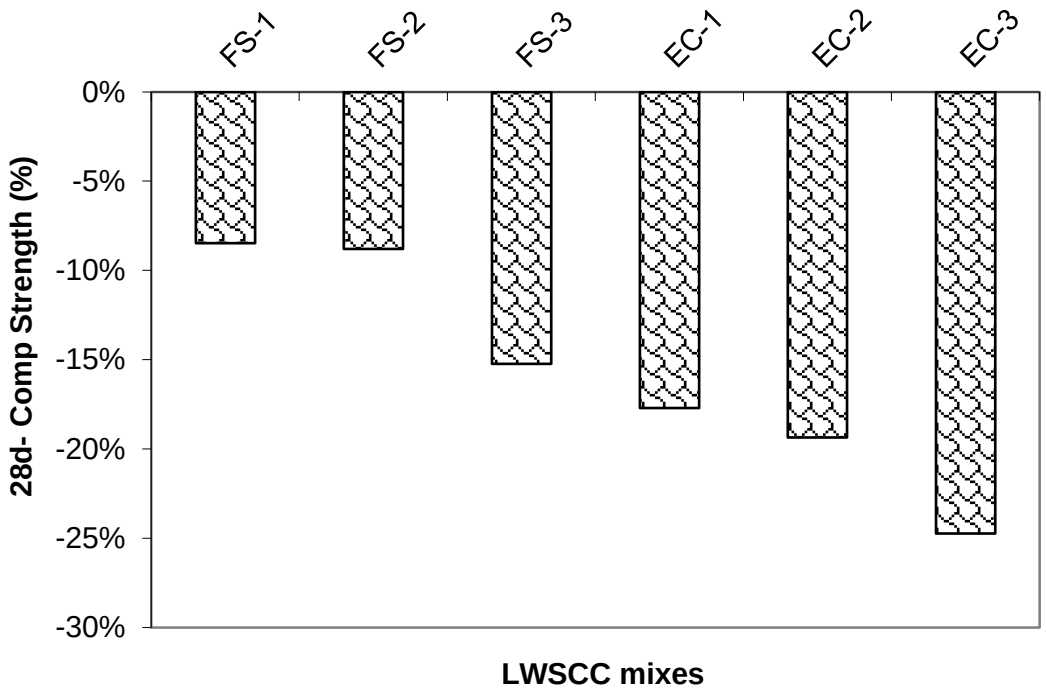

Figure 7.14 - Comparison between the 28-day comp strength of FS and EC- LWSCC mixtures against the ESH-LWSCC mixtures

Moreover, the comparison between different mixes with the same amount of binder and w/b but with different aggregates properties, suggests that the aggregates are the weak point in the concrete matrix. Compression tests also confirmed this by exhibiting aggregate fracture in the broken specimens (Figures 7.11 and 7.12).

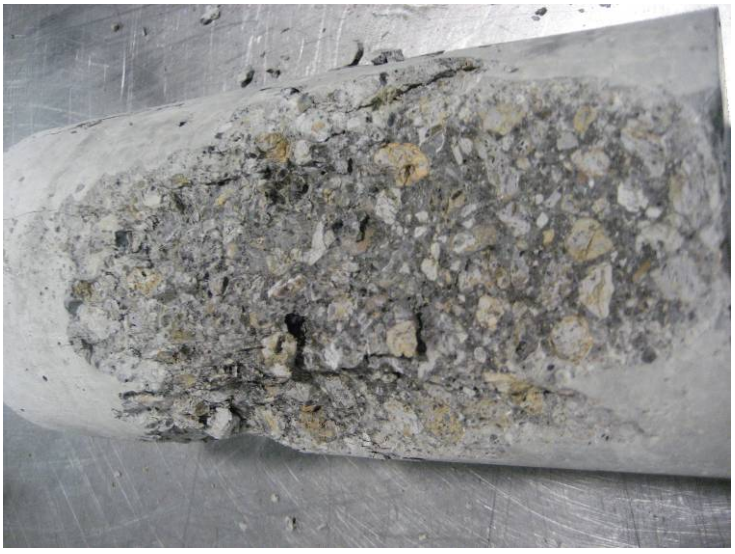

Figure 7.15 – Coarse FS aggregate fracture in the broken specimens

Figure 7.16 – Coarse ESH aggregate fracture in the broken specimens

The amount of binder and w/b were kept constant for each sub-mix in each group (1, 2 and 3) as can be seen in Table 7.1. The major change in the sub-mixes was the aggregate type and subsequently, the coarse-to-total aggregates volume ratio and these are the key factors affecting the strength of LWSCC. The absorption rate of EC was the highest (showing somewhat worst

aggregate quality) followed by ESH. However, the percentage of the coarse ESH used was the lowest in all LWSCC group mix. This was due to the superior packing density of the ESH aggregates which resulted in reduction of the coarse portion usage in the mixtures. Similar aggregate quality observation was noted in a previous LWSCC study (Kim et al. 2010). As a consequence, mixtures with EC showed lower strength than those mixtures with FS or ESH due to high percentage of comparatively weaker EC. On the other hand, ESH mixtures had higher compressive strength due to increased fine-to-total aggregates ratio allowing for more fine particles to fill up the voids to perform the role of filler. It should be noted that the coarse lightweight aggregate proportion was limited to maximum of 29.5%, 29.5% and 24.5% by volume for the FS, EC and ESH-LWSCC mixtures, respectively. These percentages were derived from the aggregate packing density test as explained in Chapter 3.

As 15% fly ash and 5% silica fume was used as supplementary cementitious material (SCM) in all LWSCC mixtures, it was found in average that the compressive strength increased by 37% from 7-day to 28-day and by 16% from 28-day to 91-day. The finely divided silica can combine with calcium hydroxide (liberated by the hydrating Portland cement) in the presence of water to form stable compounds like calcium silicates, which have cementitious properties. Such pozzolanic action of SCM contributes to the enhancement of strength and long-term durability (Hossain 1999). Figure 7.17 shows the compressive strength gain with age for the developed LWSCC mixtures, while Figure 7.18 shows the percentage increase in compressive strength at 28 and 91-day compared to the 7-day. It can be seen from Figure 7.18 that all three mixtures in each LWSCC class exhibited very similar percentage increase in strength from 7 to 28-day and from 28 to 91 -day, influenced by the fixed w/b and total binder content in each LWSCC class mixture.

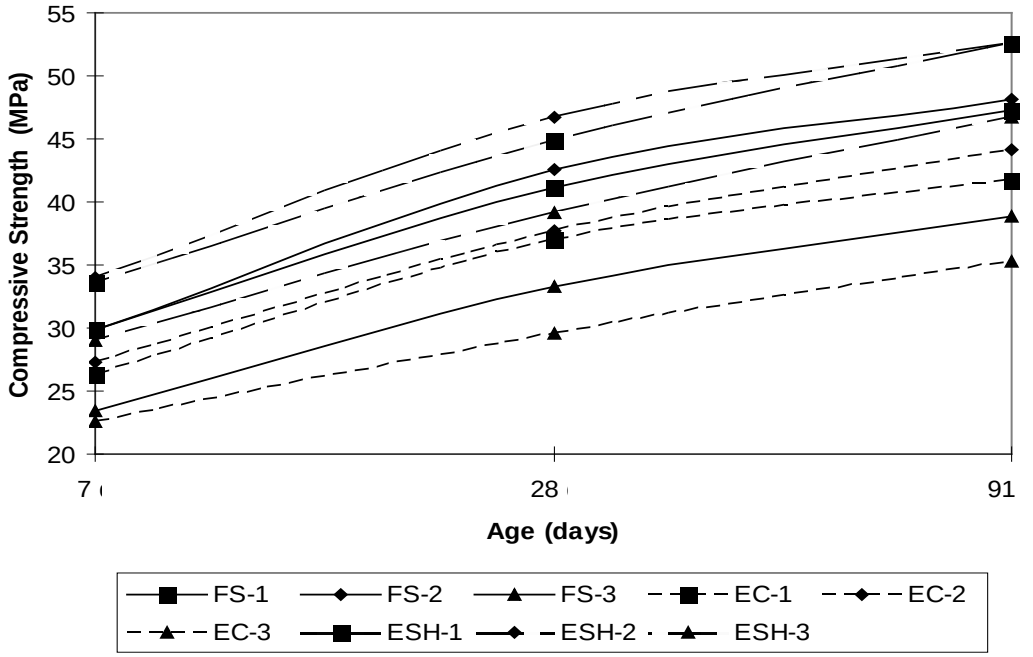

Figure 7.17 - Comparison of compressive strength gain with age for the three different LWSCC mixtures

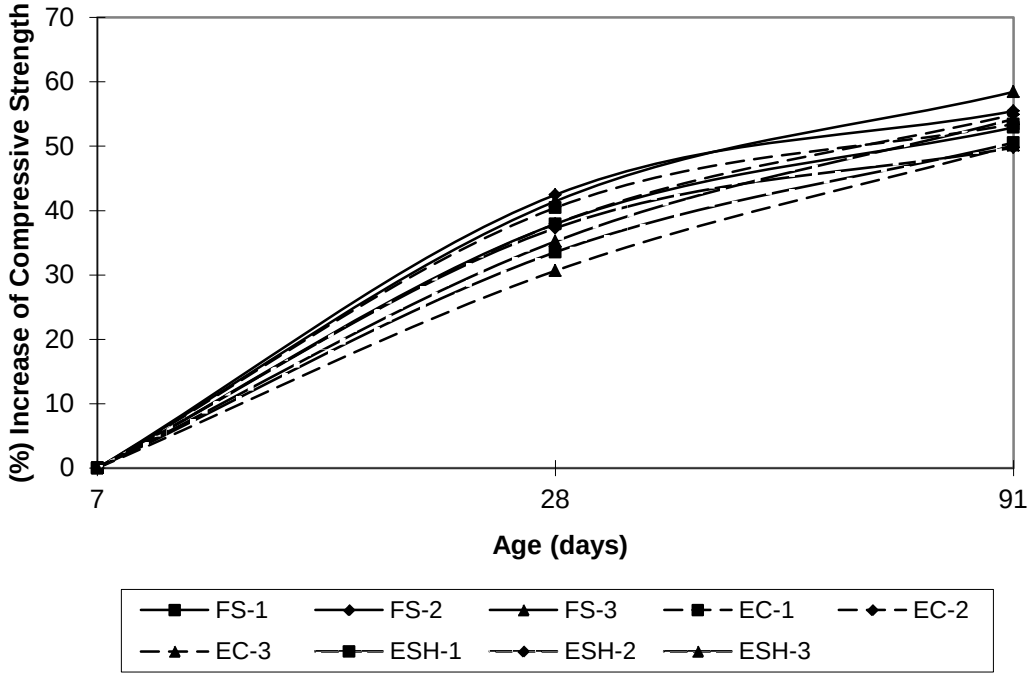

Figure 7.18 - Comparison of (%) increase of compressive strength with age for different LWSCC mixtures

On the other hand, as the w/b increased from 0.35 (in LWSCC-2 mixtures) to 0.40 (in LWSCC-3), the compressive strength was found to decrease by more than 16% for ESH mixture and more than 22% for both FS and EC mixtures. Figure 7.19 compares the compressive strength of the three different types of LWSCC mixtures at different ages.

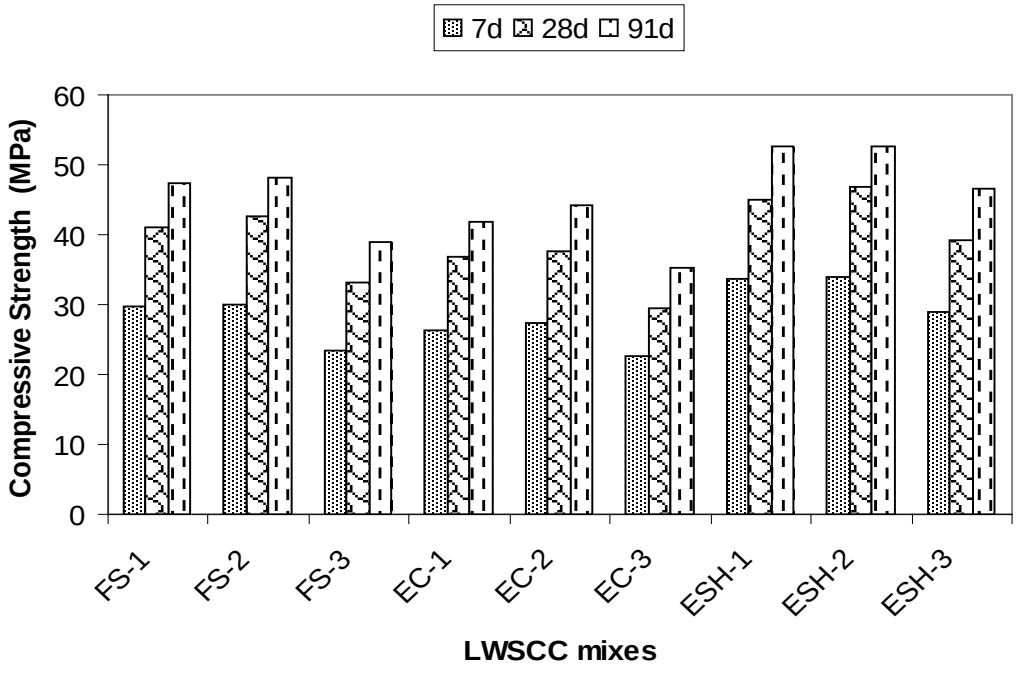

Figure 7.19 - Comparison of compressive strength of three types of LWSCC mixtures at different ages

7.3.3 LWSCC Unit Weight

The fresh, 28-day air and oven dry unit weight results of the LWSCC mixtures are summarized in Table 7.4. The fresh unit weight of the FS-LWSCC was the highest (ranging from 1909 to 1926 kg/m^3), while the EC-LWSCC mixtures had the lowest density (ranging from 1608 to 1622 kg/m^3). The density of ESH-LWSCC mixtures ranged between1794 and 1817 kg/m^3. All the 28-day air and oven dry density of LWSCC mixtures were below the 1840 kg/m^3 limit which classified all nine developed mixtures as lightweight concrete according to ACI 213R. Figure 7.20 presents the fresh, 28-day air dry and 28-day oven dry unit weight of all nine LWSCC

mixtures. Figure 7.21 presents the percentage reduction of unit weights after 28 days of air and oven drying. It can be seen that the LWSCC mixtures with EC had the highest percentage reduction in unit weight followed by mixtures with ESH. This can be attributed to the high aggregate absorption values for both EC and ESH (> 13%) compared with the lower absorption value of FS aggregates (< 8%).

Table 7.4 - Unit weight results of LWSCC mixtures

Mixture No.		Unit Weight (kg/m^3)		
		Fresh	28-day Air Dry	28-day Oven Dry
FSLWSCC-1	Mean	1909	1842	1768
	C.OV. (%)	0.70	1.50	2.50
FSLWSCC-2	Mean	1926	1847	1778
	C.OV. (%)	1.40	1.80	2.90
FSLWSCC-3	Mean	1916	1824	1741
	C.OV. (%)	1.20	2.30	2.50
ECLWSCC-1	Mean	1608	1521	1449
	C.OV. (%)	1.60	1.90	5.40
ECLWSCC-2	Mean	1622	1530	1467
	C.OV. (%)	0.80	3.90	2.30
ECLWSCC-3	Mean	1620	1519	1466
	C.OV. (%)	2.60	1.70	0.80
ESHLWSCC-1	Mean	1794	1696	1617
	C.OV. (%)	1.30	2.90	5.10
ESHLWSCC-2	Mean	1807	1706	1634
	C.OV. (%)	0.8	4.30	3.20
ESHLWSCC-3	Mean	1817	1705	1646
	C.OV. (%)	2.30	1.20	0.9

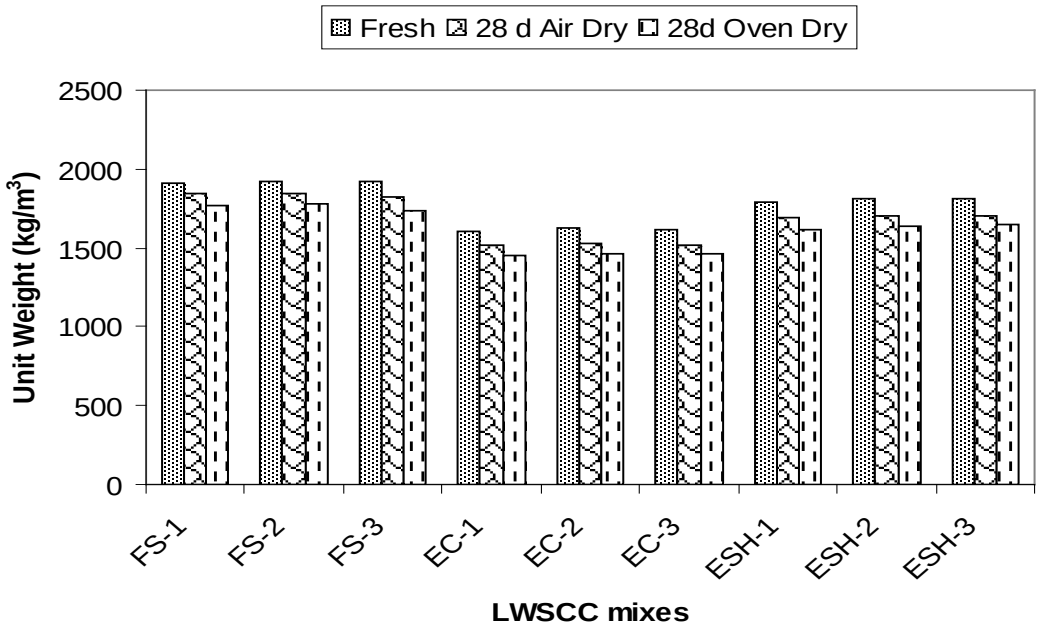

Figure 7.20 - Comparison of the unit weights values of three types of LWSCC mixtures

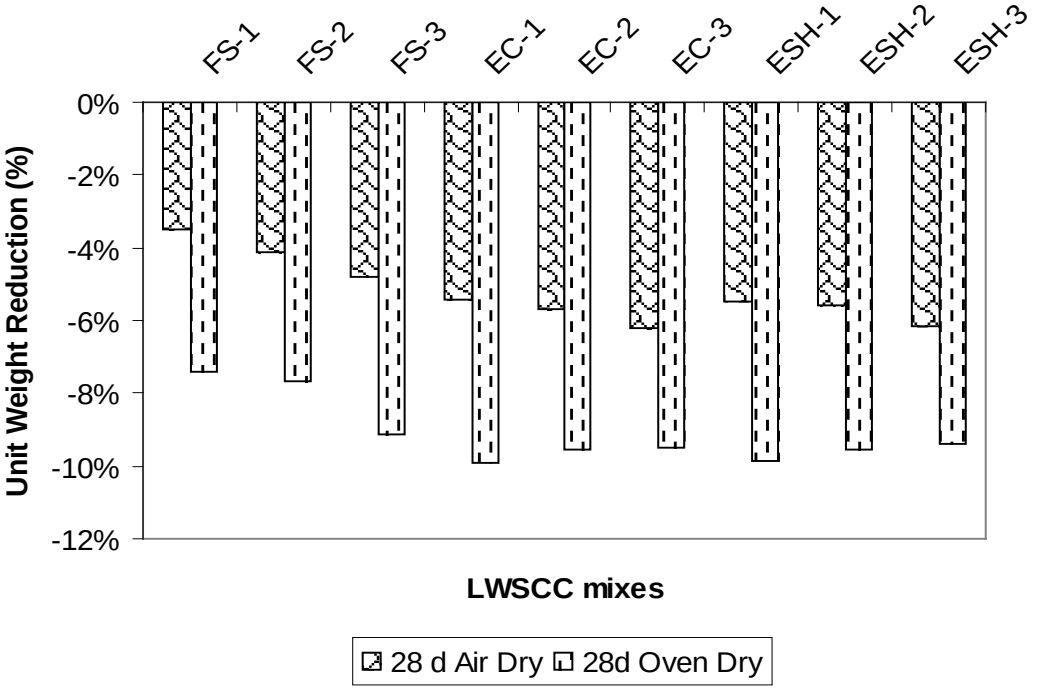

Figure 7.21 - Comparison of the reduction percentages of unit weights of three types of LWSCC mixtures

The relationship between the 28-day compressive strength and dry unit weight of concrete mixes is presented in Figure 7.22. In contrast to findings of other research studies (Kim et al. 2010; Hossain et al. 2011), no good correlation is found. More experimental data is needed to establish such relation. However, the experimental data suggests that LWSCC mixtures with relatively low dry density (1706 kg/m^3) but with high aggregate packing density (less voids) and low coarse-to-total aggregate volume ratio (as in the case of ESH-LWSCC mixtures), will produce higher compressive strength (46.7 MPa) compared to concrete mixtures with high dry density (1847 kg/m^3) such as FS-LWSCC mixtures (where the 28-day compressive strength was 42.6 MPa). The w/b and the segregation resistance percentage of LWSCC mixtures are the main contributing factors to be considered in establishing such relationship. LWSCC mixtures with high dry density but with high w/b (0.4) and low segregation resistance (≥15%) are susceptible to develop lower compressive strength even compared to low dry density mixtures.

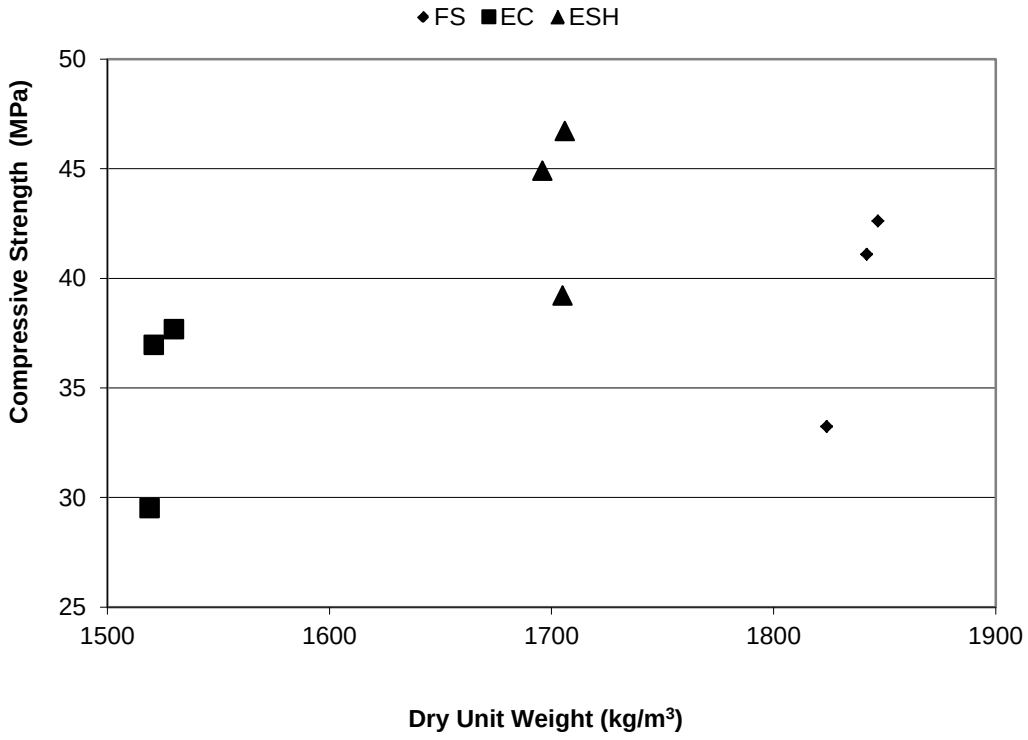

Figure 7.22 - Comparison between compressive strength and dry unit weight density of different types of LWSCC mixtures

7.3.4 LWSCC Flexural Strength

The flexural strength of LWSCC mixtures varied from 2.25 to 3.60 MPa at 7-day, 2.88 to 4.48 MPa at 28-day and 3.62 to 5.25 MPa at 91-day. These values are presented in Table 7.5, with the highest values recorded for FS-LWSCC mixes, while the lowest was recorded with mixes made with EC aggregates. Since the quality, size and volume of coarse aggregate affect the flexural strength of LWSCC mixtures, mixes made with FS showed high strength due to the fact that more coarse aggregate volume (29.5%) was used in these mixes compared to 24.5% in ESH-LWSCC mixes. The relative low quality of the coarse EC aggregates, lead to low flexural strength. Moreover, the fracture path that travels through the aggregate particles rather than around it, high w/b and trapped residual moistures can cause significant reduction in flexural strength of LWSCC mixtures. Figure 7.23 and 7.24 show the flexural test setup and LWSCC samples during testing. Figure 7.25 compares the flexural strength of the three different types of LWSCC mixtures at different ages, while the increase in flexural strength values with age is shown in Figure 7.26, while Figure 7.27 shows the percentage increase in flexural strength at 28 and 91-day compared to the 7-day for different LWSCC mixtures.

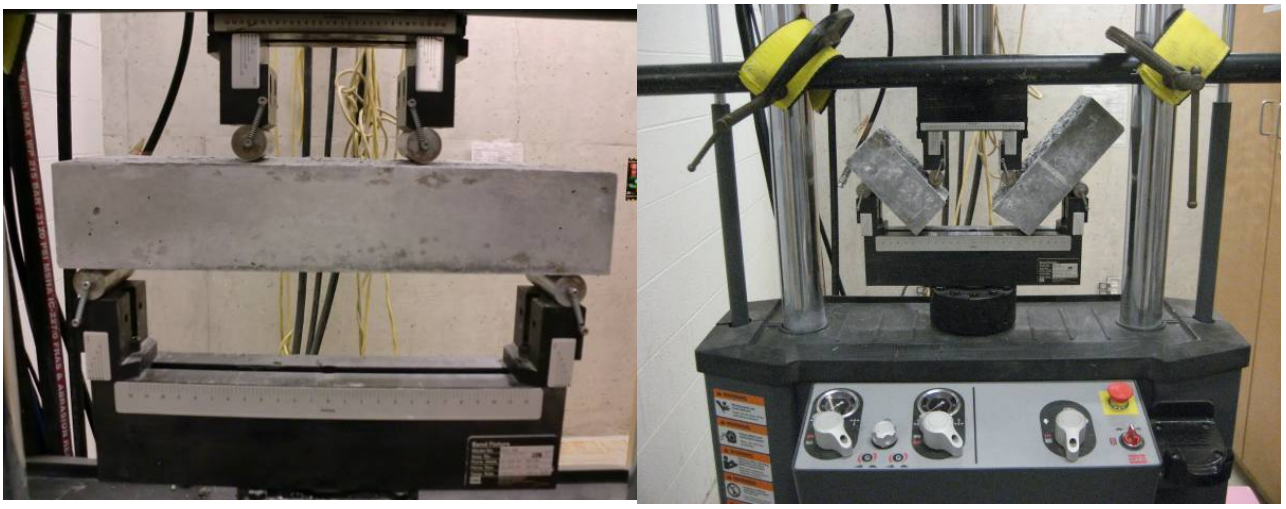

Figure 7.23 - Flexural test (4- point loading) of LWSCC beams

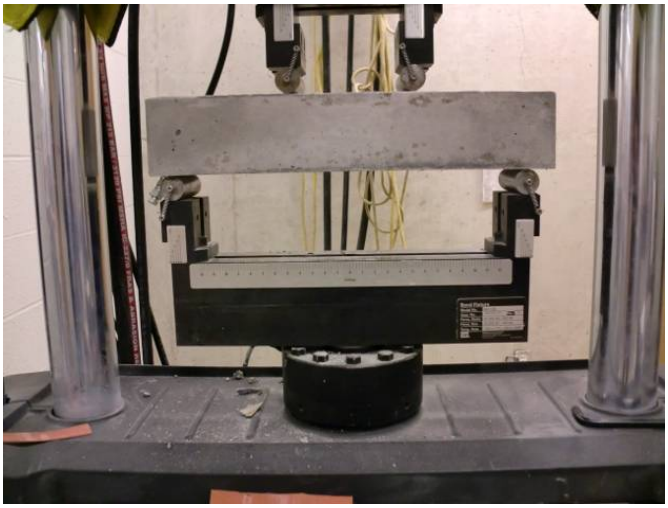

Figure 7.24 - Flexural test (4- point loading) of LWSCC beams

Table 7.5 - Flexural strength results of LWSCC mixtures

Mixture No.		Flexural Strength (MPa)		
		7-day	28-day	91-day
FSLWSCC-1	Mean	3.24	4.16	4.51
	C.OV. (%)	1.70	0.90	1.20
FSLWSCC-2	Mean	3.60	4.48	5.25
	C.OV. (%)	1.40	2.90	2.70
FSLWSCC-3	Mean	2.70	3.42	4.05
	C.OV. (%)	1.60	1.80	2.30
ECLWSCC-1	Mean	3.11	3.90	4.39
	C.OV. (%)	2.2	2.0	1.70
ECLWSCC-2	Mean	2.97	3.80	4.68
	C.OV. (%)	1.1	2.70	0.80
ECLWSCC-3	Mean	2.25	2.88	3.61
	C.OV. (%)	4.80	2.40	1.20
ESHLWSCC-1	Mean	3.06	4.08	4.68
	C.OV. (%)	2.20	2.50	0.60
ESHLWSCC-2	Mean	3.33	4.32	5.04
	C.OV. (%)	2.20	0.90	3.90
ESHLWSCC-3	Mean	2.61	3.33	4.23
	C.OV. (%)	5.20	4.0	1.7

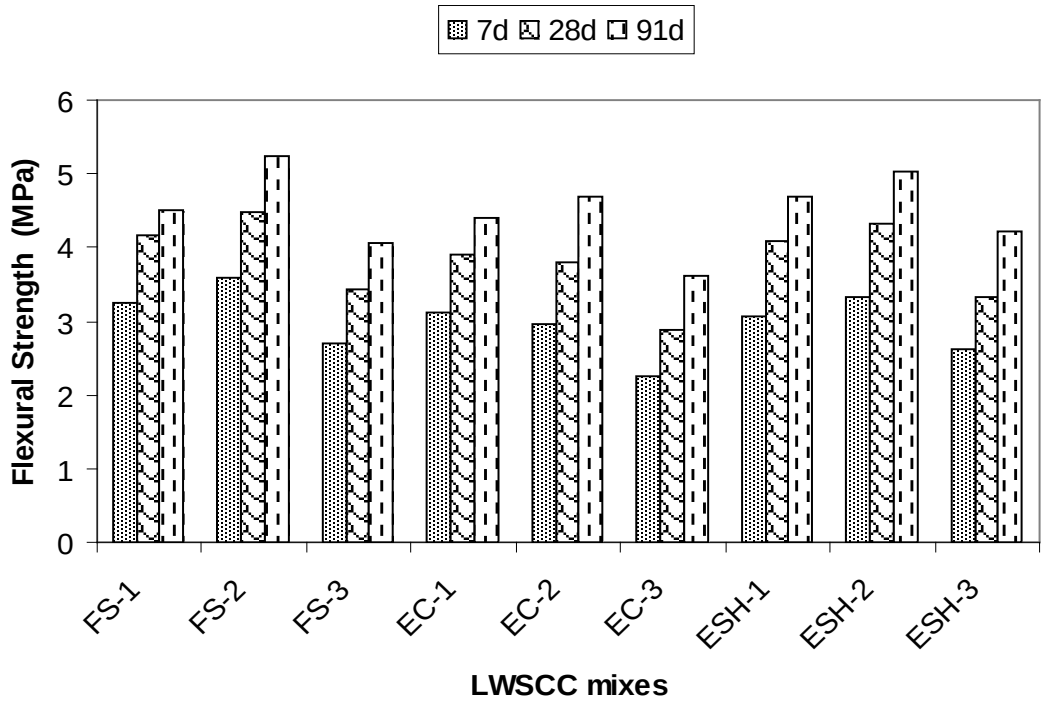

Figure 7.25 - Comparison of the flexural strength of different types of LWSCC mixtures at different ages

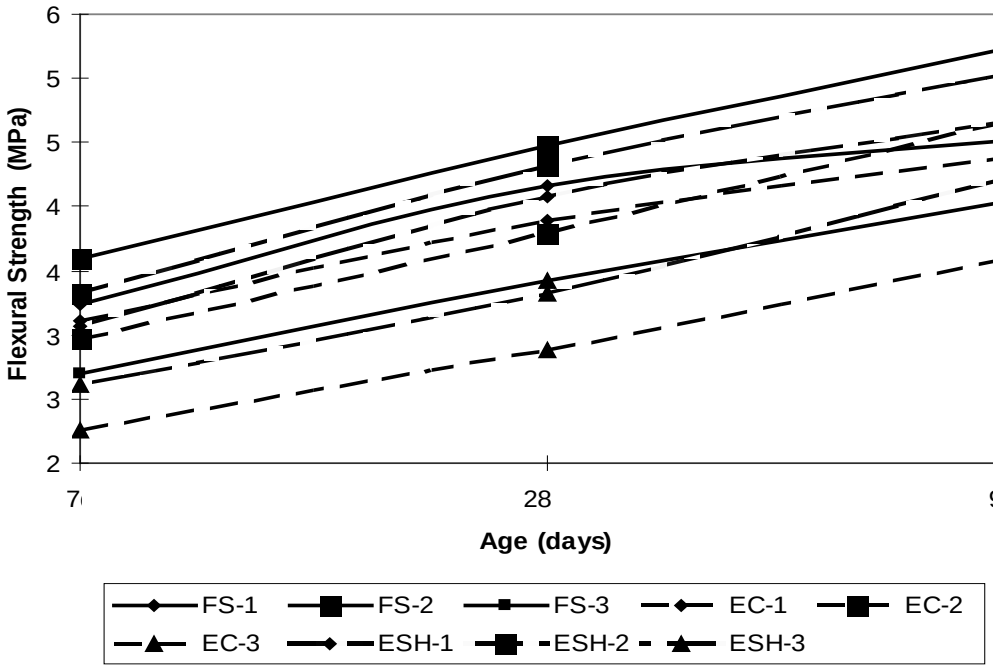

Figure 7.26 - Comparison of the flexural strength gains with age for different types of LWSCC mixtures

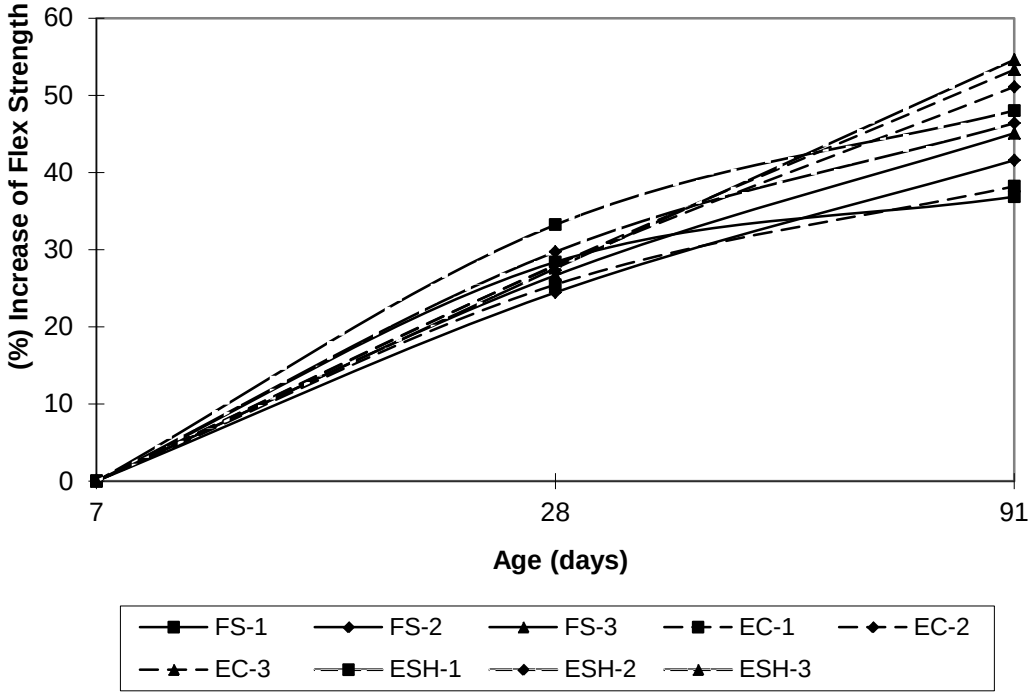

Figure 7.27 - Comparison of (%) increase of flexural strength with age for different LWSCC mixtures

Correlation between flexural and compressive strength

According to previous research studies, the flexural strength of lightweight concrete varies from 9.8 to 10.5% of the compressive strength at 28-day (Lange et al. 1995). This is found to be true also from the current study where the flexural strength of LWSCC mixtures varied from 8.5 to 10.5% of the compressive strength at 28-day.

Figure 7.28 illustrates the relationship between the compressive strength and the flexural strength at 28-day of the three different types of LWSCC mixtures made with three different lightweight aggregates having different densities and mix proportions. Based on the results of the present study, the relationship between the compressive strength (fc') and the flexural strength (fs_f) follows power law and the mathematical relationship was expressed as $fs_f = 0.1702 \times (fc')^{0.8482}$. Further, the results showed relatively low correlation with a correlation coefficient (R) of 0.75 for LWSCC mixtures. Such relatively low correlation can be attributed to the difference in coarse aggregate volume, quality of aggregates and mix design proportions of the examined data.

Nevertheless, the derived mathematical equation is quite similar to the relationship between the compressive strength and the flexural strength for normal density aggregate SCC (Sekhar and Rao 2008). It is concluded from these results that a good quality lightweight aggregate SCC can be designed to achieve hardened properties similar to those of normal density SCC.

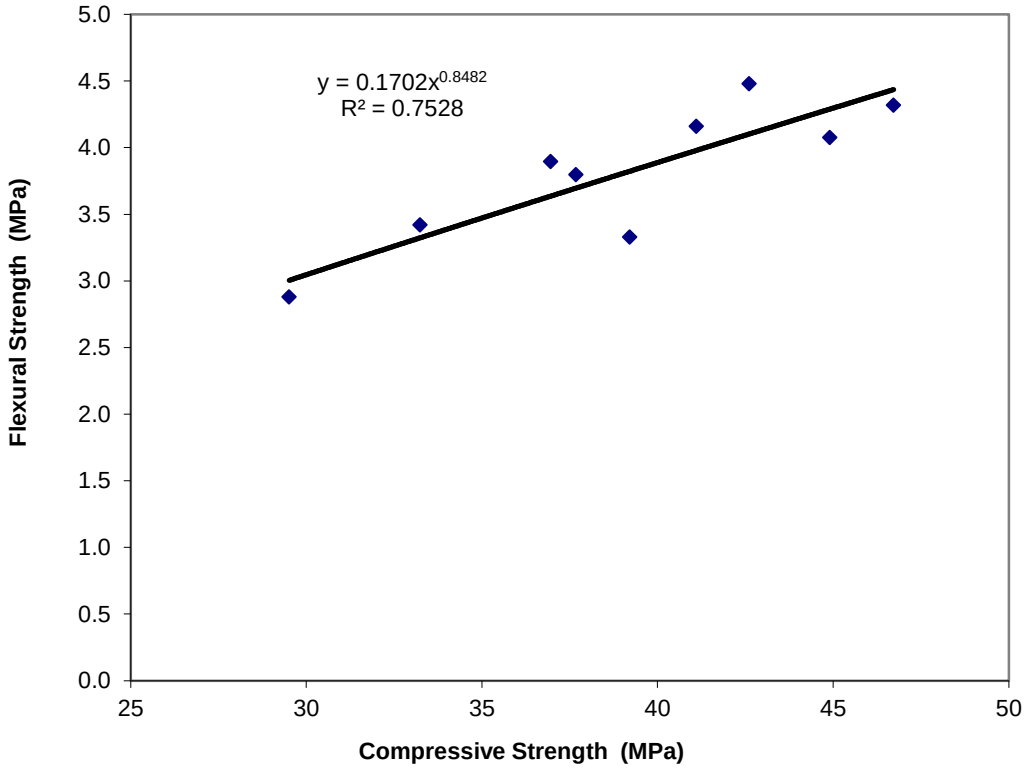

Figure 7.28 - Relationship between the 28-day compressive strength and flexural strength of LWSCC mixtures

7.3.5 LWSCC Split Tensile Strength

The splitting tensile strength is used for estimating the diagonal tension resistance of lightweight concrete in structures. The split tensile strength at different ages of three aggregate types LWSCC mixtures are presented in Table 7.6. The 28-day split tensile strength of LWSCC mixes ranged between 3.08 MPa and 1.61 MPa. Similar to the 28-day compressive strength, the highest split tensile strengths were observed for ESH-LWSCC mixtures, followed by FS-LWSCC and EC-LWSCC. Mainly, the 28-day split tensile strength of ES-LWSCC mixes 1, 2 and 3 were 12,

11 and 11% higher than that of equivalent ESH-LWSCC mixtures, respectively while 27, 37 and 40% higher than that of the equivalent EC-LWSCC, respectively. Figure 7.29 shows LWSCC cylinder during split tensile strength test. Figure 7.30 compares the split tensile strength of the three different types of LWSCC mixtures at different ages, while Figure 7.31 shows the split tensile strength development with age. Figure 7.32 illustrate the percentage increase in split tensile strength at 28 and 91-day compared to the 7-day for different LWSCC mixtures.

Figure 7.29 - Split tensile strength test of LWSCC cylinder

Table 7.6 - Split tensile strength results of LWSCC mixtures

Mixture No.		Splitting Tensile Strength (MPa)		
		7-day	28-day	91-day
FSLWSCC-1	Mean	1.98	2.55	3.00
	C.OV. (%)	2.1	2.30	1.20
FSLWSCC-2	Mean	2.28	2.78	3.15
	C.OV. (%)	1.90	2.40	2.6
FSLWSCC-3	Mean	1.66	2.03	2.40
	C.OV. (%)	1.30	4.20	2.60
ECLWSCC-1	Mean	1.79	2.24	2.55
	C.OV. (%)	1.10	2.50	2.2
ECLWSCC-2	Mean	1.82	2.25	2.63
	C.OV. (%)	3.40	1.90	1.60
ECLWSCC-3	Mean	1.34	1.61	1.88
	C.OV. (%)	1.70	2.70	1.80
ESHLWSCC-1	Mean	2.32	2.85	3.38
	C.OV. (%)	2.90	0.80	2.20
ESHLWSCC-2	Mean	2.48	3.08	3.68
	C.OV. (%)	1.50	1.20	5.3
ESHLWSCC-3	Mean	1.80	2.25	2.63
	C.OV. (%)	2.30	1.60	1.40

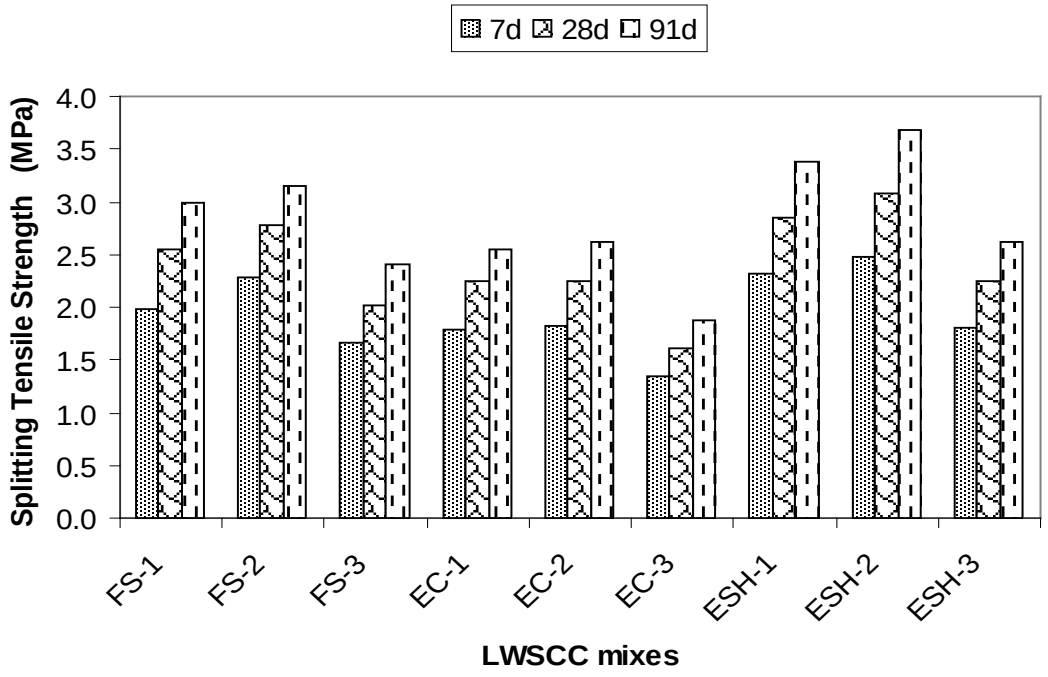

Figure 7.30 - Comparison between split tensile strength of different types of LWSCC mixtures at different ages

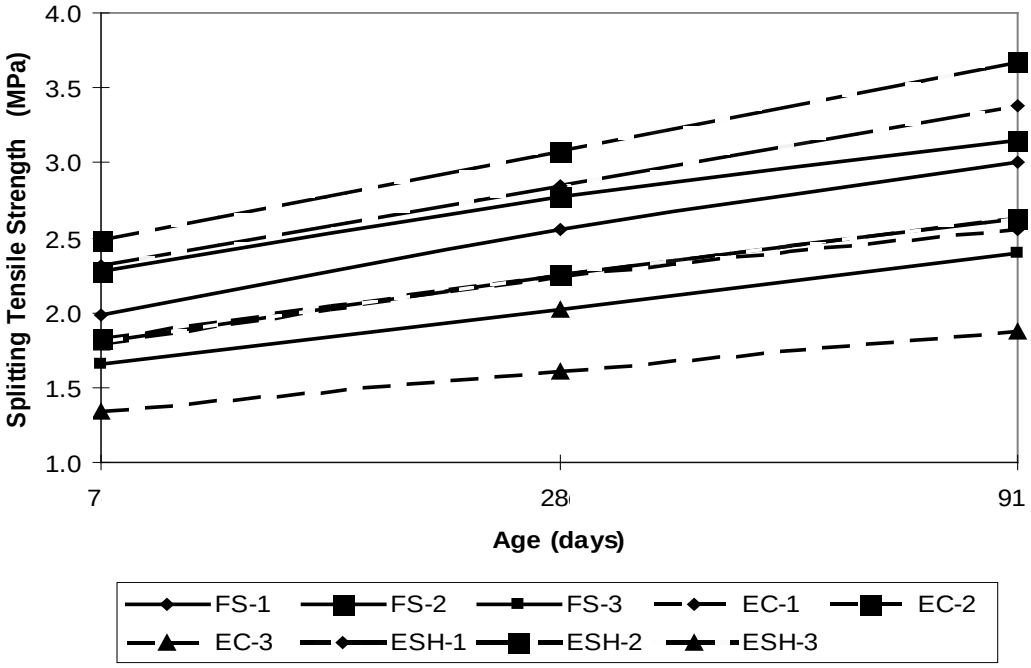

Figure 7.31 - Comparison between split tensile strength gains with age for different types of LWSCC mixtures

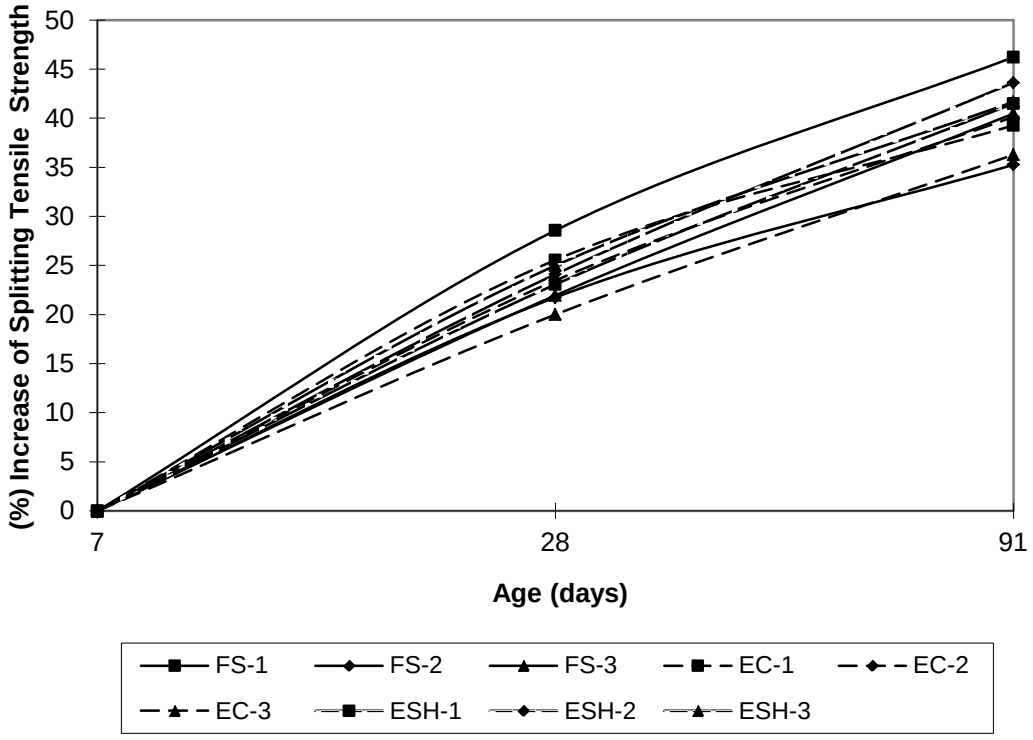

Figure 7.32 - Comparison of (%) increase of tensile strength with age for different LWSCC mixtures

Correlation between tensile and compressive strengths

According to Weigler, the compressive strength of lightweight concrete increases faster than the tensile strength. This tendency is stressed with high quality concrete. The ratio of tensile to compressive strength is normally 5 to 15% for lightweight concrete with compressive strength over 20 MPa (Weigler et al. 1972). Smeplass found that the tensile strength of lightweight concrete with natural sand as well as with lightweight sand is about the same as normal density concrete for the same strength class (Smeplass 1992). According to Curcio, the splitting tensile strength of high performance lightweight concrete is about 6 to 6.5% of the cylinder compressive strength (Curcio et al. 1998).

Figure 7.33 illustrates the relationship between the compressive strength and the splitting tensile strength at 28-day of the three different types of LWSCC mixtures. Based on the results of the present study, the relationship between the compressive strength (fc') and the splitting tensile

strength (f_{st}) at 28 follows power law and the mathematical relationship was expressed as $f_{st} = 0.0177 \times (fc')^{1.33}$ with a correlation coefficient (R) of 0.97 showing a high correlation.

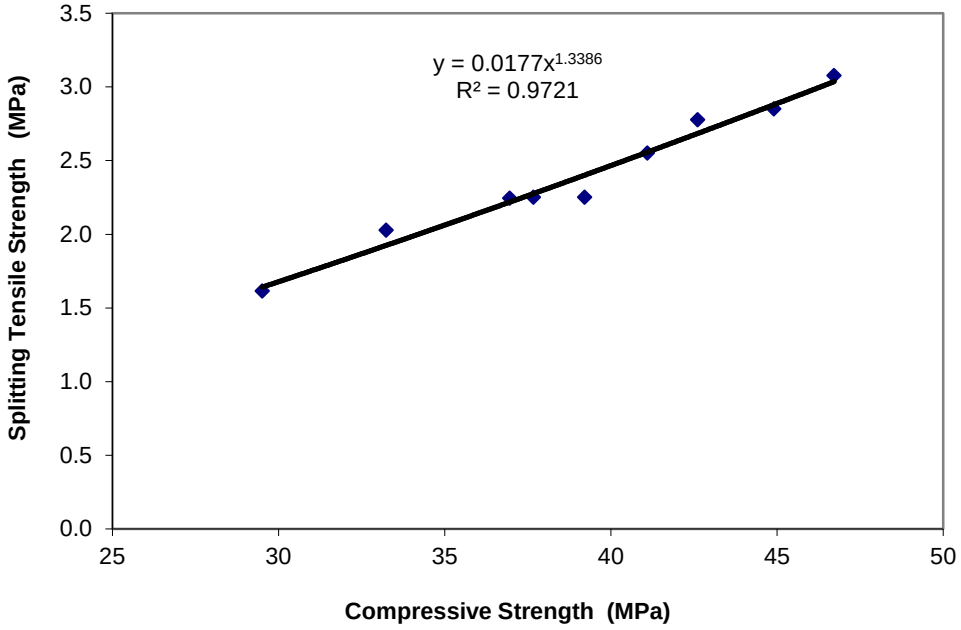

Figure 7.33 - Relationship between the 28-day compressive strength and split tensile strength of LWSCC mixtures

7.3.6 LWSCC Bond Strength and Discussion

The bond strength between the reinforcing bar and LWSCC mixtures were studied by conducting direct pullout test of a centrally embedded 15 mm diameter deformed reinforcing steel bar in 100 mm × 200 mm cylinder specimens as shown in Figure 7.34.

The bond strength between concrete and reinforcements can be obtained from the pullout load-versus-slip relation. In this research, the bond strengths obtained by pullout test were used for comparison of variables. If the measured bond strengths are to be applied for design purpose, the characteristics of pullout test need to be taken into consideration. In general, the bond stress corresponding to the maximum pullout load (the peak of a pullout load) can be regarded as the bond strength, or the ultimate bond strength. The criterion of ultimate bond strength has been widely adopted by most researchers because of its clear definition and the simplicity in bond

strength interpretation and was used in this study as well as by other researchers in similar LWSCC and lightweight concrete bond strength studies (Lachemi et al. 2009; Esfahani and Rangan 1998; Hossain, 1999).

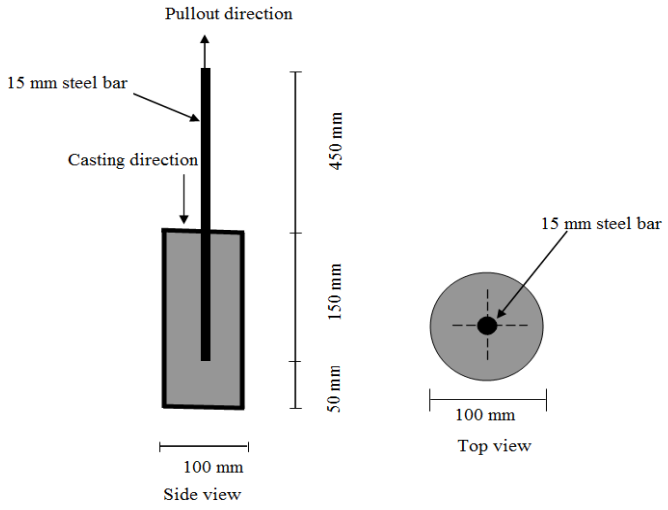

Figure 7.34 - Schematic representation of pullout test specimen

During the pullout test, the pullout load is recorded. The pullout load (P) is then converted into bond stress/strength (f_b) based on embedment length and reinforcing bar diameter using Eq. 7.1 (Lachemi et al. 2009; Esfahani and Rangan 1998; Hossain and Lachemi 2008; Hossain 2008):

$$f_b = 2P/\pi ld \qquad (7.1)$$

where f_b = bond strength (MPa); P = maximum applied load indicated by the testing machine (kN) in case of pullout/splitting failure or load at 2.5 mm slip in case of failure due to yielding of steel; l = embedment length (mm) and d = bar diameter (mm).

Effect of lightweight aggregates types on the bond strength of LWSCC mixtures

The 28-day bond strength of the investigated LWSCC mixtures is summarized in Table 7.7 along with the specimen's mode of failure. Figure 7.35 shows LWSCC pull-out test while Figure 7.36 shows the test setup and LWSCC specimens after pull-out test. Figure 7.37 compares the ultimate bond strength (average of the results of two similar tests) of LWSCC mixtures at 28-

day. It was observed that ESH-LWSCC mixtures produced the highest bond strength followed by FS-LWSCC and EC-LWSCC. Compared to ESH-LWSCC mixes 1, 2 and 3, the decrease in bond strength were about 37, 36, and 45% for FS-LWSCC 1, 2 and 3 mixes, respectively while a 49, 50 and 55% for EC-LWSCC mixes, respectively (Figure 7.38). It has been reported that the workability properties and compressive strength of concrete play a major role in the pullout bond strength (Lachemi et al. 2009; Esfahani and Rangan 1998; Hossain and Lachemi 2008; Hossain 2008, 1999). However, it should be noted that the three sub-mix in each LWSCC group were designed to have similar workability, compressive strength and ingredients- the only differences were the types of LWA and the amount of HRWRA. Therefore, the type of lightweight aggregate played a significant role in the bond strength.

Figure 7.35 - Pull-out test of LWSCC cylinders

Figure 7.36 - Pull-out test set up and LWSCC specimens after testing

Table 7.7 - 28-day bond strength results of LWSCC mixtures

Mixture No.		28-day bond Strength f_b (MPa)	Mode of Failure
FSLWSCC-1	Mean	4.20	Splitting
	C.OV. (%)	2.30	
FSLWSCC-2	Mean	4.50	Splitting
	C.OV. (%)	1.40	
FSLWSCC-3	Mean	2.70	Splitting
	C.OV. (%)	2.50	
ECLWSCC-1	Mean	3.40	Splitting
	C.OV. (%)	1.60	
ECLWSCC-2	Mean	3.50	Splitting
	C.OV. (%)	1.30	
ECLWSCC-3	Mean	2.20	Splitting
	C.OV. (%)	0.90	
ESHLWSCC-1	Mean	6.70	Splitting
	C.OV. (%)	2.10	
ESHLWSCC-2	Mean	7.00	Splitting
	C.OV. (%)	1.70	
ESHLWSCC-3	Mean	4.90	Splitting
	C.OV. (%)	1.80	

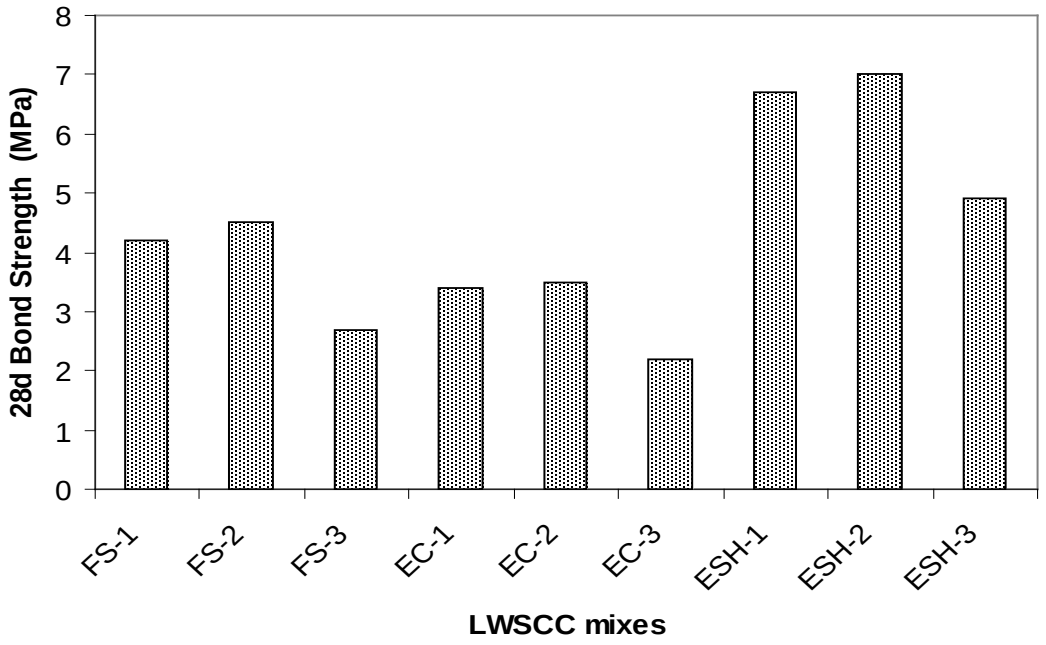

Figure 7.37 - Comparison between the 28-day bond strength of the three different types of LWSCC mixtures

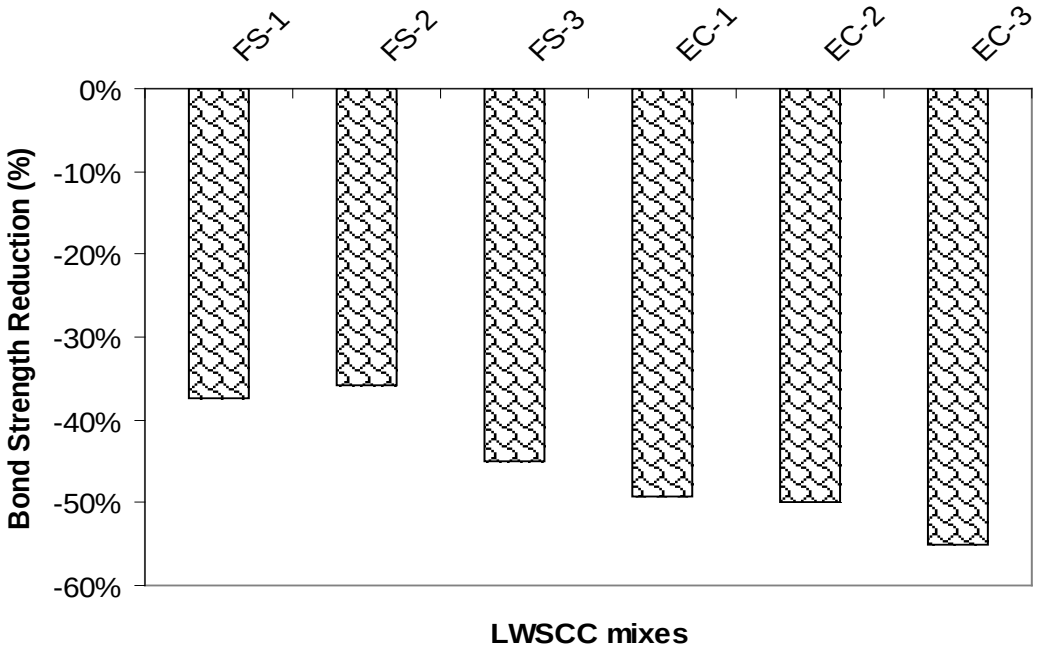

Figure 7.38 - The 28-day bond strength reduction of FS and EC- LWSCC mixtures against the ESH-LWSCC

As each of the three sub-mixes (1, 2 and 3) are made with different lightweight aggregates (Table 7.1), the LWSCC mixtures had shown quite different segregation index, where the lowest segregation resistance was observed in EC-LWSCC while the highest was for mixes made with ESH followed by FS aggregates. The same trend was observed for the compressive strength at 28-day (Table 7.3). Therefore, the bond strength values of these LWSCC mixes were different. The difference in the ultimate bond strength may be attributed to the type of lightweight aggregate, workability and the quality of the paste used for the production of LWSCC.

For this experimental investigation, all pullout specimens failed due to splitting of concrete and no pullout or yielding of steel bar failure was observed. Typical brittle splitting failure of specimens is shown in Figures 7.39 and 7.40. Failure was initiated by the formation of cracks with approximately 120^{o}C angled to each other at the loaded surface and propagated towards the free end of rebar regardless of the type of concrete mix.

Figure 7.39 - Bond failure due to splitting with cracks forming at approximately 120^{o}

Figure 7.40 - Bond failure due to splitting with cracks forming at approximately 120^{o}

According to the provisions of ACI 318 (2011), the development length of reinforcing bar for sufficient anchorage is inversely proportional to the square root of the compressive strength, implying that the bond strength should be linearly proportional to square root of the compressive strength (ACI 318 2011). In general, design provisions require longer development length for lightweight aggregate concrete.

Due to the lower strength of aggregate, LWSCC should be expected to have lower bond strength, fracture energy, and local bearing capacity than normal SCC with the same compressive strength. As a result, the bond strength of bars cast in LWSCC is lower than that that in normal SCC - that difference tending to increase at higher strength levels (Lachmei et al. 2009).

Bond stress and load-slip behaviour in LWSCC

Based on a study, LWSCC failed in two modes during pullout tests - categorized as pullout failure and splitting failure (Lachemi et al. 2009). Pullout failures are characterized by a gradual increase of load in load-slip curve up to the maximum load, followed by a gradual softening. On contrary, the load-slip curve for splitting failures is almost linear up to the peak load and then followed by a sudden failure (Figure 7.41).

For splitting failure mode, the deformed bar exhibited a small amount of slip, typically less than a 0.15 mm, when the peak load was obtained. Figure 7.42 shows the load-slip behaviour of the optimized LWSCC mixtures. The recorded behaviours of LWSCC load-slip curves were in agreement with other LWSCC study (Lachemi et al. 2009). Once the peak load was reached, the majority of the load was dropped suddenly; this abrupt decrease in bond stress was caused by the failure due to concrete cracking. Once chemical bond between rebar and concrete was broken, the remaining bond stress was maintained and resisted by ribs in the case of deformed bar.

The bond generates shear stresses along an anchored bar. For plain bars, this strength is low and the failure happens by pullout of the bar (Tepfers and Lorenzis 2003). Plain rebar exhibits the same pre-peak behaviour as deformed rebar with a very small amount of slip before peak load. The difference is that after the peak load, plain bar loses some load but holding a relatively higher load compared to the deformed bar as slip continues. Once the adhesive bond is broken,

the bond stress drops off quickly and the further resistance to pullout is provided primarily by friction. Due to the absence of ribs for mechanical resistance, overall, the bond stress of plain bar in LWSCC is relatively lower than the deformed rebar.

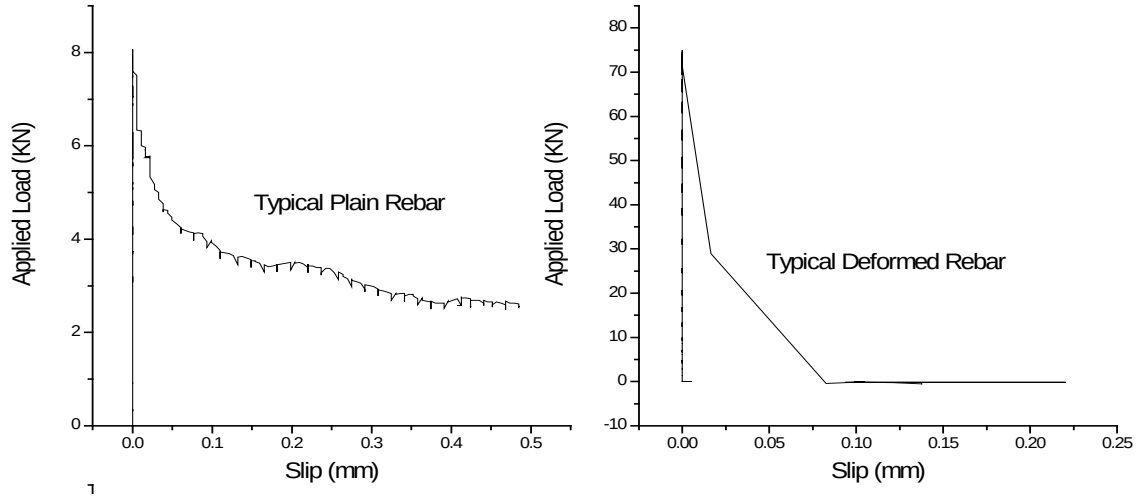

Figure 7.41 - Load-slip behaviour depending on type of rebar (Lachemi et al. 2009)

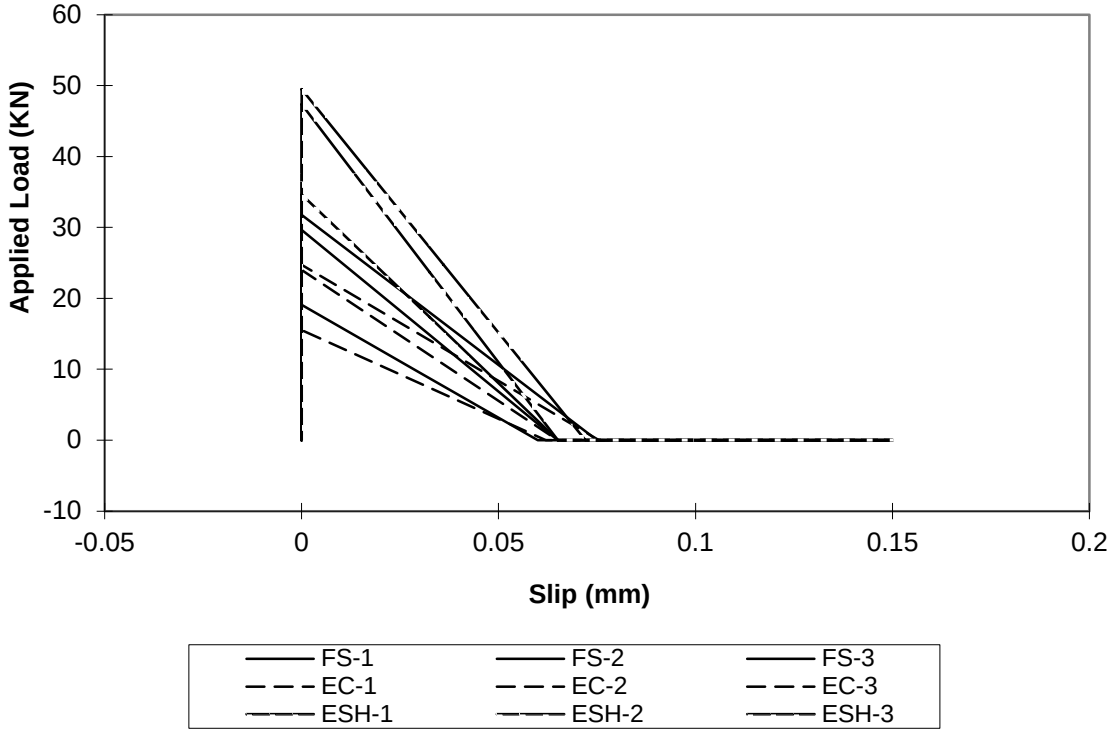

Figure 7.42 - Load-slip behaviour of LWSCC mixtures

Correlation between bond and compressive strength

The relationship between the compressive strength and the bond strength at 28-day for three different types of FS/ES/ESH LWSCC mixtures is illustrated in Figure 7.43. The relationship between the compressive strength and the bond strength at 28-day follows power law. The mathematical relationship was expressed as $f_b = 0.0004 \times (fc')^{2.5386}$ with a correlation coefficient (R^2) of 0.92 for LWSCC mixtures showing a high correlation. This is in agreement with the ACI 318 (2011) provision for the relationship of compressive strength and the bond strength for lightweight concrete.

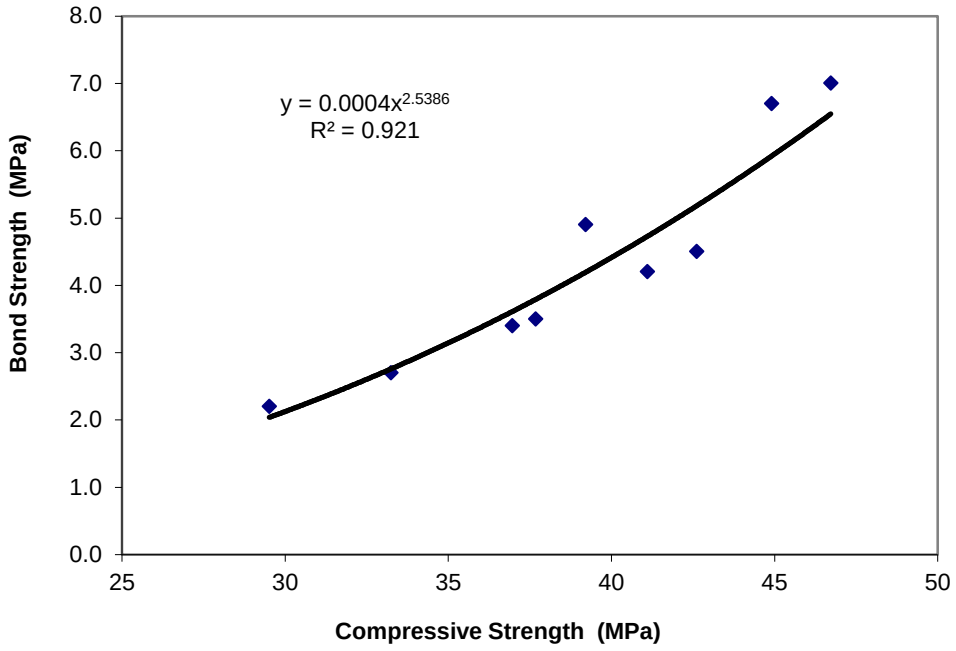

Figure 7.43 - Relationship between the 28-day compressive strength and bond strength of LWSCC mixtures

The bond strength is influenced by the shape of the bar and the strength of the concrete which is related to the quality of the aggregate and of the paste (Weigler et al. 1972). Low tensile strength can contribute to lower bond or anchorage bond stresses (Bardhan-Roy 1995). Besides, lightweight concrete is considered more brittle than normal concrete which might increase the risk of splitting cracks and delamination of the concrete cover (Bjerkeli et al. 1995). In pullout tests, the bond strength of lightweight concrete is always found to be lower than that of normal

concrete of the same strength. However, the cracking and tension stiffening behaviour of lightweight concrete is very similar to that of normal weight concrete (Walraven and Stroband 1995).

The bond stresses obtained from the experiments are compared with those obtained from various Code based models such as CSA (Equation 7.1 general and Equation 7.2 simplified) and ACI (Equation 7.3) (CSA A23 2009; ACI 318 2011):

$$l_d = 1.15 \frac{k_1 k_2 k_3 k_4}{d_{cs} + k_{tr}} \frac{f_y}{\sqrt{f'_c}} A_b \qquad (7.1)$$

$$l_d = 0.60 k_1 k_2 k_3 k_4 \frac{f_y}{\sqrt{f'_c}} d_b \qquad (7.2)$$

l_d = 0.015 (f_y d_b/$\sqrt{f_c'}$) (splitting failure) (7.3)

where,

Bar location factor, K_1

= 1.3 for horizontal reinforcement so placed that more than 300 mm of fresh concrete is cast in the member below the development length or splice

= 1.0 for other cases

Coating factor, K_2

= 1.5 for epoxy-coated reinforcement with clear cover < 3db or with clear spacing between bars being developed < 6db

= 1.2 for all other epoxy-coated reinforcement

= 1.0 for uncoated reinforcement

Concrete density factor, K_3

= 1.3 for structural low-density concrete

= 1.2 for structural semi-low density concrete

= 1.0 for normal density concrete

Bar size factor, K_4

= 0.8 for No. 20 and smaller bars and deformed wires

= 1.0 for No. 25 and larger bars

d_{cs} = the distance from the closest concrete surface to the centre of the bar being developed

K_{tr} = the factor of the contribution due to confinement

f_y = specified yield strength

A_b = area of individual bar in mm^2

d_b = nominal diameter of bar in mm

$f_c^{'}$ = compressive strength of concrete in MPa

The development length (l_d) in Eq. 7.1 and Eq. 7.2 is converted into the bond stress (u) using the following equation:

$$u = \frac{d_b f_s}{4 l_d} \tag{7.4}$$

where, d_b is the diameter of bar in mm, f_s is the peak stress developed in rebar during pullout test and l_d is the development length from Eq. 7.1 and Eq 7.2.

The bond stress in Eq 7.3 is calculated from:

$$l_d \pi d_b u = A_b f_u \tag{7.5}$$

where,

A_b = area of individual bar in mm^2

f_u = ultimate strength of the bar (MPa)

Based on the results presented in Table 7.8, it is found that Equations 7.1, 7.2 and 7.3 under-estimate the bond strength of LWSCC mixtures. This finding is in agreement with previous research studies (Hossain and Lachemi 2008). ACI and CSA based equations can therefore, be used to predict the bond strength of LWSCC mixtures.

Table 7.8 - Comparison of LWSCC bond strength using various code equations

	Experiment	**CSA A23**		**ACI 318**
Mixture No.	**28-day bond Strength f_b (MPa)**	**Eq. 7.1 (MPa)**	**Eq. 7.2 (MPa)**	**Eq. 7.3 (MPa)**
FSLWSCC-1	4.20	3.60	1.38	2.61
FSLWSCC-2	4.50	3.85	1.40	3.00
FSLWSCC-3	2.70	2.47	0.82	1.86
ECLWSCC-1	3.40	2.42	1.16	2.35
ECLWSCC-2	3.50	3.28	1.69	2.55
ECLWSCC-3	2.20	1.59	0.86	1.35
ESHLWSCC-1	6.70	4.93	2.74	4.26
ESHLWSCC-2	7.00	6.37	2.86	4.18
ESHLWSCC-3	4.90	3.62	2.08	3.15

7.4 LWSCC Mass Transport Properties Results and Discussion

7.4.1 LWSCC Porosity and Water Absorption

The absorption and porosity percentage for all LWSCC sub-mixes at the age of 28 days are presented in Table 7.9. The high absorption capacities of EC aggregates made EC-LWSCC mixtures to show higher value of absorption compared to both FS/ESH LWSCC mixtures. Mix 1 with different lightweight aggregates had absorbed more water than Mix 2 and 3 due to the presence of higher quantity of lightweight aggregates. The same applies for Mix 2 when compared to Mix 3. The absorptions of FS-LWSCC-1, EC-LWSCC-1 and ESH-LWSCC-1 were approximately 11, 7, and 16% higher than that of FS-LWSCC-3, EC-LWSCC-3 and ESH-LWSCC-3, respectively. Figure 7.44 shows LWSCC samples during absorption and porosity test. Figure 7.45 shows absorption percentage of the nine FS/EC/ESH-LWSCC mixtures. In lightweight concrete, the moisture movement is governed by the fineness of cement, the richness of the mix, the w/c and the curing environment at early ages.

Figure 7.44 - Absorption and porosity test of LWSCC specimens

Table 7.9 - Absorption and porosity results of LWSCC mixtures

Mixture No.		Absorption (%)	Porosity (%)
FSLWSCC-1	Mean	17.8	30.1
	C.OV. (%)	3.60	6.9
FSLWSCC-2	Mean	16.9	28.0
	C.OV. (%)	2.70	4.20
FSLWSCC-3	Mean	16.0	26.5
	C.OV. (%)	3.20	2.30
ECLWSCC-1	Mean	28.0	35.9
	C.OV. (%)	5.30	4.60
ECLWSCC-2	Mean	27.1	35.0
	C.OV. (%)	2.70	3.10
ECLWSCC-3	Mean	26.2	33.5
	C.OV. (%)	2.80	5.10
ESHLWSCC-1	Mean	22.2	30.8
	C.OV. (%)	2.70	3.10
ESHLWSCC-2	Mean	20.6	28.5
	C.OV. (%)	4.20	2.9
ESHLWSCC-3	Mean	19.2	27.0
	C.OV. (%)	2.50	4.30

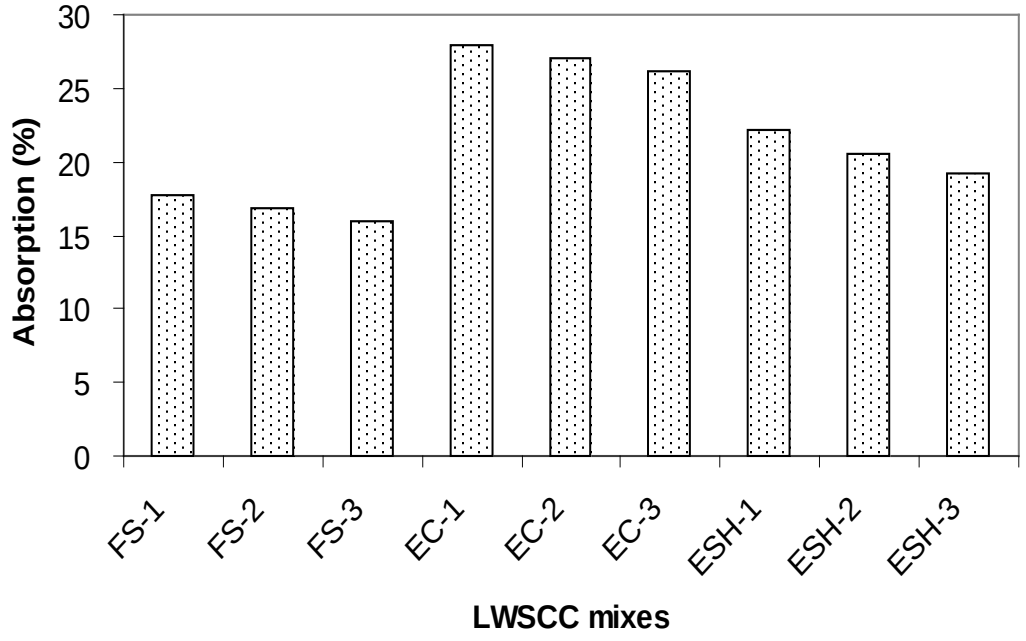

Figure 7.45 - Comparison between the absorption (%) of the three different types of LWSCC mixtures

The porosity variation of the tested LWSCCs showed similar trend as observed in the absorption test. Mix 1 for all three types of lightweight aggregates showed the highest porosity compared to Mix 2 and 3 made with the same type of lightweight aggregates. This is due to higher percentage of lightweight aggregate volume in these mixes. Mixes with EC aggregates showed the highest porosity at 36, 35 and 33.50%. This can be attributed to EC aggregates properties where the aggregate particles are more porous than both ESH and FS aggregates. Figure 7.46 shows the porosity percentage of the nine tested LWSCC mixtures. The porosity of Mix 1, 2 and 3 made with either ESH or FS is virtually the same, even though the ESH aggregates are more porous than FS. This is due to the fact that ESH-LWSCC mixes had over all less percentage of coarse aggregate and better compactability/workability and paste quality.

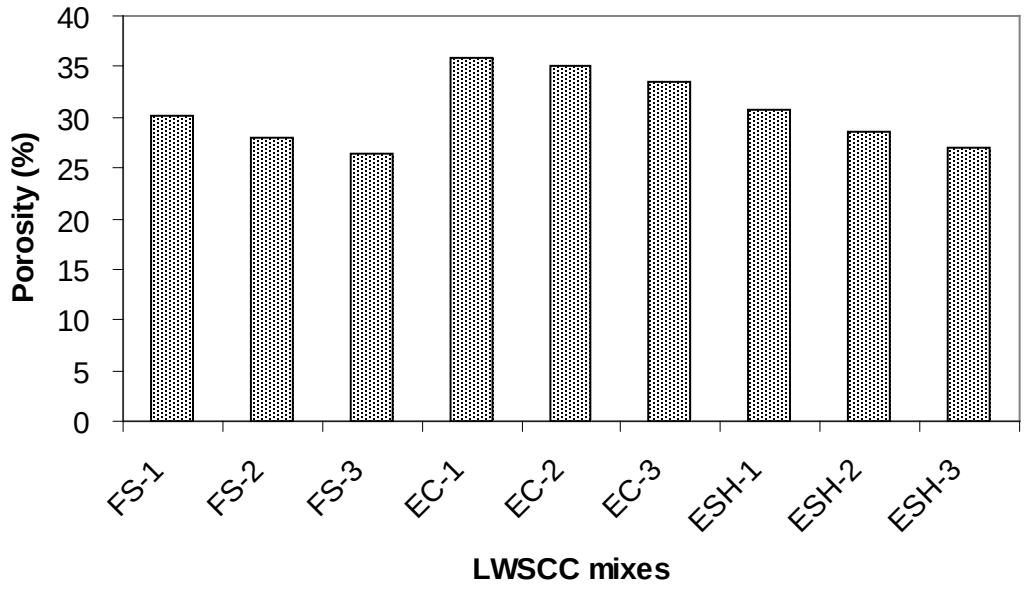

Figure 7.46 - Comparison between the porosity (%) of the three different types of LWSCC mixtures

It is worth to note that the used ASTM C 642 test method yielded absorption and porosity results higher than expected for LWSCC specimens. This can be attributed to the fact that this test method takes into account the high absorption and porosity of the used (coarse and fine) lightweight aggregates. It can be suggested that such test method is not suitable for testing lightweight concrete. Testing by electrical resistance or ultrasonic pulse velocity (UPV) would rather be suitable methods to evaluate the mass transport properties of LWSCC as confirmed by other research studies (Hwang and Hung 2005).

7.4.2 LWSCC Sorptivity

The sorptivity test measures the rate at which water is drawn into the pores of concrete. The test is based on water flowing into the concrete through large connected pores. Thus, it is considered as a relative measure of the permeability. Figure 7.47 shows the differences between porosity and permeability where lots of voids connected by very few channels represents high porosity/low permeability concrete, lots of connected voids represents high porosity and permeability (negative impact in durability), lots of isolated voids represents high porosity/non permeability concrete, and connected network of voids indicates high permeability and low

porosity. For this test, two specimens from each LWSCC mixture with dimensions of Ø100 x 50 mm cut from Ø100 x 200 mm cylinder specimens were employed. The specimens were dried in an oven at approximately 100 ± 5°C until the constant mass was obtained. Then the specimens were allowed to cool to the ambient temperature in a sealed container.

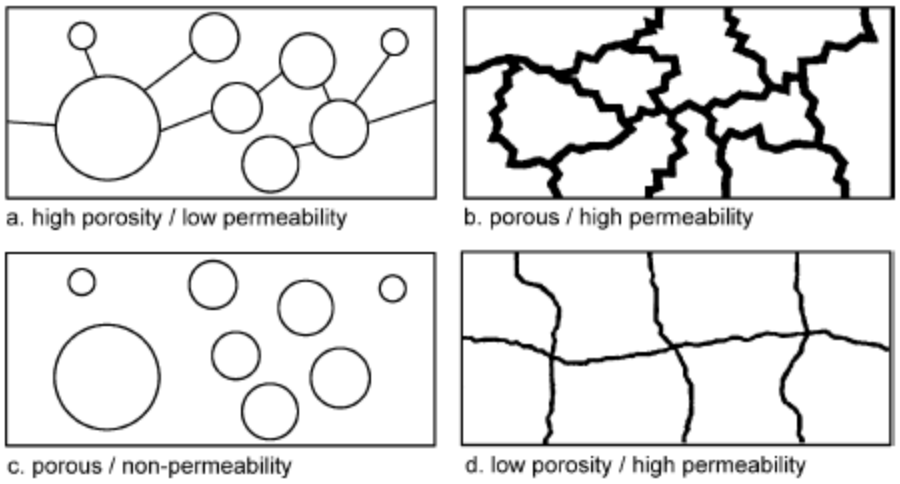

Figure 7.47 - Schematic diagram showing differences between porosity and permeability (EuroLightCon 1998)

Afterward, the sides of the specimens were sealed with non-absorptive self-adhesive strips of aluminum tape. The sorptivity test was then carried out by placing the specimens on glass rods in a tray so that their bottom surfaces up to a height of 3 mm were in contact with water, as seen in Figure 7.48. This procedure was considered to allow free water movement through the bottom surface. Figure 7.49 shows LWSCC samples during the sorptivity test.

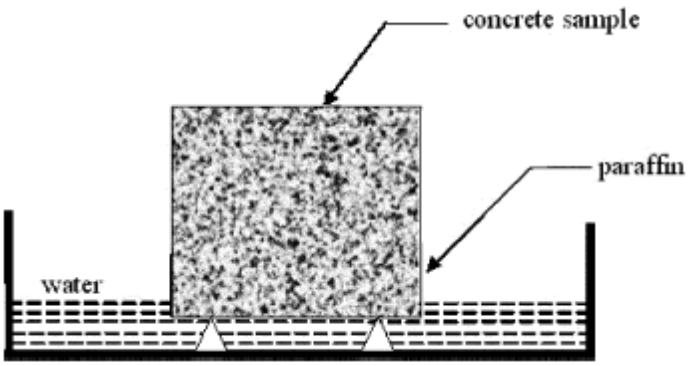

Figure 7.48 - Sorptivity measure of LWSCC

Figure 7.49 - LWSCC samples during sorptivity test

The specimens were removed from the tray and weighed at different time intervals up to 6 hours, and then every 24 hours up to 8 days to evaluate mass gain. The volume of water absorbed was calculated by dividing the mass gained by the nominal surface area of the specimen and the density of water. These values were plotted against the square root of time. The slope of the line of the best fit up to 6 hours reading was defined as the initial sorptivity coefficient of concrete, while the slope of the line from 1 day up to 8 days defined as the secondary sorptivity coefficient of concrete. The test was carried out at 28-day and 91-day.

As shown in Figure 7.50, the EC-mixes had the highest sorptivity, followed by ESH and FS mixes. According to these results, the sorptivity index of EC-LWSCC mixtures had the highest rate of initial and secondary absorptions at 0.171, 0.159 and 0.1485 mm/sec$^{0.5}$ at 28-day and 0.111, 0.112 and 0.123 mm/sec$^{0.5}$ at 91-day for mixes EC-LWSC-1, 2 and 3, respectively. All sorptivity values of ESH/FS-LWSCC mixtures were lower than those equivalent EC-LWSCC mixtures.

Similar to the absorption test, the lowest sorptivity index was observed for FS-LWSCC mixtures. In general, LWSCC mixtures made with any type of both coarse and fine lightweight aggregates exhibit much higher sorptivity index than comparable normal SCC mixture. The reduction of sorptivity with age may have beneficial effect of improving the long-term corrosion resistance of LWSCC mixtures. Figure 7.51 shows the percentage reduction in sorptivity at 91-day compared to the 28-day test results, where it was ranged from -32 to 24%. This may be attributed to the contribution of the silica fume in refinement of the pore structure of the cement matrix associated with the transformation of a network of large permeable pores into discrete, smaller, and less permeable pores. The pozzolanic reaction between SCM and calcium hydroxide takes place at a slower rate and produces a denser concrete as the age of concrete increases. The development of denser LWSCC mixture with the increase in age should exhibit lower permeability as confirmed from the 91-day sorptivity index.

A study by Hossain and Ahmed (2011) confirmed the lower permeability of lightweight concrete over normal concrete which was attributed to the development of high quality paste-aggregate ITZ at the interface, refinement of pore structure, and the progressive internal curing in LWCs.

Also it was confirmed that LWCs exhibited lower 12-week permeability because of the pozzolanic reaction that produces refinement of pore structure and a denser concrete.

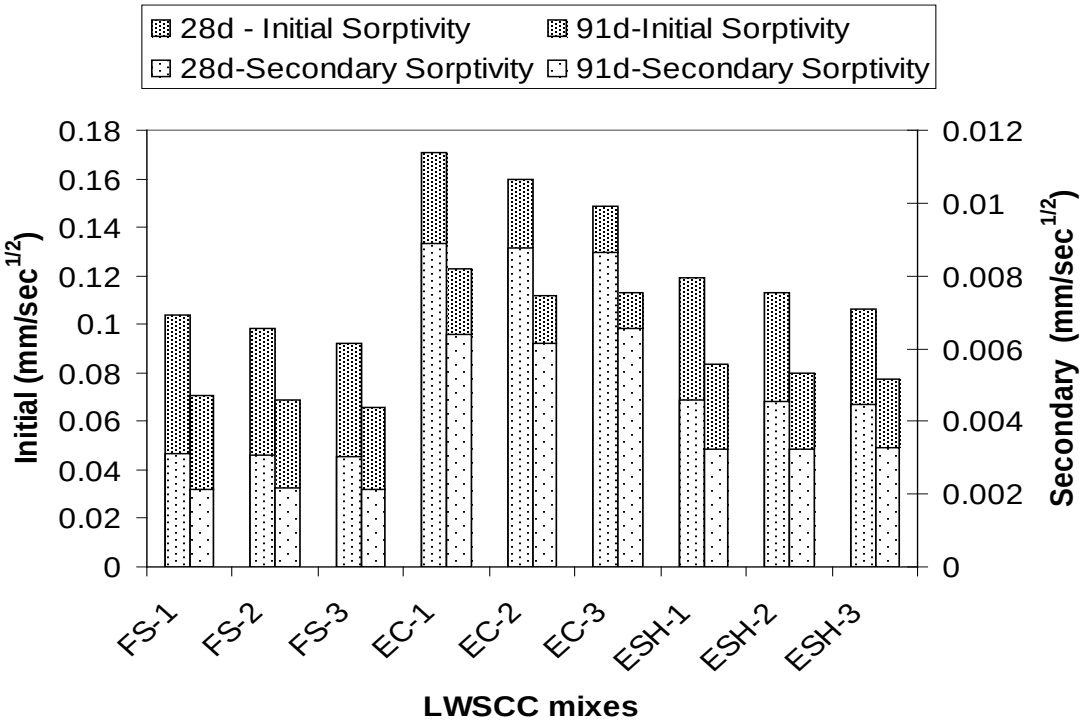

Figure 7.50 - Comparison between the 28-day and 91-day of sorptivity index of LWSCC mixtures

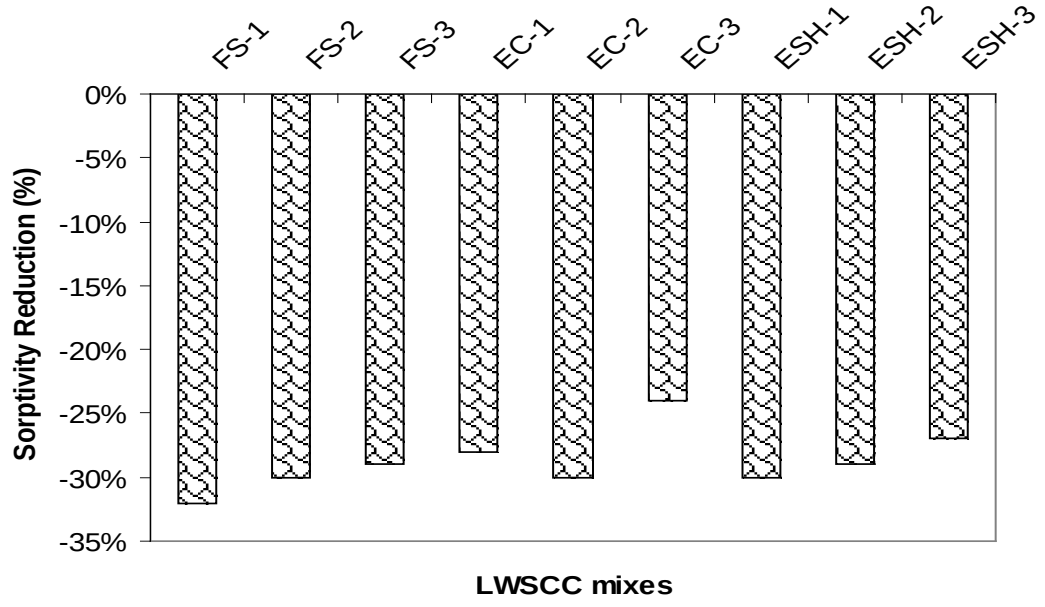

Figure 7.51 - Comparison between the 91-day sorptivity index reductions of LWSCC mixtures

7.4.3 Rapid Chloride Permeability (RCP) of LWSCC

Rapid chloride permeability (RCP) is an indication of concrete's ability to resist chloride ion penetration. RCPT is a relatively quick method to determine the chloride permeability of concrete. Permeability mainly refers to the amount of water migration through concrete when the water is under pressure or the ability of concrete to resist water penetration. Permeability of concrete is a function of permeability of paste, permeability and gradation of aggregate, paste–aggregate transition zone and paste to aggregate proportion. Permeability also depends on w/b (increase with the increase of w/b) and initial curing conditions

Before testing, the specimens must go through a conditioning process. This process removes all air from the voids in the concrete using a vacuum and then fills the voids with distilled water before they are tested. From 100 x 200 mm cylinders, 50 mm thick disc specimens were cut from the middle of each cylinder. Then, the disc specimens were transferred to the test cell, in which one face of the specimen was in touch with 0.3N NaOH solution and the other was in touch with 3% NaCl solution. A direct voltage of 60.0 ± 0.1V was applied across the faces. A data logger registered the current passing through the concrete over a 6-hour period. The test was terminated after 6 hours. Current (in amperes) versus time (in seconds) was plotted for each concrete specimen, and the area underneath the curve was integrated to obtain the charge passed (in coulombs). Figure 7.52 to 7.54 show RCPT setup, samples preparation and LWSCC samples undergoing RCPT test.

The rapid chloride ion penetrability measured at 28 and 91-day for all LWSCC mixtures is listed in Table 7.10, including the ASTM C1202 rapid chloride ion penetrability classification ranges. ASTM C 1202-10 specifies the concrete as highly permeable if the charge that passes through it is more than 4000 Coulombs. All LWSCCs mixtures showed values lower than 4000 Coulombs. The highest RCPT value was recorded for Mix 3 with EC lightweight aggregates at 3992 Coulombs. In general all LWSCC mixtures made with EC aggregates had higher RCPT value compared to LWSCC with other lightweight aggregates. The RCPT values ranged from 2489 to 3992 Coulombs at 28-day and 1220 to 1996 Coulombs at 91-day. Figure 7.55 illustrates the comparison between 28-day and 91-day RCPT values for all nine LWSCC mixes with three different lightweight aggregates.

Table 7.10 - RCPT results of LWSCC mixtures

Mixture No.		RCPT 28-day		RCPT 91-day	
		Coulombs	Rating	Coulombs	Rating
FSLWSCC-1	Mean	2489	Moderate	1220	Low
FSLWSCC-2	Mean	2315	Moderate	1088	Low
FSLWSCC-3	Mean	2758	Moderate	1379	Low
ECLWSCC-1	Mean	3715	Moderate	1635	Low
ECLWSCC-2	Mean	3596	Moderate	1726	Low
ECLWSCC-3	Mean	3992	Moderate	1996	Low
ESHLWSCC-1	Mean	2982	Moderate	1461	Low
ESHLWSCC-2	Mean	2832	Moderate	1359	Low
ESHLWSCC-3	Mean	3189	Moderate	1531	Low

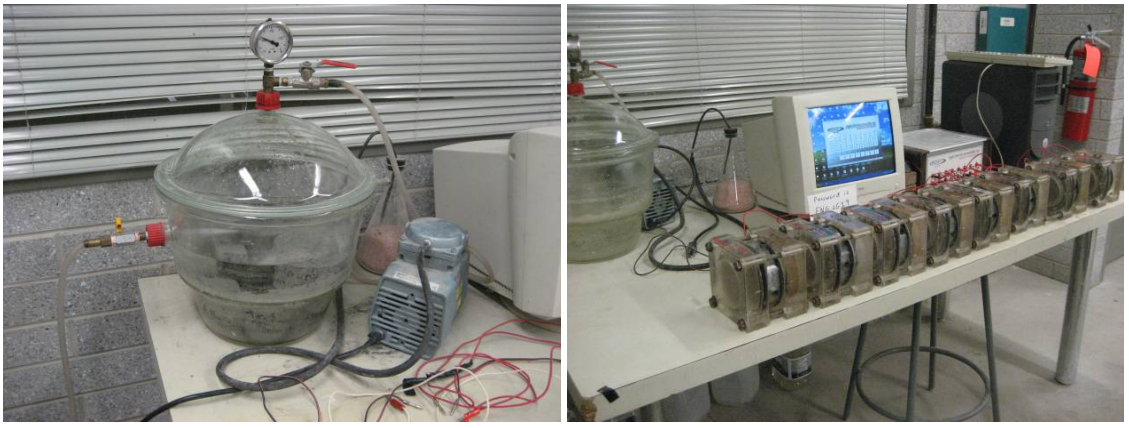

Figure 7.52 - RCPT setup and samples preparation

Figure 7.53 - LWSCC samples undergo RCPT and "Germann Proove-it" software screen

Figure 7.54 - LWSCC samples after RCPT test

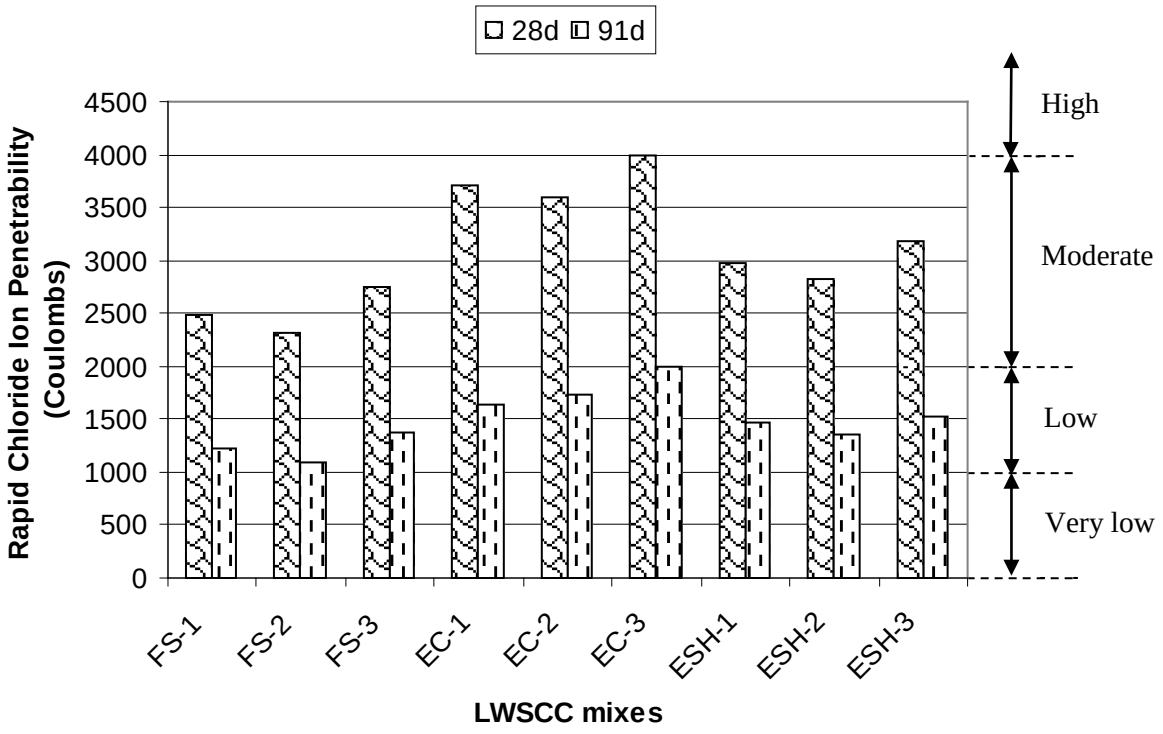

Figure 7.55 - Comparison between the 28-day and 91-day RCP values of LWSCC mixtures

Based on Table 1 of ASTM 1202-10, the chloride permeability of the LWSCCs were rated "moderate" at 28-day and "low" at 91-day. The FS-LWSCC showed much higher resistance to chloride ion permeability. The total charge that passed through the FS-LWSCC-2 specimens was approximately 1088 coulombs at 91-day, which rated this concrete as "low".

All LWSCC mixtures had 5% silica fume replacement. As such the major contribution of the silica fume (SF) has been identified to be a refinement of the pore structure of the cement matrix, involving the transformation of a network of large permeable pores into discrete, smaller, and less permeable pores. Three research studies on concretes incorporating SCM replacement confirmed the large decrease in the chloride ion permeability with the use of SCM (such as SF) due to the change in the pore structure of the hydrated cementitious system (Güneyisi et al. 2002, 2005; Gesoglu and Güneyisi 2011, 2007; Gesoglu et al. 2009).

The influence of SF on the microstructure and diffusion properties of mortar has been studied by Kostuch et al. (1993). It was observed that the average pore size significantly reduced when the cement was replaced with 20% fly ash. It was also found that SCM seemed to be effective in reducing the rate of diffusion of Cl^- and Na^+ ions in mortar. In the current study, all LWSCC mixtures showed effective decrease in the 91-day chloride ion penetrability of 44 to 50%. This is attributed to the use of SF in all LWSCCs conforming to the finding of research studies with regards to RCPT and SF where it was concluded that the interfacial transition zone of the SCC mixtures can be improved substantially by the reduction w/b and by the incorporation of silica fume (Nehdi et al. 2004).

7.4.4 LWSCC Drying Shrinkage

Moisture transport in normal SCC with dense aggregates is determined mainly by the permeability of the matrix. In LWSCC, the porous structure of the aggregates may contribute to the permeability of the concrete. At the same time the aggregates may serve as water reservoirs which may substantially affect the transport of water through the concrete. Since transport of water is the basis for the occurrence of shrinkage, the particular properties of the lightweight aggregate particles are liable to affect the shrinkage properties of LWSCC.

In order to obtain a LWSCC mixture with the same strength as a normal SCC, higher paste content may be used. This is because of the generally lower strength of the lightweight aggregates. Since the paste content largely determines the shrinkage potential of the concrete, LWSCC exhibits larger shrinkage strain than normal SCC of same strength. Figure 7.56 shows the drying shrinkage test of LWSCC prisms.

The variation of the drying shrinkage with age for the LWSCC mixtures of different lightweight aggregates is presented in Figure 7.57. The shrinkage of all LWSCC mixtures at 112-day is found to be almost at or higher than 600 microstrain. Aggregates with high absorption properties are associated with high shrinkage in concrete (ACI 221R 2001) as confirmed from the substantial increase in shrinkage with the increase of the aggregates absorptions such in cases of LWSCC mixtures with both EC and ESH.

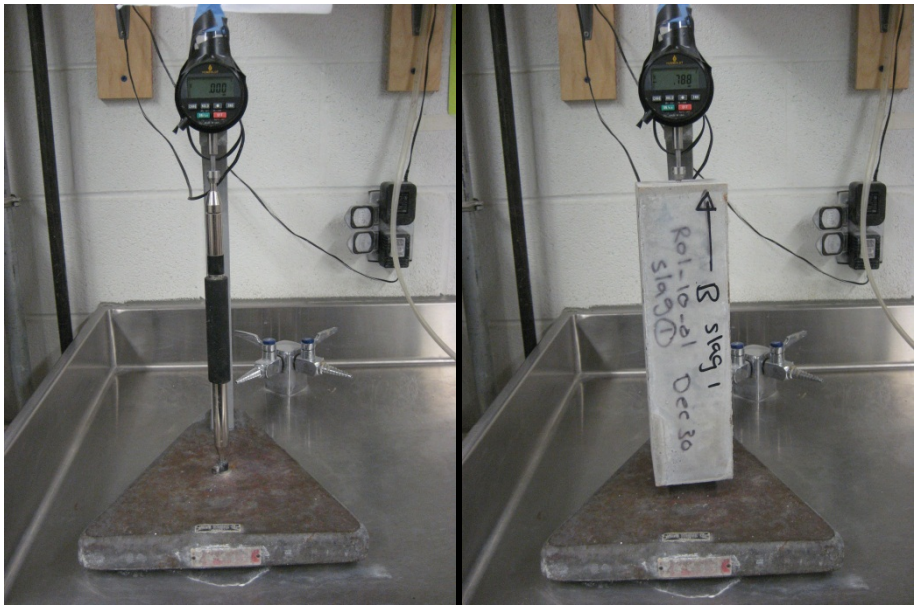

Figure 7.56 - Drying shrinkage test of LWSCC prisms

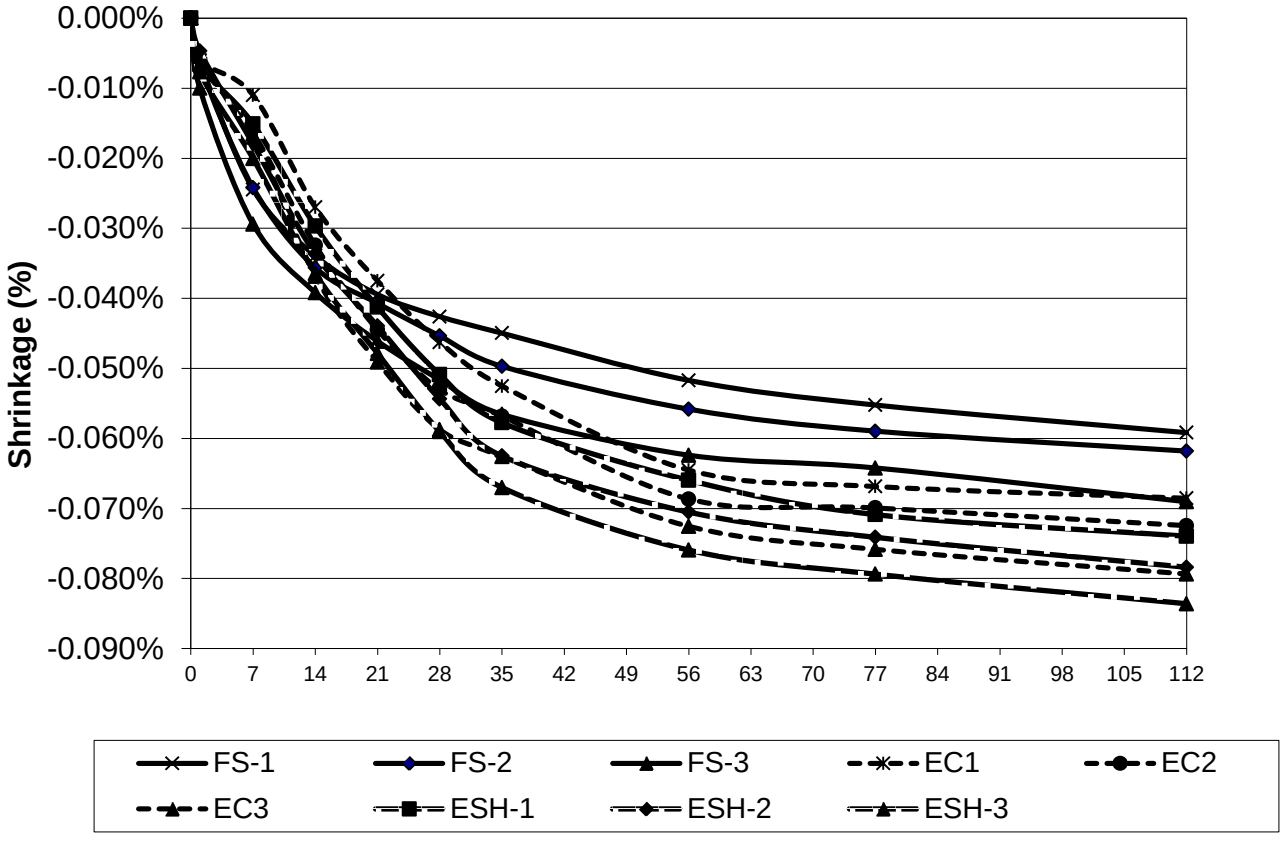

Figure 7.57 - Comparison between the drying shrinkage values of LWSCC mixtures

The binder content was constant for each group mix made with the three different lightweight aggregates. However, the percentage of coarse aggregate in the mixtures was limited to maximum 29.5%, 29.5% and 24.5% by volume for the FS, EC and ESH-LWSCC mixes, respectively. Consequently, the shrinkage was higher in the LWSCC concrete specimens having higher content of sand verses stone as in case of ESH-LWSCC mixtures as can be seen from Fig. 7.26.

The shrinkage in LWSCC mixtures 1, 2 and 3 with ESH aggregates at the age of 112-day was found to be approximately 21, 27 and 25% (mean value) higher than those made with FS aggregates, representatively. The 16-week drying shrinkage in ESH-LWSCC-1 was about 740 microstrain compared to about 590 microstrain in FS-LWSCC-1 and 690 microstrain in EC-LWSCC-1. It is suggested that the drying shrinkage of structural lightweight concrete ranges from 10 to 30% more than that of normal density concrete (Hossain and Ahmed 2011; Kostmatka et al. 2002). It is also reported that the shrinkage of lightweight concrete can be 50% greater than normal weight concrete (Manual of Lightweight Aggregate Concrete 1983). Concrete made with lightweight aggregates having open textured and irregular surface can produce a shrinkage of 1000 microstrain. Like hydration of cement, drying shrinkage is the long lasting process that depends on w/c, degree of hydration, curing temperature, relative humidity, duration of drying, aggregate properties, admixture and cement composition (Mindess and Young 1981; Brandt 1995).

The drying shrinkage is affected by twin influences of aggregate-to-binder and water-to-cement ratios. Shrinkage increases with the increase of w/c and decreases with the increase of aggregate-to-binder ratio of concrete. Previous study (Carlson 1938) showed that for each 1% increase in mixing water, concrete shrinkage increased by about 2%. For the current series of tests, when comparing Mix 1 and 3 made with same aggregates, such as for EC-LWSCC where the aggregate volume was decreased from 29.5% to 27% by volume as presented in Table 7.1, where it's related to decrease of aggregate-to-binder ratio (A/b) from 1.86 to 1.56 and the w/b is increased from 0.36 to 0.40. As a consequence, the increase in shrinkage for Mix 3 compared with Mix 1 for any type of lightweight aggregates is justified. LWSCC mixtures with both EC

and ESH aggregates showed lower initial drying shrinkage and significantly higher later drying shrinkage than LWSCC mixtures made with FS. This is possibly due to the high absorption and porosity of the EC and ESH aggregates compared to FS aggregates. The high drying shrinkage and comparatively low tensile strength may lead to the danger of shrinkage cracking. However, the danger of shrinkage cracking can be compensated by the lower modulus of elasticity of lightweight aggregates.

The highest shrinkage values were observed in ESH-LWSCCs where the aggregates had high absorption and mixtures had the lowest coarse-aggregates to binder ratio, followed closely by EC-LWSCC mixtures. The lowest shrinkage values were recorded in FS-LWSCC mixes.

It should be noted that the process of internal curing due to the supply of pore water from lightweight aggregates (coarse/fine) into the finer capillary pores of cement paste can explain the reduced early age drying shrinkage in the LWSCC mixtures, as confirmed in a study by Hossain and Ahmed (2011) investigating this aspect.

7.5 Summary

The optimized LWSCC mixtures with EC showed lower compressive strength than equivalent mixes with FS and ESH aggregates. The highest flexural strength values was recorded for the optimized LWSCC mixes made with FS, while the lowest was recorded with mixes made with EC aggregates. The highest split tensile strengths were reported for the optimized LWSCC mixtures made with lightweight ESH aggregates, followed by LWSCC mixtures made with FS, and then EC. It was observed that the optimized LWSCC mixtures with ESH aggregates produced the highest bond strength followed by mixtures made with FS, and then EC.

The high absorption capacities of EC aggregates have made the optimized EC-LWSCC mixtures to show higher value of absorption than both FS and ESH mixtures. The porosity of the tested LWSCCs showed the same trend as that of absorption test. The porosity of LWSCC mixes made ESH and FS were virtually the same even though the ESH aggregates are more porous than FS.

The EC- LWSCC mixtures exhibited the highest sorptivity, followed by ESH and then FS mixes. A reduction of sorptivity values was recorded with the increase of age. LWSCCs mixtures

showed RCPT values lower than 4000 Coulombs with the highest RCPT values recorded by EC-LWSCCs. The RCPT values were rated as “moderate” at 28-day and “low” at 91-day. The drying shrinkage of all LWSCC mixtures at 112-day was ≥ 600 microstrain. Substantial increase in shrinkage was noticed with the increase of aggregate absorption capacity as in the case of both EC and ESH LWSCCs.

CHAPTER EIGHT

8 EVALUATION OF DURABILITY ASPECTS OF LWSCC MIXTURES

8.1 Introduction

Chapter 8 presents the Phase V of this research, where three selected LWSCC mixtures made with furnace slag (FS), expanded clay (EC) and expanded shale (ESH) aggregates, were investigated for durability performance. Total nine LWSCC mixtures presented in Table 7.1 of Chapter 7 were tested for hardened air-void structure and residual bond stress after corrosion as well as resistance against corrosion, elevated temperature, freeze-thaw cycle, salt scaling and acid attack. The results are critically analyzed to examine the effect of various parameters related to mix design and testing conditions as well as to make comparative performance evaluation of LWSCC mixtures.

8.2 LWSCC Durability Performance

8.2.1 LWSCC Corrosion Resistance

Corrosion of steel reinforcement in concrete is a major aspect affecting concrete durability. When concrete is subjected to a chloride-rich environment, the chloride ions can penetrate and diffuse through the body of the concrete, ultimately reaching the steel bars and causing corrosion (Hossain 2005). Concrete that has low permeability and dense microstructure is believed to obstruct chloride diffusion through the concrete body, which helps reduce the rate of corrosion of embedded reinforcing steel.

To determine the corrosion resistance of LWSCC mixtures, a total of eighteen concrete cylinders (100 mm in diameter and 200 mm in height), reinforced axially with a single 15 mm deformed bar embedded at the centre, were used. The cylinders were divided into nine groups representing the nine selected LWSCC mixtures with three lightweight aggregates types where, each group contained two cylinders, as presented in Table 8.1.

Table 8.1 - LWSCC specimen detail for accelerated corrosion test

Number of mixes	Number of specimens per mix	Specimen size	Rebar type and size
9 LWSCC mixes as per Table 7.1	2	100 x 200 mm cylinder	15 mm deformed rebar axially embedded at the centre of the specimen

Accelerated corrosion tests have been used successfully to determine the susceptibility of reinforcing rebar to corrosion (Amleh, 2000; Hassan et al. 2009; Hossain 2005). The accelerated corrosion setup used in this investigation consisted of plastic tanks, electrolytic solution (5% sodium chloride (NaCl) by the weight of water) and steel mesh placed at the bottom of each tank.

Each cylinder was partially immersed in the electrolytic solution up to two-third of its height (to avoid direct corrosion of the bars). To eliminate any variance in the concentration of the NaC1 and PH of the solution, the electrolyte solution was changed on a weekly basis. Figure 8.1 illustrates the schematic representation of the experimental setup for the accelerated corrosion test. A potential of 12V direct current was applied across the specimens, the steel rod being the positive electrode and a steel mesh being the negative electrode.

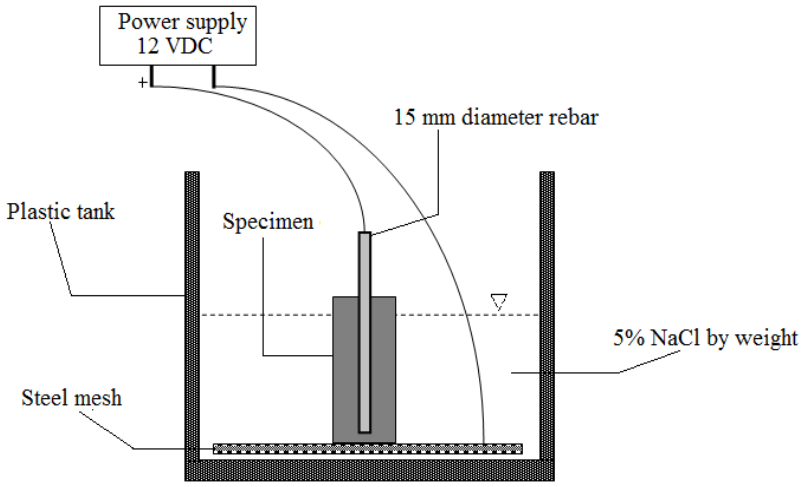

Figure 8.1 - Schematic representation of the accelerated corrosion test

During accelerated corrosion test, it is assumed that the electrical potential applied to the reinforcement attracted negatively charged chloride ions from the solution into the concrete and toward the positively charged steel bars. As the chloride ions reached the steel-concrete interface above threshold concentration, the steel surface began to corrode. The expansive products of corrosion-imposed tensile stresses on LWSCC cover resulted in cracking when the tensile stresses exceeded the tensile strength of the cover material. Cracking, especially large cracks, would allow the conductive chloride solution to come into direct contact with the steel surface, thus providing a direct current path between the reinforcement and the electrodes in solution. Therefore, a current spike, or a dramatic increase in current flow, suggests a reduction in electrical resistance following cracking in the concrete around the steel bar (Hassan et al. 2009; Guneyisi et al. 2005)

During the accelerated corrosion test, specimens were monitored periodically to record the duration it takes for corrosion cracks to appear on the surface of specimens and the current variation with time was also recorded. In this study, accelerated corrosion test was terminated after 30 days. Even though a dramatic increase in current flow of some specimens was monitored before 30 days, test was kept going up to the end of 30 days in order to make meaningful rebar mass loss comparison.

Based on Faraday (1999), the amount of corrosion is related to the electrical energy consumed and is a function of ampere and time. The amount of mass loss as an indicator of corrosion can be estimated by using Equation 8.1:

$$\text{Mass loss} = t \times i \times M / (z * F) \quad (8.1)$$

where t = the time passed (s), i = the current passed (Amperes), M = atomic weight (for iron M = 55.847 g/mol), z = ion charge (assumed 2 for $Fe \rightarrow Fe^{2+} + 2e^{-}$) and F = Faraday's constant which is the amount of electrical charge in one mole of electron (F = 96,487 Amp.sec).

Figure 8.2 shows the relationship between the current in mA and the immersion time in days for LWSCC cylinders with different lightweight aggregates. In general, the current–immersion time relationship for all LWSCC mixtures showed an initial fluctuation in the current, followed by a

gradual increase. The variation of the current in the first few days is an indication of the formation of the passive film around the reinforcing steel bar, which protects the steel from corrosion. When depassivation of the steel occurs, corrosion starts and then the rate of corrosion increases significantly (Cornet et al. 1986).

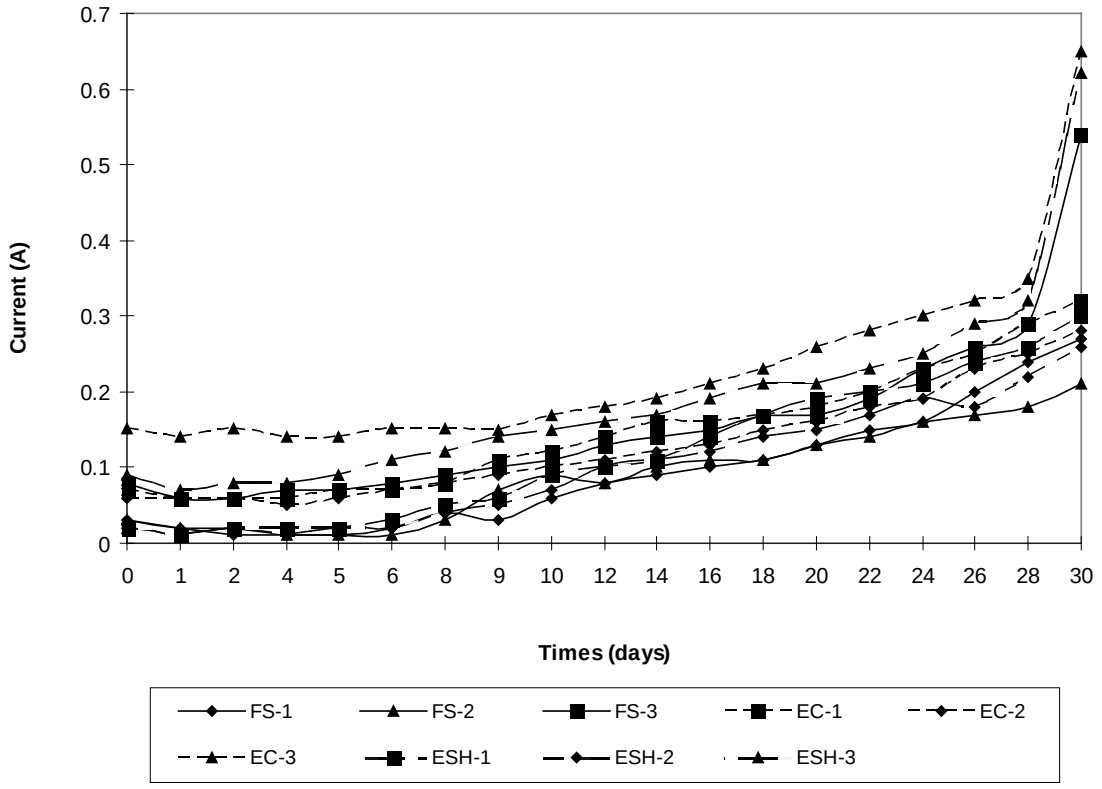

Figure 8.2 - Current–time history for LWSCC mixtures

EC-LWSCC mixtures demonstrated higher current values in the early stages of the test, approximately 0.07, 0.06 and 0.15 mA for mixes 1, 2 and 3, respectively, compared to FS-LWSCC mixes 1, 2 and 3 (which demonstrated 0.03, 0.03 and 0.08 mA, respectively) and ESH-LWSCC mixes 1, 2 and 3 (which demonstrated relatively low current values at 0.02, 0.02 and 0.09 mA, respectively). Also, the current in EC-LWSCC specimens was higher than that of comparable FS/ESH-LWSCC specimens during the entire test duration. The lower current passing through the FS/ESH-LWSCC specimens is an indication of the higher resistivity of these

concretes. Permeability of the concrete is the main factor influencing the concrete resistivity (Hope and Alan 1987). The aggregate quality, porosity and absorption plus the higher flowability and resistance to segregation of FS followed by ESH specimens were thought to be the main factors that improved the resistance and enhanced the quality of these concretes.

The increase of the slope in the time–current curve indicates the corrosion initiation, and the slope of the curve represents the rate of corrosion. EC-LWSCC specimens showed earlier corrosion initiation and a higher corrosion rate than both FS/ESH-LWSCC specimens.

Mix 3 with all types of lightweight aggregates showed the highest corrosion, fastest corrosion initiation and higher corrosion rate compared to Mixes 1 and 2. This can be attributed to higher w/b (w/b for Mixes 3 was 0.4 while Mixes 1 and 2 at 0.36 and 0.35, respectively). Lower concrete quality manifested in higher w/b and lower segregation resistance (Table 7.1) can be the reason for the lower corrosion resistance observed in these mixes. LWSCC-Mixes 3 exhibited sudden jump in the time–current curve after relatively increased slope compared to Mixes 1 and 2 which showed relatively gradual increase of the current with the time without sudden jump in 30 days.

The sudden jump in LWSCC- Mixes 3 in time–current curves was the indication of the formation of severe longitudinal crack of 1~3 mm width along the length of the embedded bar as can be seen in Figures 8.3 and 8.4.

Figure 8.3 - LWSCC specimens after accelerated corrosion test

Figure 8.4 - LWSCC specimens after accelerated corrosion test

After the corrosion test, the pull-out test was conducted on the corroded specimens to determine the bond strength and mass loss of steel rebar. The pulled out corroded bars (Figure 8.5) were cleaned with a wire brush to ensure that they were free of any adhering concrete or corrosion products, then soaked in a chemical solution (1:1 of HCl and water) according to ASTM Standards G1-03 method (ASTM G1, 2003). The clean bars were then weighed and the percentage mass loss for each bar was calculated based on Eq. 8.2.

$$\%\ \text{of mass loss} = \frac{(\text{initial weight - final weight})}{\text{initial weight}} \times 100 \tag{8.2}$$

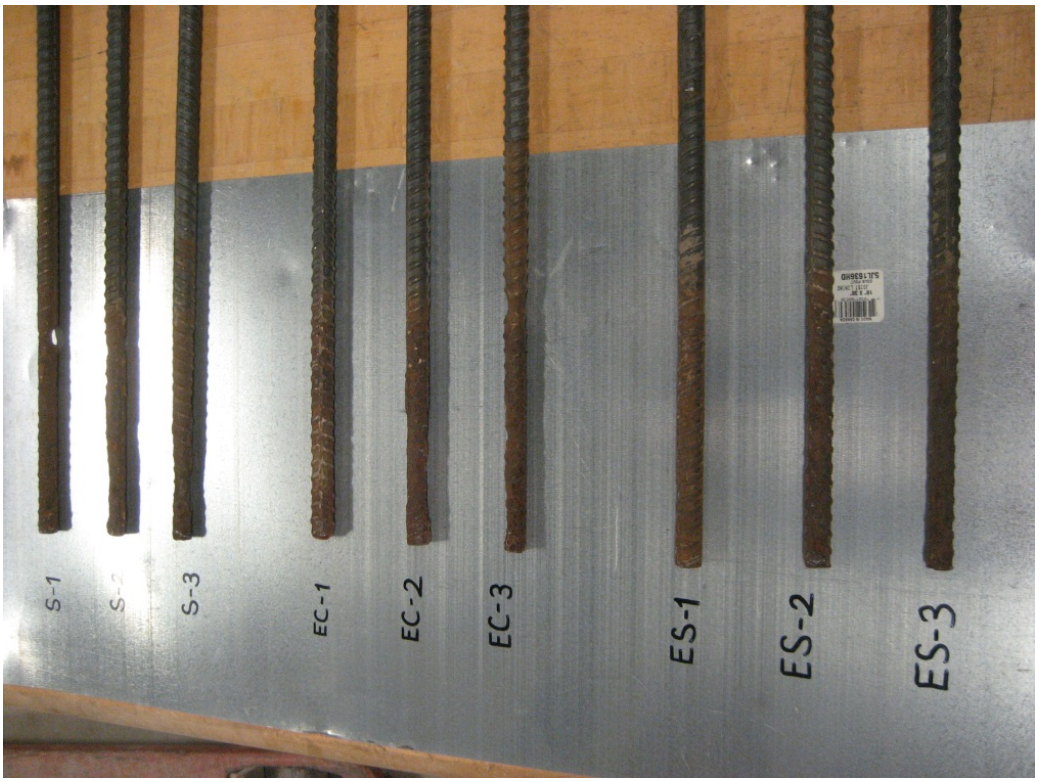

Figure 8.5 - Corroded steel rebars after undergoing the accelerated corrosion test

Bond strength and rebar mass losses of the LWSCC mixtures are presented in Table 8.2 Mass loss of rebar embedded in Mixes 3 were the highest at 68.2 g, 92.5 g, and 78.5 g for specimens made with FS, EC and ESH aggregates at the end of 30 days accelerated corrosion test, respectively. Less significant mass loss of rebar was noted for Mixes 2 with lower w/b followed by slightly higher mass loss in Mixes 1 with different aggregate types. On the other hand, bond strength loss of the all LWSCC mixtures varied between 81.1 to 91.8%, the highest bond strength loss was recorded for Mixes 3, where Mixes 1 and 2 showed relatively lower in bond strength loss. LWSCC made with EC aggregates showed the highest bond strength loss followed by LWSCC mixtures made with ESH and then FS aggregates. The reason behind very close bond strength reduction can be associated with the constant exposure time (30 days) for all LWSCC mixtures.

Table 8.2 - Bond strength loss and weight loss of steel rebar after corrosion of LWSCC specimens

Mixture No.	Loss	
	Bond strength (%)	Weight of steel rebar (g)
FSLWSCC-1	81.3	48.0
FSLWSCC-2	81.1	42.0
FSLWSCC-3	87.3	68.2
ECLWSCC-1	85.0	69.0
ECLWSCC-2	85.1	62.0
ECLWSCC-3	91.8	92.5
ESHLWSCC-1	83.3	56.0
ESHLWSCC-2	83.9	50.0
ESHLWSCC-3	89.7	78.5

The corrosion mass loss was computed using Faraday's Eq. (8.1) based on the amount electrical energy passed through the bar. The calculated mass loss was compared with the actual mass loss for each of the tested specimen after computing the total actual metal loss in the bars (Figure 8.6). The results showed that the actual mass loss was less than the theoretical mass loss for all Mixes 3, where the percentages of actual to theoretical mass loss in Mixes 1 and 2 were 108%, 100%, 99.0%, 102%, 99.5% and 106% in FSLWSCC-1, FSLWSCC-2, ECLWSCC-1, ECLWSCC-2 and ESHLWSCC-1 and ESHLWSCC-2, respectively. The mass loss based on Faraday's law generally overestimates the actual mass. This is attributed to the fact that some of the passing currents do not contribute to corrosion but are consumed while passing through the concrete cover.

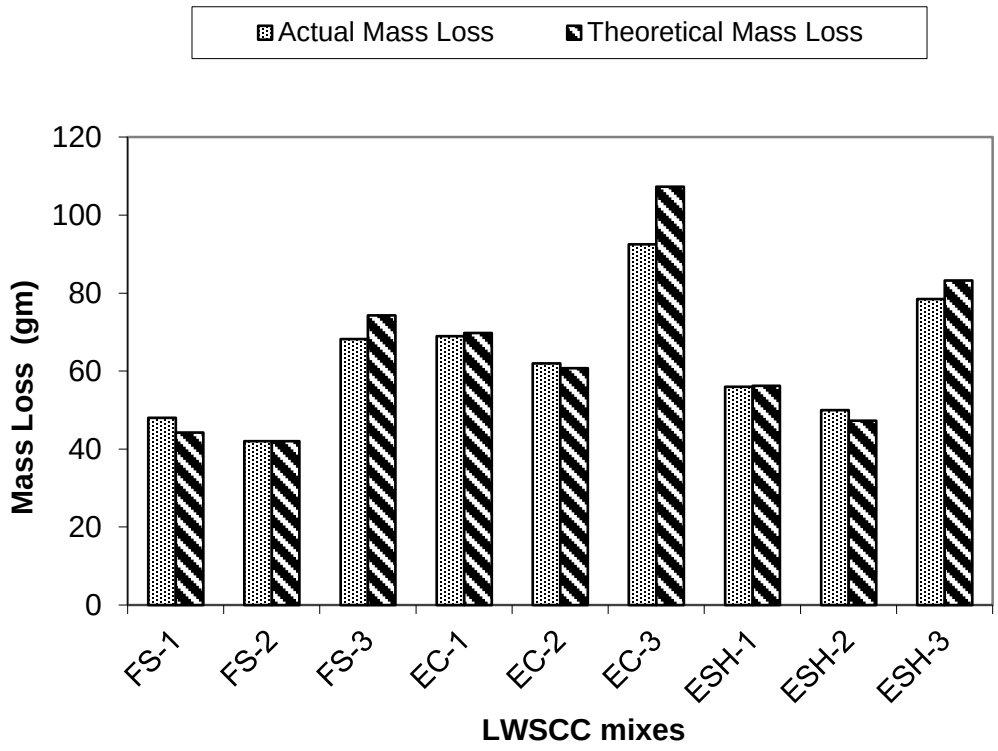

Figure 8.6 - Comparison between theoretical and actual mass loss for all LWSCC mixtures

8.2.2 Resistance LWSCCs against Elevated Temperatures

The elevated temperature resistance of the LWSCC mixtures was investigated in terms of mass loss and residual strength. For testing, 150 mm concrete cube specimens were used. The specimens were removed from molds after 24 hours of casting and then placed in a water tank at 23 ± 2°C for 28 days. For the elevated temperature resistance test, each mix specimens were divided into three groups (two specimens each), and then were heated under controlled rate (5°C/minute) in an electric furnace up to 300, 600, and 900°C. The rate of heating, however, is lower than the standard fire rate of temperature rise specified by ASTM E 119a (2012), which is approximately 600°C in the first 6.7 minutes. The specimens were then allowed to cool naturally to room temperature outside the furnace. Figure 8.7 shows the heating rate curves and duration of steady state temperatures. The heating/cooling rate depends on the lightweight properties (especially thermal conductivity) of the material. Because of lower thermal conductivity of the evaluated lightweight aggregates, additional time (lower rate of heating) is required for heating LWSCC specimens.

There are three test methods available for finding the residual compressive strength of concrete at elevated temperatures: stressed, unstressed, and unstressed residual strength test. The first two types of test are suitable for accessing the strength of concrete during high temperatures. The unstressed residual test adopted in the current study allowed the assessment of residual properties of concrete after cooling down to room temperature (Hossain and Lachemi 2007). One should note that the strength measured in this way is the smallest because the lack of transient creep and partial rehydration of the cement during and after cooling induce further damage in the concrete mass (Phan 1996).

The residual strength was found to decrease with the increase of temperature for a constant 1.5h high temperature duration, as shown in Figure 8.8. All types of LWSCC mixtures exhibited reduction in residual strength as the temperature was increased to 300^{o}C, followed by 600^{o}C and then 900^{o}C. This finding concords with several studies that investigated the properties of concrete made with lightweight aggregates when exposed to elevated temperatures (Hossain and Lachemi 2007, 2005; Hossain 1999; Sarshar and Khoury 1993).

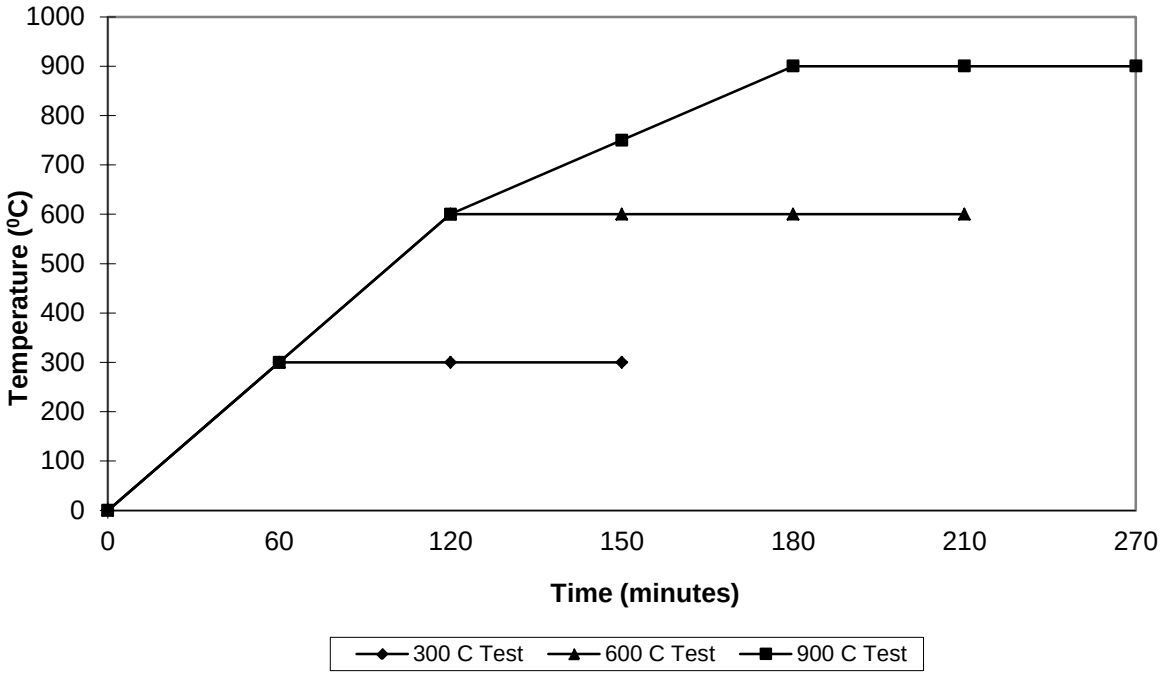

Figure 8.7 - Heating rate curves and duration of steady state temperatures

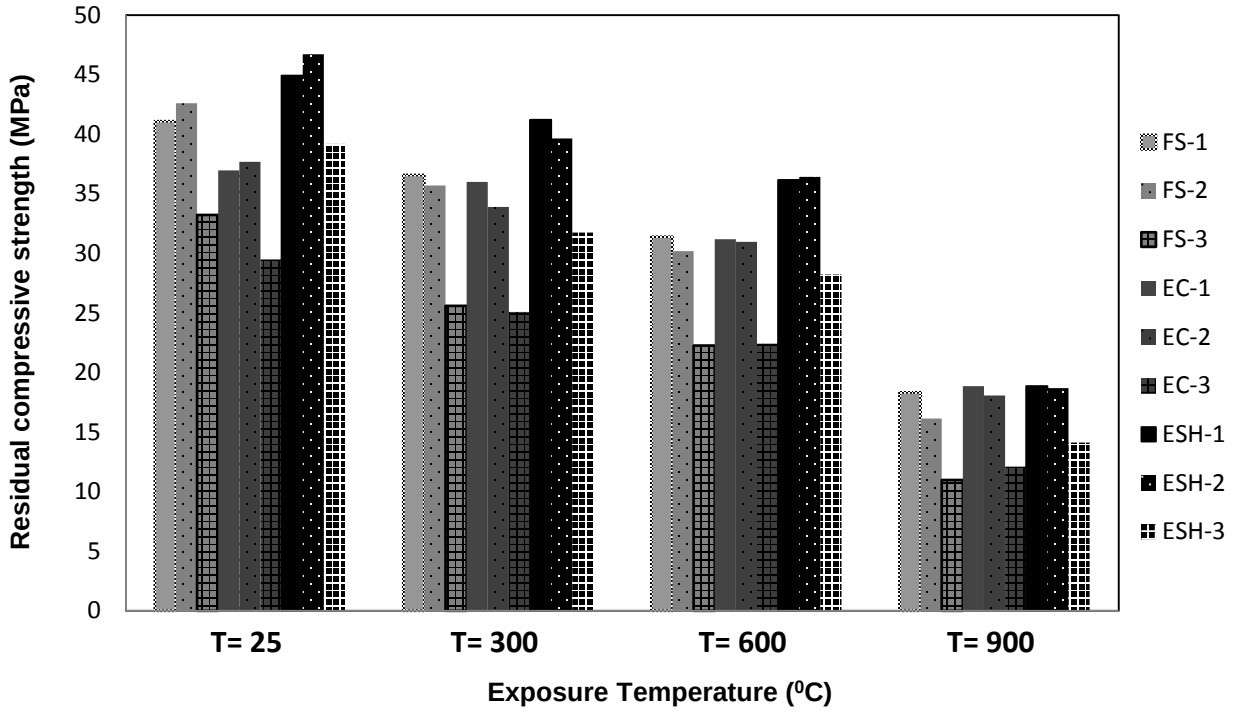

Figure 8.8 - Comparison between the residual compressive strength of LWSCC mixtures after exposure to different temperatures

Figure 8.9 shows the percentage reduction in compressive strength of LWSCC mixtures after 1.5h exposure to elevated temperature. LWSCC mixtures made with EC aggregates showed the lowest reduction in strength as the temperature was elevated. The residual strength at 300°C for EC-LWSCC-1 was approximately 97.4% of the original strength while 90% for EC-LWSCC-2 and 85% for EC-LWSCC- 3 were observed. At 600°C, the residual strength was approximately 84.4, 83 and 76% of the original strength for EC-LWSCC 1, 2 and 3, respectively. Finally, 51, 48 and 41% residual strength was recorded for EC-LWSCC 1, 2 and 3, respectively at 900°C. The highest reduction in original compressive strength was recorded for LWSCC mixtures made with FS aggregates followed by ESH aggregates.

The very low compressive strength loss noted for mix EC-LWSCC-1 at 300°C can be partially due to the strengthened hydrated cement paste during the evaporation of free water, which leads to greater Van der Waal's forces as a result of the cement gel layers moving closer to each other (Hossain and Lachemi 2007; Hossain, 1999; Dias et al. 1990; Khoury 1992).

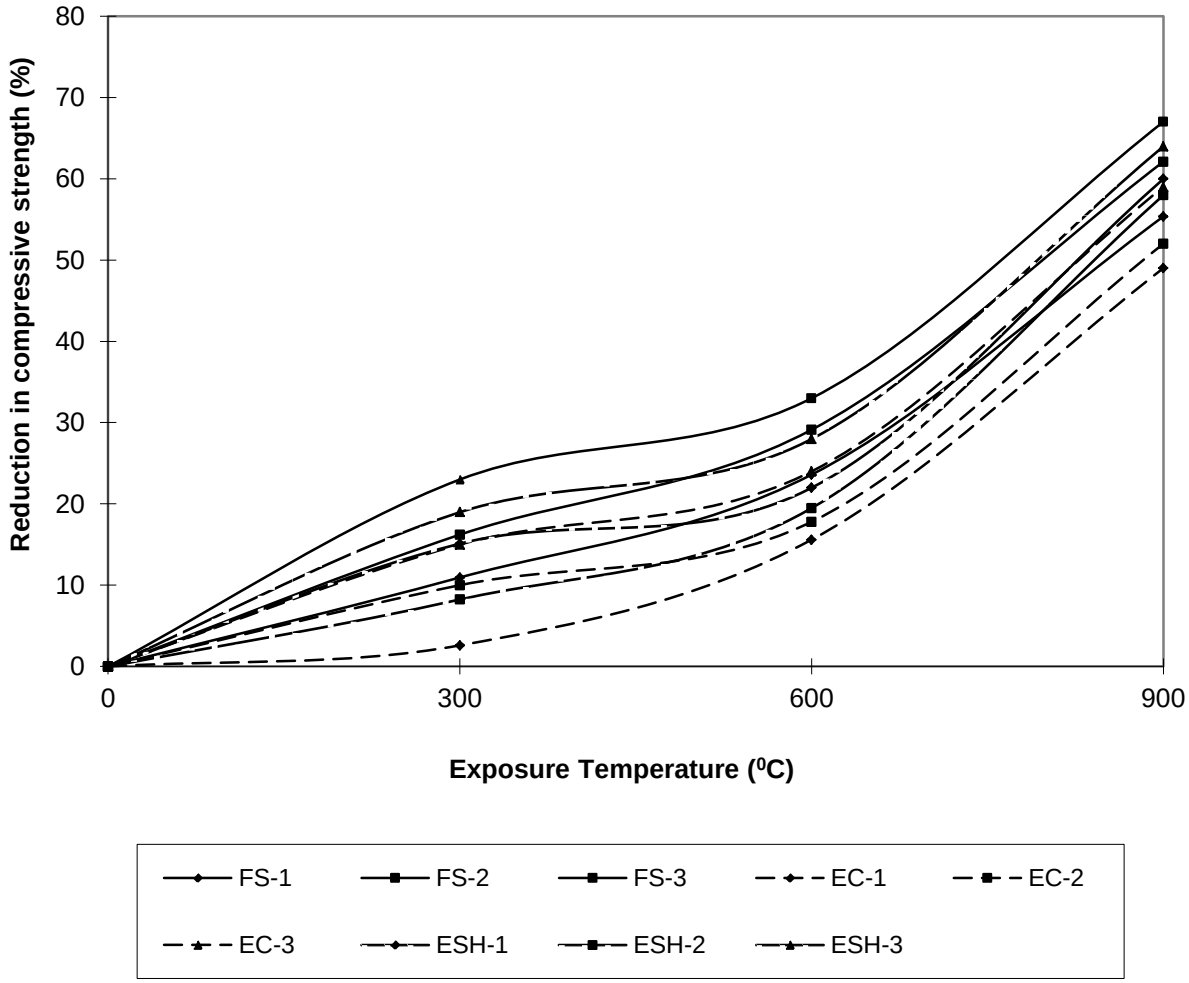

Figure 8.9 - Comparison between the reductions in compressive strength of LWSCC mixtures after exposure to different temperatures

The resistance of concrete to fire and to elevated temperature depends on many factors such as duration of fire, temperature, moisture conditions, concrete mixture (leaner or richer), and aggregate properties (Hossain and Lachemi 2007; Hossain 1999; Sarshar and Khoury 1993). Thus, the lower residual strength of Mixes 3 can be attributed to the high w/b and segregation

index and lower aggregate proportion compared to LWSCC- 1 and 2 mixtures. The strength of concrete decreases when exposed to a temperature in excess of 35°C and under conditions allowing loss of moisture content. The moisture content has a significant effect on the strength of concrete in the temperature range of approximately 28 to 600°C. The loss of strength is attributed to the loss of moisture and the degree of moisture loss depends on the duration of fire (Reinhardt et al. 2006). When concrete is exposed to high temperatures, the free water in capillary pores of the concrete, the water in C-S-H gel and chemical bond, and the water in C-S-H and sulphoaluminate evaporate. Consequently, this causes shrinkage in concrete around 300°C (Topcu and Uygunoglu 2007; Unluog˘lu et al. 2007). When the temperature above 400°C is employed, C-S-H gels decompose. Around 530°C, $Ca(OH)_2$ transforms to the anhydrate lime. Thus, the high temperature leads to cracking and decreases the compressive strength of concrete. The detrimental effects of $Ca(OH)_2$ can be eliminated by using mineral admixtures as used in this research such as fly ash. Due to the pozzolanic reaction between $Ca(OH)_2$ from cement and reactive SiO_2 from fly ash, the amount of $Ca(OH)_2$ decreases in the system. The useful contribution of fly ash and volcanic materials on high temperature resistance was proved by previous research studies (Dias et al. 1990; Sarshar and Khoury 1993).

The compressive strengths normally decrease due to mechanism of high temperature effect associated with the decomposition of C-S-H gels. The degradation of residual compressive strength due to high temperature increases with the increase in exposure temperature. Low compressive strengths are generally obtained with the increase in temperature especially above 600°C.

Lightweight aggregates should exhibit more high temperature resistance characteristics than normal aggregate concrete due to lesser tendency to spall and loss of lesser proportion of its original strength with the rise of temperature. The developed LWSCC 1, 2 and 3 mixtures with three ES/FS/ESH lightweight aggregates had shown a good high temperature resistance up to 600°C. These mixes showed only 15 to 33% compressive strength loss at 600°C for the specified duration of high temperature exposure. However, at 900°C, the residual compressive strength of

these mixtures dropped to range from 49 to 67%, with highest reduction noted for FS-LWSCC mixtures.

Figures 8.11 to 8.18 show LWSCC cubes subjected to the elevated temperature tests as well as during the visual evaluation after exposure. The superior performance of LWSCC mixtures is due to the combinations of lower thermal conductivity (leading to lower temperature rises on exposed surface), lower coefficient of thermal expansion (leading to lower forces developed under restraint) and the inherent thermal stability of these aggregates since they have already been exposed to high temperatures during manufacturing which results in high resistance to volume expansion and decomposition at elevated temperatures (Holm and Bremner 2000).

Resistance to spalling during a fire, however, is also a function of the moisture content of the concrete (Copier et al. 1983). The use of saturated lightweight aggregates would thus increase the risk of concrete spalling. The rate at which water can move through the concrete (as steam) during a fire will also affect spalling. Low vapour permeability, which will be the case for concretes with low w/b, will permit the build-up of high internal stresses as steam attempts to escape. Therefore, dry concrete is much less prone to spalling. Ultimate compressive strength tests on specimens after high temperature exposure showed that even if the specimens only show very minor spalling after exposure, the reduction in concrete strength and thus the load-bearing capacity may be severely deteriorate. The higher water content of the lightweight aggregates is a source of potentially explosive pressure during high temperature exposure if the permeability is not high enough to relieve the steam pressure that develops (Bilodeau et al. 1995). At 900°C, during the initial 0.5 hour of exposure, LWSCC specimens experienced considerable cracks as well as surface spalling at some corners. The crack width ranged between 0.15 and 0.33 mm, and spider web-like cracks were developed (Figures 8.12, 8.15 and 8.18). Also, the color of the specimens changed to a pale color (Figures 8.14 and 8.16). Surface features of LWSCC specimens exposed to 600°C also showed color changes as well as some edge cracks but not as severe as those exposed to 900°C . Figures 8.8 shows LWSCC specimens during and after elevated temperatures test, while Figures 8.9 to 8.11 show LWSCC specimens after exposure with minor surface cracking and spalling.

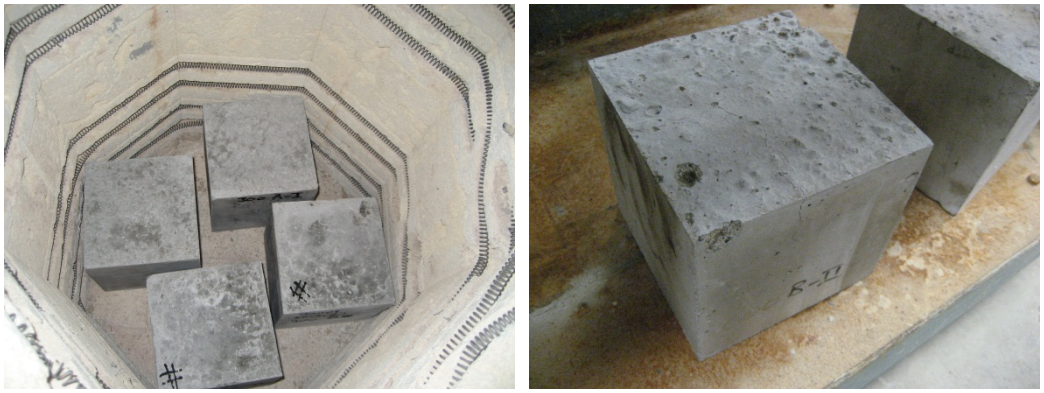

Figure 8.10 - LWSCC specimens during elevated temperatures test

Figure 8.11 - Controlled furnace used during elevated temperatures test

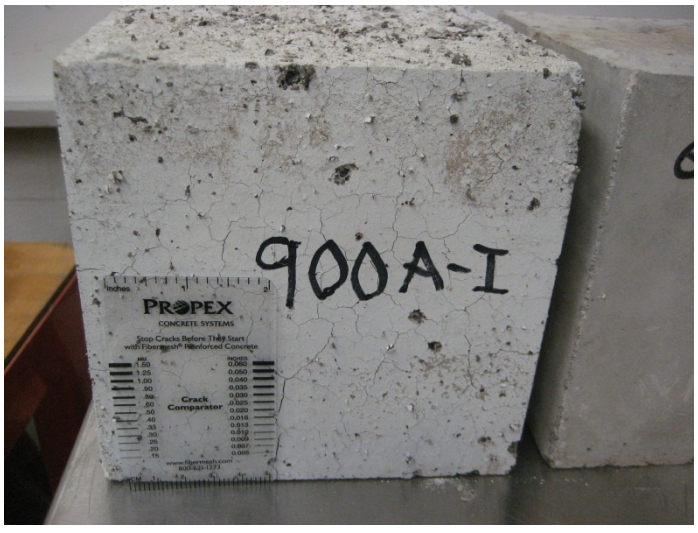

Figure 8.12 - LWSCC specimens after undergoing elevated temperatures test at 900^0C

Figure 8.13 - EC-LWSCC specimens after undergoing elevated temperatures tests

Figure 8.14 - Discoloration of EC-LWSCC specimens after undergoing the 900^{0}C temperatures test

Figure 8.15 - Surface map cracks on FS-LWSCC specimens after the 900^{0}C exposure test

Figure 8.16 - Discoloration of LWSCC specimens after specimens after the 900^{0}C exposure tests

Figure 8.17 - ESH-LWSCC specimens after the 300 and 600^{0}C exposure tests

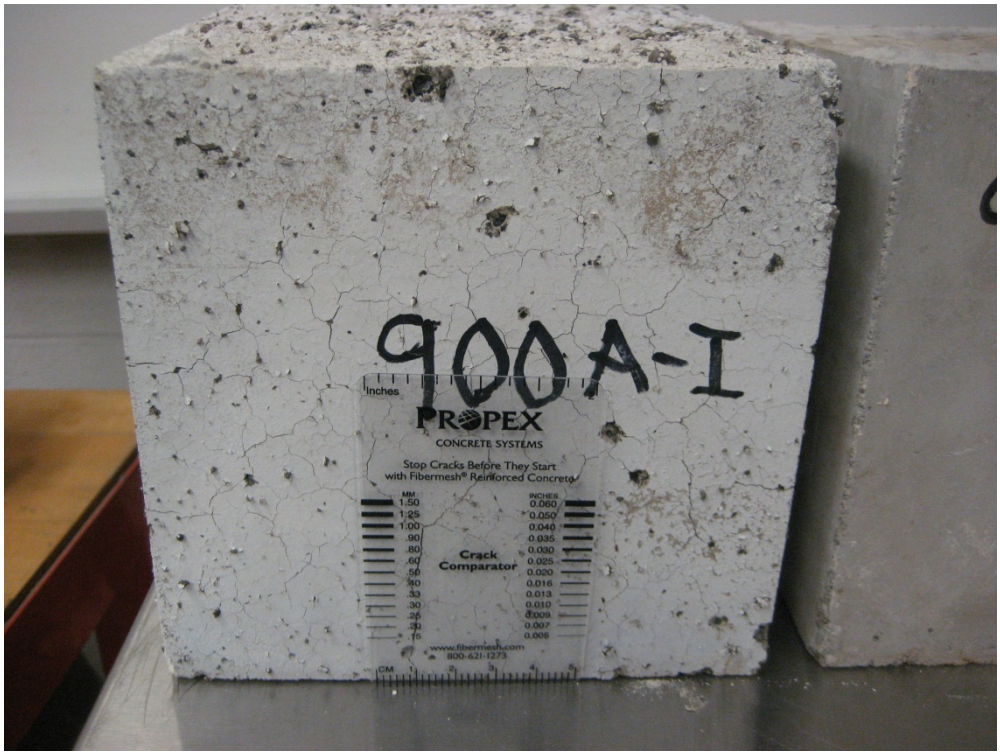

Figure 8.18 - Surface map cracks on ESH-LWSCC specimens after the 900^{0}C exposure test

The initial weights of LWSCC specimens were measured at 28-day. After the 300, 600 and 900°C temperature exposure for specific duration of 1.5 hours, the weights of the specimens were re-measured and the loss in weight (generally associated with evaporation of internal water) due to the high temperature effect was calculated. The variation of mass loss percentage (for LWSCC specimens) with temperature is presented in Figure 8.19. Similar to the compressive strength reduction due to the exposure to high temperatures, the highest weight loss was recorded for FS-LWSCC specimens. On the other hand, the lowest weight loss was recorded for mixtures made with EC followed by ESH aggregates. This can be associated with higher resistance to volume expansion and decomposition at elevated temperatures as well as the lower heat conductivity property of the EC and ESH aggregates. Mixes 3 exhibited the highest weight losses compared to Mixes 1 and 2, which can be attributed to the higher w/b and lower aggregate volume in the mixes compared to Mixes 1 and 2.

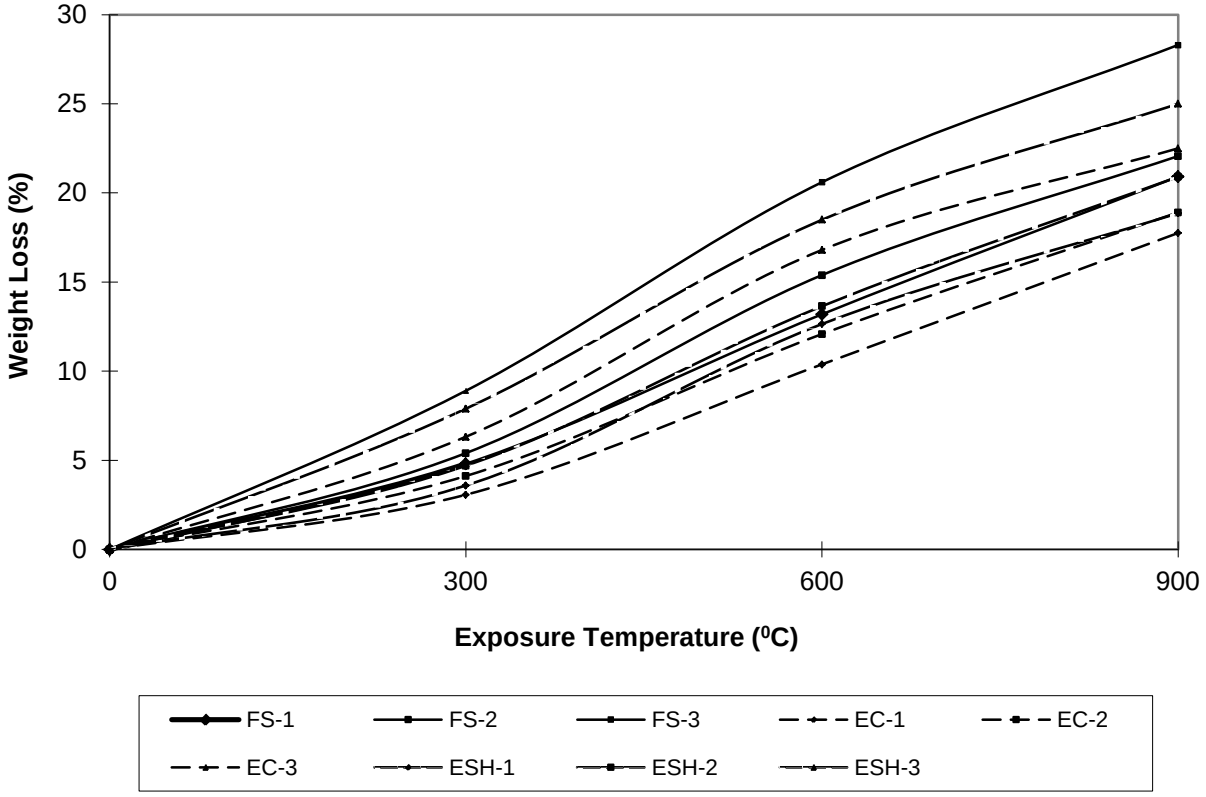

Figure 8.19 - Comparison between weight losses of LWSCC mixtures after exposure to different temperatures

In general, the rate of weight loss of LWSCC increased as the temperatures increased up to 900°C, which lead to surface microcracks and spalling. The maintained integrity of LWSCC specimens at 900°C can be attributed to the mineral structure of the used lightweight aggregates that allows less evaporation of water in C‑S‑H structure of LWSCC mixtures.

It was found that an increase in LWSCC weight loss (during elevated temperature test) is associated with reduction in compressive strength. Figures 8.20, 8.21, and 8.22 illustrate a linear relationship between the reduction in compressive strength and the weight loss of FS-LWSCC, EC-LWSCC and ESH-LWSCC mixtures, respectively. The correlation coefficient (R^2) of 0.92, 0.86 and 0.88 for FS-LWSCC, EC-LWSCC and ESH-LWSCC, respectively indicate a relatively strong correlation.

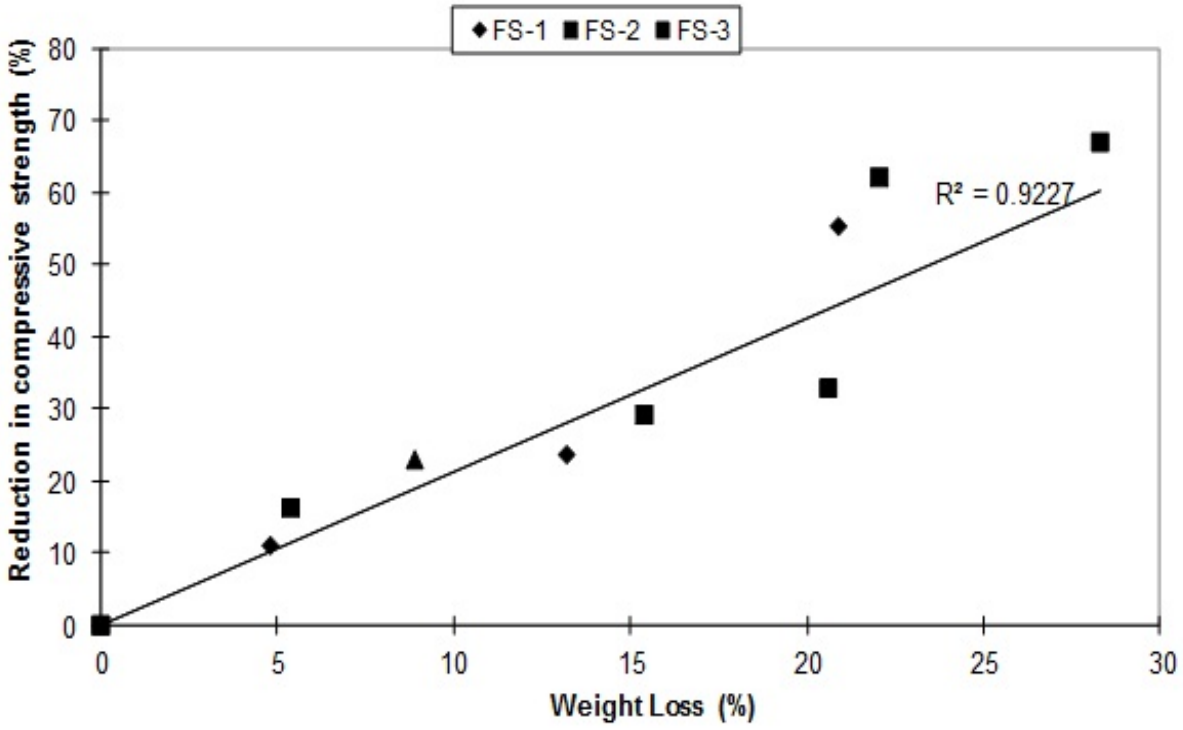

Figure 8.20 - Relationship between the weight loss and reduction in compressive strength of FS-LWSCC mixtures

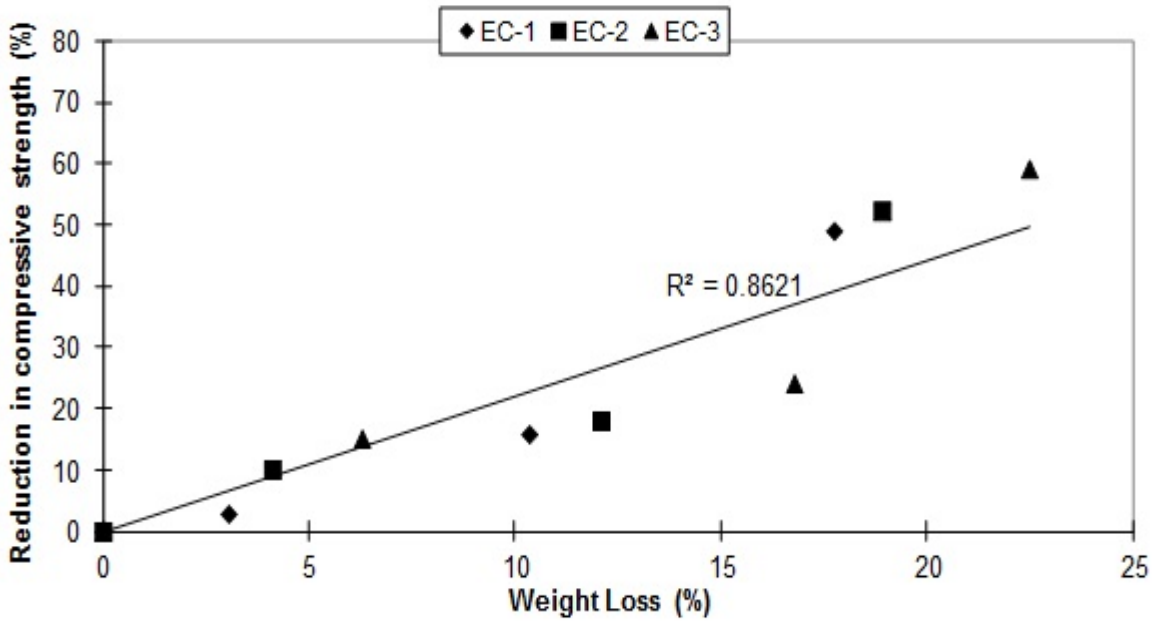

Figure 8.21 - Relationship between the weight loss and reduction in compressive strength of EC-LWSCC mixtures

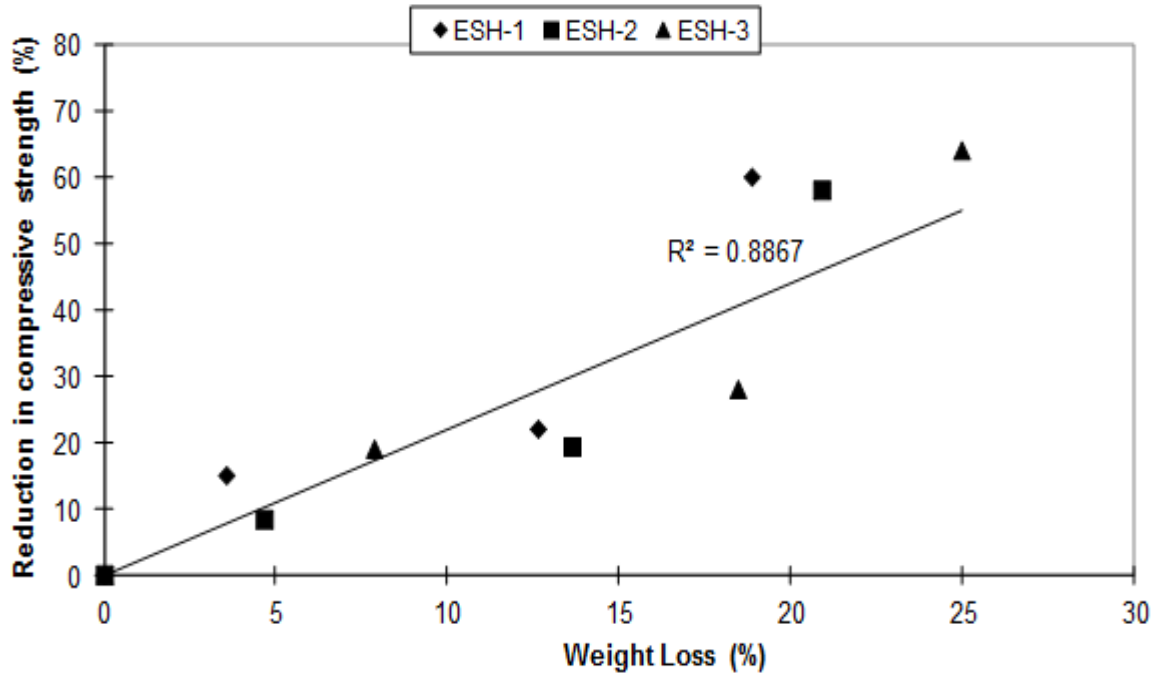

Figure 8.22 - Relationship between the weight loss and reduction in compressive strength of ESH-LWSCC mixtures

8.2.3 Salt Scaling Resistance of LWSCCs

The surface scaling resistance ratings of developed LWSCC mixtures are presented in Table 8.3 on a scale of 0 to 5 as per ASTM C672. LWSCC Mixes 3 for all three types of lightweight aggregates (with w/b equal to 0.40, high slump flow and high segregation index resulted in bleeding), exhibited the poorest salt scaling resistance with the largest mass of scaled-off materials and the worst visual scaling rating of 5 among all other LWSCC mixtures. This may be due to the non-air entrained nature, high w/b, high sorptivity and porosity of the LWSCC mixtures. This may also be due to the severity of the ASTM C672 test procedure when used to evaluate the scaling resistance of concrete incorporating supplementary cementing materials such as fly ash (Thomas 1997). On the other hand, Mixes 1 with lower w/b at 0.35 and lower permeability showed better scaling resistance with ratings of 3 for all three types of lightweight aggregates. This indicated that the scaling was slight to moderate and these concretes would be suitable for highway use. Due to the low w/b of 0.36, LWSCC mixes 2 showed moderate scaling rating of 3, 4 and 4 with FS, EC and ESH aggregates, respectively.

The average cumulative mass of scaled-off material obtained from two slabs made of each of the LWSCC mixtures after 50 cycles is shown in Figure 8.23. Inspection of the scaled-off material from the specimens showed that it consisted almost solely of hardened cement paste. Originally it was expected that porous aggregates particles would contribute significantly to the scaling of LWSCC blocks. But no ruptured stones of porous lightweight aggregates have been observed in any of these tests. Porous lightweight aggregates may however affect the salt scaling resistance indirectly, because of their high water absorption where water may be squeezed out during freezing and thereby, deteriorating the surrounding cement paste (Pigeon and Pleau 1995).

Despite the observed performance, it is well known that the processes involving salt scaling resistance are most likely physical rather than chemical (Neville 1996). According to Mindess, the exact mechanism of salt scaling is not yet clear. However, it is probably the combination of a couple of processes (Mindess et al. 2003). Mechanisms such as osmotic pressure where the difference in concentration between water in concrete pores (with and without salt) causes the water in the smaller pores to move towards the larger pores with salt. The pressure caused by the increase in water triggers the concrete to crack. Otherwise it can be the difference in thermal

strain (temperature shock) where the consumption of heat required to melt ice with salt causes a rapid drop in concrete temperature just below the surface causing damage regardless of the aggregates type or density (Mindess et al. 2003).

Further, whatever the process that causes salt scaling, it is evident that if the concrete has a low permeability, low w/c, and adequate air entrainment, it is expected to exhibit high resistance to salt scaling (Mindess et al. 2003).

Table 8.3 - Deicing salt surface scaling test results of LWSCC blocks

Mixture No.	Cumulative mass of scaled- off particles after 50 cycles (kg/m^2)	Visual rating (ASTM C672 scale 1-5)
FSLWSCC-1	0.55	3
FSLWSCC-2	0.62	3
FSLWSCC-3	0.83	4
ECLWSCC-1	0.75	3
ECLWSCC-2	0.79	4
ECLWSCC-3	0.96	5
ESHLWSCC-1	0.64	3
ESHLWSCC-2	0.71	4
ESHLWSCC-3	0.91	5

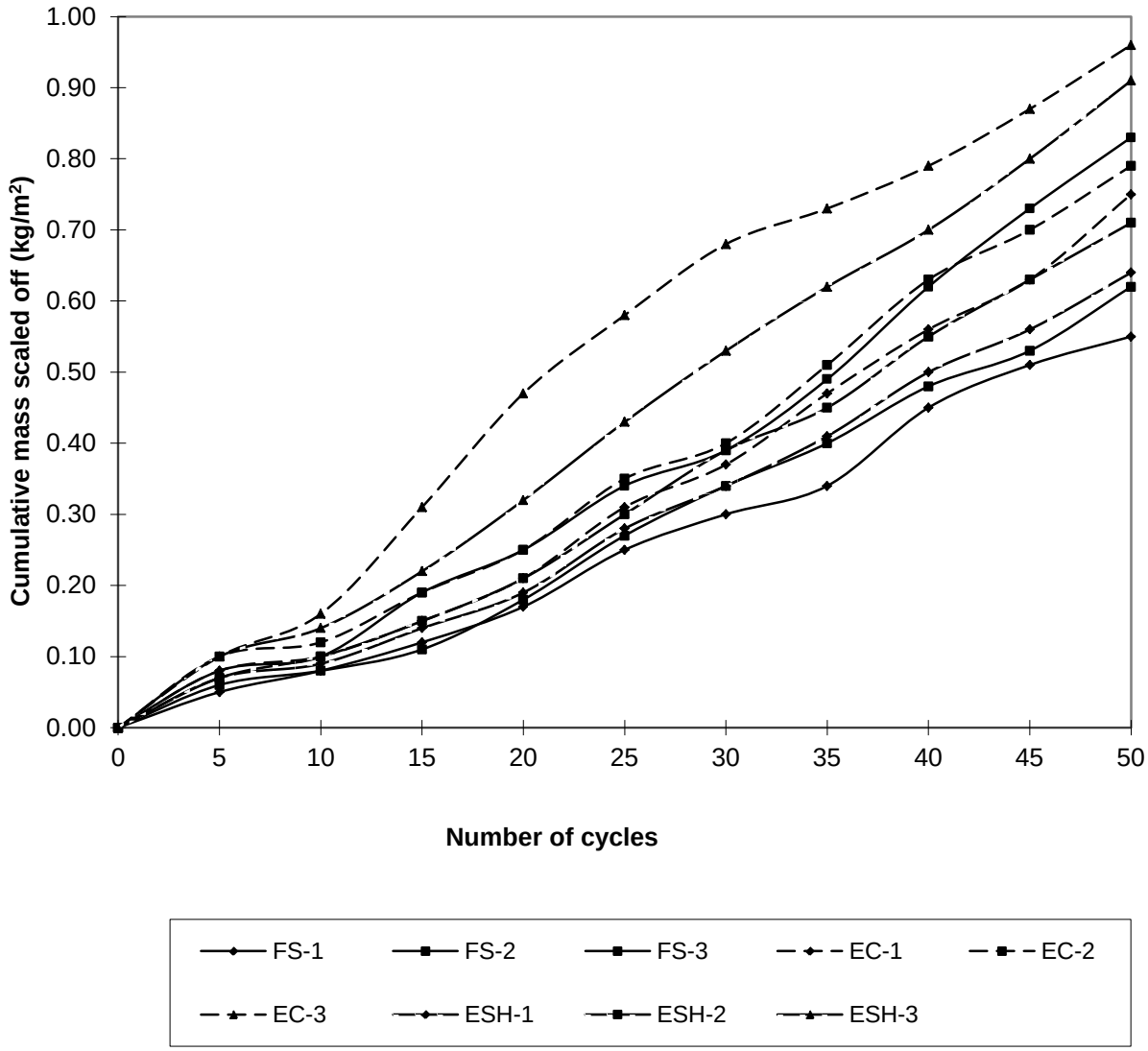

Figure 8.23 - LWSCC mixtures - Cumulative amount of scaled materials over 50 cycles

Effect of paste composition on salt scaling resistance

The use of fly ash in this study may have resulted in reduction of salt scaling resistance of LWSCC (Bleszynski et al. 2002). According to Bilodeau et al. (1994) the chemical composition of fly ash (calcium content or alkali content) had an effect on the resistance against scaling. It was found that concrete mixtures with different types of fly ash had visual rating of 5 and the amount of residue was similar after 50 cycles. On the other hand, it's believed that the use of

silica fume in this study resulted in improvement of the concrete resistance to scaling. Other studies with air and non-air lightweight concrete with various types of lightweight aggregates with w/b in the range of 0.28-0.44 and silica fume concluded that an increase in the silica fume content increases the scaling resistance of concrete (Bleszynski et al. 2002; Zhang 1989). Similar to other studies conducted by Hammer (1990) and Havdahl et al. (1993), the results of Zhang's study indicate that the lightweight aggregate do not have any impact on the frost resistance as the salt scaling is found to be in the same range for both lightweight and normal weight concretes with similar paste compositions.

In general, LWSCC mixtures made with FS showed the highest resistance to scaling due to lower porosity and absorption properties of these aggregates (i.e. high quality aggregates) compared to EC/FS LWSCC mixtures. EC-LWSCC mixtures showed the lowest resistance to scaling followed by ESH-LWSCC mixtures. This can be attributed to high permeability and low aggregate quality. As stated, the fly ash greatly reduces the salt scaling resistance of the concrete (Pigeon et al. 1996). However due to the addition of silica fume to LWSCC mixtures, this negative effect is believed to be overcome. In general, the silica fume would greatly reduce bleeding, therefore improving the surface resistance of the slab specimens. However, these are non-air entrained LWSCC specimens and this could have been a significant contributing factor to the observed performance. Air content has a significant influence on the salt scaling resistance and it is expected that an increase in amount of air should result in lower salt scaling.

It is worth noting that LWSCC is not vibrated, which limits the transport of fines and water to the surface and sidewalls of formwork (eliminate any surface finishing issues), thereby enhancing the LWSCC's resistance to deicing salt scaling compared to that of vibrated conventional concrete. Figures 8.24 to 8.28 show LWSCC specimens undergoing salt scaling tests and evaluation of samples after the test. Some blocks showed slight to moderate scaling while others such as EC-LWSCC showed some visible coarse aggregate after undergoing 50 cycles of salt scaling test.

Figure 8.24 - Controlled freezer used salt scaling test

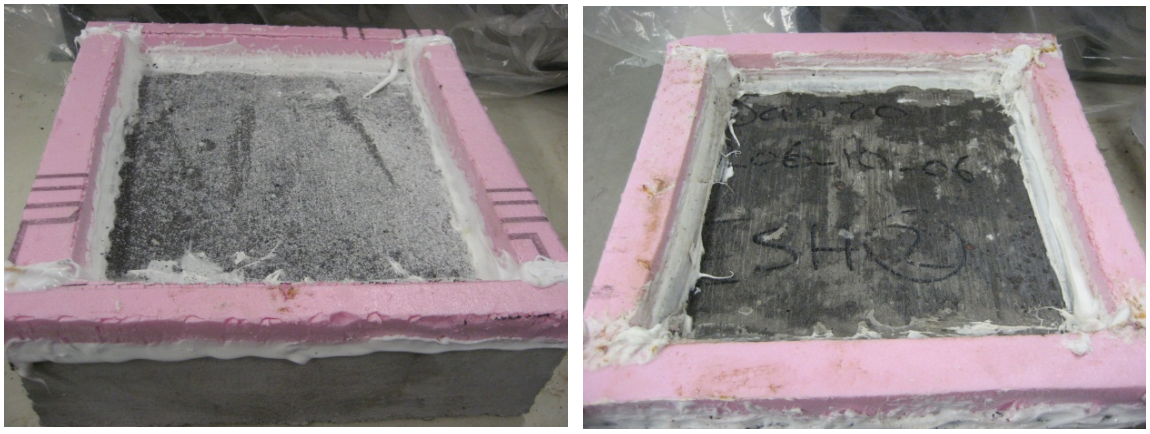

Figure 8.25 - ESH-LWSCC specimens undergoing salt scaling test

Figure 8.26 - FS/EC LWSCC specimens after undergoing salt scaling test

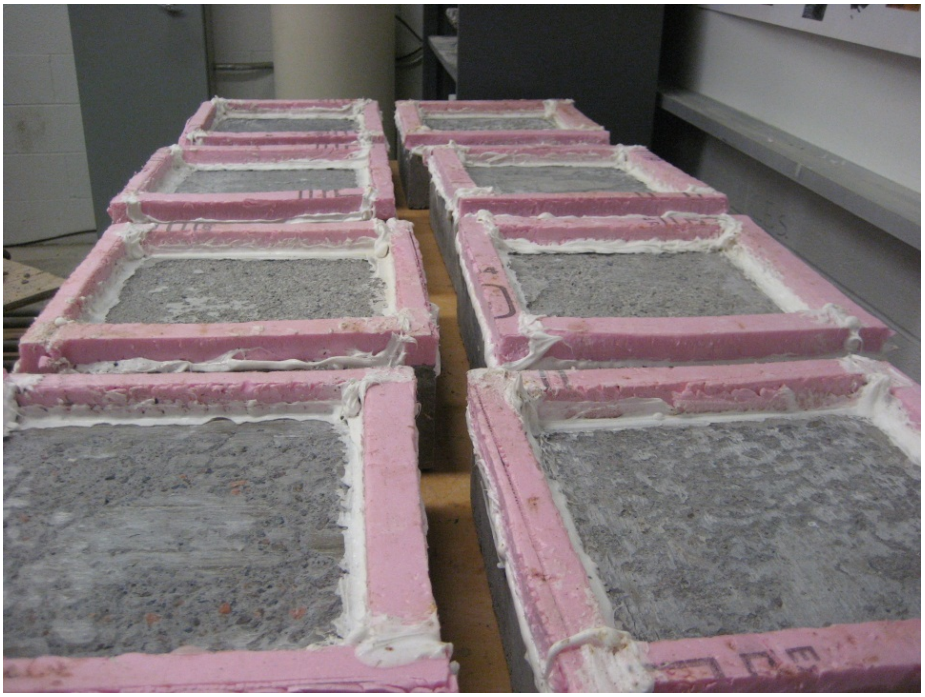

Figure 8.27 - LWSCC specimens specimen after undergoing salt scaling test

Figure 8.28 - FS/EC/ESH LWSCC specimens after undergoing salt scaling test

8.2.4 Hardened Air Void Analysis of LWSCC

One cylinder per mix was cast for conducting the hardened air void analysis of the LWSCC mixtures. These cylinders were cured the same way as the cylinders being tested for compressive strength. At the age of 28 days, the cylinder samples were saw cut length wise into two equal halves, and one cut face from each cylinder was then polished. The prepared specimens were tested for air-void parameters in accordance with the ASTM C 457-11 test method using the modified point count method at magnification of about 115 times (ASTM C 457 2011). This

procedure consists of the determination of the volumetric composition of the concrete by observation of the frequency with which areas of a given component coincide with a regular grid system of points at which stops are made to enable the determinations of composition. Based on the data collected, the air content and various parameters of the air void system are calculated. A summary of the hardened air void and spacing factor results is presented in Table 8.4. The hardened air void for LWSCC mixtures ranged between 1.8 to 2.8%, which is considered as entrapped air.

Entrained air greatly improves concrete's resistance to surface scaling caused by chemical deicers (Kosmatka et al. 2002) and also substantially enhances the concrete resistance to freeze-thaw cycles. Thus, the CSA standards A23.1-09 recommend an entrained air content between 6 and 9% (for 10 mm stone mix) for exposed concrete applications, where the air void system is required to be with a minimum of 3% air and maximum of 0.230 mm spacing factor (CSA A23.1 2009). As can been seen from the LWSCC hardened air void and spacing factor analysis, the developed mixtures did not meet CSA criteria for exposed concrete as the hardened air void was less than 3% and spacing factor was greater than of 0.230 mm. Therefore, the developed LWSCC mixtures can only be recommended for interior applications in Canada.

Table 8.4 - LWSCC hardened air void and spacing factor analysis

Mixture No.	Hardened Air void (%)	Spacing Factor (mm)
FSLWSCC-1	2.6	0.45
FSLWSCC-2	2.2	0.48
FSLWSCC-3	1.8	0.66
ECLWSCC-1	2.8	0.37
ECLWSCC-2	2.5	0.34
ECLWSCC-3	2.3	0.46
ESHLWSCC-1	2.8	0.35
ESHLWSCC-2	2.3	0.34
ESHLWSCC-3	2.1	0.53

8.2.5 Sulphuric Acid Attack Resistance of LWSCC

Sulfuric acid is one of the most destructive acids to concrete and depending on its concentration and formation manner, can cause severe degradation and damage to concrete structures which come into contact with it. This acid may be produced in soils and groundwater through the oxidation of iron sulfide minerals in the form of pyrites or marcasite (Richardson 2002).

It is commonly known that the pore structure of concrete plays a crucial role on its durability in different environmental conditions. Using silica fume would improve the resistance of concrete against a 1% sulfuric acid solution by refining the pore structure and reducing the amount of $Ca(OH)_2$, Further the C-S-H formed in concrete containing silica fume is more stable in low pH conditions (Durning and Hicks 1991). Also, in most cases, fly ash improves the durability of concrete against exposure to sulfuric acid attacks (Aydin and Baradan 2007). Both fly ash and silica fume were used in this study at 15% and 5% in all LWSCC mixtures, respectively.

The LWSCC specimens were immersed into 5% sulfuric acid solution after 28 days of curing. 8 cylinders (100 x 200 mm) were used for each of the LWSCC mixtures for the acid test. The initial weight of all the specimens was measured in accordance to ASTM C 267 (2006). The average compressive strength of two concrete samples was also measured prior to the immersion. A 700 liter container was used to immerse the specimens in sulphuric acid during the test. The immersion period of the specimens was divided into four phases. The length of each phase was 2 weeks, thus the total length/duration of the test was 8 weeks. The solution was stirred once a week to provide a uniform distribution of sulfuric acid around the submerged specimens. The pH of the solutions was monitored bi-weekly.

The performance of the degraded specimens was evaluated by measuring the weight loss and change in strength. In this study, weight of submerged cylindrical specimens was measured every two week after the removal of loose particles from their surfaces by using a steel wire brush.

Two concrete specimens from each mix were removed from the container at the end of each phase (every two weeks), then the specimens were washed smoothly with tap water. Afterwards, the specimens were placed in room temperature for 24 hours before recording the weight after

immersion and shortly after that the specimens were tested for compressive strength. A pH value of around 1.17 was recorded after two weeks of exposure and the continuous monitoring of the pH in the following weeks did not show any significant changes. It should be noted that although immersed concrete samples will increase the pH of the solutions (caused by dissolution of hydration products), due to the removal of these specimens every two weeks and the large volume of the solutions, the effect of the remaining samples on the pH value of the solutions is insignificant.

The result of the weight loss of LWSCC cylinders after different periods of exposure up to 8 weeks is illustrated in Figure 8.29. The result of each mixture is the average of the weight loss of the two specimens in an SSD condition after 8 weeks. FS-LWSCC mixtures 1, 2 and 3 showed the lowest weight loss at 6.3, 5.0 and 8.2%, respectively. This can be associated to the lower absorption and porosity of the FS aggregates. On the other hand, EC-LWSCC mixtures 1, 2 and 3 showed the highest weight loss at 10.4, 9.4 and 12.8%, respectively, followed by ESH-LWSCC mixes at 8.2, 7.0 and 10.9%, respectively. This performance was due to the EC/ESH aggregates pore characteristics and their higher absorption value.

It can also be observed that the weight loss was minimal for LWSCC mixes 1 and 2 made with all lightweight aggregates after 14 days of submerging. The reason for these may be due to the sulfuric acid being not able to penetrate deep into the LWSCC micro-structure and hence, no critical damage or effect takes place in the interfacial transition zone (ITZ) between the aggregates and hydration products. Further, the chemical reaction between the hydration products of LWSCC mixtures and the surrounding acid results in a calcium sulfate hydrate or a protective layer around the sound inner part of the concrete that has not experienced an acid attack yet. Thus, LWSCC samples will resume their regular hydration process and consequently their performance with little weight loss will reflect this phenomenon. However, Mixes 3 with different types of lightweight aggregates showed substantial weight loss compared to mixes 1 and 2 after only 2 weeks of submerging possibly due to higher w/b of 0.4 and higher segregation index close to 20%.

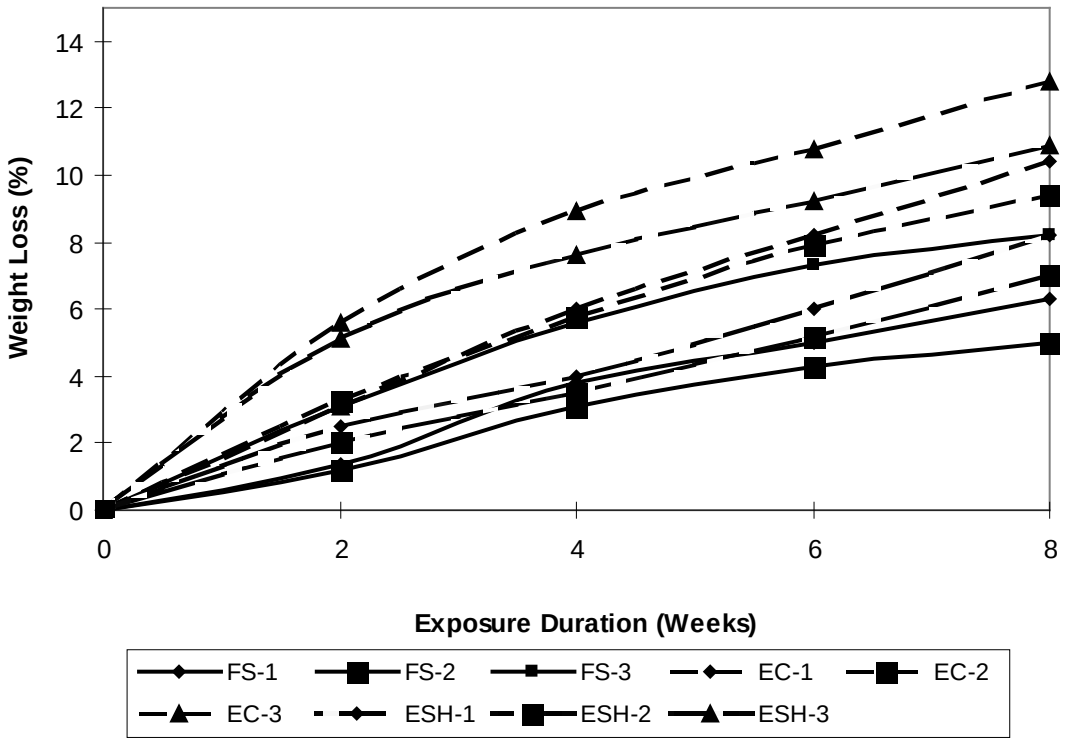

Figure 8.29 - Comparison between weight losses of LWSCC mixtures after different duration of exposure to sulfuric acid

It should be noted that evaluating the specimens by measuring the change in mass after a certain period of exposure to sulphuric acid gives more clear indication of LWSCC resistance to such aggressive conditions. Therefore, the weight loss measure is the most widely accepted method to evaluate the resistance of concrete subjected to aggressive conditions as concluded by Bassuoni and Nehdi (2007). It is stated that the weight loss measurements are more efficient than other methods for understanding and comparing the performance of different concrete mixtures.

The initial compressive strength and strength loss of LWSCC cylinders from different mixtures were measured to evaluate the performance against sulfuric acid intrusion after 2, 4, 6 and 8 weeks of immersion. It can be seen from Figure 8.30 that LWSCC mixtures 1 and 2 behaved superiorly after 2 weeks of exposure - strength was not reduced but increased by around 3% in the case of FSLWSCC-2 mixture. Unexpectedly, the average strength of the specimens for

Mixes 1 and 2 made with all types of lightweight aggregates showed no loss of strength at the end of the second cycle of immersion. Moreover, concurring with the results of the weight loss, the highest strength loss was recorded for EC-LWSCC mixtures followed by ESH-LWSCC. However, the maximum strength loss was recorded in EC-LWSCC-3 mixture after 8 weeks of exposure and with only 4.44% reduction.

The observed increase in the strength of LWSCC mixtures 1 and 2 can be the result of undisturbed continuous hydration with no damage to the inner core matrix after the end of 2 weeks of immersion period. Thus it is possible due to the inability of sulfuric acid to reach deeper into the concrete structure (only surface penetration), that the LWSCC specimens of these mixtures continued to hydrate and develop strength resulting in strength gain while immersed in the acid solution. It is suspected that the protective layer of the white gypsum (a by-product of sulfuric acid attack) which covers the surface of LWSCC specimens acted as a shielding layer to prevent more degradation of the concrete matrix. This protective layer on the surface of LWSCC specimens was stronger and had better adhesion to the surface of the specimens at the initial stages of exposure. However, it become softer in the later stages of exposure and was removed/ washed during sample evaluation, which resulted in the exposure of the concrete inner surface to more sulfuric acid attack.

The major difference between Mixes 1 and 2 versus Mixes 3 for all types of LWSCC mixes is that Mixes 3 showed consistent increasing trend of strength loss. This can be the result of higher deterioration due to sulfuric acid exposure resulting from the removal of the surface layer. Further, Mixes 3 for all aggregate types had lower concrete quality due to high w/b of 0.4 and high segregation index of around 20%. Hence, the undisturbed sound inner core of the LWSCC-3 mixtures which played a major part in strength development being reduced over time.

According to Bassuoni and Nehdi (2007), the compressive strength of concrete specimens is affected by the properties of the concrete matrix (binder type, aggregates, w/c, etc.), consolidation and curing methods, geometry and aspect ratio. The effect of the continuous hydration of the sound parts of the specimens and formation of the described protective gypsum layer on the strength development of LWSCC samples should also be taken in account.

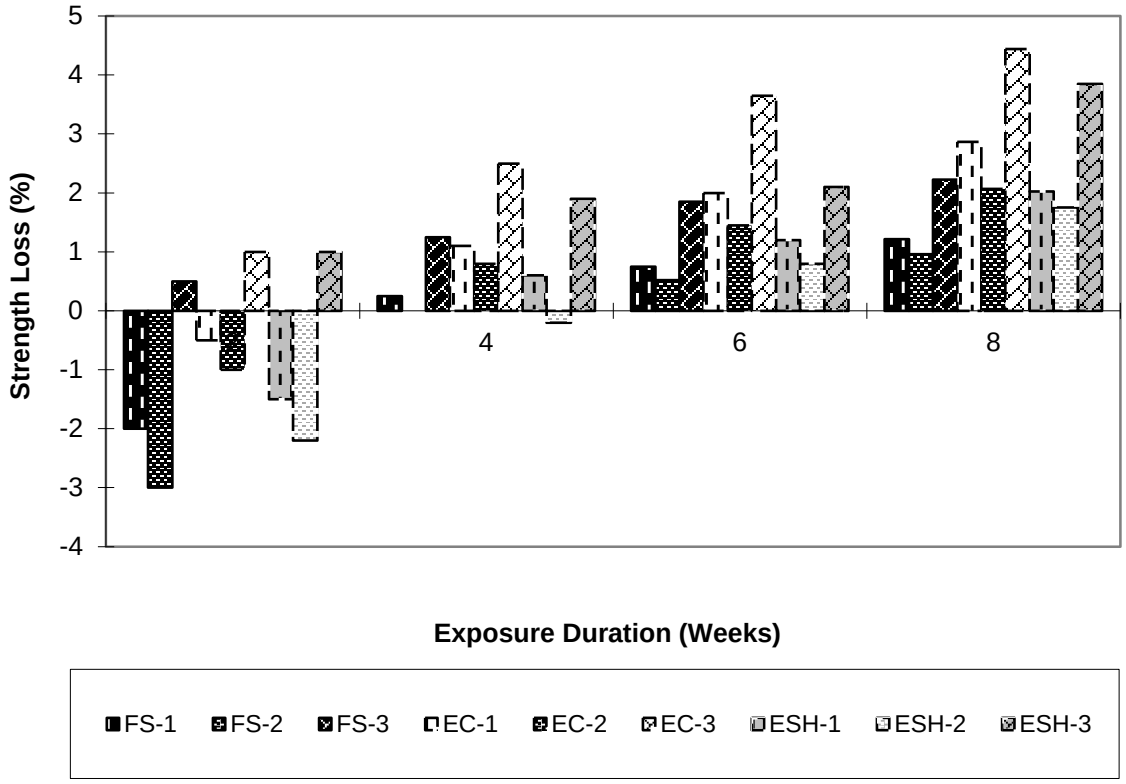

Figure 8.30 - Comparison between strength losses of LWSCC mixtures after different duration of exposure to sulfuric acid

Over all, the strength loss of LWSCC mixtures was much less than expected. The improved resistance of the LWSCC specimens is attributed to the presence of silica fume and fly ash which leads to the production of C-S-H matrix with low C/S ratio of around 1 forming dense silica gel layer, which subsequently, protects the cement paste from more deterioration. In low pH acidic environments, the C-S-H releases most of its lime while a layer that consists of silica and alumina silicate gels remains and protects the cement paste from further deterioration (Shi and Stegemann 2000). It can be concluded that due to the presence of strong protective layer, the strength of LWSCC was not greatly affected by sulphuric acid exposure (sound inner core). The hydration process was sustained and the specimens continued to gain strength. However, the observed mass loss was an indication of outer layer degradation implying possible aggressive chemical attack to the inner core affecting the integrity of the specimens with time. Figures 8.30

to 8.32 show LWSCC specimens subjected to sulfuric acid test and specimens under evaluation after the test.

Figure 8.31 - LWSCC specimens undergoing exposure to sulfuric acid

Figure 8.32 - LWSCC specimens under evaluation after exposure to sulfuric acid

Figure 8.33 - LWSCC specimens under evaluation after exposure to sulfuric acid

8.2.6 Freeze-Thaw Resistance of LWSCC

The test was performed in accordance with ASTM C 666-08 - Procedure A. However, the curing process was modified in accordance with ASTM C 330-03 due to the use of lightweight aggregate (ASTM C 666 2008 ; ASTM C 330/ M 330 2009). The LWSCC specimens were removed from moist curing at age of 14 days and allowed to dry in air for another 14 days while exposed to a relative humidity of 50% and a temperature of 23°C. Then the specimens were submerged in water for 24 hours, prior to the start of the freezing and thawing test subjected to between five/six freeze-thaw cycles in a 24 h period.

The deterioration of specimens during the freeze-thaw cycles was evaluated at the end of every 50 freeze-thaw cycles, by computing the mass loss and the relative dynamic modulus of elasticity (%) of each LWSCC specimen.

As illustrated in Figures 8.34 and 8.35 for all LWSCC mixtures, an increase in number of freeze–thaw cycles increases the mass loss and decreases the relative dynamic modulus of elasticity to a point that the mortar cover was broken up by the build-up pressure and severe deterioration was observed resulting in terminating test. Same behavior in normal lightweight aggregate concrete was reported by Pigeon and Pleau (1995). The main mechanism that results in freezing and thawing deterioration is believed to be due to hydraulic pressure development.

This mechanism occurs when water in fully saturated pores freezes causing expansion of around 9%. This expansion produces a pressure applied to the walls of the pore causing the concrete to crack (Neville 1996). Other factors that have shown to reduce concrete resistance to freezing and thawing are the addition of supplementary cementing material (Toutanji et al. 2004).

For all LWSCC mixtures the maximum percentage of weight loss ranged between 5.8 and 8.5%. The increment in the mass loss depends on the build-up pressure and the amount of pop-out materials. Significant breakage occurred during the specimen's last freezing and thawing action and the weight loss increased noticeably. The value of relative dynamic modulus dropped rapidly with the freeze-thaw cycles and went down below the ASTM limit of 60%. None of the LWSCC specimens was able complete 300 cycles of freeze-thaw. All specimens fell apart at some point during the test, due to the development of extensive pore pressures influenced by the concrete's microstructural characteristics, namely, total porosity, permeability and the pore size distribution.

Meanwhile, FS-LWSCC mixtures showed the slowest initial deterioration, lowest mass loss with steady drop in relative dynamic modulus compared to other lightweight aggregate specimens. FS-LWSCC mixtures 1, 2 and 3 had a maximum mass loss of 6.9, 5.8 and 6.2%, respectively; with a relative dynamic modulus below the ASTM C 666 limit (60%) before the specimens fell apart. After 150 cycles, FSLWSCC-1 specimens fell apart, while FSLWSCC– 2 and 3 specimens fell apart after 200 cycles.

As expected, LWSCC specimens made with EC aggregates showed the fastest initial deterioration compared to other types of lightweight aggregates. This is due to high porosity and absorption capacity of the aggregate resulting into high permeability of the concrete mixture. As the number of freeze–thaw cycles increased, the interior structure of EC-LWSCC mixtures also turned porous and the damage worsened. Large amount of fragments and powder was found. Cracks and the rough surface of EC can be seen clearly in the photograph (Figure 8.42). In contrast, FS-LWSCC mixtures suffered less damage because of its harder and denser structure. Even through the maximum mass loss was not much higher than the FS-LWSCC mixtures at 8.5, 7.6 and 8.0% for EC-LWSCC mixtures 1, 2 and 3, respectively. However, EC-LWSCC specimens quickly showed serious signs of deterioration leading to complete disintegration after

100 cycles for mix ECLWSCC-1 and after 150 cycles for mix ECLWSCC-2 and 3. The last recorded relative dynamic modulus was well below the 60% limit. The poor performance can be predominately attributed to the weak and poor quality of aggregates. As presented in Chapter 7, in comparison to other LWSCC mixtures, the porosity, water absorption, sorptivity and chloride ion penetration values are markedly higher for EC-LWSCC - most probably due to its porous microstructure.

Similarly, ESH-LWSCC specimens showed fast deterioration compared to FS-LWSCC mixtures. The maximum mass loss was 7.8, 6.5 and 7.1% for ESH-LWSCC mixtures 1, 2 and 3, respectively. Quick sign of deterioration was recorded resulting in termination of test after 100 cycles for mix ESH-LWSCC-1 and after 150 cycles for mix ECLWSCC-2 and 3 with last recorded relative dynamic modulus below the 60%.

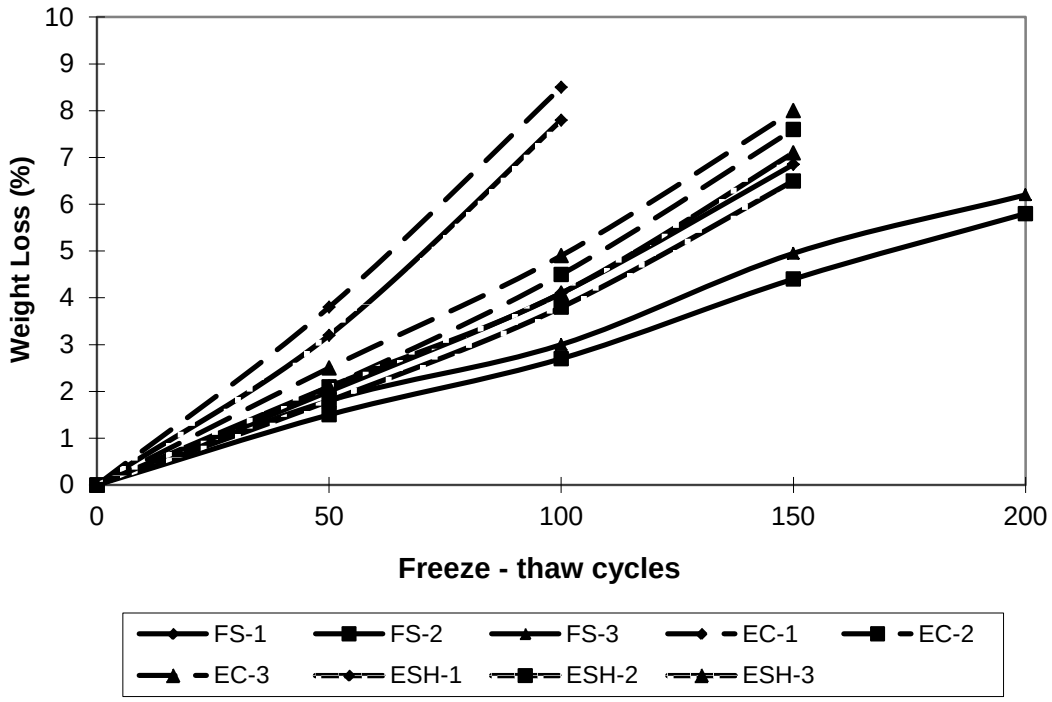

Figure 8.34 - Comparison between weight losses of LWSCC mixtures during freeze-thaw test

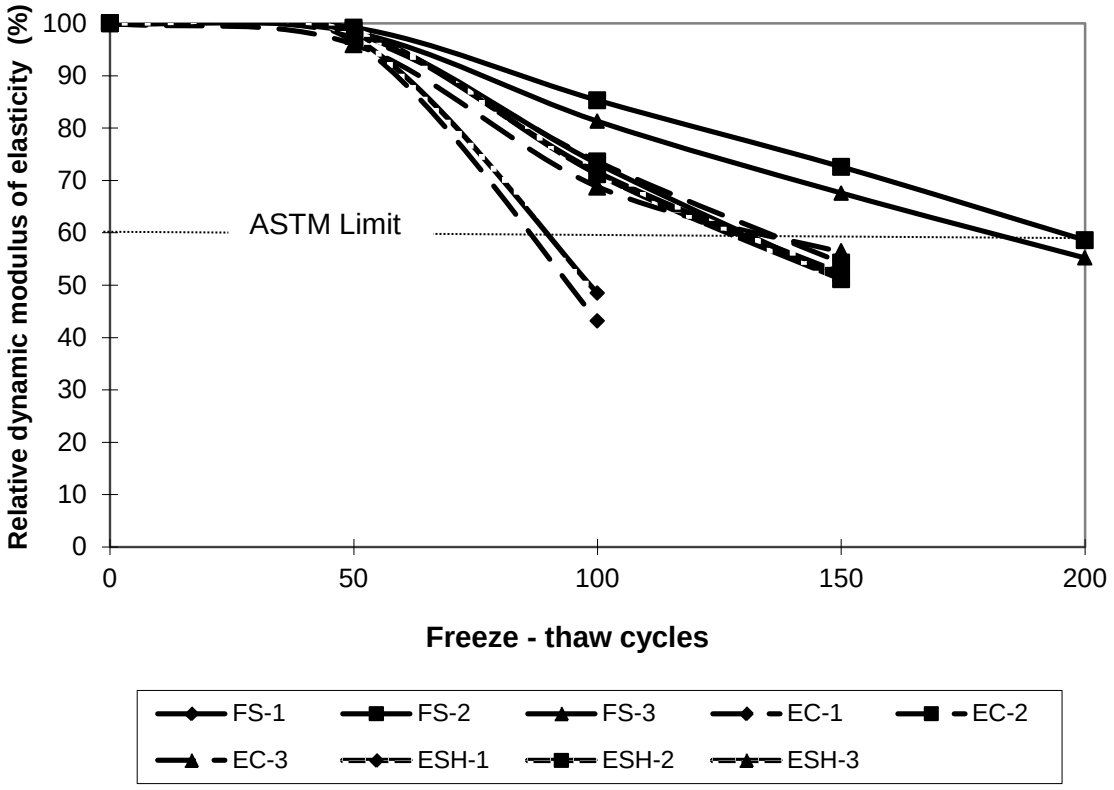

Figure 8.35 - Comparison between the relative dynamic modulus of LWSCC mixtures

Generally, mixes 1 for all lightweight aggregates showed the worst freeze-thaw resistance due to the presence of higher lightweight aggregate volume. Mixes 2 showed relatively the best performance for all types of lightweight aggregates possibly due to the low w/b at 0.35 and the low volume of lightweight aggregate. Mixes 3 showed slightly worse performance than mixes 2 (for a given aggregate type) driven by a higher w/b of 0.4.

It is worth to note that all the developed LWSCC mixtures were non-air entrained. Air entrainment and a certain level of strength (dependent on w/b) are essential for adequate resistance to cycles of freezing and thawing (Hover 2006). It has been determined that a proper amount of air entrainment can positively improve the resistance to freezing and thawing in concrete (Chatterji 2003). Use of air entraining admixtures provides small, closely spaced, and uniformly distributed air voids leading to improved freeze-thaw resistance. The average spacing factor (distance of any point in a cement paste from the periphery of an air void) for satisfactory

resistance to cycles of freezing and thawing is accepted as 0.20 mm or less (Mather 1990; Whiting and Nagi 1998). These air voids act as a relief mechanism for the water that is expelled from the capillary pores. Since the air voids are considered to be full of air, full saturation of these voids does not occur, although some water may exist (Chatterji 2003). The pressure that is accumulated by the concretes inability to expose of the water is enough for the water to surpass the membrane of the air void. Therefore, increasing the air entrainment can create enough air voids to prevent the deteriorating effect of freezing and thawing. Conversely, a great amount of air entrainment produces air voids with an increased volume and increased spacing between air voids (Chatterji 2003). An increase in size would imply that a greater amount of water can be accommodated. However, the increase in spacing results in a further distance for the water to travel before it can release the pressure. Therefore, the pressure is built up and cracks can occur in the concrete. An optimum amount or air entrainment has been determined to be between 5 to 9% (Neville 1996).

Air-entrained lightweight concrete has shown equal or better performance than normal weight concrete in freezing and thawing conditions (ACI 213 2003; Holm and Ries 2006). However, lightweight aggregates vary in quality and some do not have the proper soundness for resistance to freezing and thawing. In addition, freeze-thaw behavior is dependent on moisture content and moisture condition of the aggregates (Brite EuRam 2000). The pore size distribution and pore structure of the lightweight aggregate are important factors which relate to the ability of the aggregate particles to absorb and loose moisture. Aggregates with pores large enough to expel water easily during freezing are less prone to damage than those with small pores where easy transport of water is hindered.

On the other hand, lightweight aggregates are capable of absorbing a large amount of water relative to normal-density aggregates. Use of saturated lightweight aggregates as per standard test procedure for examining durability against freezing and thawing generally yields higher degradation in performance (ACI 213R 2003). However, these standard tests simulate relatively severe temperature gradients and the results appear to be contradicted by service record in real situation. Examination of structures that have been exposed for many years to freezing and thawing under wet conditions shows insignificant damage. One possible explanation is that the

pores in lightweight aggregate do not completely fill up even when soaked for a relatively long time in water. This is because most of the pores are not interconnected in a way that makes them readily accessible to permeation of water from the outside. Perhaps these empty pores serve as a relief mechanism to the high pressure generated during naturally occurring freezing events where the freezing gradient travels at a slow rate in a way analogous to air voids in cement paste. In contrast, the rapidly moving freezing gradient in an ASTM C 666 test may not allow enough time for the empty pore space to be effectively used (Holm and Bremner, 2000).

Figures 8.35 and 8.36 show LWSCC specimens before and during freeze-thaw cycles, while Figures 8.37 to 8.41 show some aspects of evaluating LWSCC specimens during freeze-thaw test. Figure 8.42 shows failed LWSCC specimens during freeze-thaw test.

Based on the information from available research studies, one would expect that the freeze-thaw resistance of the developed LWSCC mixtures can be significantly improved by proper air entrainment through the introduction of air-entraining admixtures. Air-entrained LWSCC mixtures can be designed to achieve fresh air between 6 and 9%, hardened air void greater than 3% and the spacing factor less than 0.230 mm (CSA A23.1 2009). Such air entrained LWSCCs will have great potential to pass the ASTM C 666 test.

Figure 8.36 - LWSCC specimens before freeze-thaw test

Figure 8.37 - LWSCC specimens undergoing freeze-thaw cycles

Figure 8.38 - Evaluating LWSCC specimens during freeze-thaw test

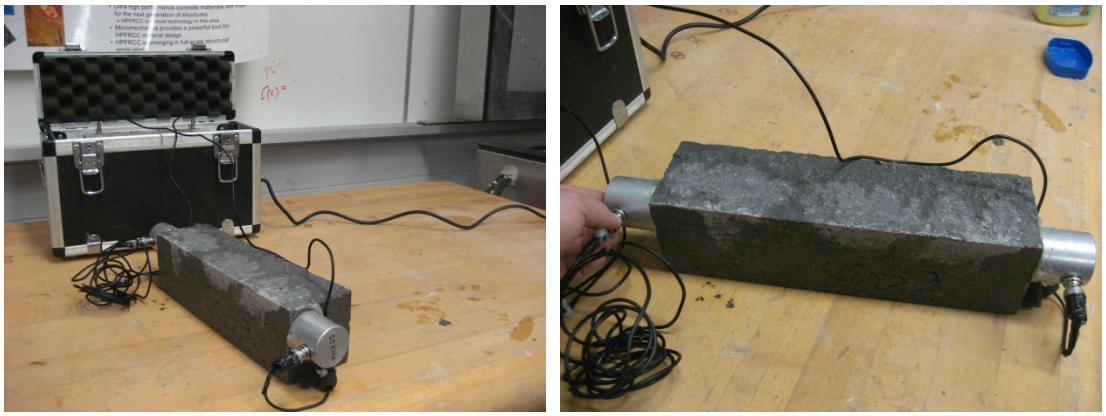

Figure 8.39 - Evaluating LWSCC specimens during freeze-thaw test

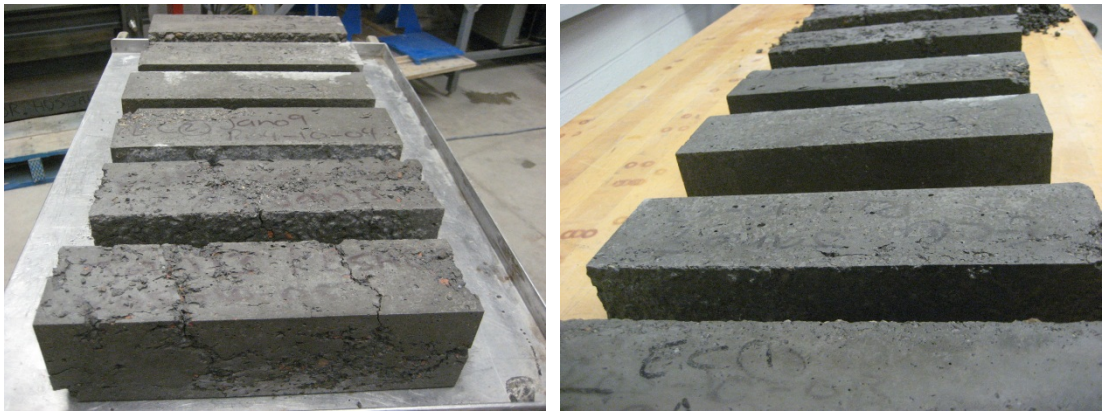

Figure 8.40 - Evaluating LWSCC specimens during freeze-thaw test

Figure 8.41 - Evaluating ESH-LWSCC specimens after freeze-thaw test

Figure 8.42 - Evaluating EC-LWSCC specimens after freeze-thaw test

Figure 8.43 - Failed LWSCC specimens during freeze-thaw test

8.3 Summary

Durability performance of developed LWSCC mixtures in terms of resistance to corrosion, chloride ion penetration, elevated temperature (fire), salt scaling and freezing-thawing are described through comprehensive series of tests.

LWSCC mixtures with EC aggregates demonstrated highest rebar mass loss due to corrosion, followed by ESH-LWSCC and FS-LWSCC. FS-LWSCC mixtures showed the highest reduction in compressive strength followed by ESH-LWSCC and EC-LWSCC when subjected to elevated temperatures of up-to 900^{o}C. LWSCC mixtures also showed good performance showing formation of no major cracking (only visible hairline cracks) and spalling after exposure to elevated temperatures. The FS-LWSCC specimens showed highest resistance to salt scaling followed by ESH-LWSCC and EC-LWSCC. The LWSCC mixtures with all three types of lightweight aggregates exhibited superior performance when exposed to sulfuric acid solution for a duration of two weeks with no strength reduction. Low resistance to freeze-thaw cycles was observed for all the developed LWSCC mixtures. However, freeze-thaw resistance of LWSCCs can be improved by air entrainment using air-entraining admixtures.

CHAPTER NINE

9 CONCLUSIONS

9.1 Summary

The properties of lightweight self-consolidating concrete (LWSCC), developed with different proportions and types of lightweight aggregates, namely, furnace slag (FS), expanded clay (EC), and expanded shale (ESH), were investigated. This research included comprehensive laboratory investigations leading to the development of statistical design models for LWSCC mixtures followed by fresh, hardened, mechanical, mass transport, and durability performance evaluation of the developed LWSCC mixtures. The research was divided into five phases described in various Chapters.

Phase I involved in-depth literature review to examine current trends and advancement in LWSCC technology. This phase included the determination of material characteristics, description of the parameters affecting fresh and hardened properties, mixture proportioning, and presentation of the fractional factorial design approach. Using three different types of lightweight aggregate (LWA) as coarse and fine aggregates, three experimental mix-design models (A, B and C) were designed. Each model consisted of twenty concrete mixtures designed using the Design Expert v.8.1 software18 (Stat-Ease Corporation 2009). Three key parameters were selected to derive mathematical models namely water to binder ratio (0.30 to 0.40), dosage of high range water reducing agent (HRWRA) (0.3 to 1.2% by total content of binder) and total binder content (410 to 550 kg/m^3) for the design of LWSCC mixtures. The responses that were modelled were slump flow, V-funnel flow time, J-ring flow diameter/height difference, L-box ratio, filling capacity, bleeding, fresh air content, setting times, segregation, unit weight and compressive strength of concrete mixtures.

Phase II presented the test results of fresh and hardened properties of 60 laboratory trials of LWSCC mixtures derived from three factorial design models incorporating expanded furnace slag, expanded clay, and expanded shale aggregates. The effect of the aggregate type, packing density and gradation on the fresh and hardened properties of LWSCC mixtures was discussed. The relative significance of primary mixture parameters and their coupled effects on relevant

properties of LWSCC were established. The potential influence of adjusting mixture variables on fresh and hardened properties was determined using the developed statistical models.

Phase III included mix proportion optimization process and validation of the statistical models. Three types of LWSCC mixtures were mathematically optimized to satisfy three classes of EFNARC (2005) industrial classifications and their performance was validated through fresh and hardened properties in order to determine suitable industrial class LWSCC mixtures. In this Phase additional experimental study was conducted to determine whether the theoretically proposed optimum mix design parameters such as water to binder ratio (w/b), HRWRA (%), and total binder (b) content can yield the desired fresh and hardened properties for LWSCCs. Ten LWSCCs mixtures from each model in Phase I, were randomly chosen and their performance was examined through the assessment of fresh and hardened properties. Optimized mixtures with the best overall performance were selected for detailed investigation in Phase IV and Phase V. Phase III concluded by validating the established statistical models.

Phase IV and **Phase V** investigated the the fresh, mechanical, mass transport and durability characteristics of the optimized industrial class LWSCC mixtures with FS, EC and ESH aggregates. Three LWSCC mix designs for each aggregate types (based on the established statistical models) providing a total of nine mixtures were investigated. **Phase IV** included the evaluation of fresh, hardened, mechanical and mass transport characteristics of LWSCC mixtures. In addition to the tests described in Phase I, other tests such as compressive /flexural/ split tensile strength, bond strength (pre/post corrosion), drying shrinkage, sorptivity, absorption, porosity and rapid chloride-ion permeability were conducted. **Phase V** examined the durability characteristics of the nine LWSCC mixtures based on hardened air void (%), spacing factor, resistance to corrosion, elevated temperature, salt scaling, freeze-thaw, and sulphuric acid attack.

9.2 Conclusions

This research involved statistical modelling, mix design development, and evaluation of mechanical/mass transport properties and durability performance of LWSCCs made with lightweight furnace slag (FS), expanded clay (EC), and expanded shale (ESH) aggregates. The following conclusions were derived from the results of the comprehensive series of investigations conducted:

- Gradation and particle shape can result in high packing density of aggregates that plays a major role in controlling the fresh properties of LWSCC mixtures. Comparatively higher packing density of ESH aggregates compared to EC aggregates resulted in the reduction of water and HRWRA demand for achieving equivalent fresh properties.

- For a given LWSCC mix proportion, mixtures made with ESH aggregates showed the highest workability, passing ability, filling capacity and segregation resistance compared to mixtures made with FS. LWSCCs made with EC aggregates showed the lowest workability, passing ability, filling capacity and segregation resistance.

- Lightweight aggregates did not contribute significantly to the compressive strength of the LWSCC mixtures rather the paste quality and bond between the paste and aggregate particles in the interfacial transition zone (ITZ) lead to high compressive strength.

- Generally, use of fine and coarse lightweight aggregates in mix proportioning yielded concretes with a 28-day air dry unit weight of less than 1840 kg/m^3, classifying them as LWSCC.

- The established relation between the slump flow and the segregation index confirmed the commonly held notion that LWSCCs with less than 500 mm slump flow should not exhibit segregation. The chances of LWSCC segregation are very high beyond a slump flow of 750 mm as the segregation index tends to be more than 20%. It is always desirable to keep the slump flow between 550 and 750 mm for a stable and homogenous LWSCC mixture.

- Based on the derived relationship between the V- funnel flow time and the segregation index, there is a higher chance for LWSCC mixture to segregate when the V- funnel flow time is under 6 sec.

- The slump flow increased with the decrease of V- funnel flow time. The chance of producing less viscous mix increases beyond a slump flow of 620 mm as the V- funnel flow time tends to be under 6 s.

- The w/b has significant influence on the overall performance of LWSCC, including fresh/ mechanical/mass transport/durability properties. In terms of fresh properties, the w/b has high influence on workability and HRWRA demand. The passing ability and filling capacity increase with the increases of w/b. For a given binder content, LWSCC mixtures made with a w/b of 0.40 w/b had higher passing ability and filling capacity compared to those made of 0.35 and 0.30. However, the segregation resistance decreases with increase in w/b. LWSCCs with low w/b (0.35) required high dosage of HRWRA for flowability. It is noted that LWSCC mixtures proportioned with w/b of less than 0.33 (regardless of HRWRA (%) or the total binder content), produced unsatisfactory fresh properties, and disqualified to be a LWSCC. On the other hand a balanced LWSCC mixture with w/b of around 0.35 made with any of the three lightweight aggregate types exhibited satisfactory workability, passing ability, filling capacity and segregation resistance.

- Overall, the w/b has significant influence on the mechanical and mass transport properties as well as the durability performance of LWSCC mixtures. LWSCC mixtures proportioned with a given type of lightweight aggregate and w/b of 0.40 developed lower compressive/flexure/splitting/tensile/bond strength, higher porosity/water absorption/sorptivity/drying shrinkage with lower resistance to chloride-ion penetration (RCPT), corrosion, elevated temperature, salt scaling and sulfuric acid attack compared to mixtures prepared with w/b of 0.35.

- In terms of fresh properties, the total binder content had influence on workability and static stability (segregation resistance) of LWSCCs. For a given w/b, the HRWRA

demand decreased with the increase of total binder content. On the other hand, segregation resistance increased with the increase of total binder content. In contrast, at fixed HRWRA (%) and w/b, the workability/passing ability/filling capacity decreased and segregation resistance increased with the increase of total binder content.

- The HRWRA (%) had significant influence on the workability and static stability of LWSCC mixtures. For a given w/b and total binder content, the workability/passing ability/filling capacity increased significantly and segregation resistance decreased with the increase of HRWRA (%). A slight reduction in viscosity (V- funnel times) was observed with the increase of HRWRA (%).

- The lowest effect of increasing the coupled parameters (w/b and HRWRA) on LWSCC fresh properties was observed with the EC-LWSCC mixtures. The highest positive effect was observed with the ESH-LWSCCs followed by the FS-LWSCCs which could be attributed to the high packing density of the mixtures and therefore, lower amount of fluidity was needed to achieve high workability.

- From ANOVA statistical analysis, it was found that both w/b and (%) of HRWRA had significant impact on the fresh properties of LWSCC mixtures. The total binder content had insignificant impact on the workability, passing ability and filling capacity of LWSCC mixtures with high to moderate aggregate packing density, namely ESH-LWSCC and FS-LWSCC, respectively. Its impact on the fresh properties of EC-LWSCC mixtures was significant. The effect of the total binder content on the segregation resistance and compressive strength of all LWSCC mixtures was classified as statistically significant.

- Air content (%) was not affected by any of the three investigated parameters. Bleed water was affected by both w/b and total binder content. However, the bleed water in LWSCC mixtures was very little; this can be attributed to the use of 5% silica fume (SF).

- The established models using the fractional factorial design approach are valid for LWSCC mixtures with w/b ranging between 0.30 and 0.40, total binder content between

410 and 550 kg/m^3 and HRWRA dosages between 0.3 to 1.2% by mass of total binder content.

- The derived statistical models and response tables are useful tools for predicting the fresh/hardened properties of LWSCC mixtures and can be used to optimize the LWSCC mixtures in a simplified and timely fashion.

- The statistical analysis and validation results of the derived models indicate that these models can be used to design LWSCCs and to facilitate the protocol for optimization of LWSCCs. The theoretical optimum mix proportions can be used to derive desirable fresh properties and compressive strength of LWSCCs.

- It was possible to produce robust LWSCC mixtures that satisfy the EFNARC criteria for SCC. Three industrial classes of LWSCC mixtures with wide range of workability performance were successfully developed. These mixtures can cover various ranges of applications, such as tunnel linings, walls, columns, vertical applications in very congested structures, and structures with complex shapes.

- The optimized EC-LWSCCs showed lower compressive strength than equivalent FS/ESH-LWSCCs due to the presence of high percentage of comparatively weaker EC lightweight aggregates. ESH-LWSCC mixtures had the highest compressive strength due to its higher fine-to-total aggregate ratio that allowed more fine particles to fill up voids, which resulted in a stronger interfacial transition zone (ITZ) between the aggregates and the paste. FS-LWSCCs had compressive strength in the range between EC-LWSCCs and ESH-LWSCCs. The reason for this difference could be attributed to the influence of the quality and percentage of lightweight coarse aggregate used.

- Good correlation was not found between the 28-day compressive strength and dry unit weight of concrete. However, the data suggested that optimized LWSCCs with relatively low dry density (1706 kg/m^3) but with high aggregate packing density (less voids) and low coarse-to-total aggregates volume ratio, as is the case of ESH-LWSCCs, will produce higher compressive strength (46.7 MPa) than concrete mixtures with high dry density

(1847 kg/m^3) such as FS-LWSCCs where the 28-day compressive strength was 42.6 MPa. Further, the w/b and the segregation resistance of LWSCCs are main factors in establishing such relationship. LWSCC mixtures with high dry density, high w/b (0.4) and low segregation resistance (>15) are susceptible to yield lower compressive strength even when compared to mixtures with lower dry densities.

- The highest flexural strength values were recorded for the optimized FS-LWSCCs and the lowest were recorded with EC-LWSCCs. The quality, size and volume of coarse aggregate affected the flexural strength of LWSCC mixtures. Mixes made with FS showed high values because more coarse aggregate volume at (28.2%) was used in these mixes compared to 24.5% in LWSCC mixes with ESH. The relative low quality of the coarse EC aggregates resulted in low flexural strength values.

- Similar to the 28-day compressive strength, due to better ITZ and bonding between the paste and the aggregates, the highest split tensile strengths were reported for the optimized ESH-LWSCC mixtures followed by FS-LWSCC and EC-LWSCC mixtures. The 28-day split tensile strength of ESH-LWSCC mixtures were in average 11% higher than that of the equivalent FS-LWSCC mixtures, and 35%, higher than that of the equivalent EC-LWSCC mixtures.

- It was observed that the optimized ESH-LWSCC mixtures produced the highest bond strength followed by FS-LWSCC and EC-LWSCC mixtures. Compared to ESH-LWSCC, the decrease in bond strength was about 40% and 51% for mixes made with FS and EC, respectively. The fresh properties (especially the segregation resistance), quality of the paste and the concrete compressive strength as well as the lightweight aggregate type played a major role in the pullout bond strength results. A relation between bond strength (f_b) and concrete compressive strength of the form $f_b = 0.0004 \times (fc')^{2.5386}$ is derived based on experimental results with a correlation coefficient (R^2) of 0.92.

- Based on the test results it is found that CSA and ACI Code based equations under-estimate the bond strength of LWSCC mixtures. Such Code based equations can therefore be used to predict the bond strength of LWSCC mixtures.

- Relatively strong correlation is established between the flexural/split tensile strength and the compressive strength of the optimized LWSCC mixtures. The flexural and split tensile strength of LWSCC mixtures were 8.5 to 10.5% and 5.5 to 6.6% of the 28-day compressive strength, respectively. On the other hand, the bond strength of LWSCC mixtures was 7.5 to 15% of the 28-day compressive strength.

- Both absorption and porosity of LWSCCs increased with increase of lightweight aggregates in the mixture. LWSCC made with EC aggregates showed the highest porosity, which can be attributed to the comparatively higher porosity of EC aggregates compared with ESH and FS aggregates.

- The porosity of LWSCCs made ESH and FS were virtually identical, even though the ESH aggregates are more porous. This is due to the fact that ESH-LWSCCs had less percentage of coarse aggregate and better compactability/workability and paste quality.

- EC-LWSCCs exhibited the highest sorptivity followed by ESH and FS-LWSCCs. According to these results, the sorptivity index of EC -LWSCC mixtures had the highest rate of absorption for both initial and secondary absorption.

- In general, LWSCC mixtures made with any type of lightweight aggregate (used as both coarse and fine) exhibited much higher sorptivity index than comparable normal SCC mixture. The reduction of sorptivity with age may have beneficial effect of improving the long-term deterioration resistance of LWSCC mixtures.

- Overall, LWSCC mixtures showed RCPT values lower than 4000 Coulombs. EC-LWSCCs had higher RCPT value than comparable ones with ES and ESH lightweight aggregates. The RCPT values for all LWSCC mixtures were classified as “moderate” at 28-day and as “low” at 91-day as per Code specifications.

- The drying shrinkage of all LWSCC mixtures at 112-day was found to be equal to or higher than 600 microstrain. Aggregates with high absorption properties are normally associated with high shrinkage in concrete. This was confirmed from the substantial increase in shrinkage with the increase of the aggregate absorption in case of both EC and

ESH-LWSCC mixtures. Also, the limited volume of coarse aggregate in the developed LWSCC mixtures prompted the overall higher drying shrinkage.

- EC-LWSCC specimens demonstrated lower resistivity by showing higher current values compared to respective FS and ESH specimens during the entire duration of accelerated corrosion test. This was also evident from the highest mass loss reinforcing bars embedded in EC-LWSCC in corrosion tests. The superior FS/ESH aggregates quality and porosity characteristics in addition to the higher flowability and better resistance to segregation of FS-LWSCC followed by ESH-LWSCC are thought to be the main factors in exhibiting improved corrosion resistance.

- The developed LWSCC mixtures with all three different types of lightweight aggregates exhibited good high temperature resistance by showing 15 to 33% compressive strength loss at 600°C. However, the residual compressive strength of LWSCCs dropped to a range from 49 to 67% at 900^{o}C with highest reduction noted for FS-LWSCCs.

- The rate of weight loss of LWSCCs increased with the increase of temperature up to 900°C accompanied by discoloration, development of surface microcracks and minor spalling at the corners. LWSCC specimens maintained their integrity even up to 900°C which can be attributed to the better mineral structure of the used lightweight aggregates causing less evaporation of water in C–S–H structure. Overall LWSCCs lightweight should exhibit better high temperature resistance characteristics than normal aggregate due to lesser tendency to spall and loss of its original strength as confirmed from this study.

- FS-LWSCC specimens showed the highest resistance to scaling due to lower porosity and absorption properties of the aggregates compared to other LWSCC specimens with EC-LWSCC showing the lowest resistance. This was attributed to high permeability and low aggregates quality of EC/ESH LWSCCs. Non-air entrained nature of the LWSCCs could have been a significant contributing factor to the observed performance. It is anticipated salt scaling resistance can be improved by using entrained air in the developed of LWSCC mixtures.

- The optimized LWSCC mixtures with all three types of lightweight aggregates behaved reasonably well after 2 weeks of exposure to sulfuric acid with no strength reduction. Moreover, concurring with the results of the weight loss, the highest strength loss due to exposure to sulfuric acid was recoded on EC-LWSCC mixtures followed by ESH-LWSCCs.

- Overall, the strength loss of LWSCC mixtures due to exposure to acid was much less than anticipated. The improved resistance of LWSCC specimens was attributed to the use of silica fume and fly ash (in the mixtures) leading to the production of C-S-H matrix of low C/S (close to 1) with dense formation of silica gel layer which subsequently protected the cement paste from progressive deterioration.

- Generally, LWSCC specimens showed low resistance to freeze-thaw cycles due to non-air entrained nature of the concrete mixtures. For all LWSCC mixtures, the maximum percentage of weight loss due to freeze-thaw cycles ranged between 5.8 and 8.5%. The value of relative dynamic elasticity modulus dropped rapidly with the freeze-thaw cycles and went down below the ASTM limit of 60%. Although none of the LWSCC specimens survived up to 300 cycles of freeze-thaw due to the development of extensive pore pressures associated with typical lightweight aggregate microstructural characteristics (total porosity, pore size distribution etc.) distinct from normal-weight aggregate. However, freeze-thaw resistance of LWSCC mixtures can be improved through air entrainment using air-entraining admixtures.

- Developed LWSCC mixtures incorporating EC, FS and ESH aggregates have great potential to be used in practical construction applications. The use of such LWSCCs can lead to sustainable construction through reduction of noise pollution, better heat/sound insulation, reduction of structural dead load and cost savings.

- In addition, the significant contributions of the research can be summarized as follows:

    - Developed models and guidelines (which are not currently available) which can be used by the construction industry to design LWSCC mixtures and optimize

certain fresh and hardened properties. This will ensure a speedy mix design process and reduce the number of trials needed to achieve LWSCC mix specifications.

- Overall, this research established a technology for the production of LWSCCs which will guide engineers, researchers and manufacturers to develop future high performance LWSCC mixtures with different types of lightweight aggregates.

9.3 Recommendations for Further Research

The following recommendations are provided for future research studies:

- It is suggested to extend the derived statistical models to investigate the influence of mixture proportioning and material characteristics that were not considered in the factorial design of workability, mechanical and mass transport properties, as well as durability performance of LWSCCs. These parameters can include the maximum size of aggregates, varying gradation/shape of aggregates, possible combinations of lightweight aggregates such as (FS and EC) or (FS and ESH), other types of lightweight aggregates such as pumice or expanded slate as well as combinations of lightweight aggregates and normal sand in order to develop LWSCC mixtures that are suitable for all types of practical applications.

- Given that LWSCCs can exhibit up to 30% higher drying shrinkage compared to normal density SCC, it is important to investigate the compatibility of shrinkage reducing admixtures with HRWRA in order to simultaneously obtain better workability and reduced drying shrinkage.

- It is important to develop methods to measure the absorption, porosity, water absorption rate (sorptivity) of LWSCCs since current ASTMS methods C642 and C1585 are not compatible and applicable to lightweight aggregate concrete as confirmed from the results of current research. For example, testing by electrical resistance and ultrasonic pulse velocity (UPV) are better methods to evaluate the mass transport properties of LWSCC.

- Investigations on LWSCC mixtures by incorporating air entraining admixtures are to be conducted in order to improve durability properties especially salt-scaling and freeze-thaw resistance characteristics. It is also equally important to analyze micro-structural aspects and interfacial transition zone (ITZ) characteristics of LWSCC mixtures.

- It is important to evaluate fresh, mechanical and durability properties of LWSCC mixtures through production in the field. This will facilitate the development of design, production and performance specifications for the developed LWSCCs.

- Undertake comprehensive investigations on LWSCC structural elements subjected to mechanical (static, dynamic, fatigue and creep) and environmental (marine, fire etc.) loadings to evaluate performance and formulate design specifications.

APPENDIX

Appendix A

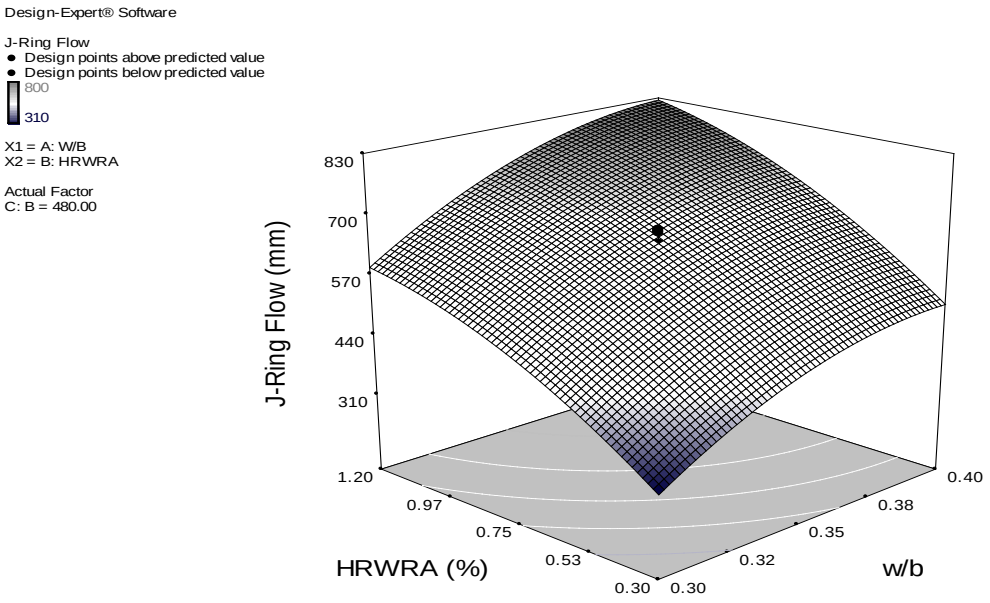

Effect of w/b, HRWRA and total binder content at 480kg/m^3 on J-ring FS-LWSCC mixes

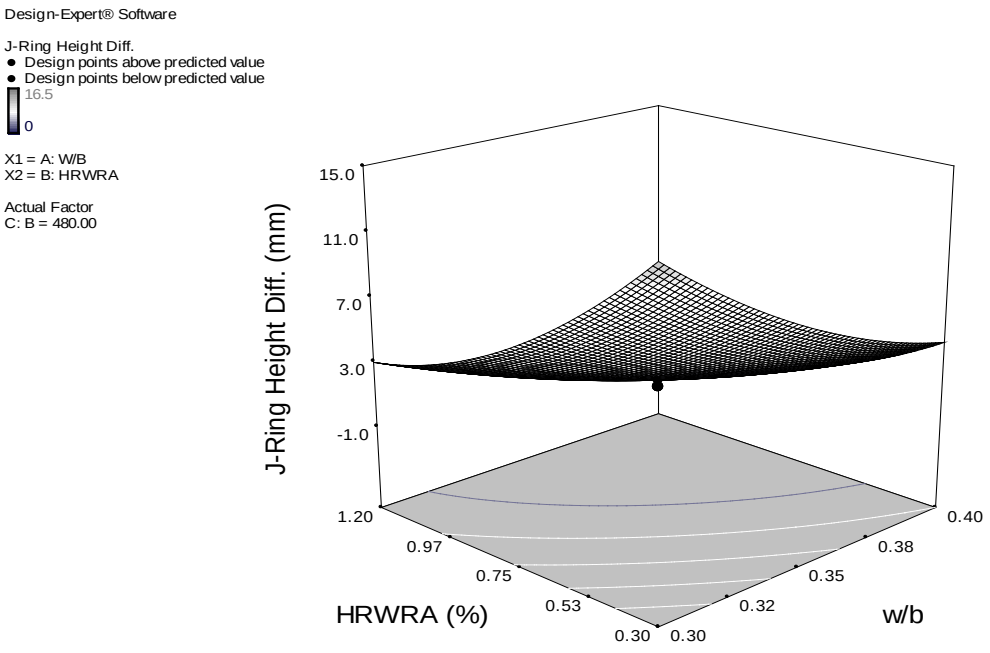

Effect of w/b, HRWRA and total binder content at 480kg/m^3 on the J-ring height difference of FS-LWSCC mixes

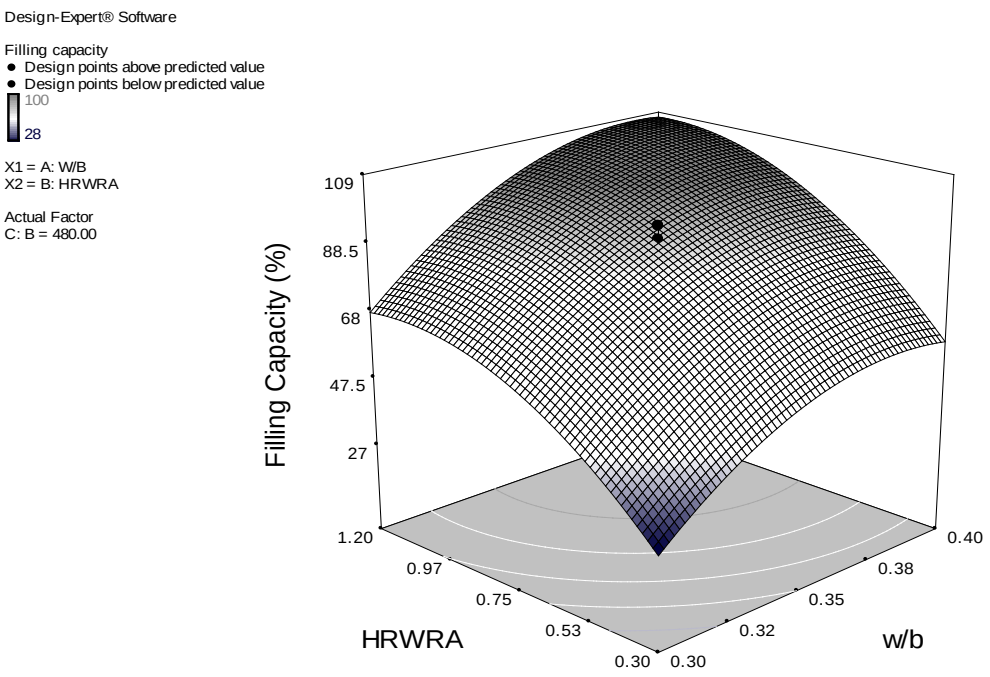

Effect of w/b, HRWRA and total binder content at 480kg/m^3 on the filling capacity of FS-LWSCC mixes

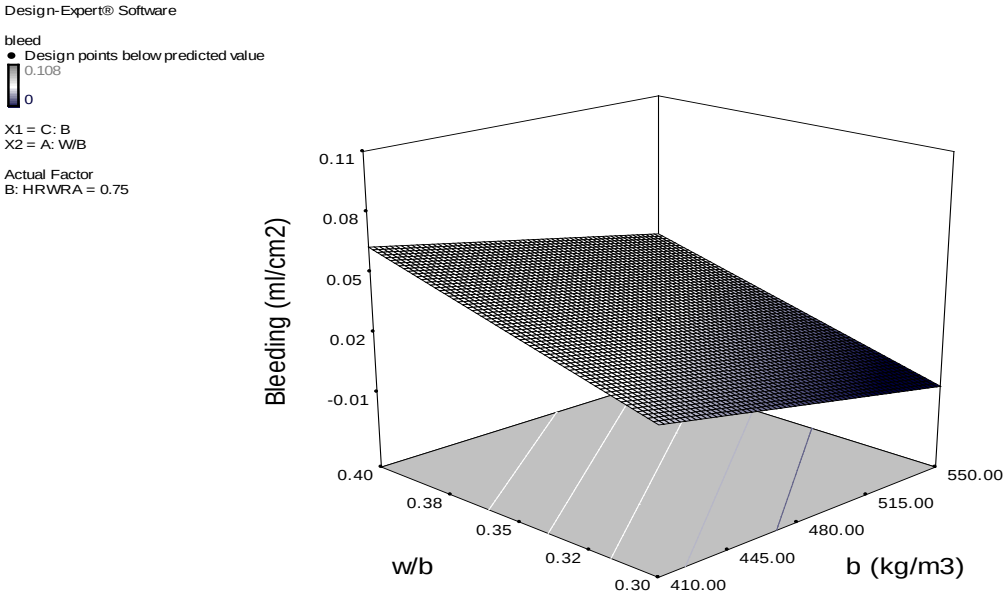

Effect of w/b, b and HRWRA at 0.75% on the bleed of FS-LWSCC mixes

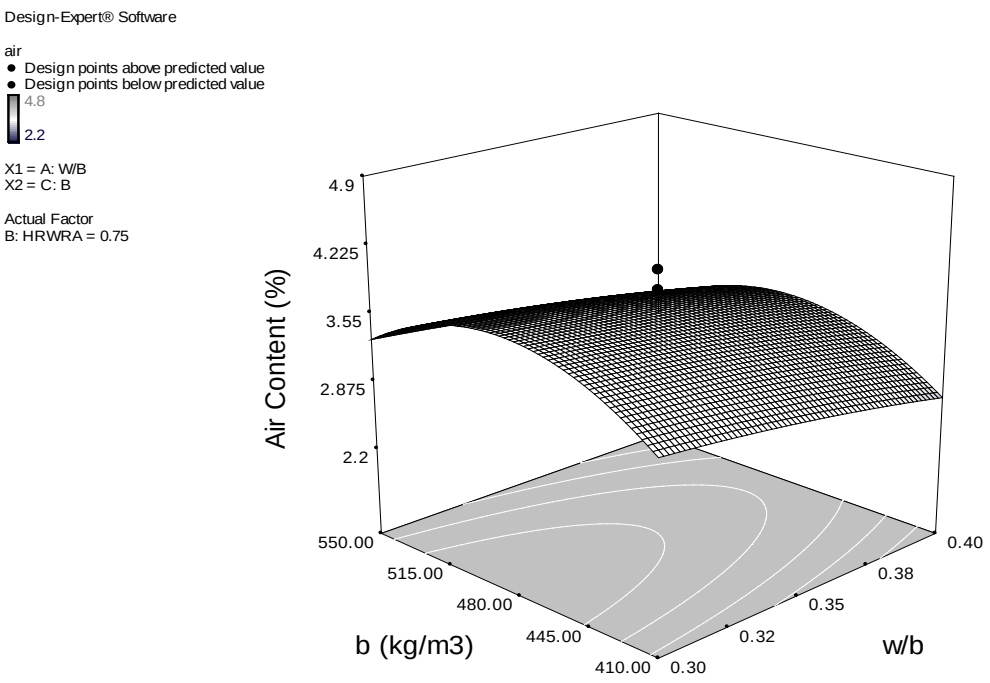

Effect of w/b, b and HRWRA at 0.75% on the air content of FS-LWSCC mixes

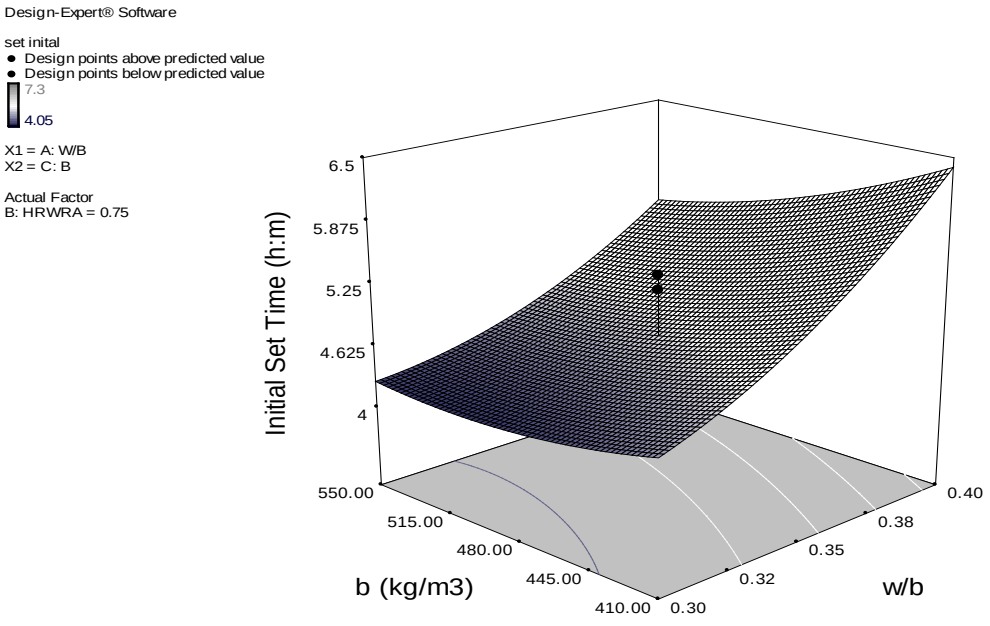

Effect of w/b, b and HRWRA at 0.75% on the initial set time of FS-LWSCC mixes

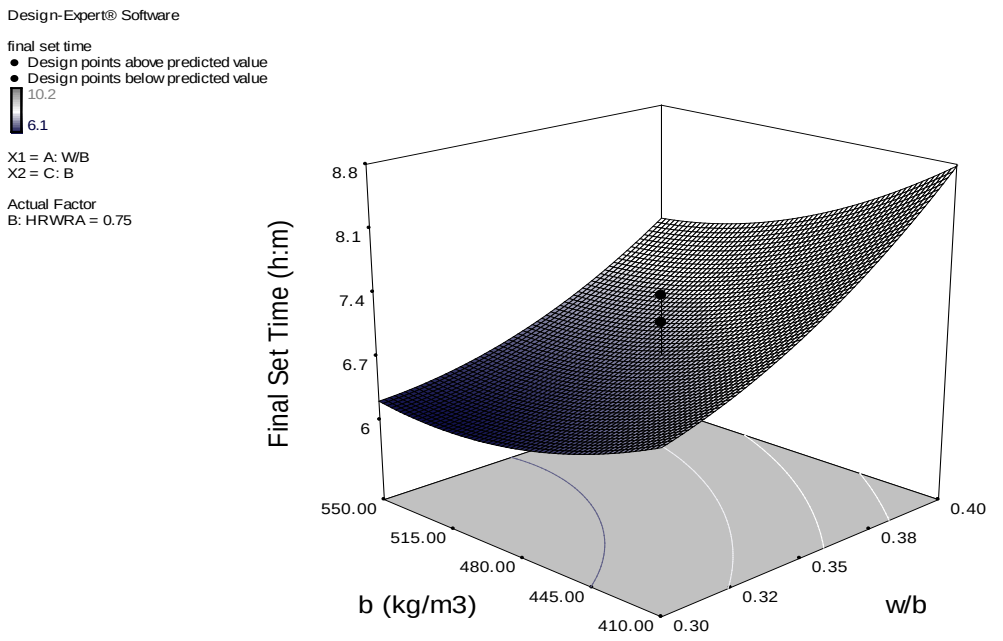

Effect of w/b, b and HRWRA at 0.75% on the final set time of FS-LWSCC mixes

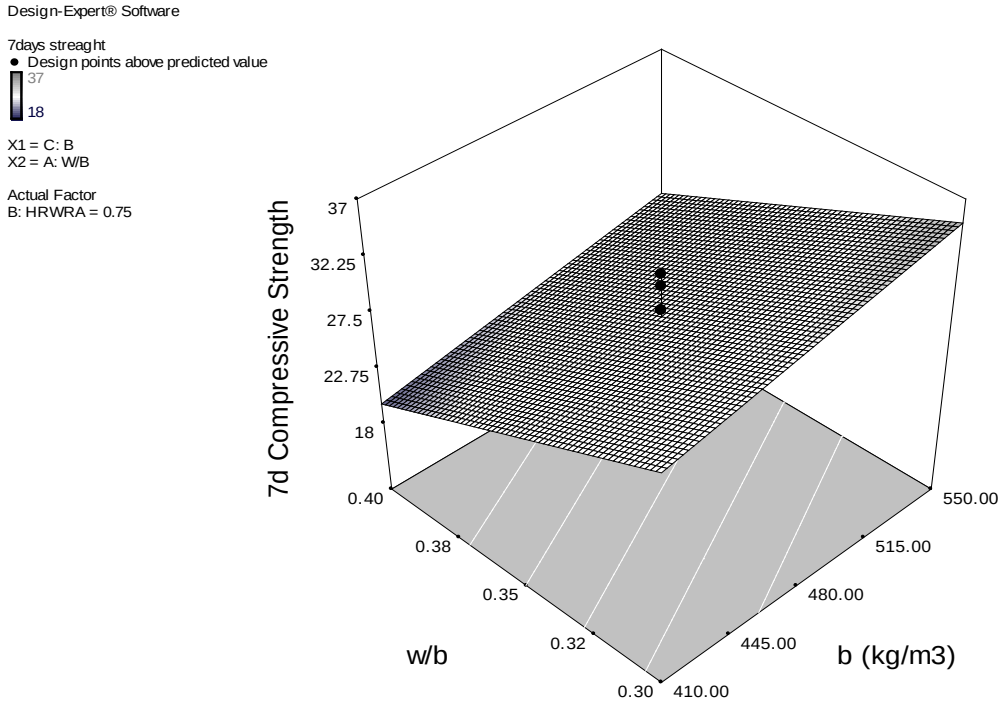

Effect of w/b, b and HRWRA at 0.75% on the 7d compressive strength of FS-LWSCC mixes

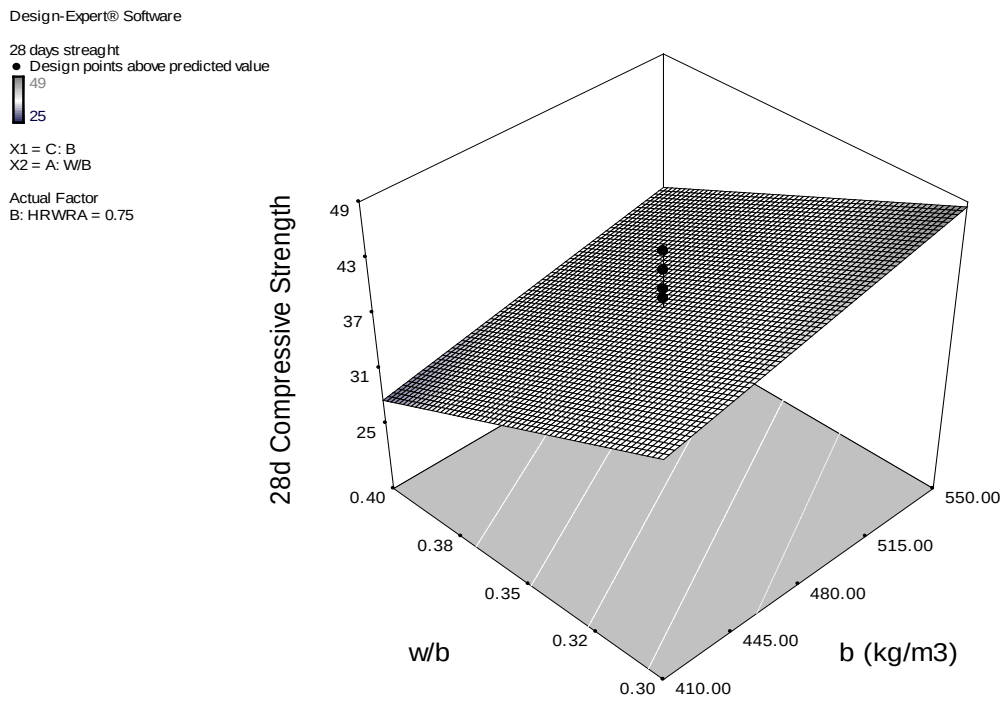

Effect of w/b, b and HRWRA at 0.75% on the 28d compressive strength of FS-LWSCC mixes

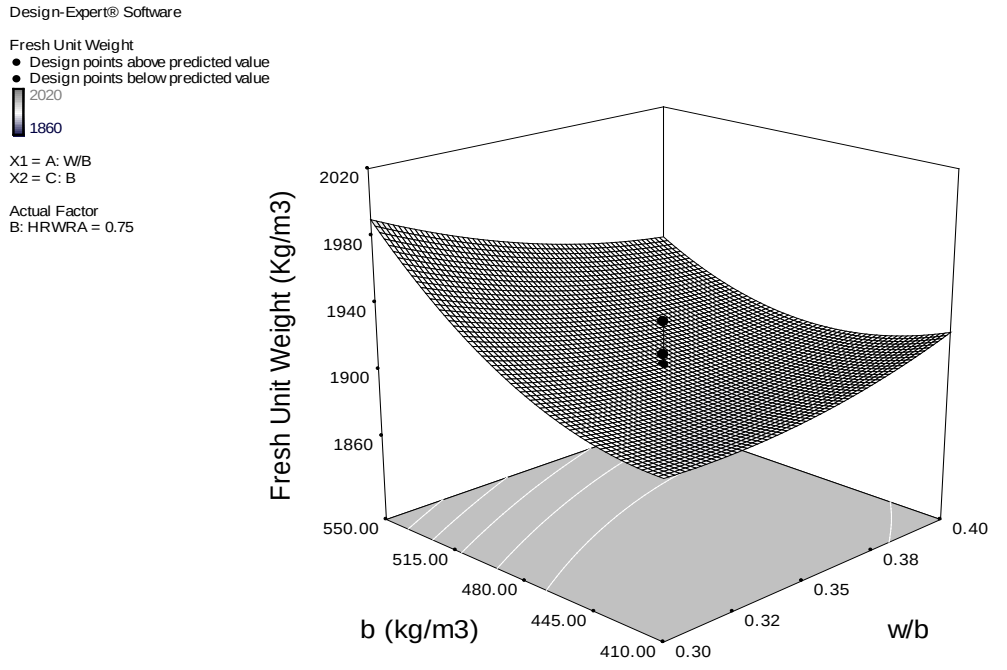

Effect of w/b, b and HRWRA at 0.75% on fresh unit weight of FS-LWSCC mixes

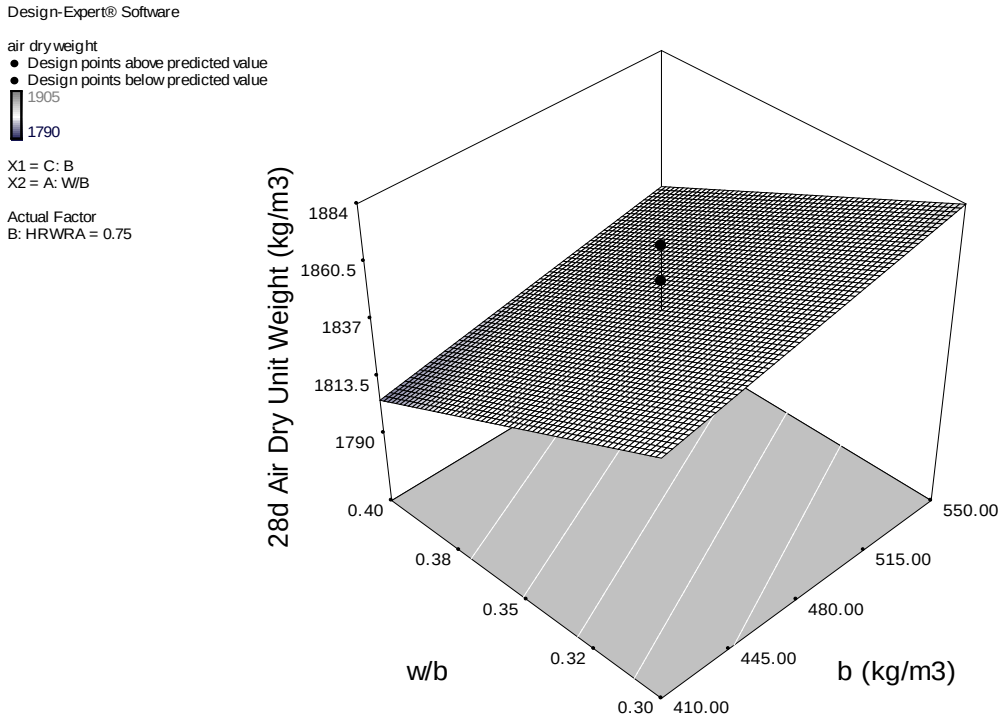

Effect of w/b, b and HRWRA at 0.75% on the 28d air dry unit weight of FS-LWSCC mixes

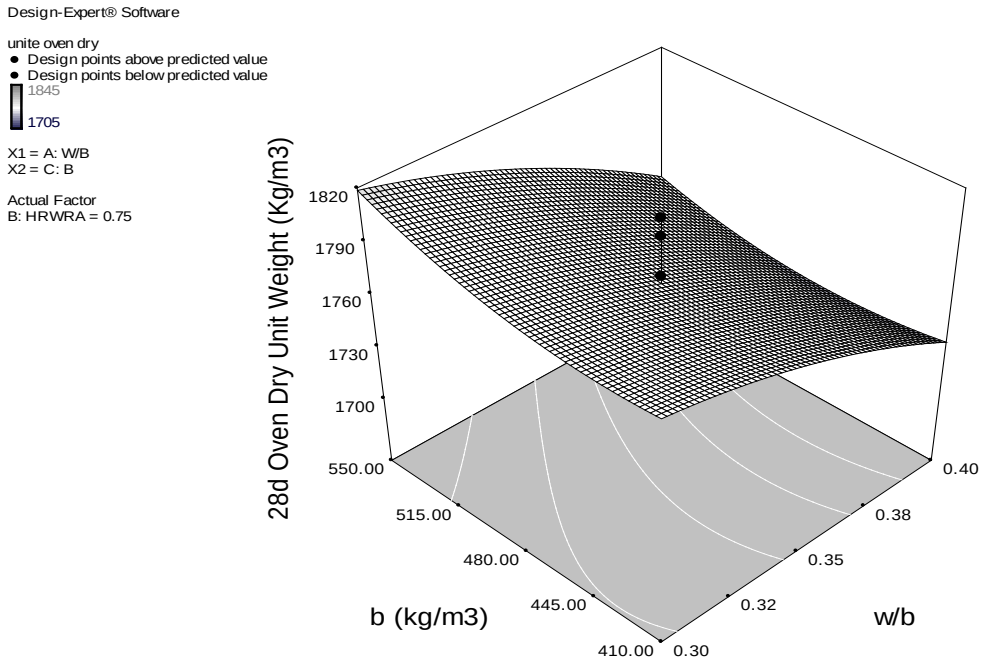

Effect of w/b, b and HRWRA at 0.75% on the 28d oven dry unit weight of FS-LWSCC mixes

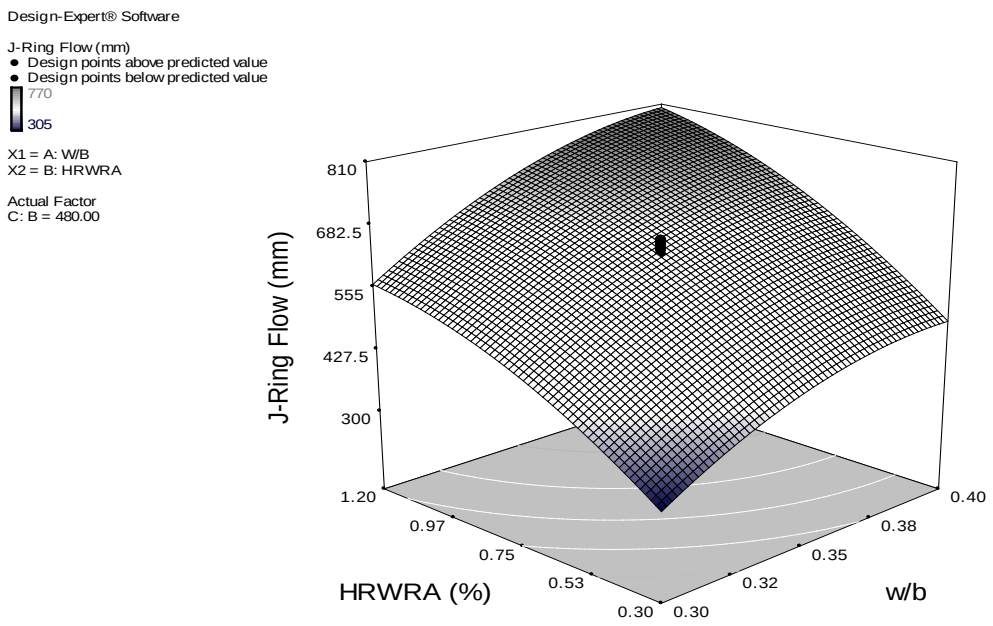

Effect of w/b, HRWRA and total binder content at 480kg/m^3 on J-ring EC-LWSCC mixes

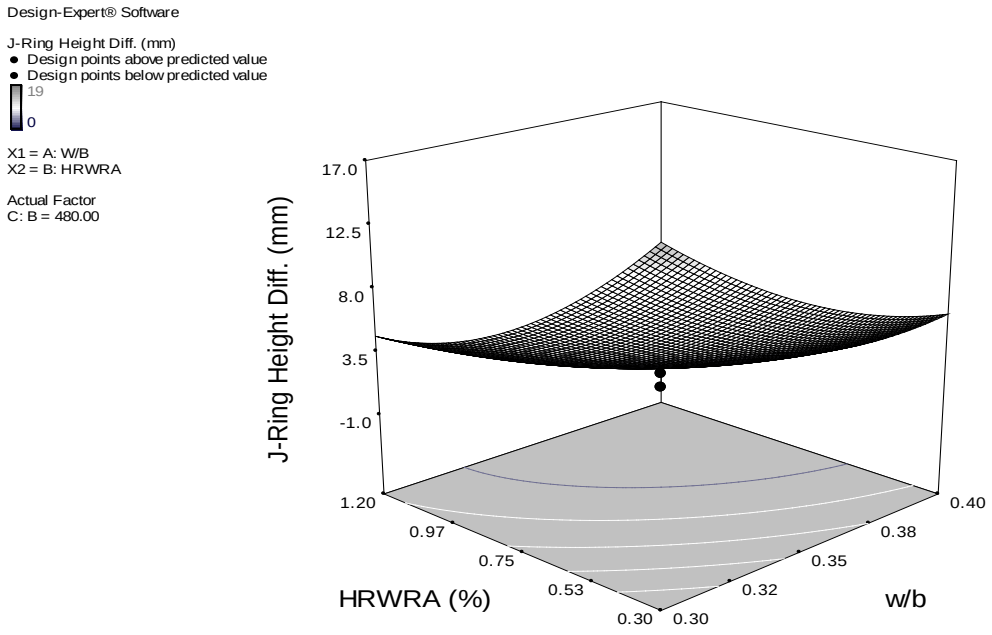

Effect of w/b, HRWRA and total binder content at 480kg/m^3 on the J-ring height difference of EC-LWSCC mixes

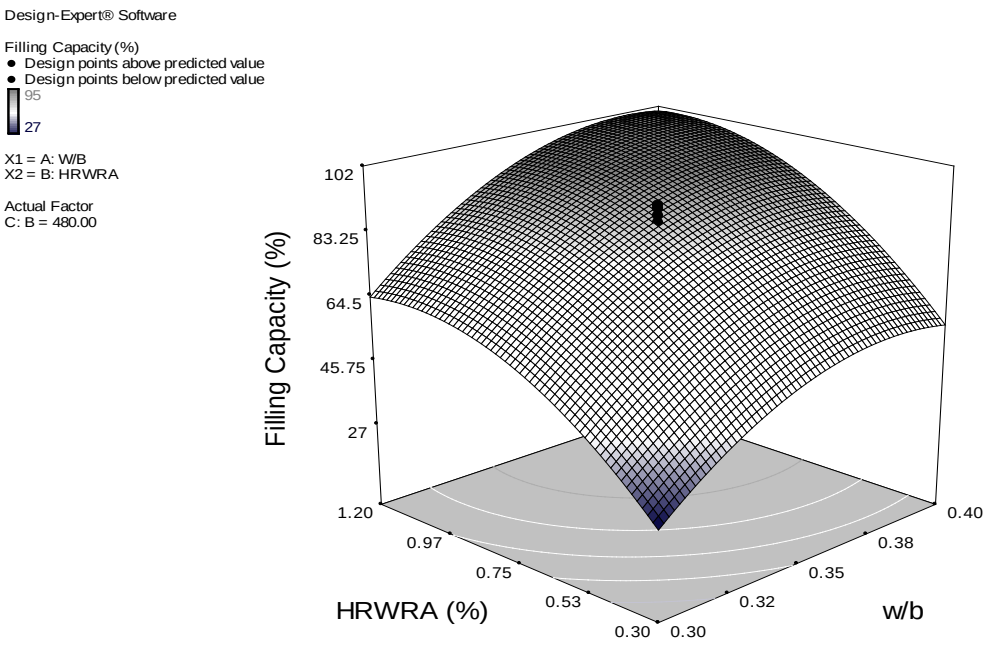

Effect of w/b, HRWRA and total binder content at 480kg/m^3 on the filling capacity of EC-LWSCC mixes

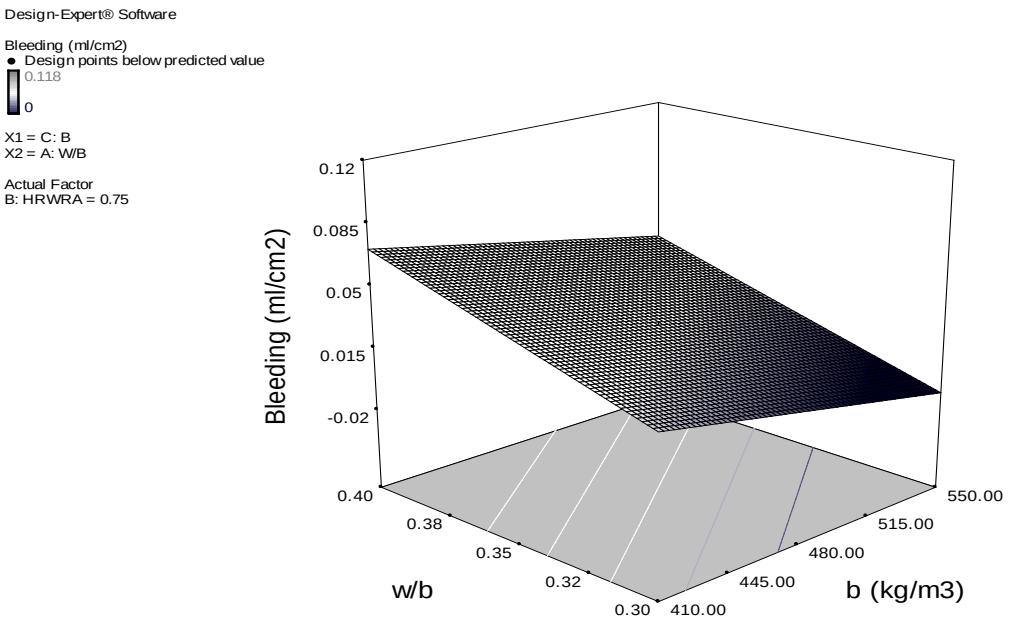

Effect of w/b, b and HRWRA at 0.75% on the bleed of EC-LWSCC mixes

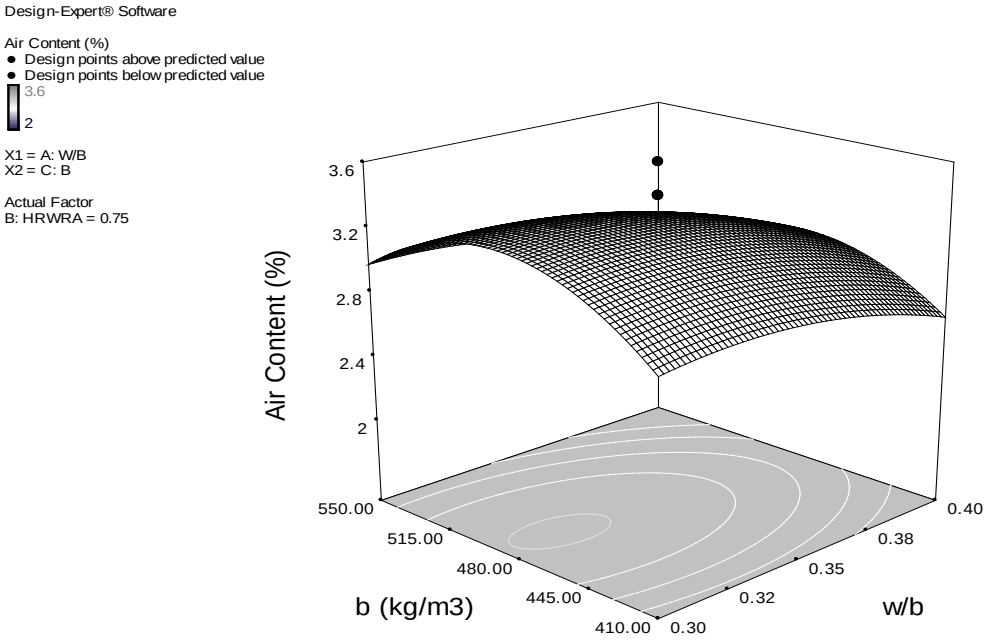

Effect of w/b, b and HRWRA at 0.75% on the air content of EC-LWSCC mixes

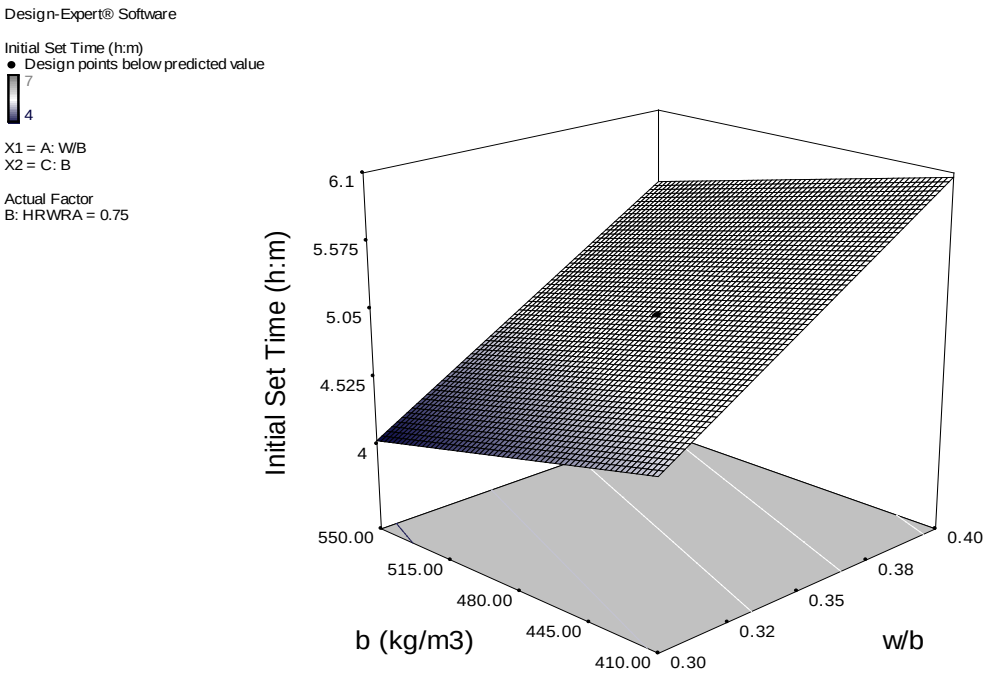

Effect of w/b, b and HRWRA at 0.75% on the initial set time of EC-LWSCC mixes

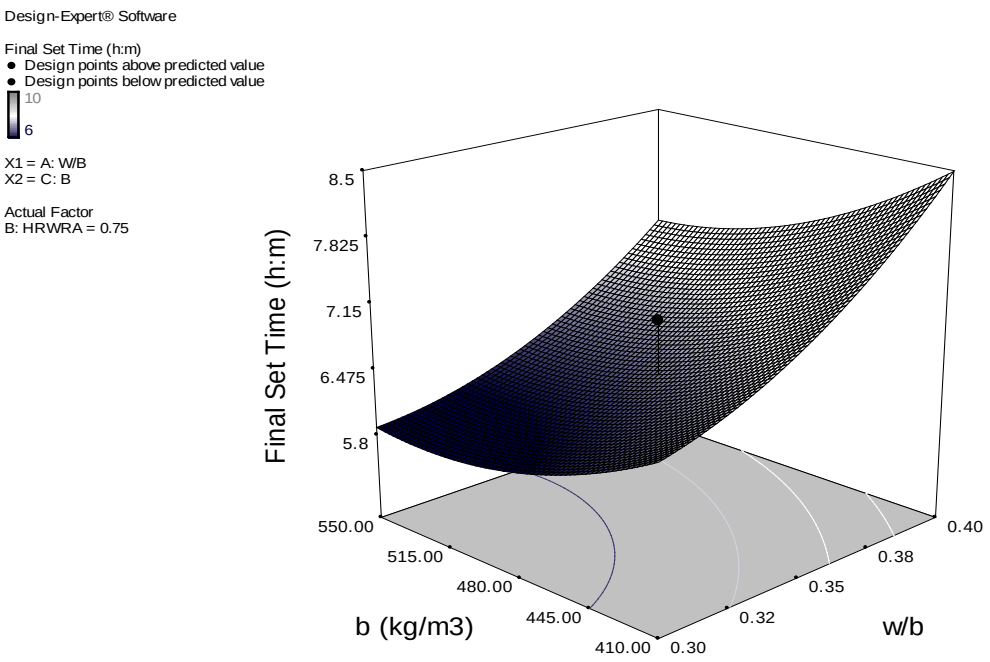

Effect of w/b, b and HRWRA at 0.75% on the final set time of EC-LWSCC mixes

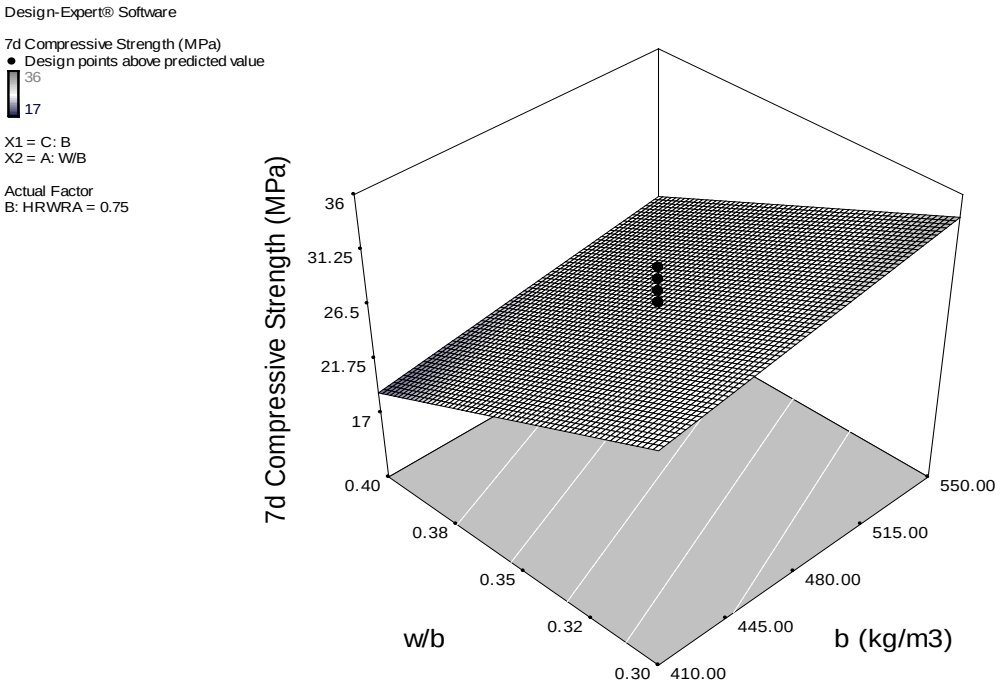

Effect of w/b, b and HRWRA at 0.75% on the 7d compressive strength of EC-LWSCC mixes

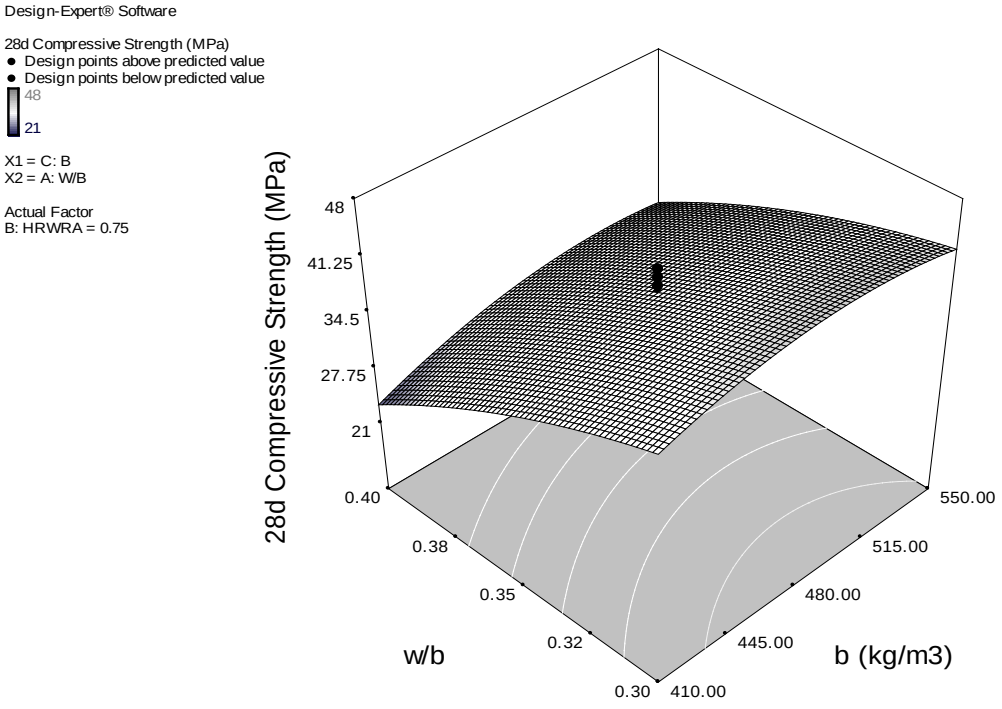

Effect of w/b, b and HRWRA at 0.75% on the 28d compressive strength of EC-LWSCC mixes

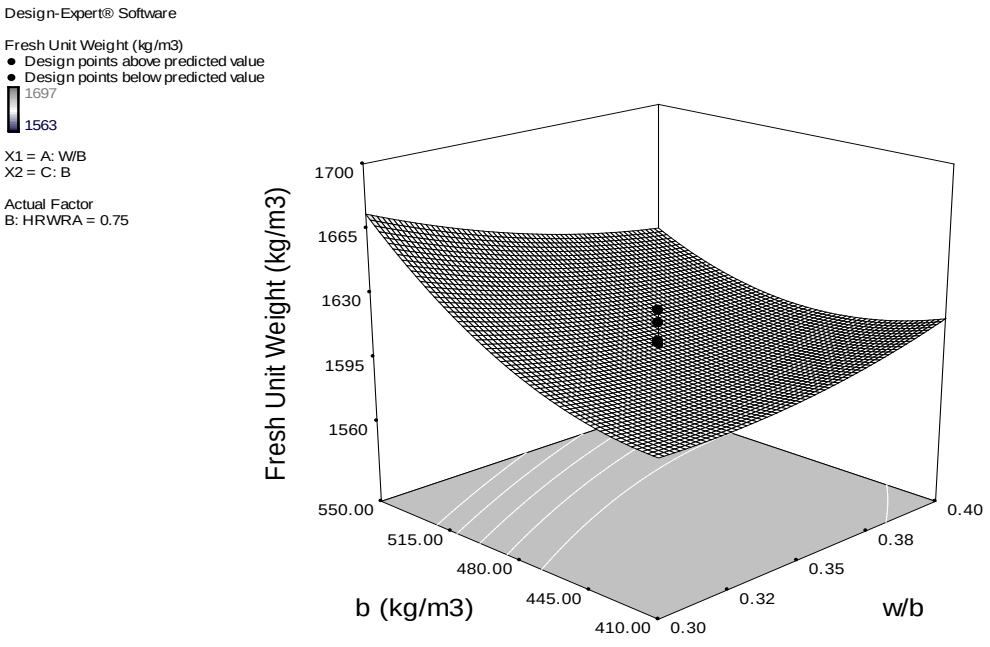

Effect of w/b, b and HRWRA at 0.75% on fresh unit weight of EC-LWSCC mixes

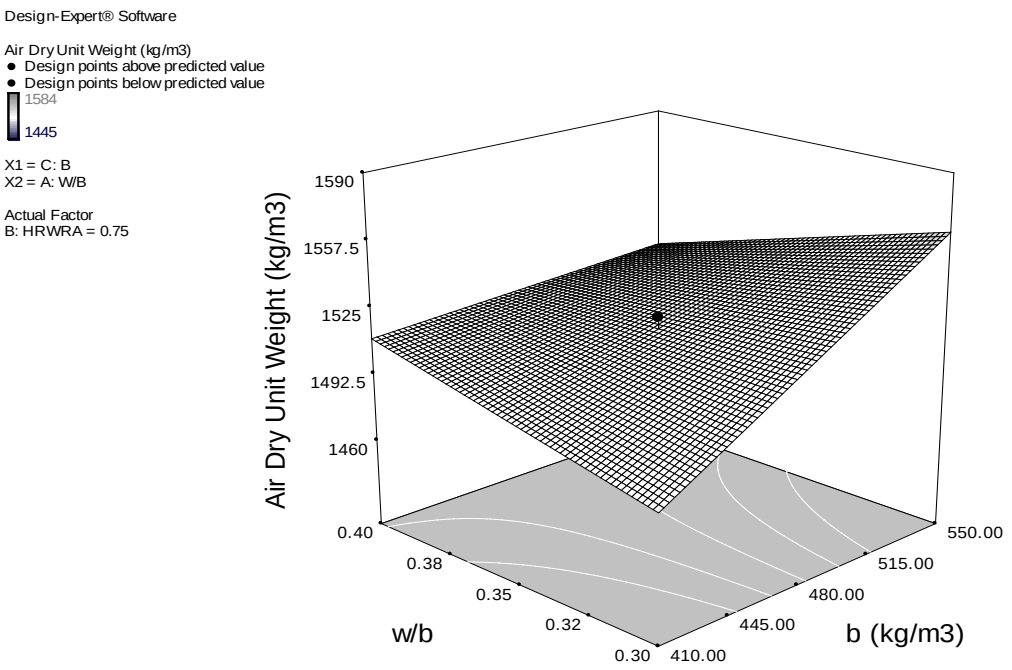

Effect of w/b, b and HRWRA at 0.75% on the 28d air dry unit weight of EC-LWSCC mixes

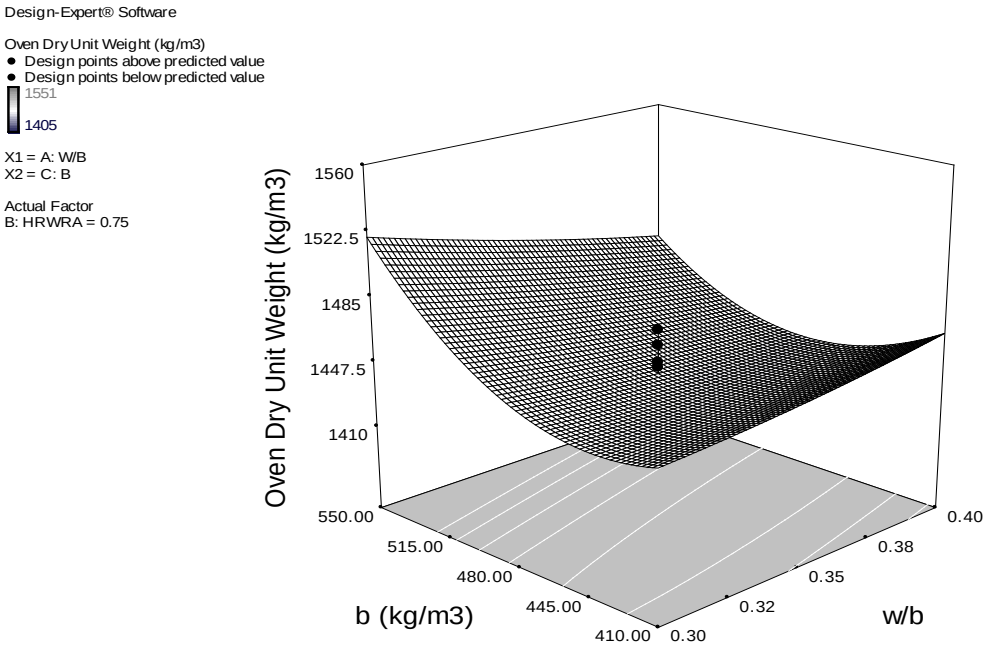

Effect of w/b, b and HRWRA at 0.75% on the 28d oven dry unit weight of EC-LWSCC mixes

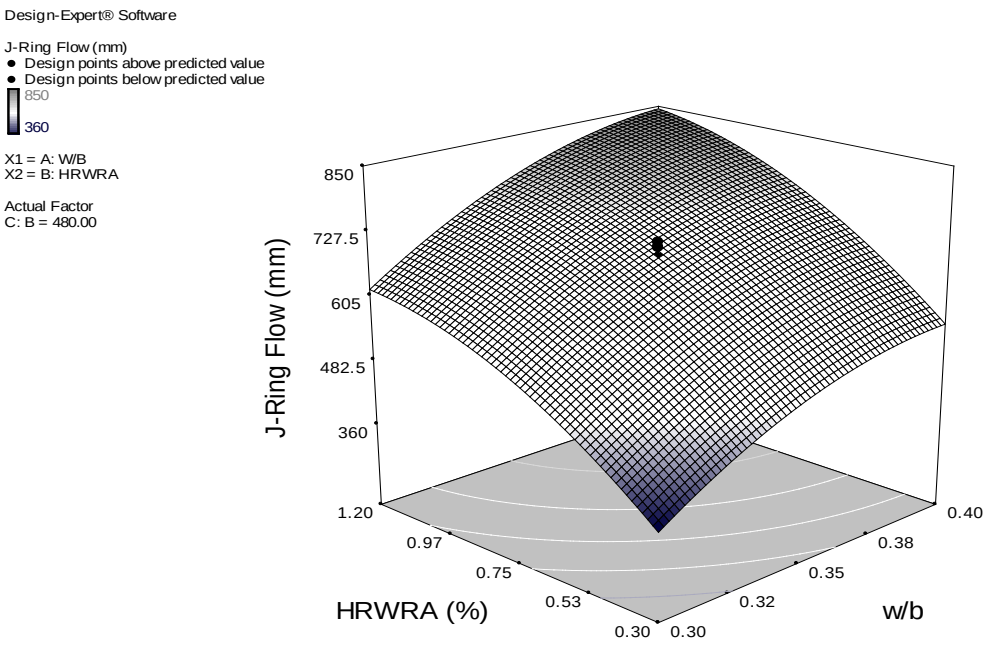

Effect of w/b, HRWRA and total binder content at 480kg/m^3 on J-ring ESH-LWSCC mixes

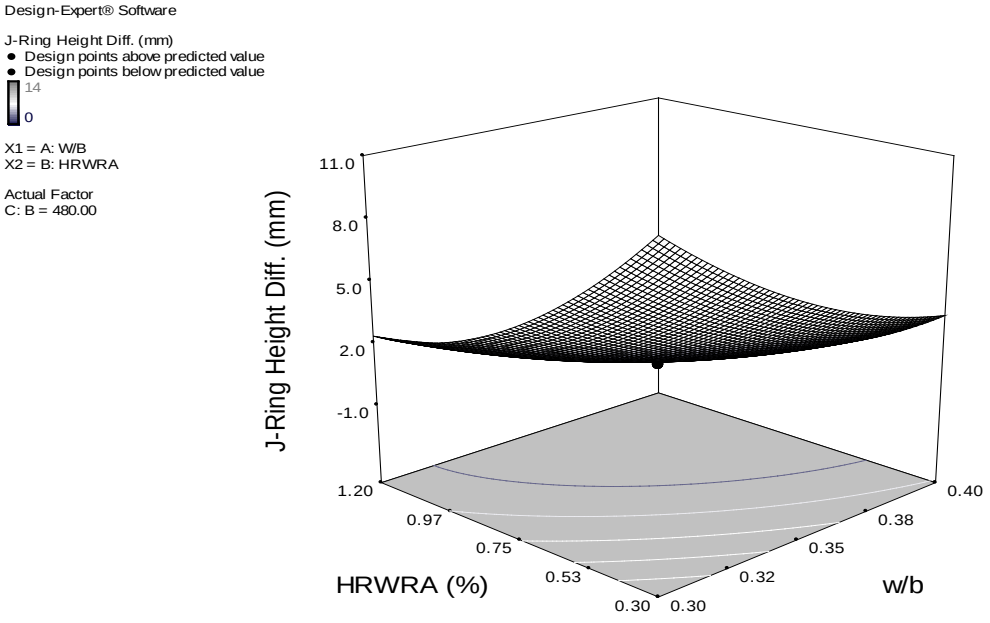

Effect of w/b, HRWRA and total binder content at 480kg/m^3 on the J-ring height difference of ESH-LWSCC mixes

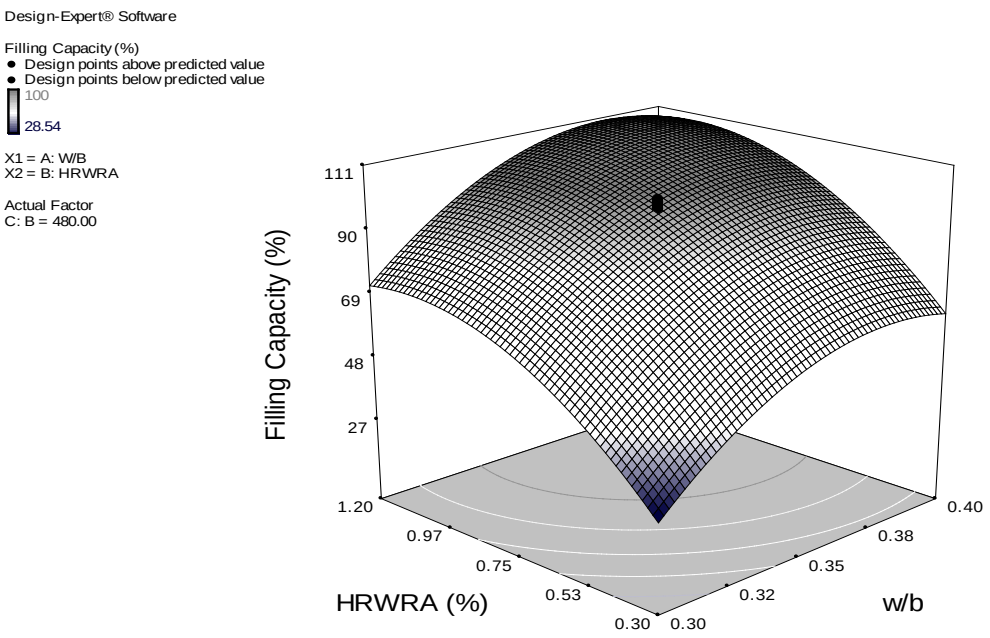

Effect of w/b, HRWRA and total binder content at 480kg/m^3 on the filling capacity of ESH-LWSCC mixes

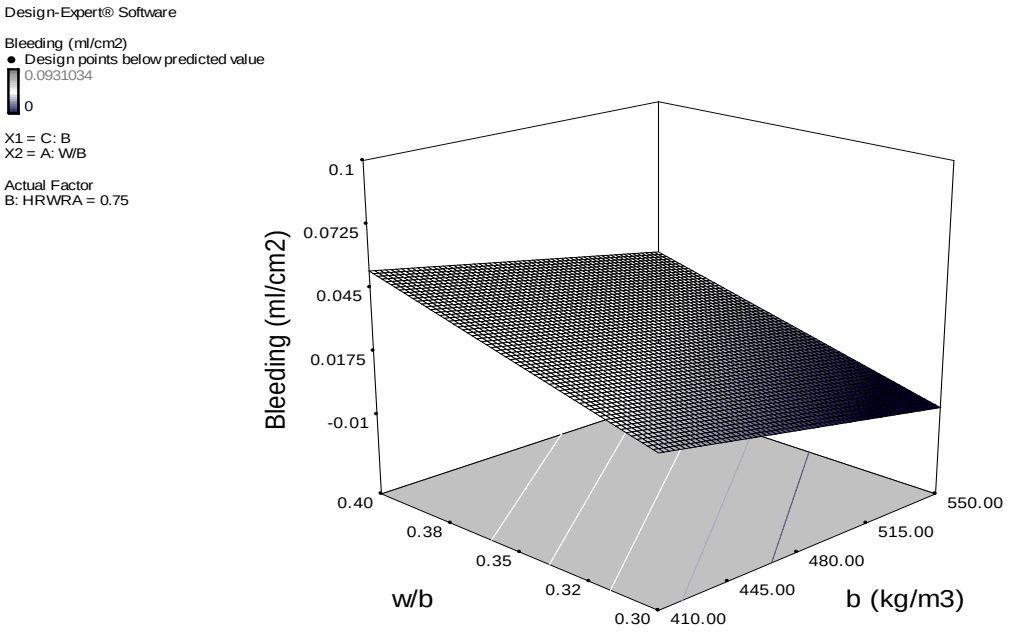

Effect of w/b, b and HRWRA at 0.75% on the bleed of ESH-LWSCC mixes

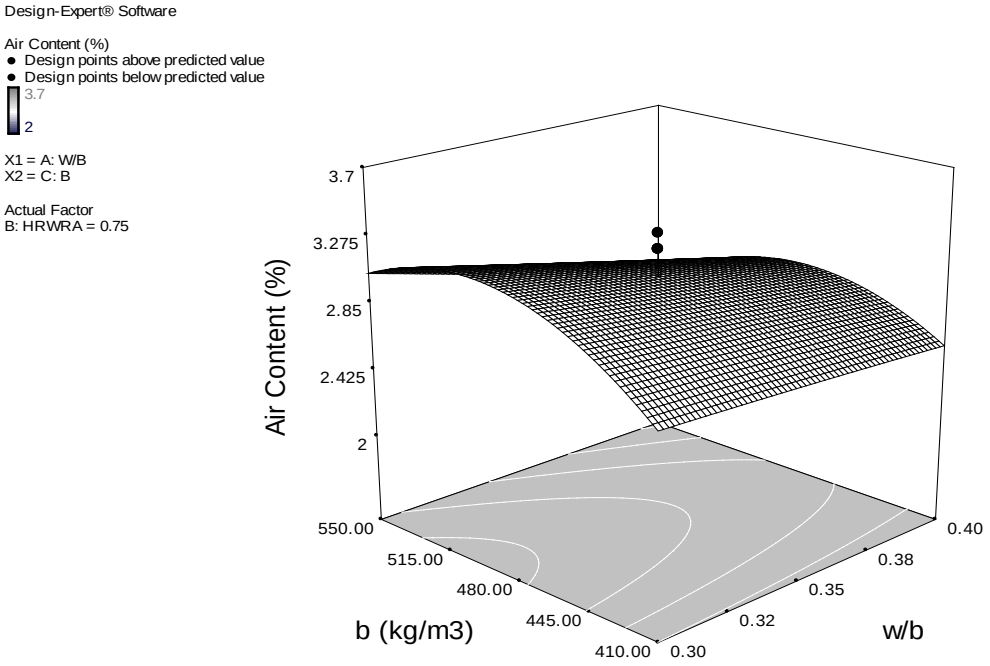

Effect of w/b, b and HRWRA at 0.75% on the air content of ESH-LWSCC mixes

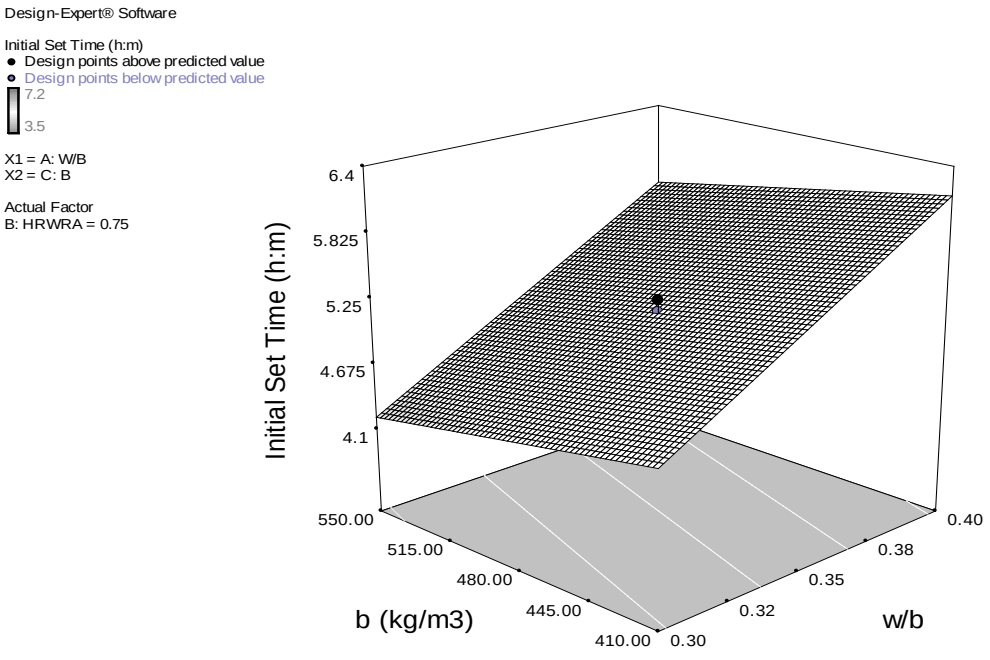

Effect of w/b, b and HRWRA at 0.75% on the initial set time of ESH-LWSCC mixes

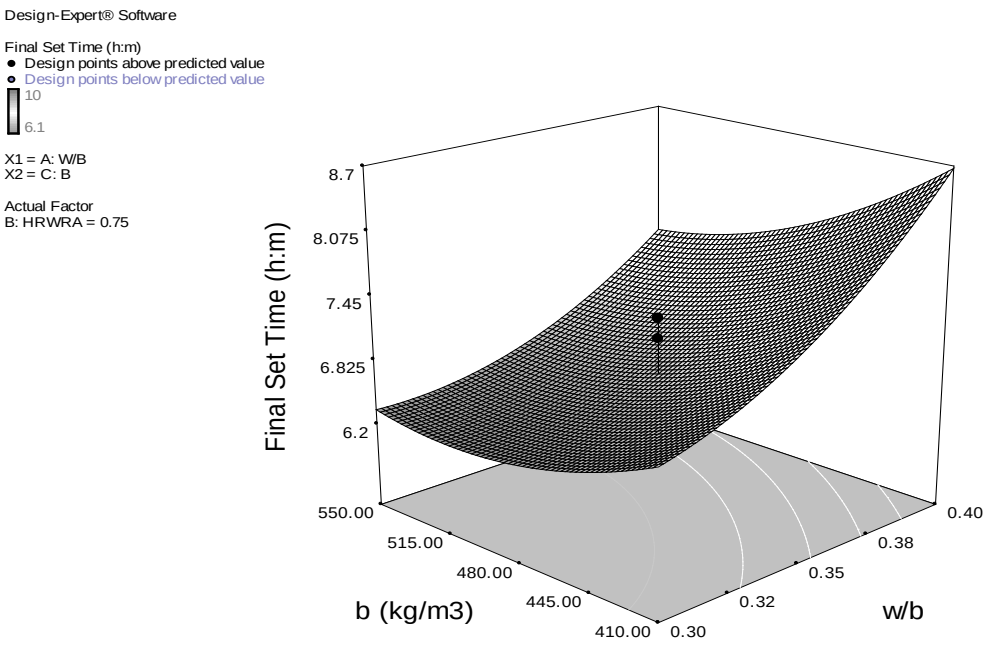

Effect of w/b, b and HRWRA at 0.75% on the final set time of ESH-LWSCC mixes

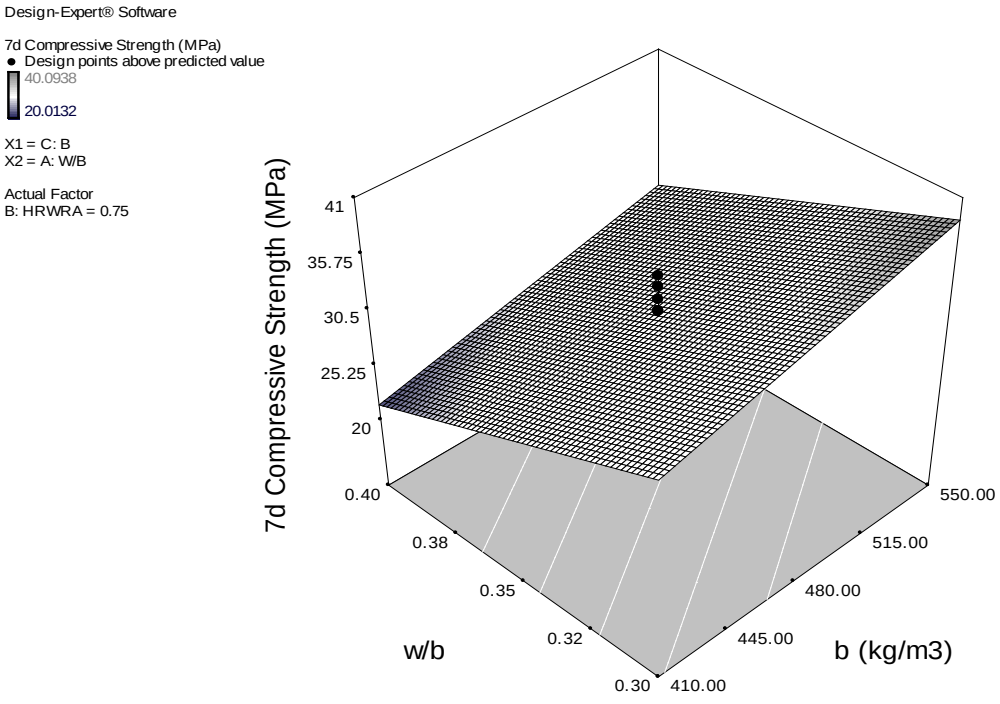

Effect of w/b, b and HRWRA at 0.75% on the 7d compressive strength of ESH-LWSCC mixes

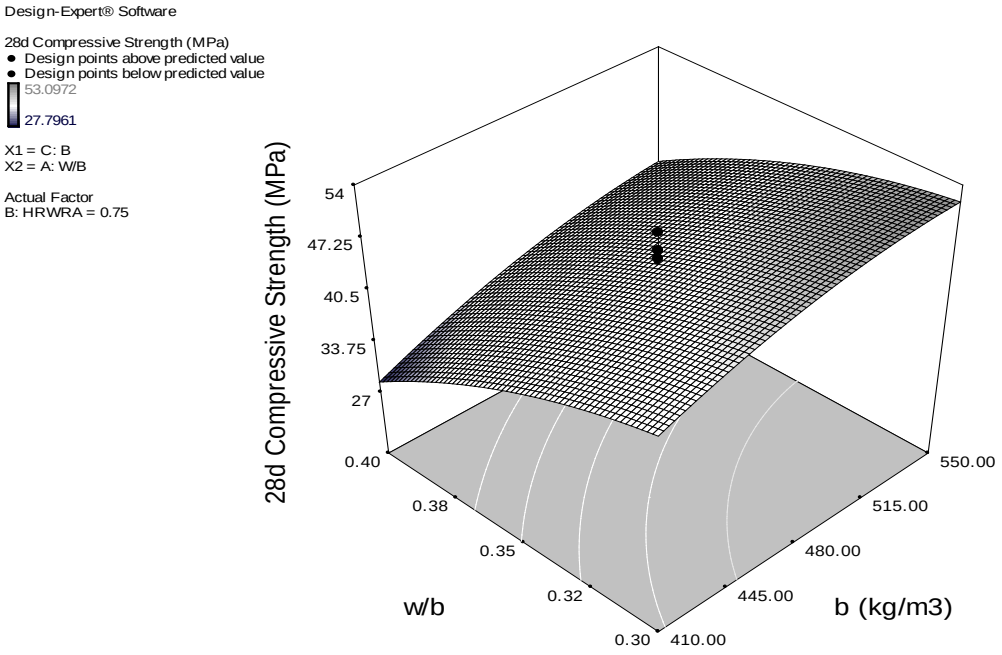

Effect of w/b, b and HRWRA at 0.75% on the 28d compressive strength of ESH-LWSCC mixes

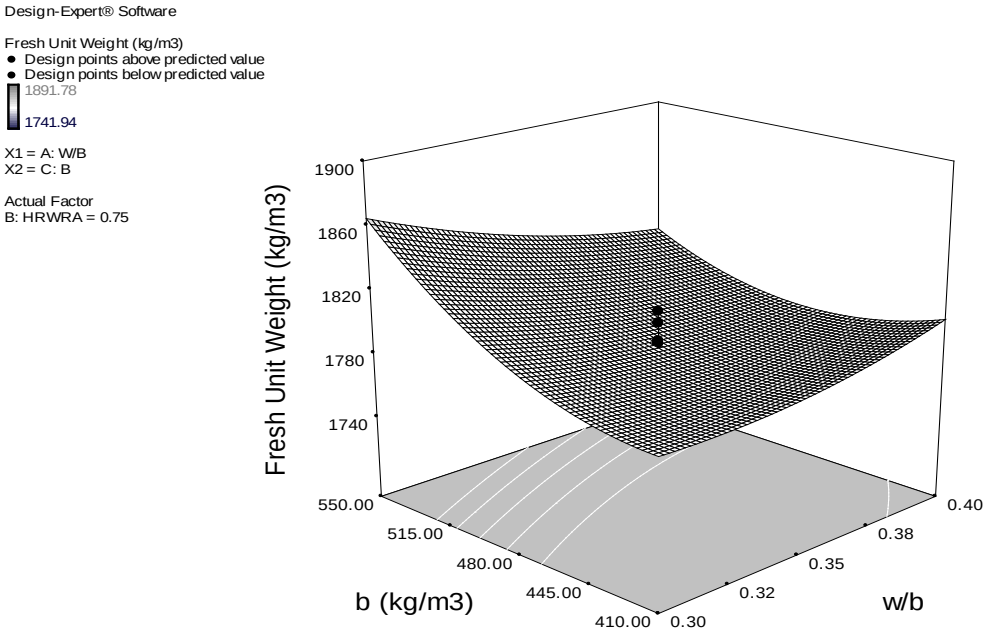

Effect of w/b, b and HRWRA at 0.75% on fresh unit weight of ESH-LWSCC mixes

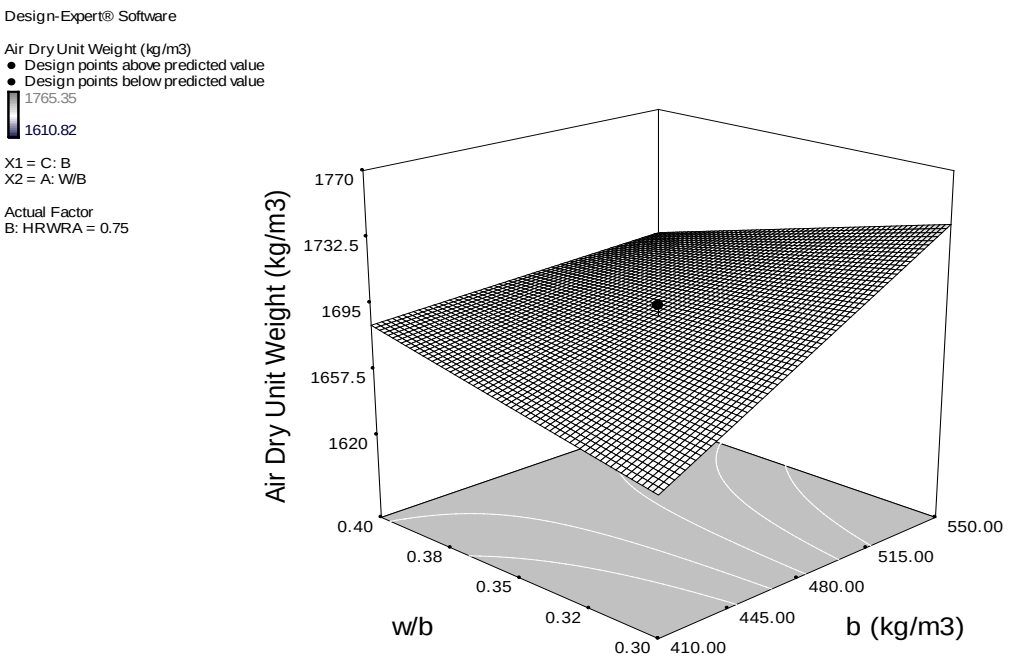

Effect of w/b, b and HRWRA at 0.75% on the 28d air dry unit weight of ESH-LWSCC mixes

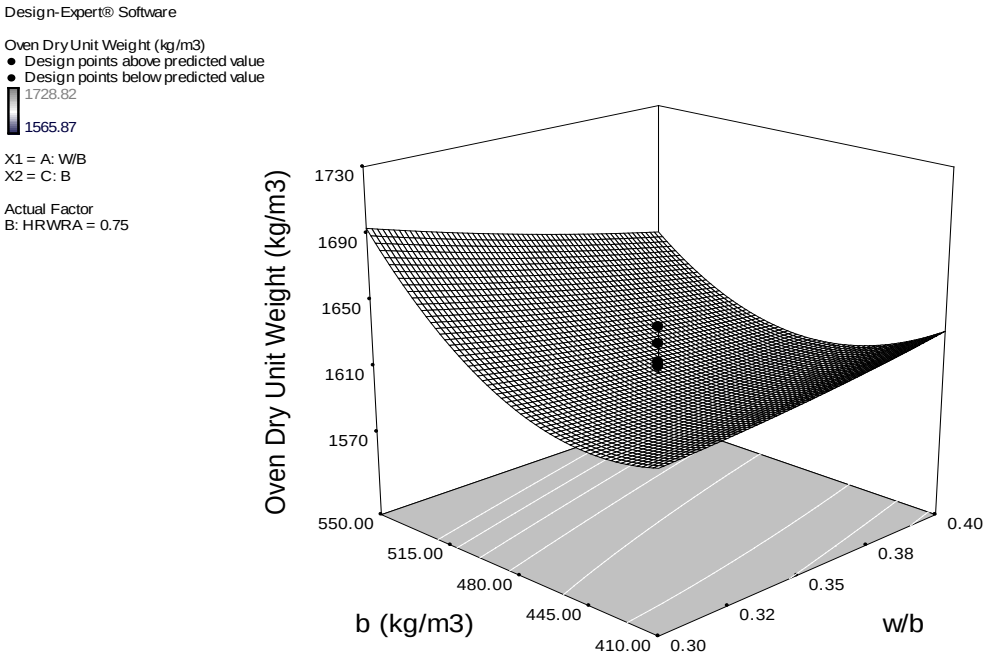

Effect of w/b, b and HRWRA at 0.75% on the 28d oven dry unit weight of ESH-LWSCC mixes

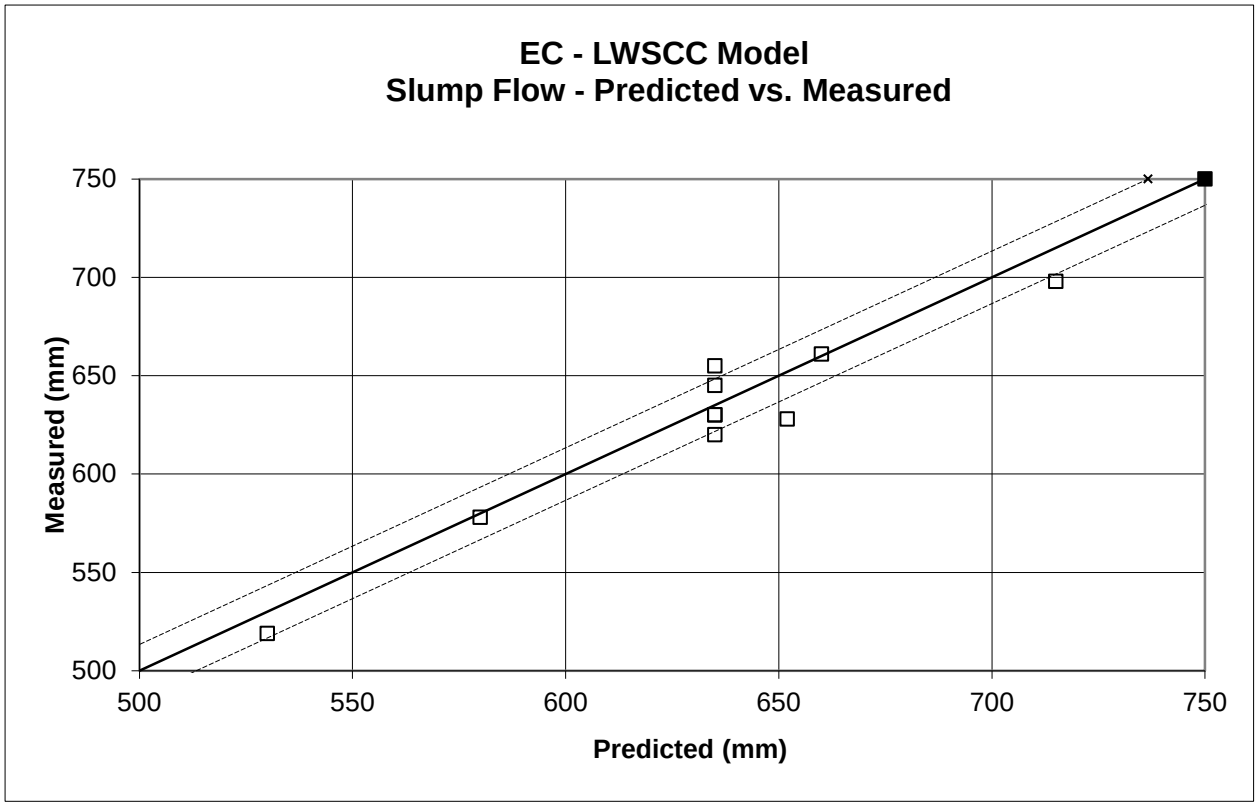

Predicted vs. measured slump flow values of EC-LWSCC model

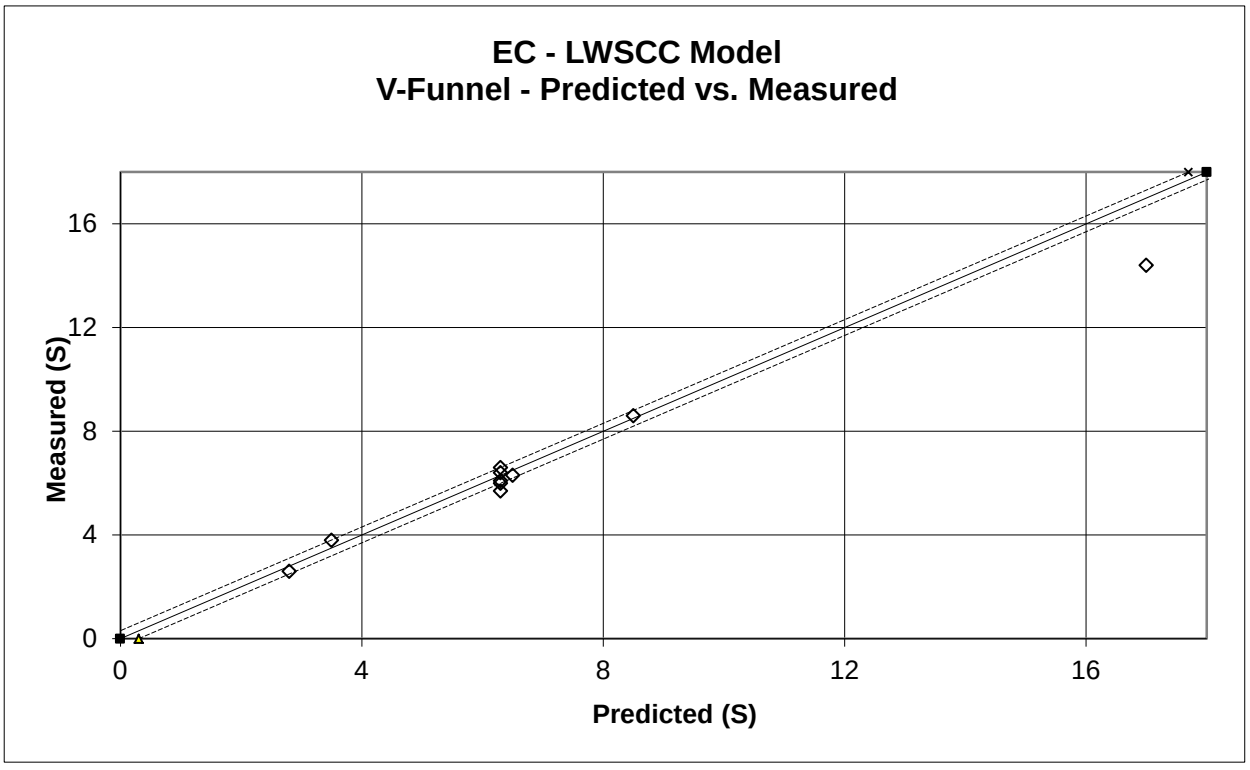

Predicted vs. measured V-funnel values of EC-LWSCC model

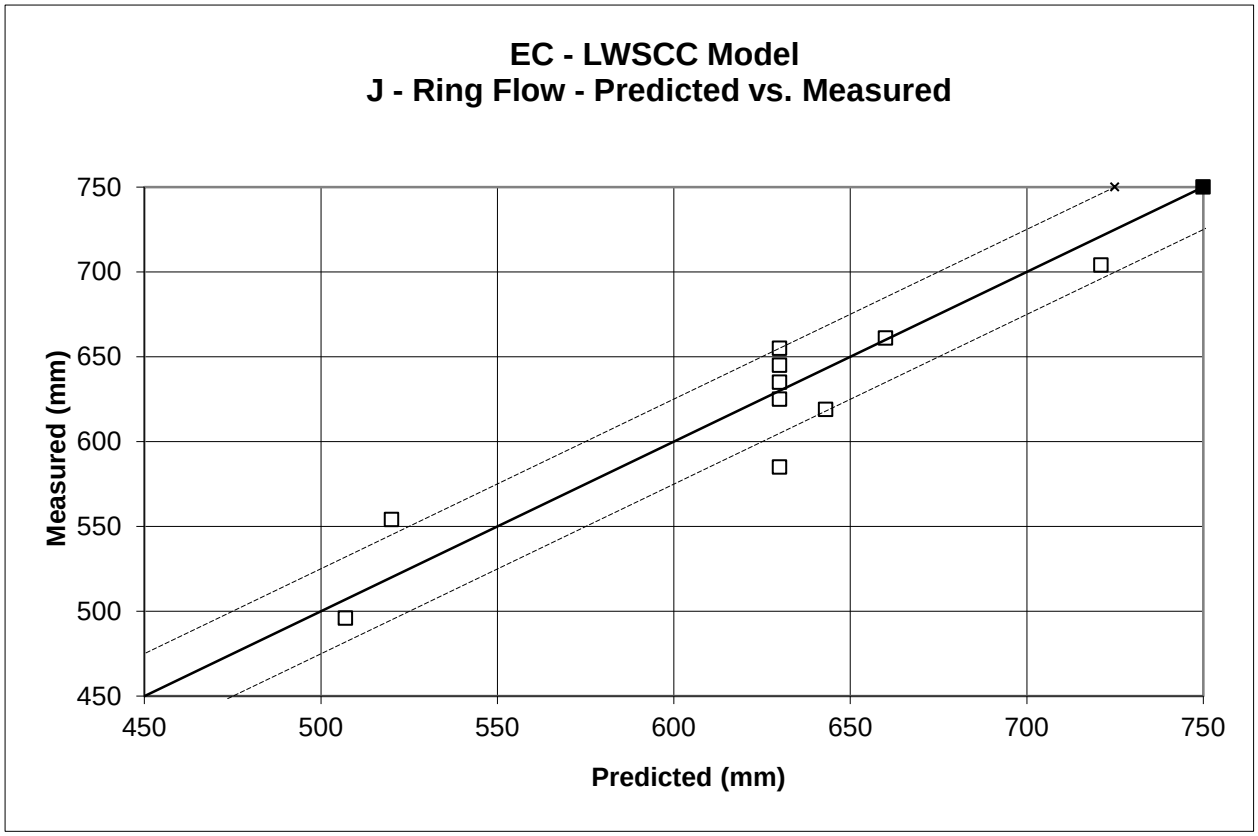

Predicted vs. measured J-ring values of EC-LWSCC model

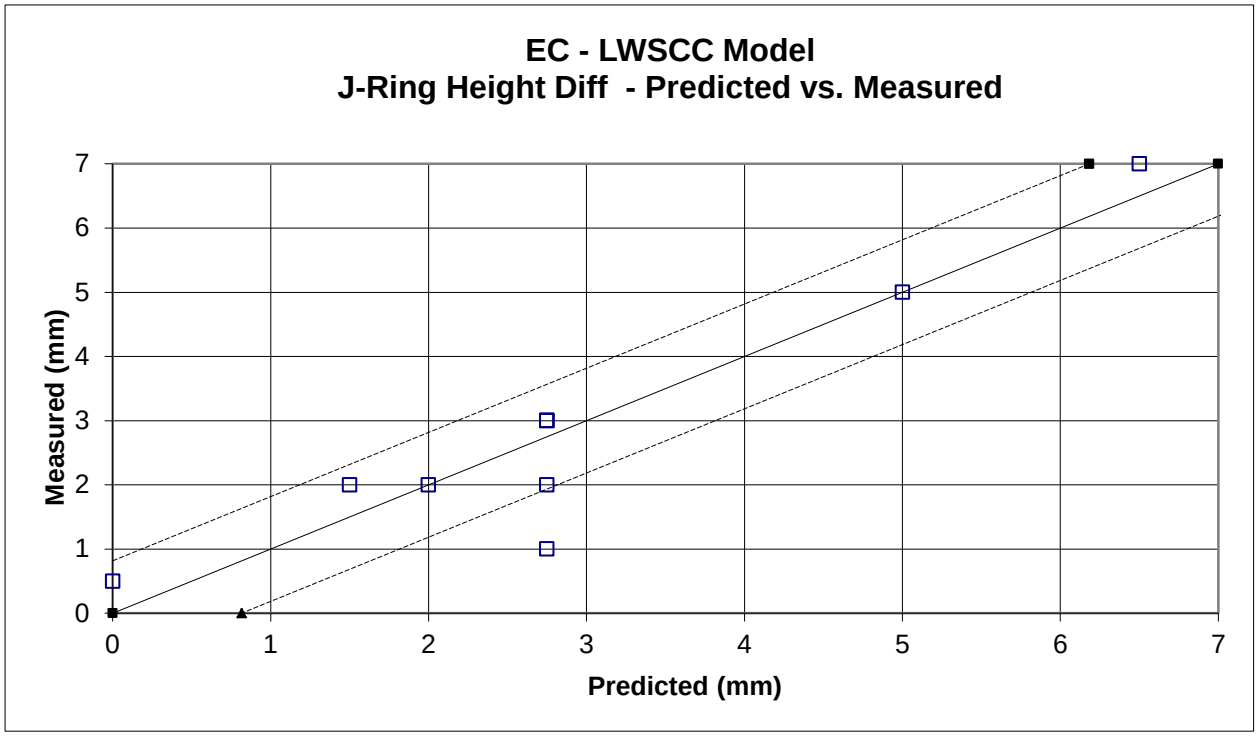

Predicted vs. measured J-ring height diff values of EC-LWSCC model

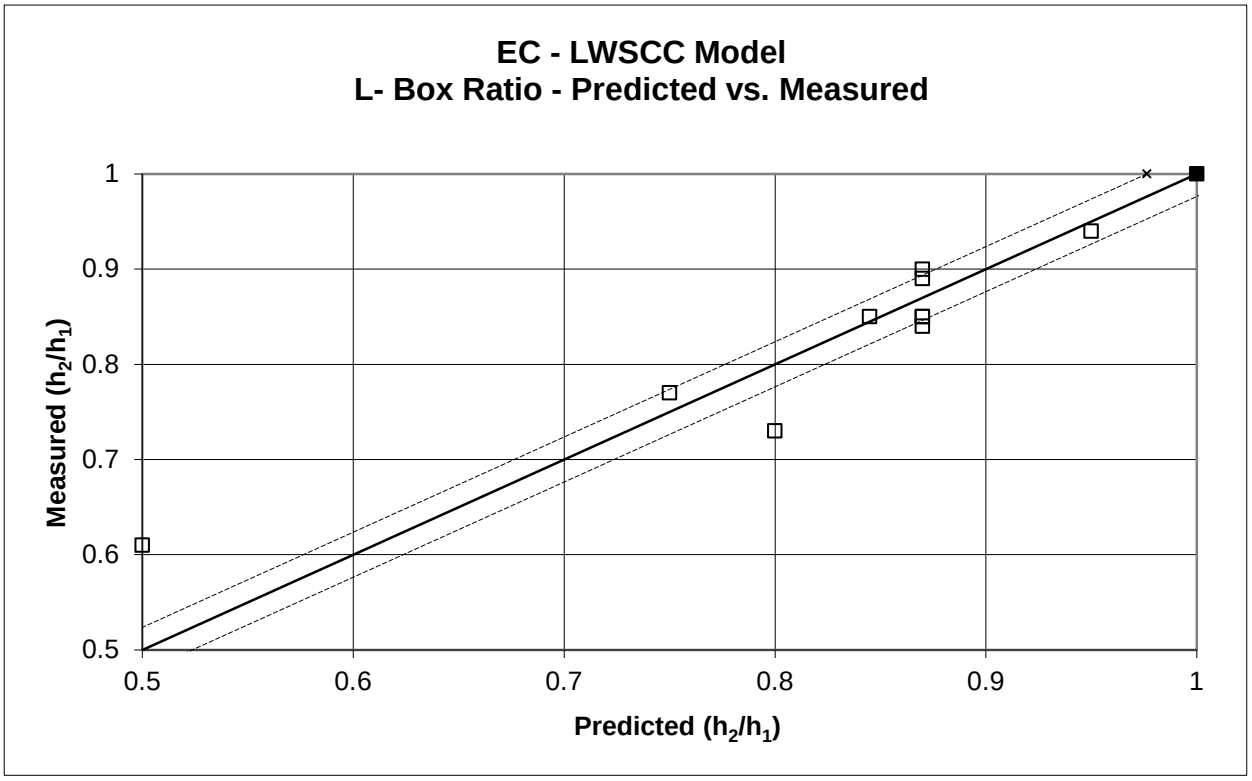

Predicted vs. measured L-box values of EC-LWSCC model

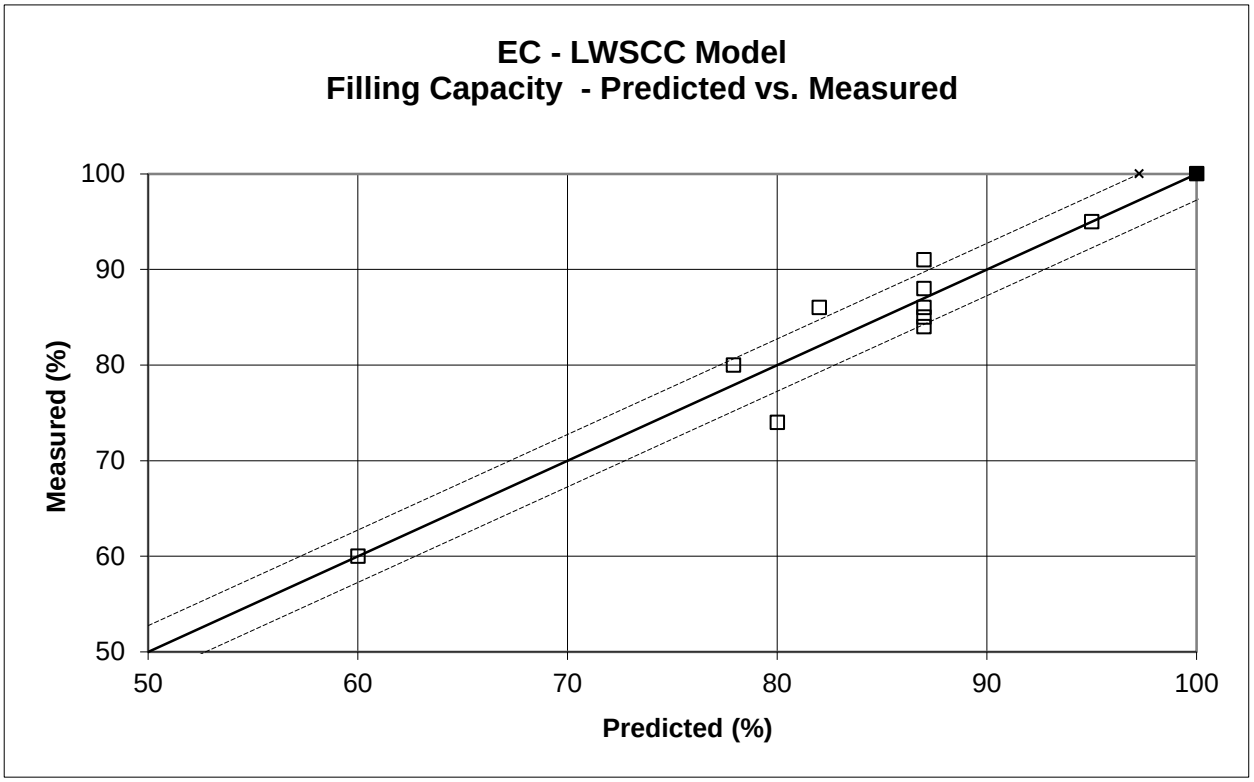

Predicted vs. measured filling capacity values of EC-LWSCC model

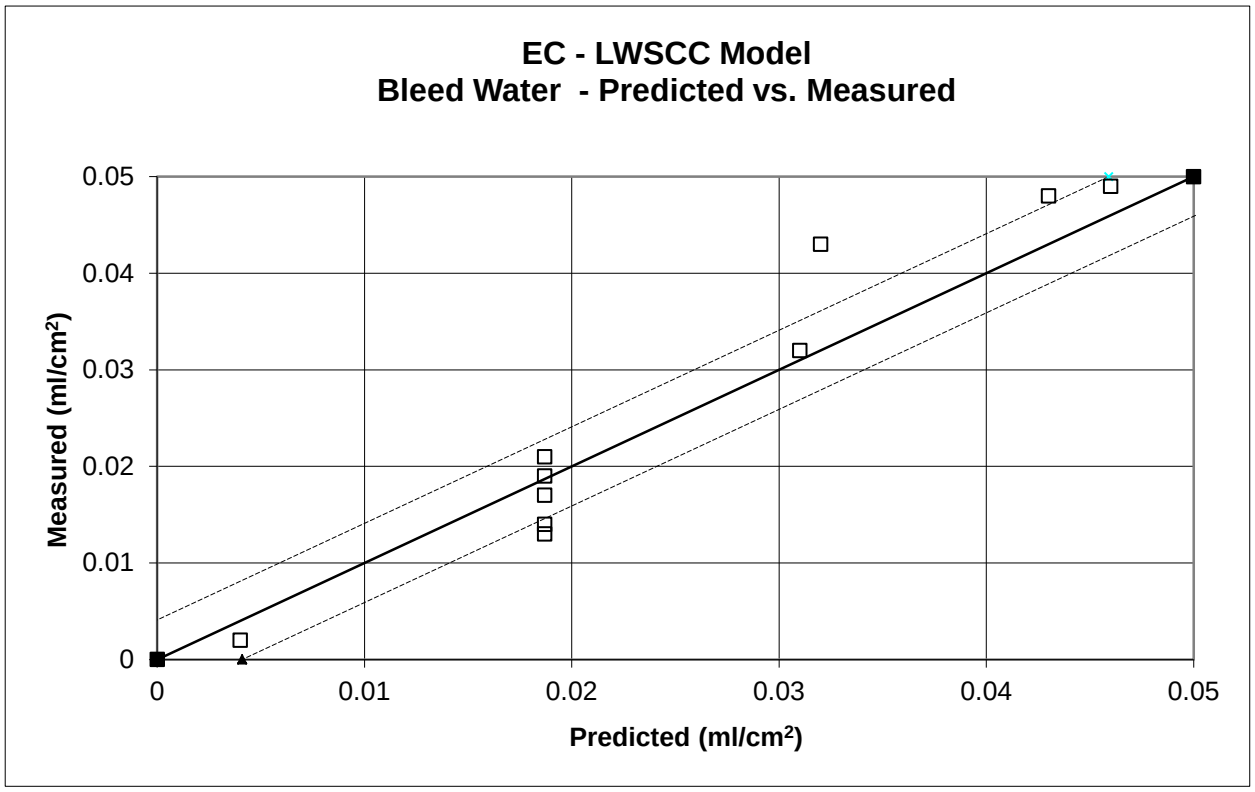

Predicted vs. measured bleed water values of EC-LWSCC model

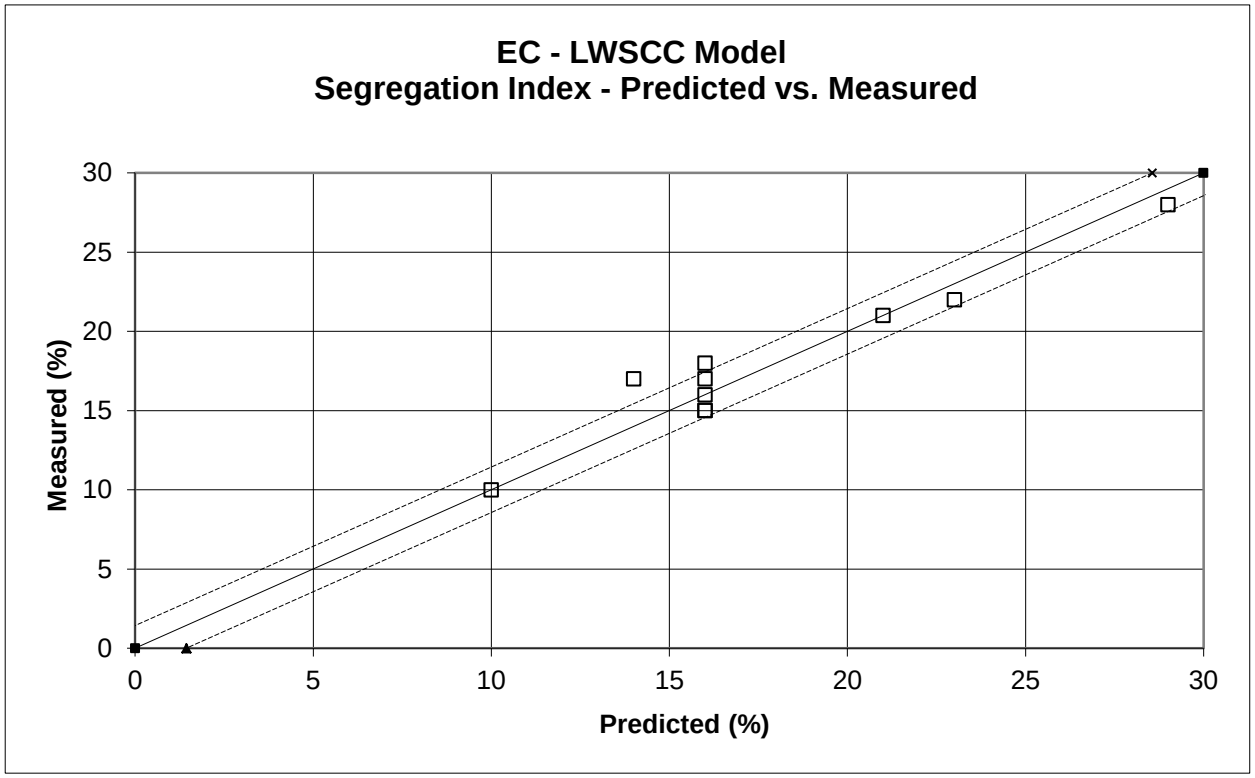

Predicted vs. measured segregation index values of EC-LWSCC model

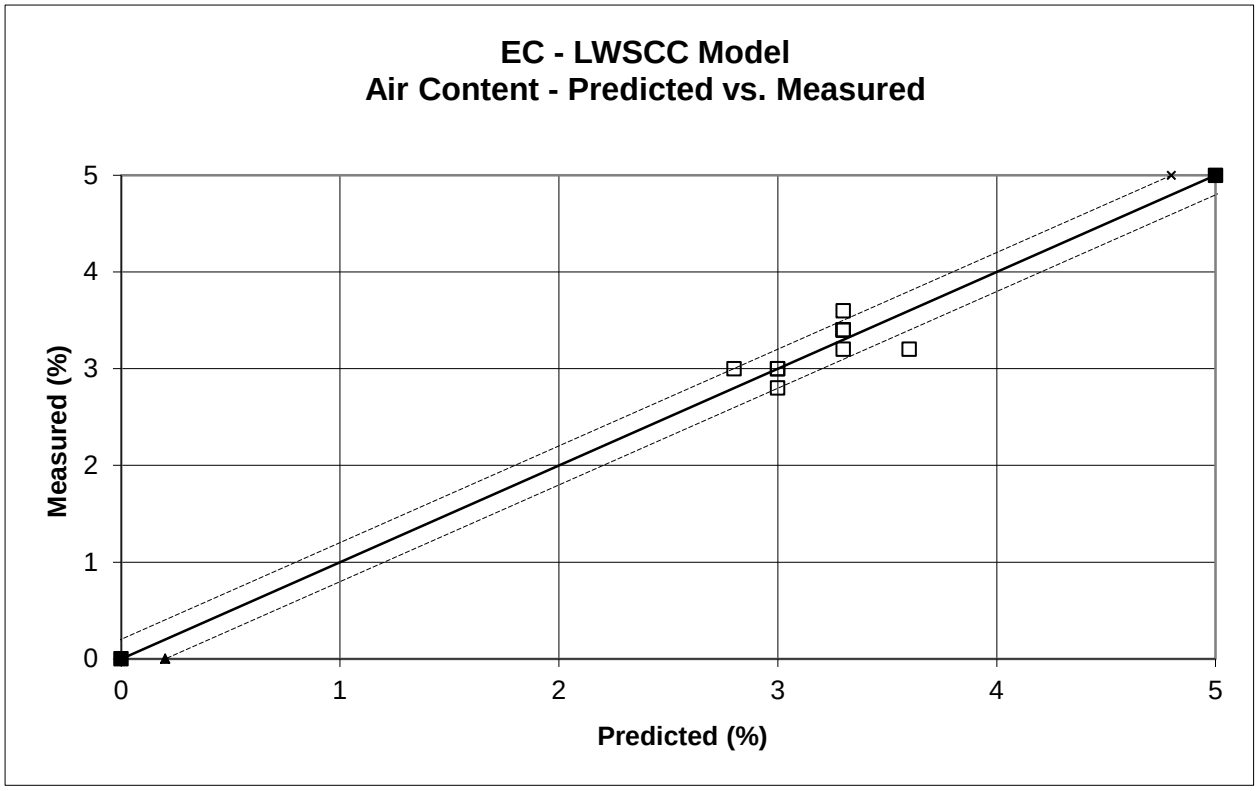

Predicted vs. measured air content values of EC-LWSCC model

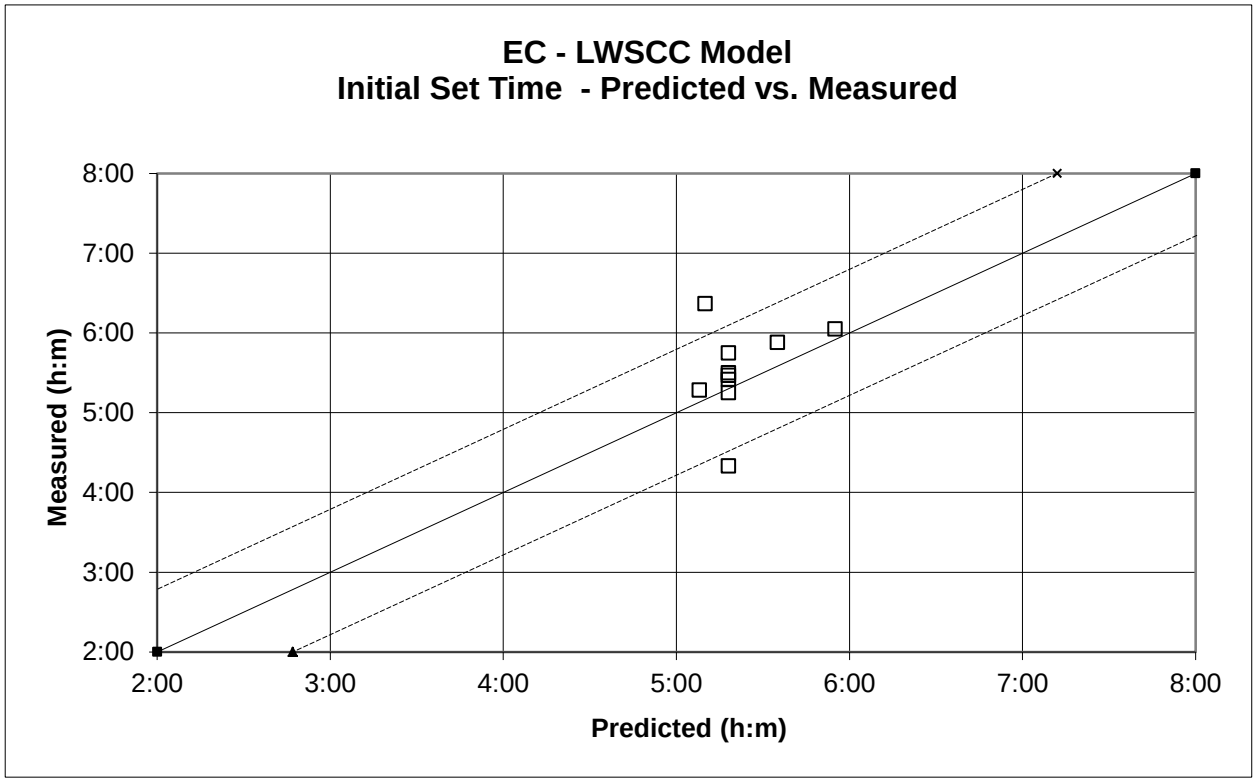

Predicted vs. measured initial set time values of EC-LWSCC model

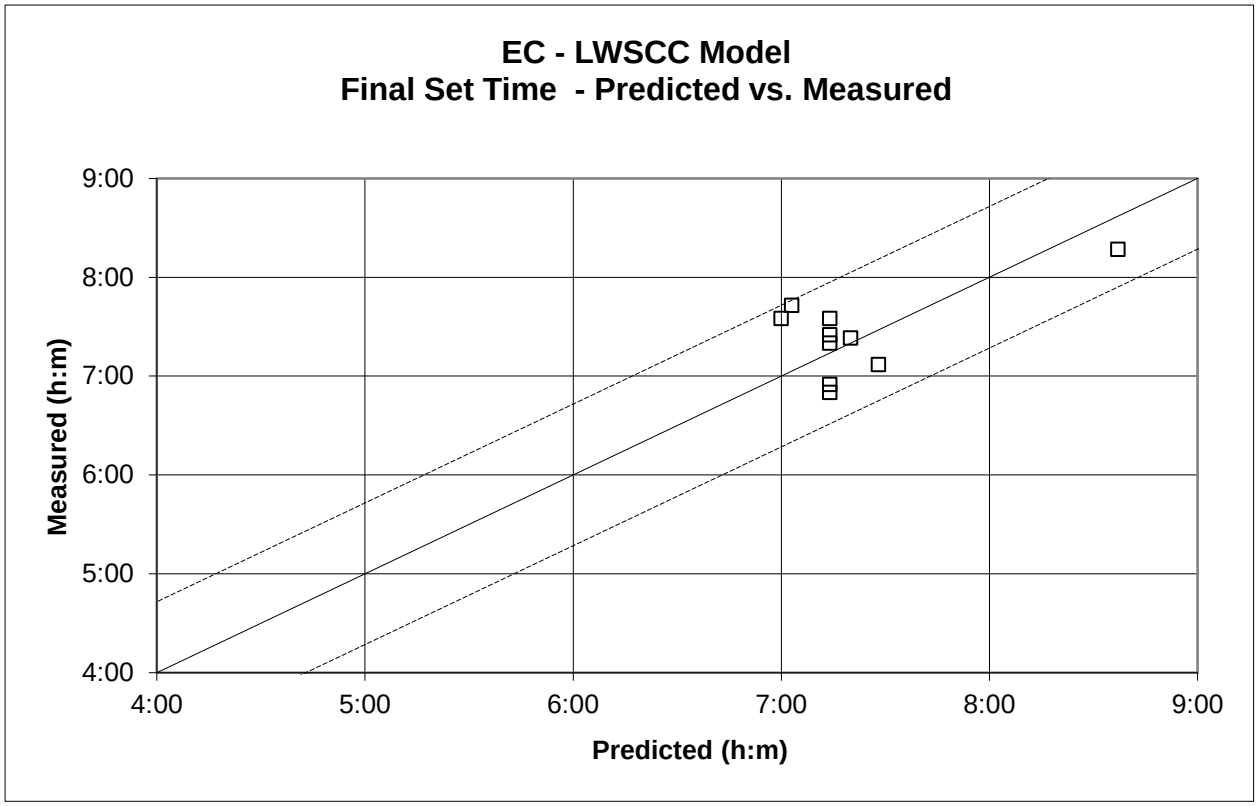

Predicted vs. measured final set time values of EC-LWSCC model

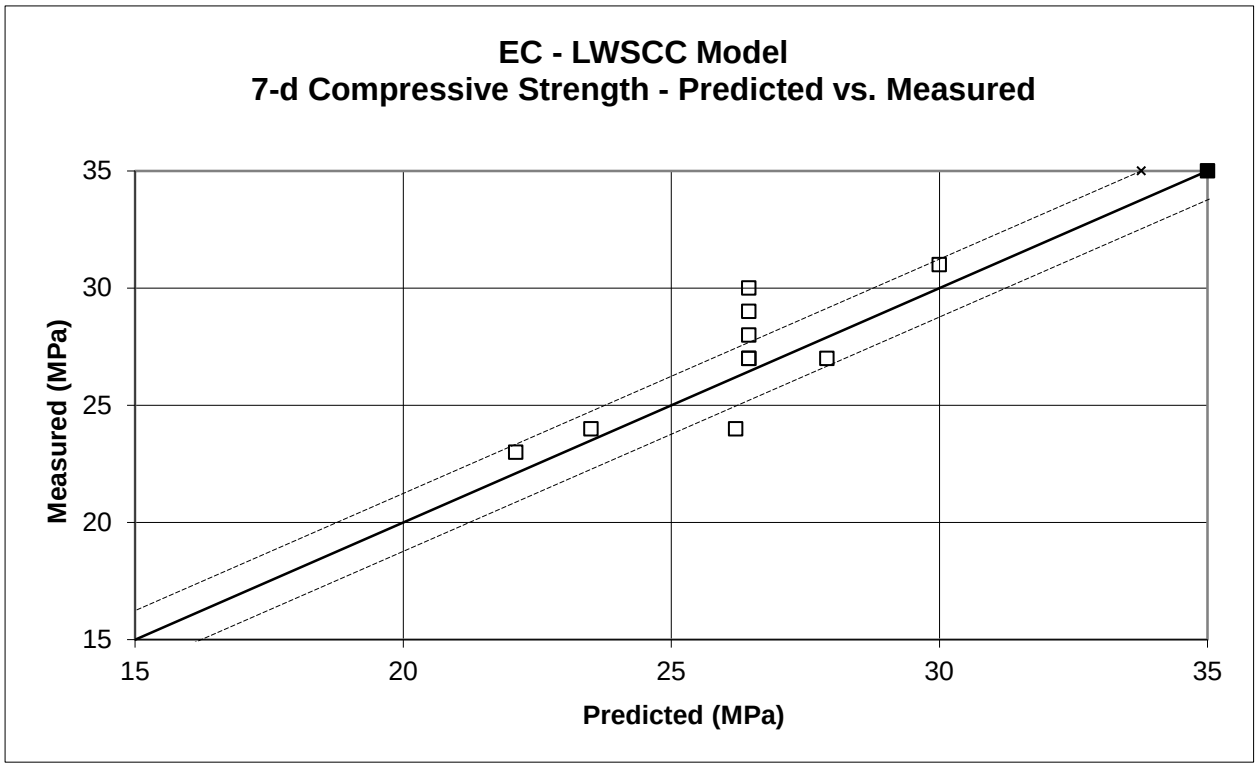

Predicted vs. measured 7d compressive strength of EC-LWSCC model

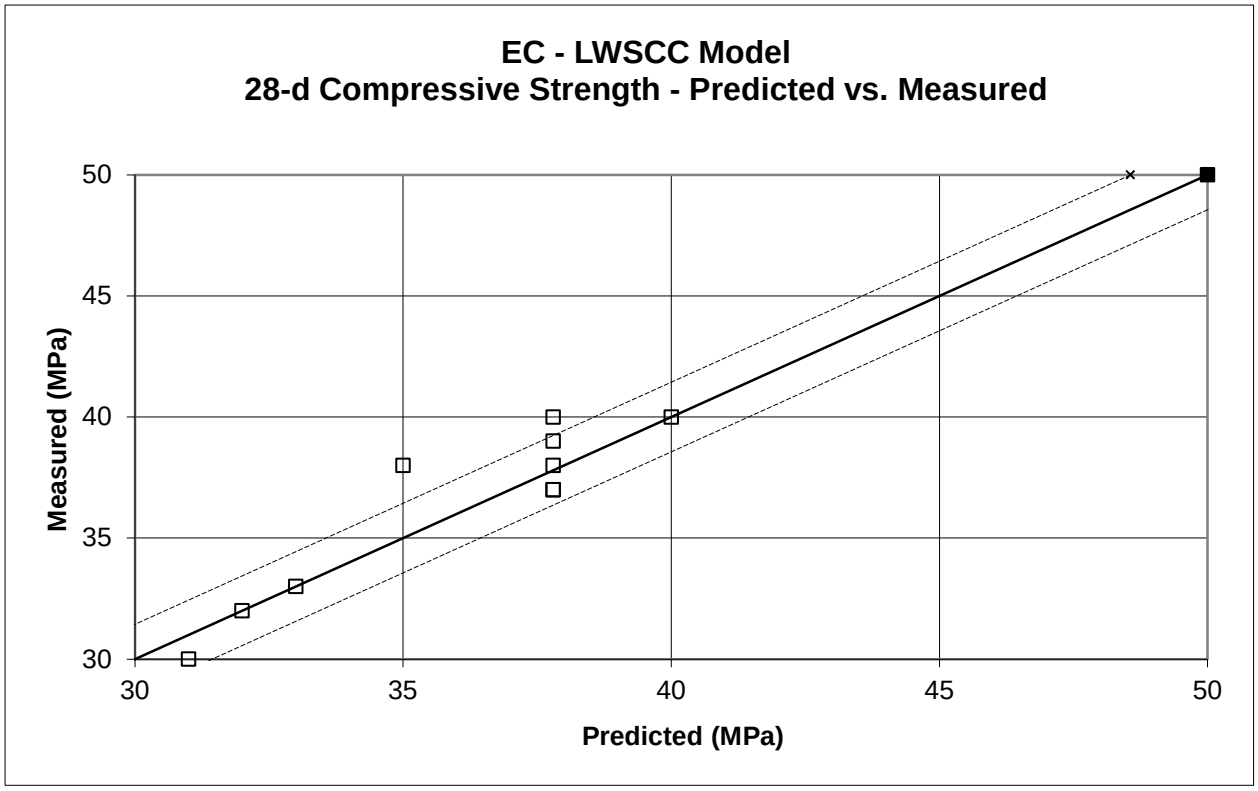

Predicted vs. measured 28d compressive strength of EC-LWSCC model

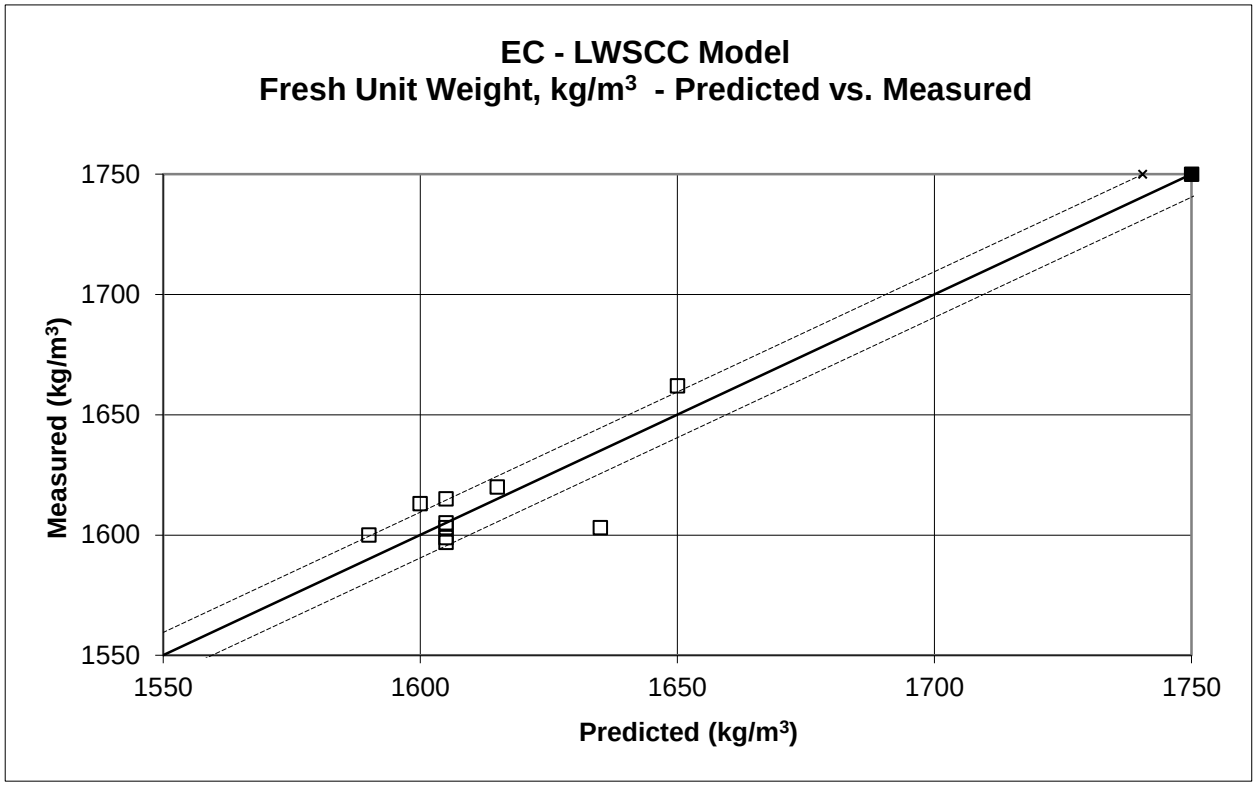

Predicted vs. measured fresh unit weight of EC-LWSCC model

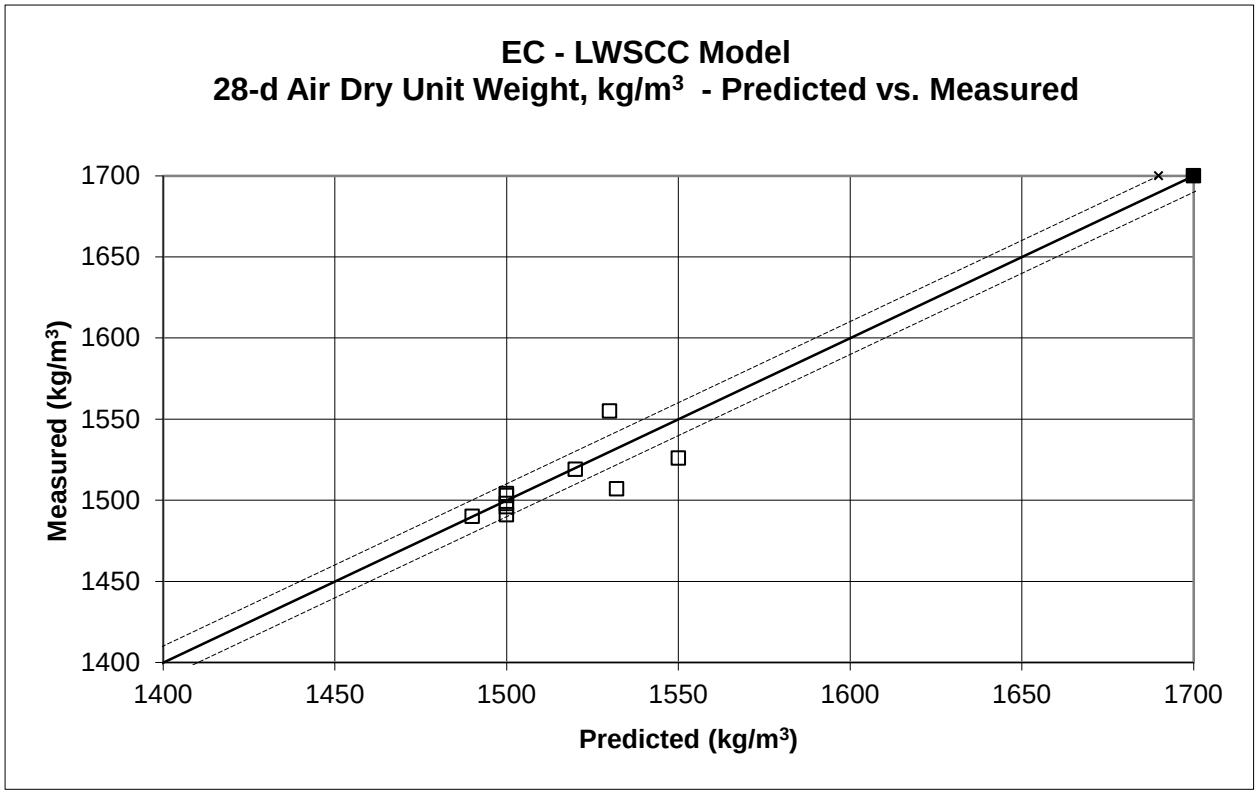

Predicted vs. measured 28d air dry unit weight of EC-LWSCC model

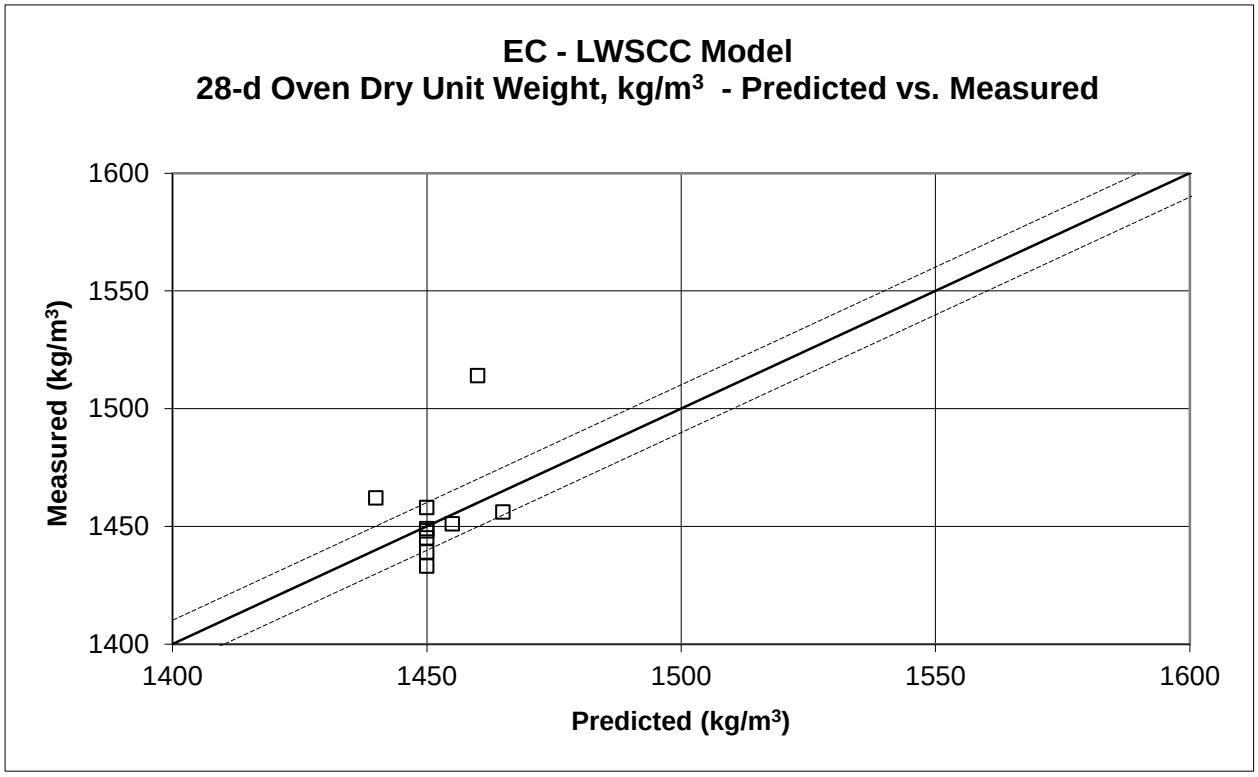

Predicted vs. measured 28d oven dry unit weight of EC-LWSCC mode

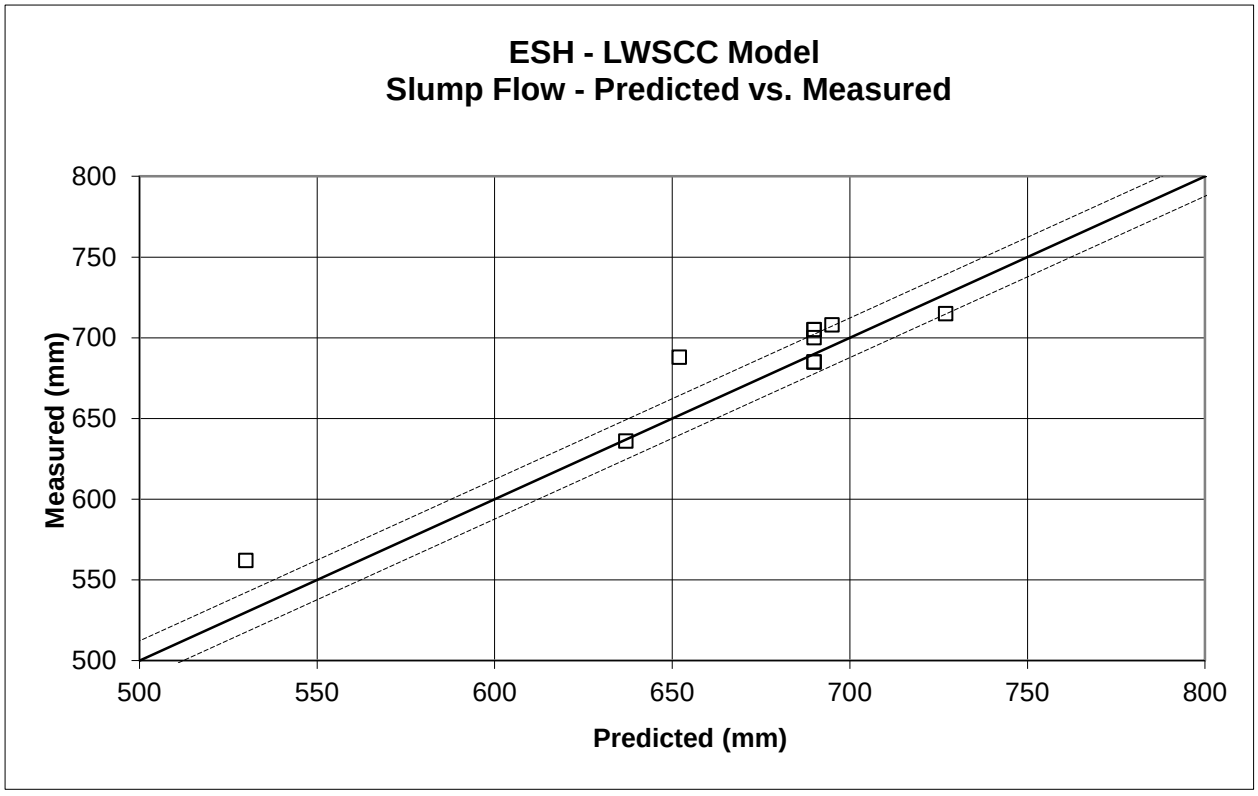

Predicted vs. measured slump flow values of ESH-LWSCC model

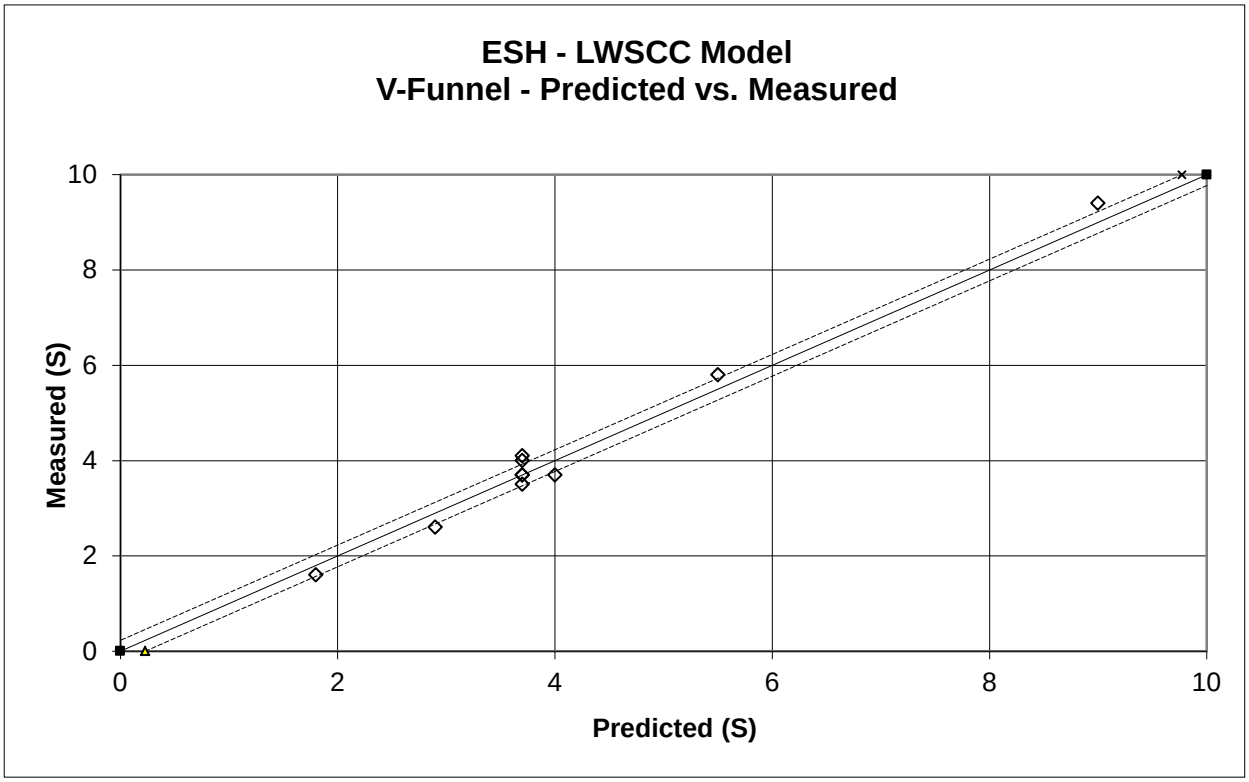

Predicted vs. measured V-funnel values of ESH-LWSCC model

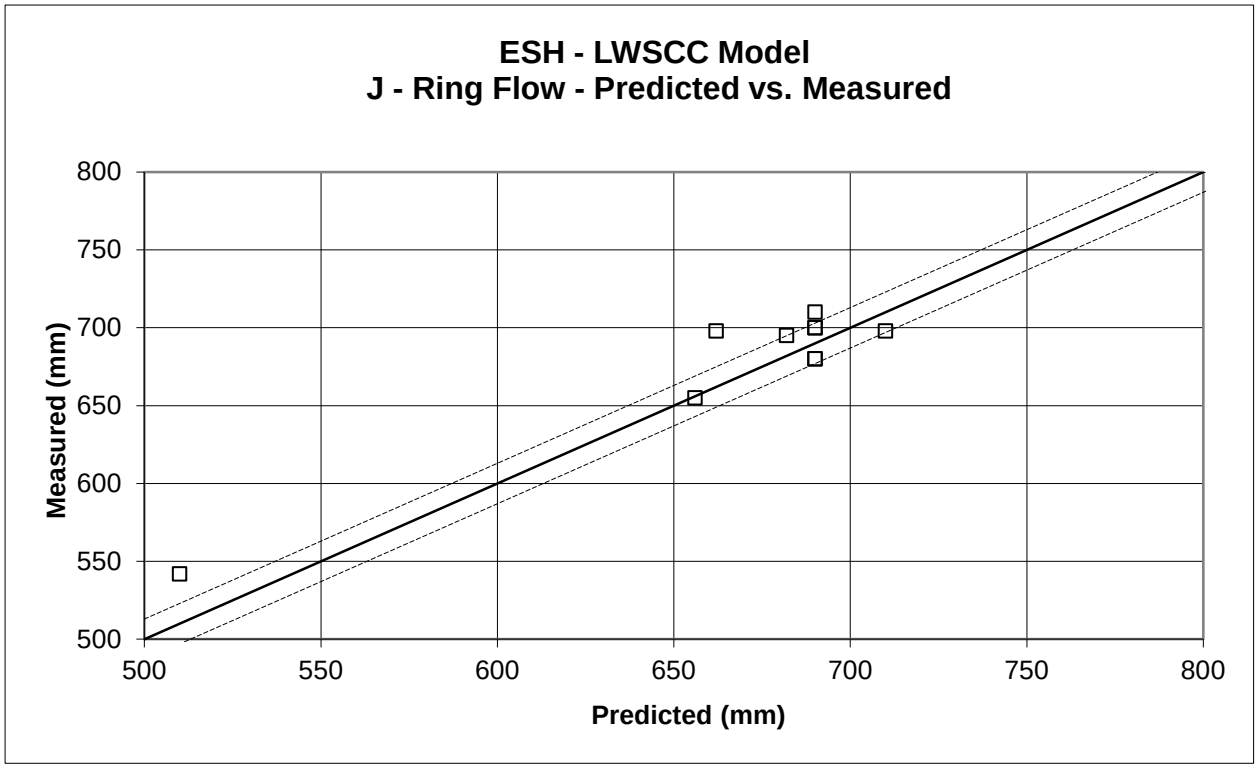

Predicted vs. measured J-ring values of ESH -LWSCC model

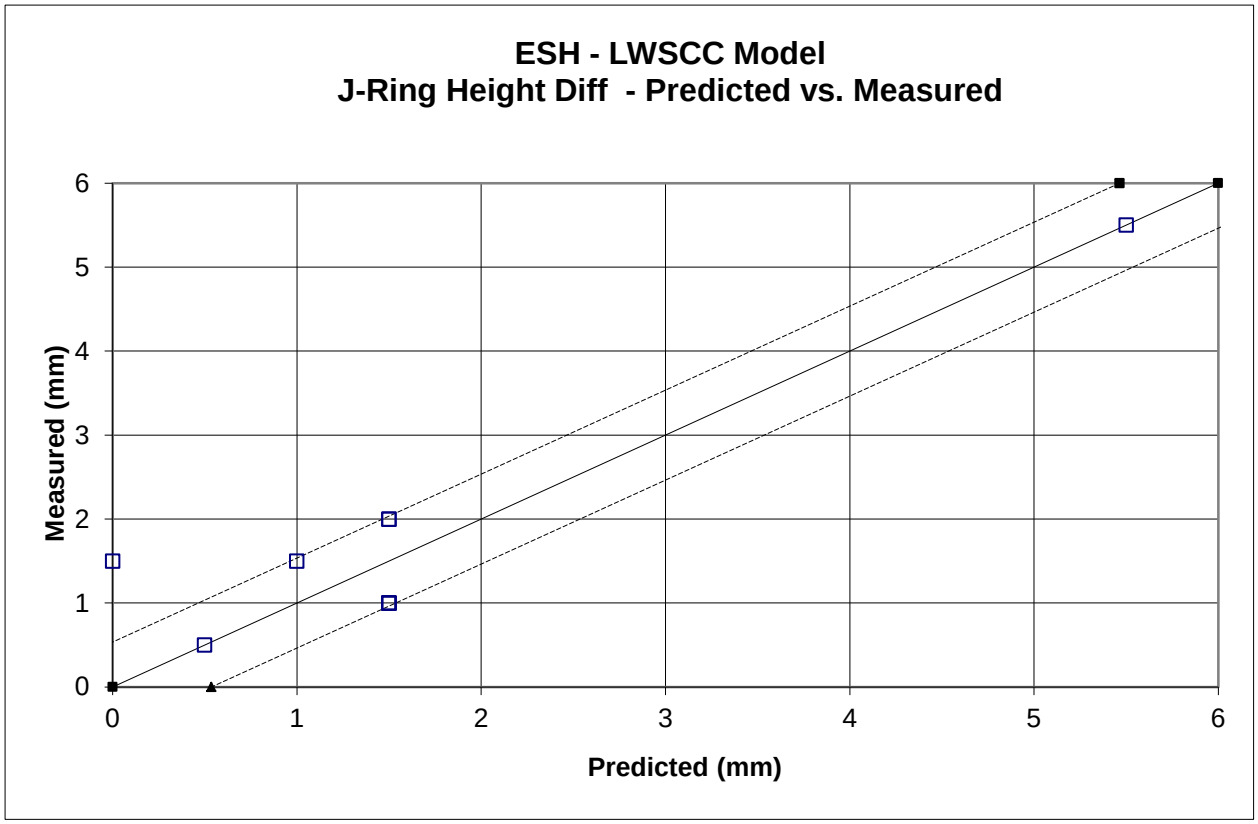

Predicted vs. measured J-ring height diff values of ESH-LWSCC model

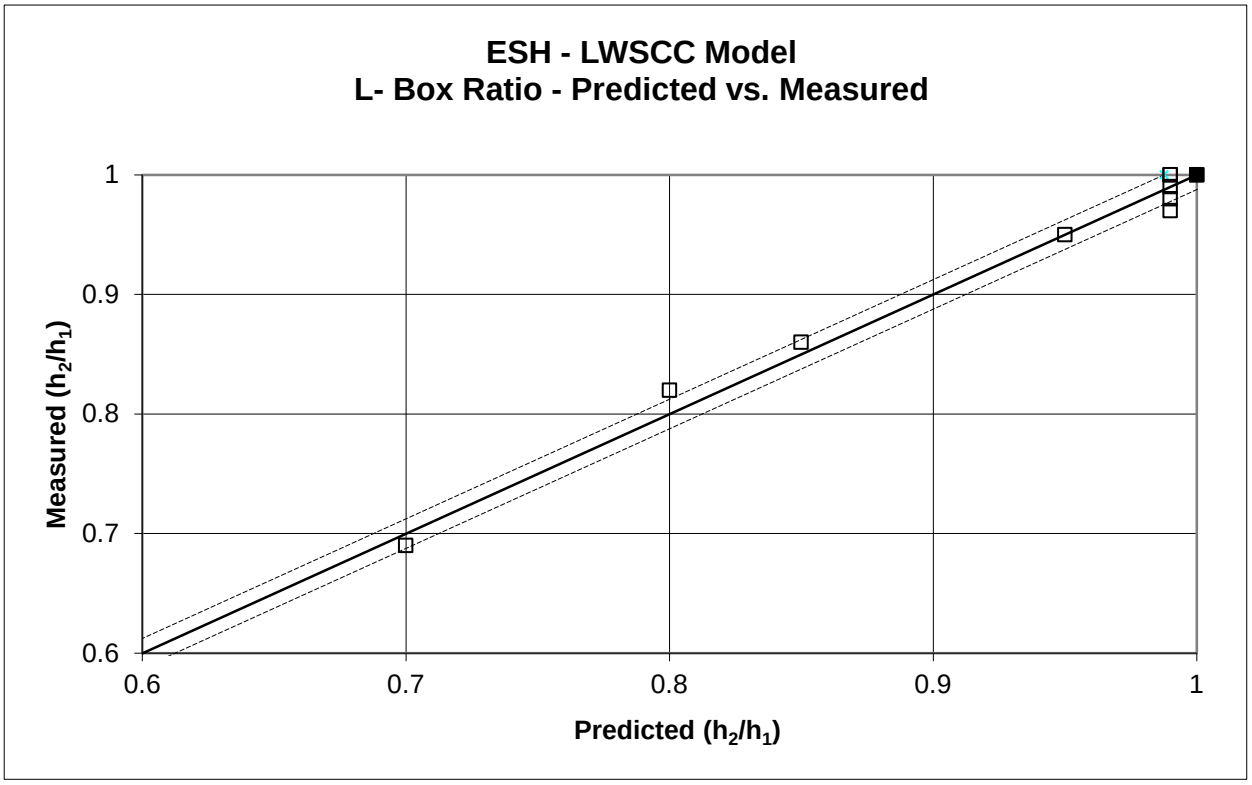

Predicted vs. measured L-box values of ESH -LWSCC model

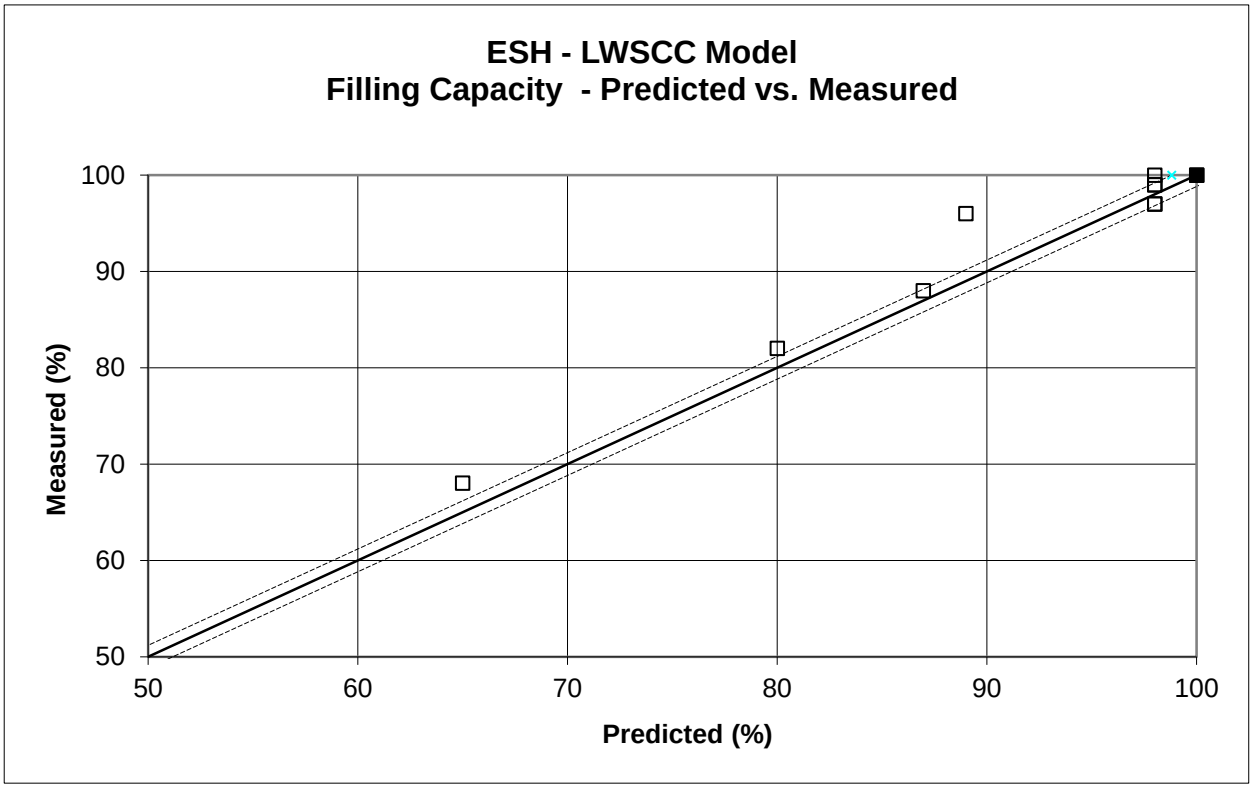

Predicted vs. measured filling capacity values of ESH-LWSCC model

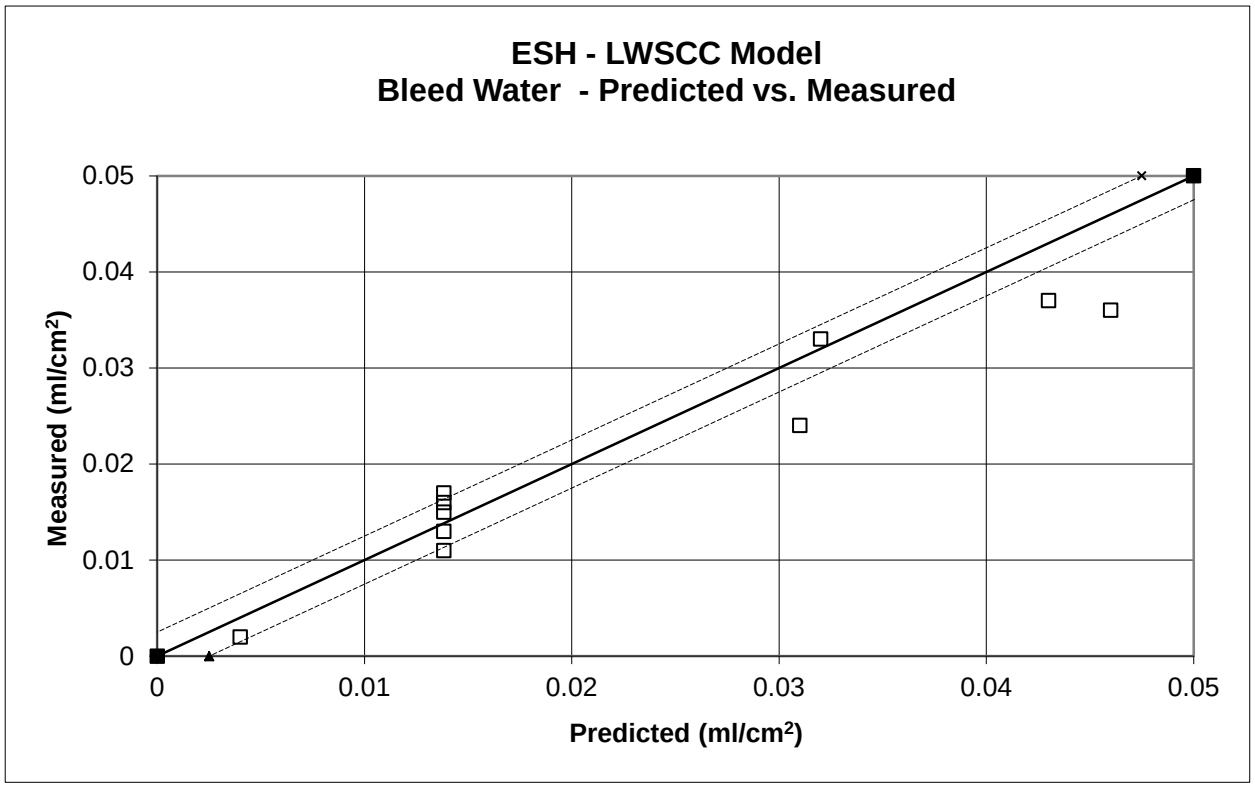

Predicted vs. measured bleed water values of ESH-LWSCC model

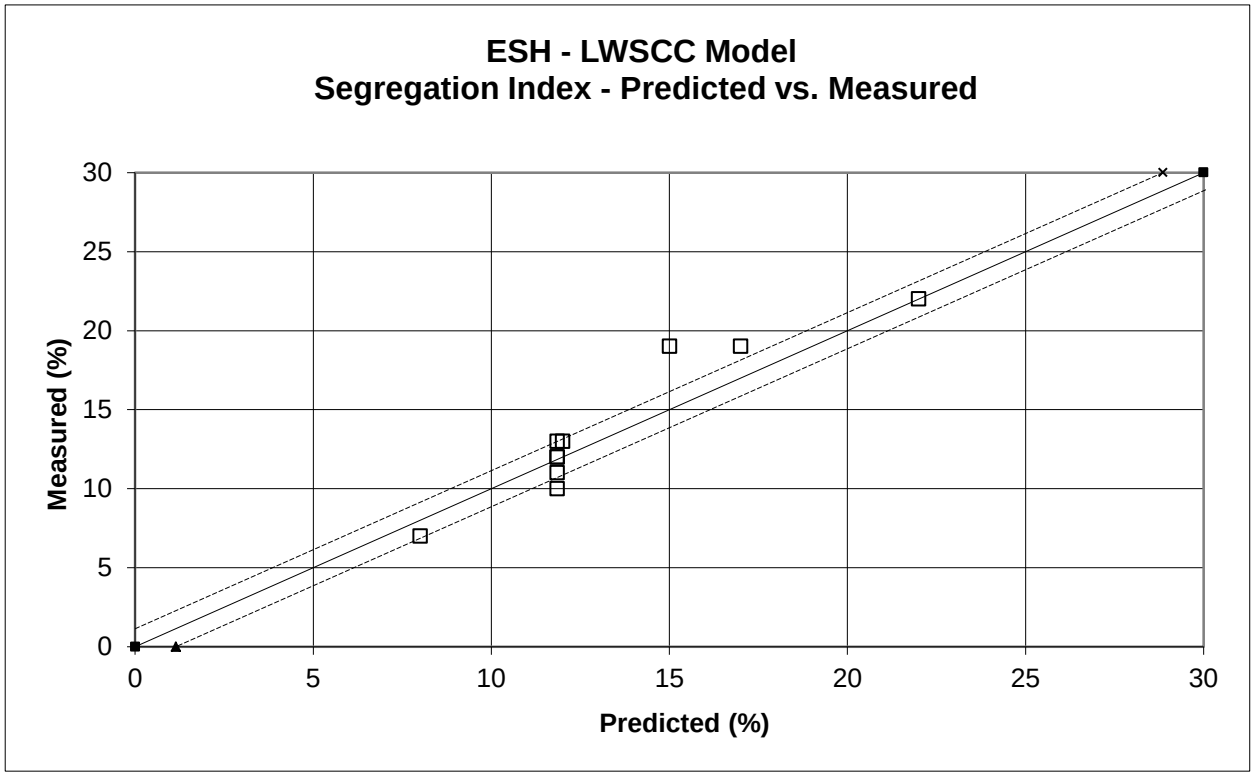

Predicted vs. measured segregation index values of ESH-LWSCC model

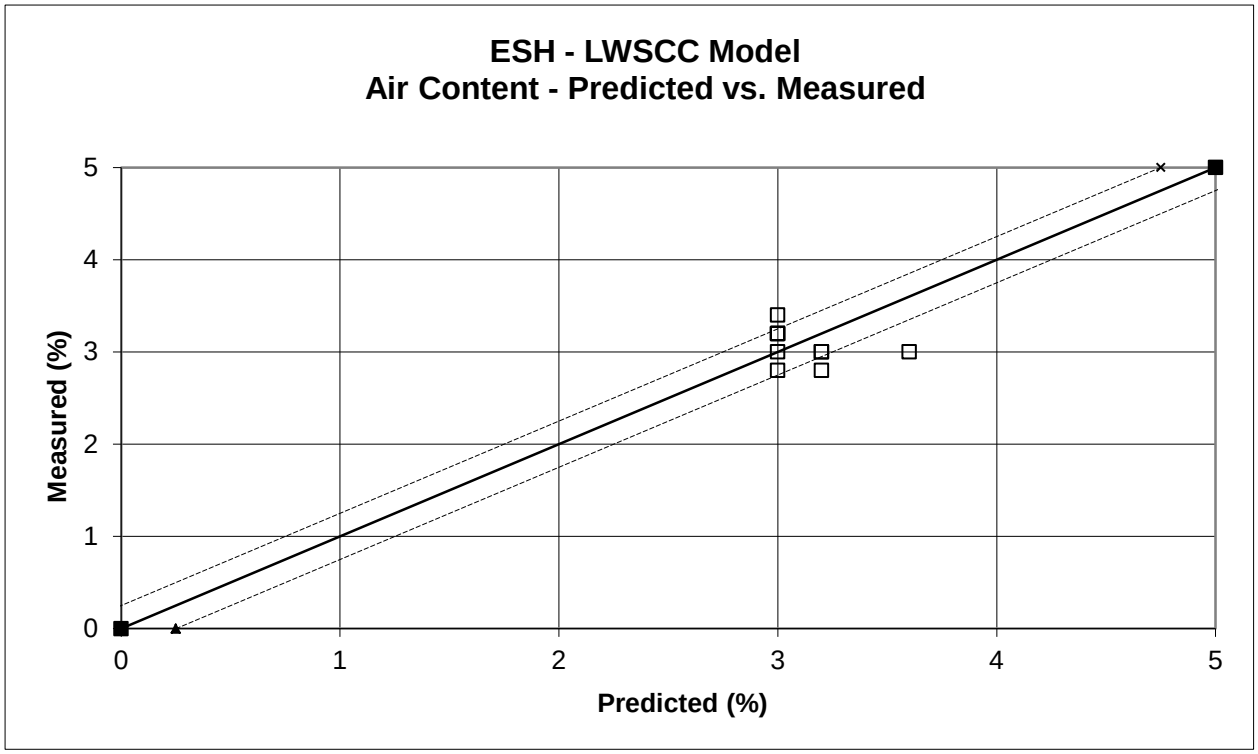

Predicted vs. measured air content values of ESH-LWSCC model

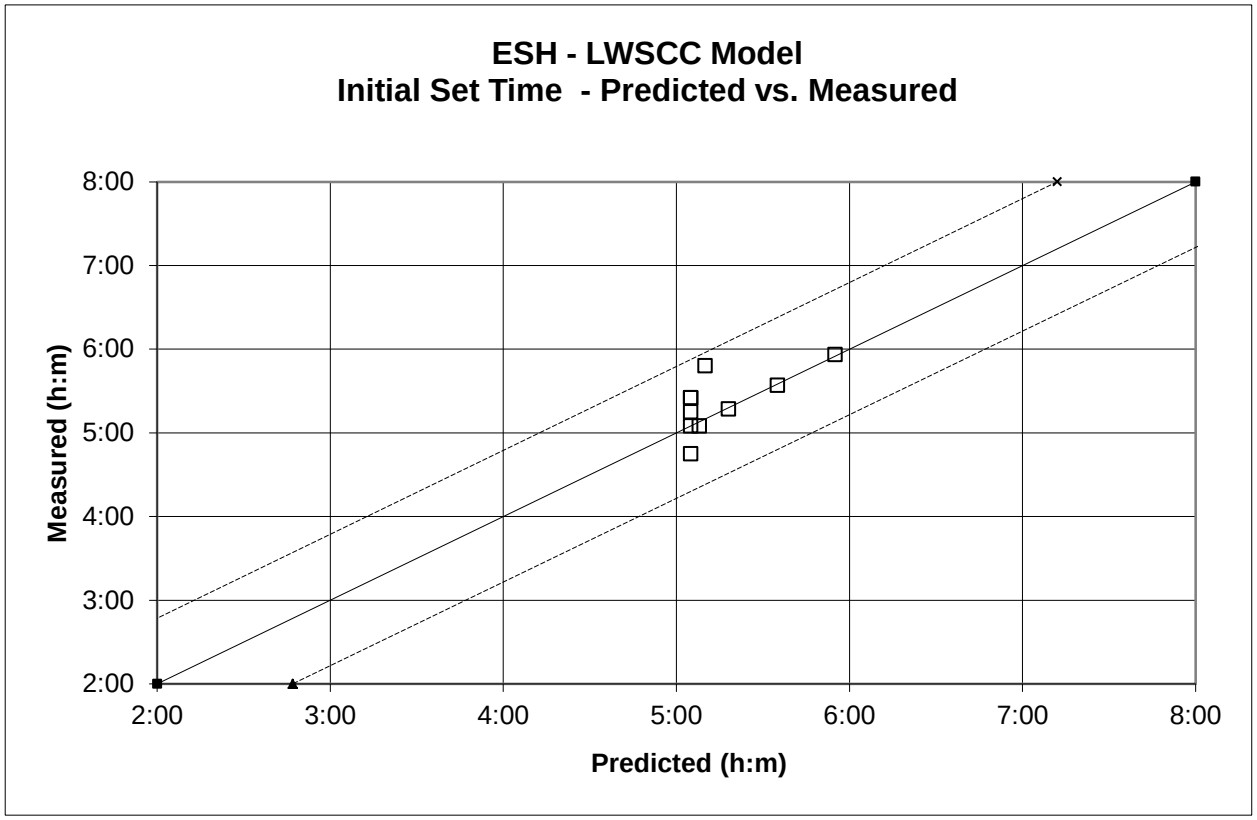

Predicted vs. measured initial set time values of ESH-LWSCC model

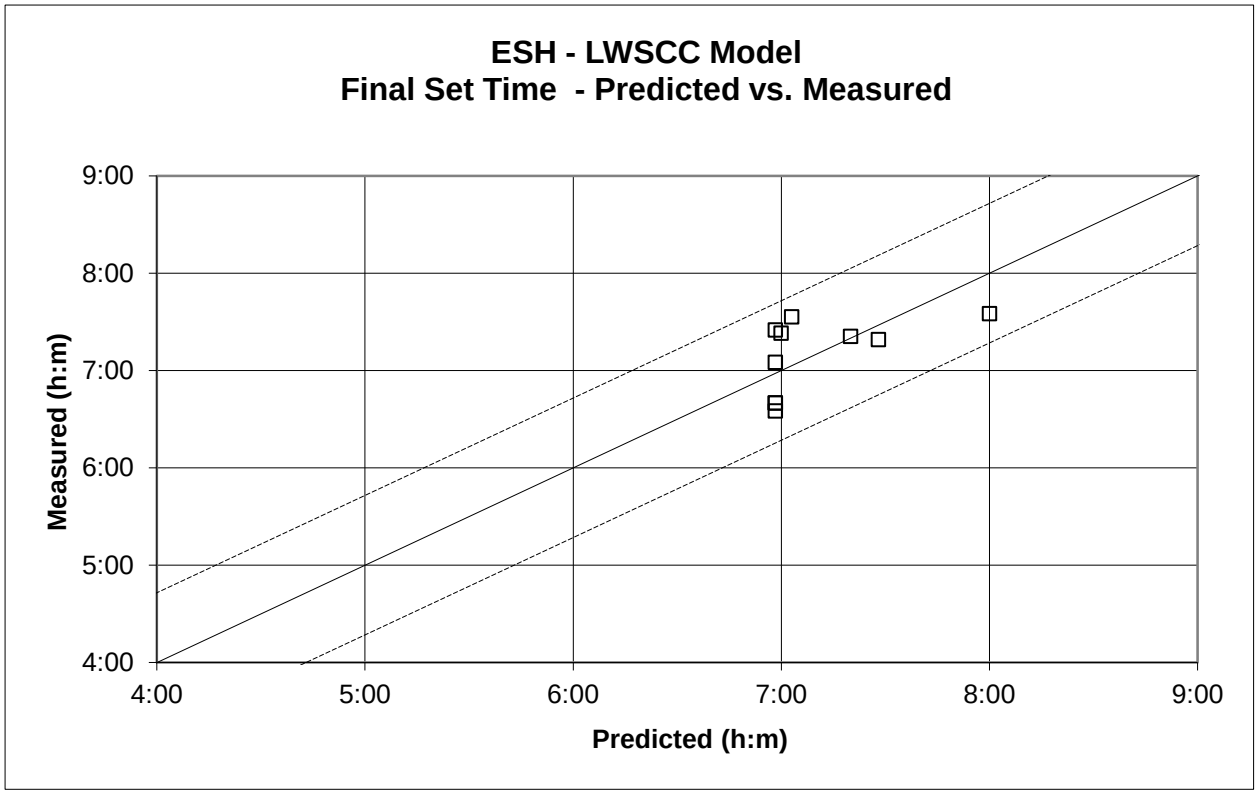

Predicted vs. measured final set time values of ESH-LWSCC model

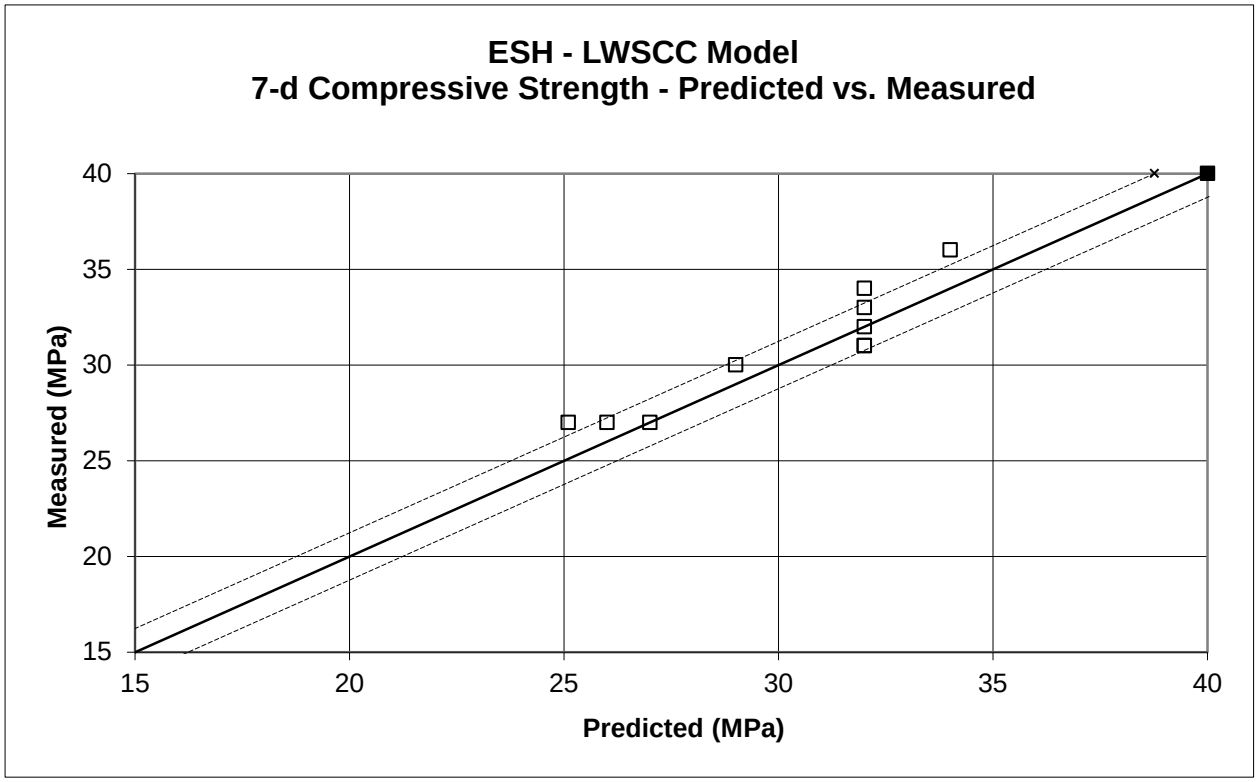

Predicted vs. measured 7d compressive strength of ESH-LWSCC model

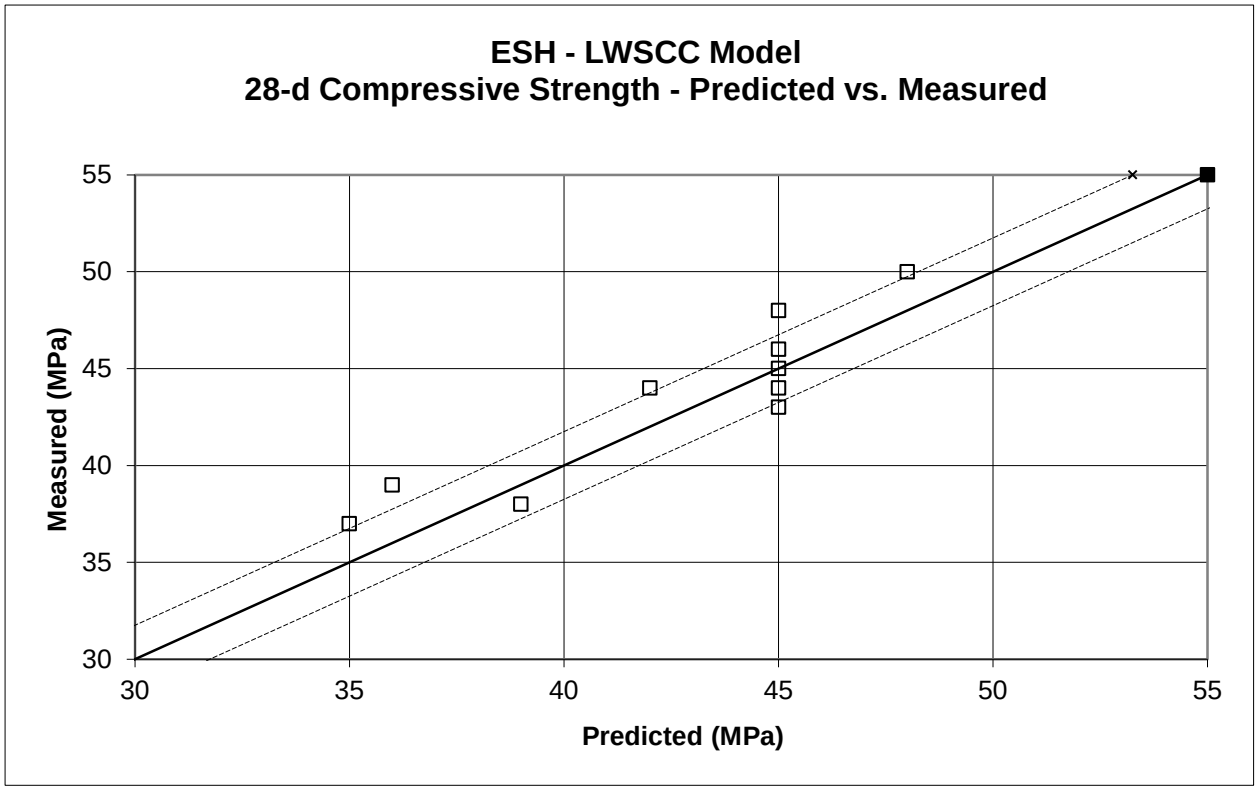

Predicted vs. measured 28d compressive strength of ESH-LWSCC model

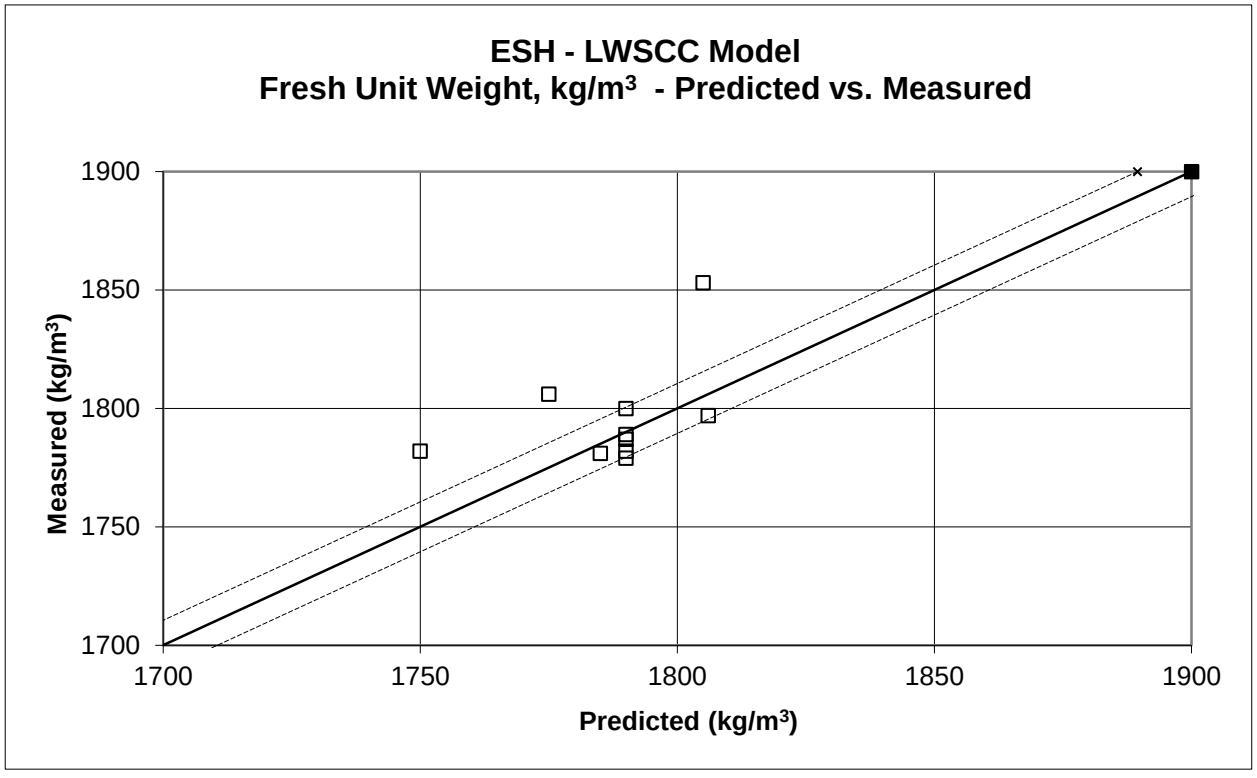

Predicted vs. measured fresh unit weight of ESH-LWSCC model

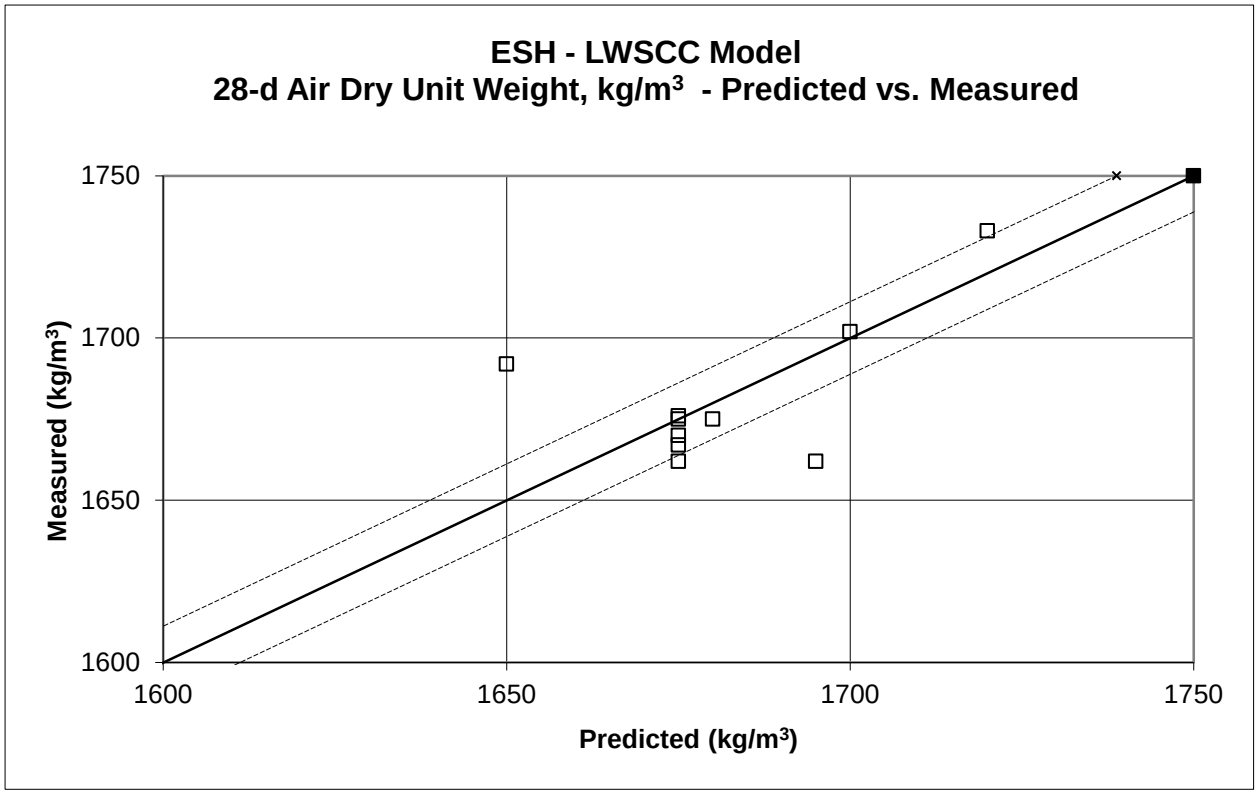

Predicted vs. measured 28d air dry unit weight of ESH-LWSCC model

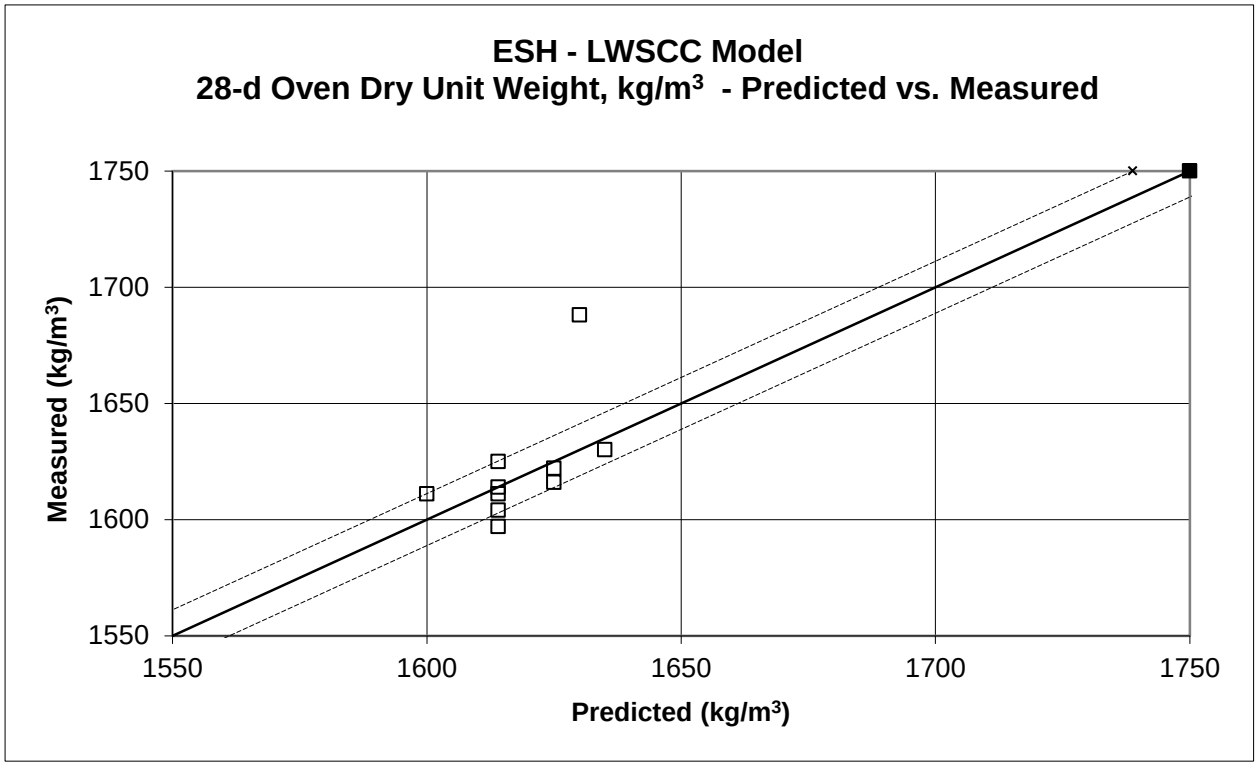

Predicted vs. measured 28d oven dry unit weight of ESH-LWSCC model

REFERENCES

ACI Committee 437, (2007), “Test Load Magnitude, Protocol and Acceptance Criteria”, American Concrete Institute, Farmington Hills, Michigan, U.S.A, pp. 83.

ACI Committee 363, (1998), “Guide to Quality Control and Testing of High-Strength Concrete”, American Concrete Institute, Farmington Hills, Michigan, U.S.A.

ACI Committee 318, (2002) “Building Code Requirements for Structural Concrete”, American Concrete Institute, Farmington Hills, Michigan, U.S.A.

ACI Committee 318, (2008), “Building Code Requirements for Structural Concrete”, American Concrete Institute, Farmington Hills, Michigan, U.S.A. pp. 151.

ACI Committee 318, (2011), “Building Code Requirements for Structural Concrete”, American Concrete Institute, Farmington Hills, Michigan, U.S.A. pp. 151.

ACI Committee 237R, (2007), “Self-Consolidating Concrete”, American Concrete Institute, Farmington Hills, Michigan, U.S.A. pp.30.

ACI Committee 234R, (1996), “Guide for the Use of Silica Fume in Concrete”, American Concrete Institute, Farmington Hills, Michigan, U.S.A. pp.1-2.

ACI Committee 221R, (2001), “Guide for Use of Normal Weight and Heavyweight Aggregates in Concrete”, American Concrete Institute, pp. 29.

ACI Committee 213R, (2003), “Guide for Structural Lightweight-Aggregate Concrete”, American Concrete Institute Farmington Hills, Michigan, U.S.A. pp.38.

ACI Committee 213, (1987), “Guide for Structural Lightweight-Aggregate Concrete”, American Concrete Institute, Farmington Hills, Michigan, U.S.A. pp 27.

ACI Committee 211.2, (1998), “Standard Practice for Selecting Proportions for Structural Lightweight Concrete”. American Concrete Institute, Farmington Hills, Michigan, U.S.A. pp. 18.

ACI Committee 209, (1997), “Prediction of Creep, Shrinkage, and Temperature effects in Concrete Structures.” American Concrete Institute, Farmington Hills, Michigan, U.S.A. pp. 47.

Aggarwal, P., Siddique, R., Aggarwal, Y., and Gupta, M.S., (2008), “Self-Compacting Concrete - Procedure for Mix Design”, Leonardo Electronic Journal of Practices and Technologies, ISSN 1583-1078, Issue. 12, pp. 15-24.

Aitcin, P.C., and Neville, A.M., (1993), “High Performance Concrete Demystified”, Concrete International, Vol. 15, No. 1, pp. 21-26.

Amleh, L., (2000), “Bond Deterioration of Reinforcing Steel in Concrete Due to Corrosion”, A thesis submitted to the Faculty of Graduate Studies and Research in partial fulfillment of requirements for the degree of Doctor of Philosophy, McGill University, Montreal, Canada.

ASTM C1621 / C1621 M, (2009) “Standard Test Method for Passing Ability of Self-Consolidating Concrete by J-Ring”, American Society for Testing and Materials, West Conshohocken, Pennsylvania, U.S.A.

ASTM C1611 / C1611 M, (2009), “Standard Test Method for Slump Flow of Self-Consolidating Concrete”, American Society for Testing and Materials, West Conshohocken, Pennsylvania, U.S.A.

ASTM C1585, (2011), “Standard Test Method for Measurement of Rate of Absorption of Water by Hydraulic-Cement Concretes”, Cement Standards and Concrete Standards, Book of Standards Volume: 04.02, pp. 1-6.

ASTM C1202, (2010), “Standard Test Method for Electrical Indication of Concrete’s Ability to Resist Chloride Ion Penetration”, American Society for Testing and Materials, West Conshohocken, Pennsylvania, U.S.A.

ASTM C900, (2006), “Standard Test Method for Pullout Strength of Hardened Concrete”, Cement Standards and Concrete Standards, pp. 1-10.

ASTM C672, (2003), “Standard Test Method for Scaling Resistance of Concrete Surfaces Exposed to Deicing Chemicals”, (Withdrawn 2012).

ASTM C666/ C666 M, (2008), “Standard Test Method for Resistance of
Concrete to Rapid Freezing and Thawing”, West Conshohocken, Pennsylvania, U.S.A, pp. 1-6.

ASTM C642, (2006) “Standard Test Standard Test Method for Density, Absorption, and Voids in Hardened Concrete”, American Society for Testing and Materials, West Conshohocken, Pennsylvania, U.S.A.

ASTM C618, (2008), “Standard Specification for Coal Fly Ash and Raw or Calcined Natural Pozzolan for Use in Concrete”, Cement Standards and Concrete Standards, pp. 1-3.

ASTM C567, (2011), “Standard Test Method for Determining Density of Structural Lightweight Concrete”, Cement Standards and Concrete Standards, pp. 1-3.

ASTM C512 / C512 M, (2010) “Standard Test Method for Creep of Concrete in Compression,” American Society for Testing and Materials, West Conshohocken, Pennsylvania, U.S.A.

ASTM C496 / C496 M, (2011), “Standard Test Method for Splitting Tensile Strength of Cylindrical Concrete Specimens”, American Society for Testing and Materials, West Conshohocken, Pennsylvania, U.S.A.

ASTM C494, (2011), “Standard Specification for Chemical Admixtures for Concrete, Cement Standards and Concrete Standards, pp. 1-10.

ASTM C469 / C469 M, (2011), “Standard Test Method for Static Modulus of Elasticity and Poisson’s Ratio of Concrete in Compression,” American Society for Testing and Materials, West Conshohocken, Pennsylvania, U.S.A.

ASTM C457, (2011), “Standard Test Method for Microscopical Determination of Parameters of the Air-Void System in Hardened Concrete”, American Society for Testing and Materials, West Conshohocken, Pennsylvania, U.S.A.

ASTM C403 / C403 M, (2008) “Standard Test Method for Time of Setting of Concrete Mixtures by Penetration Resistance”, West Conshohocken, Pennsylvania, U.S.A, pp. 1-6.

ASTM C267, (2006), “Standard Test Methods for Chemical Resistance of Mortars, Grouts, and Monolithic Surfacings and Polymer Concretes”, Masonry Standards, pp. 1-6.

ASTM C330, (2009), “Standard Specification for Lightweight Aggregates for Structural Concrete”, Cement Standards and Concrete Standards, pp. 1-4.

ASTM C232 / C232M, (2009), “Standard Test Methods for Bleeding of Concrete”, American Society for Testing and Materials, West Conshohocken, Pennsylvania, U.S.A.

ASTM C231 / C231M, (2010), “Standard Test Method for Air Content of Freshly Mixed Concrete by the Pressure Method”, American Society for Testing and Material, West Conshohocken, Pennsylvania, U.S.A.

ASTM C215 / C215M, (2008), “Standard Test Method for Fundamental Transverse, Longitudinal, and Torsional Resonant Frequencies of Concrete Specimens”, American Society for Testing and Materials, West Conshohocken, Pennsylvania, U.S.A. pp. 1-7.

ASTM C173 / C173M, (2010), “Standard Test Method for Air Content of Freshly Mixed Concrete by the Volumetric Method”, Cement Standards and Concrete Standards, Book of Standards Volume: 04.02, pp. 1-8.

ASTM C157 / C157M, (2008), “Standard Test Method for Length Change of Hardened Hydraulic-Cement Mortar and Concrete,” American Society for Testing and Materials, West Conshohocken, Pennsylvania, U.S.A. pp. 1-7.

ASTM C143 / C143M, (2010), “Standard Test Method for Slump of Hydraulic Cement Concrete”, American Society for Testing and Materials, West Conshohocken, Pennsylvania, U.S.A. pp. 1-4.

ASTM C138 / C138M, (2010), “Standard Test Method for Density (Unit Weight), Yield, and Air Content (Gravimetric) of Concrete”, Cement Standards and Concrete Standards, pp.1-4.

ASTM C127, (2007) “Standard Test Method for Density, Relative Density (Specific Gravity), and Absorption of Coarse Aggregate”, Cement Standards and Concrete Standards, pp.1-6.

ASTM C128, (2007), “Standard Test Method for Density, Relative Density (Specific Gravity), and Absorption of Fine Aggregate”, Cement Standards and Concrete Standards, pp.1-7.

ASTM C78 / C78M, (2010), “Standard Test Method for Flexural Strength of Concrete (Using Simple Beam with Third-Point Loading)”, Cement Standards and Concrete Standards, pp. 1-4.

ASTM C39 / C39M, (2011), “Standard Test Method for Compressive Strength of Cylindrical Concrete Specimens”, American Society for Testing and Materials, West Conshohocken, Pennsylvania, U.S.A. pp. 1-7.

ASTM C29, (2009), “Standard Test Method for Bulk Density ("Unit Weight") and Voids in Aggregate”, Cement Standards and Concrete Standards, pp. 1-5.

ASTM E119, (2012), “Standard Test Methods for Fire Tests of Building Construction and Materials”, Fire Standards and Flammability Standards, pp. 1-34.

ASTM G1, (2003), “Standard Practice for Preparing, Cleaning, and Evaluating Corrosion Test Specimens”, Corrosion Standards and Wear Standards, pp. 1-9.

Assaad, J.J., and Khayat, K.H., (2006), “Effect of Viscosity-Enhancing Admixtures on Formwork Pressure and Thixotropy of Self-Consolidating Concrete”, ACI Materials Journal, Vol. 103, Issue 4, pp. 280-287.

Assaad, J., and Khayat, K.H., (2004), “Assessment of Thixotropy of Self-Consolidating Concrete and Concrete-Equivalent-Mortar—Effect of Binder Composition and Content”, ACI Materials Journal, Vol. 101, Issue 5, pp. 400-408.

Assaad, J., Khayat, K. H., and Daczko, J., (2004), “Evaluation of Static Stability of Self-Consolidating Concrete,” ACI Materials Journal, Vol. 101, Issue 3, pp. 207-215.

Assaad, J., Khayat, K. H., and Mesbah, H., (2003), “Variations of Formwork Pressure with Thixotropy of Self-Consolidating Concrete,” ACI Materials Journal, Vol. 100, Issue 1, pp. 29-37.

Assaad, J., Khayat, K. H., and Mesbah, H., (2003), “Assessment of Thixotropy of Flowable and Self-Consolidating Concrete,” ACI Materials Journal, Vol. 100, Issue 2, pp. 99-107.

Aydin, S., and Baradan, B., (2007), “Effect of Pumice and Fly Ash Incorporation on High Temperature Resistance of Cement Based Mortars”, Cement and Concrete Research, Vol. 37, Issue. 6, pp. 988–995.

Bailey, J., Schindler, A., and Brown, D., (2005), “An Evaluation of the Use of Self-Consolidating Concrete (SCC) for Drilled Shaft Applications”, Auburn, Alabama, No. 1, pp. 4-18.

Bardhan-Roy, B.K., (1995), “Lightweight Aggregate Concrete in the UK”, CEB/FIP International Symposium on Structural Lightweight Aggregate Concrete, Sandefjord, Norway, pp. 52-69.

Bardhan-Roy, B.K., (1993), “Structural Lightweight Aggregate Concrete”, Chapter 7, Lightweight Concrete for Special Structures, Edited by J. L. Clarke, Chapman and Hall.

Bassuoni, M.T., and Nehdi, M.L., (2007), “Resistance of Self-Consolidating Concrete to Sulfuric Acid Attack with Consecutive pH Reduction”, Cement and Concrete Research, Vol. 37, No. 7, pp. 1070-1084.

Bennenk, W., (2002), “(SCC) Self Consolidating Concrete in Daily Precast Concrete Practice,” Betonwerk und Fertigteil-Technik, Germany, Vol. 34, Issue. 4.

Big River Industries, (2012), (http://www.bigriverind.com), August, 13th, 2011.

Bilodeau, A., Chevrier, R., Malhotra, V.M., and Hoff, G., (1995), “Mechanical Properties, Durability and Fire Resistance of High Strength Lightweight Concrete”, International Symposium on Structural Lightweight Aggregate Concrete, Sandefjord, Norway, pp. 432-443.

Bilodeau, A., Silvasundaram, V., Painter, K., and Malhotra, V., (1994), “Durability of Concrete Incorporating High Volumes of Fly Ash from Sources in the U.S.”, ACI Materials Journal, Vol. 91, No. 1, pp. 3-12.

Bjerkeli, L., Hansen, E.A., and Thorenfeldt, E., (1995), “Tension Lap Splices in High Strength LWA Concrete.” CEB/FIP International Symposium on Structural Lightweight Aggregate Concrete, Sandefjord, Norway, pp. 131-142. Ed. I. Holand, et al.

Bleszynski, R., Hooton, D., Thomas, M., and Rogers, C., (2002), “Durability of Ternary Blend Concrete with Silica Fume and Blast-Furnace Slag: Laboratory and Outdoor Exposure Site Studies”, ACI Materials Journal, Vol. 99, Issue. 5, pp. 499.

Bouzoubaa, N., and Lachemi, M., (2001), “Self-Compacting Concrete Incorporating High Volumes of Class F Fly Ash Preliminary Results”, Cement and Concrete Research, Vol. 31, Issue. 2, pp. 413-420.

Brandt, A. M., (1995), “Cement-Based Composites: Materials, Mechanical Properties and Performance”, Publisher E& FN Spon, ISBN 0419191100.

Bremner, T. W., Holm, T.A., and McInerney, J.M., (1992), “Influence of Compressive Stress on the Permeability of Concrete”, American Concrete Institute, Holm TA, Vaysburd AM, editors. Structural lightweight concrete performance. SP-136. Farmington Hills, Michigan pp. 345-356.

Brite EuRam, (2000), “Task 9 End Product, Guidelines” Edited by: Mr. Lars-Göran Tviksta Internet website (http://www.cege.ucl.ac.uk/__data/assets/pdf_file/0016/3607/task9.pdf) of Brite EuRam, 2000; pp. 48.

Cather, R., (2003), “Concrete and Fire Exposure”, Advanced Concrete Technology-Concrete Properties, Edited by John Newman and Ban Choo, ISBN 0 7506 5104 0.

Carlson R. W., (1938), “Drying Shrinkage of Concrete as Affected by Many Factors”, Proceedings of the 41st Annual Meeting of the ASTM, Vol. 38, part II, Philadelphia. pp. 419 - 440.

Chatterji, S., (2003), “Freezing of Air-Entrainment Cement-Based Materials and Specific Actions of Air-Entraining Agents”, Cement and Concrete Composites, Vol. 25, No. 7, pp. 759-765.

Caijun, S., and Yanzhong, W., (2005), “Mix Proportioning and Properties of Self-Consolidating Lightweight Concrete Containing Glass Powder”, ACI Material Journal, Vol. 102, Issue. 5, pp. 355–363.

Comité Euro-international du Béton (CEB), (1993), “CEB-FIP Model Code”, Vol. 3, ISBN.288394010X.

Chia, K.S. and Zhang, M.H., (2004), “Effect of Chemical Admixtures on Rheological Parameters and Stability of Fresh Lightweight Aggregate Concrete”, Magazine of Concrete Research, Vol. 56, No. 8, pp. 465 - 473.

Chia, K.S., and Zhang, M.H., (2002), “Water Permeability and Chloride Penetrability of High Strength Lightweight Aggregate Concrete”, Cement and Concrete Research, Vol. 32, Issue 4, pp. 639 - 645.

Chia, K.S., and Zhang, M.H., (2001), “Water Permeability and Chloride Penetrability of High-Strength Lightweight Aggregate Concrete”, Cement and Concrete Research, Vol. 32, No. 4, pp. 639 – 645.

Choi, Y., Kim, Y., Shin, H., and Moon, H., (2006), “An Experimental Research on the Fluidity and Mechanical Properties of High-Strength Lightweight Self-Compacting Concrete,” Cement and Concrete Research, Vol. 36, No. 9, pp. 1595 - 1602.

Choi, B.S, Scanlon, A., and Johnson, P. A., (2004), "Monte Carlo Simulation of Immediate and Time-Dependent Deflections of Reinforced Concrete Beams and Slabs," ACI Structural Journal, Vol. 101, Issue 5, pp. 633 - 641.

Copier, W., (1983), "The Spalling of Normal and Lightweight Concrete Exposed to Fire," Paper Presented at the Fall Convention of the American Institute", Proceedings published in the Fire Safety of Concrete Structures, American Concrete Institute, Detroit, M.I, pp. 308.

Cornet, I., Ishikawa, T., and Bresler, B., (1986), "The Mechanism of Steel Corrosion Structure", Materials Protection, Vol. 3, No. 7, pp. 44 - 47.

Curcio, F., Galeota, D., Gallo, A., and Giammatteo, M., (1998), "High-performance Lightweight Concrete for the Precast Prestressed Concrete Industry", Proceeding. 4th International CANMET/ACI/JCI Symposium, To-kushima, Japan, pp. 389 - 406.

CSA A23.3, (2009), "Canadian Standard Association" Design of concrete structures. Canadian Standard Association, Rexdale, Ontario, Canada.

De Lorenzis, L., and Tepfers, R., (2003), "Comparative Study of Models on Confinement of Concrete Cylinders with Fiber-Reinforced Polymer Composites", Journal of Composites for Construction, Vol. 7, Issue 3, pp. 219 - 237.

Design Expert V.8.1 statistical software, (2011), (http://www.statease.com/dx8descr.html), October, 14th, 2011.

Dias, W.P.S., Khoury, G.A., and Sullivan, P.J.E., (1990), "Mechanical Properties of Hardened Cement Paste Exposed to Temperatures up to 700°C", ACI Materials Journal, Vol. 87, Issue 2, pp.160 - l166.

Ding, Y.N., Liu, S.G., Zhang Y., and Thomas. A., (2008), "The Investigation on the Workability of Fibre Cocktail Reinforced Self-Compacting High Performance Concrete", Construction Building Materials, Vol. 22, Issue 7, pp. 1462 - 1470.

Domone, P.L., (2006), "Self-Compacting Concrete: An Analysis of 11 Years of Case Studies", Cement and Concrete Composites, Vol. 28, Issue 2, pp. 197 - 208.

Durning, T. A., and Hicks, C., (1991), "Using Microsilica to Increase Concrete's Resistance to Aggressive Chemicals", Concrete International, Vol. 13, No. 3, pp. 42- 48.

Dymond B.Z, Carin L. Roberts-Wollmann C. L, and Cousins T. E, (2009), "Shear Strength of a PCBT-53 Girder Fabricated with Lightweight Self-Consolidating Concrete", Virginia Department of Transportation, Richmond, VA.

Dymond, B.Z, (2007), "Shear Strength of APcbt-53 Girder Fabricated With Lightweight, Self-Consolidating Concrete" Master's Thesis, Virginia Tech, Blacksburg, VA.

EFNARC, (2005), "The European Guidelines for Self Compacting Concrete", Specification, Production and Use The Self-Compacting Concrete European Project Group, pp. 63.

EFNARC, (2002), "Specification and Guidelines for Self-Compacting Concrete," European Association for Producers and Applicators of Specialist Building Products, Surrey United Kingdom, ISBN 0-9539733-4-4, (http://www.efnarc.org/pdf/SandGforSCC.PDF), pp. 32.

ESCSI, (2004), "Moisture Dynamics in Lightweight Aggregate and Concrete", Salt Lake City, Utah, Publication No. 9349, pp. 12.

ESCSI, (2011), (www.escsi.org), May, 10th, 2011.

Emission Test Report, (1985), “Environmental Protection Agency”, Plant K6, from Calciners and Dryers in Mineral Industries - Background Information Standards, EPA-450/3-85-025a, U.S.A, Research Triangle Park, North Carolina.

EN12350-8, (2010), “Testing Fresh Concrete. Part 8. Self-Compacting Concrete. Slump-Flow Test”, European Committee for Standardization, ISBN 978 0 580 69212 3, pp. 1-9.

EN12350-9, (2010), “Testing Fresh Concrete, Part 9, Self-Compacting Concrete. V-funnel test”, European Committee for Standardization.

EN12350-10, (2010), “Testing Fresh Concrete-Part 10: Self-Compacting Concrete- L-box Test”, European Committee for Standardization.

EN1097-6, (2000), Tests for Mechanical and Physical Properties of Aggregates. Determination of Particle Density and Water Absorption”, European Committee for Standardization.

ESCSI, (1971), “Expanded Shale Clay and Slate Institute”, Lightweight Concrete, History, Applications, Economy, Salt Lake City, Utah, pp. 44.

ESCSI, Expanded Shale Clay and Slate Institute (2011), (www.escsi.org/), September 26th, 2011.

Esfahani, M.R., Lachemi, M., and Kianoush, M.R., (2008), “Top-Bar Effect of Steel Bars in Self-Consolidating Concrete (SCC)”, Cement and Concrete Composites, Vol. 30, Issue. 1, pp. 152-160.

Esfahani, M.R., and Rangan, B.V., (1998), “Local Bond Strength of Reinforcing Bars in Normal Strength and High Strength Concrete (HSC)”, ACI Structure Journal, Vol. 95, Issue 2, pp. 96–106.

EuroLightCon, (2000), “Properties of LWAC Made With Light Weight Aggregate Concrete,” Project No. BE96-3942, pp. 38.

EuroLightCon, (1998), “Definitions and International Consensus Report”, Economic design and Construction with Lightweight Aggregate Concrete, Document BE96-3942/R1, (http://www.sintef.no/static/BM/projects/EuroLightCon/BE3942R01.pdf), pp. 69.

Faraday, M., and Day, P. (1999) “The Philosopher's Tree: A Selection of Michael Faraday's Writings”. CRC Press. P.71. ISBN 978-0-7503-0570-9.

FIP, (1983), “Manual of Lightweight Aggregate Concrete”, 2nd Edition, London: Surrey University Press.

Garrecht, H., Gilka-Botzow, A., and Helm, G., (2010) “Precast Wall Panels Of Lightweight Concrete”, Betonwerk und Fertigteil-Technik (BFT), Germany, Vol. 76, No. 2, pp. 111 – 124.

Gamal, E.A., (2007), “A Study on the Performance of Lightweight Self-Consolidated Concrete”, Housing and Building National Research Center Journal, Vol. 3, No. 3, pp. 10-22.

Gesoğlu, M., and Güneyisi, E., (2011), “Permeability Properties of Self-Compacting Rubberized Concretes” Construction and Building Materials, Vol. 25, No. 8, pp. 3319–3326.

Gesoğlu, M., Güneyisi, E., and Ozbay, E., (2009), “Properties of Self-Compacting Concretes Made with Binary, Ternary, and Quaternary Cementitious Blends of Fly Ash, Blast Furnace Slag, and Silica Fume”, Construction and Building Materials, Vol. 23, Issue. 5, pp. 1847–1854.

Gesoğlu, M., and Güneyisi, E., (2007), “Strength Development and Chloride Penetration in Rubberized Concretes with and without Silica Fume,” Materials and Structures, Vol. 40, Issue. 9, pp. 953-964.

Gosset, W.S., (1908), “The Probable Error of a Mean – Student’s t Distribution”, Statistics in Biometrika.

Grubl, P., (1979), “Mix Design of Lightweight Aggregate Concrete for Structural Purposes”, The International Journal of Lightweight Concrete, Vol. 1, Issue. 2, pp. 63-69.

Güneyisi, E., Gesoğlu, M., and Ozbay, E., (2010), “Strength and Drying Shrinkage Properties of Self-Compacting Concretes Incorporating Multi-System Blended Mineral Admixtures” Construction and Building Materials, Vol. 24, Issue. 10, pp. 1878–1887.

Güneyisi, E., and Mermerdas, K., (2007), “Comparative Study on Strength, Sorptivity, and Chloride Ingress Characteristics of Air-Cured and Water- Cured Concretes Modified with Metakaolin,” Materials and Structures, Vol. 40, Issue. 10, pp. 1161-1171.

Güneyisi, E., Özturan, T., and Lu, M.G., (2005), “A Study on Reinforcement Corrosion and Related Properties of Plain And Blended Cement Concretes Under Different Curing Conditions”, Cement And Concrete Composites, Vol. 27, Issue. 4, pp. 449-461.

Güneyisi, E., Özturan, T., and Gesoðlu, M., (2002), “Laboratory Investigation of Chloride Permeability for High Performance Concrete Containing Fly Ash and Silica Fume”, International Congress, Challenges of Concrete Construction, Dundee, Scotland, pp. 295-305.

Ghezal, A., and Khayat, K. H., (2002), “Optimizing Self-Consolidating Concrete with Limestone Filler by Using Statistical Factorial Design Methods”, ACI Materials Journal, Vol. 99, Issue 3, pp. 264-272.

Haist, M., Mechtcherine, V., Beitzel, H., and Muller, H., (2003), “Retrofitting of Building Structures using Pumpable Self-compacting Lightweight Concrete”, 3rd International RILEM Symposium on Self-Compacting Concrete, Reykyavik, Iceland, pp.776 – 785.

Hammer, T., (1990), “Marine Concrete Structures Exposed to Hydrocarbon Fire”, Spalling Resistance of Lightweight Aggregate Concrete, SINTEF-Report No. STF25 A90009, Trondheim, pp. 8.

Hans W. R., and Michael S., (2006) “Self-Consolidating Concrete in Fire” ACI Materials Journal, Vol. 103, Issue 2, pp. 130 – 135.

Harding, M.A., (1995), “Using Structural Lightweight Concrete Should Pose Few Problems for Knowledgeable Contractors”, Structural Lightweight Aggregate Concrete, Publication No. C950618.

Hassan, A.A.A., Hossain, K.M.A., and Lachemi, M., (2009), “Corrosion Resistance of Self-Consolidating Concrete in Full-Scale Reinforced Beams”, Cement and Concrete Composites, Vol. 31, Issue 1, pp. 29-38.

Havdahl, J., Hammer, T.A., Justnes, H., and Smeplass, S., (1993), “LWA Concrete for Floaters, SP5 Durability, Report 5.1 Rebar Corrosion and Frost Resistance”, SINTEF report STF70 A93042, Trondheim, Norway.

Her-Yung, W., (2009), “Durability of Self-Consolidating Lightweight Aggregate Concrete Using Dredged Silt,” Construction and Building Materials, Vol. 23, Issue 6, pp. 2332 - 2337.

Holm, T. A., and Ries, J., (2006), “Lightweight Concrete and Aggregates”, Significance of Tests and Properties of Concrete and Concrete Making Materials, STP 169D, ASTM International, West Conshohocken, Pennsylvania, U.S.A., pp. 548 - 560.

Holm, T.A., and Bremner T.W., (2000), “State-Of-The-Art-Report on High-Strength, High-Durability Structural Low-Density Concrete for Applications in Severe Marine Environments”, U.S. Army Corps of Engineers, Report No. ERDC/SL TR-00-3, pp. 116.

Holm, T. A., (1980), “Physical Properties of High Strength Lightweight-Aggregate Concrete,” Second International Congress of Lightweight Concrete, London, pp. 10.

Holm, T. A., (1980), “Performance of Structural Lightweight Concrete in a Marine Environment,” Performance of Concrete in Marine Environment, SP-65, V. M. Malhotra, Edited., American Concrete Institute, Farmington Hills, Michigan., pp. 589 - 608.

Hope, B., and Alan K., (1987), “Corrosion of Steel In Concrete Made With Slag Cement”, ACI Materials Journal, Vol. 84, Issue 5, pp. 525 – 531.

Hossain, K. M. A., (2009), “Influence of Extreme Curing Conditions on Compressive Strength and Pulse Velocity of Lightweight Pumice Concrete”, Computers and Concrete, Vol.6, No.6, pp. 437-450.

Hossain, K.M.A., (2008), “Bond characteristics of Plain and Deformed Bars in Pumice Based Lightweight Concrete”, Construction and Building Materials, Vol. 22, No. 7, pp. 1491-1499.

Hossain, K.M.A., (2006), “High Strength Blended Cement Concrete Incorporating Volcanic Ash”, Cement and Concrete Composites, Vol. 28, Issue. 6, pp. 535-545.

Hossain, K.M.A., (2006), “Performance of Volcanic Ash and Pumice Based Blended Cements in Sulfate and Sulfate–Chloride Environments”, Advances in Cement Research, Vol. 18, Issue 2, pp.71–82.

Hossain, K. M. A., (2006), “Blended Cement and Lightweight Concrete using Scoria: Mix Design, Strength, Durability and Heat Insulation Characteristics”, International Journal of Physical Sciences (IJPS), Vol.1, No.1 (2006), pp. 5-16.

Hossain, K.M.A., (2005), "Chloride Induced Corrosion Of Reinforcement in Volcanic Ash and Pumice Based Blended Concrete", Cement and Concrete Composites, Vol. 27, Issue. 3, pp. 381-390.

Hossain, K. M. A., (2004a), "Properties of Volcanic Scoria Based Lightweight Concrete", Magazine of Concrete Research, Vol. 56, No. 2, pp. 111-120.

Hossain, K. M. A., (2004b), "Development of Volcanic Pumice Based Lightweight Concrete", Magazine of Concrete Research, Vol. 56, No. 2, pp. 99-109.

Hossain, K. M. A., (2003), "Behaviour of Volcanic Pumice Based Thin Walled Composite Filled Columns under Eccentric Loading", Structural Engineering and Mechanics- International Journal, Vol. 16, No. 1, pp. 63-82.

Hossain, K.M.A., (1999), "Bond in Lightweight Volcanic Pumice Concrete", Proceedings of the 7th East Asia-Pacific conference on structural engineering and construction (EASEC7), 27-29 August, Kochi University of Technology, Japan, Vol. 2, pp. 1460–1465.

Hossain, K.M.A., (1999), "Fire Resistance of Lightweight Volcanic Pumice Concrete", Proceeding of the 24th OWICS Conference, "21st century Concrete and Structures", 5-26 August, Singapore, pp. 201-208.

Hossain, K.M.A., (1999) "Performance of Volcanic Ash Concrete in Marine Environment," Proceedings of 24th OWICS Conference, "21st Century Concrete and Structures", 25-26 August, Singapore, pp. 209-214.

Hossain, K. M. A., (1999), "Fire Durability of Lightweight Volcanic Pumice Concrete with Special Reference to Thin Walled Filled Sections", Durability of Building Material and Components 8, Canadian Institute for Scientific and Technical Information (CISTI), NRC Research Press, NRC No. 42738, Vol. 1-4, pp.149-158, (ISBN 0-660-17737-4).

Hossain, K.M.A., and Saifuddin, A., (2011), “Lightweight Concrete Incorporating Volcanic Ash-Based Blended Cement and Pumice Aggregate”, Journal of Materials in Civil Engineering, Vol. 23, No. 4, pp. 493 - 498.

Hossain, K.M.A., and Ahmed, S., (2011), “Lightweight Concrete Incorporating Volcanic Ash Based Blended Cement and Pumice Aggregate”, ASCE Journal Of Materials In Civil Engineering, American Society Of Civil Engineers Vol. 23, Issue 4, pp. 493-498.

Hossain, K.M.A., Ahmed, S., and Lachemi, M., (2011), “Lightweight Concrete Incorporating Pumice Based Blended Cement and Aggregate: Mechanical and Durability Characteristics”, Construction and Building Materials, Vol. 25, Issue. 3, pp. 1186-1195.

Hossain, K. M. A., and Lachemi, M., (2010), “Fresh, Mechanical, and Durability Characteristics of Self-Consolidating Concrete Incorporating Volcanic Ash”, ASCE Journal Materials in Civil Engineering, Vol. 22, No.7, pp. 651-657.

Hossain, K. M. A., and Lachemi, M., (2008), “Bond Behaviour of Self-Consolidating Concrete with Mineral and Chemical Admixtures”, Journal of Materials in Civil Engineering, Vol. 20, No. 9, pp. 899-1561.

Hossain, K.M.A., and Lachemi, M., (2007), “Characteristics of Self-Consolidating Concrete Incorprating Volcanic Ash”, 32nd Conference on Our World in Concrete and Structures, 28-29 August 2007, Singapore, pp. 28-29.

Hossain, K.M.A., and Lachemi, M., (2007), “Mixture Design, Strength, Durability, and Fire Resistance of Lightweight Pumice Concrete”, ACI Materials Journal, Vol. 104, Issue 5, PP. 449-457.

Hossain, K.M.A., and Lachemi, M., (2006), “Development of Volcanic Ash Concrete: Strength,

Durability, and Micro-structural Investigations," ACI Materials Journal, Vol. 103, Issue 1, pp. 11-17.

Hossain, K.M.A., and M. Lachemi, M., (2006), "Time Dependent Equations For The Compressive Strength of Self-Consolidating Concrete Through Statistical Optimization", Computers and Concrete, Vol. 3, No. 4, pp. 249-260.

Hossain, K. M. A., and Lachemi, M., (2005), "Lightweight Concrete with Pumice Aggregate: Mix Design and Fire Durability", 1st Canadian Conference on Effective Design of Structures, McMaster University, Hamilton, Ontario, Canada, July 10 – 13.

Hossain, K. M. A., and Lachemi, M., (2005), "Thermal Conductivity and Acoustic Performance of Volcanic Pumice Based Composites", Materials Science Forum, Vol. 480-481, pp. 611-616 (ISBN: 0-87849-962-8).

Hover, K.C., (2006), "Air Content and Density of Hardened Concrete", Significance of Tests and Properties of Concrete and Concrete Making Materials, STP 169D, ASTM International, West Conshohocken, Pennsylvania, U.S.A. pp. 288-308.

Hubertova, M., and Hela, R., (2011), "Durability of Light-Weight Expanded Clay Aggregate Concrete", World Academy of Science, Engineering and Technology, Vol. 58, pp. 390-395.

Hubertova, M., and Hela, R., (2007), "The Effect of Metakaolin and Silica Fume on the Properties of Lightweight Self-Consolidating Concrete", ACI Materials Journal, American Concrete Institute, Detroit, pp. 35-48.

Hwang, S.D., and Khayat, K.H., (2006), "Performance of Hardened Self-Consolidating Concrete Designated for Repair Applications", ACI SP-233, Workability of SCC: Roles of Its Constituents and Measurement Techniques, Ed. Shi, C., Khayat, K.H.

Hwang, S., Khayat, K., and Bonneau, O., (2006), “Performance-Based Specifications of Self-Consolidating Concrete Used in Structural Applications,” ACI Materials Journal, Vol. 103, Issue 2, pp. 121-129.

Hwang, C.L., and Hung, M.F., (2005), “Durability Design and Performance of Self-Consolidating Lightweight Concrete”, Construction and Building Materials, Vol. 19, pp. 619-626.

Illinois Department of Transportation, (2005), “Standard Test Method for Static Segregation of Hardened Self-Consolidating Concrete Cylinders”, Illinois Test Procedure SCC-6, Peoria, Illinois, U.S.A.

Japan Society of Civil Engineers (JSCE), (1998) “Recommendations for Construction of Self-Compacting Concrete”, Japan Society of Civil Engineers, Issue 30 pp. 40.

Japanese Society of Civil Engineers (JSCE), (1999), “Recommendation for Self- Compacting Concrete”, JSCE Concrete Engineering Series 31, T. Omoto and K. Ozawa, Eds., 77 pp.

Japanese Society of Civil Engineers (JSCE), (1998), “Recommendation for Construction of Self-Compacting Concrete”, Technical Session: Recommendations and Materials, pp. 417-437.

Japanese Society of Civil Engineering (JSCE), (1998) “Guide to construction of high flowing Concrete”, Gihoudou publication, Tokyo, Japan.

Karahan, O., Hossain, K. M. A., Ozbay, E., Lachemi, M., Sancak, E., (2012), “Effect of Metakaolin Content on the Properties Self-Consolidating Lightweight Concrete”, Construction and Building Materials, Vol. 31, No.6, pp. 320-325.

Kaffetzakis, M., and Papanicolaou, C. (2011), “Fiber-Reinforce Pumice Aggregate Self compacting Concrete”, Proceedings of the fib Symposium, Session 2A, Concrete Technology, 8-10 June, Prague, Czech Republic, ISBN 978-80-87158-29-6.

Khayat, K.H., (2000), “Optimization and Performance of Air-Entrained, Self-Consolidating Concrete”, ACI Materials Journal, Vol. 97, Issue 5, pp. 226-535.

Khayat, K.H., (1999), “Testing and Performance of Self-Compacting Concrete”, ACI Materials Journal, Vol. 96, Issue 3, pp. 346-353.

Khayat, K. H., (1998), “Use of Viscosity-Enhancing Admixtures in Cement- Based Systems-An Overview”, Cement and Concrete Composites, Vol. 20, No. 2, pp. 171-188.

Khayat, K. H., (1998), “Use of Viscosity-Modifying Admixture to Reduce Top-Bar Effect of Anchored Bars Cast with Fluid Concrete”, ACI Materials Journal, Vol. 95, Issue 2, pp. 158-167.

Khayat, K.H., Assaad, J., and Daczko, J., (2004), “Comparison of Field-Oriented Test Methods to Assess Dynamic Stability of Self-Consolidating Concrete”, ACI Materials Journal, Vol. 101, No. 3, pp. 207-215.

Khayat, K.H., and Assaad, J., (2004), “Assessment of Thixotropy of Self-Consolidating Concrete And Concrete-Equivalent-Mortar - Effect of Binder Composition and Content”, ACI Materials Journal, Title no. 101-M45, pp. 400-408.

Khayat, K.H., Lovric, D., Obla, K., and Hill, R., (2002), “Stability Optimization and Performance of Self-Consolidating Concrete Made with Fly Ash”, First North American Conference on the Design and Use of Self-Consolidating Concrete, November 12-13, ACI, Chicago, Illinois, pp. 215-223.

Khayat, K.H., Paultre, P., and Tremblay, S., (2001), "Structural Performance and In-place Properties of Self-consolidating Concrete used for Casting Highly Reinforced Columns", ACI Materials Journal, Vol. 98, Issue 5, pp. 371-378.

Khayat, K.H., Bickley, J., and Lessard, M., (2000), "Performance of Self-Consolidating Concrete for Casting Basement And Foundation Walls", ACI Materials Journal, Vol. 97, Issue 3, pp. 374-380.

Khayat, K.H., Ghezal, A., and Hadriche, M.S., (2000), "Utility of Statistical Models in Proportioning Self-Consolidating Concrete", Proceedings of the First International RILEM Symposium on Self-Compacting Concrete, Stockholm, Sweden, pp. 345-359.

Khayat, K.H., Hu, C., and Monty, H., (1999), "Proceeding First International RILEM Symposium", SCC, Stockholm, Sweden.

Khayat, K.H., Ghezal, A., and Hadriche, M.S., (1999), "Factorial Design Models for Proportioning Self-Consolidating Concrete", Materials and Structures, Vol. 32, pp. 679-686.

Khayat, K.H., Yahia, A., and Sonebi, M., (1999), "Applications of Statistical Models for Proportioning Under Water Concrete", ACI Materials Journal, Vol. 96, Issue 6, pp. 634-640.

Khayat, K.H., Yahia, A., and Sonebi, M., (1998), "Applications of Statistical Models for Proportions of Underwater Concrete", Forth CANMET ACI JCI International Conference on Recent Advances in Concrete Technologu, Supplementary Papers, October 02-04, Tohushima, Japan. pp. 95-113.

Khayat, K. H., Ghezal, A., and Hadriche, M. S., (1998) "Development of Factorial Design Models for Proportioning Self-Consolidating Concrete", Nagataki Symposium on Vision of Concrete: 21st Century, V. M. Malhotra, June, Tokushima, Japan, pp. 173-197.

Khokhrin, N.K., (1973), “The Durability of Lightweight Concrete Structural Members”. Kuibyshev, USSR.

Khoury, G.A., (1992), “Compressive Strength of Concrete at High Temperatures: a Reassessment”, Magazine of Concrete Research, Vol. 44, Issue. 161, pp. 291-309.

Kilic, A., Atis, C.D., Yasar, E., and Ozcan, F., (2003), “High-Strength Lightweight Concrete Made with Scoria Aggregate Containing Mineral Admixtures”, Cement and Concrete Research, Vol. 33, No. 10, pp. 1595–1599.

Kim, Y.J., Choi, Y.W., and Lachemi, M., (2010), “Characteristics of Self-Consolidating Concrete Using Two Types of Lightweight Coarse Aggregates”, Construction and Building Materials, Vol. 24, Issue 1, pp. 11-16.

Klieger, P. (1957), “Curing Requirements for Scale Resistance of Concrete”, Research Department Bulletin RX082, Portland Cement Association. Website: (http://www.portcement.org/pdf_files/RX082.pdf).

Koehler, E.P., and Fowler, D.W., (2007), “Aggregates in Self-Consolidating Concrete”, Final report ICAR project108: Aggregates in self-consolidating concrete. Aggregates Foundation for Technology, Research, and Education (AFTRE), the University of Texas, Austin.

Koehler, E.P., and Fowler, D.W., (2006) “Mixture Proportioning Procedure for Self-consolidating Concrete”, International Center for Aggregates Research (ICAR), Research Report 108-1, International Center for Aggregates Research, University of Texas at Austin, Texas, USA, 2006, 21pp.

Kostuch, J.A., Walters, G.V., and Jones, T.R., (1993), “High Performance Concrete Incorporating Metakaolin - A review”, Concrete 2000. University of Dundee, pp. 1799-1811.

Kosmatka, S.H., Kerkhoff, B., Panarese, W.C., Macleod, N.F., and McGrath, R.J., (2002), "Design and Control of Concrete Mixtures", Engineering Bulletin 101, 7th Edition, Cement Association of Canada, pp. 356.

Kowalsky, M.J., Priestley, M.J.N., and Seible, F., (1999), "Shear and Flexural Behavior of Lightweight Concrete Bridge Columns in Seismic Regions", ACI Structural Journal, Vol. 96, Issue 1, pp. 136-148.

Kwan, A.K.H., and Fung, W.W.S., (2009), "Packing density measurement and modelling of fine aggregate and mortar", Cement and Concrete Composites, Publisher: Elsevier Ltd, Vol. 31, Issue 6, pp. 349-357.

Lessard, M., Talbot, C., Phelan, W.S., and Baker, D., (2002), "Self-Consolidating Concrete Solves Challenging Placement Problems at the Pearson International Airport in Toronto, Canada", 1st North American Conference on the Design and Use of Self-Consolidating Concrete (SCC) Rosemont, November 12-13, ACI, Chicago, Illinois, pp. 12-13.

Lachemi, M., Bae, S., Hossain, K.M.A., and Sahmaran, M., (2009), "Steel - Concrete Bond Strength of Lightweight Self-Consolidating Concrete", Materials and Structures, Vol. 42, Issue. 7, pp. 1015-1023.

Lachemi, M., Hossain, K.M.A., Patel, R., Shehata, M., and Bouzouba, N., (2007), "Prediction of flow behaviour of high volume fly ash self-consolidating concrete from the rheology of paste and mortar", Magazine of Concrete Research, Vol. 59, Issue. 7, pp. 517-528.

Lachemi, M., Hossain, K.M.A., and Lambros V.B, (2006), "Axial Load Behavior of Self-Consolidating Concrete-Filled Steel Tube Columns in Construction and Service Stages", ACI Structural Journal, Vol. 103, Issue 1, pp. 38 - 47.

Lachemi, M., Hossain, K.M.A., Lambros, V., Nkinamubanzi, P.C., and Bouzoubaa, N., (2004), "Self-Compacting Concrete Incorporating New Viscosity Modifyng Admixtures", Cement and Concrete Research, Vol. 34, Issue 6, pp. 917-926.

Lachemi, M., Hossain, K.M.A., Lambros, V., Nkinamubanzi, P.C., and Bouzoubaâ, N., (2004), "Performance of New Viscosity Modifying Admixtures in Enhancing the Rheological Properties of Cement Paste", Cement and Concrete Research, Vol. 34, No. 2, pp. 185-193.

Lachemi, M., Hossain, K.M.A., Lambros, V., and Bouzoubaâ, N., (2003), "Development of Cost-Effective Self-Compacting Concrete Incorporating Fly Ash, Slag or Viscosity-Modifying Admixtures", ACI Materials Journal, Vol. 100, Issue 5, pp. 419 – 425.

Lafarge North America, (2012), (http:www.lafarge.com), May, 11th, 2011.

Lange, C., Riutort, T., and Lebris, J., (1995), "Lightweight Concrete for A Cable-Stayed Bridge – The Iroise Bridge in Brest", International Symposium on Lightweight Aggregate Concrete, 20-24 June, Sandefjord, Norway, pp. 287-298.

Lessard, M., Sarkar, S.L., Ksinsik, D.W., and Aitcin, P.C., (1992), "Long-Term Behaviour of Silica Fume Concrete International", Vol. 14, No. 4, pp. 25-30.

Lo, T., and Cui, H.Z., (2004), "Effect of Porous Lightweight Aggregate on Strength Of Concrete", Materials Letters, Vol. 58, pp. 916– 919.

Lo, T., Tang, P., Cui, H., and Nadeem, A., (2007), "Comparison of Workability and Mechanical Properties of Self-Compacting Lightweight Concrete and Normal Self-Compacting Concrete" Materials Research Innovations, Vol. 11, No. 1, pp. 45-50.

Maage, M., and Smeplass, S., (2000), "Structural LWAC", Specification and Guideline for Materials and Production, 2nd Int. Symposium on Structural Lightweight Aggregate Concrete,

(Eds. Helland S., Holand I. and Smeplass S.), June, Kristiansand, Norway, pp. 18-22 Norwegian Concrete Association, pp. 802-810.

Maghsoudi, A.A., Mohamad, S., and Maghsoudi, M., (2011), "Mix Design and Mechanical Properties of Self-Compacting Light Weight Concrete", International Journal of Civil Engineering, Vol. 9, No. 3, pp. 231-236.

Malhotra, V.M., (2004), "Role of Supplementary Cementing Materials and Superplasticisers in Reducing Greenhouse Gas", Emissions, ICFRC, Chennai, India: Allied Publishers Private Ltd.

Malhotra, V.M., (2002), "High-Performance High Volume Fly Ash Concrete", ACI Concrete International, Vol. 24, Issue 7, pp. 1-5.

Malhotra V.M., (2002), "Introduction: Sustainable Development and Concrete Technology", ACI Concrete International, Vol. 24, Issue 7, pp. 22.

Malhotra V.M., (1999), "Making Concrete "Greener with Fly Ash", ACI Concrete International, Vol. 21, Issue 5, pp. 61-66.

Manual of Lightweight Aggregate Concrete, (1983), Fédération internationale de la précontrainte., Publisher: Glasgow: Surry University Press; New York: Halsted Press, ISBN: 0470274840, pp. 259.

Martin, D.J., (2003), "Economic Impact of SCC in Precast Applications", First North American Conference on the Design and Use of Self-Consolidating Concrete, Evanston, November 12-13, ACI, Chicago, Illinois. pp. 147-152.

Mather, B., (1990), "How to Make Concrete That Will Be Immune to the Effects of Freezing and Thawing", Paul Klieger Symposium on Performance of Concrete, American Concrete Institute, Farmington Hill, Michigan, supplementary papers, Vol. 122, pp. 1-8.

Mechtcherine, V., Lieboldt, M., and Butler, M., (2010), “Application of Textile Reinforced Concrete (TRC) in Prefabrication”, Proceedings of ACI Spring Convention Chicago, U.S.A.

Mechtcherine, V., Haist, M., Hewener, A., and Muller, H.S., (2001), “Self-compacting Lightweight Concrete- A New High-Performance Building Material”, Proceedings of the 2nd Int. Symposium on Self-Compacting Concrete, 23-25 October, Kochi, Japan, pp. 23-25.

Melby, K., Jordet, E., and Hansvold, C., (1996), “Long-span Bridges In Norway Constructed in High-Strength LWA Concrete”, Elsevier, pp. 845-849.

Mehta, P.K., (1997), “Durability – Critical Issues for the Future”, ACI Concrete International, Vol. 19, Issue 7, pp. 27-33.

Mehta, P.K., and Monteiro, P.J.M., (1993), “Concrete-Structure, Properties, and Materials”, 2nd Edition, Prentice Hall, Englewood Cliffs, N.J., pp. 548.

Mehta, P., (1986), “Concrete Structure Properties and Materials, Prentice Hall, Englewood Cliffs, NJ, ISBN 0-13-175621-4, pp. 548.

Mehta, P.K., (1980), “Durability of Concrete in Marine Environment”, A Review”, performance of Concrete in Marine Environment, ACI SP-65, V.M. Malhotra, Ed., pp. 1-20 .

Melby, K., Jordet, E., and Hansvold, C., (1996), “Long-Span Bridges in Norway Constructed In High-Strength LWA Concrete”, Elsevier, pp. 845-849.

Midgley, H.G., and Illston, J.M., (1983), “Stone Comments on the Microstructure of Hardened Cement pastes”, Cement and Concrete Research, Vol. 13, Issue. 2, pp. 197-206.

Mindess, S., Young, J.F., and Darwin, D., (2003), “Concrete 2nd edition Prentice Hall”, Upper Saddle River, New Jersey, pp. 644.

Mindess, S., and Young, J.F., (1981), “Concrete. New York: Prentice-Hall” Engle-Wood Cliffs, New Jersey, pp. 76-86, 95-99 and 566-567.

Müller, H.S., and Haist, M., (2004), “Self-Compacting Lightweight Concrete”, Erste Allgemeine Bauaufsichtliche Zulassung, Betonwerk und Fertigteil-Technik, pp. 8-17.

Müller H.S. and Haist, M., (2002), “Self-compacting Lightweight Concrete”, Technology and use. Concrete Plant Precast Technology, Vol. 71, Issue. 2, pp. 29–37.

Müller, H.S., and Guse, U., (2000), “Concrete Technology Development: Important Research Results and Outlook In The New Millennium”, Concrete Plant and Precast Technology, Vol. 66, No.1, pp. 32-45.

Muller-Rochholz, J., (1979), “Determination of the Elastic Properties of Lightweight Aggregate by Ultrasonic Pulse Velocity Measurements”, International Journal of Lightweight Concrete, Lancaster, U.K, Vol. 1, Issue 2, pp. 87-90.

Muthukumar, M., and Mohan, D., (2004), “Optimization of Mechanical Properties of Polymer Concrete and Mix Design Recommendation Based on Design Of Experiments”, Journal of Applied Polymer Science, Vol. 94, Issue. 3, pp. 1107-1116.

Nagataki, S., and Fujiwara, H., (1995), “Self-Compacting Property of Highly Flowable Concrete”, V.M. Malhotra (Ed.), ACI SP, American Concrete Institute, Farmington Hills, Mich., Vol. 154, pp. 301-314.

Naik, T. R., Kraus, R. N., Chun Y., Canpolat, F., and Ramme, B. W., (2005), “Use Of Limestone Quarry By-Products for Developing Economical Self-Compacting Concrete” Presented and Published at the CANMET/ACI (SDCC-38) Three-Day International Symposium on Sustainable Development of Cement and Concrete, October 5-7, 2005, Toronto, CANADA.

Nehdi, M., Pardha, M., and Koshowski, J., (2004), "Durability of Self-Consolidating Concrete Incorporating High-Volume Replacement Composite Cements", Cement and Concrete Research, Vol. 34, Issue 11, pp. 2103-2112.

Nehdi, M.L., and Summer, J., (2002), "Optimization of Ternary Cementitious Mortar Blends Using Factorial Experimental Plans. Material and Structures Journal, Vol. 35, Issue 8, pp 495-503.

Naik, T.R., Ramme, B.W., and Kolbeck, H.J., (1990), "Filling Abandoned Underground Facilities with CLSM Fly Ash Slurry," ACI Concrete International, Vol. 12, Issue 7, pp. 19-25.

Newman, J.B., (1993), "Properties of Structural Lightweight Concrete", Structural Lightweight Concrete, London, Chapman and Hall, pp. 1-17.

Neville, A.M., (1996), "Properties of Concrete", 4th edition, Pearson Higher Education, Prentice Hall, New Jersey.

Neville, A. M., (1995), "Properties of Concrete", Fourth Edition, Longman Group Ltd., Harlow, England, ISBN: 0582230705, pp. 844.

Nishi, S., Oshio, A., Sone, T., and Shirokuni, S., (1980), "Water Tightness of Concrete Against Sea Water", Journal of The Central Research Laboratory., Onada Cement Co., Tokyo, Vol. 32, No. 104, pp. 40-53.

Newman, J.B., (1993), "Properties of Structural Lightweight Concrete in Structural Lightweight Concrete", Ed. J.L. Clarke, Blackie, Chapman & Hall, London, pp. 19-44.

Noumowe, A., Carre, H., Daoud, A., and Toutanji, H., (2006), "High-Strength Self Compacting Concrete Exposed to Fire Test," Journal of Materials in Civil Engineering, Vol. 18, No. 6 pp. 754.

NSA, (2006), "The Construction Material of Choice," National Slag Association, (http:www.nationalslagassoc.org), May, 25th, 2011.

Ohno, H., Kawall, T., Kuroda, Y., and Ozawa, K., (1993), "Development of Vibration Free High Strength Lightweight Concrete and Its Application", Proceedings FIP Symposium, October 17-20, Kyoto, Japan, Vol. 1 pp. 297-304.

Okamura, H., (2003), "Self-Compacting Concrete", Journal of Advanced Concrete Technology, Vol. 1, No. 1, pp. 5-15.

Okamura, H., and Ouchi, M., (1995), "Mix Design for Self-Compacting Concrete," Concrete Library of Japan Society of Civil Engineers, No. 25, pp. 107-120.

Ouchi, M., Nakamura, S., Osterberg, T., Hallberg, S., and Lwin, M., (2003), "Applications of Self-Compacting Concrete in Japan, Europe and the United States", United States Department of Transportation - Federal Highway Administration – Infrastructure, pp. 20.

Ozbay, E., Gesoglu, M., and Guneyisi, E., (2010), "Transport Properties Based Multi-Objective Mix Proportioning Optimization of High Performance Concretes", Materials and Structures, Vol. 44, No. 1, pp. 139-154.

Ozyildirim, C., (2009), "Durability of Structural Lightweight Concrete", LWC Bridges Workshop, pp. 1-14.

Phan, L, (1996), "Fire Performance of High Strength Concrete", A Report of The State-Of-The-Art. Technical Report, Building and Fire Research Laboratory, National Institute of Standards and Technology, Maryland.

Papanicolaou, C., and Kaffetzakis, M., (2009), “Pumice Aggregate Self-Compacting Concrete (PASCC)”, 16th Conference on Concrete Materials and Structures, Technical Chamber of Greece, 21-23 October, Paphos, Cyprus, pp. 21-23.

Patel, R., Hossain, K.M.A., Shehata, M., Bouzoubaâ, N., and Lachemi, M., (2004), “Development of Statistical Models for Mixture Design of High-Volume Fly Ash Self-Consolidating Concrete”, ACI Materials Journal, Vol. 101, Issue 4, pp. 294-302.

PC, (1995), “Prestressed Concrete Institute”, PCI Design Handbook, 5th Edition, Chicago, Illinois, pp. 614.

Persson, B., (2004), “Fire Resistance of Self-Compacting Concrete, SCC,” Materials and Structures, Vol. 7, No. 10, pp. 575-584.

Persson B., (2003), “Internal Frost Resistance And Salt Frost Scaling of Self-Compacting Concrete”, Cement and Concrete Research, Vol. 33, Issue. 3, pp. 373-379.

Persson, B., (2003), “Self-Compacting Concrete at Fire Temperatures”, Report TUBM 3110, Division of Building Materials, Lund Institute of Technology, Lund, pp. 200.

Persson, B., (1999), “Creep, Shrinkage, and Elastic Modulus of Self Compacting Concrete,” RILEM Proceedings PRO 7. pp. 239-250.

Petersson, Ö., and Skarendahl, Å., (1999), “Self-Compacting Concrete”, Proceedings of the first international RILEM-Symposium, Stockholm, Sweden, 786 pages.

Pigeon, M., Azzabi, M., and Pleau, R., (1996), “Can Microfibers Prevent Frost Damage?”, Cement and Concrete research, Vol. 26, No. 8, pp. 1163-1170.

Pigeon, M., Talbot, C., Marchaud, J., and Hornain, H., (1996), “Surface Microstructure and Scaling Resistance of Concrete,” Cement and Concrete Research, Vol. 26, No. 10, pp. 1555-1566.

Pigeon, M., and Pleau, R., (1995), “Durability of Concrete in Cold Climates”, Publisher: (Spon Press), 1st edition, London, 244 pages.

Powers, T.E., Copeland, L.E., and Mann H.M., (1959), “Capillary Continuity of Discontinuity in Cement Pastes,” Journal Portland Cement Research and Development Labs, No. 2, pp. 38-48.

Pradeep, G., (2008) “Response Surface Method”, Publisher: (VDM Verlag), ISBN #: 3639011856, 76 pages.

Raghavan, K.P., Sarma B.S., and Chattopadhyay D., (2002), “Creep, Shrinkage and Chloride Permeability Properties of Self-Consolidating Concrete”, First North America Conference on the design and use of Self-Consolidating Concrete, Evanston, November 12-13, ACI, Chicago, Illinois, U.SA pp. 307-311.

Reinhardt, H.W., and Michael, S., (2006), “Self-Consolidating Concrete in Fire” ACI Materials Journal, Vol. 103, Issue 2, pp. 130-135.

Richardson, M.G., (2002), “Fundamentals of Durable Reinforced Concrete”, Publisher: Taylor and Francis (Spon Press), pp. 272.

Ries, J. P., Speck J., and Harmon K. S., (2010), “Lightweight Aggregate Optimizes the Sustainability of Concrete, Through Weight Reduction, Internal Curing, Extended Service Life, and Lower Carbon Footprint” National Ready Mixed Concrete Association, Concrete Sustainability Conference, April 13-15 at Arizona State University (ASU), Tempe, AZ, U.S.A.

Sahmaran, M., Lachemi, M., Khandaker, M., Hossain, A., and Li, V.C., (2009), “Internal Curing of Engineered Cementitious Composites For Prevention of Early Age Autogenous Shrinkage Cracking”, Cement and Concrete Research Vol. 39, Issue. 10, pp. 893–901.

Sarkar, S.L., and Aitcin, P.C., (1987), “Comparative Study of the Microstructures of Normal and Very High-Strength Concerts Cement”, Concrete and Aggregates, Board Vol. 32, pp. 285-297.

Sarshar, R., and Khoury, G.A., (1993), “Material and Environmental Factors Influencing the Compressive Strength Of Unsealed Cement Paste and Concrete At High Temperatures”, Magazine of Concrete Research, Vol. 45, Issue 162, pp. 51-61.

Swedish Ceramic Institute (SCI), (2003), “Surface Chemistry and Rheology”, http://www.keram.se/eng/pdf/surface_chemistry.pdf, May.

Schmidt, S.R, and Launsby, R.G., (1994), “Understanding Industrial Designed Experiments”, Fourth Edition, edited by M.J Kiemele, Air Academic press, Colorado springs, Chapter 3, pp. 1-48.

Sekhar, T.S., and Rao, P.S., (2008), “Relationship between Compressive, Split Tensile, Flexural Strength of Self Compacted Concrete”, International Journal of Mechanics and Solids, Vol. 3, No. 2, pp. 157-168.

Shi, C., Wu, Y., and Riefler, C., (2006), “Self-consolidating Lightweight Concrete”, A Field Demonstration Using Insulating Concrete Forms”, Concrete International, Vol. 28, pp. 40-43.

Shi, C.J., and Wu, Y.Z, (2005), “Mixture Proportioning and Properties of Self-Consolidating Lightweight Concrete Containing Glass Powder”, ACI Material Journal, Vol. 102, Issue 5, pp. 355 - 363.

Shi, C., and Yang, X., (2005), “Design and Application of Self-Consolidating Lightweight Concretes,” Design And Application Of Self-Compacting Lightweight Concretes. China 1st International Symposium on Design, Performance and Use of Self-Consolidating Concrete. Yu Z, Shi C, Khayat KH, Xie Y, editors, RILEM Publication SARL, Paris, France. pp. 55-64.

Shi, C., and Stegemann, J.A., (2000), "Acid Corrosion Resistance Of Different Cementing Materials”, Cement and Concrete Research, Vol. 30, No. 5, pp. 803-808.

Smeplass, S., (1992), “Mechanical Properties - Lightweight Concrete”, Report 4.5, High Strength Concrete”. SP4 - Materials Design, SINTEF.

Smeplass, S., (1992), Materialutvikling Høyfast Betong, Report 5.6 “Effect of the Aggregate Type on the Compressive Strength and E-modulus of the Aggregate”, SINTEF-report STF70 A92051 Trondheim, Norway.

Sonebi, M., (2004a), “Medium Strength Self-Compacting Concrete Containing Fly Ash: Modelling Using Factorial Experimental Plans”, Cement and Concrete Research, Vol. 34, No. 7, pp. 1199-1208.

Sonebi, M., (2004b), “Applications of Statistical Models in Proportioning Medium strength Self-Compacting Concrete”, ACI Materials Journal, Vol. 34, Issue 5, pp. 339-346.

Sonebi, M., (2003), “Medium Strength Self-Compacting Concrete Containing Fly Ash: Modelling Using Factorial Experimental Plans,” Cement and Concrete Research, Vol. 34, Issue. 7, pp. 1199-1208.

Sonebi, M., (2001), “Factorial Design of Modelling Mix Proportion Parameters of Underwater Composite Cement Grouts”, Cement and Concrete Research, Vol. 31, No. 11, pp. 1553-1560.

Sonebi, M., (2001), "Effect of Silica Fume, Fly Ash and Water-to-binder Ratio on Bond Strength of Under Water, Self-Consolidating Concrete," Proceedings of the 7th CANMET ACI International Conference on Fly Ash, Silica Fume, Slag and Natural Pozzolans in Concrete, July 22-27, Chennai (Madras), India, pp. 595-610.

Sonebi, M., Grünewald, S., and Walraven, J., (2007), "Filling Ability and Passing Ability of Self-Consolidating Concrete" ACI Materials Journal, Vol. 104, Issue 2, pp. 162-170.

Sonebi, M., Svermova, L., and Bartos, P.J.M., (2004), "Factorial Design for Cement Slurries Containing Limestone Powder for Self-Consolidating SIFCON," ACI Materials Journal, Vol. 101, Issue 2, pp. 136-145.

Sonebi, M., Tamimi, A.K., and Bell, D., (2000), "Analysis of the Performance of Fresh Concrete Produced with Polysaccharide Gum and Superplasticizer Using Plunge and Orimet Tests", Proceedings of the 14th International Conference on Building Materials, 20-23 September, Tagung, Weimar, Allemagne, Germany, Vol. 1, pp. 147-156.

Sonebi, M., Batro, P., Zhu, W., Gibb, J., and Tamimi, A., (2000), "Properties of Hardened Concrete", Task 4, final report, Advance Concrete Masonry Center, University of Paisley, Scotland, United Kingdom, pp. 6-73.

Sonebi, M., Tamimi, A.K., Bartos, P.J.M., (2000), "Application of Fractural Models to Predict the Effect of Anti-Washout Admixture, Superplasticizer and Cement on Slump, Flow time and Washout Resistance if Underwater Concrete," Materials and Structures, Vol. 33, No. 229, pp. 317-323.

Sonebi, M., Bartos, P.J.M., Zhu, W., Gibbs, J., and Tamimi, A., (2000), "Final Report Task 4, Hardened Properties of SCC," Brite-EuRam, Contract No. BRPRTC96- 0366, Hardened Properties of SCC, pp. 75.

Sonebi, M., Bartos, P.J.M., and Khayat, K.H, (1999), “Assessment of Washout Resistance of Underwater Concrete: A Comparison between CRD C 61 and New MC-1 Tests,” Materials and Structures, Vol. 32, No. 218, pp. 273-281.

Sonebi, M., and Bartos, P.M.J., (1999), “Hardened SCC and its Bond with Reinforcement,” Proceedings of RILEM International Symposium on Self- Compacting Concrete, Å. Skarendahl and Ö. Petersson, Eds., Stockholm, Sweden, pp. 275-290.

Stat-Ease Corporation, (2009), “Design-Expert 8.1 Software for Design of Experiments, Stat-Ease”, Statistics Made Easy, Minneapolis, U.S.A.

Su, N., And Miao, B., (2003), “A new Method for The Mix Design of Medium Strength Flowing Concrete with Low Cement Content”, Cement and Concrete Composites, Vol. 25, Issue. 2, pp. 215–222.

Tarun, R.N., Rudolph, N.K., Yoon-moon, C., Fethullah, C., and Bruce, W.R., (2005), “Use of Limestone Quarry By-Products for Developing Economical Self-Compacting Concrete”, Center for By-Products Utilization, Report No. CBU-2005-14.

Tepfers, R., and Lorenzis, L.D., (2003), “Bond of FRP Reinforcement in Concrete." Mechanics of composite materials, Vol. 39(4), pp. 315-328.

Thomas, M.D.A., (1997), “Laboratory and Field Studies of Salt Scaling in Fly Ash Concrete”, Proceedings of the International RILEM Workshop on Resistance of Concrete to Freezing and Thawing With or Without De-Icing Chemicals, Essen, Germany, pp. 21-30.

Thomas, H., (1994), “Lightweight Concrete and Aggregates,” Significance of Tests and Properties of Concrete and Concrete-Making Materials, STP 169C, ASTM, Philadelphia, PA, pp. 522-532.

The Concrete Countertop Institute (CCI), (2006) “Lightweight Concrete Mixes”, (http://www.concretecountertopinstitute.com/modules/), July, 15th, 2011.

TXI aggregate company, (2011), (http://www.txi.com/), September 25th, 2011, 1341 West Mockingbird Lane Dallas, TX 75247, United States.

Topcu, I.B., and Uygunoglu, T., (2010), “Effect of Aggregate Type on Properties of Hardened Self-Consolidating Lightweight Concrete (SCLC)” Construction and Building Materials, Vol. 24, Issue 7, pp. 1286–1295.

Topcu, I.B., and Uygunoglu, T., (2007), “Properties of Autoclaved Lightweight Aggregate Concrete”, Building and Environment, Vol. 42, Issue 12, pp. 4108–4116.

Topcu, I.B., (1997), "Semi-Lightweight Concretes Produced by Volcanic Ash", Cement and Concrete Research, Vol. 27, Issue. 1, pp. 15-21.

Toutanji, H., Delatte, N., Aggoun S. Duval, R., and Danson, A., (2004), “Effect of Supplementary cementitous Materials on the compressive strength and durability of short-term cured concrete,” Cement and Concrete Research, Vol. 34, Issue. 2, pp. 311-319.

Umehara H., Uehara T., Enomoto Y., and Oka S., (1994), “Development and usage of lightweight high performance concrete” Proceeding of International Conference on high performance concrete (supplementary papers), Singapore, American Concrete Institute, Detroit, USA, pp. 339 – 353.

Uygunoglu, T., and Topcu, I.B., (2009), “Thermal expansion of self-consolidating normal and lightweight aggregate concrete at elevated temperature”, Construction and Building Materials, Vol. 23, Issue 9, pp. 3063–3069.

Walraven, J.C., and Stroband, J., (1995), “Bond, Tension Stiffening and Crack Width Control in Lightweight Concrete”, CEB/FIP International Symposium on Structural Lightweight Aggregate Concrete, Sandefjord, Norway, pp. 256–266. Editors: I. Holand, et al.

Wang, H.Y., (2009), “Durability of Self-Consolidating Lightweight Aggregate Concrete Using Dredged Silt”, Construction and Building Materials, Vol. 23, Issue 6, pp. 2332-2337.

Weber, S., and Reinhardt, H.W., (1995), “A Blend of Aggregate to Support Curing of Concrete”, CEB/FIP International Symposium on Structural Lightweight Aggregate Concrete”, Sandefjord, Norway, pp. 662-671.

Weigler, H., Karl, S., and Lieser, P., (1972), “The Bending Load Capacity of Reinforced Lightweight Concrete”, Betonwerk und Fertigteil-Technik Vol. 38, No. 5, pp. 324-334 and No. 6, pp. 445-449.

Weiss, D.J., (2006), “Analysis of Variance and Functional Measurement”, 1st edition, Oxford University Press, New York, pp. 271.

Whitcomb, P.J., and Anderson, M.J., (2004), “RSM Simplified: Optimizing Processes Using Response Surface Methods For Design of Experiments”, Productivity Press, New York, pp. 292.

Whiting, D.A., and Nagi, M.A., (1998), “Manual of Control of Air Content in Concrete”, Portland Cement Association, Skokie, Illinois.

Wu, Z., Zhang, Y., Zheng J., and Ding,Y., (2009), “An Experimental Study on The Workability of Self-Compacting Lightweight Concrete”, Construction and Building Materials, Vol. 23, pp. 2087-2092.

Yanai, S., Sakata, N., Nobuta, Y., and Okamoto, T, (1999), "Study on Mix Proportion for Self - Compacting High Performance Lightweight Aggregate Concrete" 2nd International Symposium on Structural Lightweight Aggregate Concrete, Kristiansand, Norway. pp. 18-22.

Yeginobali, A., Sobolev, K.G., Soboleva, S.V., and Tokyay, M., (1998), "High Strength Natural Lightweight Aggregate Concrete with Silica Fume", Vol. 178, pp. 739-758.

Yao, S.X., and Gerwick, B.C., (2006), "Development of Self-Compacting Lightweight Concrete for RFP Reinforced Floating Concrete Structures", US Army Corps of Engineers Research and Development Center, Technical Report, San Francisco, California, U.S.A.

Zhang, M.H., and Malhotra, V.M., (1995), "Characteristic of a Thermally Activated Alumino Silicate Pozzolanic Material and Its Use In Concrete", Cement and Concrete Research, Vol. 25, No. 8, pp. 1713-1725.

Zhang, M.H., and Gjørv, O.E., (1995), "Properties of High-strength Lightweight Concrete", CEB/FIP International Symposium on Structural Lightweight Aggregate Concrete, Sandefjord, Norway, pp. 683-693.

Zhang, M.H., (1989), "Microstructure and Properties of High Strength Lightweight Concrete", PhD Thesis, The Norwegian University of Science and Technology, N-7034, Publisher, Trondheim, Norway.

Zhu, W., Sonebi, M., Bartos, P.J.M., (2004), "Bond and Interfacial Properties of Reinforcement in Self-Compacting Concrete," Materials and Structures, Vol. 37, No. 7, pp. 442-448.

Zhu W., and Bartos P, (2003), "Permeation Properties of Self-Compacting Concrete", Cement and Concrete, Vol. 33, No.6, pp. 921–926.

Zhu, W., Gibbs, J.C., and Bartos, P.J.M., (2001), “Uniformity of In-Situ Properties of Self-Compacting Concrete in Full-Scale Structural Elements,” Cement and Concrete Composites, Vol. 23, No. 1, pp. 57-64.